EVALUATION OF

Hydrogen/Fluorine/Lithium,

Hydrogen/Fluorine, and

Hydrogen-Lithium/Fluorine

UPPER STAGES

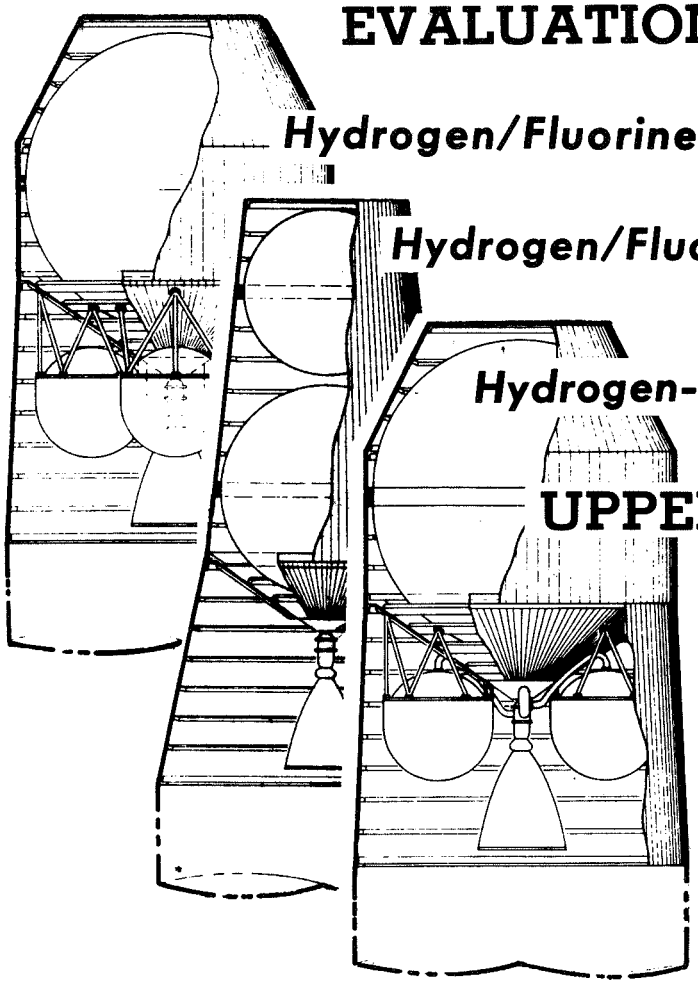

TR-AE-70-29

JUNE 25, 1970

SPACE DIVISION CHRYSLER CORPORATION

TECHNICAL REPORT TR-AE-70-29

EVALUATION OF HYDROGEN/FLUORINE/LITHIUM, HYDROGEN/FLUORINE, AND HYDROGEN-LITHIUM/FLUORINE UPPER STAGES

July 25, 1970

Approved by: G. M. Joseph
G. M. Joseph
Study Manager

Approved by: C. E. Tharratt
C. E. Tharratt, Manager
Advanced Vehicle Systems

Prepared for

The National Aeronautics and Space Administration,
Office of Advanced Research and Technology,
Washington, D. C., under Contract NASw-1965,
Tripropellant Stage Study

CHRYSLER CORPORATION SPACE DIVISION, P. O. BOX 29200
NEW ORLEANS, LOUISIANA 70129

FOREWORD

This report was prepared by the Chrysler Corporation Space Division, New Orleans, Louisiana, and contains the results of a study performed for the National Aeronautics and Space Administration, Office of Advanced Research and Technology, under contract NASw-1965, "Tripropellant Stage Study".

ACKNOWLEDGEMENTS

The Tripropellant Stage Study was performed under the direction of Dr. Robert S. Levine, NASA Headquarters, telephone (202) 962-1703.

Propulsion company support was provided by Rocketdyne Division, North American Rockwell Corporation. Specific contributions included parametric performance, size, and weight data for fluorine-hydrogen engines. This support was quite valuable to the study and was much appreciated.

Chrysler Corporation Space Division personnel responsible for major contributions to the study included:

G. M. Joseph - Study Manager, telephone (504) 255-2395

J. D. Magness - Technical Leader, Stage Design and Structures

R. C. Pocklington - Technical Leader, Performance and Mission Analysis

P. D. Thompson - Technical Leader, Propulsion and Mechnical Systems

TABLE OF CONTENTS

Paragraph	Title	Page
	Section 1 - INTRODUCTION	
1.1	General	1-1
1.2	Study Objectives	1-1
1.3	Summary of Results	1-2
1.3.1	Engine Parameter Optimization	1-2
1.3.2	Stage Sizing and Performance Comparisons	1-3
1.3.2.1	Direct Injection Missions	1-3
1.3.2.2	Long Duration Missions	1-4
1.3.2.2.1	Single-Burn Missions	1-4
1.3.2.2.2	Two-Burn Missions	1-4
1.3.2	Implications of Slush Hydrogen	1-4
	Section 2 - STUDY APPROACH	
2.1	General	2-1
2.2	Sizing Computer Program Description	2-2
2.2.1	General	2-2
2.2.2	Stage Configurations	2-5
2.2.3	Structural Systems	2-13
2.2.4	Thermal Protection Systems	2-15
2.2.4.1	Cryogenic Storage	2-15
2.2.4.2	Lithium Storage	2-20
2.2.5	Meteoroid Protection	2-21
2.2.5.1	Meteoroid Environment	2-21
2.2.5.2	Design Meteoroid Mass	2-22
2.2.5.3	Meteoroid Shield Model	2-26
2.2.5.4	Method of Analysis	2-28
2.2.6	Reaction Control System (RCS)	2-30
2.2.7	Propellant Feedlines	2-32
2.2.8	Engine Data	2-33
2.2.9	Electric Heater and Power System	2-34
2.2.10	Miscellaneous Weights	2-34
2.2.11	Contingency Weight	2-35

TABLE OF CONTENTS (continued)

Paragraph	Title	Page
	Section 3 - STUDY RESULTS	
3.1	General	3-1
3.2	Direct Injection Missions	3-1
3.2.1	Data and Assumptions	3-1
3.2.2	Engine Parameter Optimization	3-5
3.2.2.1	Example Tripropellant Stage Engine Parameter Optimization	3-5
3.2.2.2	Example Bipropellant Stage Engine Parameter Optimization	3-11
3.2.2.3	Example Gel Stage Engine Parameter Optimization	3-11
3.2.2.4	Example Stage Weight Optimization	3-11
3.3	Stage Comparisons	3-15
3.3.1	Atlas/Centaur Booster Results	3-15
3.3.2	Atlas Booster Results	3-23
3.3.3	Titan IIID/Centaur Booster Results	3-26
3.3.4	Titan IIID Booster Results	3-26
3.3.5	260-Inch SRM/S-IVB Booster Results	3-45
3.4	Long-Duration Missions	3-65
3.4.1	Data and Constraints	3-65
3.4.2	Single-Burn Mission Results	3-68
3.4.3	Multiple-Burn Mission Results	3-71
3.5	Sensitivity Studies	3-87
3.5.1	Thermal Protection	3-87
3.5.1.1	Effect of Propellant Load	3-87
3.5.1.2	Implications of Stage Mass Ratio	3-87
3.5.1.3	Effect of Coast Time	3-90
3.5.1.4	Effect of Insulation External Surface Temperature	3-91
3.5.1.5	Effects of Thermal Conductivity	3-91
3.5.1.6	Advantages of Slush Hydrogen	3-94
3.5.2	Meteoroid Shield Sensitivity Analysis	3-95
	Section 4 - CONCLUSIONS AND RECOMMENDATIONS	

TABLE OF CONTENTS (continued)

Appendix	Title	Page
A	NOMENCLATURE	A-1
B	DEFINITIONS	B-1
C	OPTIMIZATION CHARTS	C-1
D	METEOROID SHIELD ANALYSIS	D-1
E	BOOSTER VELOCITY INCREMENT VERSUS PAYLOAD	E-1
F	DESIGN CHARTS	F-1

LIST OF ILLUSTRATIONS

Figure	Title	Page
2-1	Typical Launch Vehicle Performance Capability	2-4
2-2	Method of Locating the Stage's Center of Gravity	2-6
2-3	Spacing Constraints	2-7
2-4	Tripropellant Configurations 111 and 121	2-8
2-5	Tripropellant Configurations 112 and 122	2-9
2-6	Tripropellant Configurations 113 and 123	2-10
2-7	Tripropellant Configuration 114	2-10
2-8	Bipropellant and Gel Configurations	2-11
2-9	Four Alternate Bipropellant Configurations	2-12
2-10	Tank Support Concepts	2-14
2-11	Spider Beam Thrust Structure Concept	2-15
2-12	A Typical Thermal Optimization	2-18
2-13	Meteoroid Environment Model	2-22
2-14	Whipple's "Bumper Shield" Concept	2-26
2-15	Meteoroid Shield Model	2-28
2-16	A Typical Meteoroid Shield Analysis	2-30
2-17	Model Used to Compute Mass Moment of Inertia	2-31
2-18	Tripropellant Feedline Geometry	2-32
2-19	Bipropellant Feedline Geometry	2-33
2-20	Electric Heater Weight	2-34
2-21	Additional Power System Weight	2-35
3-1	Payload Variation with Chamber Pressure (Atlas/Centaur/Tripropellant)	3-5
3-2	Payload and Corresponding Chamber Pressure Variation with Expansion Ratio (Atlas/Centaur/Tripropellant)	3-6
3-3	Engine Parameter Optimization Summary (Atlas/Centaur/Tripropellant)	3-6
3-4	Payload Variation with Percent Hydrogen (Atlas/Centaur/Tripropellant)	3-7
3-5	Payload Variation with Chamber Pressure (Atlas/Centaur/Bipropellant)	3-7
3-6	Engine Parameter Optimization Summary (Atlas/Centaur/Bipropellant)	3-8

LIST OF ILLUSTRATIONS (continued)

Figure	Title	Page
3-7	Payload Variation with Chamber Pressure (Atlas/Centaur/Gel)	3-8
3-8	Payload and Corresponding Chamber Pressure Variation with Percent Hydrogen (Atlas/Centaur/Gel)	3-9
3-9	Engine Parameter Optimization Summary (Atlas/Centaur/Gel)	3-9
3-10	Payload Variation with Stage Weight, Direct Injection Missions (Atlas/Centaur)	3-12
3-11	Stage Cost Estimating Relationship	3-13
3-12	Cost Effectiveness Stage Size Selection (Atlas/Centaur)	3-14
3-13	Stage Size Comparison (Atlas/Centaur)	3-14
3-14	Direct Injection Mission (Atlas/Centaur)	3-15
3-15	Tripropellant Stage (Atlas/Centaur)	3-21
3-16	Bipropellant Stage (Atlas/Centaur)	3-22
3-17	Gel Stage (Atlas/Centaur)	3-22
3-18	Payload Variation with Mission Velocity, Direct Injection Mission (Atlas)	3-25
3-19	Payload Corresponding to Optimum Cost Effective Stage Size (Atlas)	3-25
3-20	Tripropellant Stage (Atlas)	3-32
3-21	Bipropellant Stage (Atlas)	3-33
3-22	Gel Stage (Atlas)	3-34
3-23	Payload Variation with Mission Velocity, Direct Injection Mission (Titan IIID/Centaur)	3-36
3-24	Tripropellant Stage (Titan IIID/Centaur)	3-42
3-25	Bipropellant Stage (Titan IIID/Centaur)	3-42
3-26	Gel Stage (Titan IIID/Centaur)	3-43
3-27	Payload Variation with Mission Velocity, Direct Injection Mission (Titan IIID)	3-45
3-28	Tripropellant Stage (Titan IIID)	3-51
3-29	Bipropellant Stage (Titan IIID)	3-52
3-30	Gel Stage (Titan IIID)	3-53
3-31	Payload Variation with Mission Velocity, Direct Injection Mission (260-Inch SRM/S-IVB)	3-55
3-32	Tripropellant Stage (260-Inch SRM/S-IVB)	3-61
3-33	Bipropellant Stage (260-Inch SRM/S-IVB)	3-62
3-34	Gel Stage (260-Inch SRM/S-IVB)	3-63
3-35	Alternate Bipropellant Stage (260-Inch SRM/S-IVB)	3-65
3-36	External Profiles of Stages for Single-Burn, Long Duration Mission	3-70
3-37	Two-Burn Mission Payload Capability (260-Inch SRM/S-IVB)	3-78

LIST OF ILLUSTRATIONS (continued)

Figure	Title	Page
3-38	Two-Burn, Tripropellant Stage (260-Inch SRM/S-IVB)	3-80
3-39	Two-Burn, Bipropellant Stage (260-Inch SRM/S-IVB)	3-80
3-40	Two-Burn, Gel Stage (260-Inch SRM/S-IVB)	3-81
3-41	Effect of Propellant Load on Thermal Mass Penalty	3-88
3-42	Implications of Stage Mass Ratio on Thermal Mass Penalty	3-89
3-43	Effects of Coast Time on Thermal Mass Penalty	3-90
3-44	Effects of External Temperature on Thermal Mass Penalty	3-91
3-45	Effects of Thermal Conductivity on Thermal Mass Penalty	3-92
3-46	Effects of Insulation Thermal Conductivity for Shadow-Shielded Hydrogen Tank	3-93
3-47	Advantages of Slush Hydrogen	3-94

LIST OF TABLES

Table	Title	Page
1-1	Optimum Engine Characteristics	1-3
1-2	Direct Injection Missions Payload Summary	1-3
2-1	Upper Stage Sizing Program-Subroutine Listing Summary	2-2
2-2	Constraints on Stage Configuration Geometry	2-5
2-3	Miscellaneous Subsystem	2-35
3-1	Design Constraints for Direct Injection Missions	3-2
3-2	Prime Structure Design Data for Direct Injection Missions	3-3
3-3	Tankage Design Data for Direct Injection Missions	3-4
3-4	Major Stage Characteristics Summary, Atlas/ Centaur Booster, Direct Injection	3-16
3-5	Engine Data Summary, Atlas/Centaur Booster, Direct Injection	3-17
3-6	Design Data Summary, Bipropellant Stage, Atlas/ Centaur Booster, Direct Injection	3-18
3-7	Design Data Summary - Gelled H_2/Li Stage, Atlas/ Centaur Booster, Direct Injection	3-19
3-8	Design Data Summary - Tripropellant Stage, Atlas/ Centaur Booster, Direct Injection	3-20
3-9	Weight Statement Comparison, Atlas/Centaur Booster, Direct Injection Mission	3-24
3-10	Major Stage Characteristics Summary, Atlas Booster, Direct Injection	3-27
3-11	Engine Data Summary, Atlas Booster, Direct Injection	3-28
3-12	Design Data Summary - Bipropellant Stage, Atlas Booster, Direct Injection	3-29
3-13	Design Data Summary, Gelled H_2/Li Stage, Atlas Booster, Direct Injection	3-30
3-14	Design Data Summary - Tripropellant Stage, Atlas Booster, Direct Injection	3-31
3-15	Weight Statement Comparison, Atlas Booster, Direct Injection Mission	3-35

LIST OF TABLES (continued)

Table	Title	Page
3-16	Major Stage Characteristics Summary, Titan IIID/ Centaur Booster, Direct Injection	3-37
3-17	Engine Data Summary, Titan IIID/Centaur Booster, Direct Injection	3-38
3-18	Design Data Summary - Bipropellant Stage, Titan IIID/Centaur Booster, Direct Injection	3-39
3-19	Design Data Summary - Gelled H_2/Li Stage, Titan IIID/Centaur Booster, Direct Injection	3-40
3-20	Design Data Summary - Tripropellant Stage, Titan IIID/Centaur Booster, Direct Injection	3-41
3-21	Weight Statement Comparison, Titan IIID/Centaur Booster, Direct Injection Mission	3-44
3-22	Major Stage Characteristics Summary, Titan IIID Booster, Direct Injection	3-46
3-23	Engine Data Summary, Titan IIID Booster, Direct Injection	3-47
3-24	Design Data Summary - Bipropellant Stage, Titan IIID Booster, Direct Injection	3-48
3-25	Design Data Summary - Gelled H_2/Li Stage, Titan IIID Booster, Direct Injection	3-49
3-26	Design Data Summary - Tripropellant Stage, Titan IIID Booster, Direct Injection	3-50
3-27	Weight Statement Comparison, Titan IIID Booster, Direct Injection Mission	3-54
3-28	Major Stage Characteristics Summary, 260-Inch SRM/S-IVB Booster, Direct Injection	3-56
3-29	Engine Data Summary, 260-Inch SRM/S-IVB Booster, Direct Injection	3-57
3-30	Design Data Summary - Bipropellant Stage, 260-Inch SRM/S-IVB Booster, Direct Injection	3-58
3-31	Design Data Summary - Gelled H_2/Li Stage, 260-Inch SRM/S-IVB Booster, Direct Injection	3-59
3-32	Design Data Summary - Tripropellant Stage, 260-Inch SRM/S-IVB Booster, Direct Injection	3-60
3-33	Weight Statement Comparison, 260-Inch SRM/S-IVB Booster, Direct Injection Mission	3-64
3-34	Single-Burn Interplanetary Mission Data	3-65
3-35	Two-Burn Interplanetary Mission Data	3-66
3-36	Design Constraints for Interplanetary Missions	3-66
3-37	Prime Structure Design Data for Interplanetary Missions	3-67
3-38	Tankage Design Data for Interplanetary Missions	3-67

LIST OF TABLES (continued)

Table	Title	Page
3-39	Meteoroid Protection Data for Interplanetary Missions	3-68
3-40	Weight Statement Comparison, Single-Burn Mars Retro (12,000 lb Gross Weight)	3-69
3-41	Major Stage Characteristics Summary, 120-Inch Booster, Single-Burn Interplanetary Mission	3-72
3-42	Engine Data Summary, 120-Inch Diameter Single-Burn, Interplanetary Mission	3-73
3-43	Design Data Summary - Bipropellant Stage, 120-Inch Diameter Booster, Single-Burn, Interplanetary Mission	3-74
3-44	Design Data Summary - Gelled H_2/Li Stage, 120-Inch Diameter Booster, Single-Burn, Interplanetary Mission	3-75
3-45	Design Data Summary - Tripropellant, 120-Inch Diameter Booster, Single-Burn, Interplanetary Mission	3-76
3-46	Effects of Favorable Thermal Analysis Criteria on Stage Comparisons	3-77
3-47	Weight Statement Comparison, 260-Inch SRM/S-IVB Booster, Two-Burn Mars Retro	3-79
3-48	Major Stage Characteristics Summary, 260-Inch SRM/S-IVB Booster, Two-Burn, Interplanetary Mission	3-82
3-49	Engine Data Summary, 260-Inch SRM/S-IVB Booster, Two-Burn, Interplanetary Mission	3-83
3-50	Design Data Summary - Bipropellant Stage, 260-Inch SRM/S-IVB Booster, Two-Burn, Interplanetary Mission	3-84
3-51	Design Data Summary - Gelled H_2/Li Stage, 260-Inch SRM/S-IVB Booster, Two-Burn, Interplanetary Mission	3-85
3-52	Design Data Summary - Tripropellant Stage, 260-Inch SRM/S-IVB Booster, Two-Burn, Interplanetary Mission	3-86
3-53	Summary of Meteoroid Shield Sensitivity to Backup Sheet Selection	3-95
3-54	Summary of Meteoroid Shield Sensitivity to Design Criteria	3-96

Section 1
INTRODUCTION

1.1 GENERAL

One of the highest performing propellant combinations to be investigated is the tripropellant lithium/fluorine/hydrogen. This advanced propellant combination, which offers more than a 10 percent improvement in theoretical specific impulse over the best performing bipropellant (fluorine/hydrogen), was the subject of a recent engine study by Rocketdyne under contract NASw-1838. The purpose of the present stage study was to investigate the requirements for integrating this propellant into a complete stage and to determine the resultant performance capabilities. This report describes the work accomplished and the results obtained during the study. Included herein are a description of the methods used to accomplish the study, performance comparisons between tripropellant and fluorine/hydrogen upper stages, which have been optimized for use on five different boosters for both direct injection and long duration missions, and the results of sensitivity studies accomplished for the thermal and meteoroid protection systems.

1.2 STUDY OBJECTIVES

The objective of this study was to determine if a lithium/fluorine/hydrogen tripropellant stage would be sufficiently attractive to merit further technology development, and to identify the technology areas for future study. To accomplish this objective, the technical effort was divided into two parts. The purpose of Part I was to provide a direct and reliable comparison between the tripropellant $Li/F_2/H_2$ stage and a comparable F_2/H_2 bipropellant stage for a wide range of missions and boosters. Using the results obtained, design criteria was to be selected for a conceptual design to be prepared in the Part II study effort. The conceptual design studies were intended to: a) identify technology development requirements; b) enable comparisons with other systems (e.g., nuclear); c) identify any special GSE, handling, transportation or fabrication problems; and d) to provide a baseline configuration to assist NASA in the planning of related study work.

Early in the study, it became evident that the tripropellant stage had a relatively poor mass fraction* – low enough to offset the advantage of its very high specific impulse. Consequently, the question arose of whether a higher payload might be

*Mass Fraction = W_{PROP}/W_{STAGE}

achieved for the tripropellant system by combining the hydrogen and lithium into the same tank, thereby saving some of the lithium tank, insulation and meteoroid shield weights. This was a compromise since the specific impulse is less and a third agent (e.g., methane) is required to gel the hydrogen so that the lithium would remain in suspension and homogeneously distributed. However, to ensure a thorough investigation of the merits of the fluorine/lithium/hydrogen system, this approach was added to the Part I scope of work. Hereinafter, the two-tank tripropellant system will be referred to as the "Gel" stage. This designation is merely one of convenience and is not intended to imply that gelling the hydrogen to suspend the lithium is necessarily better than using a slurry.

1.3 SUMMARY OF RESULTS

To ensure that reliable conclusions were obtained in this study with respect to the relative attractiveness of the tripropellant stage, the following major tasks were accomplished:

1) The optimum combination of engine characteristics, e.g., mixture ratio, area ratio and chamber pressure was determined for each stage investigated as a function of mission requirement (i.e., mission velocity and coast time), stage size and launch vehicle.

2) Each stage (tripropellant, gel and bipropellant) was sized to achieve both the maximum payload and optimum cost effective payload as a function of mission requirement and booster vehicle.

3) For the missions involving a long coast, additional sensitivity studies were conducted to evaluate the implications of uncertainties in the thermal and meteoroid protection system analyses.

4) The merits of using slush hydrogen was investigated for both the direct injection and long duration missions.

The results of these studies are summarized in the following paragraphs.

1.3.1 ENGINE PARAMETER OPTIMIZATION

Table 1-1 summarizes the optimum engine characteristics for the three stages. The values are presented as a range since the optimums were found to be dependent upon both mission requirement and stage size.

Although the engine parameters were selected on the basis of stage performance rather than engine performance, negligible penalties would have been incurred had optimum (theoretical) engine characteristics been chosen. The final selection should strongly consider engine costs and development risks as they relate to the attainment of attaining the engine performance upon which the study results are predicated.

Table 1-1. Optimum Engine Characteristics

Stage/Engine Parameter	Chamber Pressure (psia)	Area Ratio	Percent Hydrogen
Tripropellant	750-1000	160:1	23-28
Bipropellant	800-950	100:1 to 150:1	*
Gel	800-1000	125:1 to 160:1	22-25

*Mixture ratio was assumed to be 12:1 for the bipropellant stage.

1.3.2 STAGE SIZING AND PERFORMANCE COMPARISONS

1.3.2.1 Direct Injection Missions

Table 1-2 compares the payload capability of the three stages for three mission velocities and five different boosters. Each payload corresponds to a stage that has been optimized for the particular booster and mission velocity identified. The optimum stage sizes were found to be a function of mission velocity as well as launch vehicle. The results show that the tripropellant stage does not have a significant payload advantage over a fluorine/hydrogen bipropellant stage for any of the boosters investigated, and that the tripropellant and gel stages are comparable for direct injection missions – at least from a payload standpoint.

Table 1-2. Direct Injection Missions Payload Summary

Velocity (Ft/Sec) \ Booster		Payload (Pounds)				
		*Atlas Centaur	Atlas	*Titan IIID Centaur	Titan IIID	260" SRM S-IVB
36,140 (Earth Escape)	BI	4,200	4,510	**	12,700	39,500
	TRI	4,400	4,260	**	13,100	40,500
	GEL	4,350	4,520	**	13,000	39,500
48,500 (≈0.3 AU Probe)	BI	900	300	3,900	3,680	13,800
	TRI	990	***	4,110	3,600	14,500
	GEL	970	140	4,070	3,800	13,700
54,500 (≈0.2 AU Probe)	BI	120	***	2,200	1,300	7,300
	TRI	125	***	2,210	1,480	7,600
	GEL	150	***	2,080	1,470	6,950

*Gross Weight above Centaur limited to 12,000 lb.
**Kick stage does not improve booster's performance
***No capability

1.3.2.2 Long Duration Missions

1.3.2.2.1 Single Burn Missions

The mission assumed for this analysis consisted of a single burn to achieve a velocity increment of 8000 fps after a 205-day coast. This is roughly analogous to a braking (retro) maneuver into a low orbit about the planet Mars. A stage size of 12,000 pounds, including payload and interstage, was assumed for all three propellant combinations. This size is intermediate to the optimum for the 260-inch SRM/S-IVB and Titan IIID boosters which are about 14,000 and 10,000 pounds, respectively. Thus, the results of the 12,000-pound stage study are applicable to a wide range of boosters.

The results showed that the fluorine/hydrogen bipropellant stage had a payload of 5266 pounds, which compared to 4642 pounds for the tripropellant stage and 5112 pounds for the gel stage. The poorer performance of the tripropellant and gel stages is due almost entirely to the very high thermal and meteoroid protection requirements for these stages as compared to the fluorine/hydrogen bipropellant stage. The requirement for increased protection results from the relatively larger hydrogen tanks required for the gel and the tripropellant stages, and the additional requirement of having to protect the lithium tank in the tripropellant stage.

Additional studies were conducted to determine if the uncertainties in the thermal and meteoroid protection requirements could lead to erroneous conclusions. These sensitivity studies showed that any differences due to these uncertainties would not change the relative attractiveness of the stages. However, they did indicate that the payload capability of the gel stage might be comparable to the bipropellant stage under the most optimistic assumptions regarding the thermal protection system requirements.

1.3.2.2.2 Two-Burn Missions

A mission requiring two burns was assumed to illustrate the effect of requiring more than one burn from the upper stage. A mission was postulated which required that the booster (in this case a 260-inch SRM/S-IVB) and upper stage deliver a total of 46,000 fps of which 8,000 fps was specified as being required after a 205-day coast. The remaining 38,000 fps was to be shared between the booster and the upper stage. Payload was determined for the three types of stages as functions of stage size. The results showed that, relatively, the tripropellant stage compared even less favorably with the bipropellant than for the single burn mission. The results of these analyses are shown in paragraph 3.4.

1.3.2 IMPLICATIONS OF SLUSH HYDROGEN

The investigation of the potential merits of using slush hydrogen was not, per se, one of the objectives of this study. However, the implications of using slush hydrogen was examined, for both the direct injection and long-duration missions, to determine if its use would affect any of the conclusions arrived at in this study. For direct injection missions it was found that the payload of the bipropellant and tripro-

propellant stages would be increased by approximately 5 and 10 percent, respectively. For long duration missions it was found that the increased thermal capacity of slush hydrogen would enable significant reductions in the thermal protection system weights. The use of slush hydrogen for the long duration missions was found to be especially intriguing since there would be minimal special stage design requirements to incorporate it. This is because the slush would all be melted prior to igniting the main engines (assuming a one-burn mission).

Even though the use of slush hydrogen was relatively more beneficial to the tripropellant and gel stages than to the bipropellant stage, its use does not increase payloads enough to make the tripropellant stage as attractive as the bipropellant stage for missions involving a long coast.

Section 2
STUDY APPROACH

2.1 GENERAL

Before reliable conclusions could be drawn concerning the relative merits of a hydrogen/fluorine/lithium tripropellant stage when compared with the bipropellant fluorine/hydrogen stage, each stage had to be efficiently sized and its major characteristics selected to ensure that maximum performance would be attained for the particular mission of interest. Even a cursory examination of the basic design requirements for the bipropellant and tripropellant stages shows that the use of assumed mass fractions (or even trend-curve derived mass fractions in the case of the tripropellant stage) or ground-ruled engine operating parameter selections (e.g., P_c, ϵ, MR) could lead to significant errors in performance predictions. Moreover, the results obtained could be biased in favor of one stage or the other. Therefore, to accomplish the stage comparisons previously described, and to ensure that conclusions could be interpreted reliably, the design parameters for each stage evaluated in this study were optimized from a payload standpoint. Thus, for each combination of propellant load, missions specification, and launch vehicle the optimum engine parameters were determined (i.e., P_c, ϵ, MR, percent H_2 and, where pertinent, the number of engines). The optimum amount of meteoroid protection and thermal insulation were also evaluated. Weights for structural, power, electrical, GN&C, propulsion and miscellaneous subsystems were estimated to be compatible with the mission requirements of the particular stage investigated. These weights were determined parametrically with sufficient accuracy to permit satisfactory performance predictions.

To facilitate handling of the large number of variables associated with the wide range of missions and alternate boosters investigated, a digital computer program was used. The program has the capability to accomplish stage optimization for a specified mission considering the following major variables or constraints and their interdependent relationships:

1) Engine parameters (P_c, ϵ, MR, percent H_2, I_{sp}, ηI_{sp}),
2) Number of coast periods and time duration of each,
3) Thermal control and meteoroid protection requirements,
4) Jettisonable weights (sized internal to program) and jettison time (either interstage, shroud, or both),

5) Power system requirements and weights,

6) Propulsion system weights (including pressurization, propellant residuals, feed system, RCS, propellant orientation, etc.),

7) Astrionics including GN&C subsystems,

8) Miscellaneous weights,

9) Payload above the stage,

10) Dimensional constraints (e.g., maximum diameter),

11) Design constraints (e.g., minimum skin gauges), and

12) Structure design.

The following paragraphs describe the computer program and illustrate the manner in which it was used for this study.

2.2 SIZING COMPUTER PROGRAM DESCRIPTION

2.2.1 GENERAL

The sizing computer program which was used in this study comprises numerous smaller subprograms and subroutines that are used to analyze the requirements for the various systems which make up an upper stage. Table 2-1 provides a listing of the more important subroutines included in the program.

Table 2-1. Upper Stage Sizing Program-Subroutine Listing Summary

STGSIZ	-	Main subroutine which handles the program control, determines the stage geometry and size, and selects the optimum stage for each mission.
THERM	-	Optimizes the cryogenic tankage on the basis of minimum weight. Determines ullage pressure, thermal insulation thickness, tank weight, pressurization system weight, and boiloff and vent time where pertinent.
XINSUL	-	Optimizes the lithium tank on the basis of minimum weight. Computes initial lithium temperature, thermal insulation weight, tank weight, pressurization system weight and addendum heater and electrical power system weight.
METEOR	-	Establishes meteoroid protection requirements and determines the optimum shield geometry and weight.
STRUCT	-	Computes the weight of the shell and interstage.
THRST	-	Determines the thrust cone and spider beam weights.
RCS3	-	Determines the weight of reaction control propellant required and the entire subsystem weight on the basis of a limit cycle.

The program is designed to permit the determination of: 1) the optimum engine parameters for a given stage, and 2) the optimum size upper stage for a specified mission and booster. The engine parameter optimization is accomplished by means of a series of "do-loops" within the program which vary the engine parameters one at a time and determine the corresponding payloads. For example, if five values were assumed for each of the four parameters (P_c, ϵ, F_2/LI, and percent H_2), then 625 (5x5x5x5) payloads (and their corresponding stages) will be determined. These data can be cross plotted to find the optimum engine parameters as well as to identify payload sensitivity to off-optimum selections.

The determination of the optimum stage size for a given booster and mission is handled slightly different than is commonly done. The usual approach is to assume different propellant loadings and to calculate payload and stage size as a function of propellant load. In this program, however, stage gross weight*, defined below, is assumed as the independent variable and stage size, payload, interstage weight and propellant load are all computed as dependent variables. This is done to allow the velocity split between the booster and upper stage to be determined in a straight forward manner. Figure 2-1 shows a typical launch vehicle performance capability plot; i.e., payload (or gross weight above the booster) versus velocity. The total mission velocity is defined as:

$$1)\quad \Delta V_{MISSION} = \Delta V_{Booster} + \Delta V_{Upper\ Stage\text{-}Transfer} + \Delta V_{Upper\ Stage\text{-}Retro}$$

Thus, if the upper stage gross weight is specified then the velocity which will be obtained from the booster can be determined from figure 2-1 and the total velocity requirement of the upper stage can be determined from equation 1. Knowing the specific impulse (corresponding to a particular combination of engine parameters) and the velocity requirements, the propellant load requirements can be computed as follows, assuming a maximum of two burns (e.g., transfer and breaking maneuvers):

$$\mu_{TRANS} = \exp\left[\frac{\Delta V_{TRANSFER}}{g_c\ Isp}\right]$$

$$\mu_{RETRO} = \exp\left[\frac{\Delta V_{BREAKING}}{g_c\ Isp}\right]$$

$$W_{PROP_1} = \left[\frac{\mu_{TRANS\text{-}1}}{\mu_{TRANS}}\right]\left[W_{IGNITION} - W_{STARTUP}\right]$$

*$W_{Gross} = W_{Stage} + W_{Payload} + W_{Interstage}$

$$W_{PROP_2} = \left[\frac{\mu_{RETRO}^{-1}}{\mu_{RETRO}}\right]\left[\left(\frac{1}{\mu_{TRANS}}\right) W_{IGNITION} - W_{BOILOFF_2} = \right.$$

$$\left. - W_{SHUTDOWN} - \left(\frac{\mu_{TRANS}^{-1}}{\mu_{TRANS}}\right) W_{STARTUP}\right]$$

$$W_{PROP_{TOTAL}} = \left\{W_{PROP_1} + W_{PROP_2}\right\} \phi$$

where ϕ is a factor accounting for residuals.

Based on this total calculated propellant load, various geometries are considered for tradeoff within the program. For each of these geometries the inert weights are determined and the geometry which yields maximum payload is selected. Payload is determined by subtracting from the assumed gross weight the propellant load and all of the inert weights. The remainder is payload, which, if the mission requirements are too severe, may be less than zero. The optimum gross weight and, hence, stage size and propellant load, are determined simply by varying assumed gross weights until a critical point (e.g., maximum) is obtained in a plot of payload vs. gross weight.

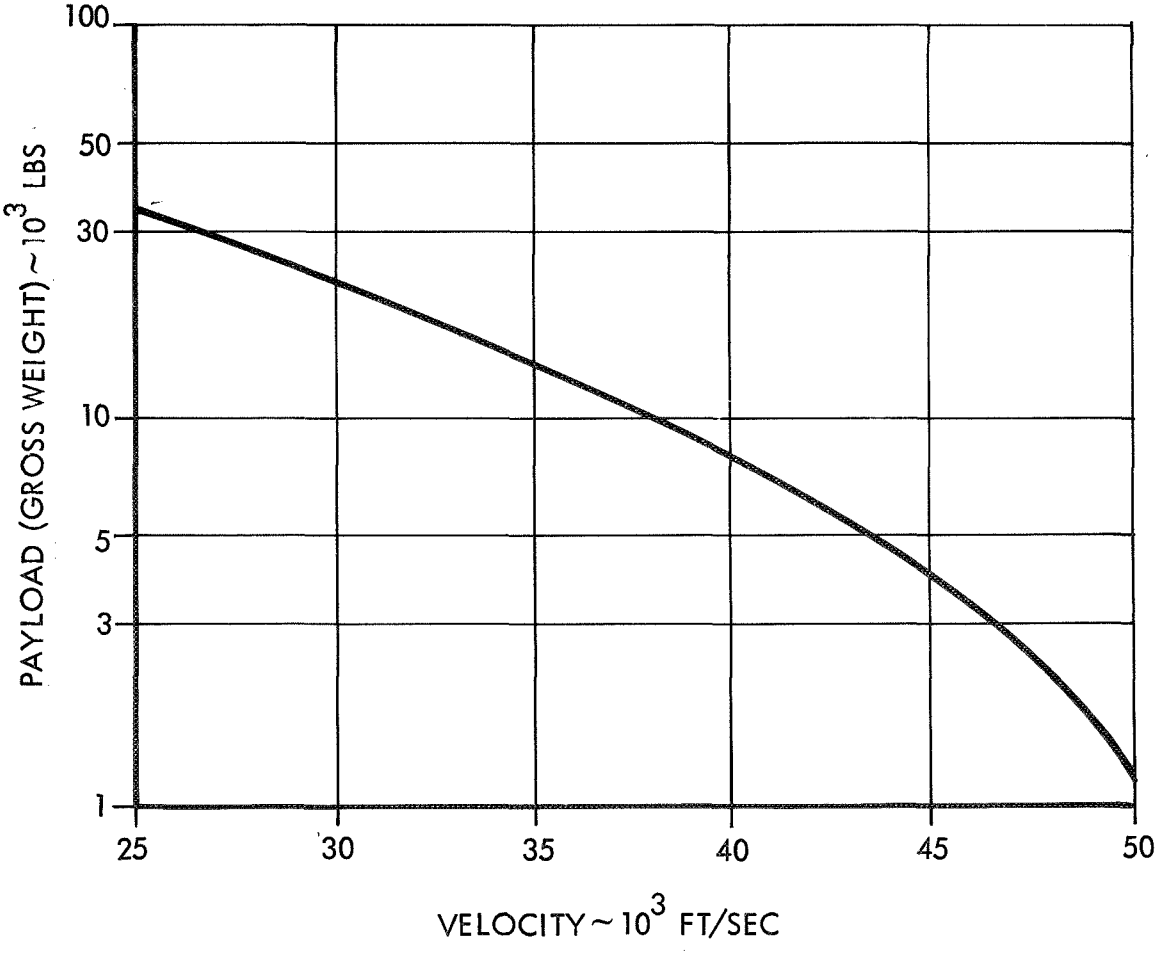

Figure 2-1. Typical Launch Vehicle Performance Capability

The following paragraphs discuss the various tripropellant and bipropellant stage geometries which are incorporated into the program and the structural, thermal protection, meteoroid protection, reaction control system and other subroutines which are used.

2.2.2 STAGE CONFIGURATIONS

The stage sizing computer program has the capability of analyzing seven tripropellant configurations and three bipropellant geometries. The program considers each configuration possible for a given type of propellant combination. It then selects for further analysis only those configurations in which it is possible to package the necessary amount of propellant while adhering to certain geometric constraints. The program computes the payload for each of the remaining configurations and selects the one with the highest payload.

Any geometric constraint will have a major influence on the selection of a particular configuration. The constraints used in the program are listed in table 2-2. The one which has the largest impact on the general type of configuration considered is the requirement that the stage's center of gravity be located along its longitudinal axis. This reduces any controllability problem which might result on a single engine stage having an offset center of gravity.

Table 2-2. Constraints on Stage Configuration Geometry

Constraint	Major Area Affected
Center of gravity	Number of fluorine and lithium tanks
Maximum stage diameter	Type of hydrogen tank Number of Fluorine and lithium tanks Maximum engine expansion ratio
Shell to tank spacing	Type of Hydrogen tank Number of fluorine and lithium tanks
Tank to tank spacing	Number of fluorine and lithium tanks
Engine to tank spacing	Type of thrust structure interstage size
Engine exit to booster spacing	Interstage size
Booster/interstage diameter	Interstage size

On configurations having a single lithium tank, the center of gravity requirement is satisfied by locating the lithium tank beneath the hydrogen tank and as far from the stage longitudinal axis as possible. The lithium tank is not permitted to extend past the periphery of the hydrogen tank. Figure 2-2 depicts the general arrangement of the lithium and fluorine tanks. The position of the fluorine tank(s) is computed so that the moments balance about the vehicle's centerline. The lithium and fluorine tanks are positioned so that they are diametrically opposed on the configurations having only a single fluorine tank. On the single lithium tank, multiple fluorine tank configurations, the same balance technique is used but the tanks are spread to the circumference of the hydrogen tank to allow the engine to be submerged.

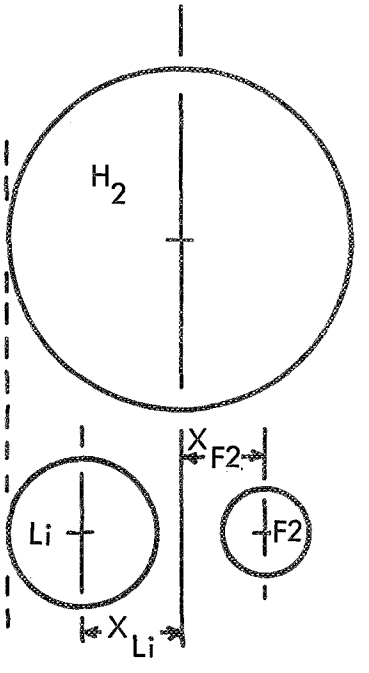

$W_{Li} X_{Li} = N_{F2} W_{F2} X_{F2}$

N IS NUMBER OF TANKS

W IS PROPELLANT WEIGHT

X IS DISTANCE FROM CENTERLINE

Li IS THE LITHIUM

F2 IS THE FLUORINE

Figure 2-2. Method of Locating the Stage's Center of Gravity

Balancing the center of gravity is simplified on the configurations having multiple fluorine and lithium tanks. The two fluorine tanks are diametrically opposed and are located 90 degrees from the two lithium tanks. All tanks are located as far from the vehicle centerline as possible.

The maximum stage diameter is a constraint in order to permit the entire payload, stage and interstage, to be shrouded if desired. If an unshrouded configuration is to be considered, the diameter of the booster is used as the maximum stage diameter. Depending upon the total propellant load and the mixture ratio, this constraint determines the type of hydrogen tank (i.e., spherical or cylindrical) and the number of fluorine and lithium tanks. The maximum engine expansion ratio is limited by the stage diameter because, during stage separation, the engine nozzle passes through the upper interstage opening, the diameter of which is determined by the stage diameter.

The shape of the hydrogen tank is also affected to a small extent by the various spacing constraints used in the program. Figure 2-3 shows the constraints used in defining the configuration geometry. The shell-to-tank spacing criteria ensures that the thermal insulation and meteoroid shields will fit between the shell and the hydrogen tank. Similarly, the tank-to-tank spacing is used to make clearances for the thermal and meteoroid protection systems on the fluorine and lithium tanks, and to ensure adequate room for the propellant feedlines.

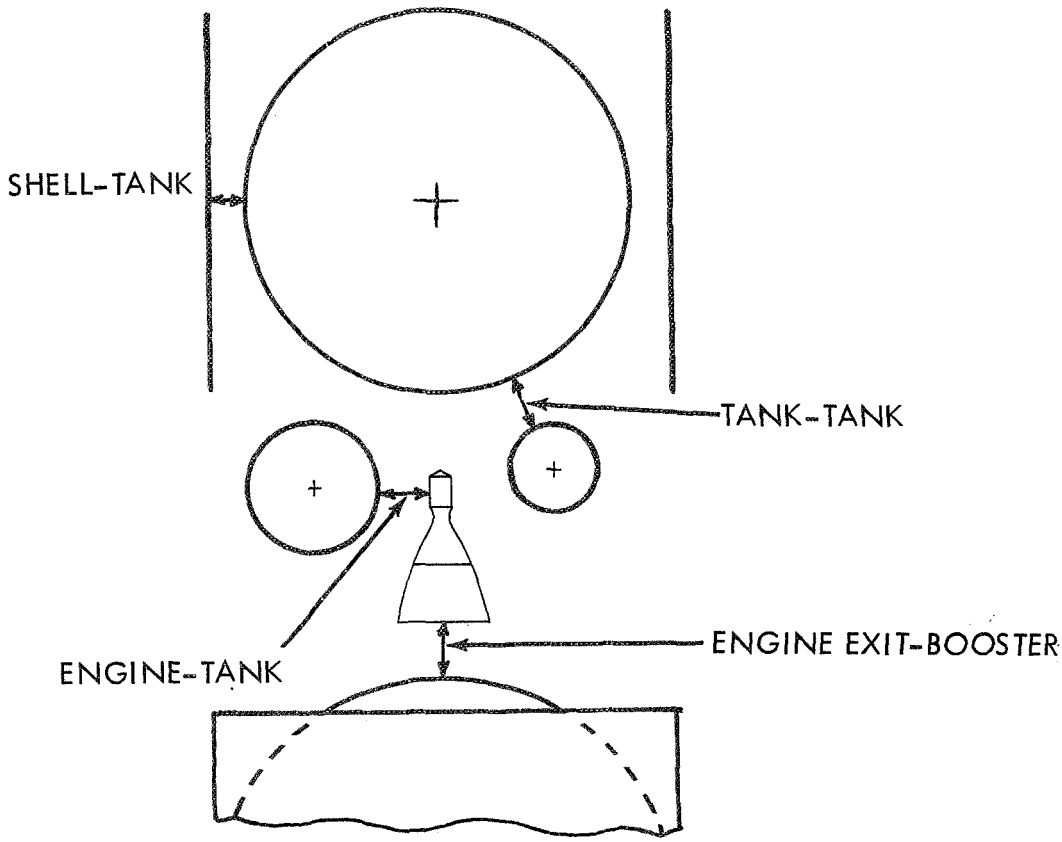

Figure 2-3. Spacing Constraints

The engine-to-tank clearance criteria is used to check engine submergibility on the thrust cone configurations. Basically, this is a constant coefficient, which, when multiplied by the engine's throat diameter, established the maximum diameter for accommodating the engine thrust chamber, turbopumps and plumbing. The program checks the possibility of engine submergence on each configuration by determining if a cylinder of this radius will fit between the fluorine and lithium tanks.

The engine exit-to-booster spacing establishes the clearance between the engine exit plane and the uppermost part of the launch vehicle. Using this spacing constraint it is possible to establish the correct interstage length for configurations where the booster's upper tank dome extends beyond the forward skirt on the launch vehicle.

The booster/interstage diameter is used to establish the lower diameter of the interstage.

The seven tripropellant configurations considered, consist of stages having a single hydrogen tank and a combination of one or two fluorine and lithium tanks. The thrust structure on each of these basic tankage arrangements can either be a thrust cone or a spider beam, depending upon whether multiple engines are used or a single engine can be submerged between the fluorine and lithium tanks.

Although there is a program option whereby two or four engines can be specified, the program normally selects the fewest number of engines needed to provide a specified thrust-to-weight ratio. A maximum thrust of 50,000 pounds per engine was used for the study because engine data in excess of this amount was not available.

The first two tripropellant configurations are depicted in figure 2-4. Each comprises one hydrogen tank, one fluorine tank, and one lithium tank. The hydrogen tank is spherical and determines stage diameter; however, if a sphere will not fit within the maximum allowable diameter, the tank radius is set equal to the maximum permitted and a cylindrical section is added to give the necessary volume. Both the fluorine and lithium tanks are spherical and are located at the maximum possible distance from the vehicle's longitudinal axis, while maintaining the center-of-gravity criteria previously discussed. The centers of the lithium and fluorine tanks in the thrust cone configuration are located at different stations in order to maintain the necessary clearances between the tanks, the engine, and the thrust cone.

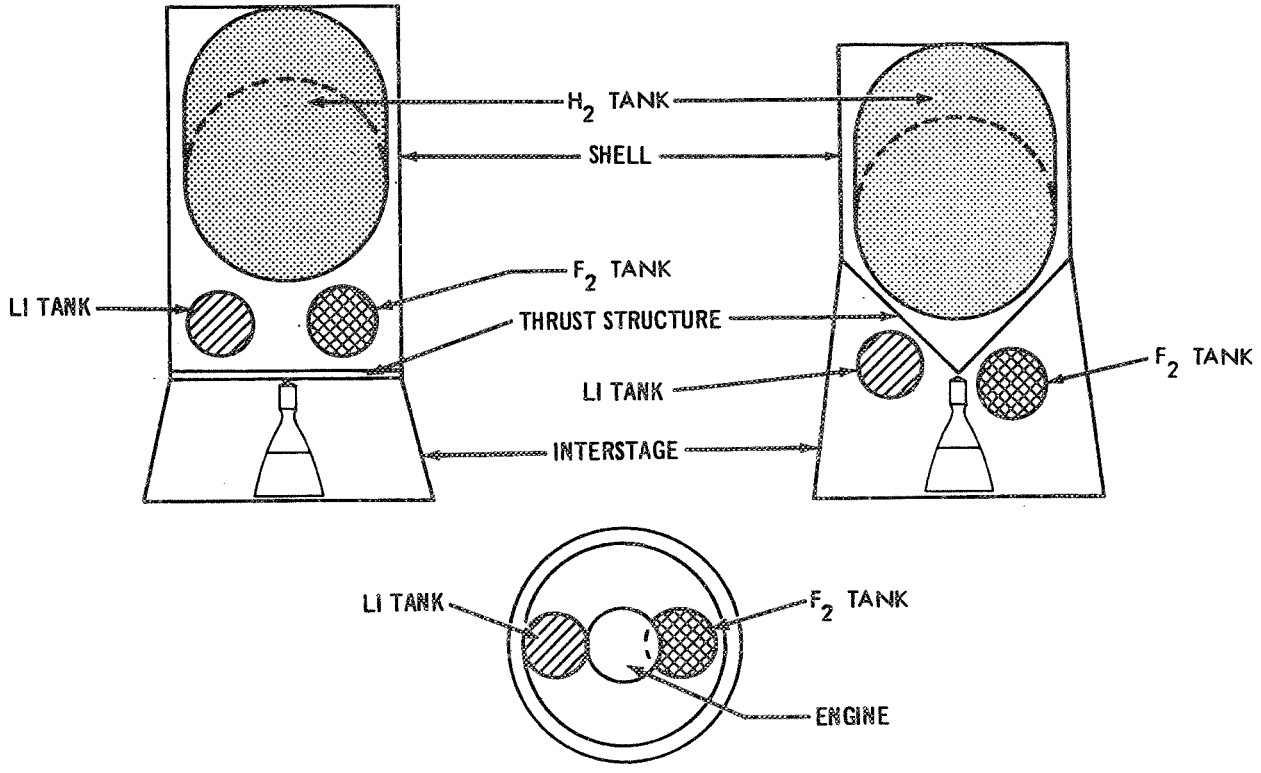

Figure 2-4. Tripropellant Configurations 111 and 121

The second set of tripropellant configurations evaluated by the program are shown in figure 2-5. These are essentially the same as the two preceding configurations, except that two spherical fluorine tanks are used instead of one. The fluorine tanks are located along the periphery of the hydrogen tank while maintaining center-of-gravity criteria discussed in the previous paragraphs. This geometry was generally found to be best for long coast missions.

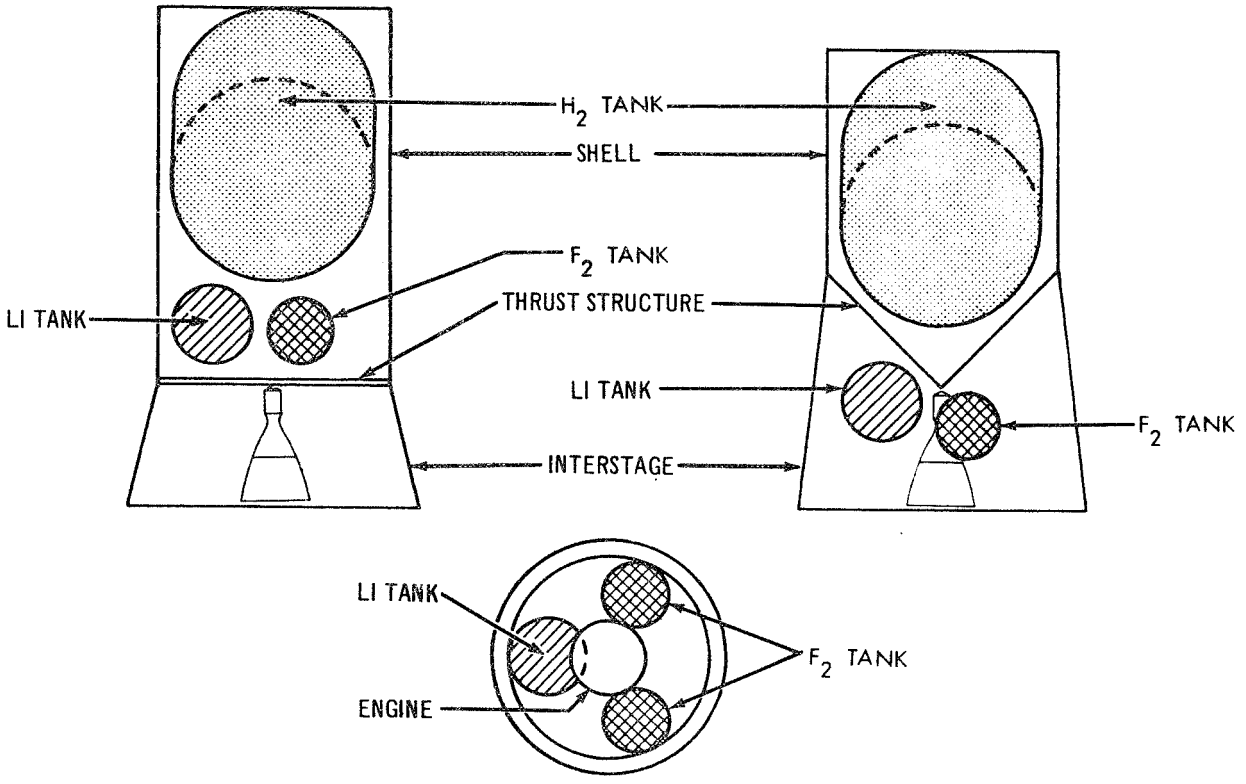

Figure 2-5. Tripropellant Configurations 112 and 122

In general, the next three tripropellant configurations were found to be preferrable for the direct injection missions where the extra thermal mass penalty associated with the multiple lithium tanks was negligible. The first two of the configurations are depicted in figure 2-6 as having two spherical lithium tanks and two spherical fluorine tanks. The lithium and fluorine tanks are all located at the periphery of the hydrogen tank. Checks in the program verify that sufficient space exists to submerge the engine on the thrust cone variation.

The final tankage arrangement evaluated for the tripropellant stage, figure 2-7, is similar to that of the last two configurations. This stage has two cylindrical fluorine and two cylindrical lithium tanks located along the perimeter of the hydrogen tank. Each of the four tanks have identical radii, which are the largest possible without violating the required tank-to-shell clearances. The cylindrical lengths are computed to give the necessary tank volumes. There is no thrust cone version of this tankage arrangement.

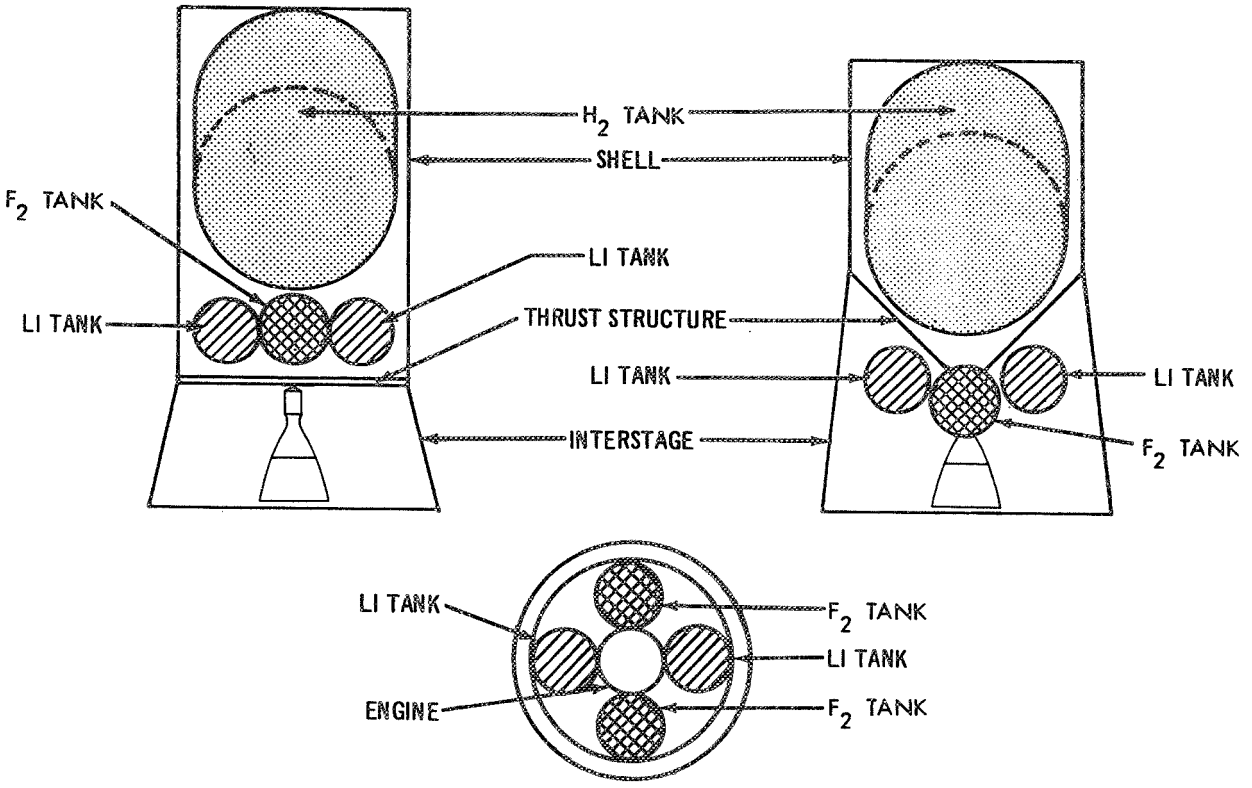

Figure 2-6. Tripropellant Configurations 113 and 123

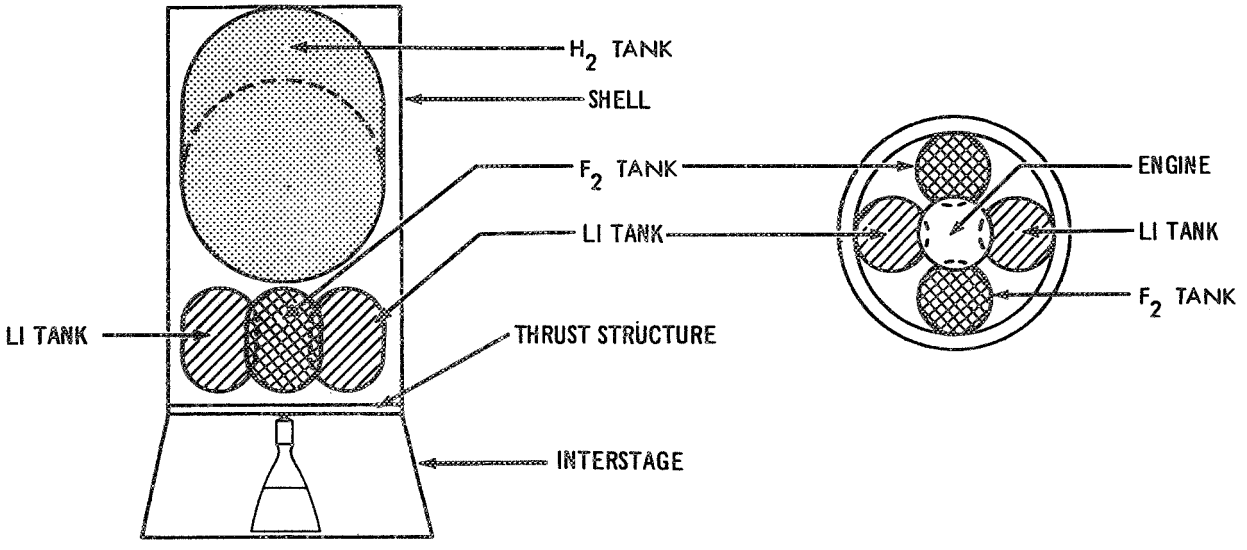

Figure 2-7. Tripropellant Configuration 114

The three bipropellant configurations evaluated in the sizing program are depicted in figure 2-8. They all have tandum tankage with the smaller (volume) tank on top, and all three employ a conical type thrust structure. The only difference between each of these configurations is the shell shape. The first version has spherical tanks and a frustum type shell. The second configuration also has spherical tanks, but has a shell consisting of a cylindrical section and a frustum of a cone. This shell arrangement is used to satisfy the maximum stage radius criteria, in the event the lower diameter of the frustum is larger than allowed. The last version has a cylindrical shell and either spherical or cylindrical propellant tanks.

The program computes the size and shape of each propellant tank on the basis of the volume required and the geometric constraints previously discussed. The program automatically selects the particular bipropellant version which will satisfy these requirements. The selection order of preference is from left to right, as shown in figure 2-8.

The three bipropellant configurations were used also for the gelled H_2/Li configurations.

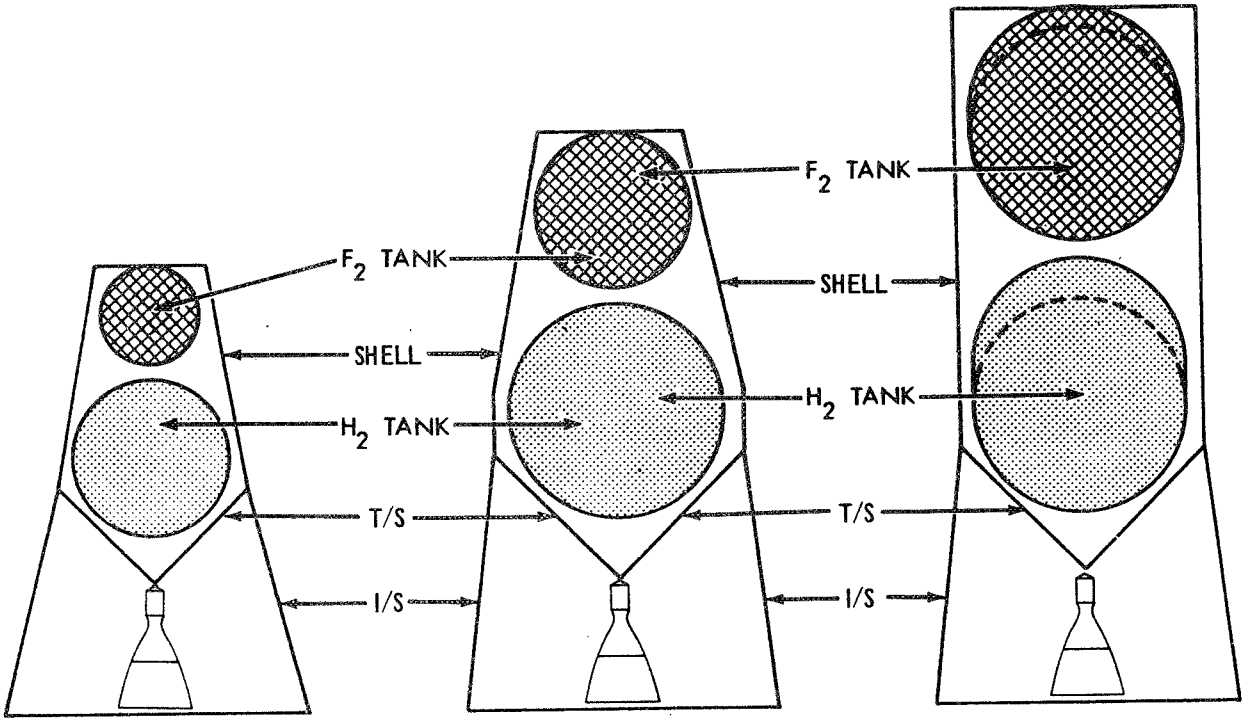

Figure 2-8. Bipropellant and Gel Configurations

Evaluation of configurations was not limited to the sizing program. Once the optimum engine parameters and propellant loads were determined using the program, several alternate bipropellant configurations were manually evaluated. Figure 2-9 illustrates four of the 12,000 pound gross weight configurations considered for use with the Atlas/Centaur launch vehicle. The configurations comprise: 1) a spherical

hydrogen tank and a toroidal fluorine tank, 2) a spherical hydrogen tank and two spherical fluorine tanks, 3) two cylindrical hydrogen tanks and two cylindrical fluorine tanks, and 4) toroidal hydrogen and fluorine tanks. The design analyses performed on these configurations showed that they had a negligible payload advantage over those configurations considered in the sizing program; that is, the weight saved in the shell and interstage structure were balanced by increased in the weights of the tank and tank supports.

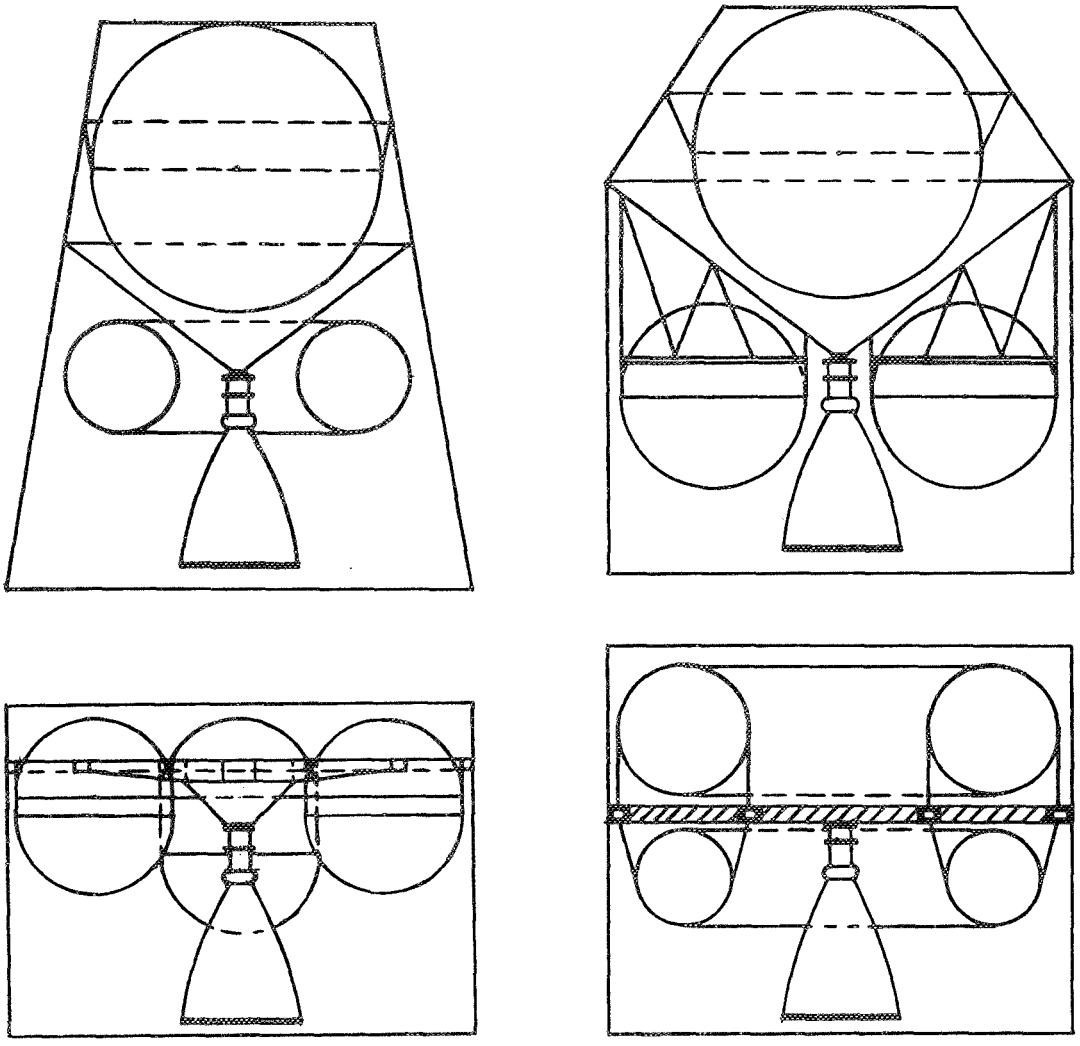

Figure 2-9. Four Alternate Bipropellant Configurations

Considering larger gross weight stages, such as those for a 260-inch S-IVB launch vehicle, alternate configurations similar to these would have given slightly better payloads than configurations derived from the computer program. The most efficient design for the heavier gross weight stages was the one with four cylindrical tanks.

The thrust cone proved to be the most efficient structure with the separate and common bulkhead tandem tank designs, and with most toroidal tank designs. The spider beam thrust structure proved most efficient for stages with multiple engines and multiple tanks.

2.2.3 STRUCTURAL SYSTEMS

Five basic structural components were analyzed to determine their respective weights for each stage configuration evaluated by the program. (See figures 2-4 through 4-8.) These basic parts are: 1) propellant tankage, 2) shell, 3) interstage, 4) thrust structure, and 5) tank supports. Propellant tank weights were computed in accordance with geometric dictates using internal pressure as the design criteria and adhering to minimum allowable skin gauge constraints.

Weights for the shell, thrust cone type thrust structure, and interstage are computed by first determining what a monocoque design would weigh, and then applying a manually derived complex-to-monocoque structure weight ratio factor to the monocoque weight. The monocoque weights are computed using dimensional data calculated in special geometry subroutines as outlined in paragraph 2.2.2; and design criteria (i.e, loads) based on a simplified mass distribution model for each configuration and inputed axial and lateral accelerations. The complex/monocoque weight ratios and the accelerations were inputed to the program for each booster as a function of upper stage gross weight, thereby accounting for the influence of upper stage size on stage mass fraction.

This approach has several advantages over the use of trend curves (e.g., interstage weight vs. propellant load) to estimate structure weights:

1) Weight variation may be determined for alternate arrangements which have different dimensions, even though propellant load may be the same. This permits a more accurate and reliable optimization of parameters such as engine mixture ratio which may not change propellant load significantly, but which can alter the stage dimensions.

2) Any desired degree of accuracy can be achieved simply by reevaluating the input monocoque-to-complex-structure weight ratio factors and rerunning the cases of interest.

3) Various structural design concepts can be examined (e.g., sheet-stringer, honeycomb, truss) since the weight ratio factor is manually determined.

4) A minimum of "hand" analyses are required since it is rarely necessary to manually determine weight factors for more than one typical stage in the size range of interest; whereas, as many as 750 stages may be sized with the computer to obtain a complete optimization.

Weights for the tank supports are determined for each propellant tank as a function of the weight being supported. The determination of the proper relationship was accomplished in a separate side study in which several concepts were considered. These included monocoque skirts, scalloped skirts, semi-monocoque skirts, and truss-to-ring structure, which are depicted in figure 2-10.

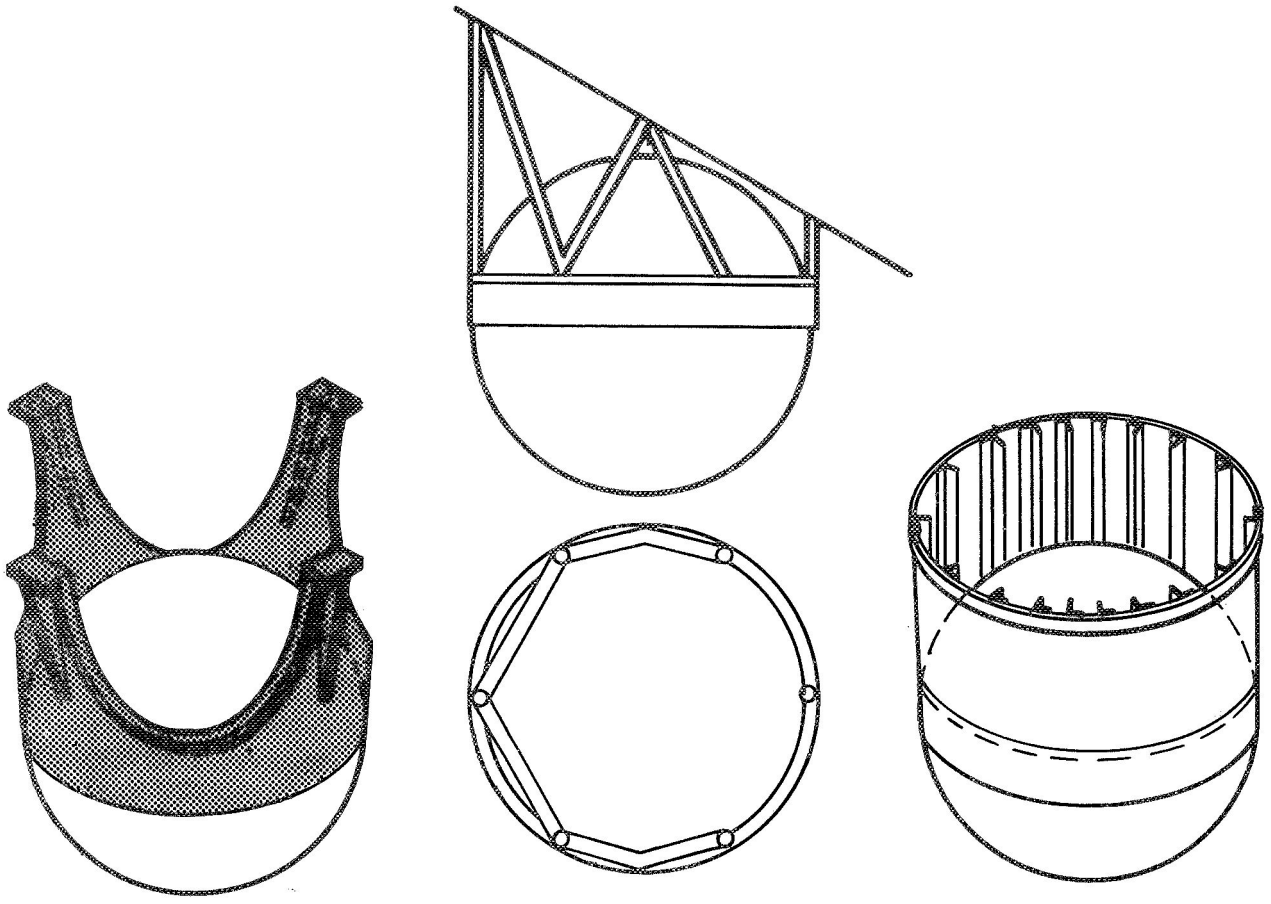

Figure 2-10. Tank Support Concepts

Approximately half of the tripropellant configurations considered in the program employ a beam type thrust structure. The concept for this thrust structure is assumed to be a conventional spider beam, ring frame and/or cross beam structural arrangement while the engine mount is assumed to be a conventional gimbal fitting. A particular structural arrangement is assumed for each number-of-engines case considered for the stage. The concept assumed for each number-of-engines case is shown in figure 2-11. The weight equations for each concept were developed for the computer program with the following assumptions: 1) geometry of beams is as shown in figure 2-11, 2) beam sections are rectangular, 3) section is stable so material yield controls, and 4) engine attach points are located at the centerline of maximum inscribed circle for all engine sizes.

Weight equations for other shapes (i.e., rectangular tube, square tube) were developed and sufficient cases were analyzed to plot conversion coefficients as functions of required thrust level. These conversion coefficients (presented in appendix F) are used as inputs to the program. The rectangular tube weight would equal the conversion coefficient times the rectangular block weight that is programmed.

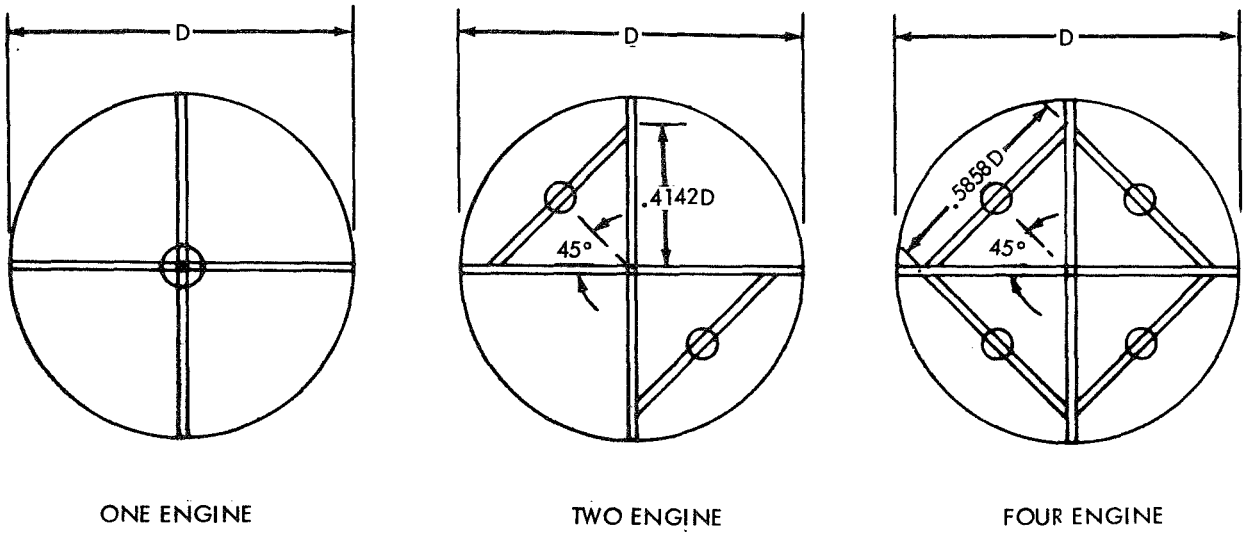

Figure 2-11. Spider Beam Thrust Structure Concept

2.2.4 THERMAL PROTECTION SYSTEMS

Two subroutines are used for the analysis of the thermal protection system requirements. One is specifically tailored to the analysis of cryogenic storage (e.g., hydrogen and fluorine), or more generally for propellants which receive heat during storage, and the other is used to analyze the requirements for storing propellants which give off heat during storage - in this case, molten lithium. Since the analysis methods are different for these two programs they are discussed separately in the following paragraphs.

2.2.4.1 Cryogenic Storage

The approach used in this analysis is based on the criteria of minimizing the thermal mass penalty (TMP). The following five equations show the development of the analytical definition of TMP as used in this program:

1) $W_G = W_{PL} + W_{ST} + W_{INSUL} + W_{TANKS} + W_{PRESS} + W_{PROP}$

ASSUME W_{ST} = CONSTANT

W_{PROP} = CONSTANT

2) $$\Delta V = g_c \, ISP \, \ln \frac{W_G - W_{B.O.}}{W_G - W_{PROP}}$$

3) $$\text{Exp}\left[\frac{\Delta V}{g_c I_{SP}}\right] = \mu = \frac{W_G - W_{B.O.}}{W_G - W_{PROP}}$$

$$= \frac{W_{HL} + W_{ST} + W_{TANKS} + W_{PRESS} + W_{PROP} + W_{INSUL} - W_{B.O.}}{W_{HL} + W_{ST} + W_{INSUL} + W_{TANK} + W_{PRESS}}$$

4) $$W_{HL} = -W_{ST} - W_{INSUL} + \frac{W_{PROP}}{\mu-1} - \frac{W_{B.O.}}{\mu-1} - W_{TANKS} - W_{PRESS}$$

AND

5) $$TMP = W_{TANK} + W_{PRESS} + \frac{W_{B.O.}}{\mu-1} + W_{INSUL}$$

The two main assumptions made in deriving these equations are: 1) that the weight of structure other than tanks is constant, and 2) the total weight of propellant initially loaded (including boil-off) is constant. The derivation itself is straightforward and shows that the thermal mass penalty is a function of:

a) Tank weight, which varies with the selected tank design pressure and the propellant density at vent conditions,

b) Pressurization system weight, which is roughly a function of total tank volume and pressure at burnout,

c) Insulation weight, and

d) Boil-off weight divided by $(\mu-1)$, where μ is the stage mass ratio.

A summary of the primary equations used in the thermal analysis are listed below:

1) $$W_{B.O.} = \frac{-kA\,(T_{VENT} - T_{OUT})\,(\alpha x+1)}{\lambda x}\left\{\tau_M - \left[\frac{W_P C_L (DTP) + \phi_x W_P h_S}{-kA\,(T-T_o)}\right]\frac{x}{(\alpha x+1)}\right\}$$

WHERE $$DTP = T_{VENT} - T_{INITIAL} \text{ OR } T_{VENT} - T_{RPT}$$

$$\bar{T} = (T_{VENT} + T_{INITIAL})\ 1/2$$

2) $$W_{INSUL} = A\rho_1 x$$

3) $$\frac{\partial W_{HL}}{\partial x} = 0 = -A\rho_1 - \frac{1}{\mu - 1}\frac{\partial W_{B.O.}}{\partial x}$$

4) $$x_{opt} = \left\{ \frac{\left[\frac{-kA}{\lambda}(T_{VENT} - T_{OUT})\right]\tau_M}{[\mu - 1]A\rho_1} \right\}^{1/2}$$ VENTED SYSTEMS

5) $$x_{REQ} = \tau_M \Big/ \left\{ \left[\frac{W_P C_L DTP + \phi_x W_P h_S}{-kA(T - T_o)} \right] - \alpha\tau_M \right\}$$ NON-VENTED SYSTEMS

The first equation relates the weight of boiloff to the propellant, the insulation properties and the boundary conditions. This expression is readily derived from fundamental thermodynamic equations, recognizing that the fraction of heat which enters through the insulation (B) is related to insulation thickness by the approximate relationship.

$$B = \frac{1}{\alpha x + 1}$$

The heat conduction constant, α, may be estimated using the results of existing nodal analyses of similar configurations examined in other studies.

The second equation is the relationship for the weight of insulation, where x is the insulation thickness. The optimum insulation thickness (maximum payload) can be found by taking the derivative of payload with respect to insulation thickness and setting this equal to zero, as depicted in the third equation.

The last two equations show the relationships used to determine the optimum insulation thickness for a vented system, and the required thickness for a non-vented system, respectively. The second to last equation is based on the first three equations, which assume that only the boiloff and insulation weights are functions of insulation thickness. While this assumption is not precisely correct, it is considered adequate for preliminary design purposes.

The program logic is set up to optimize the thermal protection system requirements by determining the thermal mass penalty for vented and non-vented systems as a function of vent temperature. See figure 2-12 for an example. This figure illustrates the results of a typical thermal optimization. These data are presented in terms of item weight as a function of vent temperature for both the vented and non-vented cases. The criteria used for this example analysis are as follows:

a) Weight of hydrogen: 1000 lb

b) Mission duration: 4920 hr (205 days)

c) Stage mass ratio: 1.5 (dimensionless)

d) Insulation external temperature: 450° R

e) Heat conduction constant (α): 1.0 (dimensionless)

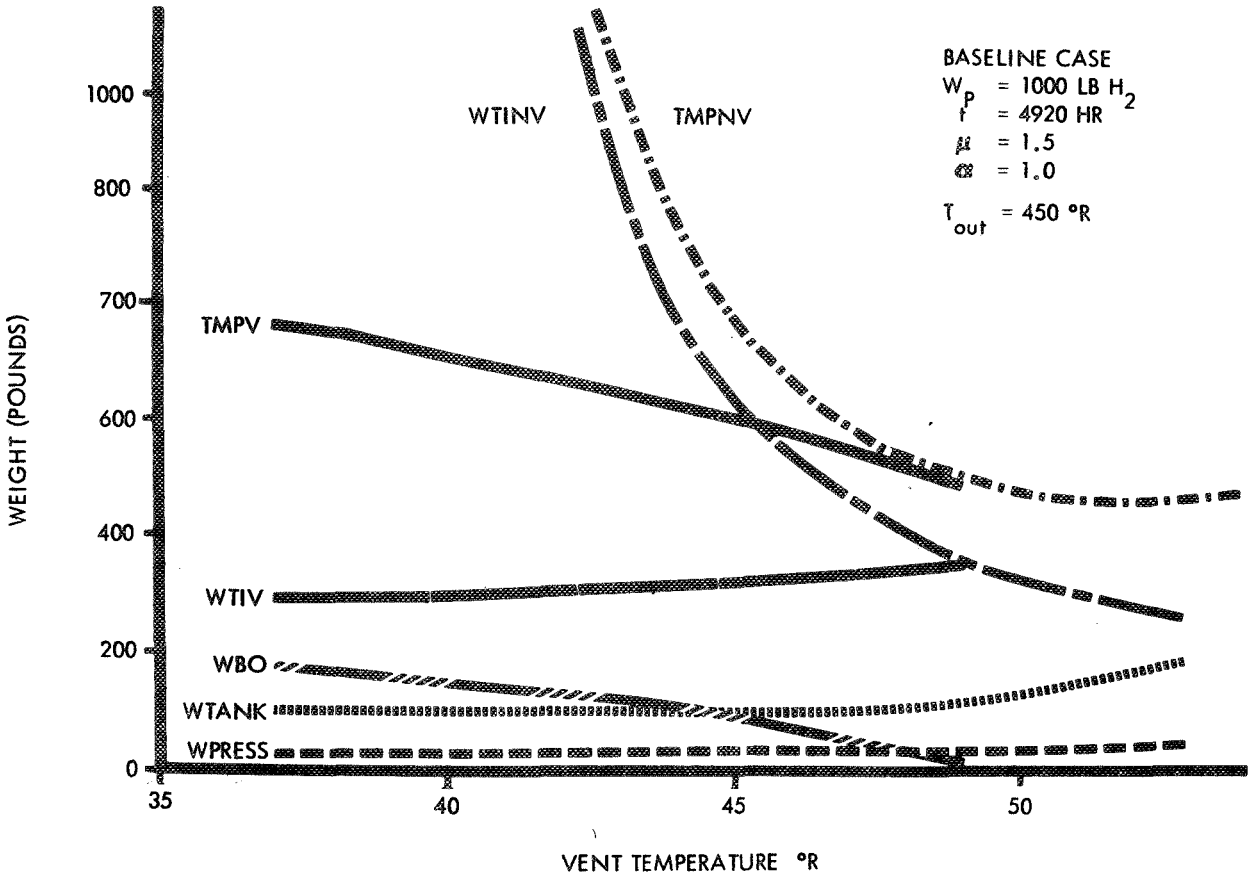

Figure 2-12. A Typical Thermal Optimization

The results show that the pressurization system weight has little influence on the optimization, and tank weight has no effect, except at the higher vent temperature where it begins to rapidly increase. This rapid increase is due to two factors. First, at lower pressures (vent temperatures) the tank skin gauges are determined by minimum gauge requirements, while at higher vent temperatures the skin gauge is a direct function of pressure. Second, the volume of the tank begins to increase very rapidly at higher temperatures because of the higher rate of hydrogen density change with respect to temperature near the triple point.

Both boiloff and the total thermal mass penalty decrease for the vented system as the temperature is increased; however, the insulation weight increases slightly.

Optimum insulation thickness for a non-vented system decreases exponentially with increased vent temperature such that at about 52° R the minimum weight system is obtained.

It should be noted, however, that the non-vented system is not necessarily always the minimum weight system for a 1000-pound propellant load. Factors which tend to increase the thermal problem - such as higher mission times, higher insulation thermal conductivities and greater mission velocities - will tend to shift the favorability to the vented systems. This will be discussed in subsequent paragraphs.

Apart from the option of using either vented or non-vented systems, the program also has options which permit the use of slush (partially frozen) propellant and has analysis capability for missions with up to two burns and two coasts. It will be shown later in this report that multiple burn missions with a long second coast incur very high thermal mass penalties. This results from the fact that with multiple burns the remaining propellant after the first burn receives approximately the same amount of heat as a fully loaded tank, but it has a reduced thermal capacity to accept it.

The thermal subroutine input data requirements are summarized as follows:

a) Material Data*

1. Propellant physical and thermodynamic properties
2. Tank material properties
3. Insulation thermal conductivity and density
4. Tank land factors

b) Boundary Conditions

1. Fraction slush
2. Total propellant load
3. Propellant consumption for 1st and 2nd burns
4. First and second coast durations
5. Insulation external temperature
6. Initial propellant temperature
7. Stage mass ratio for last burn
8. Number of tanks

c) Constraints

1. Tank minimum skin gauges
2. Tank safety factor
3. Minimum allowable ullage at last ignition
4. Pressure in excess of vapor pressure to meet pump NPSH requirements
5. Maximum allowable tank radius

d) Other Data*

1. Parametric pressurization system weights
2. Heating constant, α = f (propellant load)

*Much of these data are in bivariate or trivariate arrays.

The program data outputs are summarized as follows:

a) Boil-off weight

b) Pressure system weight

c) Tank weight

d) Tank dimension (e.g., radius and cylinder lengths)

e) Tank cap and cylindrical section skin gauges and weights

f) Tank design pressure

g) Insulation thickness

h) Insulation weight

i) Thermal mass penalty

j) Heating rates during 1st and 2nd coasts

k) Initial conditions at the end of the 1st burn and start of 2nd coast

2.2.4.2 Lithium Storage

This program determines the optimum combination of insulation thickness, initial propellant temperature, and a heater system (including all associated power generation and conversion weights) to keep a propellant at a temperature greater than or equal to a predetermined value. In accomplishing this, the program has appropriate provisions for determining the effect of initial propellant temperature (viz. lithium temperatures) on tank weights and for specifying insulation thermal conductivity as a function of average insulation temperature (a necessity for accurate analysis of systems using high temperature super insulations). As with the low temperature thermal optimizations previously discussed, this program can analyze requirements for a two-burn/two-coast mission as well as a single burn mission with only one coast.

Primary input data requirements for this program are summarized as follows:

a) Allowable stress in tank as a function of temperature

b) Tank surface area

c) Insulation thermal conductivity as a function of temperature

d) Insulation density

e) Propellant properties

f) Heater, power and distribution weight as a function of power and energy requirements

g) Insulation external temperature

h) First and second coast durations

i) Propellant consumption for 1st and 2nd burns

Data outputs for the lithium storage program are summarized as follows:

a) Optimum initial propellant temperature

b) Optimum insulation thickness and weight

c) Heater, power and distribution system weight*

d) Power and energy requirements for heater (i.e., watts and watthours)

As a general rule, lithium storage requirements for direct injection missions optimize without the use of an auxiliary heater system, but the long duration missions require one if minimum weight is to be achieved.

2.2.5 METEOROID PROTECTION

Spacecraft on long duration missions are subjected to encounters with meteoroids that could cause considerable damage to vital parts of the vehicle. To ensure adequate mission reliability it is, therefore, necessary to provide some type of protection against this hazard.

The most promising technique for protecting vital components and structures is to erect a thin bumper shield a short distance from the item to be protected. The shield serves to disintegrate the incoming meteoroid, allowing only a relatively diffuse debris cloud to strike the component. With the bumper shield, the rear wall need only withstand the impact of a cloud instead of a solid incoming meteoroid.

Since the results of the meteoroid shield analysis would influence the study conclusion for only the long duration (coast) missions, analyses were performed for only the single burn retro and two-burn interplanetary missions.

Subsequent paragraphs describe the meteoroid environment and shield models used in conducting this analysis. The results are presented in section 3, paragraph 3.2.

2.2.5.1 Meteoroid Environment

The meteoroid flux varies considerably during the course of a year. The total activity comprises two components: 1) a fairly constant sporadic component, and 2) a varying component associated with meteoroid streams. The second component, or stream flux, has well defined recurring peaks associated with the individual meteoroid streams. The intensity of these streams can vary up to 20 times that of the background, or sporadic flux.

The meteoroid environment model selected for this study was that proposed by Burbank, Cour-Palais, and McAllum[1]. Mathematically the unshielded meteoroid fluxes of this model can be expressed as follows:

*This item may be any heat generating system (e.g., a gas generator) whose weight may be expressed as a function of either power or energy.

(1) Burbank, P.B., Cour-Palais, B.G., and McAllum, W.E., "A Meteoroid Environment for Near-Earth, Cislunar, and Near Lunar Operations", NASA TN-D-2747, Manned Spacecraft Center, April 1965.

$$\log_{10} N = -1.34 \log_{10} M - 2.68 \log_{10} V - 6.465 + \log_{10} F$$

where

N is the cumulative flux, or particles per unit area - unit time (number of particles per square foot per day)

M is the meteoroid mass (grams)

V is the average sporadic meteoroid velocity (30 km/sec) at the geocentric velocity of the meteoroid stream (kilometers per second)

F is the ratio of accumulative meteoroid stream flux to the sporadic meteoroid flux - equal to unity for the sporadic flux equation.

Figure 2-13 depicts this meteoroid flux-mass relationship graphically. Also presented are fluxes which have masses an order of magnitude greater (10X) and less (0.1X) than the nominal (1X). These were used in evaluating the sensitivity of the meteoroid shield design to the environment; the results of which are discussed in section 3, paragraph 3.5.

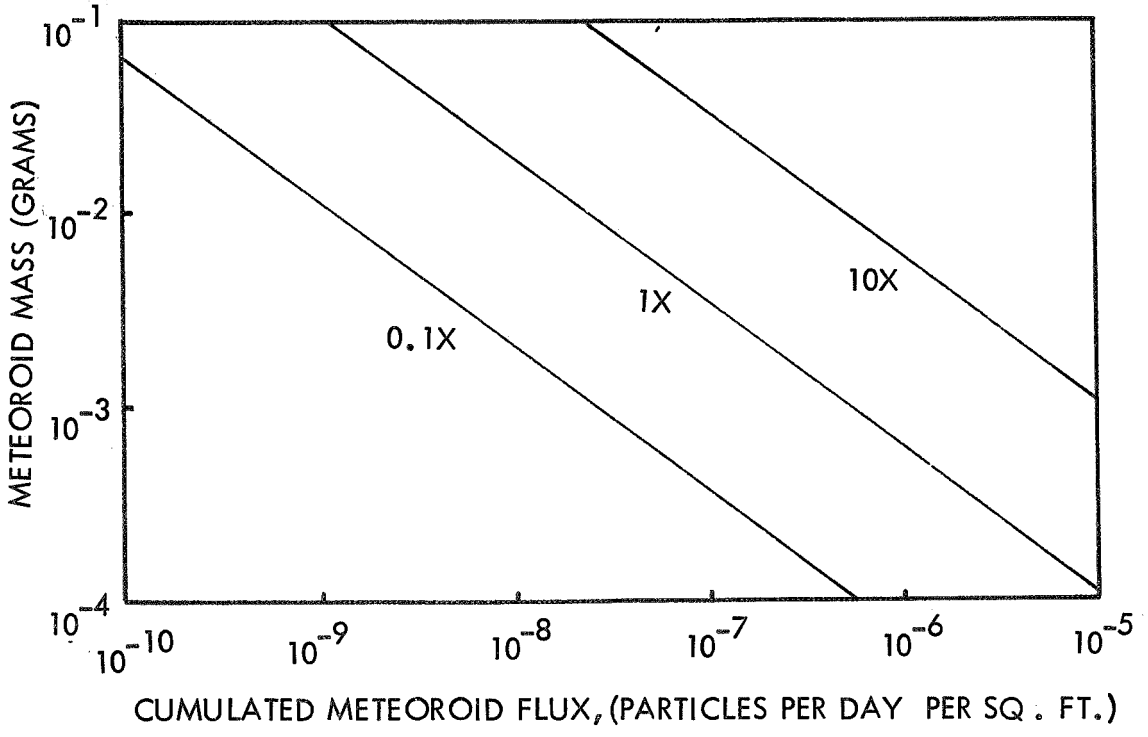

Figure 2-13. Meteoroid Environment Model

2.2.5.2 Design Meteoroid Mass

The present method of protecting a space vehicle from meteoroid damage is to ensure that the meteoroids do not impact directly on vital components. This is accomplished by designing the protective shield so that the largest meteoroid which would probably be encountered during the mission will not penetrate the shield. The

method used in this study for determining this design meteoroid mass is basically that set forth by Kessler, and Patterson[2].

The probability of encountering a meteoroid having a specific design mass is a function of the meteoroid flux, the area exposed and the time spent in the environment. Mathematically this can be expressed as,

$$P_o = \exp(-NAT)$$

where

P_o is the probability of not being hit

N is the cumulative flux (number of particles per day per square foot)

A is exposed area (square feet)

and

T is the time exposed to the environment (days).

In the previous section it was shown that the form of the mass-flux equation is:

$$N = \alpha M^{-\beta} V^{-\delta} F$$

where

α is the meteoroid flux-mass constant ($\alpha = 2.917 \times 10^{-6}$ = antilog of 6.465)

β is the exponent of the mass in the flux-mass relation (1.34)

δ is the exponent of the velocity (2.68)

N is the cumulative flux (particles per day per square foot)

M is the mass (grams)

V is the average velocity (kilometers per second)

F is the ratio of stream to sporadic fluxes

By combining the two previous equations it is possible to obtain the following relationship for the design meteoroid flux:

$$M^{\beta} = \frac{-A\alpha FT}{V^{\delta} \log_e P_o}$$

(2) Kessler, D.J., and Patterson, R.L., "Determination of Design Meteoroid Mass for a Sporadic and Stream Meteoroid Environment", NASA TN D-2828, Manned Spacecraft Center, May 1965.

In general, the ratio of stream to sporadic fluxes (F) is time dependent, so

$$FT = \int_{T_1}^{T_2} F(T)\, dT$$

where the time interval is

$$T = T_2 - T_1$$

Thus, it is possible to express the design meteoroid mass as a function of time:

$$M^{\beta} = \frac{-A\alpha}{V^{\delta} \log_e P_o} \int_{T_1}^{T_2} F(T)\, dT$$

Letting μ be the meteoroid flux parameter,

$$\mu = \frac{\alpha}{V^{\delta}} \int_{T_1}^{T_2} F(T)\, dt$$

it is possible to rewrite the expression for the design meteoroid flux as:

$$M = \frac{-A\mu}{\log_e P_o}.$$

Since there are two basic parts to the meteoroid - sporadic and stream - it is possible to sum their effects to get the total design mass:

$$M^{\beta} = (\mu_{SP}) \left(\frac{-A}{\log_e P_o}\right) + (\mu_{ST}) \left(\frac{-A}{\log_e P_o}\right)$$

where μ_{SP} is the meteoroid flux parameters for the sporadic portion and μ_{ST} is the meteoroid flux parameter for the stream portion.

Simplifying the above expression yields the following:

$$M^{\beta} = \left[\mu_{SP} + \mu_{ST}\right] \left[\frac{-A}{\log_e P_o}\right]$$

In a similar fashion it is possible to add the combined effect of all active meteoroid streams:

$$M_{ST}^{\beta} = \mu_{ST1}\left[\frac{-A}{\log_e P_o}\right] + \mu_{ST2}\left[\frac{-A}{\log_e P_o}\right] + \cdots$$

$$\cdots + \mu_{STn}\left[\frac{-A}{\log_e P_o}\right]$$

That is,

$$M_{ST}^{\beta} = \sum_{i=1}^{n} \mu_{STi}\left[\frac{-A}{\log_e P_o}\right]$$

The expression for the design mass can be rewritten as:

$$M^{\beta} = \left[\mu_{SP} + \sum_{i=1}^{\eta} \mu_{STi}\right]\left[\frac{-A}{\log_e P_o}\right]$$

and thereby account for not only the sporadic flux, but the flux due to all simultaneously active streams during the time interval under consideration.

It is a simple matter to compute the design mass the sporadic flux, which is time-invariant. However, computation of the design mass for the stream fluxes is more difficult since they vary from day to day and stream to stream. Since the exact mission times (day or month) were not known, the stream flux parameters given by Kessler and Patterson[2] were time-averaged, that is:

$$M^{\beta} = \left[\mu_{SP} + \bar{\mu}_{ST}\right]\left[\frac{-A}{\log_e P_o}\right]$$

where

$$\bar{\mu}_{ST} = \frac{T}{365}\sum_{i=1}^{n} \mu_{ST\,i} = \frac{T}{365}\sum_{i=1}^{n} \frac{\alpha}{V^{\delta}} \int_{o}^{365} F(T)\, dT$$

or

$$\bar{\mu}_{ST} = 1.70 \times 10^{-11}\, T$$

The sporadic meteoroid flux parameter given by Kessler and Patterson[2] is:

$$\mu_{SP} = 3.63 \times 10^{-11}\, T$$

Therefore, the expression for the design meteoroid mass becomes:

$$M = \left\{ 5.33 \times 10^{-11} \left[\frac{-AT}{\log_e P_o} \right] \right\}^{1/1.34}$$

2.2.5.3 Meteoroid Shield Model

Whipple's bumper shield concept was used as a means of protecting the stages from meteoroid damage, since this is the most promising technique. Basically, this concept consists of a thin outer shield and a primary or backup structure. The thin shield which surrounds the space vehicle, see figure 2-14, fragments the incoming meteoroid into a relatively diffuse cloud of smaller particles. The debris then impinges on a second backup wall or sheet. Since the backup wall is impacted by the diffuse debris cloud, the damage done to the spacecraft itself is much less than if it had been struck directly by the meteoroid.

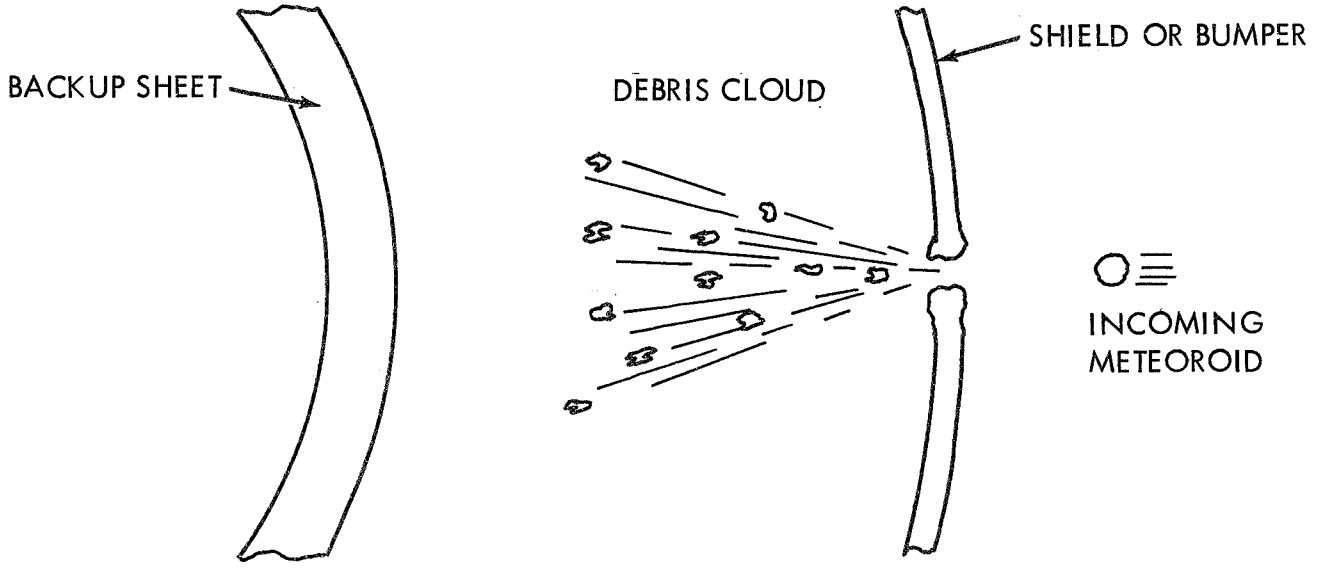

Figure 2-14. Whipple's "Bumper Shield" Concept

The most important element in this type of meteoroid protection system is the shield or bumper, since it controls the physical state of the debris in the cloud. The cloud consists not only of the disintegrated meteoroid, but a significant amount of shield material. The debris, from both the shield and the meteoroid, can take the form of solid particles, liquid droplets, vapors, or some combination. Since it is evident that an all-gaseous debris cloud would produce the least damage to the backup sheet, it is desirable to design the shield to vaporize the debris. In order to accomplish this it is necessary to look at the phenomena through which it can be achieved.

Cour-Palais[3] reasons that the impact of a hypervelocity meteoroid on a shield produces intense compressive shock waves which travel forward in the shield and rearward in the particle. Since the shock waves are not isentropic, they increase the internal energies of both the shield and meteoroid. When the internal energy of debris exceeds its fusion energy or sublimation energy, the debris either becomes molten or vaporizes.

The maximum internal energy increase will occur when the unloading wave, which is reflected from the rear surface of the shield, overtakes the compressive wave in the meteoroid as the latter reaches the rear end of the particle. Therefore, the shield should be designated to a thickness which is proportional to the particle diameter. According to Cour-Palais[3] the optimum shield thickness falls between one and 0.2 of the meteoroid diameter. However, he states that because there are more small particles in the meteoroid population than the size corresponding to this optimum ratio, a shield thickness in the order of 0.3 of the meteoroid diameter should be used. Mathematically, this can be expressed as:

$$t_s = 0.3D$$

where

t_s is the thickness of the bumper or shield (centimeters)

D is the diameter of the meteoroid (centimeters).

When the shield thickness falls outside the optimum region ($0.1 \leq t_s/D \leq 0.2$), the design of the backup sheet is governed by solid fragments in the meteoroid and the shield debris. The Manned Space Center's emperical formula for the nonoptimum regions, which was used to calculate the backup wall requirements, is given by the following equation[3]:

$$t_b = 0.075 \frac{m^{1/3} V}{S^{1/2}} \left(\frac{70000}{\delta}\right)^{1/2}$$

where

m is the meteoroid mass (grams)

V is the meteoroid velocity (kilometers per second)

S is the spacing between the shield and backup wall (centimeters)

δ is the 0.2 percent yield stress for the backup material (pounds per square inch)

(3) Cour-Palais, B.G., "Meteoroid Protection by Multiwall Structures", AIAA Paper No. 69-372, AIAA Hypervelocity Impact Conference, Cincinnati, Ohio, April 30-May 2, 1969, American Institute of Aeronautics and Astrionics, New York.

Although the above expression was developed from data based on the impact of glass particles on 2024-T3 aluminum sheets without a filler, it has been shown to be valid for other shield materials[3]. The reference also states that the constant coefficient of the equation could depend on both the shield material and meteoroid densities. Since the validity of this dependence has not been established, it was not used in computing the backup wall requirements.

2.2.5.4 Method of Analysis

Since the results of the meteoroid shield analysis would influence the study conclusions for only the long duration (coast) missions, meteoroid shield analyses were performed for only the single-burn retro and two-burn interplanetary missions. Analyses were performed to determine the requirements and weights of only the propellant tank shields. It was felt that protection for other subsystems, such as electronic packages, would constitute only a small fraction of the entire meteoroid shield weight, and hence were neglected since they would not affect the study conclusions.

Whipple's bumper shield concept previously discussed was used as a model for the meteoroid shield. As illustrated in figure 2-15, the thermal insulation was located between the backup wall and the shield. A computer routine was used to determine the meteoroid protection requirements and to optimize the shield weight on each stage evaluated. This was accomplished by selecting the shield spacing - the location of the shield relative to the backup wall - which yielded minimum weight, while maintaining several geometric constraints.

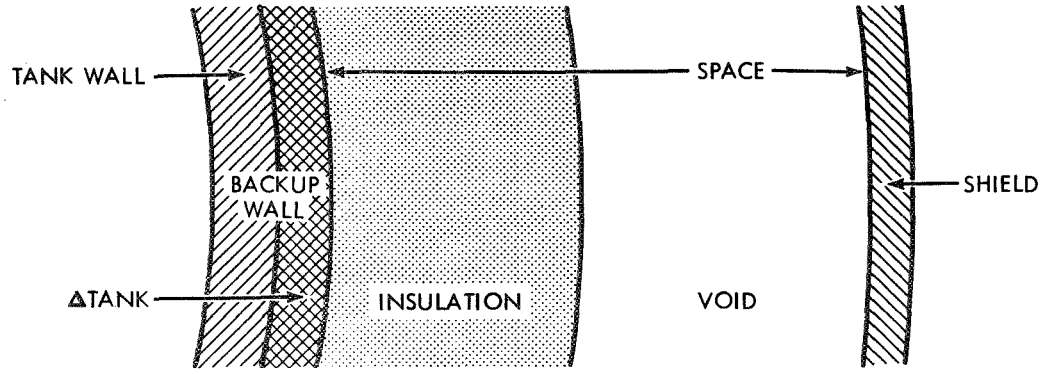

Figure 2-15. Meteoroid Shield Model

The backup wall thickness requirements were computed using MSC's empirical relation. (See paragraph 2.2.5.3.) To minimize the weight of the meteoroid protection, the pressurized propellant tank walls were used as the backup sheet. Figure 2-15 shows the backup wall as consisting of the tank wall and a "Δ tank". In cases where the computed backup sheet thickness exceeded the tank wall thickness, the tank walls were designed to the meteoroid criteria and not the tank pressures. However, while the weight of the pressure designed tank wall was not considered

to be part of the meteoroid protection system, the weight associated with any increase in the tank wall (Δ tank) was included in the total meteoroid shield weight and not the tank weight. The impact on the study results of selecting a common backup wall instead of a separate one is discussed in section 3, paragraph 3.3.

The required shield or bumper thickness was assumed to be 0.30 times the diameter of the design meteoroid. Although this will not give the optimum thickness, it will yield results which are accurate enough for the preliminary designs conducted in this study. The reasons for this are two-fold. First, as discussed in paragraph 2.2.5.3, even though the optimum shield thickness range is between 0.10 and 0.20 particle diameters, the shield is usually designed to a slightly higher value; and second, even at a shield thickness-to-meteoroid diameter ratio of 0.30, a large number of shield thickness were found to fall below the allowable minimum skin gauges and had to be designed to a higher ratio. The computer routine checked skin gauge of each shield to ensure that the minimum gauges were satisfied.

The computer routine determined the spacing between the shield and the backup sheet which yielded the minimum total weight (shield + Δ tank) which could fit within the specified configuration geometry. For the purpose of this study, the spacing was required to be at least the thickness of the thermal insulation and was not permitted to exceed a distance which would locate the shield outside a maximum radius established by the restrictions placed on propellant tank spacing.

The complex relationships between the geometric, structural, and minimum weight requirements can best be illustrated by examples. The results of typical meteoroid shield analyses are presented in figure 2-16, for the hydrogen tanks on typical bipropellant and tripropellant stages. The meteoroid shields were designed for a 0.995 probability of no penetrations during the 205-day mission.

The analysis of the bipropellant hydrogen tank indicated that the required shield thickness (0.023 inches) was less than minimum skin gauge (0.025 inches) and therefore it was necessary to make the shield thicker and heavier than actually required for meteoroid protection. On the bipropellant stage, the minimum total weight occurred at a shield spacing of 4 inches. This optimum point was well within the two geometric constraints.

However, this was not the case for the hydrogen tank on the tripropellant stage, where the minimum weight occurred at a spacing of 1.74 inches, which was incompatible with the geometric (insulation) restrictions. The shield was therefore located at a spacing equal to the thickness of the thermal insulation (3.04 inches), which maintained the criteria of minimum weight within the specified geometric constraints. This was necessary because of the relatively thick tank wall and large amount of thermal insulation required on the larger tank on the tripropellant stage.

In the case of the tripropellant stage shield, the required shield thickness (0.029 inches) exceeded the minimum skin gauge. This was due to the larger design meteoroid required for the larger surface area of the tripropellant's tank.

An analyses was conducted on each of the propellant tanks on the bipropellant, gel, and tripropellants stages evaluated. The results of the analyses for selected

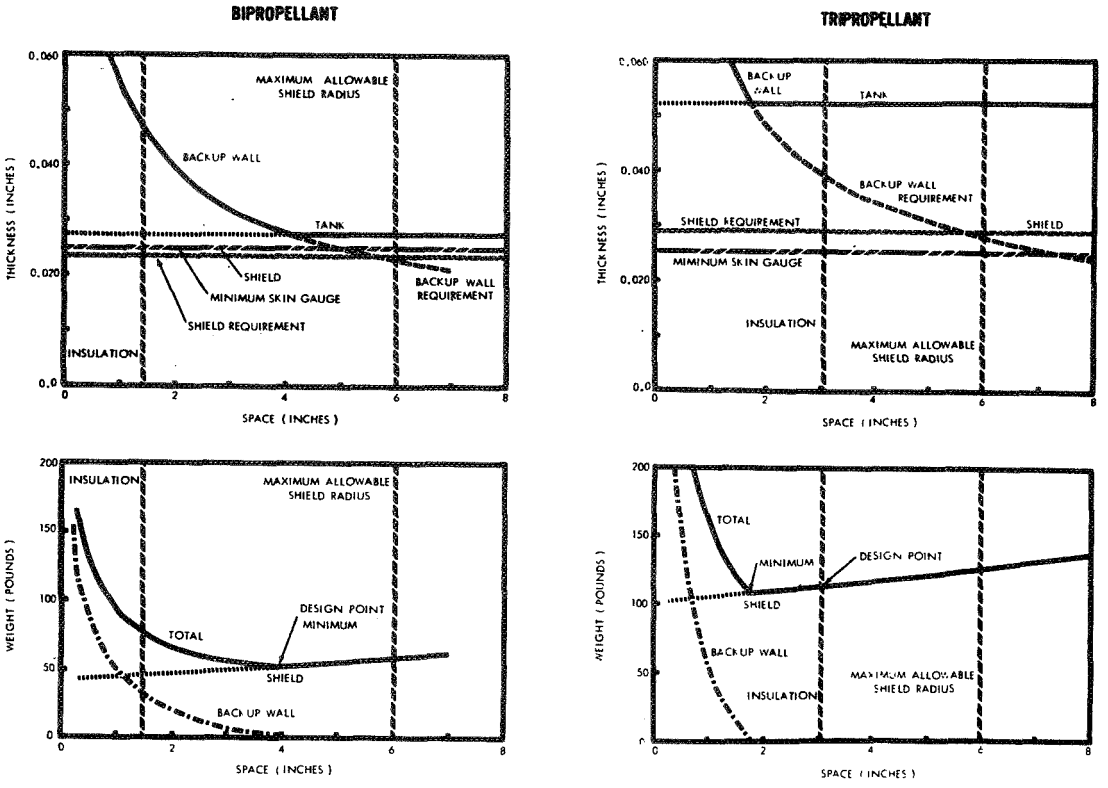

Figure 2-16. A Typical Meteoroid Shield Analysis

configurations are presented in section 3, paragraph 3.2, for both the single- and two-burn, interplanetary missions.

2.2.6 REACTION CONTROL SYSTEM (RCS)

The reaction control system (RCS) weights are based on a simple limit-cycle (pulse type thruster operation) where vehicle attitude and rates are sensed by inertial position and rate sensors. Deviations from the desired position or a rate of change of attitude produce error signals. When these signals exceed certain preset switching values, the appropriate thrusters are fired to provide a correcting impulse which drives the errors toward zero. The inertia of the vehicle, and the delays in thrust buildup and decay cause the vehicle to oscillate between the switching values, thereby requiring on-off thruster operation.

The size of the RCS is established using the following criteria:

1) Limit cycle of ±5.00 degrees about all axes

2) Angular velocity of 0.01 deg/sec about all axes

3) Angular acceleration of 0.003 rad/sec about the axis having the minimum inertia, and

4) Monopropellant thrusters having a steady state specific impulse of 180 seconds.

The weight of propellant consumed during the mission is found from the following equation: (4)

$$W_P = \frac{\pi}{180}\left(\frac{\omega^2}{\Theta I_{sp}}\right)\left[\left(\frac{I_{xx}}{r_{xx}}\right)+\left(\frac{I_{yy}}{r_{yy}}\right)+\left(\frac{I_{zz}}{r_{zz}}\right)\right]T$$

where

ω is the angular velocity in deg/sec

Θ is the limit cycle in degrees

I_{sp} is average specific impulse in seconds

T is the mission duration in seconds

I is the moment of inertia in slug-ft^2

and

xx, yy, and zz denote the pitch, yaw and roll axes, respectively.

To facilitate calculation of the inertias, it was assumed that the payload was a uniform solid cone, and that the engine and stage were homogeneous solid cylinders. The basic geometry used, and the individual weights included in each section are depicted in figure 2-17.

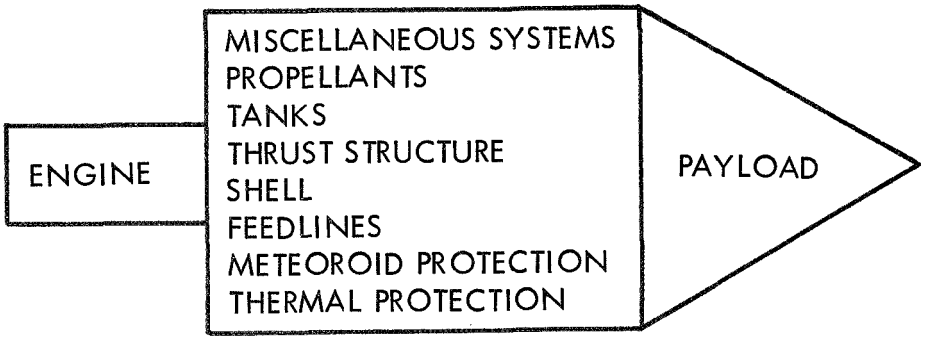

Figure 2-17. Model Used to Compute Mass Moment of Inertia

The total RCS weight was assumed to be directly proportional to the weight of propellant consumed during the mission.

(4) Schneider, E. J., "A Parametric Study of Attitude Control System (ACS) Design for a Space Vehicle," Report TB-EE-65-27, Chrysler Corporation Space Division, New Orleans, Louisiana, March 2, 1966.

Preliminary analyses indicated that the entire system would weigh approximately 25 to 30 percent more than the propellant. Therefore, the total RCS weight was computed from the following equation:

$$W_{RCS} = 1.30\ W_p$$

Any error introduced by the use of this technique would be small and would not affect the conclusions of the study.

2.2.7 PROPELLANT FEEDLINES

The weight of individual propellant feedlines is based on lengths and diameters, calculated to satisfy the tank geometry and flow requirements, respectively. The diameter of each feedline was sized to provide the necessary flowrate at a specified feedline flow velocity.

Estimates of the length of the tripropellant lines were made using the geometry shown in figure 2-18. The hydrogen feedline was assumed to be a straight line running directly from the bottom of the hydrogen tank to the gimbal point on the engine. The fluorine and lithium feedlines have identical geometries. These lines utilize dip tubes which run from the bottom of each propellant tank to the top, then horizontally to the centerline of the stage, and finally to the engine's gimbal point.

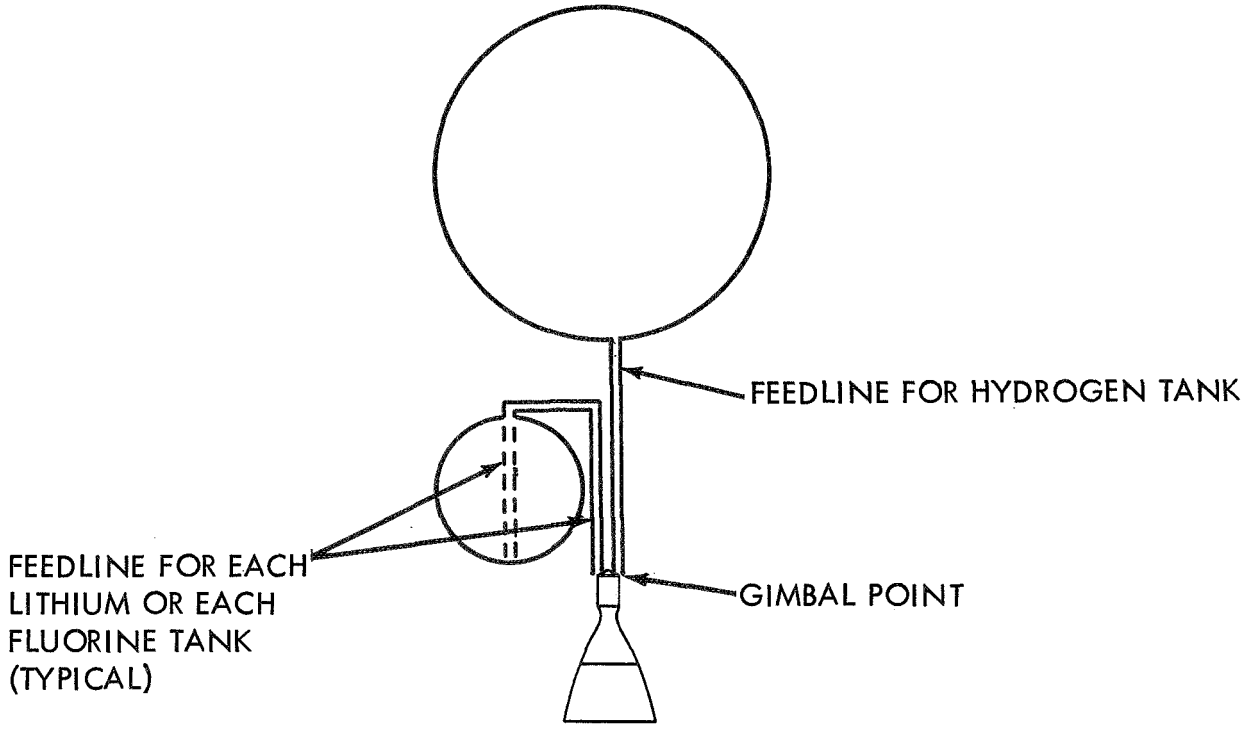

Figure 2-18. Tripropellant Feedline Geometry

The feedline lengths on the bipropellant stage were calculated in a similar manner. Figure 2-19 shows the feedline geometry used on the bipropellant stage. The lower tank feedline was assumed to run directly from the tank bottom to the engine gimbal point. The feedline length for the forward or smaller tank was estimated by assuming it ran along the stage centerline from the bottom of the upper tank to the top dome of the lower tank, then along the lower tank periphery to the stage centerline at the lower tank bottom dome, and finally to the engine gimbal point along the stage longitudinal axis.

The total line length required for each propellant was assumed to be directly proportional to the number of tanks; that is, one feedline for each tank.

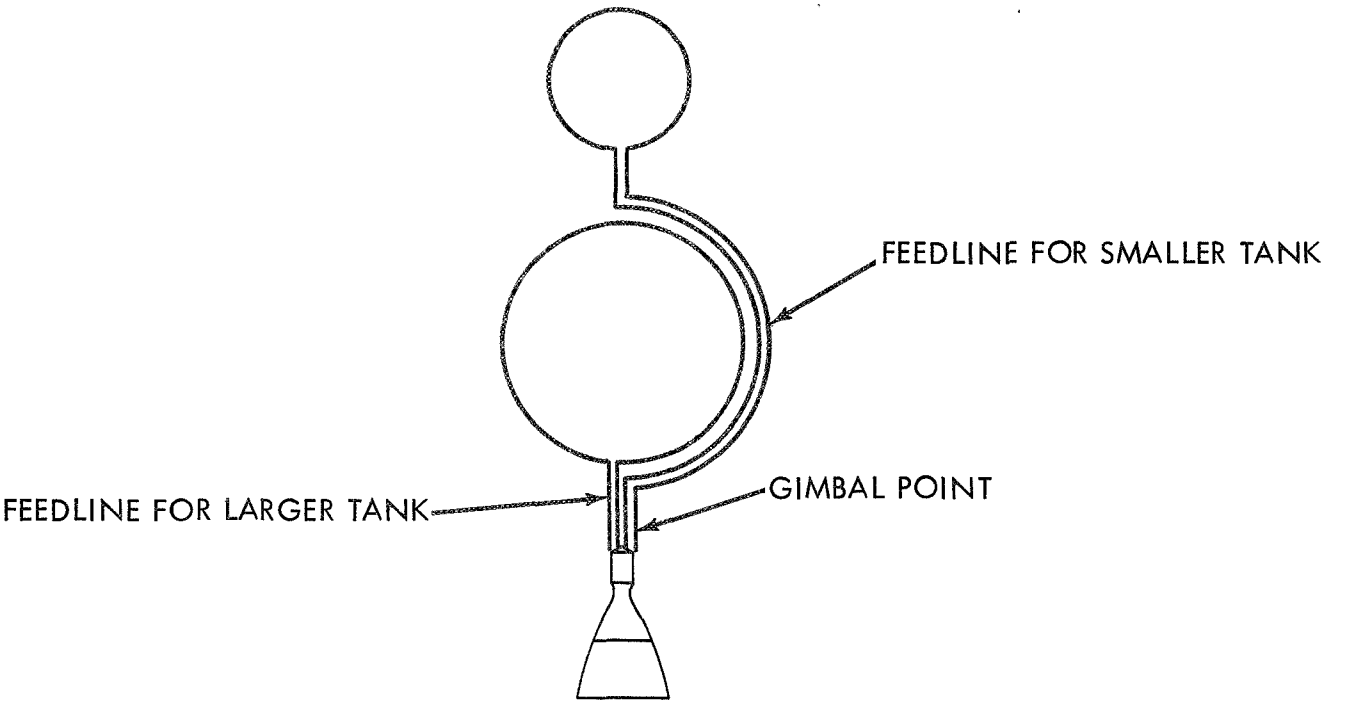

Figure 2-19. Bipropellant Feedline Geometry

2.2.8 ENGINE DATA

The parametric tripropellant engine system performance, weight, and geometry data used in optimizing the engine parameters and stage size, was obtained from a Rocketdyne tripropellant engine study[5]. Similar parametric data were obtained from Rocketdyne for hydrogen-fluorine bipropellant engines[6].

(5) Huntsinger, J. P., "Tripropellant Engine System Study, Final Report," Report R-7877, Rocketdyne, North American Rockwell Corporation, Canoga Park, California, May 1969.

(6) Letter from S. F. Iacobellis to G. M. Joseph, "F_2/H_2 Engine Parametric Data," RC 13995, Rocketdyne Division, North American Rockwell Corporation, Canoga Park, California, November 3, 1969.

For stage comparison studies, the thrust chamber tapoff cycle was used for both the bipropellant and tripropellant engines.

2.2.9 ELECTRIC HEATER AND POWER SYSTEM

On long duration missions, lithium must be kept in a liquid stage, that is, above its freezing point. The thermal analysis of the lithium tank calculated the quantity of heat necessary to keep the lithium molten. During this study it was assumed that this thermal energy would be supplied by electric heaters. The parametric data used by the sizing program to determine the weight of heaters required is shown in figure 2-20. The weight of the additional electric power system needed to supply energy for the heaters was not reflected in the electrical group weights given under miscellaneous weights, paragraph 2.2.10. The addition of a power system to supply the heaters was computed by the sizing program. Figure 2-21 presents the data used to estimate the additional power system weight required for the heaters.

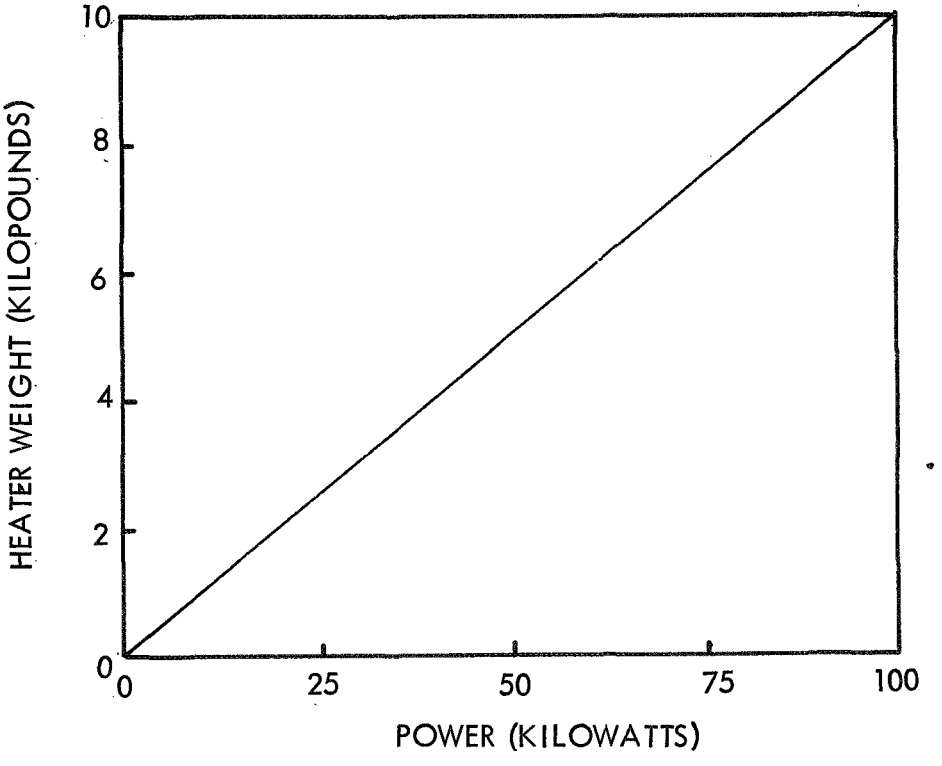

Figure 2-20. Electric Heater Weight

2.2.10 MISCELLANEOUS WEIGHTS

The subsystem weights depicted in table 2-3 were included in the sizing analysis as miscellaneous inert weights. Although the weight of these subsystems could be dependent on stage size, any variation would be small. Therefore, these weights were held constant during the study.

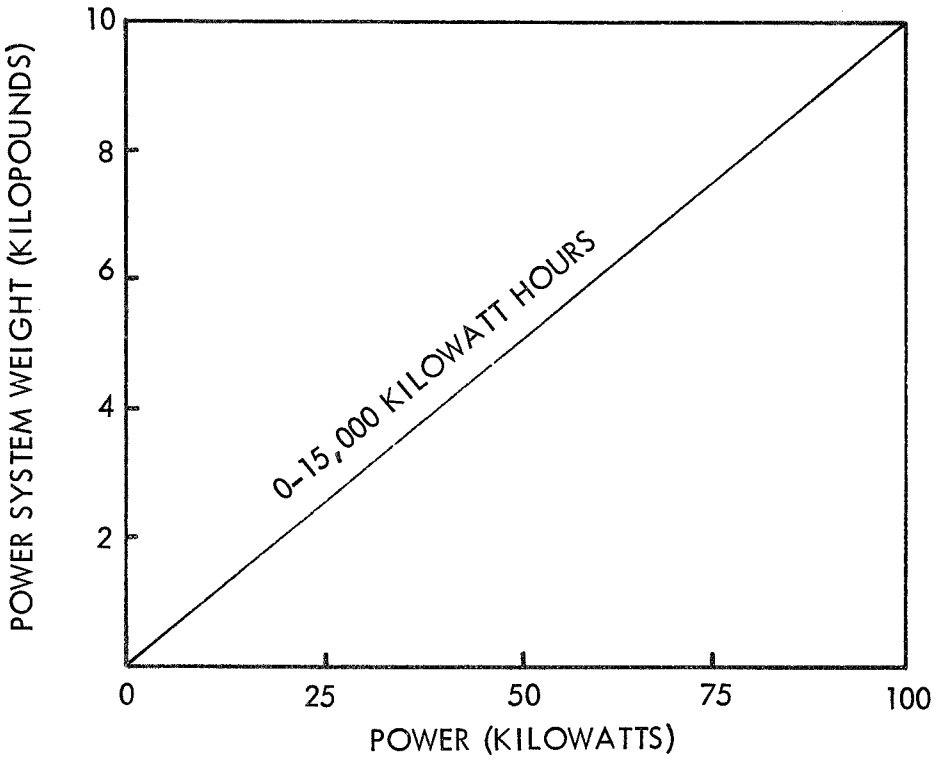

Figure 2-21. Additional Power System Weight

Table 2-3. Miscellaneous Subsystem

Subsystem	Weight (pounds)
Guidance Group	220
Electrical Group	180
Communication Group Instrumentation Group	120
Destruct Group	20
Propellant Utilization System	50
Hydraulic and Pneumatic System	60
Total Miscellaneous Weight	650

2.2.11 CONTINGENCY WEIGHT

The sizing program computed a contingency weight for each of the stages evaluated during this study. It was assumed that the contingency weight would be 7.5 percent of the total dry stage weight (i.e., gross weight less payload, interstage, and propellant).

Section 3
STUDY RESULTS

3.1 GENERAL

The two general classes of missions analyzed during the study were: 1) direct injection, and 2) long duration. The basic difference between these is that the direct injection missions have a very short coast prior to the single burn of the upper stage; whereas the long duration missions have a coast period of several months before the final upper stage burn.

The results of the direct injection missions and the long duration missions are presented in paragraphs 3.2-3.3 and 3.4, respectively.

3.2 DIRECT INJECTION MISSIONS

The basic direct inject mission profile consisted of a booster delivering the upper stage and payload to a velocity increment corresponding to the gross weight. After burnout, the booster is jettisoned and the upper stage is ignited after a short coast in order to supply the remaining velocity increment necessary to fulfill the mission requirements. Direct injection missions were investigated for total mission velocities ranging from earth escape to velocities corresponding to zero payload for each particular booster/gross weight combination. The five boosters investigated for the direct injection missions were: 1) Atlas/Centaur, 2) Atlas, 3) Titan IIID/Centaur, 4) Titan IIID, and the 260-Inch SRM/S-IVB. The results of the direct injection mission analyses and stage engine parameter optimization for these missions is presented, along with the basic data and assumptions, in the remainder of paragraph 3.2.

3.2.1 DATA AND ASSUMPTIONS

The constraints, guidelines and pertinent design data used for the direct injection mission studies are summarized in tables 3-1 through 3-3. Mission velocities ranging from earth escape to that corresponding to zero payload for the launch vehicle (booster plus upper stage) were investigated. A coast time of 0.5 hours and a stage thrust-to-weight ratio of 0.7 were assumed for all direct injection mission analyses.

Table 3-1. Design Constraints for Direct Injection Missions

Constraint \ Booster	Atlas	Atlas-Centaur	Titan IIID	Titan IIID Centaur	260-Inch SRM S-IVB
Booster Diameter (In.)	120	120	120	120	260
Lower Interstage Diameter (In.)	120	120	120	120	260
Maximum Stage Diameter (In.)	112	112	112	112	252
Shell-Tank Spacing (In.)	2	2	2	2	2
Tank-Tank Spacing (In.)	6	6	6	6	6
Engine-Tank Spacing Factor	4.0	4.0	4.0	4.0	4.0
Engine-Booster Spacing (In.)	6	6	6	6	6
Engine Gimbal Angle (Deg)	3	3	3	3	3
Thrust to Weight Ratio	0.7	0.7	0.7	0.7	0.7
Axial Acceleration (G's)	*	*	*	*	*
Lateral Acceleration (G's)	0.05	0.05	0.05	0.05	0.05
Payload Density (lb/ft^3)	25	25	25	25	25
Inert Weight Contingency (%)	7.5	7.5	7.5	7.5	7.5

*A function of gross weight, see appendix F.

Table 3-2. Prime Structure Design Data for Direct Injection Missions

Structure / Data	Shell	Interstage	Thrust Cone	Spider Beam
Material	Aluminum	Aluminum	Aluminum	Aluminum
Material Strength (psi)	67,000	67,000	67,000	46,000
Safety Factor	1.25	1.25	1.25	1.10
Monocoque to Complex Structure Weight Ratio	*	*	*	N/A
Spider Beam Multiplication Factor	N/A	N/A	N/A	*

*A function of booster and gross weight, see appendix F.

Table 3-3. Tankage Design Data for Direct Injection Missions

Data \ Propellant	Hydrogen	Fluorine	Lithium
Tank			
Material	Aluminum	Aluminum	Maraging Steel
Allowable Stress (psi)	50,000	50,000	*
Safety Factor	1.1	1.1	1.1
Minimum Skin Gauge (In.)	0.025	0.025	0.015
Land Factor	1.1	1.1	1.1
Thermal Protection			
Initial Temperature (°R)	36	150	**
Fraction Slush (%)	0	0	N/A
Insulation Thermal Conductivity (btu/hr-ft-°R)	0.010	0.010	*
Insulation Density (lb/ft^3)	3.2	3.2	8.0
External Insulation Temperature (°R)	500	500	500
Heater Weights (lb)	N/A	N/A	***
Miscellaneous			
Minimum Ullage Volume (%)	5	5	5
Residual Fraction (%)	1	1	1
Pressure Delta to Ensure NPSH (psi)	10	10	10
Feedline Flow Velocity (Fps)	25	25	25
Tank Support Factor	0.015	0.010	0.020

*A function of lithium temperature, see appendix F.

**Optimized by sizing program.

***See section 2.2.9.

3.2.2 ENGINE PARAMETER OPTIMIZATION

Before reliable conclusions could be made about the relative merits of the tripropellant and bipropellant stages, each stage had to be efficiently sized and its major stage characteristics selected to ensure that maximum performance was attained for the particular mission of interest. Figures 3-1 through 3-9, which are discussed below, illustrate typical engine parameter optimizations for the tripropellant, bipropellant and gel stages. This type of optimization was accomplished for each mission and booster investigated during the study.

The results, which are for the Atlas/Centaur, are discussed in the following paragraphs as a means of illustrating the approach used in this study. Appendix C, however, contains the working papers and graphs relative to the selection of the optimum characteristics for stages designed for use atop the other boosters.

3.2.2.1 Example Tripropellant Stage Engine Parameter Optimization

The engine parameter optimizations presented for the tripropellant stage are for a gross weight (i.e. stage, payload and interstage) of 12,000 pounds and a direct injection earth escape mission (ΔV = 36,140 fps). In figure 3-1, payload is presented as a function of chamber pressure, at an area ratio of 150:1, for a family of percentage of hydrogen curves.

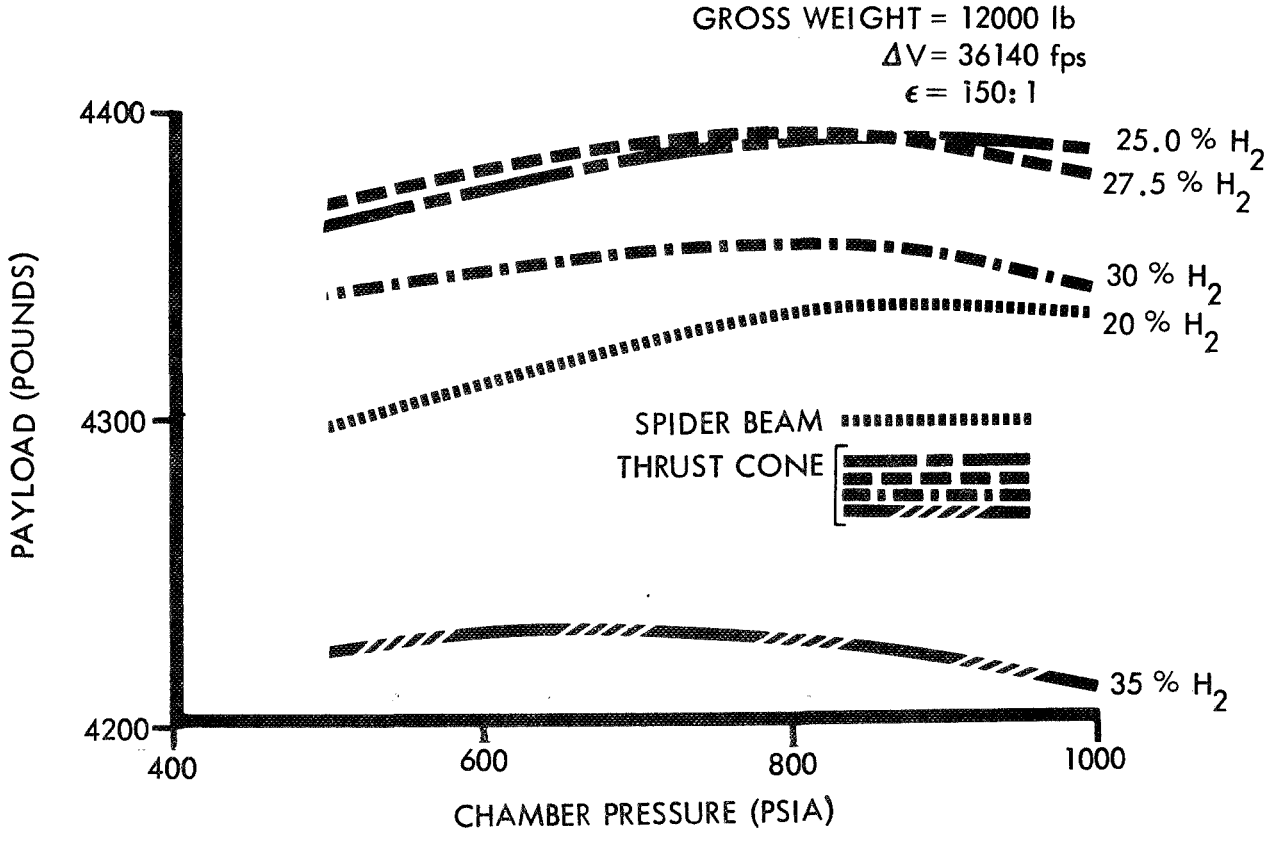

Figure 3-1. Payload Variation with Chamber Pressure (Atlas/Centaur/Tripropellant)

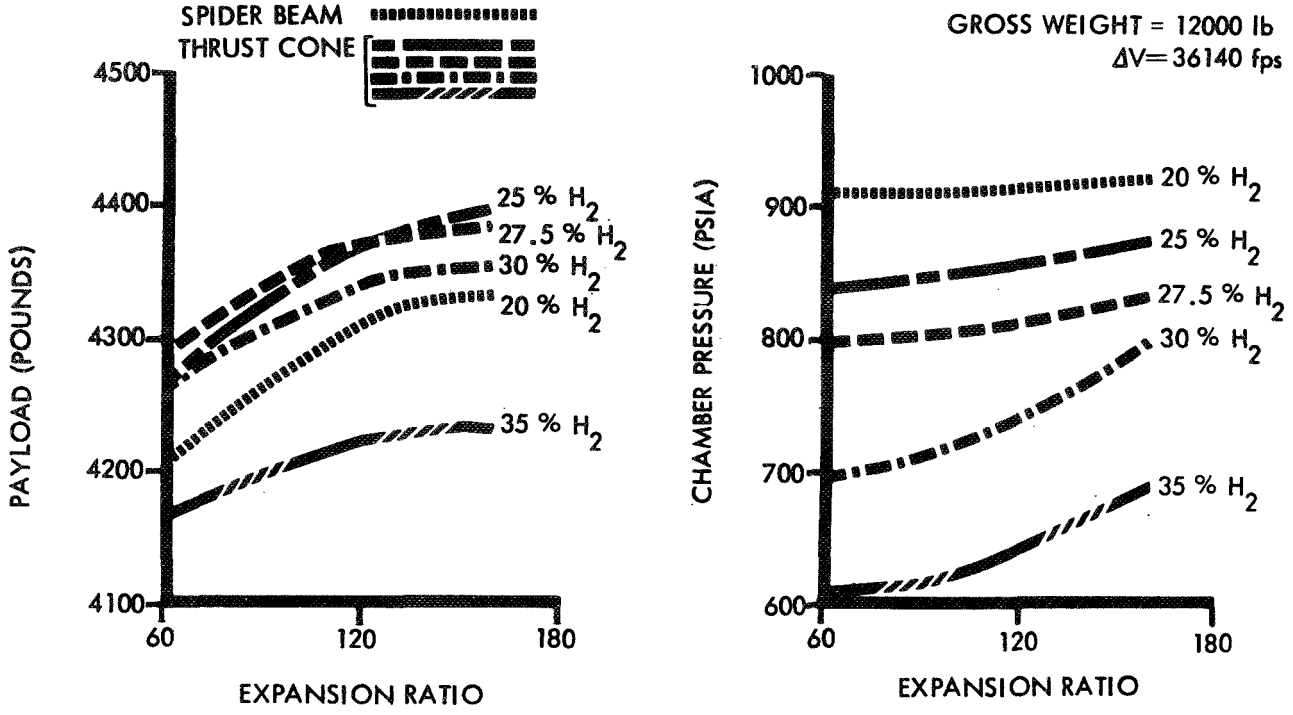

Figure 3-2. Payload and Corresponding Chamber Pressure Variation with Expansion Ratio (Atlas/Centaur/Tripropellant)

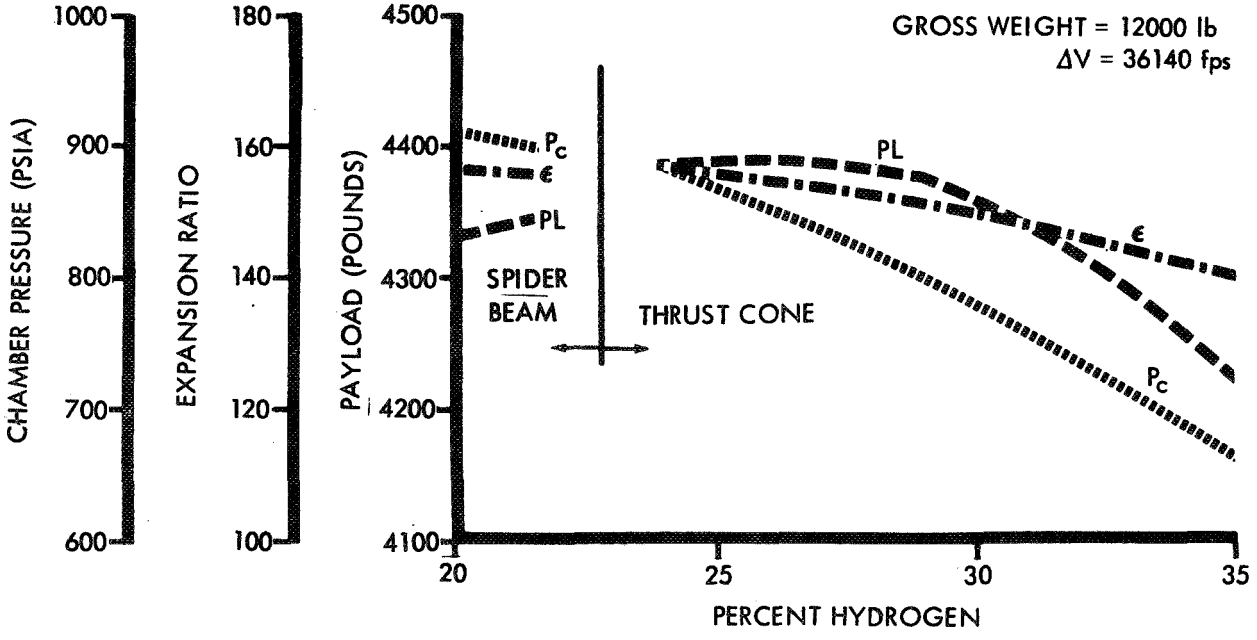

Figure 3-3. Engine Parameter Optimization Summary (Atlas/Centaur/Tripropellant)

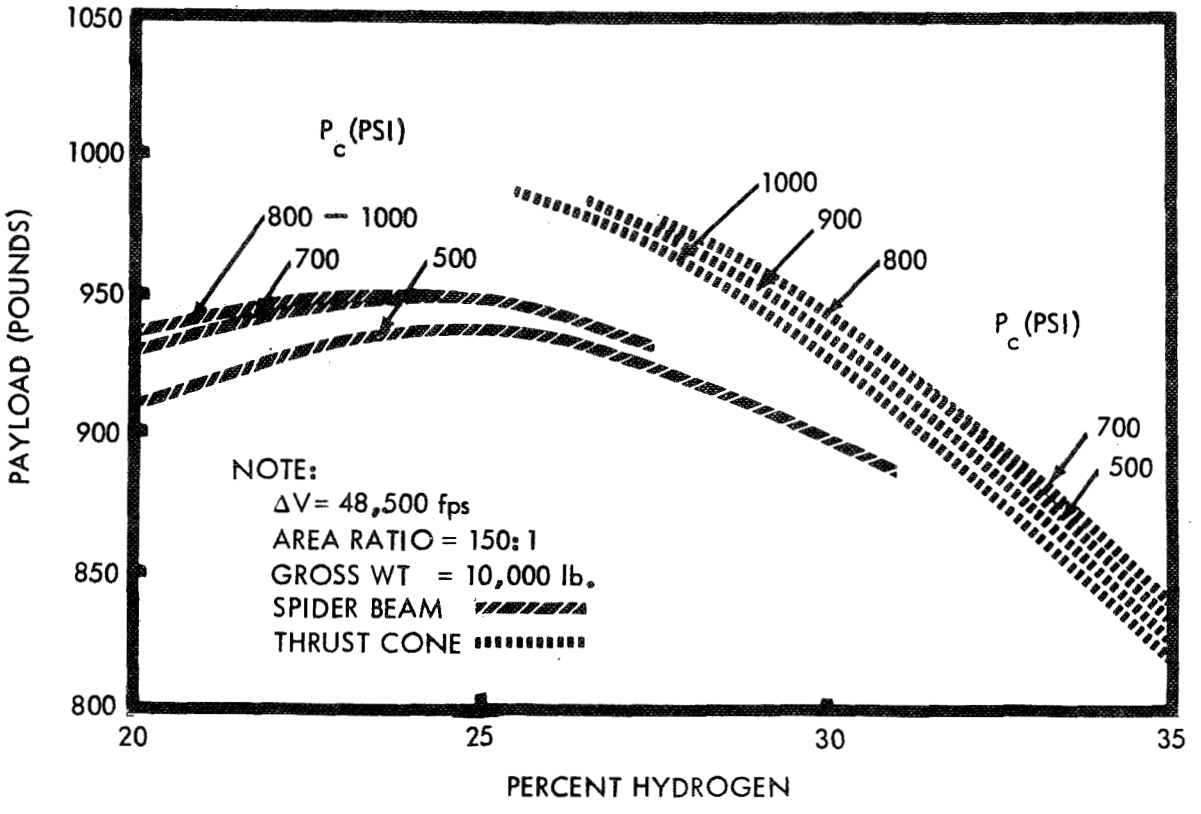

Figure 3-4. Payload Variation with Percent Hydrogen (Atlas/Centaur/Tripropellant)

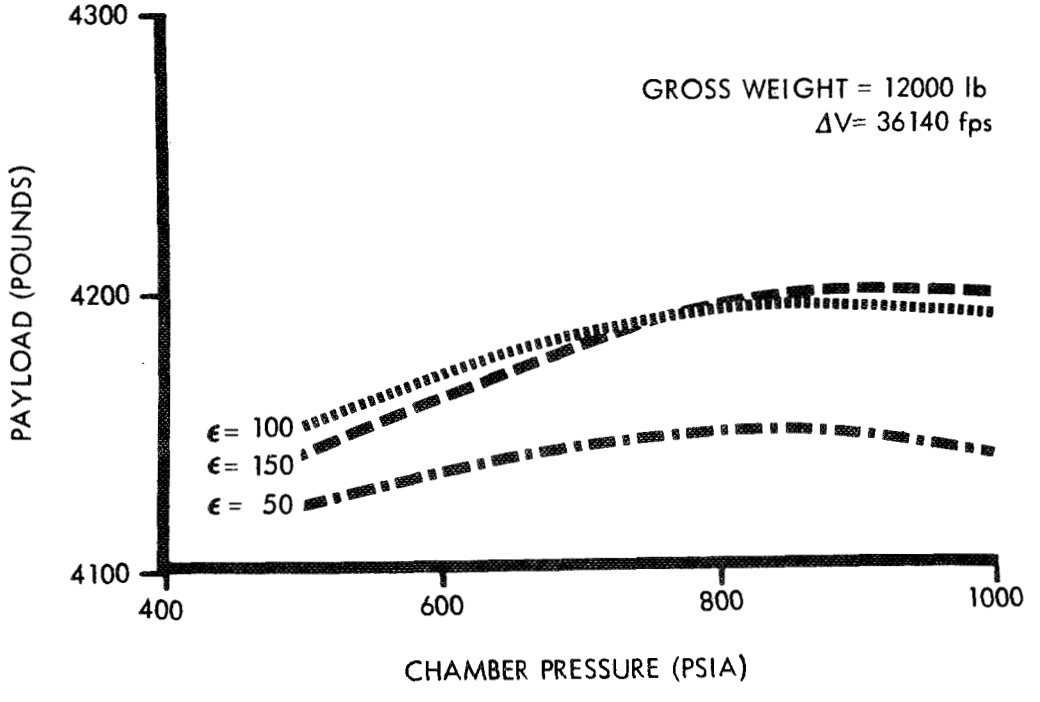

Figure 3-5. Payload Variation with Chamber Pressure (Atlas/Centaur/Bipropellant)

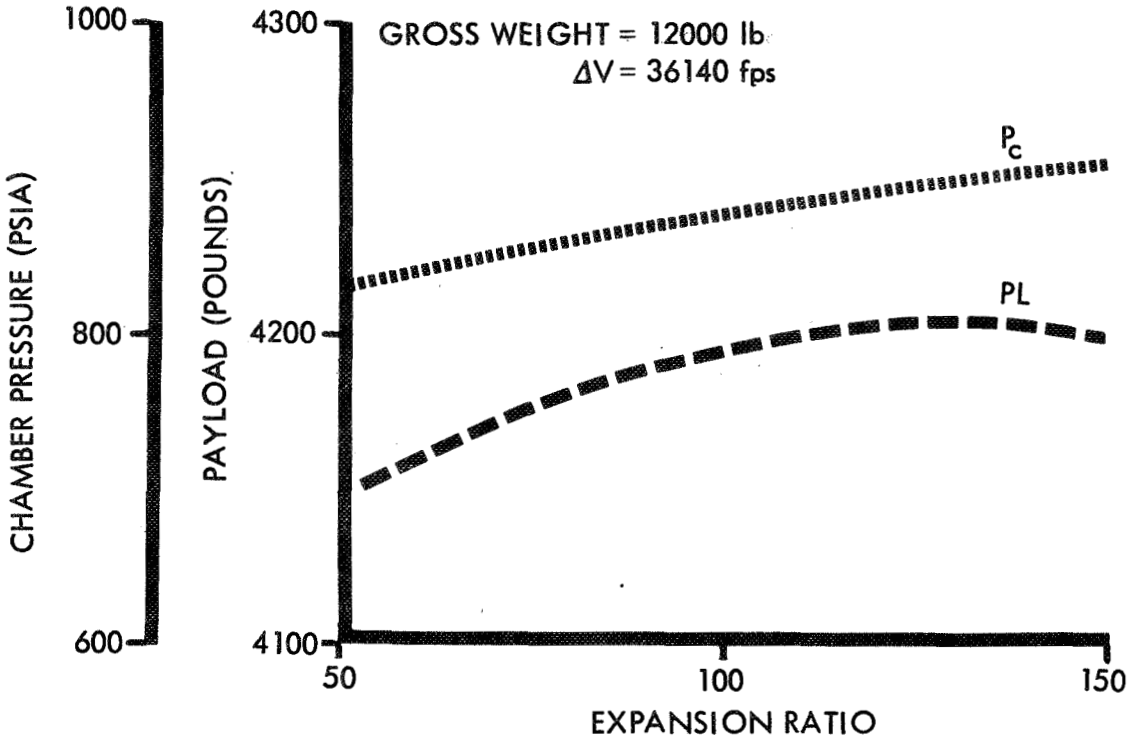

Figure 3-6. Engine Parameter Optimization Summary (Atlas/Centaur/Bipropellant)

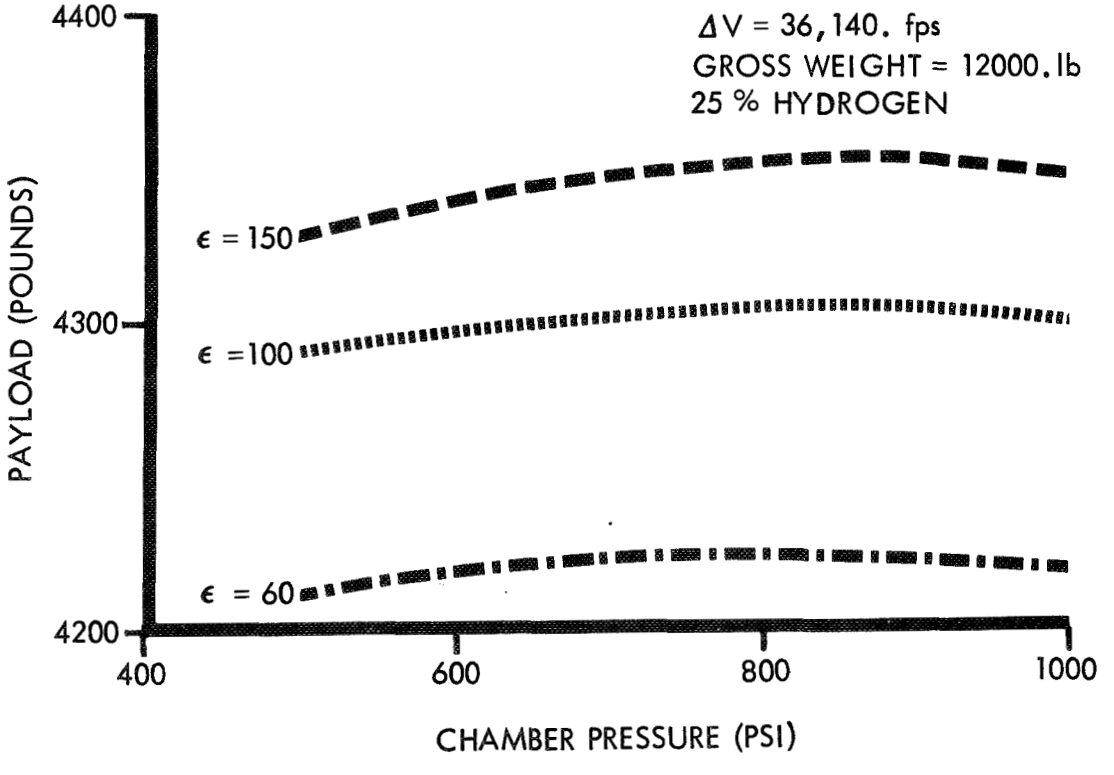

Figure 3-7. Payload Variation with Chamber Pressure (Atlas/Centaur/Gel)

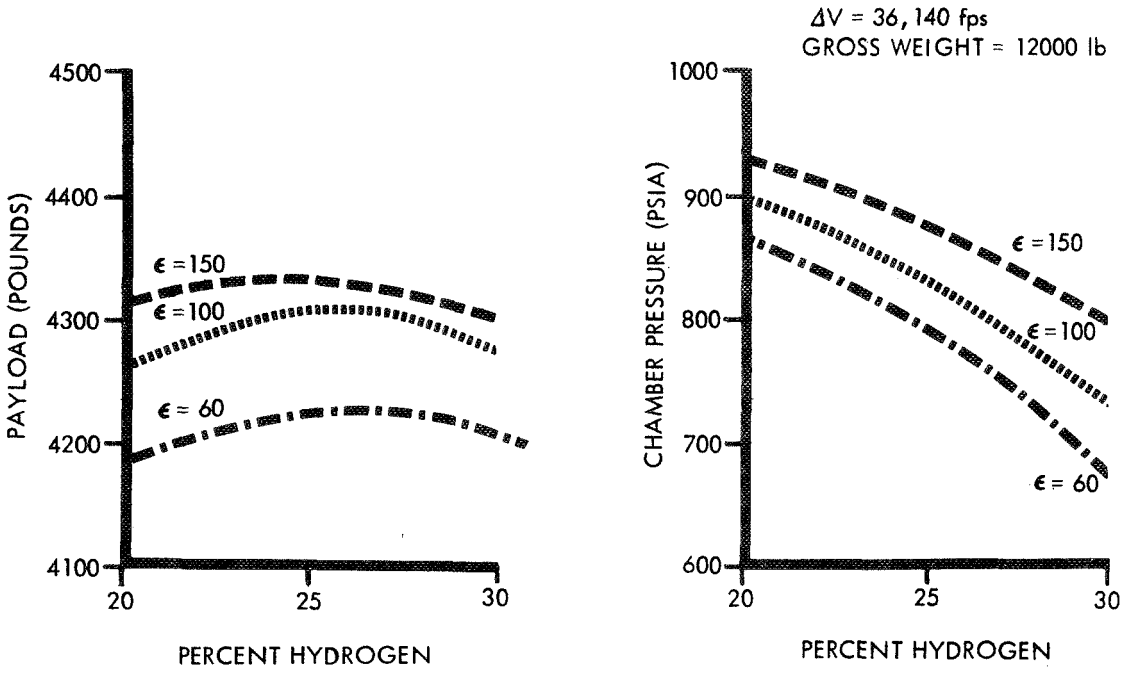

Figure 3-8. Payload and Corresponding Chamber Pressure Variation with Percent Hydrogen (Atlas/Centaur/Gel)

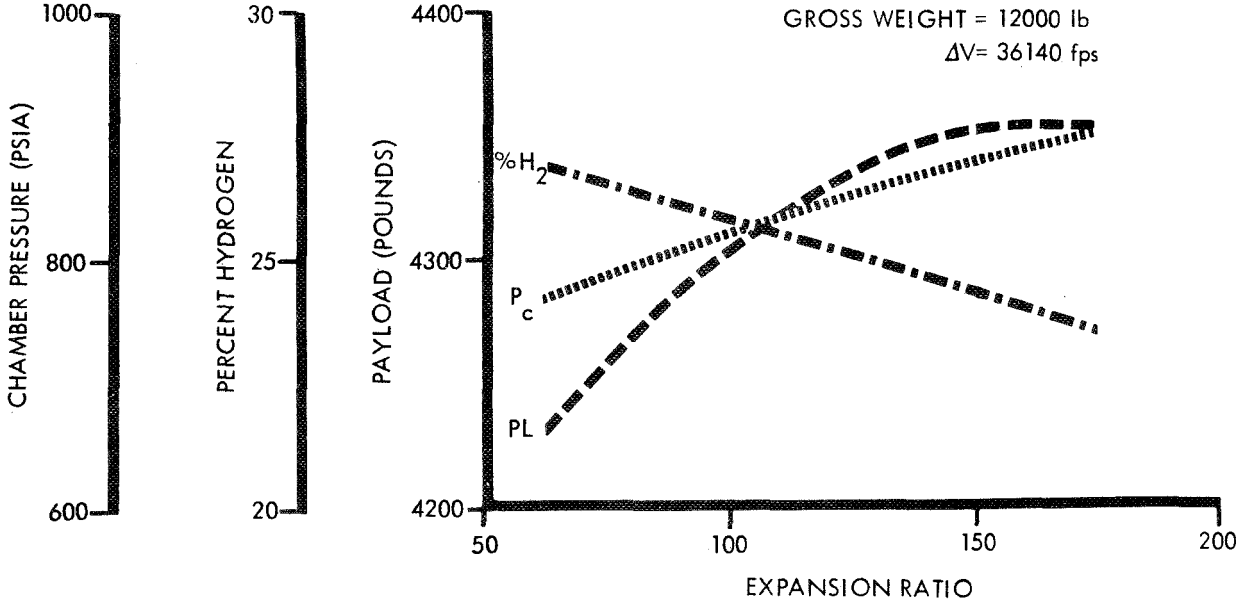

Figure 3-9. Engine Parameter Optimization Summary (Atlas/Centaur/Gel)

The results show that optimum chamber pressure is dependent upon the percentage of hydrogen investigated. Also, the results show that the absolute value of the payload is relatively insensitive to chamber pressure over the entire range investigated.

Figure 3-2 presents payload and the corresponding optimum chamber pressure as a function of area ratio for various percentages of hydrogen. These curves were obtained by cross-plotting data from payload vs. chamber pressure curves (at different area ratios) similar to that illustrated in the previous figure.

The dashed line shown for the 20 percent hydrogen case indicates that insufficient clearance was available to permit using a thrust cone configuration, therefore, a spider beam configuration was necessary.

The scale on the payload curve has been expanded to show the critical points in the curve more clearly, and that the actual variation in payload is small.

The engine parameter optimization for the tripropellant stage is summarized in figure 3-3, which presents maximum payloads and the corresponding optimum area ratios and chamber pressures for a range of hydrogen percentages.

The optimum engine parameters for this stage were found to be the following (see figure 3-3):

a) Percent hydrogen = 26
b) Expansion ratio = 155:1
c) Chamber pressure = 850 PSIA

However, as noted in the previous figures, only small penalties are incurred if it is necessary to select values slightly different from the optimums indicated.

The results presented in figure 3-3 are for a 12,000 lb gross weight stage and a mission velocity of 36,140 fps. The optimum values for the engine parameters are slightly dependent on stage size and mission velocity; however, if the chamber pressure is over 750 psia, with an area ratio greater than 125:1 and a 25(±2.5) percent hydrogen, the resultant stage will be very close to the optimum.

The results presented in the three previous figures were based on stages with propellant loads that permit the use of the more efficient submerged engine-thrust cone geometry. However, for other propellant loadings this is not always possible, as is illustrated in figure 3-4. Here the payload is presented as a function of hydrogen percentages for a family of chamber pressures. These data show that the use of a thrust cone is restricted to hydrogen percentages which are greater than 25 or 27 percent, but that the maximum payload would have occurred at lower percentages if the thrust cone type geometry could have been used.

In making payload comparisons, which will be discussed later in this report, the configuration or stage geometry that yields the maximum payload for the specific mission being investigated is selected. In some cases this was the spider beam version since the thrust cone geometries were precluded (because of geometric constraints) for the higher percentages of hydrogen (which have a relatively low specific impulse).

3.2.2.2 Example Bipropellant Stage Engine Parameter Optimization

Figure 3-5 presents payload as a function of chamber pressure for a 12,000-pound (gross weight), fluorine/hydrogen stage on an Atlas/Centaur booster, and optimized for an earth escape (36,140 fps) mission. A family of curves corresponding to three different expansion ratios are shown to illustrate this effect. A cross-plot of the critical points from these curves yields the results shown in figure 3-6, where the maximum payload and the corresponding optimum chamber pressure are presented as a function of expansion ratio. These results show that the optimum chamber pressure and the optimum area ratio are approximately 900 psia and 130:1, respectively. Once again, the payload scale has been expanded to more clearly indicate the maximum point on the curve; the total payload variation between an area ratio of 50:1 and 150:1 is only about one percent.

All bipropellant stage parameter optimizations have been accomplished assuming a mixture ratio of 12:1. This was done since compatible engine data were not available at other mixture ratios. If the optimization of mixture ratios had been accomplished, it is possible that the bipropellant stage would demonstrate slightly higher payload potential than those presented herein.

3.2.2.3 Example Gel Stage Engine Parameter Optimization

Figure 3-7 shows the variation in payload, for the gel stage on an Atlas/Centaur booster as a function of chamber pressure and expansion ratio. For this example the percent (of total load) hydrogen was held constant at 25 percent, and gross weight (i.e., stage, interstage, and payload) was held constant at 12,000 pounds. The mission was a direct injection earth escape mission (ΔV = 36,140 fps). As with the tri-propellant, payload is seen to be relatively insensitive to chamber pressure.

Figure 3-8 presents payload and optimum chamber pressure as a function of percentage of hydrogen and expansion ratio. These data are obtained by cross plotting the optimums obtained from a family of charts, similar to the previous one, for a range of hydrogen percentages.

The results show that the optimum hydrogen percentages lie around 25 (±3) percent, and that the optimum chamber pressure decreases with increasing percentage of hydrogen and decreasing expansion ratio.

Figure 3-9 shows maximum payload and the corresponding optimum chamber pressure and hydrogen percentages as a function of expansion ratio. The results show that maximum payload is obtained for an expansion ratio of 160:1, a chamber pressure of 890 psia, and 24 percent hydrogen. However, it should be pointed out that the payload scale has been exaggerated to aid in identifying the maximum payload point. In terms of absolute values, the total payload range covered varies by less than 3 percent.

3.2.2.4 Example Stage Weight Optimization

The engine parameter optimizations discussed in the previous paragraphs were all for a 12,000-pound gross weight (i.e., stage, payload, and interstage) and a 36,140 fps mission velocity. Figure 3-10 was prepared by cross plotting the optimum

payloads at other mission velocities and gross weights. All three propellant combinations are represented in the figure.

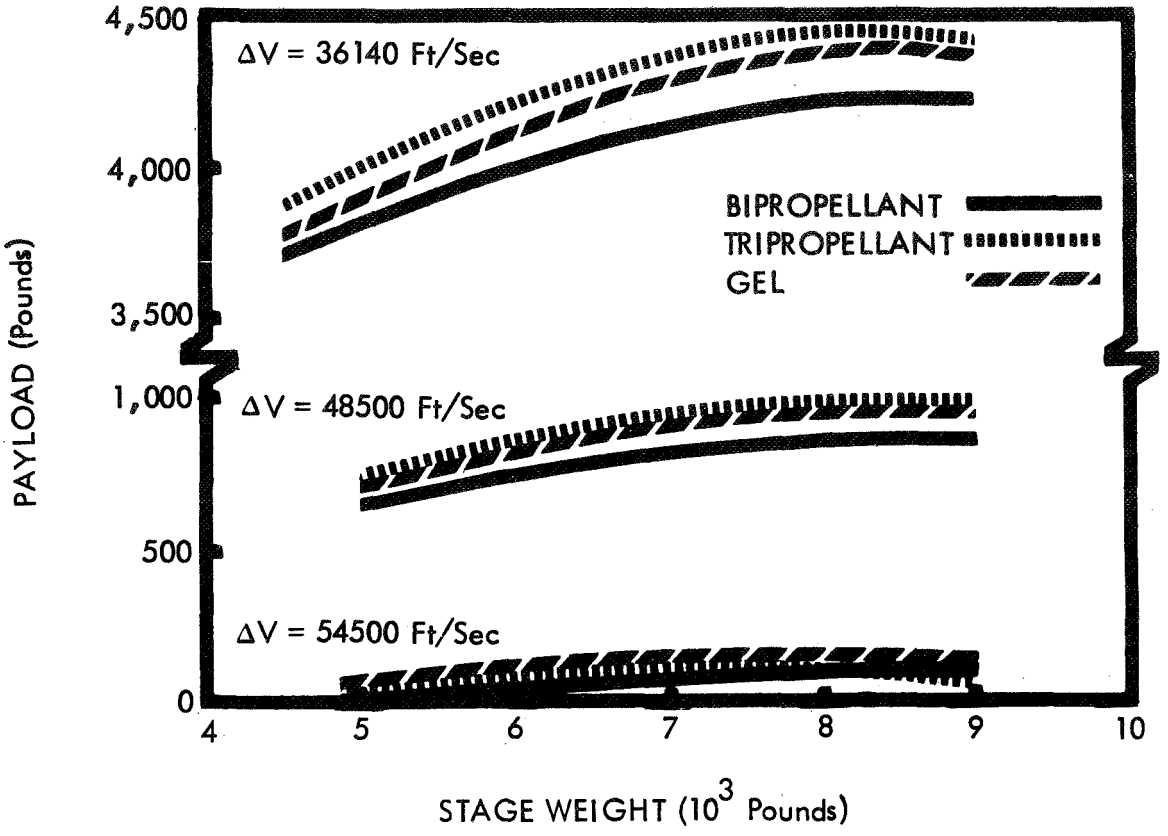

Figure 3-10. Payload Variation with Stage Weight, Direct Injection Missions (Atlas/Centaur)

From an inspection of the curves, two trends become evident. First, the optimum stage size for higher mission velocities is slightly less than those for escape velocities. Second, the payload sensitivity to stage size is small for variations of $\pm$ 15 percent about the optimum stage size.

Similar results were noted for the stage sizings accomplished for the other boosters investigated during the study.

In some cases, it was necessary to increase the size of a stage by 25 to 30 percent just to gain a few percents in payload. Thus, the stages with the maximum payload are not necessarily optimum from a cost effectiveness standpoint and it was felt that comparisons of stage capabilities based on maximum payload could be misleading. For this reason, a different type of comparison is needed to give some indication of how the stage comparisons would look when made on the basis of optimum cost effectiveness.

The relationship shown in figure 3-11 was used to estimate the cost of all stages as a function of inert weight. Cost effectiveness (dollars per pound of payload) versus gross weight plots were prepared using the results of stage sizing analyses and the stage costs data shown here.

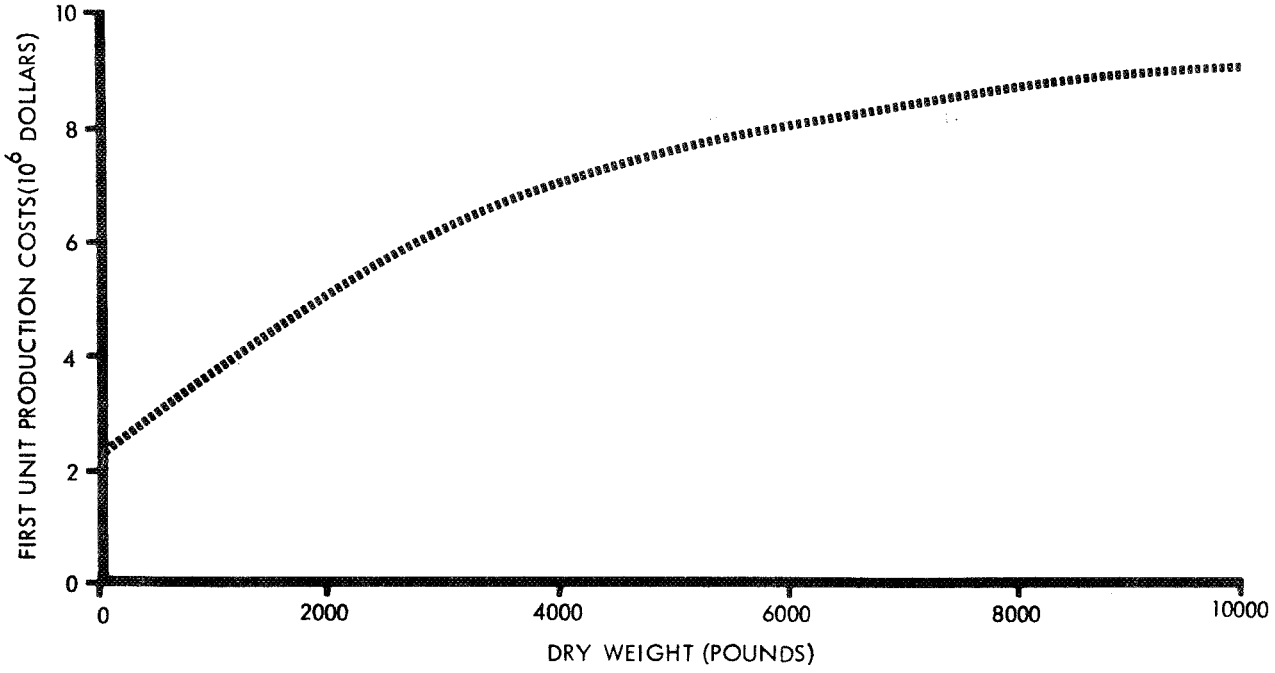

Figure 3-11. Stage Cost Estimating Relationship

Figure 3-12 shows an example cost effectiveness plot for each of the stages when used with the Atlas/Centaur. The examples presented are for a mission velocity of 48,500 fps. The results show that the bipropellant stage optimizes at a slightly higher weight than either the tripropellant or gel stages. The relationship between payload and cost effective-optimized stage sizes will be presented later; however, before proceeding, a word of caution with regard to interpreting these results is in order. The absolute values of cost effectiveness for the different stages should not be used as a basis for comparing the relative merits of the stages. The parameter which is of significance and may be compared with validity is the payload, which corresponds to optimum cost effective stage size.

The data shown in figure 3-12 are for one mission velocity. Figure 3-13 shows the effect of mission velocity on the optimum stage size from both a maximum payload and optimum cost effective standpoint. Curves are shown for each of the three stages. A comparison of the two plots shows: 1) that the cost effective stage sizes are smaller than those corresponding to the maximum payload stage; and 2) that the difference between the two varies with mission velocity. In subsequent paragraphs, payloads for the three stages are presented as a function of mission velocity for each of the five boosters investigated. The relationship between maximum and cost effective payloads will be discussed in each case.

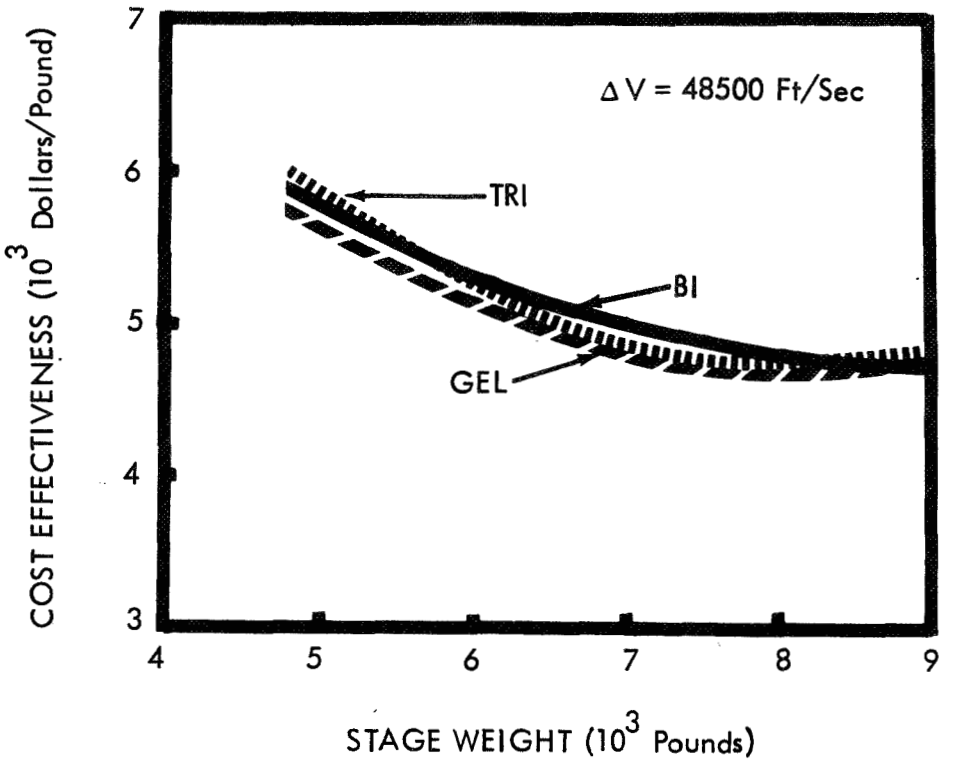

Figure 3-12. Cost Effectiveness Stage Size Selection (Atlas/Centaur)

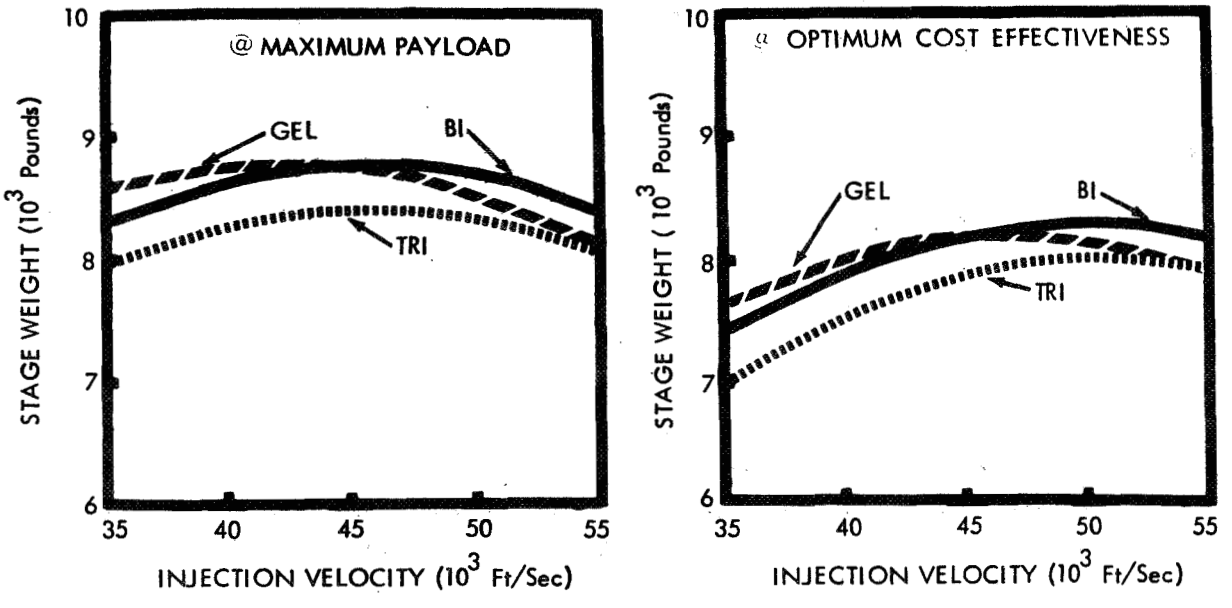

Figure 3-13. Stage Size Comparison (Atlas/Centaur)

3.3 STAGE COMPARISONS

3.3.1 ATLAS/CENTAUR BOOSTER RESULTS

Maximum payload versus total mission velocity is shown in figure 3-14 for each of the three propellant combinations investigated. The payloads given represent the maximum attainable at each mission velocity and hence do not necessarily correspond to identically sized stages.

The results show that the tripropellant stage enjoys a payload advantage over the bipropellant ranging from about 200 pounds for an escape mission to approximately 30 pounds for a total mission velocity requirement of 50,000 fps. The comparison between the gel and the tripropellant is a toss-up except for velocities above 50,000 fps, where the gel stage has a slightly better capability.

For this booster, the difference between the maximum payloads and payloads corresponding to optimum cost effectiveness is negligible and is not presented. However, the data may be found in appendix C.

A summary of the major stage characteristics of the tripropellant, bipropellant and gel stages is given in table 3-4. These data correspond to a 12,000 pound gross weight stage and are for stages sized to achieve earth escape velocity (36,140 fps).

Table 3-5 is a summary of the optimum engine parameters selection and tables 3-6 through 3-8 summarize the major design characteristics for the three stages. The data given in these tables are strictly applicable to the specified mission and stage gross weight; however, in general, these data are representative of the stages designed for other missions.

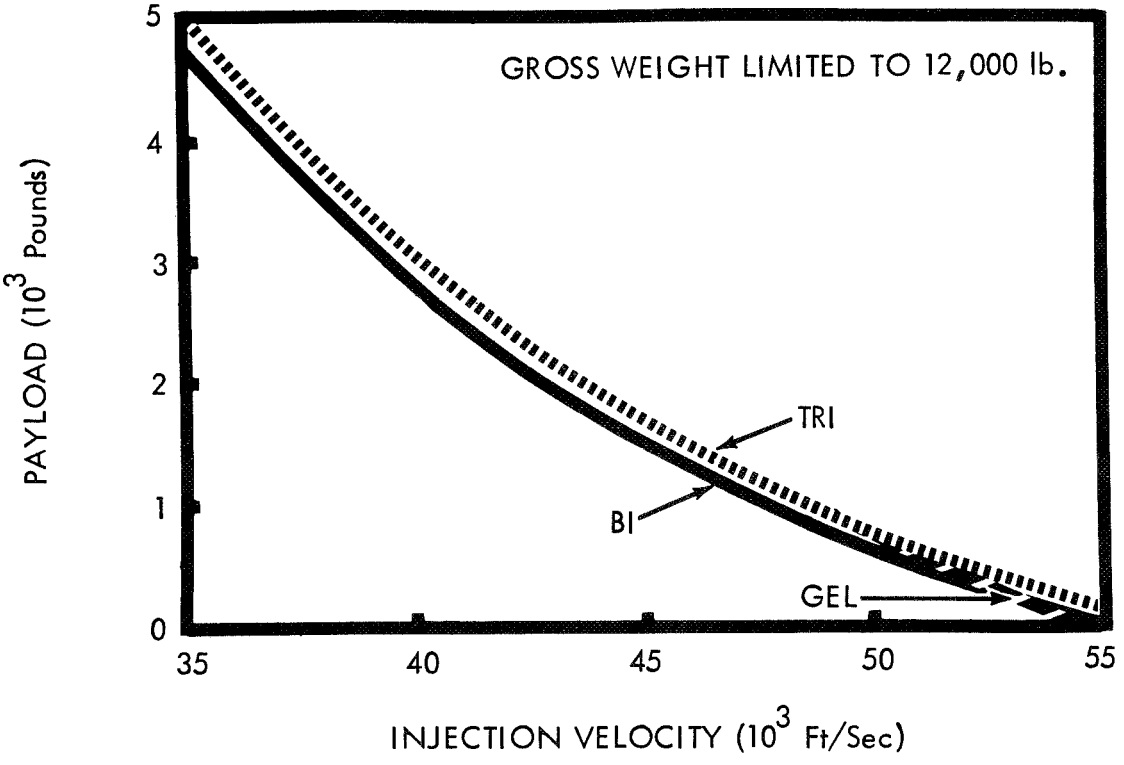

Figure 3-14. Direct Injection Mission (Atlas/Centaur)

Table 3-4. Major Stage Characteristics Summary - Atlas/Centaur Booster, Direct Injection

Total Mission Velocity:	36140 fps
Stage Velocity Increment - First Burn:	11390 fps
Stage Velocity Increment - Second Burn:	0.0 fps
First Coast Time:	0.5 hrs
Second Coast Time:	0.0 hrs
Gross Weight:	12, 000 lb

Stage	Bipropellant	Gelled H_2/Li	Tripropellant
Payload (lb)	4197	4350	4387
Specific Impulse (sec)	467.62	509.17	521.17
Thrust (lb)	8315	8280	8282
Interstage Weight (lb)	122	172	169
Total Stage Weight (lb)	7681	7479	7444
Inert Stage Weight (lb)	1279	1463	1524
Total Propellant Weight (lb)	6402	6015	5920
Propellant Consumed			
First Burn (lb)	6302	5923	5829
Second Burn (lb)	N/A	N/A	N/A
Residual Propellant Weight (lb)	64	60	60
Stage Mass Ratio	2.145	2.015	1.982
Stage Payload Fraction	0.349	0.362	0.366
Stage Structural Ratio	0.174	0.203	0.212
Stage Velocity Ratio	0.763	0.701	0.684
Stage Thrust to Weight Ratio	0.7	0.7	0.7

Table 3-5. Engine Data Summary, Atlas/Centaur Booster, Direct Injection

Stage	Bipropellant	Gelled H_2/Li	Tripropellant
Thrust (lb)	8315	8280	8282
Specific Impulse (sec)	467.62	509.17	521.17
Expansion Ratio	150	150	150
Chamber Pressure (psi)	1000	800	800
F_2/Li Mixture Ratio	N/A	2.740	2.740
Percent Hydrogen	7.692	25.0	25.0
Weight (lb)	115	139	139
Length (In.)	48.1	53.9	53.9
Exit Diameter (In.)	29.6	33.0	33.0

Table 3-6. Design Data Summary - Bipropellant Stage, Atlas/Centaur Booster, Direct Injection

Propellant Tank	Hydrogen	Fluorine
Propellant Weights		
Usable (lb)	485	5817
Residual (lb)	5	59
Boiloff (lb)	0	0
Startup/Shutdown (lb)	3	33
Total Load (lb)	493	5909
Tankage		
Number of Tanks	1	1
Volume (ft^3)	130.5	66.5
Radius (In.)	37.76	30.15
Cylinder Length (In.)	0	0
Dome Thickness (In.)	0.0275	0.0250
Cylinder Thickness (In.)	N/A	N/A
Design Pressure (psi)	N/A	N/A
Thermal		
Initial Temperature (°R)	36	150
Vent Temperature (°R)	46	155
Insulation Thickness (In.)	0.34	0.19
Number of Kilowatts	N/A	N/A
Number of Kilowatt-hours	N/A	N/A
Meteoroid Shield		
Meteoroid Design Mass (gm)	N/A	N/A
Meteoroid Diameter (cm)	N/A	N/A
Shield Thickness (In.)	N/A	N/A
Spacing (In.)	N/A	N/A
Backup (Δ Tank) Thickness (In.)	N/A	N/A

Table 3-7. Design Data Summary - Gelled H_2/Li Stage, Atlas/Centaur Booster, Direct Injection

Propellant Tank	Hydrogen	Fluorine
Propellant Weights		
Usable (lb)	2668	3254
Residual (lb)	27	33
Boiloff (lb)	0	0
Startup/Shutdown (lb)	15	18
Total Load (lb)	2710	3305
Tankage		
Number of Tanks	1	1
Volume (ft^3)	414.6	37.3
Radius (In.)	54.0	24.41
Cylinder Length (In.)	6.24	0
Dome Thickness (In.)	0.0258	0.0250
Cylinder Thickness (In.)	0.0516	N/A
Design Pressure (psi)	43	28
Thermal		
Initial Temperature (°R)	36	150
Vent Temperature (°R)	42	156
Insulation Thickness (In.)	0.43	0.21
Number of Kilowatts	N/A	N/A
Number of Kilowatt-hours	N/A	N/A
Meteoroid Shield		
Meteoroid Design Mass (gm)	N/A	N/A
Meteoroid Diameter (cm)	N/A	N/A
Shield Thickness (In.)	N/A	N/A
Spacing (In.)	N/A	N/A
Backup (Δ Tank) Thickness (In.)	N/A	N/A

Table 3-8. Design Data Summary - Tripropellant Stage, Atlas/Centaur Booster, Direct Injection

Propellant Tank	Hydrogen	Fluorine	Lithium
Propellant Weights			
Usable (lb)	1457	3203	1169
Residual (lb)	15	33	12
Boiloff (lb)	0	0	0
Startup/Shutdown (lb)	8	17	6
Total Load (lb)	1480	3253	1187
Tankage			
Number of Tanks	1	2	2
Volume (ft^3)	377.2	18.4	20.2
Radius (In.)	53.78	19.64	20.28
Cylinder Length (In.)	0	0	0
Dome Thickness (In.)	0.02831	0.0250	0.0150
Cylinder Thickness (In.)	N/A	N/A	N/A
Design Pressure (psi)	48	29	50
Thermal			
Initial Temperature (°R)	36	150	1040
Vent Temperature (°R)	43	157	N/A
Insulation Thickness (In.)	0.35	0.22	0.24
Number of Kilowatts	N/A	N/A	N/A
Number of Kilowatt-hours	N/A	N/A	N/A
Meteoroid Shield			
Meteoroid Design Mass (gm)	N/A	N/A	N/A
Meteoroid Diameter (cm)	N/A	N/A	N/A
Shield Thickness (In.)	N/A	N/A	N/A
Spacing (In.)	N/A	N/A	N/A
Backup (Δ Tank) Thickness (In.)	N/A	N/A	N/A

Figures 3-15 through 3-17 show external profiles of the three stages as designed to interface with the Atlas/Centaur. A sheet stringer design is depicted for the major structure of the stages except for the tank supports of tripropellant and gel stages which use struts to support the lithium and fluorine tanks. Judicious use of honeycomb and composite structures could result in slightly lower structural weights for all of these configurations; however, the savings would be relatively small. Further, since the differences in inert weight of the three stages would hardly change at all, the analyses necessary to incorporate composite and honeycomb structures was not undertaken.

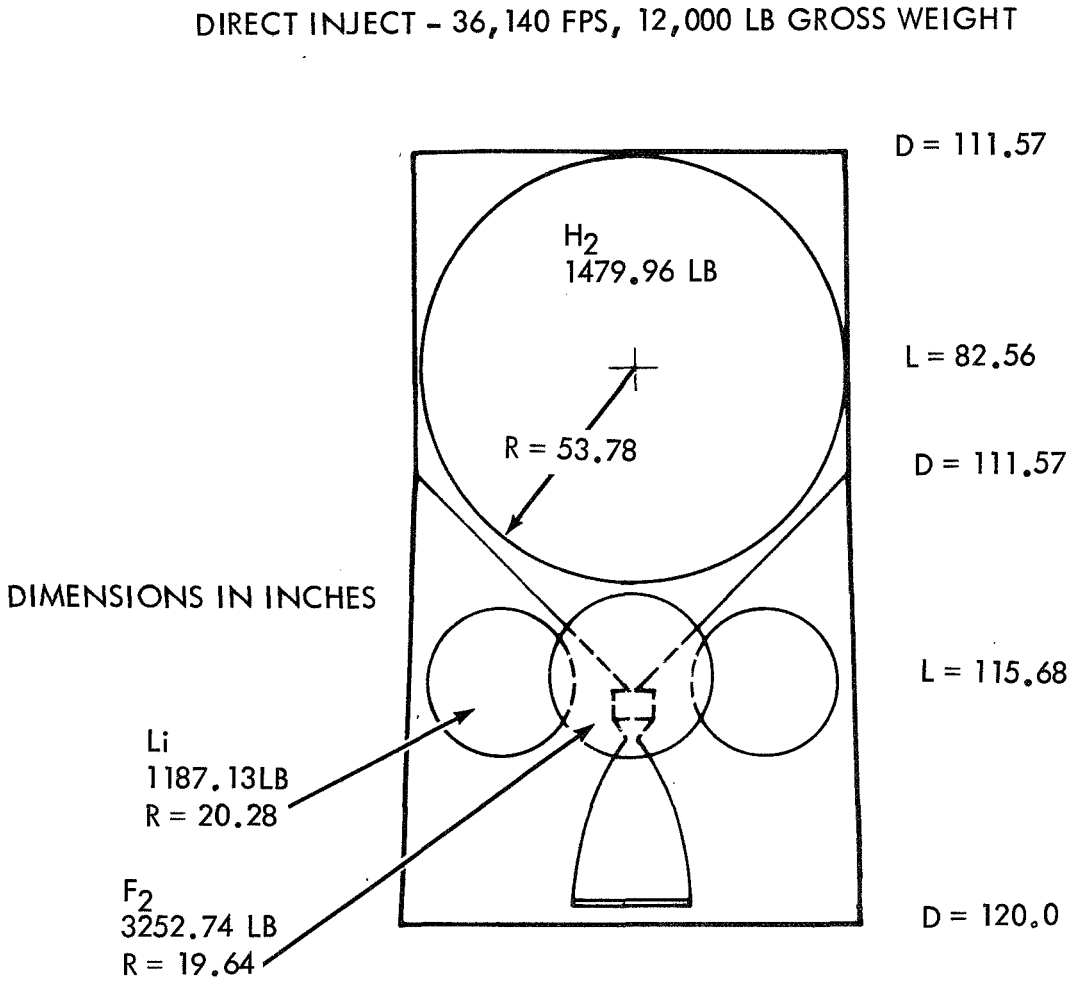

Figure 3-15. Tripropellant Stage (Atlas/Centaur)

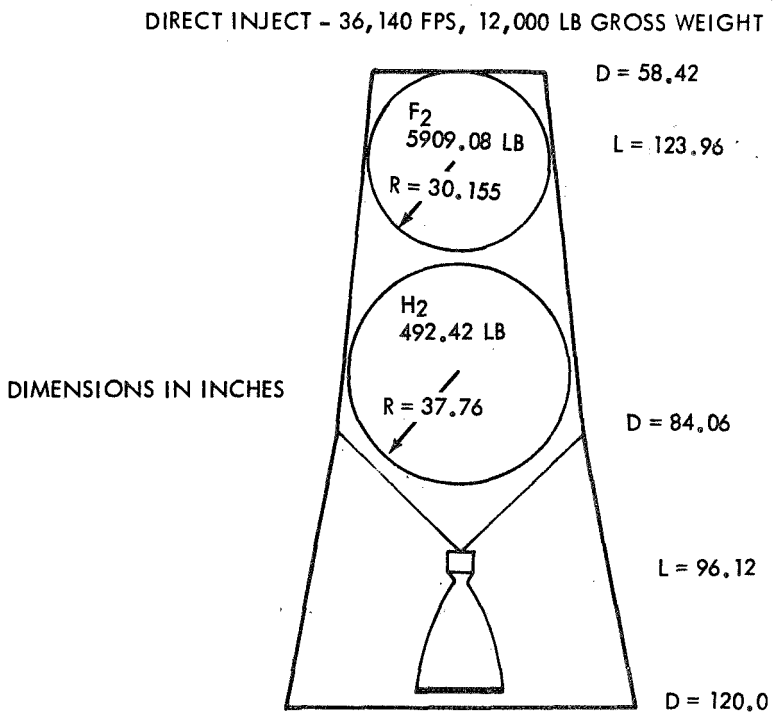

Figure 3-16. Bipropellant Stage (Atlas/Centaur)

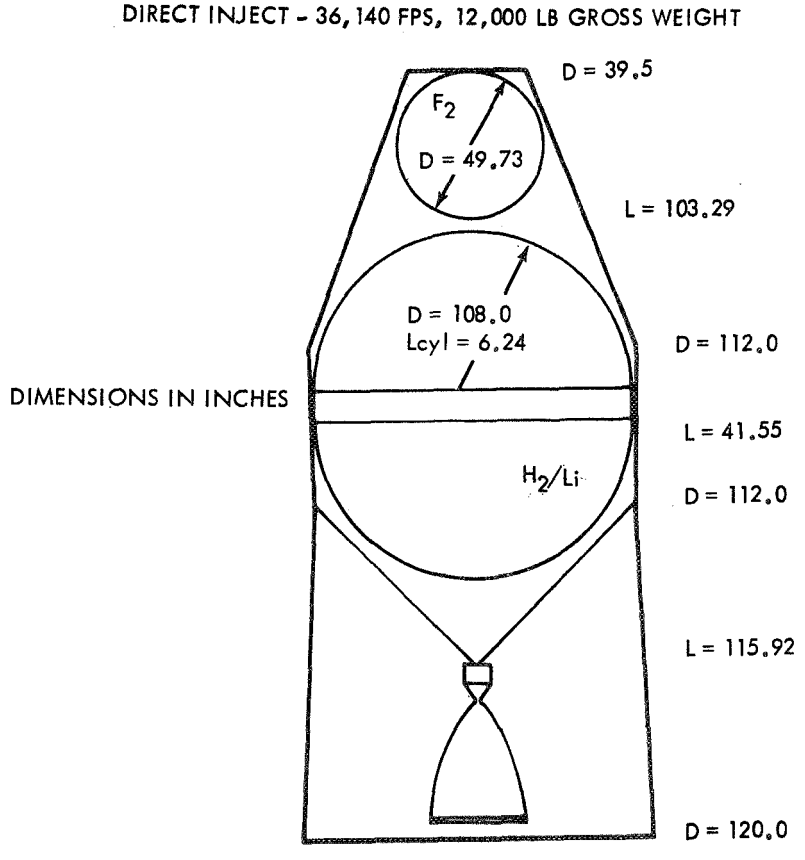

Figure 3-17. Gel Stage (Atlas/Centaur)

A weight statement comparing the three stages shown in the previous figures is given in table 3-9. All stages have a gross weight, including payload, of 12,000 pounds, which approximates the upper limit that the Centaur stage can structurally take. The structural weights given are based on "hand" analyses using the propellant loads and engine characteristics determined by the sizing program. The payloads, therefore, are slightly different from those presented in the optimization plots shown earlier. It should be noted, however, that the difference in payloads between the hand analyses and the sizing program is less than 2 percent. Because they are so close, it is considered that the sizing and optimization plots for these stages can be used with confidence, for comparative purposes, to evaluate the relative merits of the three alternates.

In general, the major difference found between the sizing program weight estimates and the hand checks was in the weights determined for the fluorine tank supports in the bipropellant stage. The computer program estimates were consistently higher than necessary. However, the difference was not enough to warrant repeating the sizing and optimization analyses for this stage to reflect reduced tank support weights.

3.3.2 ATLAS BOOSTER RESULTS

Figure 3-18 presents maximum payload as a function of mission velocity for each of the three stages atop the Atlas booster. In this configuration, the bipropellant stage has a larger payload capability than the tripropellant stage over the velocity range for which there is some finite payload capability. Poor performance of the tripropellant stage may be traced to the geometries which result as a consequence of imposing a maximum stage diameter constraint of 120 inches.

Optimum size stages for the Atlas booster have propellant loads between 25,000 and 30,000 pounds. To accommodate this much propellant in the tripropellant stage it is necessary to use long cylindrical lengths in all propellant tanks which of course greatly increases the length of the stage. Furthermore, since it is not possible to submerge the engines between the fluorine and lithium tanks, a spider beam thrust structure must be used instead of a lighter thrust cone; this also adds to the overall stage length.

Payloads corresponding to the optimum cost effective stage sizes (see figure 3-19) show almost the same results and trends as the plots of maximum payload. The only difference is a slight downward displacement for missions requiring a low ΔV. The comparison between maximum payload and optimum cost effective payloads for this example shows the greatest difference of any of the boosters investigated. Therefore, the same type of comparison will not be shown for the other boosters.

Table 3-9. Weight Statement Comparison, Atlas/Centaur Booster, Direct Injection Mission

Description	Tripropellant Stage		Bipropellant Stage		Gel Stage	
Structure		509		349		475
Shell	90		96		96	
Interstage	134		111		134	
Tankage	(159)		(91)		(146)	
Hydrogen		120		58		123
Fluorine		14		33		23
Lithium		25		-		-
Tank Supports	(82)		(31)		(55)	
Hydrogen		10		8		15
Fluorine		40		23		40
Lithium		32		-		-
Thrust Structure	44		20		44	
Propulsion		309		230		267
Engine	139		115		139	
RCS System	13		13		13	
Pressurization System	59		53		54	
Prop. Supply System	98		49		61	
Miscellaneous Weights		650		650		650
Thermal Insulation		39		15		34
Nominal Dry Stage Weight		1,507		1,244		1,426
Contingency (at 7.5%)	113		93		107	
Limit Dry Weight		1,620		1,337		1,533
Jettison Weight	134		111		134	
Residual Propellant	59		64		60	
Stage Weight at Burnout		1,545		1,290		1,459
Propellant Consumption	5,920		6,402		6,015	
Stage Weight at Liftoff		7,540		7,739		7,548
Payload		4,460		4,261		4,452
Gross Weight Above Booster		12,000		12,000		12,000

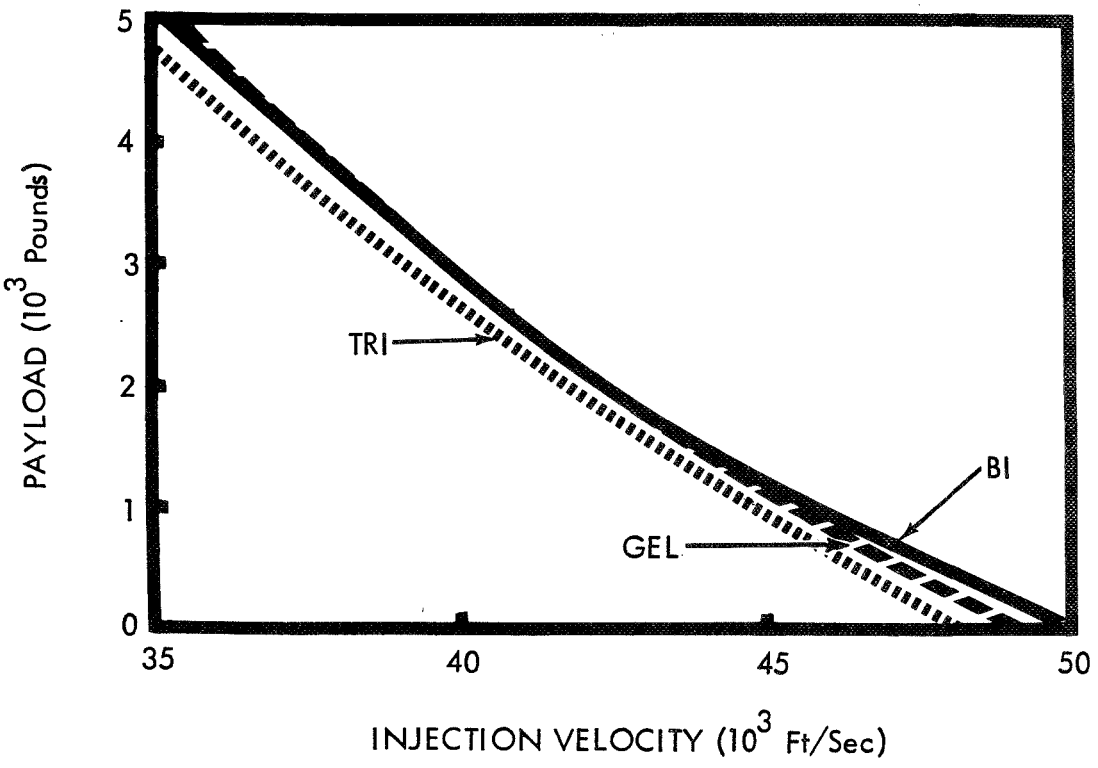

Figure 3-18. Payload Variation with Mission Velocity, Direct Injection Mission (Atlas)

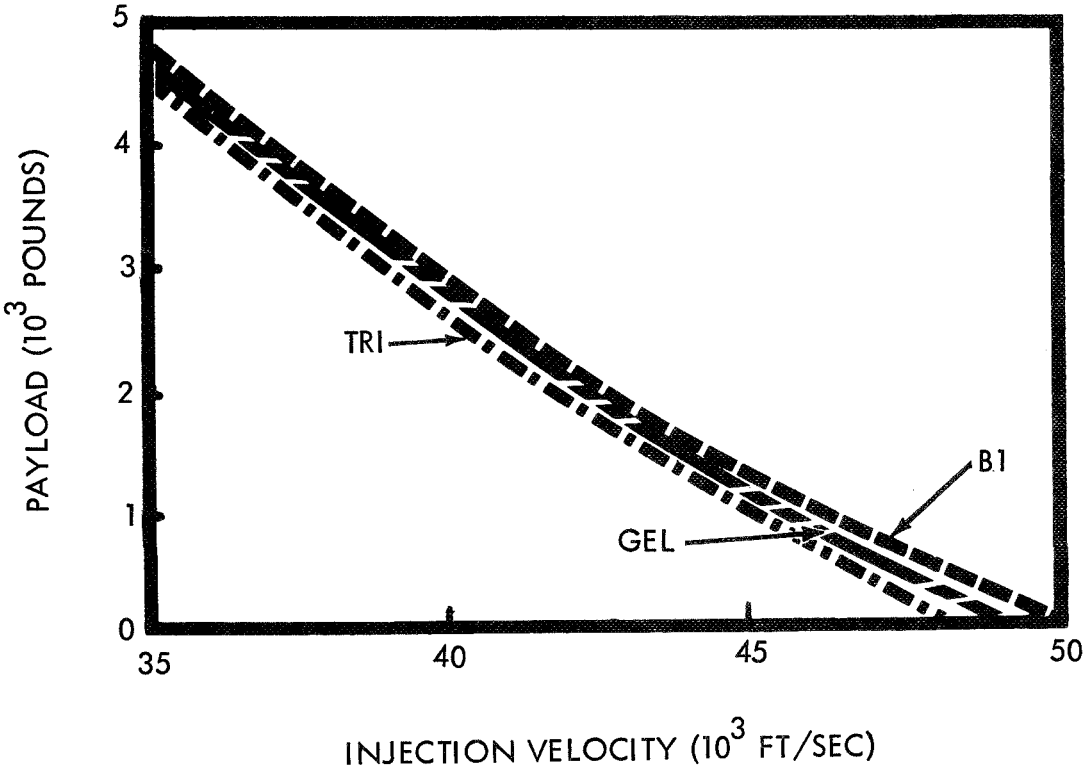

Figure 3-19. Payload Corresponding to Optimum Cost Effective Stage Size (Atlas)

For purposes of illustrating the differences between the stages, comparisons of pertinent design data are given in tables 3-10 through 3-14. An earth escape mission was assumed for this comparison, and all stages have a gross weight of 30,000 pounds. The 30,000 pounds gross weight does not correspond to either the maximum payload or optimum cost effective stage for any of the three propellant combinations; however, it is a convenient size to illustrate differences between the stages. It is also very close to the optimum cost effective size for all three stages. (See appendix C for detail optimization charts.)

Figures 3-20 through 3-22 depict the external profiles of these stages. The more noteworthy feature of these is the poor packaging efficiency which results with the tripropellant design. It is this characteristic which accounts for the relatively poor performance of the tripropellant stage when used with the Atlas booster.

A comparative weight statement of the three stages is given in table 3-15.

3.3.3 TITAN III-D/CENTAUR BOOSTER RESULTS

Figure 3-23 presents the performance comparison of the three stages using a Titan III-D/Centaur booster. The payloads shown do not represent the theoretical maximums which could be obtained. This is because it was assumed that the maximum weight which could be interfaced with the Centaur stage was 12,000 pounds; and, therefore, the results are constrained to stages where weight does not exceed 12,000 pounds including payload and interstage. This constraint lowers the payload at the lower velocities by about 900 pounds; however, it does not effect the relative comparison between stages.

The results show that the tripropellant and gel stages have a slight payload advantage over the bipropellant stage at lower velocities, but that the difference disappers at higher velocities.

Tables 3-16 through 3-20 provide summaries of the major stage characteristics, engine parameter selection and computed design data for the three stages. A mission velocity of 48,500 fps was selected for these comparisons since, at lower velocities, slight improvement in payload over the basic booster does not warrant the addition of a new upper stage.

Figures 3-24 through 3-26 are sketches of these stages and table 3-21 is a comparative weight statement. In general, comments already made relative to stages designed for the Atlas/Centaur are applicable to the Titan IIID/Centaur.

3.3.4 TITAN III-D BOOSTER RESULTS

Figure 3-27 shows the relative payload capabilities of the stages when coupled with the Titan III-D booster. The comparison shows that the gel and tripropellant stages have slightly greater payloads than the bipropellant stage for velocities below about 45,000 fps. For higher velocity missions the bipropellant stage has the advantage.

Table 3-10. Major Stage Characteristics Summary - Atlas Booster, Direct Injection

Total Mission Velocity:	36140 fps
Stage Velocity Increment - First Burn:	22040 fps
Stage Velocity Increment - Second Burn:	0.0 fps
First Coast Time:	0.5 hrs
Second Coast Time:	0.0 hrs
Gross Weight:	30, 000 lb

Stage	Bipropellant	Gelled H_2/Li	Tripropellant
Payload (lb)	4280	4375	4218
Specific Impulse (sec)	469.64	509.51	521.51
Thrust (lb)	20778	20746	20840
Interstage Weight (lb)	318	363	228
Total Stage Weight (lb)	25401	25262	25554
Inert Stage Weight (lb)	2320	3062	3501
Total Propellant Weight (lb)	23083	22200	22053
Propellant Consumed			
First Burn (lb)	22763	21897	21753
Second Burn (lb)	N/A	N/A	N/A
Residual Propellant Weight (lb)	231	222	220
Stage Mass Ratio	4.348	3.871	3.752
Stage Payload Fraction	0.143	0.146	0.141
Stage Structural Ratio	0.100	0.129	0.145
Stage Velocity Ratio	1.469	1.354	1.322
Stage Thrust to Weight Ratio	0.7	0.7	0.7

Table 3-11. Engine Data Summary, Atlas Booster, Direct Injection

Stage	Bipropellant	Gelled H_2/Li	Tripropellant
Thrust (lb)	20778	20746	20840
Specific Impulse (sec)	469.64	509.51	521.51
Expansion Ratio	150	150	150
Chamber Pressure (psi)	1000	800	800
F_2/Li Mixture Ratio	N/A	2.749	2.74
Percent Hydrogen	7.692	25.0	25.0
Weight (lb)	298	366	367
Length (In.)	70.9	88.6	88.7
Exit Diameter (In.)	46.8	53.2	53.4

Table 3-12. Design Data Summary - Birpropellant Stage, Atlas Booster, Direct Injection

Propellant Tank	Hydrogen	Fluorine
Propellant Weights		
Usable (lb)	1751	21012
Residual (lb)	18	213
Boiloff (lb)	0	0
Startup/Shutdown (lb)	7	82
Total Load (lb)	1776	21307
Tankage		
Number of Tanks	1	1
Volume (ft^3)	446.8	239.2
Radius (In.)	54.0	46.2
Cylinder Length (In.)	12.2	0
Dome Thickness (In.)	0.0258	0.0250
Cylinder Thickness (In.)	0.516	N/A
Design Pressure (psi)	43	26
Thermal		
Initial Temperature (°R)	36	150
Vent Temperature (°R)	42	154
Insulation Thickness (In.)	0.38	0.16
Number of Kilowatts	N/A	N/A
Number of Kilowatt-hours	N/A	N/A
Meteoroid Shield		
Meteoroid Design Mass (gm)	N/A	N/A
Meteoroid Diameter (cm)	N/A	N/A
Shield Thickness (In.)	N/A	N/A
Spacing (In.)	N/A	N/A
Backup (Δ Tank) Thickness (In.)	N/A	N/A

Table 3-13. Design Data Summary - Gelled H_2/Li Stage, Atlas Booster, Direct Injection

Propellant Tank	Hydrogen	Fluorine
Propellant Weights		
Usable (lb)	9865	12031
Residual (lb)	100	122
Boiloff (lb)	0	0
Startup/Shutdown (lb)	37	45
Total Load (lb)	10002	12198
Tankage		
Number of Tanks	1	1
Volume (ft^3)	1500.3	137.2
Radius (In.)	54.0	38.40
Cylinder Length (In.)	210.9	0.0
Dome Thickness (In.)	0.0250	0.0250
Cylinder Thickness (In.)	0.0428	0.0250
Design Pressure (psi)	36	27
Thermal		
Initial Temperature (°R)	36	150
Vent Temperature (°R)	40	155
Insulation Thickness (In.)	0.48	0.15
Number of Kilowatts	N/A	N/A
Number of Kilowatt-hours	N/A	N/A
Meteoroid Shield		
Meteoroid Design Mass (gm)	N/A	N/A
Meteoroid Diameter (cm)	N/A	N/A
Shield Thickness (In.)	N/A	N/A
Spacing (In.)	N/A	N/A
Backup (Δ Tank) Thickness (In.)	N/A	N/A

Table 3-14. Design Data Summary - Tripropellant Stage, Atlas Booster, Direct Injection

Propellant Tank	Hydrogen	Fluorine	Lithium
Propellant Weights			
Usable (lb)	5438	11952	4362
Residual (lb)	55	121	44
Boiloff (lb)	0	0	N/A
Startup/Shutdown (lb)	20	44	16
Total Load (lb)	5513	12117	4422
Tankage			
Number of Tanks	1	2	2
Volume (ft^3)	1357.5	68.2	75.4
Radius (In.)	54.0	20.61	20.61
Cylinder Length (In.)	184.1	60.8	70.1
Dome Thickness (In.)	0.0250	0.0250	0.0150
Cylinder Thickness (In.)	0.0428	0.0250	0.0150
Design Pressure (psi)	36	27	50
Thermal			
Initial Temperature (°R)	36	150	1040
Vent Temperature (°R)	40	155	N/A
Insulation Thickness (In.)	0.44	0.22	0.24
Number of Kilowatts	N/A	N/A	86.7
Number of Kilowatt-hours	N/A	N/A	6.23
Meteoroid Shield			
Meteoroid Design Mass (gm)	N/A	N/A	N/A
Meteoroid Diameter (cm)	N/A	N/A	N/A
Shield Thickness (In.)	N/A	N/A	N/A
Spacing (In.)	N/A	N/A	N/A
Backup (Δ Tank) Thickness (In.)	N/A	N/A	N/A

DIRECT INJECT - 36,140 FPS, 30,000 LB GROSS WEIGHT

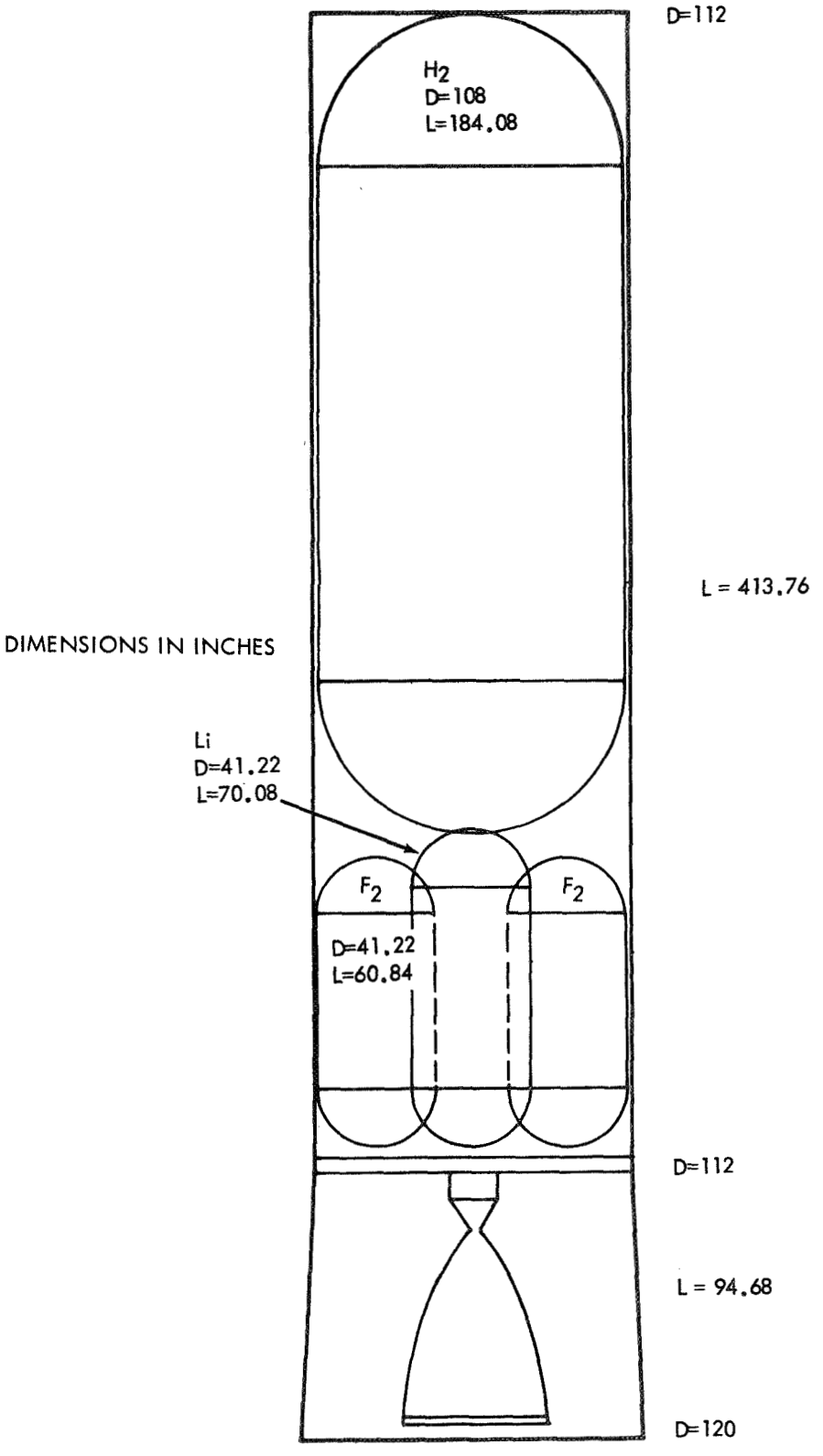

Figure 3-20. Tripropellant Stage (Atlas)

DIRECT INJECT - 36,140 FPS, 30,000 LB GROSS WEIGHT

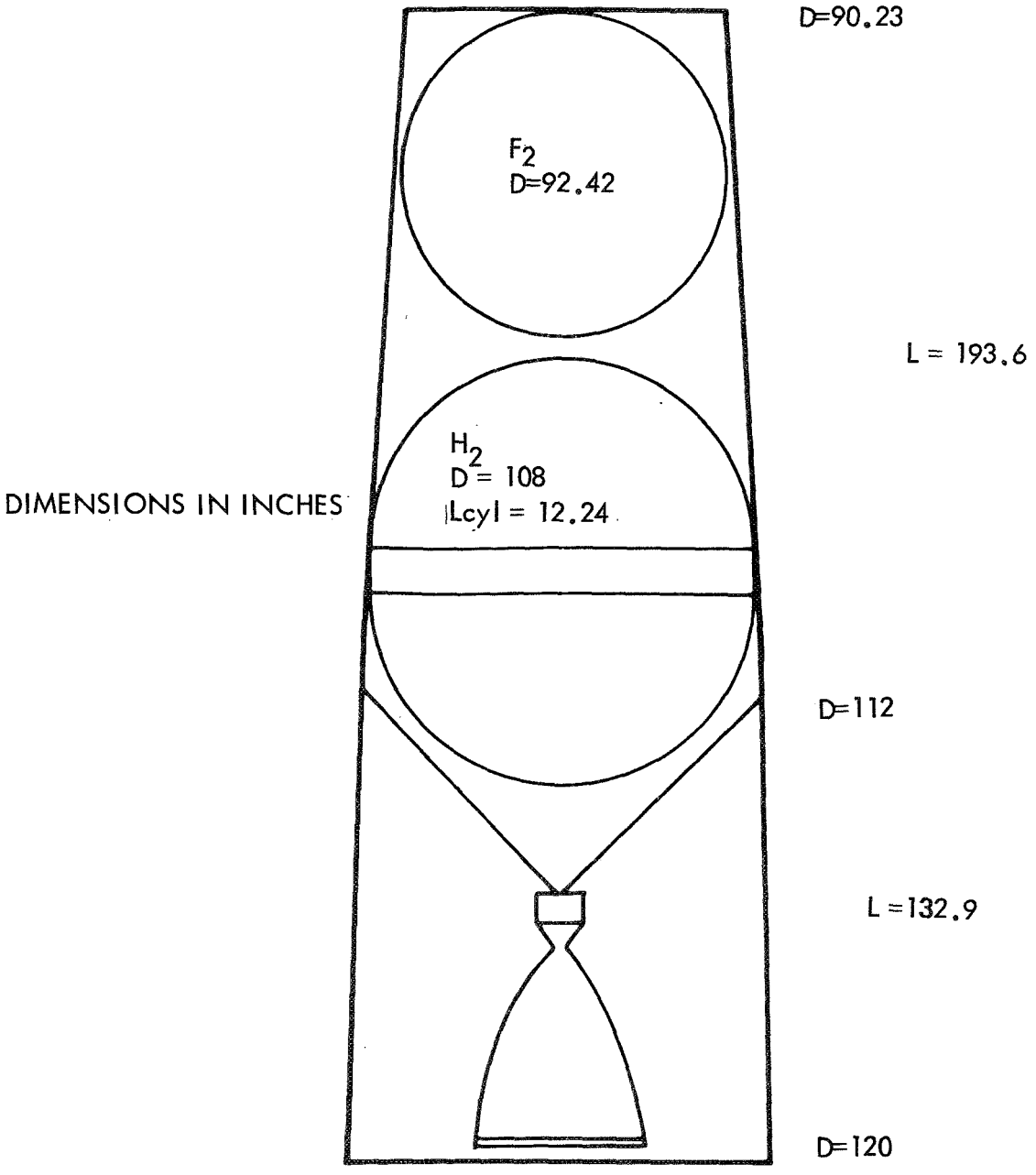

Figure 3-21. Bipropellant Stage (Atlas)

DIRECT INJECT - 36,140 FPS,
30,000 LB GROSS WEIGHT

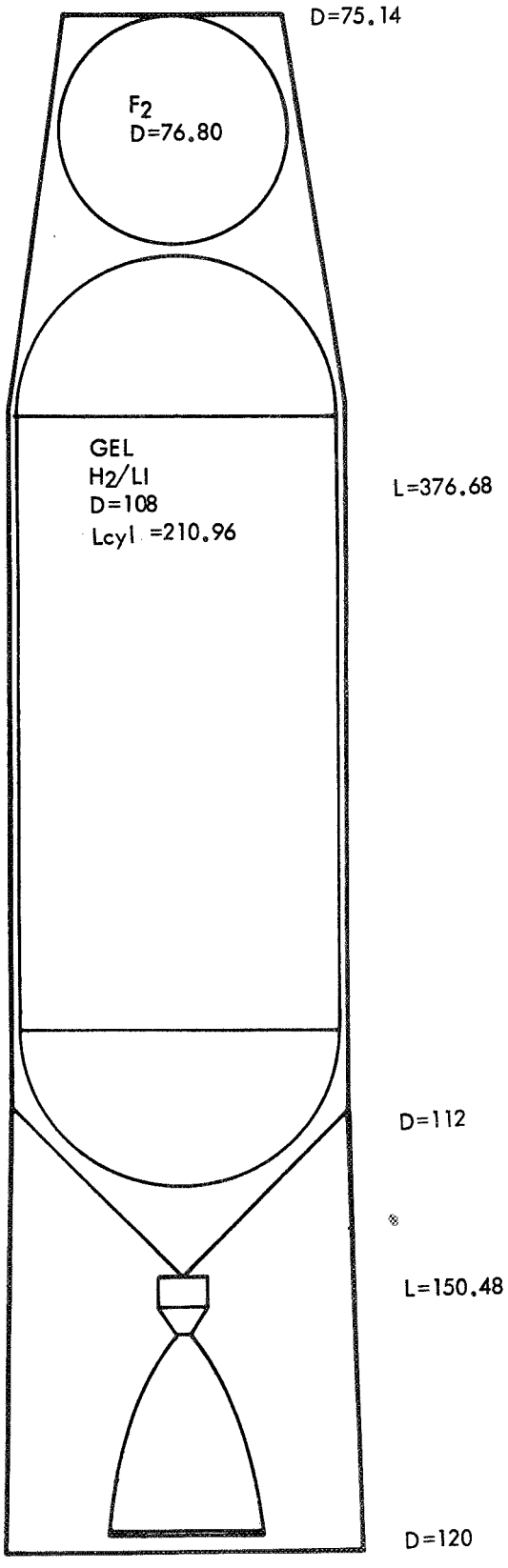

DIMENSIONS IN INCHES

Figure 3-22. Gel Stage (Atlas)

Table 3-15. Weight Statement Comparison, Atlas Booster, Direct Injection Mission

Description	Tripropellant Stage		Bipropellant Stage		Gel Stage	
Structure		1,842		992		1,650
Shell	699		295		558	
Interstage	228		318		363	
Tankage	(633)		(213)		(517)	
Hydrogen		418		135		463
Fluorine		77		78		54
Lithium		138		-		-
Tank Supports	(153)		(104)		(150)	
Hydrogen		75		27		110
Fluorine		48		77		40
Lithium		30		-		-
Thrust Structure	130		62		62	
Propulsion		717		552		618
Engine	367		298		366	
RCS System	13		13		13	
Pressurization System	161		135		142	
Prop. Supply System	176		106		97	
Miscellaneous Weights		650		650		650
Thermal Insulation		124		37		102
Nominal Dry Stage Weight		3,333		2,231		3,020
Contingency (at 7.5%)	251		173		232	
Limit Dry Weight		3,584		2,404		3,252
Jettison Weight	228		318		363	
Residual Propellant	221		231		222	
Stage Weight at Burnout		3,577		2,317		3,111
Propellant Consumption	22,053		23,083		22,200	
Stage Weight at Liftoff		25,637		25,487		25,452
Payload		4,363		4,513		4,548
Gross Weight Above Booster		30,000		30,000		30,000

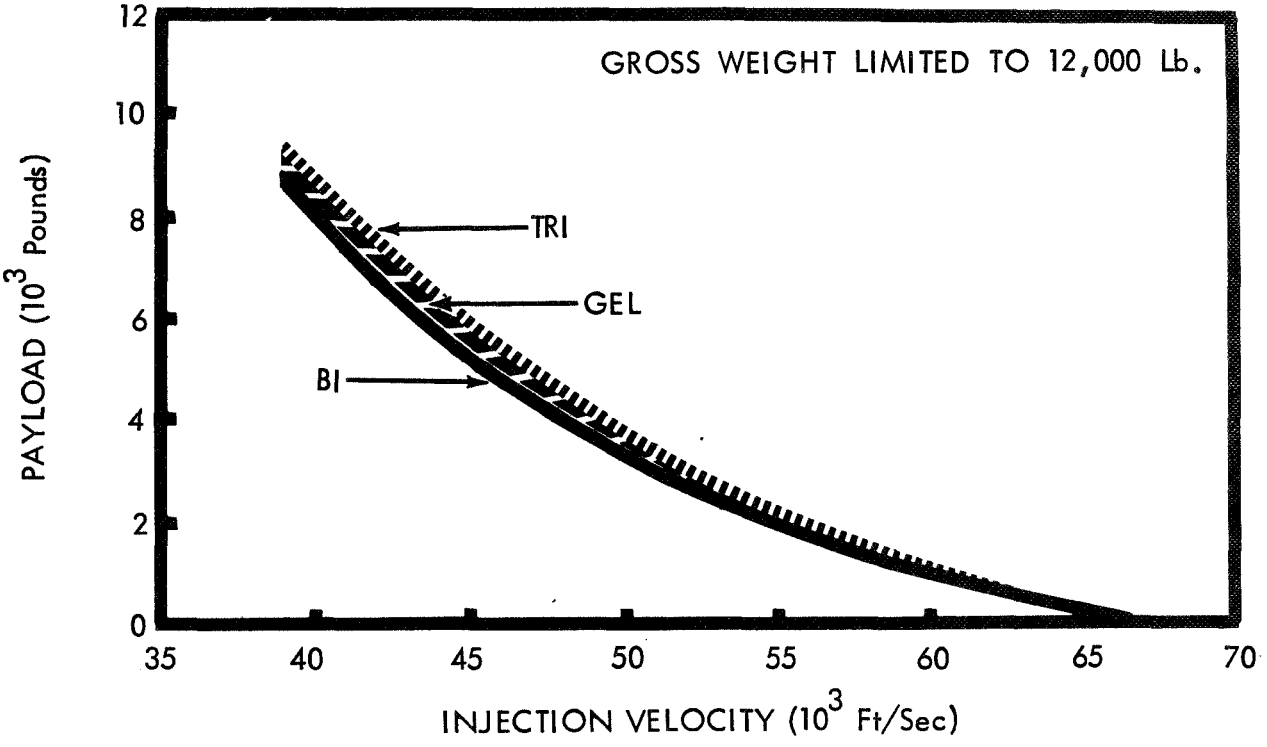

Figure 3-23. Payload Variation with Mission Velocity, Direct Injection Mission (Titan IIID/Centaur)

Table 3-16. Major Stage Characteristics Summary - Titan IIID/Centaur Booster, Direct Injection

Total Mission Velocity:	48500 fps
Stage Velocity Increment - First Burn:	12200 fps
Stage Velocity Increment - Second Burn:	0.0 fps
First Coast Time:	0.5 hrs
Second Coast Time:	0.0 hrs
Gross Weight:	12, 000 lb

Stage	Bipropellant	Gelled H_2/Li	Tripropellant
Payload (lb)	3902	4064	4112
Specific Impulse (sec)	467.62	509.17	521.17
Thrust (lb)	8322	8292	8295
Interstage Weight (lb)	111	155	150
Total Stage Weight (lb)	7987	7781	7738
Inert Stage Weight (lb)	1284	1469	1523
Total Propellant Weight (lb)	6702	6312	6215
Propellant Consumed			
First Burn (lb)	6600	6261	6121
Second Burn (lb)	N/A	N/A	N/A
Residual Propellant Weight (lb)	66	63	62
Stage Mass Ratio	2.264	2.117	2.081
Stage Payload Fraction	0.325	0.339	0.323
Stage Structural Ratio	0.169	0.196	0.204
Stage Velocity Ratio	0.817	0.750	0.733
Stage Thrust to Weight Ratio	0.7	0.7	0.7

Table 3-17. Engine Data Summary, Titan IIID/Centaur Booster, Direct Injection

Stage	Bipropellant	Gelled H_2/Li	Tripropellant
Thrust (lb)	8322	8292	8295
Specific Impulse (sec)	467.62	509.17	521.17
Expansion Ratio	150	150	150
Chamber Pressure (psi)	1000	800	800
F_2/Li Mixture Ratio	N/A	2.740	2.740
Percent Hydrogen	7.692	25.0	25.0
Weight (lb)	115	139	139
Length (In.)	48.1	54.0	54.0
Exit Diameter (In.)	29.6	33.0	33.0

Table 3-18. Design Data Summary - Bipropellant Stage, Titan IIID/ Centaur Booster, Direct Injection

Propellant Tank	Hydrogen	Fluorine
Propellant Weights		
Usable (lb)	508	6092
Residual (lb)	5	62
Boiloff (lb)	0	0
Startup/Shutdown (lb)	2	33
Total Load (lb)	515	6187
Tankage		
Number of Tanks	1	1
Volume (ft^3)	136.7	69.6
Radius (In.)	38.84	30.62
Cylinder Length (In.)	0	0
Dome Thickness (In.)	0.0279	0.0250
Cylinder Thickness (In.)	N/A	N/A
Design Pressure (psi)	66	27
Thermal		
Initial Temperature (°R)	36	150
Vent Temperature (°R)	46	155
Insulation Thickness (In.)	0.33	0.19
Number of Kilowatts	N/A	N/A
Number of Kilowatt-hours	N/A	N/A
Meteoroid Shield		
Meteoroid Design Mass (gm)	N/A	N/A
Meteoroid Diameter (cm)	N/A	N/A
Shield Thickness (In.)	N/A	N/A
Spacing (In.)	N/A	N/A
Backup (Δ Tank) Thickness (In.)	N/A	N/A

Table 3-19. Design Data Summary - Gelled H_2/Li Stage, Titan IIID/ Centaur Booster, Direct Injection

Propellant Tank	Hydrogen	Fluorine
Propellant Weights		
Usable (lb)	2801	3416
Residual (lb)	28	34
Boiloff (lb)	0	0
Startup/Shutdown (lb)	15	18
Total Load (lb)	2843	3468
Tankage		
Number of Tanks	1	1
Volume (ft^3)	435.0	39.1
Radius (In.)	54.0	25.27
Cylinder Length (In.)	10.0	0
Dome Thickness (In.)	0.0258	0.0250
Cylinder Thickness (In.)	0.0516	N/A
Design Pressure (psi)	43	28
Thermal		
Initial Temperature (°R)	36	150
Vent Temperature (°R)	42	156
Insulation Thickness (In.)	0.42	0.20
Number of Kilowatts	N/A	N/A
Number of Kilowatt-hours	N/A	N/A
Meteoroid Shield		
Meteoroid Design Mass (gm)	N/A	N/A
Meteoroid Diameter (cm)	N/A	N/A
Shield Thickness (In.)	N/A	N/A
Spacing (In.)	N/A	N/A
Backup (Δ Tank) Thickness (In.)	N/A	N/A

Table 3-20. Design Data Summary - Tripropellant Stage, Titan IIID/Centaur Booster, Direct Injection

Propellant Tank	Hydrogen	Fluorine	Lithium
Propellant Weights			
Usable (lb)	1530	3363	1228
Residual (lb)	16	34	12
Boiloff (lb)	0	0	0
Startup/Shutdown (lb)	8	18	6
Total Load (lb)	1554	3415	1246
Tankage			
Number of Tanks	1	2	2
Volume (ft^3)	391.0	19.3	21.2
Radius (In.)	54.0	19.96	20.61
Cylinder Length (In.)	1.8	0	0
Dome Thickness (In.)	0.0258	0.0250	0.0150
Cylinder Thickness (In.)	0.0516	N/A	N/A
Design Pressure (psi)			
Thermal			
Initial Temperature (°R)	36	150	1040
Vent Temperature (°R)	42	157	N/A
Insulation Thickness (In.)	0.40	0.22	0.24
Number of Kilowatts	N/A	N/A	32.1
Number of Kilowatt-hours	N/A	N/A	5.61
Meteoroid Shield			
Meteoroid Design Mass (gm)	N/A	N/A	N/A
Meteoroid Diameter (cm)	N/A	N/A	N/A
Shield Thickness (In.)	N/A	N/A	N/A
Spacing (In.)	N/A	N/A	N/A
Backup (Δ Tank) Thickness (In.)	N/A	N/A	N/A

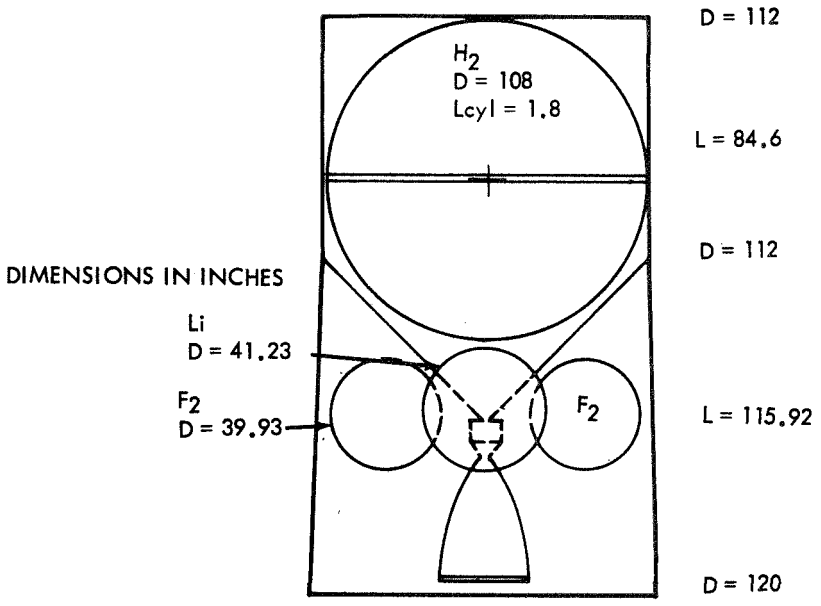

Figure 3-24. Tripropellant Stage (Titan IIID/Centaur)

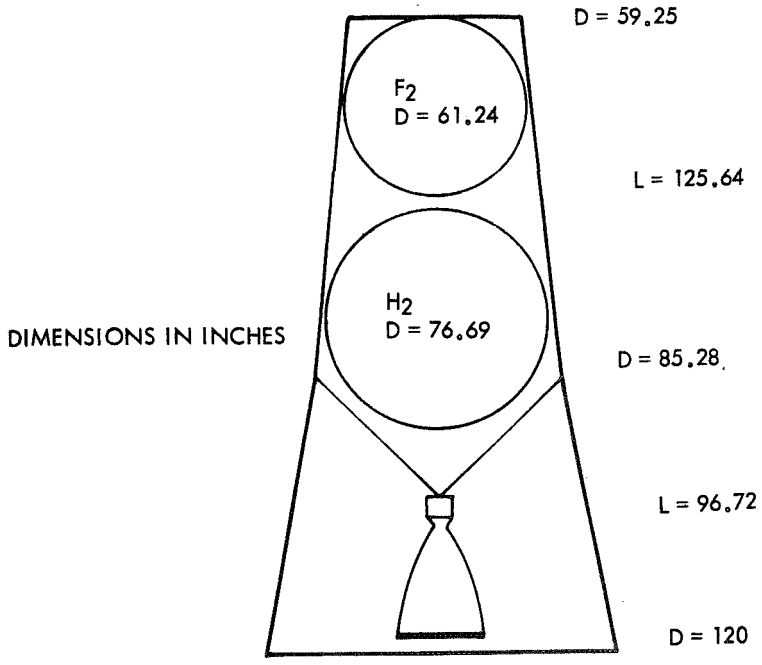

Figure 3-25. Bipropellant Stage (Titan IIID/Centaur)

DIRECT INJECT - 48,500 FPS, 12,000 LB GROSS WEIGHT

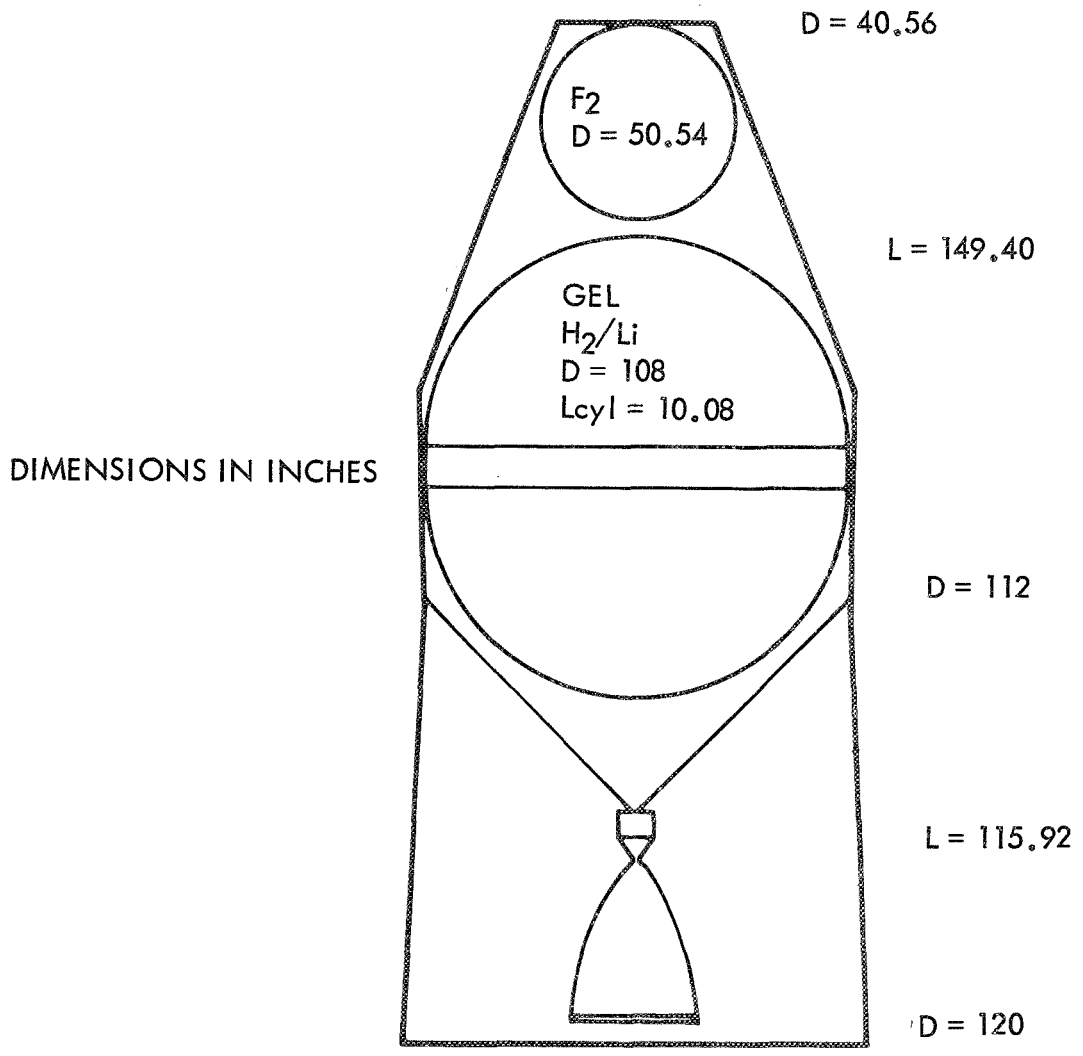

Figure 3-26. Gel Stage (Titan IIID/Centaur)

Table 3-21. Weight Statement Comparison, Titan IIID/Centaur Booster, Direct Injection Mission

Description	Tripropellant Stage		Bipropellant Stage		Gel Stage	
Structure		592		341		529
Shell	87		77		118	
Interstage	151		111		155	
Tankage	(194)		(94)		(154)	
Hydrogen		114		60		131
Fluorine		29		34		23
Lithium		51		-		-
Tank Supports	(116)		(35)		(58)	
Hydrogen		14		9		17
Fluorine		55		26		41
Lithium		47		-		-
Thrust Structure	44		24		44	
Propulsion		312		233		269
Engine	139		115		139	
RCS System	13		13		13	
Pressurization System	60		55		56	
Prop. Supply System	100		50		61	
Miscellaneous Weights		650		650		650
Thermal Insulation		44		16		34
Nominal Dry Stage Weight		1,598		1,240		1,482
Contingency (at 7.5%)	120		93		111	
Limit Dry Weight		1,718		1,333		1,593
Jettison Weight	151		111		155	
Residual Propellant	62		67		63	
Stage Weight at Burnout		1,629		1,289		1,501
Propellant Consumption	6,215		6,703		6,312	
Stage Weight at Liftoff		7,933		8,036		7,905
Payload		4,067		3,964		4,095
Gross Weight Above Booster		12,000		12,000		12,000

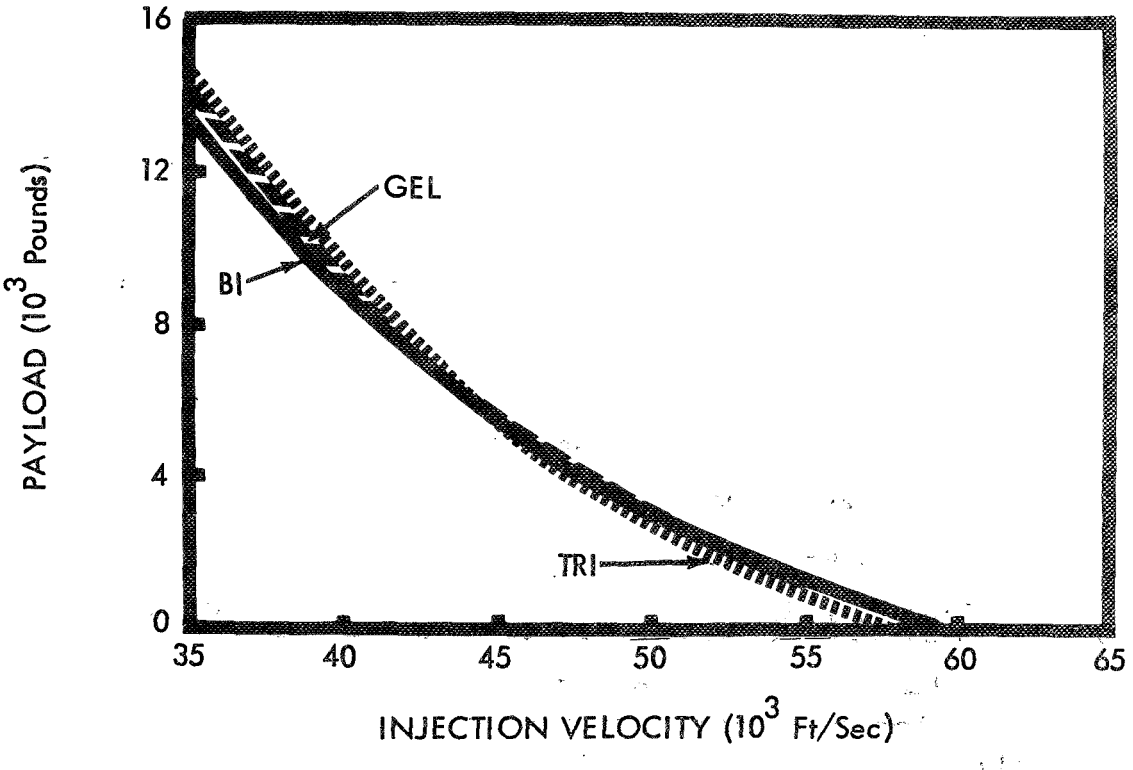

Figure 3-27. Payload Variation with Mission Velocity, Direct Injection Mission (Titan IIID)

As with the Atlas booster results, a gross weight of 30,000 pounds and a mission velocity of 36,140 fps (earth escape) have been selected for purposes of illustrating the differences between the stages and their major design features. Again, this particular size is not optimum from either a maximum performance or cost effectiveness standpoint. (See appendix C for additional data regarding optimizations at various mission velocities.)

Tables 3-22 through 3-26 summarize the major characteristics of these 30,000 pound stages. Sketches of the stages are shown in figures 3-28 through 3-30 and a comparative weight statement is given in table 3-27.

3.3.5 260-INCH SRM/S-IVB BOOSTER RESULTS

The largest booster investigated was the 260-Inch Solid Rocket Motor (SRM)/ S-IVB. The results, shown in figure 3-31, indicate similar trends to those observed with the Titan III-D. The tripropellant stage has a slight payload advantage over the other two stages for velocities up to about 60,000 fps. At higher velocities, the bi-propellant stage is the most attractive.

The maximum size stage, for which one engine could be used, was about 70,000 pounds, including payload and interstage. This gross weight was selected as a convenient size for purposes of comparing the stages.

Tables 3-28 through 3-32 summarize the major characteristics and design data for the stages.

Table 3-22. Major Stage Characteristics Summary - Titan IIID Booster, Direct Injection

Total Mission Velocity:	48500 fps
Stage Velocity Increment - First Burn:	24000 fps
Stage Velocity Increment - Second Burn:	0.0 fps
First Coast Time:	0.5 hrs
Second Coast Time:	0.0 hrs
Gross Weight:	30000 lb

Stage	Bipropellant	Gelled H_2/Li	Tripropellant
Payload (lb)	3547	3699	3554
Specific Impulse (sec)	469.65	509.51	521.52
Thrust (lb)	20864	20843	20902
Interstage Weight (lb)	194	224	140
Total Stage Weight (lb)	26260	26078	26306
Inert Stage Weight (lb)	2230	2891	3295
Total Propellant Weight (lb)	24029	23186	23012
Propellant Consumed			
First Burn (lb)	23700	22873	22701
Second Burn (lb)	N/A	N/A	N/A
Residual Propellant Weight (lb)	240	231	229
Stage Mass Ratio	4.957	4.368	4.221
Stage Payload Fraction	0.118	0.123	0.118
Stage Structural Ratio	0.094	0.119	0.134
Stage Velocity Ratio	1.600	1.474	1.440
Stage Thrust to Weight Ratio	0.7	0.7	0.7

Table 3-23. Engine Data Summary - Titan IIID Booster, Direct Injection

Stage	Bipropellant	Gelled H_2/Li	Tripropellant
Thrust (lb)	20864	20843	20902
Specific Impulse (sec)	469.65	509.51	521.52
Expansion Ratio	150	150	150
Chamber Pressure (psi)	1000	800	800
F_2/Li Mixture Ratio	N/A	2.740	2.740
Percent Hydrogen	7.692	25.0	25.0
Weight (lb)	299	368	369
Length (In.)	71.1	88.7	88.8
Exit Diameter (In.)	46.9	53.4	53.4

Table 3-24. Design Data Summary - Bipropellant Stage, Titan IIID Booster, Direct Injection

Propellant Tank	Hydrogen	Fluorine
Propellant Weights		
Usable (lb)	1823	21877
Residual (lb)	18	222
Boiloff (lb)	0	0
Startup/Shutdown (lb)	7	82
Total Load (lb)	1848	22181
Tankage		
Number of Tanks	1	1
Volume (ft^3)	465.2	249.0
Radius (In.)	54.0	46.83
Cylinder Length (In.)	15.7	0.0
Dome Thickness (In.)	0.0258	0.0250
Cylinder Thickness (In.)	0.0516	N/A
Design Pressure (psi)	43	26
Thermal		
Initial Temperature (°R)	36	150
Vent Temperature (°R)	42	154
Insulation Thickness (In.)	0.38	0.16
Number of Kilowatts	N/A	N/A
Number of Kilowatt-hours	N/A	N/A
Meteoroid Shield		
Meteoroid Design Mass (gm)	N/A	N/A
Meteoroid Diameter (cm)	N/A	N/A
Shield Thickness (In.)	N/A	N/A
Spacing (In.)	N/A	N/A
Backup (Δ Tank) Thickness (In.)	N/A	N/A

Table 3-25. Design Data Summary - Gelled H_2/Li Stage, Titan IIID Booster, Direct Injection

Propellant Tank	Hydrogen	Fluorine
Propellant Weights		
Usable (lb)	10305	12568
Residual (lb)	104	127
Boiloff (lb)	0	0
Startup/Shutdown (lb)	37	45
Total Load (lb)	10446	12740
Tankage		
Number of Tanks	1	1
Volume (ft^3)	1566.9	143.3
Radius (In.)	54.0	38.96
Cylinder Length (In.)	223.6	0
Dome Thickness (In.)	0.0250	0.0250
Cylinder Thickness (In.)	0.0428	N/A
Design Pressure (psi)	36	27
Thermal		
Initial Temperature (°R)	36	150
Vent Temperature (°R)	40	155
Insulation Thickness (In.)	0.48	0.15
Number of Kilowatts	N/A	N/A
Number of Kilowatt-hours	N/A	N/A
Meteoroid Shield		
Meteoroid Design Mass (gm)	N/A	N/A
Meteoroid Diameter (cm)	N/A	N/A
Shield Thickness (In.)	N/A	N/A
Spacing (In.)	N/A	N/A
Backup (Δ Tank) Thickness (In.)	N/A	N/A

Table 3-26. Design Data Summary - Tripropellant Stage, Titan IIID Booster, Direct Injection

Propellant Tank	Hydrogen	Fluorine	Lithium
Propellant Weights			
Usable (lb)	5675	12474	4552
Residual (lb)	57	126	46
Boiloff (lb)	0	0	N/A
Startup/Shutdown (lb)	20	44	17
Total Load (lb)	5753	12644	4615
Tankage			
Number of Tanks	1	2	2
Volume (ft^3)	1416.5	71.1	78.7
Radius (In.)	104.0	20.61	20.61
Cylinder Length (In.)	195.2	64.7	74.4
Dome Thickness (In.)	0.0250	0.0250	0.0150
Cylinder Thickness (In.)	0.0428	0.0250	0.0150
Design Pressure (psi)	36	27	50
Thermal			
Initial Temperature (°R)	36	150	1040
Vent Temperature (°R)	40	155	N/A
Insulation Thickness (In.)	0.44	0.22	0.24
Number of Kilowatts	N/A	N/A	90.0
Number of Kilowatt-hours	N/A	N/A	6.26
Meteoroid Shield			
Meteoroid Design Mass (gm)	N/A	N/A	N/A
Meteoroid Diameter (cm)	N/A	N/A	N/A
Shield Thickness (In.)	N/A	N/A	N/A
Spacing (In.)	N/A	N/A	N/A
Backup (Δ Tank) Thickness (In.)	N/A	N/A	N/A

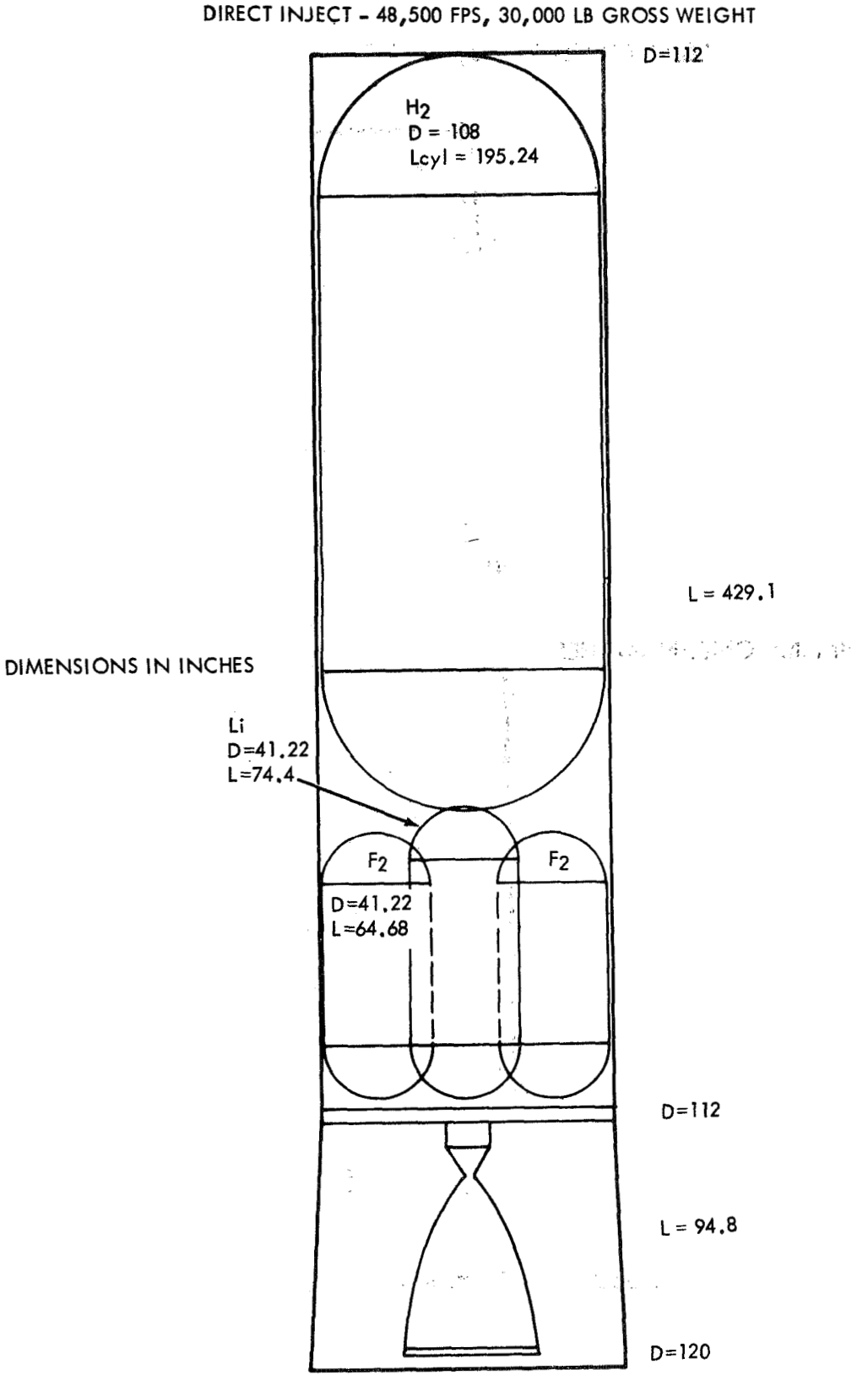

Figure 3-28. Tripropellant Stage (Titan IIID)

DIRECT INJECT - 48,500 FPS, 30,000 LB GROSS WEIGHT

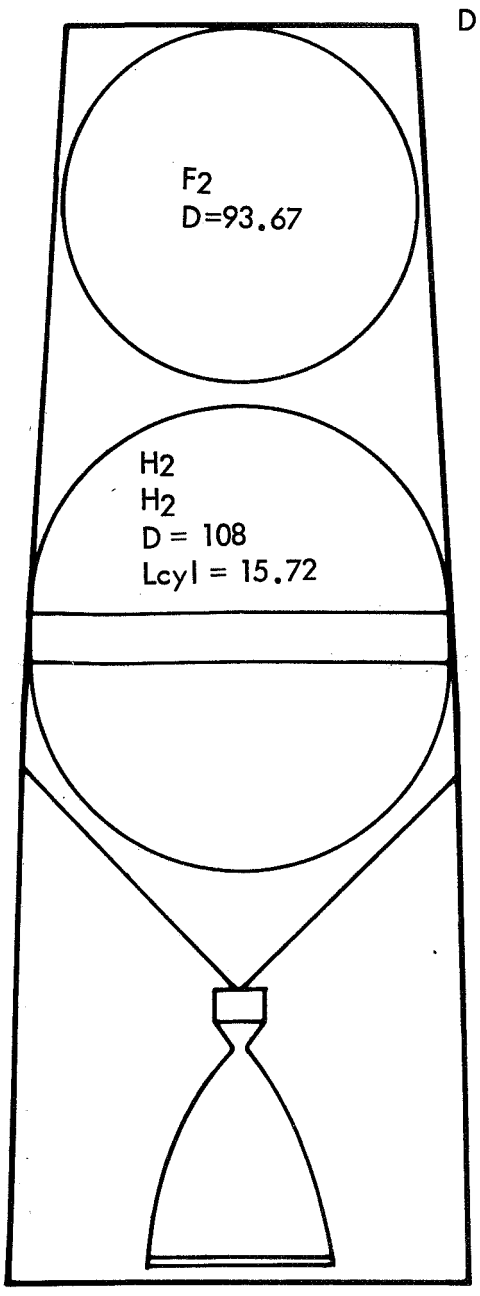

DIMENSIONS IN INCHES

Figure 3-29. Bipropellant Stage (Titan IIID)

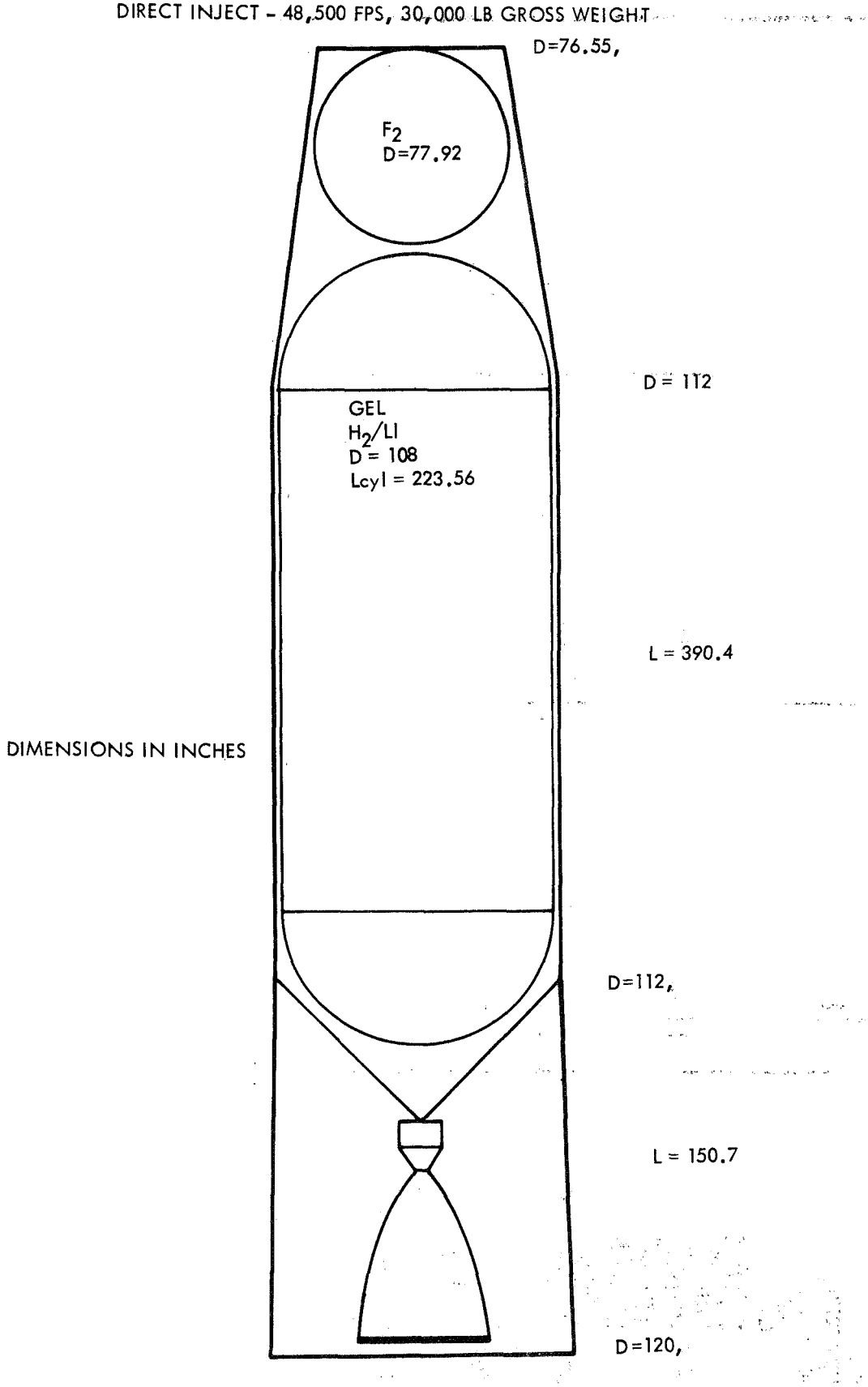

Figure 3-30. Gel Stage (Titan IIID)

Table 3-27. Weight Statement Comparison, Titan IIID Booster, Direct Injection Mission

Description	Tripropellant Stage		Bipropellant Stage		Gel Stage	
Structure		1,571		780		1,346
Shell	435		182		349	
Interstage	140		194		224	
Tankage	(660)		(222)		(541)	
Hydrogen		437		142		485
Fluorine		80		80		56
Lithium		143		-		-
Tank Supports	(190)		(120)		(170)	
Hydrogen		85		35		121
Fluorine		70		85		49
Lithium		35		-		-
Thrust Structure	146		62		62	
Propulsion		730		558		675
Engine	369		299		368	
RCS System	13		13		13	
Pressurization System	167		140		147	
Prop. Supply System	181		106		147	
Miscellaneous Weights		650		650		650
Thermal Insulation		128		37		105
Nominal Dry Stage Weight		3,079		2,025		2,776
Contingency (at 7.5%)	231		158		214	
Limit Dry Weight		3,310		2,183		2,990
Jettison Weight	140		194		224	
Residual Propellant	230		240		232	
Stage Weight at Burnout		3,400		2,229		2,992
Propellant Consumption	23,011		24,029		23,187	
Stage Weight at Liftoff		26,321		26,212		26,177
Payload		3,679		3,788		3,823
Gross Weight Above Booster		30,000		30,000		30,000

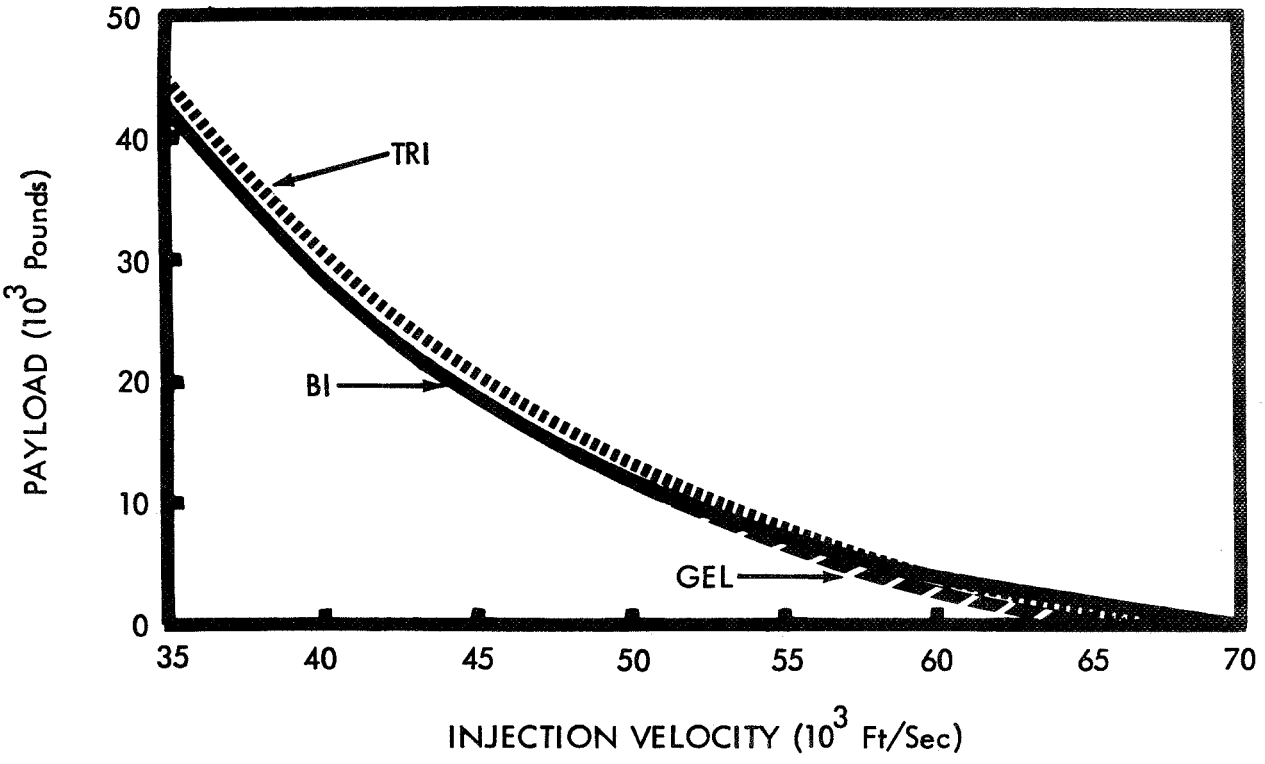

Figure 3-31. Payload Variation with Mission Velocity, Direct Injection Mission (260-Inch SRM/S-IVB)

Table 3-28. Major Stage Characteristics Summary - 260-Inch SRM/S-IVB Booster, Direct Injection

Total Mission Velocity:	48500 fps
Stage Velocity Increment - First Burn:	20200 fps
Stage Velocity Increment - Second Burn:	0.0 fps
First Coast Time:	0.5 hrs
Second Coast Time:	0.0 hrs
Gross Weight:	70000 lb

Stage	Bipropellant	Gelled H_2/Li	Tripropellant
Payload (lb)	13482	13345	14171
Specific Impulse (sec)	471.49	501.76	521.96
Thrust (lb)	48145	47635	47745
Interstage Weight (lb)	1221	1951	1793
Total Stage Weight (lb)	55297	54704	54036
Inert Stage Weight (lb)	4000	5478	5679
Total Propellant Weight (lb)	51297	49226	48357
Propellant Consumed			
First Burn (lb)	50580	48544	47690
Second Burn (lb)	N/A	N/A	N/A
Residual Propellant Weight (lb)	513	493	484
Stage Mass Ratio	3.823	3.524	3.355
Stage Payload Fraction	0.193	0.191	0.202
Stage Structural Ratio	0.082	0.109	0.114
Stage Velocity Ratio	1.341	1.259	1.210
Stage Thrust to Weight Ratio	0.7	0.7	0.7

Table 3-29. Engine Data Summary, 260-Inch SRM/S-IVB Booster, Direct Injection

Stage	Bipropellant	Gelled H_2/Li	Tripropellant
Thrust (lb)	48145	47635	47745
Specific Impulse (sec)	471.49	501.76	521.96
Expansion Ratio	150	150	150
Chamber Pressure (psi)	1000	1000	800
F_2/Li Mixture Ratio	N/A	2.740	2.740
Percent Hydrogen	7.692	20.0	25.0
Weight (lb)	763	918	921
Length (In.)	104.9	118.4	132.7
Exit Diameter (In.)	71.5	71.8	80.5

Table 3-30. Design Data Summary - Bipropellant Stage, 260-Inch SRM/S-IVB Booster, Direct Injection

Propellant Tank	Hydrogen	Fluorine
Propellant Weights		
Usable (lb)	3891	46689
Residual (lb)	39	474
Boiloff (lb)	0	0
Startup/Shutdown (lb)	16	188
Total Load (lb)	3946	47351
Tankage		
Number of Tanks	1	1
Volume (ft^3)	971.6	531.6
Radius (In.)	73.73	60.30
Cylinder Length (In.)	0	0
Dome Thickness (In.)	0.0292	0.0250
Cylinder Thickness (In.)	N/A	N/A
Design Pressure (psi)	36	26
Thermal		
Initial Temperature (°R)	36	150
Vent Temperature (°R)	40	154
Insulation Thickness (In.)	0.43	0.12
Number of Kilowatts	N/A	N/A
Number of Kilowatt-hours	N/A	N/A
Meteoroid Shield		
Meteoroid Design Mass (gm)	N/A	N/A
Meteoroid Diameter (cm)	N/A	N/A
Shield Thickness (In.)	N/A	N/A
Spacing (In.)	N/A	N/A
Backup (Δ Tank) Thickness (In.)	N/A	N/A

Table 3-31. Design Data Summary - Gelled H_2/Li Stage, 260-Inch SRM/S-IVB Booster, Direct Injection

Propellant Tank	Hydrogen	Fluorine
Propellant Weights		
Usable (lb)	20093	28451
Residual (lb)	204	288
Boiloff (lb)	0	0
Startup/Shutdown (lb)	78	111
Total Load (lb)	20375	28851
Tankage		
Number of Tanks	1	1
Volume (ft^3)	2724.9	323.9
Radius (In.)	103.96	51.12
Cylinder Length (In.)	0	0
Dome Thickness (In.)	0.0374	0.0250
Cylinder Thickness (In.)	N/A	N/A
Design Pressure (psi)	33	26
Thermal		
Initial Temperature (°R)	36	150
Vent Temperature (°R)	39	154
Insulation Thickness (In.)	0.46	0.14
Number of Kilowatts	N/A	N/A
Number of Kilowatt-hours	N/A	N/A
Meteoroid Shield		
Meteoroid Design Mass (gm)	N/A	N/A
Meteoroid Diameter (cm)	N/A	N/A
Shield Thickness (In.)	N/A	N/A
Spacing (In.)	N/A	N/A
Backup (Δ Tank) Thickness (In.)	N/A	N/A

Table 3-32. Design Data Summary - Tripropellant Stage, 260-Inch SRM/S-IVB Booster, Direct Injection

Propellant Tank	Hydrogen	Fluorine	Lithium
Propellant Weights			
Usable (lb)	11922	26204	9563
Residual (lb)	121	266	97
Boiloff (lb)	0	0	0
Startup/Shutdown (lb)	46	100	37
Total Load (lb)	12089	26570	9697
Tankage			
Number of Tanks	1	2	2
Volume (ft^3)	2946.9	149.5	164.9
Radius (In.)	106.72	39.51	40.82
Cylinder Length (In.)	0	0	0
Dome Thickness (In.)	0.0384	0.0250	0.0150
Cylinder Thickness (In.)	N/A	N/A	N/A
Design Pressure (psi)	33	27	50
Thermal			
Initial Temperature (°R)	36	150	1015
Vent Temperature (°R)	39	155	N/A
Insulation Thickness (In.)	0.40	0.15	0.24
Number of Kilowatts	N/A	N/A	31.5
Number of Kilowatt-hours	N/A	N/A	1.81
Meteoroid Shield			
Meteoroid Design Mass (gm)	N/A	N/A	N/A
Meteoroid Diameter (cm)	N/A	N/A	N/A
Shield Thickness (In.)	N/A	N/A	N/A
Spacing (In.)	N/A	N/A	N/A
Backup (Δ Tank) Thickness (In.)	N/A	N/A	N/A

Figures 3-32 to 3-34 depict external profiles of the three stages, and table 3-33 gives a comparative weight statement. The bipropellant stage weights are predicated on the tandem tank design. However, if one of the alternate bipropellant designs discussed in section 2 (such as that shown in figure 3-35) were used, the bipropellant stage performance would have been slightly better than indicated.

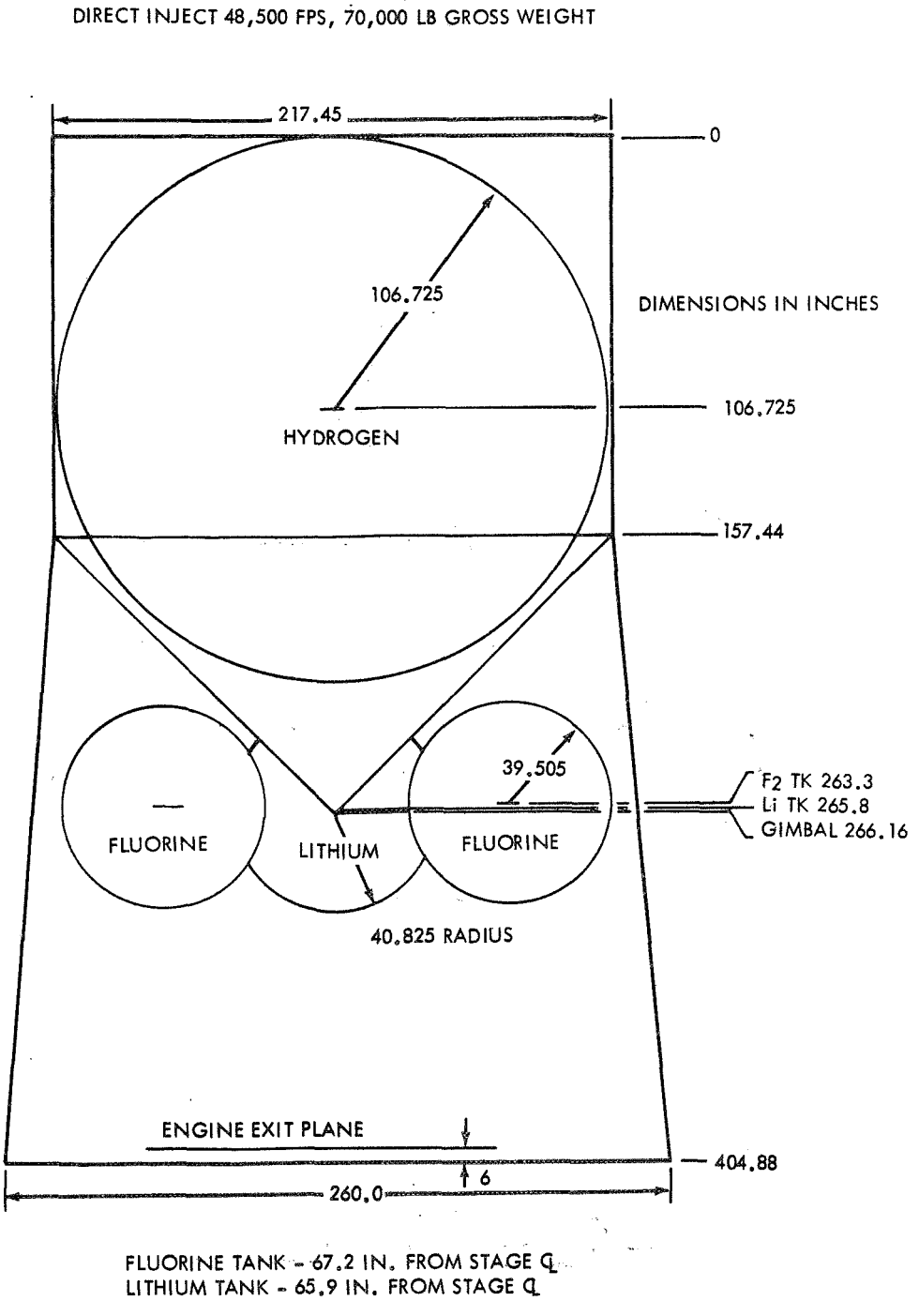

Figure 3-32. Tripropellant Stage (260-Inch SRM/S-IVB)

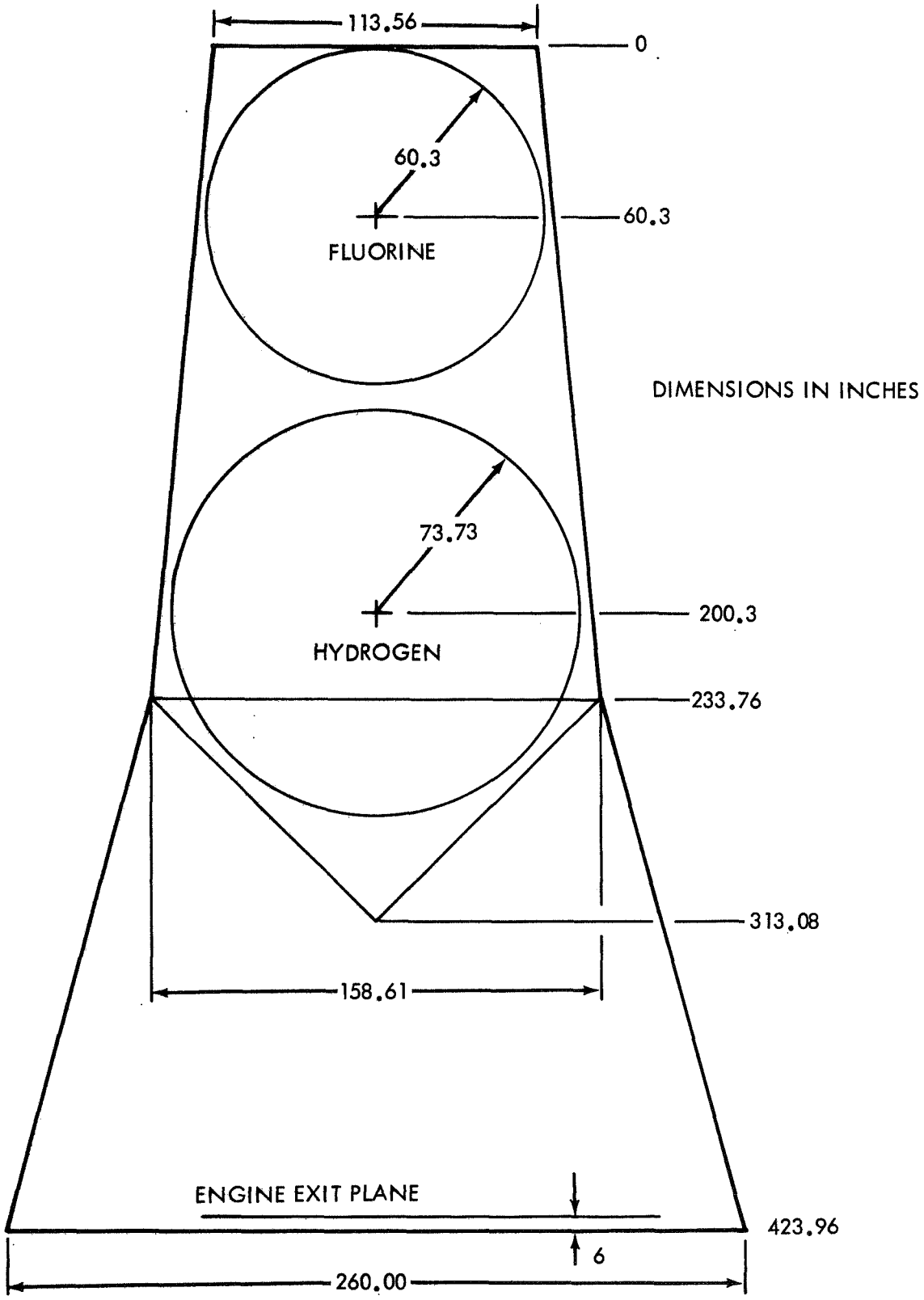

Figure 3-33. Bipropellant Stage (260-Inch SRM/S-IVB)

DIRECT INJECT - 48,500 FPS, 70,000 LB GROSS WEIGHT

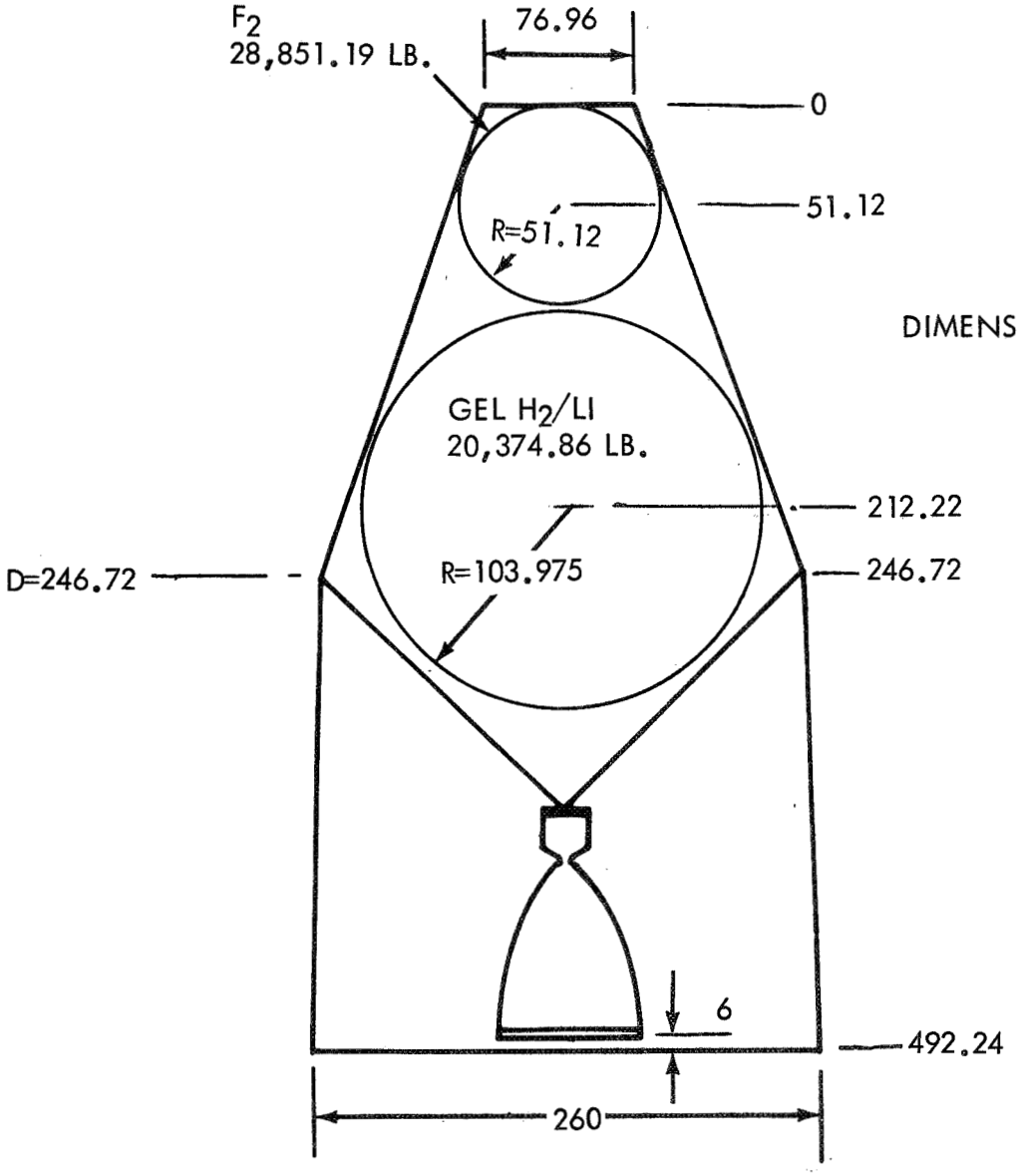

Figure 3-34. Gel Stage (260-Inch SRM/S-IVB)

Table 3-33. Weight Statement Comparison, 260-Inch SRM/S-IVB Booster, Direct Injection Mission

Description	Tripropellant Stage		Bipropellant Stage		Gel Stage	
Structure		3,345		2,578		4,046
Shell	343		712		917	
Interstage	1,135		979		1,600	
Tankage	(953)		(365)		(687)	
Hydrogen		639		232		591
Fluorine		114		133		96
Lithium		200		-		-
Tank Supports	(537)		(262)		(346)	
Hydrogen		177		60		229
Fluorine		200		202		117
Lithium		160		-		-
Thrust Structure	377		260		496	
Propulsion		1,704		1,254		1,469
Engine	921		763		918	
RCS System	13		13		13	
Pressurization System	323		265		273	
Prop. Supply System	447		213		265	
Miscellaneous Weights		650		650		650
Thermal Insulation		162		65		125
Nominal Dry Stage Weight		5,861		4,547		6,290
Contingency (at 7.5%)	440		341		472	
Limit Dry Weight		6,301		4,888		6,762
Jettison Weight	1,135		979		1,600	
Residual Propellant	484		513		492	
Stage Weight at Burnout		5,650		4,422		5,654
Propellant Consumption	48,357		51,297		49,226	
Stage Weight at Liftoff		54,658		56,185		55,988
Payload		15,342		13,815		14,012
Gross Weight Above Booster		70,000		70,000		70,000

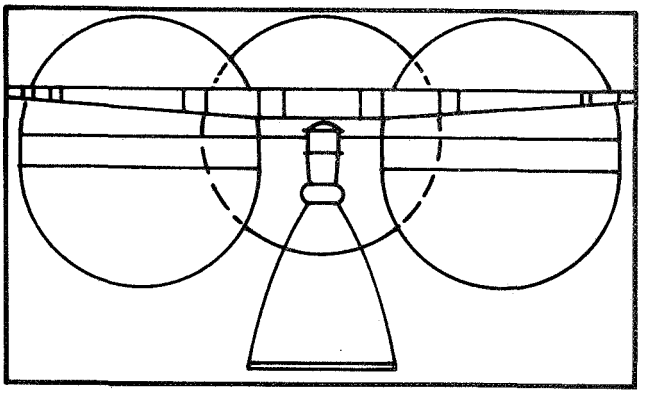

Figure 3-35. Alternate Bipropellant Stage (260-Inch SRM/S-IVB)

3.4 LONG-DURATION MISSIONS

Two long duration missions were investigated during the study. Basically, they consisted of either a single or a two-burn by the upper stage. The basic single-burn mission profile consisted of a booster placing the upper stage and payload on a Mars trajectory. After separating from the booster, the upper stage and payload coasted to the vicinity of Mars where a single retro burn placed the upper stage and payload into orbit around Mars.

The two-burn mission was also of the Mars orbiter type. One difference between the two missions was that the upper stage of the two-burn mission would provide some portion of the velocity increment required to place itself and the payload on an Earth-Mars trajectory. As in the case of the direct injection missions, the velocity level provided by the upper stage was a function of the gross weight above the booster. The only other difference between the one and two-burn interplanetary missions was that the two-burn stage coasted with only a partial propellant load before restarting in the vicinity of Mars.

3.4.1 DATA AND CONSTRAINTS

The constraints, guidelines and pertinent design data used for the long duration mission studies are summarized in tables 3-34 through 3-39. A coast time of 0.5 hours after booster separation (prior to the initial burn) and an initial thrust-to-weight ratio of 0.7 was assumed for all long duration mission analyses.

Table 3-34. Single-Burn Interplanetary Mission Data

Parameter	Value
Total Mission Velocity	8000 Fps
Coast Time	4920 Hours
Retro Velocity Increment	8000 Fps
Gross Weight	12,000 lb

Table 3-35. Two-Burn Interplanetary Mission Data

Parameter	Value
Total Mission Velocity	46,000 Fps
First Coast Time	0.5 Hour
First Burn Velocity Increment	Computed
Second Coast Time	4920 Hours
Second Burn (Retro) Velocity Increment	8000 Fps

Table 3-36. Design Constraints for Interplanetary Missions

Constraint \ Booster	1-Burn 120-Inch Diameter	2-Burn 260-Inch SRM S-IVB
Booster Diameter (In.)	120	260
Lower Interstage Diameter (In.)	120	260
Maximum Stage Diameter (In.)	112	252
Shell-Tank Spacing (In.)	6	6
Tank-Tank Spacing (In.)	6	9
Engine-Tank Spacing Factor	4.0	4.0
Engine-Booster Spacing (In.)	6	6
Engine Gimbal Angle (Deg)	3	3
Thrust to Weight Ratio	0.7	0.7
Axial Acceleration (G's)	*	*
Lateral Acceleration (G's)	0.5	0.05
Payload Density (lb/ft^3)	25	25
Inert Weight Contingency (%)	7.5	7.5

*A function of gross weight, see appendix F.

Table 3-37. Prime Structure Design Data for Interplanetary Missions

Data \ Structure	Shell	Interstage	Thrust Cone	Spider Beam
Material	Aluminum	Aluminum	Aluminum	Aluminum
Material Strength (psi)	67,000	67,000	67,000	46,000
Safety Factor	1.25	1.25	1.25	1.1
Monocoque to Complex Structure Weight Ratio	*	*	*	N/A
Spider Beam Multiplication Factor	N/A	N/A	N/A	*

*A function of booster and gross weight, see appendix F.

Table 3-38. Tankage Design Data for Interplanetary Missions

Data \ Propellant	Hydrogen	Fluorine	Lithium
Tank			
Material	Aluminum	Aluminum	Maraging Steel
Allowable Stress (psi)	50,000	50,000	*
Safety Factor	1.1	1.1	1.1
Minimum Skin Gauge (In.)	0.025	0.025	0.015
Land Factor	1.1	1.1	1.1
Thermal Protection			
Initial Temperature (°R)	36	150	**
Fraction Slush (%)	0	0	N/A
Insulation Thermal Conductivity (btu/hr-ft-°R)	2.5×10^{-5}	3.0×10^{-5}	*
Insulation Density (lb/ft^3)	4.5	4.5	18.0
External Insulation Temperature (°R)	400	400	400
Heater Weights (lb)	N/A	N/A	***
Miscellaneous			
Minimum Ullage Volume (%)	5	5	5
Residual Fraction (%)	1	1	1
Pressure Delta to Ensure NPSH (psi)	10	10	10
Feedline Flow Velocity (Fps)	25	25	25
Tank Support Factor	0.015	0.010	0.020

*A function of lithium temperature, see appendix F.
**Optimized by sizing program.
***See section 2.2.9.

Table 3-39. Meteoroid Protection Data for Interplanetary Missions

Design Criteria	Value
Probability of No Puncture	0.995
Meteoroid Velocity	20.0 Km/sec
Meteoroid Density	0.50 g/cc
Ratio of Shield Thickness to Meteoroid Diameter	0.30
Shield Material	Same as Tank
Backup Sheet Material	Same as Tank

3.4.2 SINGLE-BURN MISSION RESULTS

The single-burn mission studied was a hypothetical one consisting of a requirement to achieve a velocity increment of 8000 fps after a 205-day coast. This would roughly correspond to a breaking maneuver to circularize a spacecraft into a low orbit about Mars. A gross weight of 12,000 pounds, including payload and interstage, was used for this analysis since it is intermediate to the optimum size stages for use with the Titan IIID/ Centaur and 260-Inch SRM/S-IVB boosters, which are about 10,000 and 14,000 pounds, respectively. Therefore, the conclusions pertinent to a 12,000 pound stage may be applied to either the Titan IIID/Centaur or 260-Inch SRM/S-IVB.

Table 3-40 is a comparative weight statement for the three stages optimized for this mission; figure 3-36 shows the external profiles for these three stages. All stages are shown with a space frame design for the prime structure. This approach permits radiating heat from the tanks and results in lower average insulation external temperatures (i.e., smaller thermal mass penalties for the H_2 and F_2 tanks) than would be obtained with solid semi-monocoque or honeycomb type structures.

The tripropellant configuration is depicted with one lithium tank only, instead of the two used for the direct injection missions. This geometry is preferred because the thermal mass penalty, associated with keeping the lithium molten, is so high when two tanks are used that the increased insulation and heater/power system weights necessary to accommodate the increased surface area more than offset the slight reduction in space frame weight gained through the use of two lithium tanks.

The gel stage is shown with the same tankage arrangement as was previously depicted for the direct injection mission. It differs only in the use of a space frame design for the prime structure.

The configurations shown for the bipropellant assumes a tandem tank arrangement; however, other geometries involving toroids or multiple fluorine tanks are also attractive.

Table 3-40. Weight Statement Comparison, Single-Burn Mars Retro (12,000 lb Gross Weight)

Description	Tripropellant Stage		Bipropellant Stage		Gel Stage	
Structure		639		365		599
Shell	175		76		107	
Interstage	79		115		147	
Tankage	(266)		(123)		(248)	
Hydrogen		209		94		227
Fluorine		24		29		21
Lithium		33		-		-
Tank Supports	(63)		(24)		(53)	
Hydrogen		9		5		18
Fluorine		36		19		35
Lithium		18		-		-
Thrust Structure	56		27		44	
Propulsion		365		294		346
Engine	140		115		138	
RCS System	74		68		75	
Pressurization System	69		63		76	
Prop. Supply System	82		48		57	
Miscellaneous Weights		843		738		783
Thermal Insulation		712		186		281
Nominal Dry Stage Weight		2,559		1,583		2,009
Contingency (at 7.5%)	192		119		151	
Limit Dry Weight		2,751		1,702		2,160
Jettison Weight	79		115		147	
Residual Propellant	46		50		48	
Stage Weight at Burnout		2,718		1,637		2,061
Propellant Consumption	4,598		4,984		4,712	
Stage Weight at Liftoff		7,349		6,686		6,872
Payload		4,651		5,314		5,128
Gross Weight Above Booster		12,000		12,000		12,000

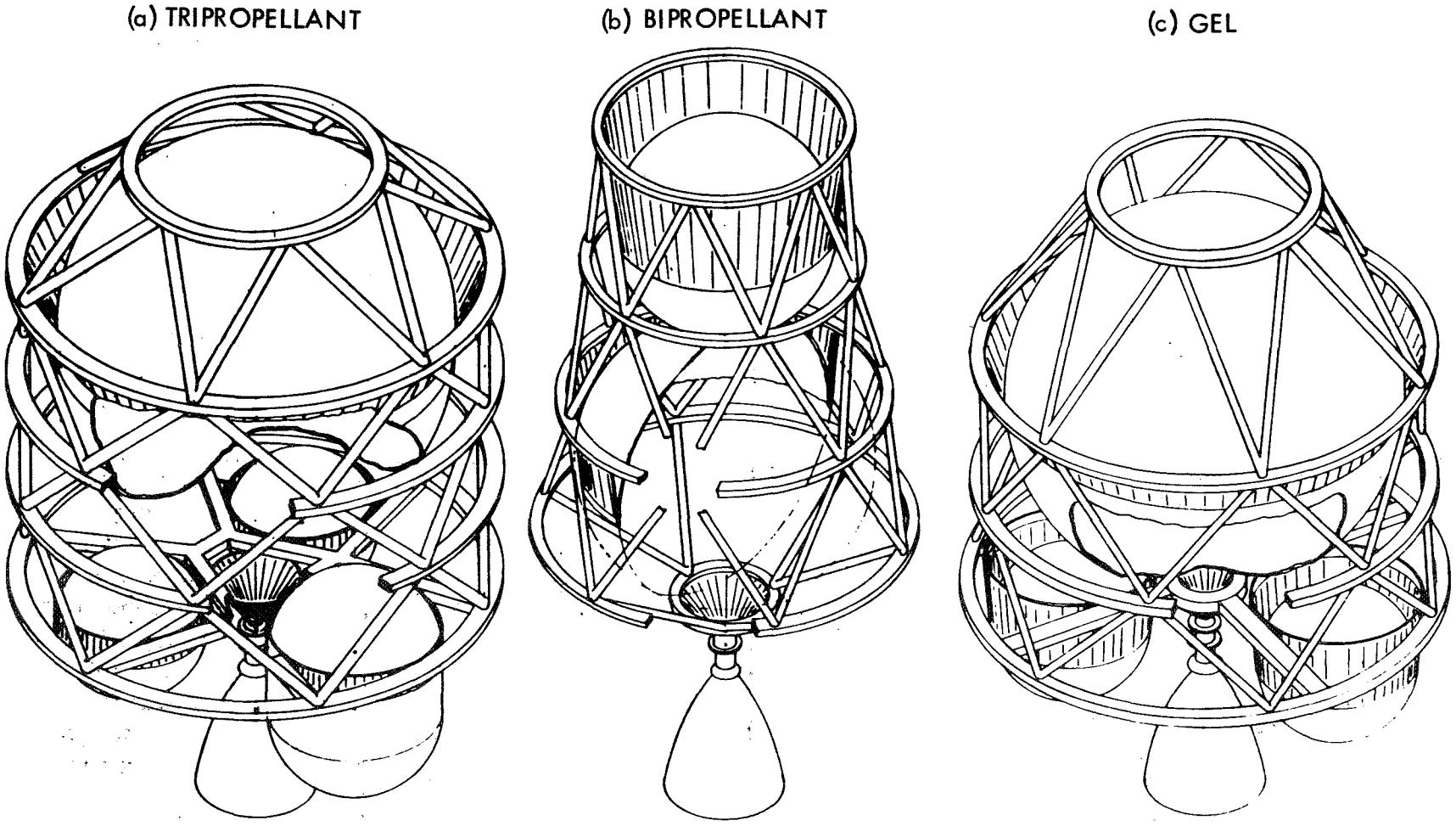

Figure 3-36. External Profiles of Stages for Single-Burn, Long Duration Mission

Tables 3-41 through 3-45 summarize the pertinent stage characteristics, engine data and design data for the three single-burn stages.

An inspection of the results of these analyses identifies the high thermal protection requirements of the $F_2/Li/H_2$ stages as the major contributors to relatively poor performance of these stages when compared to the bipropellant F_2/H_2 stage. To determine if a more favorable thermal protection system design criteria would shift the advantage to the $H_2/Li/F_2$ stages, the long-coast cases were re-run. For this second analysis, the parameters used as input to the thermal optimization portion of the sizing program were changed to reflect a reduced thermal mass penalty. These parameter changes are noted in table 3-46.

The results of the analysis (shown in the lower half of table 3-46) indicates that each stage considered has significant payload gains. With the more favorable thermal design criteria, the gel stage is the most attractive (by about 1 percent) followed by the bipropellant and finally the tripropellant. Most of the payload gains are attributable to the use of slush hydrogen. For long coast missions the high thermal capacity of slush tends to reduce the insulation requirements, resulting in lower optimum tank design pressures. Smaller tanks also result because the density of hydrogen is greater at the lower tank vent temperatures.

From this analysis it may be concluded that any uncertainties which may exist in the thermal protection system design are not large enough to change the payload advantage in favor of the tripropellant stage.

3.4.3 MULTIPLE BURN MISSION RESULTS

For the two-burn mission, a total mission velocity of 46,000 fps (including booster ΔV) was assumed. Of this 46,000 fps, 8000 fps was specified as a requirement after a 205-day coast. The 260-Inch SRM/S-IVB booster was assumed for the booster, and the upper stages were optimized for stage weights ranging from 10,000 to 40,000 pounds. Results of these analyses are given in figure 3-37. Payloads are presented as a function of stage size for the three alternate upper stages. Data are given for results based on the baseline and favorable thermal analysis criteria. (See table 3-46 for identification of favorable thermal analysis criteria.) Results show that the tripropellant stage suffers significantly when compared to the bipropellant for both the baseline and favorable thermal analysis criteria.

If stage sizes greater than 40,000 pounds had been investigated there would have been a critical point, or optimum stage size, for use atop the 260-Inch SRM/S-IVB booster. (Optimum stage weight would occur between 40,000 and 95,000 pounds.)

Stages having a 50,000 pound gross weight (35,000 to 40,000 pound stage weights) were arbitrarily selected to present typical stage characteristics. Table 3-47 depicts the comparative weight statements for the three stages illustrated in figures 3-38 through 3-40. The major stage, engine and design characteristics of these three stages are presented in tables 3-48 through 3-52.

Table 3-41. Major Stage Characteristics Summary - 120-Inch Booster, Single-Burn, Interplanetary Mission

Total Mission Velocity:	8000 fps
Stage Velocity Increment - First Burn:	8000 fps
Stage Velocity Increment - Second Burn:	0.0 fps
First Coast Time:	0.5 hrs
Second Coast Time:	4920.0 hrs
Gross Weight:	12000 lb

Stage	Bipropellant	Gelled H_2/Li	Tripropellant
Payload (lb)	5266	5112	4642
Specific Impulse (sec)	467.62	501.30	521.17
Thrust (lb)	8320	8297	8345
Interstage Weight (lb)	115	147	79
Total Stage Weight (lb)	6619	6741	7279
Inert Stage Weight (lb)	1635	2029	2681
Total Propellant Weight (lb)	4983	4712	4598
Propellant Consumed			
First Burn (lb)	4898	4632	4520
Second Burn (lb)	N/A	N/A	N/A
Residual Propellant Weight (lb)	35	33	33
Stage Mass Ratio	1.712	1.652	1.620
Stage Payload Fraction	0.439	0.426	0.387
Stage Structural Ratio	0.252	0.305	0.372
Stage Velocity Ratio	0.538	0.512	0.482
Stage Thrust to Weight Ratio	0.7	0.7	0.7

Table 3-42. Engine Data Summary, 120-Inch Diameter, Single-Burn Interplanetary Mission

Stage	Bipropellant	Gelled H_2/Li	Tripropellant
Thrust (lb)	8320	8297	8345
Specific Impulse (sec)	467.62	501.3	521.17
Expansion Ratio	150	150	150
Chamber Pressure (psi)	1000	1000	800
F_2/Li Mixture Ratio	N/A	2.740	2.740
Percent Hydrogen	7.692	20.0	25.0
Weight (lb)	115	137	140
Length (In.)	48.1	48.1	54.1
Exit Diameter (In.)	29.6	29.7	33.2

Table 3-43. Design Data Summary - Bipropellant Stage, 120-Inch Diameter Booster, Single-Burn, Interplanetary Mission

Propellant Tank	Hydrogen	Fluorine
Propellant Weights		
Usable (lb)	377	4521
Residual (lb)	4	46
Boiloff (lb)	0	0
Startup/Shutdown (lb)	3	32
Total Load (lb)	384	4599
Tankage		
Number of Tanks	1	1
Volume (ft^3)	116.7	53.5
Radius (In.)	36.37	26.06
Cylinder Length (In.)	0	0
Dome Thickness (In.)	0.0484	0.0250
Cylinder Thickness (In.)	N/A	N/A
Design Pressure (psi)	121	43
Thermal		
Initial Temperature (°R)	36	150
Vent Temperature (°R)	53	168
Insulation Thickness (In.)	3.68	1.04
Number of Kilowatts	N/A	N/A
Number of Kilowatt-hours	N/A	N/A
Meteoroid Shield		
Meteoroid Design Mass (gm)	0.00238	0.00148
Meteoroid Diameter (cm)	0.209	0.178
Shield Thickness (In.)	0.025	0.025
Spacing (In.)	3.68	3.99
Backup (Δ Tank) Thickness (In.)	0	0

Table 3-44. Design Data Summary - Gelled H_2/Li Stage, 120-Inch Diameter Booster, Single-Burn, Interplanetary Mission

Propellant Tank	Hydrogen	Fluorine
Propellant Weights		
Usable (lb)	1917	2715
Residual (lb)	19	28
Boiloff (lb)	0	0
Startup/Shutdown (lb)	14	19
Total Load (lb)	1950	2762
Tankage		
Number of Tanks	1	1
Volume (ft^3)	309.0	32.2
Radius (In.)	50.0	23.67
Cylinder Length (In.)	1.3	0
Dome Thickness (In.)	0.0604	0.0250
Cylinder Thickness (In.)	0.1209	N/A
Design Pressure (psi)	110	43
Thermal		
Initial Temperature (°R)	36	150
Vent Temperature (°R)	52	168
Insulation Thickness (In.)	3.12	1.25
Number of Kilowatts	N/A	N/A
Number of Kilowatt-hours	N/A	N/A
Meteoroid Shield		
Meteoroid Design Mass (gm)	0.00367	0.00117
Meteoroid Diameter (cm)	0.241	0.165
Shield Thickness (In.)	0.0285	0.0250
Spacing (In.)	3.12	3.42
Backup (Δ Tank) Thickness (In.)	0.0	0.0

Table 3-45. Design Data Summary - Tripropellant, 120-Inch Diameter Booster, Single-Burn, Interplanetary Mission

Propellant Tank	Hydrogen	Fluorine	Lithium
Propellant Weights			
Usable (lb)	1130	2483	906
Residual (lb)	11	25	9
Boiloff (lb)	0	0	N/A
Startup/Shutdown (lb)	8	18	7
Total Load (lb)	1149	2526	923
Tankage			
Number of Tanks	1	2	1
Volume (ft^3)	327.0	14.8	31.3
Radius (In.)	50.0	18.27	23.46
Cylinder Length (In.)	5.28	0	0
Dome Thickness (In.)	0.0517	0.0250	0.0150
Cylinder Thickness (In.)	0.1034	N/A	N/A
Design Pressure (psi)	94	50	50
Thermal			
Initial Temperature (°R)	36	150	990
Vent Temperature (°R)	50	170	N/A
Insulation Thickness (In.)	3.04	1.48	3.00
Number of Kilowatts	N/A	N/A	1.0
Number of Kilowatt-hours	N/A	N/A	4973
Meteoroid Shield			
Meteoroid Design Mass (gm)	0.00376	0.00083	0.00128
Meteoroid Diameter (cm)	0.243	0.147	0.170
Shield Thickness (In.)	0.0287	0.0250	0.0201
Spacing (In.)	3.04	2.72	3.00
Backup (Δ Tank) Thickness (In.)	0.0	0.0	0.0

Table 3-46. Effects of Favorable Thermal Analysis Criteria on Stage Comparisons

THERMAL ANALYSIS CRITERIA

Criteria	Baseline	Favorable
Thermal Conductivity (H_2 Tank)	2.5×10^{-5} btu/ft-hr-°R	2.0×10^{-5} btu/ft-hr-°R
Thermal Conductivity (F_2 Tank)	3.0×10^{-5} btu/ft-hr-°R	2.0×10^{-5} btu/ft-hr-°R
Insulation Density (H_2 and F_2 Tanks)	4.5 lb/ft^3	3.0 lb/ft^3
Insulation Density (Li Tank)	18.0 lb/ft^3	9.0 lb/ft^3
Insulation External Temperature	400.0°R	300.0°R
Fraction Slush (H_2 only)	0.0	0.6
Initial H_2 Temperature	36.0°R	24.9°R

EFFECT ON STAGE COMPARISON

Item	Tripropellant		Bipropellant		Gel (20% H_2)	
	Baseline	Favorable	Baseline	Favorable	Baseline	Favorable
Insulation Weight	510.2	233.8	186.3	48.8	281.2	61.3
Hydrogen	261.8	64.7	59.4	38.6	258.3	53.9
Fluorine	32.3	8.7	26.9	10.2	22.9	7.4
Lithium	216.1	160.4	-	-	-	-
Li Heater/Power System Weight	202.4	153.3	-	-	-	-
Tank Weight	266.6	147.2	122.6	77.5	247.6	104.6
Hydrogen	209.2	103.1	93.8	49.0	227.1	84.3
Fluorine	24.4	11.9	28.8	28.5	20.5	20.3
Lithium	33.0	32.2	-	-	-	-
Other Inert Weights	2213.9	1757.2	1441.5	1396.8	1646.8	1575.5
Total Inert Weight	(2759.9)	(2291.5)	(1750.4)	(1523.1)	(2175.6)	(1741.4)
Payload	(4642.2)	(5117.9)	(5266.4)	(5492.1)	(5112.4)	(5546.6)
% Payload Change	10.2%		4.3%		8.5%	

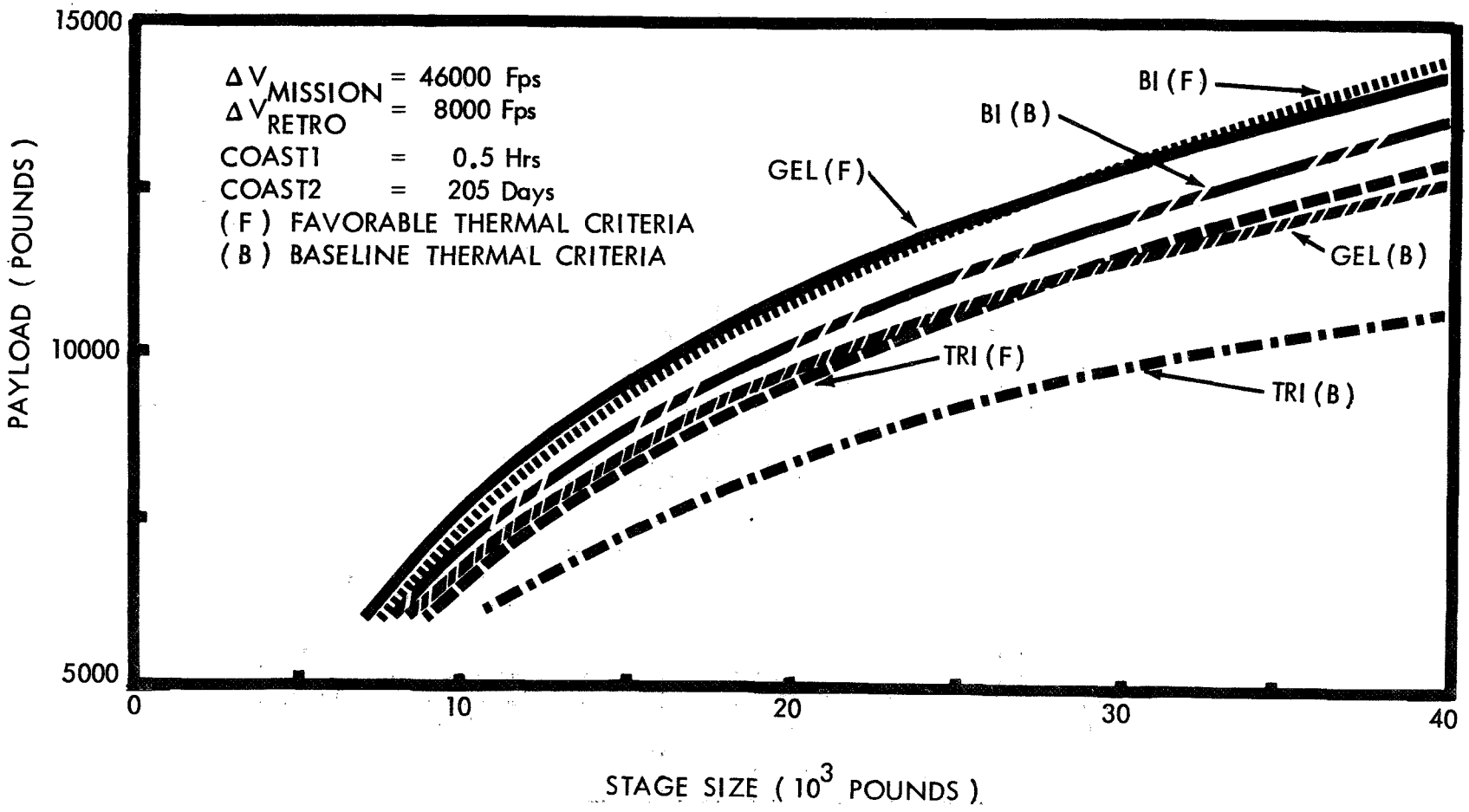

Figure 3-37. Two-Burn Mission Payload Capability (260-Inch SRM/S-IVB)

Table 3-47. Weight Statement Comparison, 260-Inch SRM/S-IVB Booster, Two-Burn Mars Retro

Description	Tripropellant Stage		Bipropellant Stage		Gel Stage	
Structure		2,856		1,716		2,802
Shell	380		353		472	
Interstage	926		689		1,023	
Tankage	(951)		(350)		(737)	
Hydrogen	725		250		668	
Fluorine	82		100		69	
Lithium	144		-		-	
Tank Supports	(341)		(187)		(233)	
Hydrogen	116		40		152	
Fluorine	135		147		81	
Lithium	90		-		-	
Thrust Structure	258		137		337	
Propulsion		1,638		1,329		1,551
Engine	645		528		644	
RCS System	507		499		592	
Pressurization System	151		137		113	
Prop. Supply System	335		165		202	
Miscellaneous Weights		1,443		967		1,154
Thermal Insulation		2,889		562		960
Nominal Dry Stage Weight		8,826		4,574		6,467
Contingency (at 7.5%)	662		343		485	
Limit Dry Weight		9,488		4,917		6,952
Jettison Weight	926		689		1,023	
Residual Propellant	299		319		306	
Stage Weight at Burnout		8,861		4,547		6,235
Propellant Consumption	29,866		31,853		30,564	
Stage Weight at Liftoff		39,354		36,770		37,516
Payload		10,646		13,230		12,484
Gross Weight Above Booster		50,000		50,000		50,000

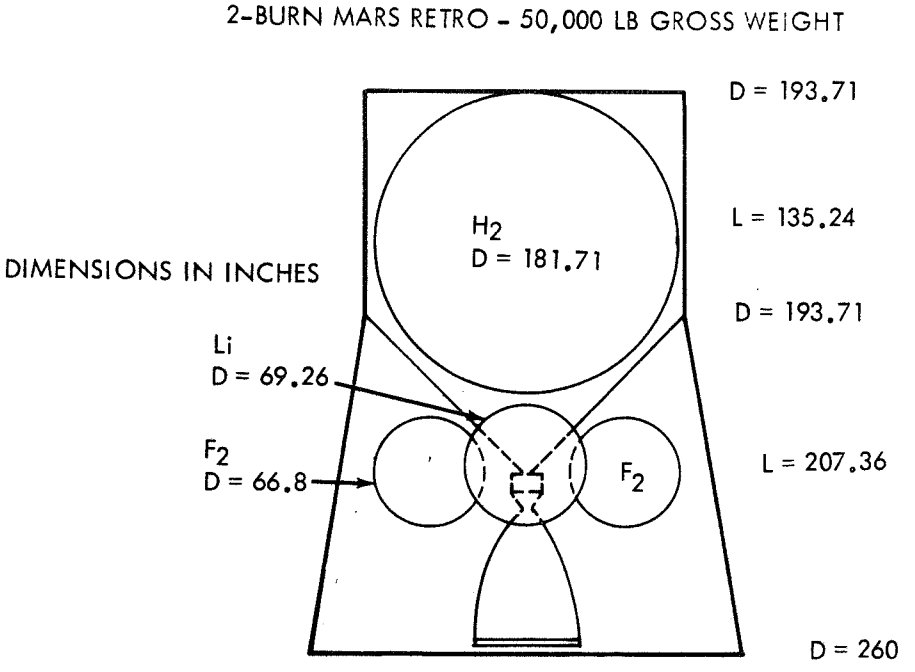

Figure 3-38. Two-Burn, Tripropellant Stage (260-Inch SRM/S-IVB)

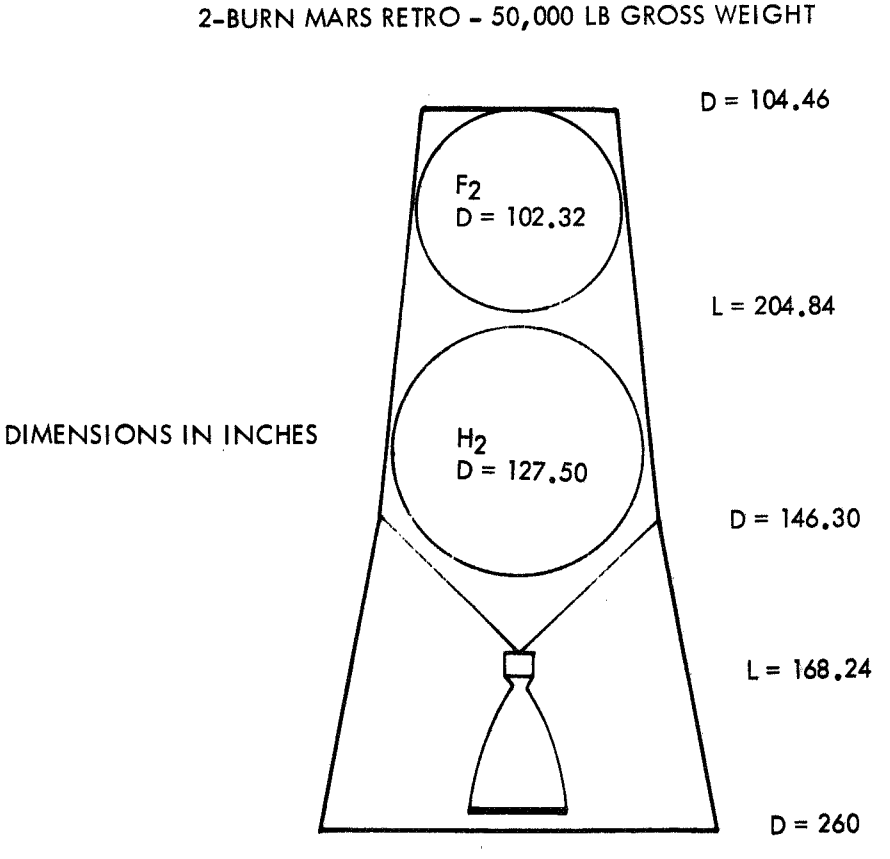

Figure 3-39. Two-Burn, Bipropellant Stage (260-Inch SRM/S-IVB)

2-BURN MARS RETRO - 50,000 LB GROSS WEIGHT

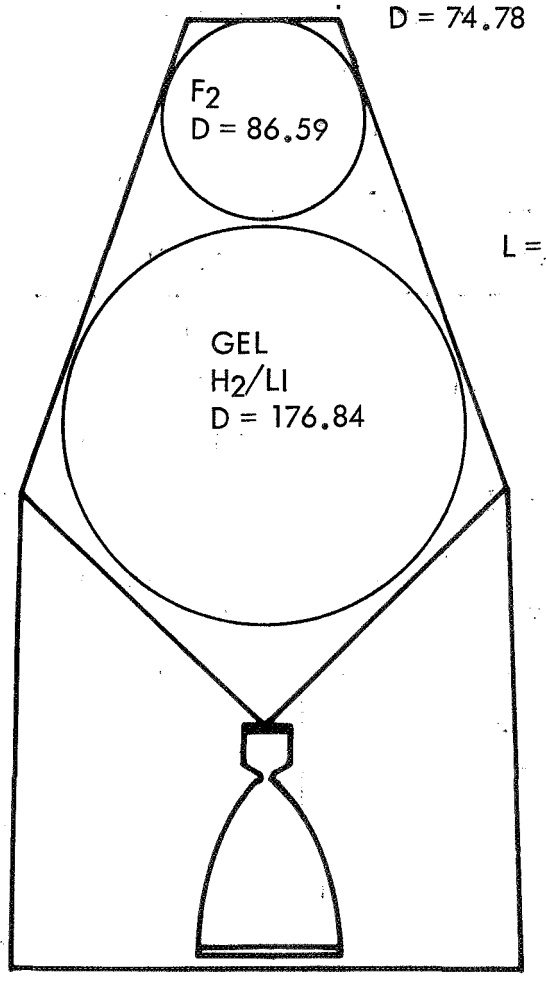

DIMENSIONS IN INCHES

Figure 3-40. Two-Burn, Gel Stage (260-Inch SRM/S-IVB)

Table 3-48. Major Stage Characteristics Summary - 260-Inch SRM/S-IVB Booster, Two-Burn, Interplanetary Mission

Total Mission Velocity:	46000 fps
Stage Velocity Increment - First Burn:	7150 fps
Stage Velocity Increment - Second Burn:	8000 fps
First Coast Time:	0.5 hrs
Second Coast Time:	4920.0 hrs
Gross Weight:	50000 lb

Stage	Bipropellant	Gelled H_2/Li	Tripropellant
Payload (lb)	13114	12294	10598
Specific Impulse (sec)	470.67	501.54	521.44
Thrust (lb)	34517	34282	34351
Interstage Weight (lb)	689	1023	926
Total Stage Weight (lb)	36197	36683	38476
Inert Stage Weight (lb)	4344	6121	8612
Total Propellant Weight (lb)	31853	30562	29863
Propellant Consumed			
First Burn (lb)	18544	17518	17017
Second Burn (lb)	12481	12107	12006
Residual Propellant Weight (lb)	318	305	297
Stage Mass Ratio	2.793	2.636	2.531
Stage Payload Fraction	0.262	0.246	0.212
Stage Structural Ratio	0.124	0.169	0.228
Stage Velocity Ratio	1.027	0.969	0.929
Stage Thrust to Weight Ratio	0.7	0.7	0.7

Table 3-49. Engine Data Summary, 260-Inch SRM/S-IVB Booster, Two-Burn, Interplanetary Mission

Stage	Bipropellant	Gelled H_2/Li	Tripropellant
Thrust (lb)	34517	34282	34351
Specific Impulse (sec)	470.67	501.54	521.44
Expansion Ratio	150	150	150
Chamber Pressure (psi)	1000	1000	900
F_2/Li Mixture Ratio	N/A	2.740	2.740
Percent Hydrogen	7.692	20.0	25.0
Weight (lb)	527	644	645
Length (In.)	89.1	98.2	104.5
Exit Diameter (In.)	60.1	59.6	63.3

Table 3-50. Design Data Summary - Bipropellant Stage, 260-Inch SRM/S-IVB Booster, Two-Burn, Interplanetary Mission

Propellant Tank	Hydrogen	Fluorine
Propellant Weights		
Usable (lb)	2386	28638
Residual (lb)	26	292
Boiloff (lb)	217	0
Startup/Shutdown (lb)	23	271
Total Load (lb)	262	29201
Tankage		
Number of Tanks	1	1
Volume (ft^3)	628.1	324.6
Radius (In.)	63.75	51.16
Cylinder Length (In.)	0	0
Dome Thickness (In.)	0.0421	0.0261
Cylinder Thickness (In.)	N/A	N/A
Design Pressure (psi)	60	46
Thermal		
Initial Temperature (°R)	36	150
Vent Temperature (°R)	45	169
Insulation Thickness (In.)	3.40	1.28
Number of Kilowatts	N/A	N/A
Number of Kilowatt-hours	N/A	N/A
Meteoroid Shield		
Meteoroid Design Mass (gm)	0.00515	0.00356
Meteoroid Diameter (cm)	0.270	0.239
Shield Thickness (In.)	0.0319	0.0282
Spacing (In.)	3.40	5.96
Backup (Δ Tank) Thickness (In.)	0	0.0024

Table 3-51. Design Data Summary - Gelled H_2/Li Stage, 260-Inch SRM/S-IVB Booster, Two-Burn, Interplanetary Mission

Propellant Tank	Hydrogen	Fluorine
Propellant Weights		
Usable (lb)	12262	17363
Residual (lb)	128	177
Boiloff (lb)	350	0
Startup/Shutdown (lb)	113	160
Total Load (lb)	12862	17700
Tankage		
Number of Tanks	1	1
Volume (ft^3)	1675.6	196.8
Radius (In.)	88.42	43.29
Cylinder Length (In.)	0	0
Dome Thickness (In.)	0.0584	0.0250
Cylinder Thickness (In.)	N/A	N/A
Design Pressure (psi)	60	28
Thermal		
Initial Temperature (°R)	36	150
Vent Temperature (°R)	45	180
Insulation Thickness (In.)	3.54	0.90
Number of Kilowatts	N/A	N/A
Number of Kilowatt-hours	N/A	N/A
Meteoroid Shield		
Meteoroid Design Mass (gm)	0.00823	0.00276
Meteoroid Diameter (cm)	0.316	0.219
Shield Thickness (In.)	0.0373	0.0259
Spacing (In.)	3.54	5.956
Backup (Δ Tank) Thickness (In.)	0	0.0002

Table 3-52. Design Data Summary - Tripropellant Stage, 260-Inch SRM/S-IVB Booster, Two-Burn, Interplanetary Mission

Propellant Tank	Hydrogen	Fluorine	Lithium
Propellant Weights			
Usable (lb)	7256	15947	5820
Residual (lb)	76	162	59
Boiloff (lb)	279	0	N/A
Startup/Shutdown (lb)	66	145	53
Total Load (lb)	7677	16254	5932
Tankage			
Number of Tanks	1	2	2
Volume (ft^3)	1817.9	90.3	100.7
Radius (In.)	90.85	33.40	34.63
Cylinder Length (In.)	0	0	0
Dome Thickness (In.)	0.0599	0.0250	0.0150
Cylinder Thickness (In.)	N/A	N/A	N/A
Design Pressure (psi)	60	28	50
Thermal			
Initial Temperature (°R)	36	150	990
Vent Temperature (°R)	45	180	N/A
Insulation Thickness (In.)	3.62	1.17	3.00
Number of Kilowatts	N/A	N/A	4.4
Number of Kilowatt-hours	N/A	N/A	21,690
Meteoroid Shield			
Meteoroid Design Mass (gm)	0.00857	0.00191	0.00217
Meteoroid Diameter (cm)	0.319	0.194	0.202
Shield Thickness (In.)	0.0378	0.0250	0.0239
Spacing (In.)	3.62	4.74	3.00
Backup (Δ Tank) Thickness (In.)	0	0	0

3.5 SENSITIVITY STUDIES

The results of the long duration mission studies (paragraph 3-4) showed the thermal and meteoroid protection systems were the largest individual contributors to the inert weight of the stages. Since there is always some uncertainty in these particular subsystem analyses (and hence the resultant weight estimates) for stages designed for a long duration coast, it is appropriate to discuss the sensitivity of a stage's performance and selected design features to the assumptions and/or criteria used in the analyses. An understanding of these sensitivities is very helpful in acquiring a higher degree of confidence in any conclusions arrived at with respect to the relative merits of competing stages. Sensitivity analyses are also useful in assessing areas for further trade-off and identifying, quantitatively, the advantages of improving the state-of-art in certain areas; e.g., use of slush hydrogen, better insulation, etc. The sensitivity analyses conducted on the thermal control and meteoroid protection subsystems are discussed in the following paragraphs.

3.5.1 THERMAL PROTECTION

3.5.1.1 Effect of Propellant Load

Figure 3-41 shows the variation in thermal mass penalty, optimum insulation thickness and optimum tank design pressure as a function of propellant load. The criteria assumed for this analysis are as follows:

a) Insulation thermal conductivity: 2.5×10^{-5} BTU/ft-hr-°R
b) Insulation density: 4.5 lb/ft^3
c) Heat conduction factor (a): 1.0
d) Insulation external temperature: 450° R
e) Mission duration: 205 days

The results indicate that the thermal mass penalty and optimum tank pressure vary in an almost linear relationship with propellant load. However, the optimum insulation thickness is seen to decrease rapidly at first and then level off to about 2 3/4 inches for propellant loads above 2,000 pounds. Although not evident from the chart, the non-vented system had a smaller thermal mass penalty than the vented system over the range investigated.

3.5.1.2 Implications of Stage Mass Ratio

The boiloff contribution to the thermal mass penalty is equal to $W_{BO}/(\mu-1)$. Hence the penalties associated with boiloff decrease as the stage mass ratio, $\mu = \exp\left(\frac{\Delta V}{g_c \, ISP}\right)$, increases. This has the effect of making the vented systems attractive for high velocity missions, while the non-vented systems are more favorable for low velocity missions. This is illustrated in figure 3-42, which depicts thermal mass penalty, optimum insulation thickness and boiloff as a function of vent temperature for stage mass (μ) varying from 1.5 to 10.0. These plots show that as the stage mass ratio is increased, the optimum insulation thickness for a vented system decreases. As the corresponding boiloff increases the resultant

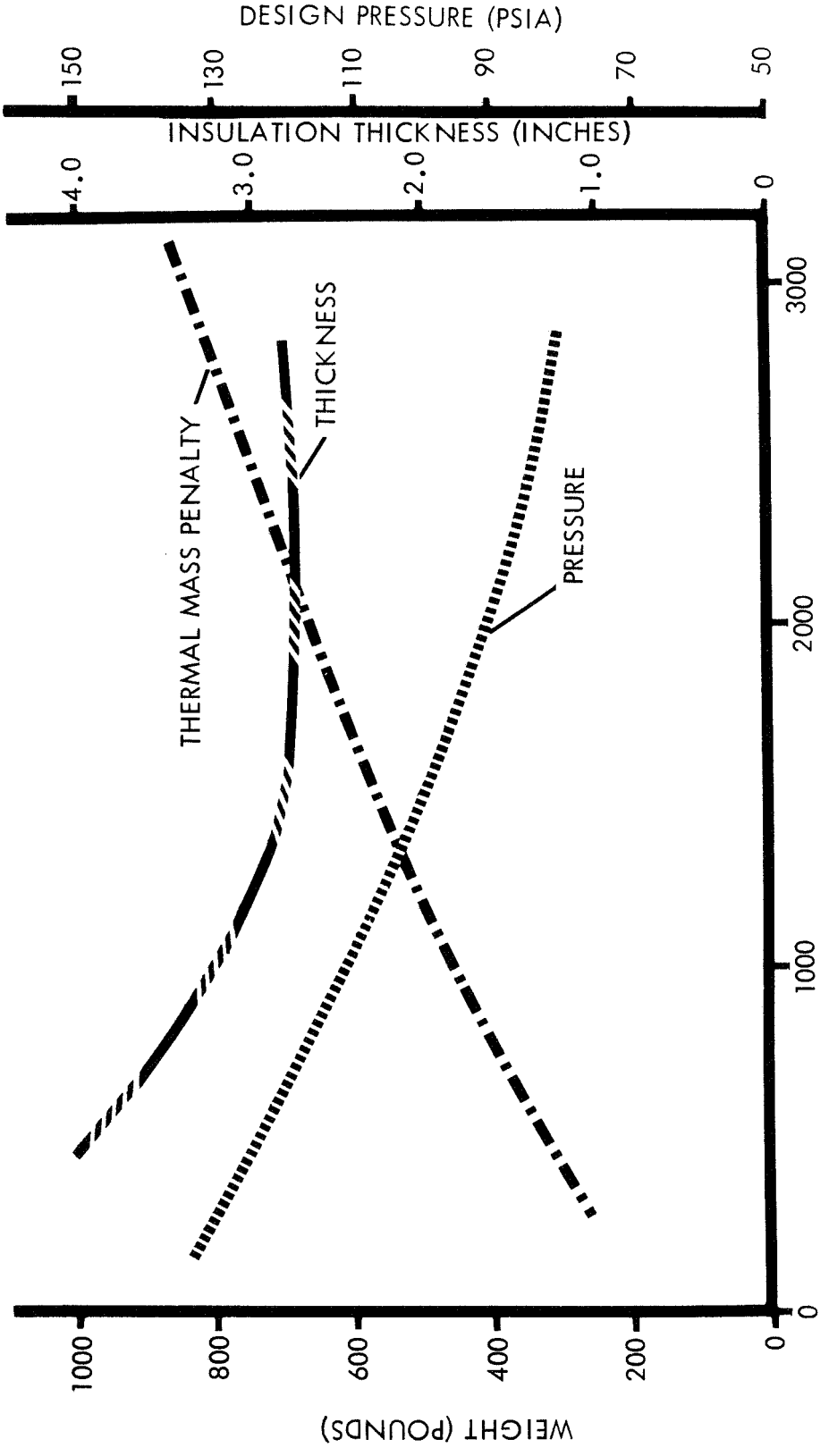

Figure 3-41. Effect of Propellant Load on Thermal Mass Penalty

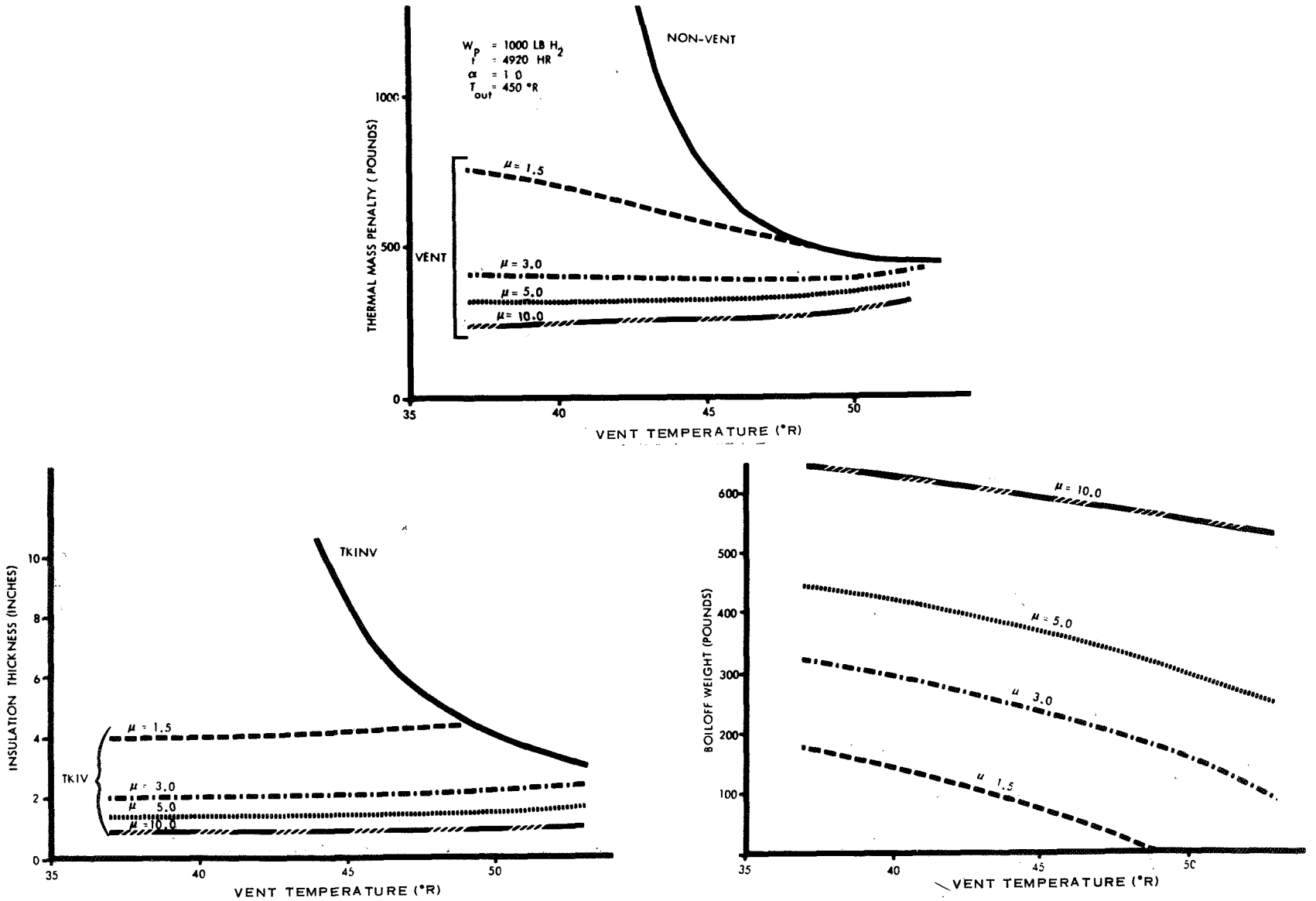

Figure 3-42. Implications of Stage Mass Ratio on Thermal Mass Penalty

thermal mass penalty for the vented systems decreases. From a weight standpoint, the figure shows that a vented system is desired for stage mass ratios greater than 3.0. Also, the optimum vent temperature (design pressure) decreases with increasing values of stage mass ratio.

The criteria used for this analysis are the same as used for the assessment of the effects of changing the propellant load, except that the amount of hydrogen was fixed at 1000 pounds.

3.5.1.3 Effect of Coast Time

The effect of mission duration on the thermal mass penalty and optimum insulation thickness is shown in figure 3-43. The results show that both parameters behave in an almost linear fashion with coast time. The slope of the thickness curve ($\partial TKI/\partial \Upsilon$) is 0.75 inches per 1000 hours. The slope of the mass penalty curve ($\partial TMP/\partial \Upsilon$) is about 65 pounds per 1000 hours, which is not insignificant when compared to the payload capability of a stage with 1000 pounds of hydrogen. These results point out the need for including the changes in thermal protection system requirements when selecting mission profiles since coast times are related to velocity requirements.

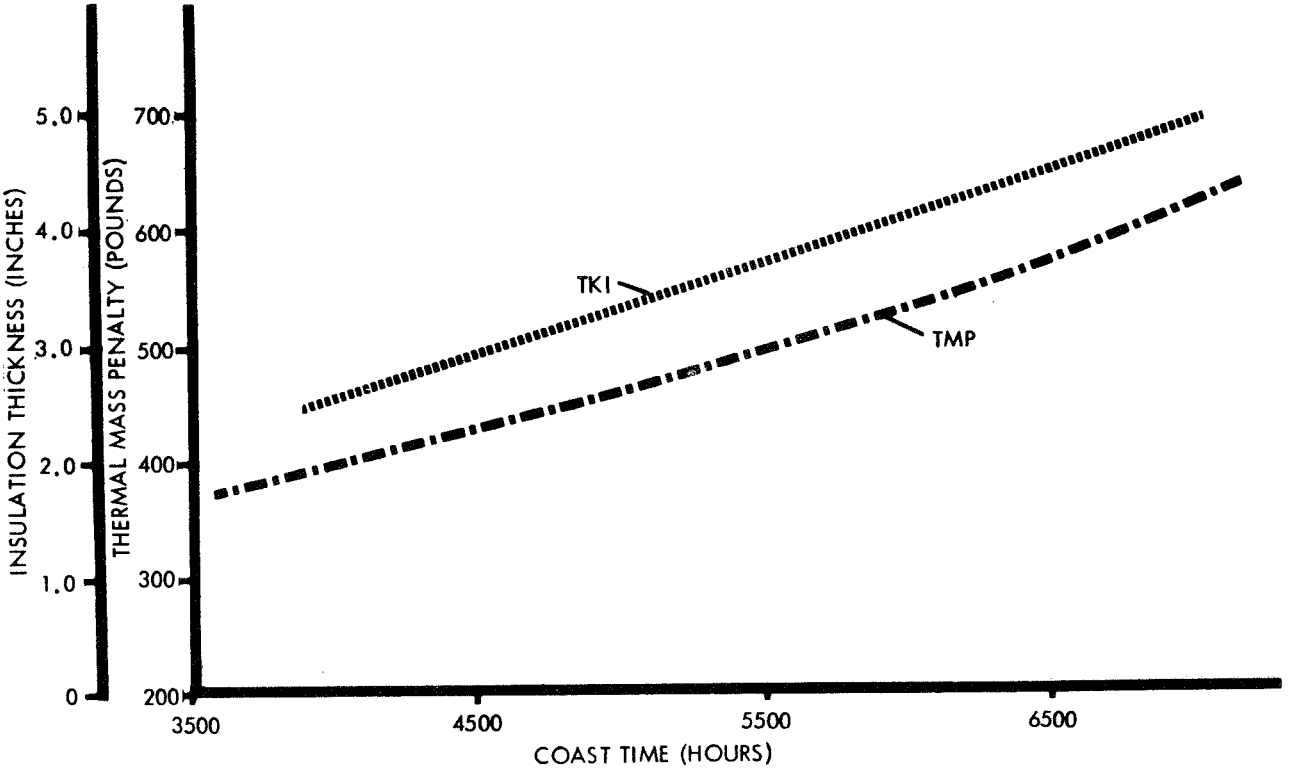

Figure 3-43. Effects of Coast Time on Thermal Mass Penalty

3.5.1.4 Effect of Insulation External Surface Temperature

The temperature of the external surface of the insulation is dependent on many factors. These include tank orientation with respect to the sun, surface α/ϵ ratios, view factors and conduction paths from other structure in the spacecraft, mission profile, etc. Figure 3-44 shows the sensitivity of the thermal mass penalty (TMP) and insulation thickness to changes in insulation external temperature. Both parameters vary almost linearly with temperature and have fairly steep slopes. The $\partial TMP/\partial T_{out}$ is about 85 pounds per 100° R and $\partial TKI/\partial T_{out}$ is about 0.60 inches per 100° R.

In conducting the sizing analyses for alternate stages for a long duration mission, an external temperature of 400° R was assumed, which approximately corresponds to the equilibrium temperature of a spinning black sphere on a Mars trajectory. In practice it should be possible to obtain much lower temperatures through shadow shielding techniques and the judicious selection of surface coatings (α/ϵ ratios).

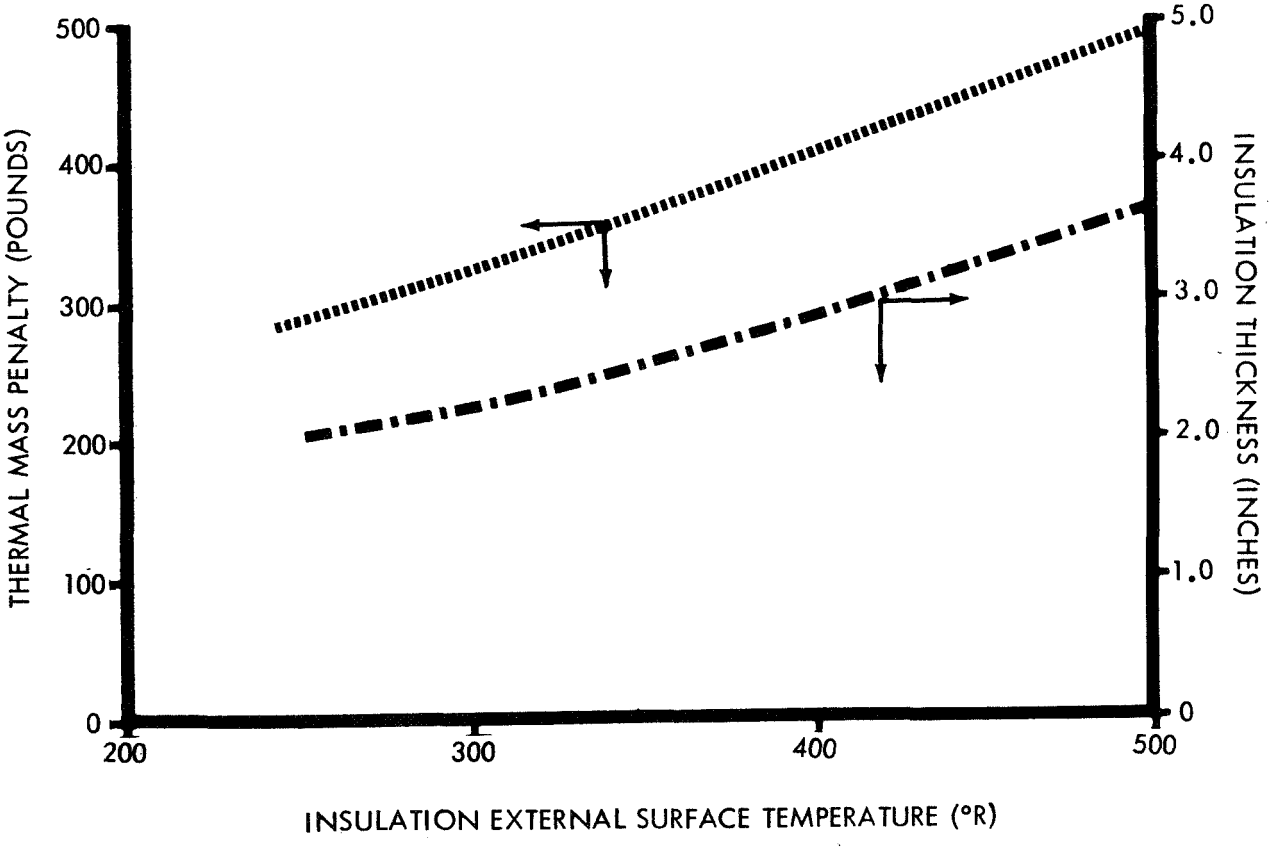

Figure 3-44. Effects of External Temperature on Thermal Mass Penalty

3.5.1.5 Effects of Thermal Conductivity

The influence of thermal conductivity on the TMP and optimum insulation thickness is presented in figure 3-45. For thermal conductivities below 6.5×10^{-5} BTU/ft-hr-°R, the non-vented system is optimum and the curves are seen to be almost linear. At higher thermal conductivities, vented systems become more attractive where the slope of both the TMP and insulation thickness curves begin to decrease.

Although not indicated on the chart, the difference between TMP for the vented and non-vented systems begins to increase rapidly as the value of thermal conductivity increases. For example, at a thermal conductivity of 11.0^{-5} BTU/ft-hr-°R the non-vented system weights almost 2500 pounds more than the vented system. Since the non-vented system is preferred from an operational and reliability standpoint, the importance of developing low thermal conductivity insulations is evident.

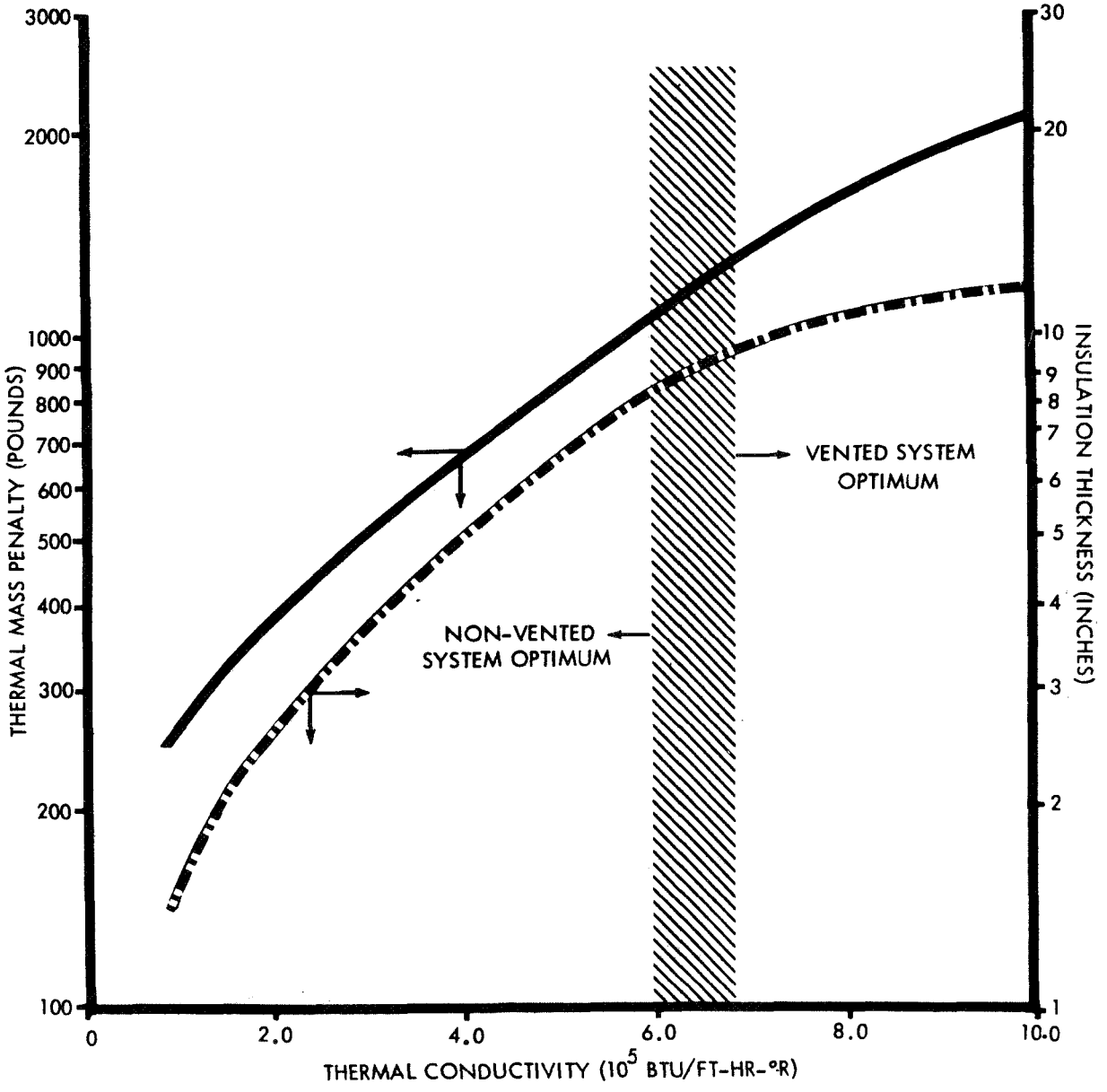

Figure 3-45. Effects of Thermal Conductivity on Thermal Mass Penalty

The results shown in figure 3-45 are applicable only for those cases where the insulation external temperature is 450° R and the hydrogen load is 1000 pounds. If shadow shielding techniques are employed it would be possible to reduce the insulation external temperature to below 100° R. Figure 3-46 presents the same type data as figure 3-45 except that, for these analyses, an external temperature of 75° R has been assumed. The weight penalty associated with a shadow shield, or other device to achieve this temperature, has not been included. From this plot it becomes evident that employing a shadow shield not only results in a reduced insulation weight, but also increases the range over which non-vented systems are optimum.

Of perhaps equal importance is the fact that greatly reduced insulation thicknesses are required for a given thermal conductivity. Recent studies of super insulation have indicated that the insulation thermal conductivity is directly proportional to thickness.

Although a tradeoff between using shadow shields or accepting higher insulation external temperatures was not conducted in this study, results in this sensitivity analysis indicates that such a tradeoff would definitely be pertinent. The potential savings obtained in insulation and tank weights are of the same order as the weight required for a shadow shield. Also the use of a shadow shield may obviate the necessity for developing an insulation having low thermal conductivities for thicknesses exceeding 3 inches.

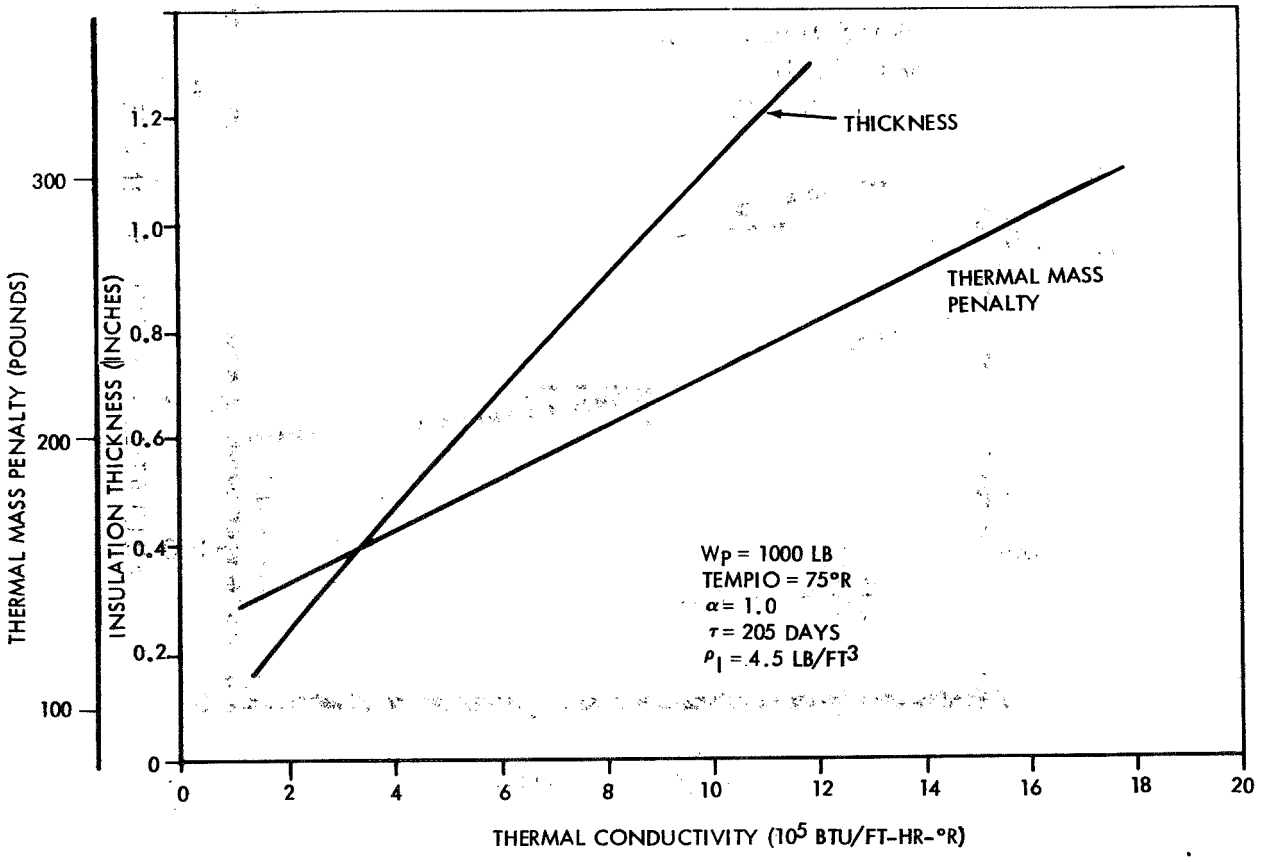

Figure 3-46. Effects of Insulation Thermal Conductivity for Shadow-Shielded Hydrogen Tank

3.5.1.6 Advantages of Slush Hydrogen

It was pointed out in paragraph 3.3 that the use of slush hydrogen in stages designed for direct injection could result in attractive payload gains for both the bipropellant and tripropellant configurations because of increased hydrogen density. Slush hydrogen also offers the possibility of signficant payload increases for long duration missions. However, in this case the advantage stems from the high thermal capacity of slush hydrogen rather than from increased density. Figure 3-47 shows the thermal mass penalty and optimum insulation thickness as a function of the fraction of the hydrogen which is slush. The mass penalty and insulation thickness for the baseline case are also indicated to serve as reference points. As indicated in figure 3-47, a weight saving of 100 to 200 pounds is possible for a stage with a hydrogen load of 1000 pounds.

Since the tripropellant stage has more hydrogen than the bipropellant stage, the use of slush should have a greater relative benefit to the tripropellant stage.

The potential savings attendant with using slush hydrogen are sufficiently large to make its use competitive with using shadow shields. At least one additional advantage is that stage orientation needed for effective use of shadow shields is not required for slush hydrogen.

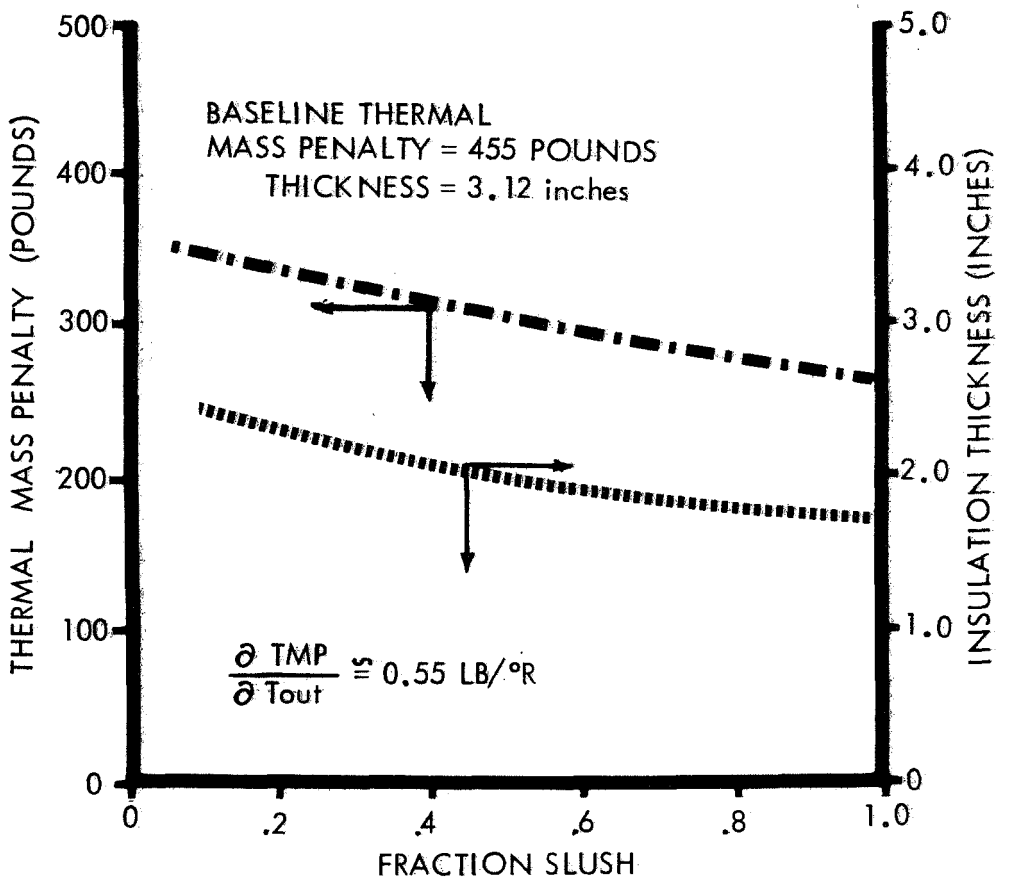

Figure 3-47. Advantages of Slush Hydrogen

3.5.2 METEOROID SHIELD SENSITIVITY ANALYSIS

A meteoroid shield weight sensitivity analysis was conducted to aid in assessing any uncertainties in the weights estimated for meteoroid protection. The use of pressurized propellant tank walls as the shield backup sheet is one area of uncertainty. This model was selected over a separate backup wall since this would provide a greater relative benefit to the tripropellant stage. Table 3-53 summarizes the results of an analysis conducted to determine what influence this selection might have on the study results. From this table it may be concluded that the use of a separate wall for the backup sheet would result in an increase in the bipropellant stage payload advantage on long duration missions.

Additional sensitivity analyses were conducted to determine what affect uncertainties in meteoroid environment and other design criteria would have on the study conclusions. A summary of the results of these analyses are presented in table 3-54. This table depicts the nominal design criteria used as a study baseline, as well as data on each side of the baseline value. The table indicates that changes in some of the parameters, such as meteoroid velocity, will have a negligible effect on the weight of the meteoroid protection system; while other design criteria, such as the mass-flux model, could increase the weight by a factor of three. Although this is considerable, any uncertainty in the design criteria could not change the payload advantage in favor of the tripropellant stage.

It should be noted that these data cannot be used to generate influence coefficients since many of the shield weights presented in the table are sized by constraints (e.g., minimum skin gauge or insulation thickness). More detailed results are presented in the appendix D.

Table 3-53. Summary of Meteoroid Shield Sensitivity to Backup Sheet Selection

Stage	Meteoroid Shield Weight* (pounds)			
	Single-Burn Mission		Two-Burn Mission	
	Separate Wall	Tank Wall	Separate Wall	Tank Wall
Bipropellant	159	88	580	319
Gelled H_2/Li	249	133	949	504
Tripropellant	339	194	1384	792

*For study baseline criteria.

Table 3-54. Summary of Meteoroid Shield Sensitivity to Design Criteria

Design Criteria		Meteoroid Shield Weight (pounds)					
		Single-Burn Mission			Two-Burn Mission		
Criteria	Value	Bipropellant	Gelled H_2/Li	Tripropellant	Bipropellant	Gelled H_2/Li	Tripropellant
Probability of No Puncture	0.990	86	118	170	263	429	675
	0.995*	88	133	194	319	504	792
	0.999	133	198	298	567	807	1283
Ratio of Shield-Backup Sheet Spacing to Meteoroid Diameter	0.2	88	119	157	263	363	560
	0.3*	88	133	194	319	504	792
	0.4	108	170	249	424	673	1046
Meteoroid Mass-Flux Model	0.1X	82	116	163	242	348	532
	1X*	88	133	194	319	504	792
	10X	203	319	501	961	1419	2181
Meteoroid Velocity (Km/sec)	10	82	130	190	297	489	776
	20*	88	133	194	319	504	792
	30	99	141	213	406	551	886
Meteoroid Density (G/cc)	0.25	103	161	238	400	636	989
	0.50*	88	133	194	319	504	792
	1.00	88	119	170	265	415	649

*Study baseline

Section 4

CONCLUSIONS AND RECOMMENDATIONS

The conclusions arrived at during the Part I studies are as follows:

1) The tripropellant stage shows no significant payload advantage over the F_2/H_2 bipropellant stage for direct injection missions,

2) The tripropellant stage is not as attractive as a F_2/H_2 stage for missions involving a long coast,

3) The tripropellant and gel stages have comparable performance for direct injection missions,

4) The gel stage is superior to the tripropellant stage and comparable to the bipropellant stage for missions with a long coast, and

5) The use of slush hydrogen results in significant payload gains for all stages and missions.

Since the Part I analyses showed that the $Li/H_2/F_2$ tripropellant combination does not have sufficient merit, relative to the F_2/H_2 (bipropellant), to warrant its development into a stage, it is Chrysler's recommendation that further studies of the tripropellant stage not be undertaken.

Appendix A

NOMENCLATURE

GENERAL

BI	Bipropellant Stage
D	Tank or Stage Diameter
GEL	A two-tank tripropellant stage, referred to as the "Gel" stage. This designation is merely one of convenience and is not intended to imply that gelling hydrogen to suspend the lithium is necessarily better than using a slurry (see section 1.2).
$\% H_2$	Weight percent hydrogen
Isp or ISP	Specific Impulse
L	Length
Lcyl	Length of cylindrical portion of propellant tank
MR	Fluorine-Lithium mixture ratio (by weight)
N_{F2}	Number of fluorine tanks
Pc	Chamber pressure.
TRI	Tripropellant stage
W	Weight
W_{GROSS}	Gross weight; the total weight above the booster (payload, total stage and interstage)
W_{F2}	Weight of fluorine (per tank)
W_{Li}	Weight of lithium
W_{PROP}	Total propellant load
W_{STAGE}	Total stage weight (excluding payload and interstage).
X_{F2}	Distance from the centerline of the stage to the center of the fluorine tank
X_{Li}	Distance from the centerline of the stage to the center of the lithium tank
ΔV	Velocity increment
ϵ	Engine nozzle expansion ratio or area ratio
η_{Isp} or η_{ISP}	Specific impulse efficiency
μ_{TRANS}	The stage mass ratio for burn required to meet the total launch vehicle velocity increment. (Total mission velocity for the direct injection missions.)

GENERAL (continued)

μ_{RETRO}	The stage mass ratio associated with the maneuver at the end of an interplanetary flight. (The first burn for single-burn, long duration missions, or the second burn of two-burn long duration missions.)
ϕ	A factor in the velocity equations which accounts for propellant residuals

THERMAL

A	Area
C_L	Heat capacity of the propellant
g_c	Universal gravitation constant (32.17 ft/sec^2)
h_s	Heat of fusion of the propellant
TEMPIO	Temperature on the outer surface of the thermal insulation
$T_{INITIAL}$	Initial propellant temperature
TKI	Thickness of thermal insulation
TMP	Thermal mass penalty
TMPNV	Thermal mass penalty associated with a non-vented system
TMPV	Thermal mass penalty associated with a vented system
T_O or T_{OUT}	Temperature on outer surface of thermal insulation
T_{RPT}	Propellant's triple-point temperature
T_{VENT}	Propellant temperature at which tank vents
WBO or $W_{B.O.}$	Weight of boiloff
W_G	Gross weight (See W_{GROSS})
W_{INSUL}	Weight of thermal insulation
W_P	Weight of propellant
W_{PL}	Weight of payload (above stage)
WPRESS or W_{PRESS}	Pressurization system weight

THERMAL (continued)

W_{ST}	Inert or structural weight
WTANK or W_{TANKS}	Weight of propellant tanks
WTINV	Weight of thermal insulation for a non-vented system.
WTIV	Weight of thermal insulation for a vented system.
x	Thermal insulation thickness
x_{opt}	optimum thickness for thermal insulation (vented systems)
x_{REQ}	required thermal insulation thickness (non-vented systems)
α	Heat conduction constant
β	Fraction of heat entering through insulation
τ	Heat of vaporization
μ	Stage mass ratio
ρ_I	Thermal insulation density
T_m	Mission duration
ϕ_x	Fraction of propellant which is slush

METEOROID

A	Exposed area
F	Ratio of stream to sporadic fluxes
M	Meteoroid mass
N	Cumulative flux (particles per unit time per unit area)
P_o	Probability of not receiving a meteoroid hit
S	Spacing between the shield and the backup sheet
T	Time
T_1 and T_2	Time interval of exposure
t_b	Backup sheet thickness
V	Meteoroid velocity
α	Meteoroid flux-mass constant
β	Exponent of the mass in the flux-mass relationship

METEOROID (continued)

δ	Exponent of the velocity in the flux-mass relationship
μ	Meteoroid flux parameter
μsp	Sporadic meteoroid flux parameter
μst	Flux parameter for the meteoroid stream
$\overline{\mu} st$	Average meteoroid stream flux parameter for duration of the mission.
σ	The 0.2 percent yield stress for the backup sheet material

REACTION CONTROL

Isp	Average specific impulse
I_{xx}, I_{yy} and I_{zz}	Moment of inertia about the pitch, yaw and roll axes, respectively.
r_{xx}, r_{yy}, and r_{zz}	Moment arms along the pitch, yaw and roll axes, respectively.
T	Mission duration
W_P	Weight of RCS propellant
W_{RCS}	Weight of entire system
Θ	Limit cycle
ω	Angular velocity

Appendix B

DEFINITIONS

GROSS WEIGHT

(Payload) + (Total Stage Weight) + (Interstage Weight)

THRUST TO WEIGHT RATIO

$$\frac{\text{(Total Stage Thrust)}}{\text{(Gross Weight)} - \text{(Interstage Weight)} - \text{(Boiloff During First Coast)}}$$

TOTAL STAGE WEIGHT

(Gross Weight) - (Payload) - (Interstage Weight)

INERT STAGE WEIGHT

(Total Stage Weight) - (Total Propellant Weight)

STAGE PAYLOAD FRACTION

$$\frac{\text{(Payload)}}{\text{(Gross Weight)}}$$

STAGE MASS RATIO

$$\frac{\text{(Numerator)}}{\text{(Denominator)}}$$

STAGE STRUCTURAL RATIO (LESS PAYLOAD)

$$\frac{\text{(Denominator)} - \text{(Payload)}}{\text{(Numerator)} - \text{(Payload)}}$$

STAGE VELOCITY RATIO

$$\log_e \frac{\text{Numerator}}{\text{Denominator}}$$

NUMERATOR

(Gross Weight) - (Interstage Weight)

- 1/2 (RCS Propellant Weight)

DENOMINATOR

(Gross Weight) - (Interstage Weight)

- 1/2 (RCS Propellant Weight)
- (Boiloff During First and Second Coasts)
- (Number of Starts) · (Startup and Shutdown Losses)
- (Weight of Propellant Consumed at 100% Thrust During First and Second Burns)

Appendix C
OPTIMIZATION CHARTS

Booster	Page
Atlas	
Tripropellant	C-1
Gel	C-9
Bipropellant	C-16
Atlas/Centaur	
Tripropellant	C-19
Gel	C-36
Bipropellant	C-47
Titan IIID	
Tripropellant	C-53
Gel	C-76
Bipropellant	C-92
Titan IIID/Centaur	
Tripropellant	C-103
Gel	C-111
Bipropellant	C-117
260-Inch SRM/S-IVB	
Tripropellant	C-119
Gel	C-125
Bipropellant	C-130

BOOSTER: ATLAS
ΔV (MISSION): 36,140 FPS
ΔV (RETRO): N/A FPS
GROSS WT: 35,000 lb

CASE: 2C5T01
☐ H2/F2
☒ H2/F2/LI

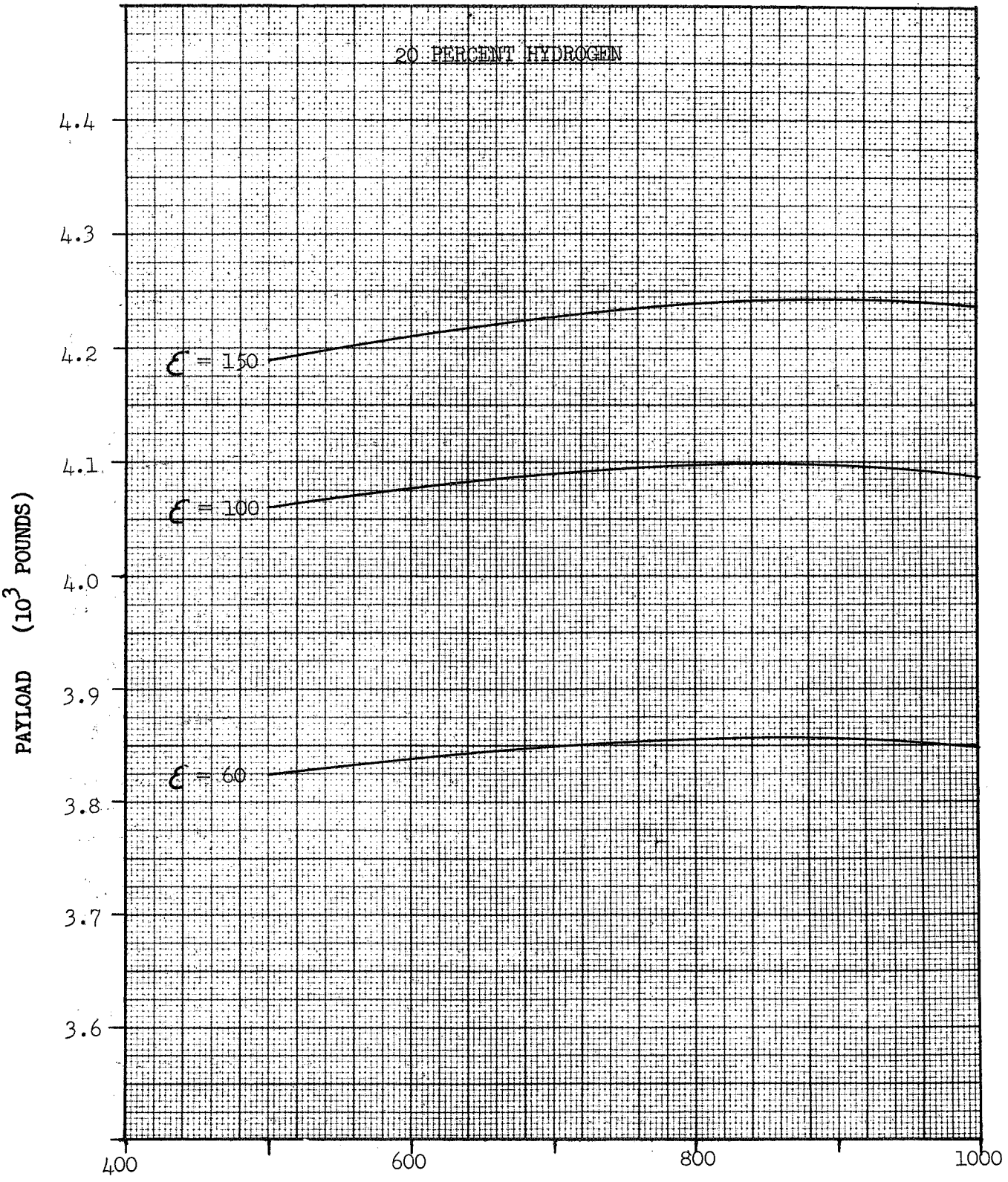

BOOSTER: ATLAS
ΔV (MISSION): 36,140 FPS
ΔV (RETRO): N/A FPS
GROSS WT: 35,000 lb

CASE: 2C5701
☐ H2/F2
☒ H2/F2/LI

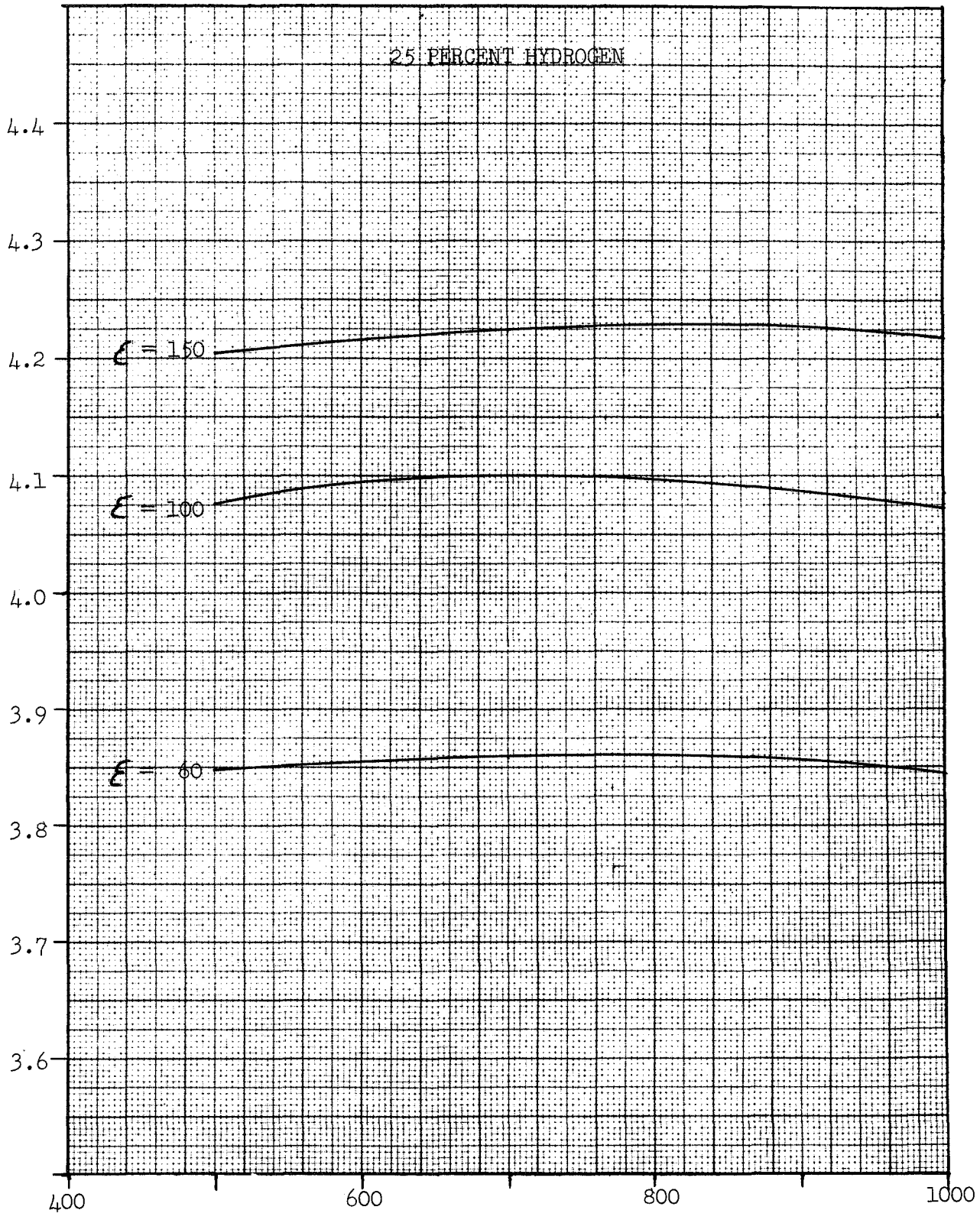

BOOSTER: ATLAS
ΔV (MISSION): 36,140 FPS
ΔV (RETRO): N/A FPS
GROSS WT: 35,000 lb

CASE: 205701
☐ H2/F2
☒ H2/F2/LI

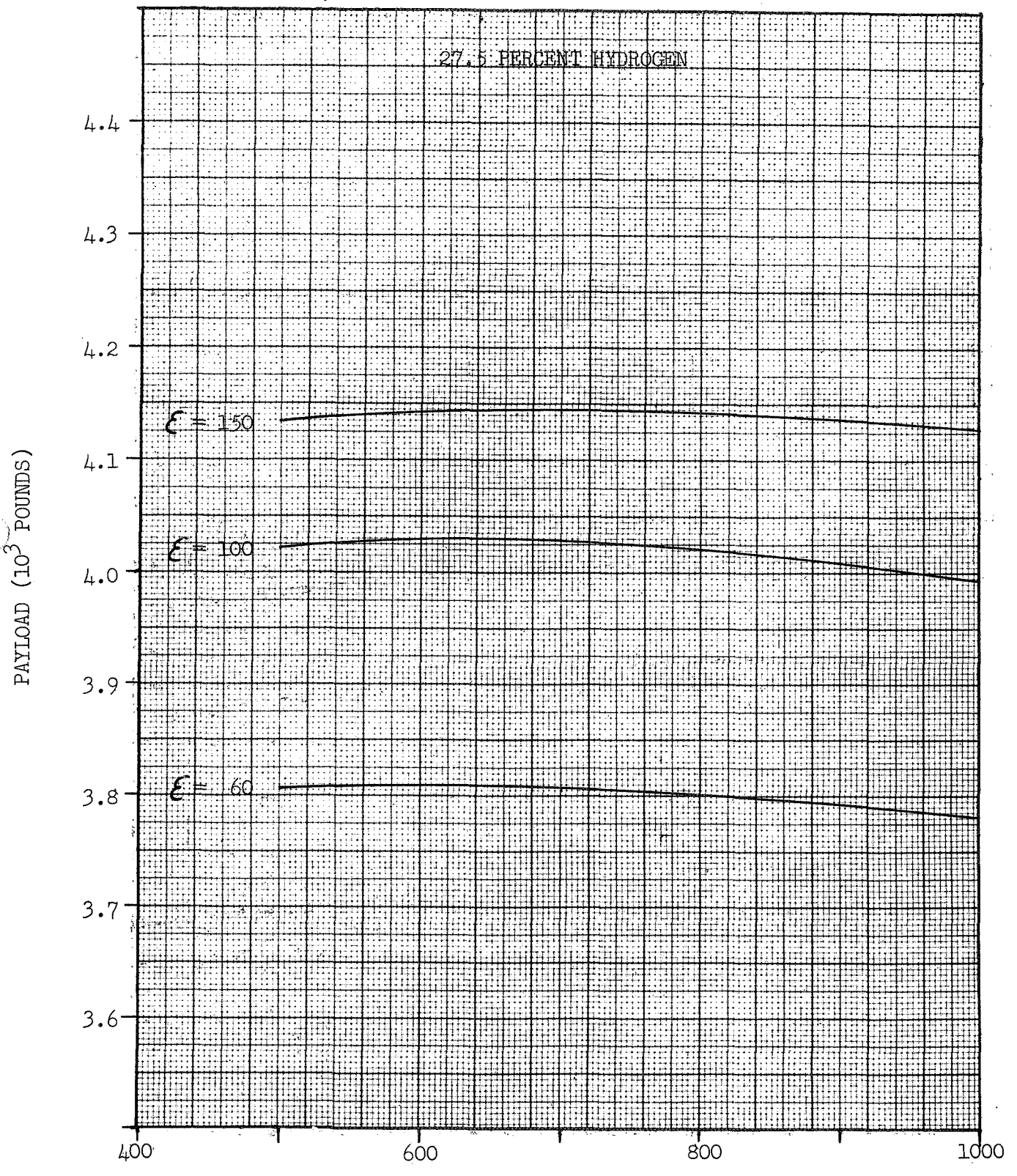

BOOSTER: ATLAS
ΔV (MISSION): 36,140 FPS
ΔV (RETRO): N/A FPS
GROSS WT: 35,000 lb

CASE: 205T01
[ ] H2/F2
[x] H2/F2/LI

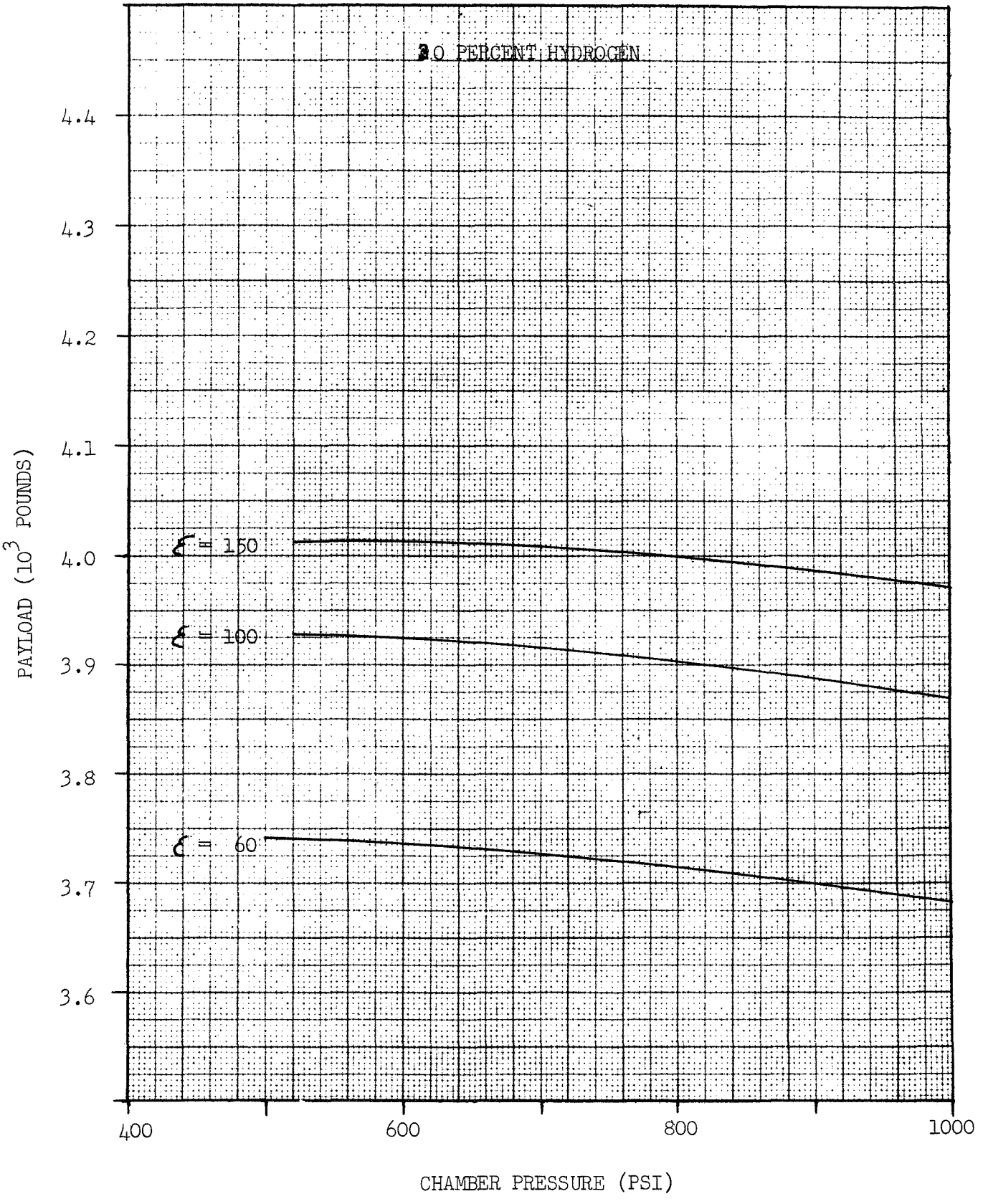

BOOSTER: ATLAS
ΔV (MISSION): 36,140 FPS
ΔV (RETRO): N/A FPS
GROSS WT: 35,000 lb

CASE: 205T01
☒ H2/F2
☒ H2/F2/LI

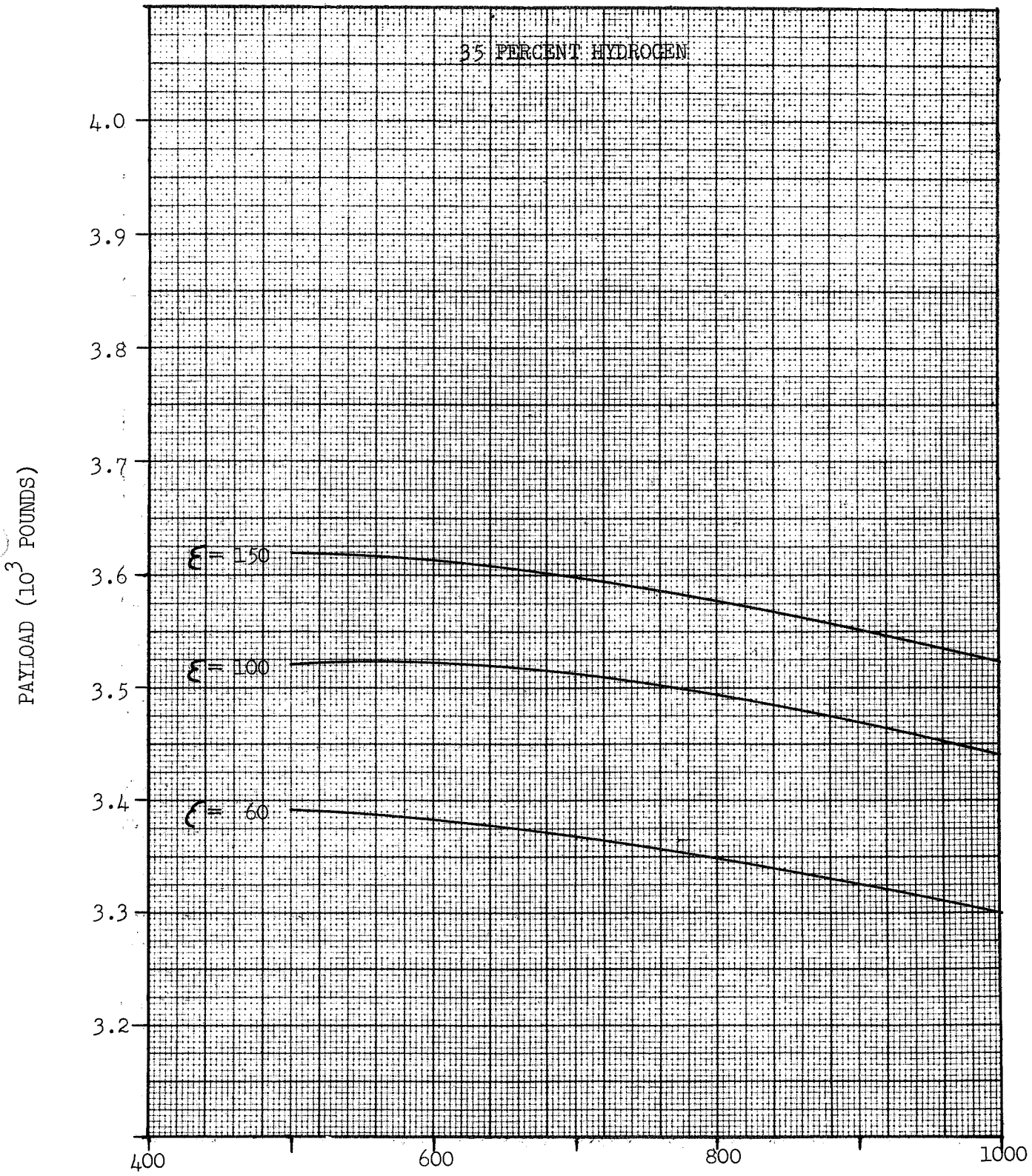

BOOSTER: ATLAS
ΔV (MISSION): 36,140 FPS
ΔV (RETRO): N/A FPS
GROSS WT: 35,000 lb

CASE: 2C5T01
☐ H2/F2
☒ H2/F2/LI

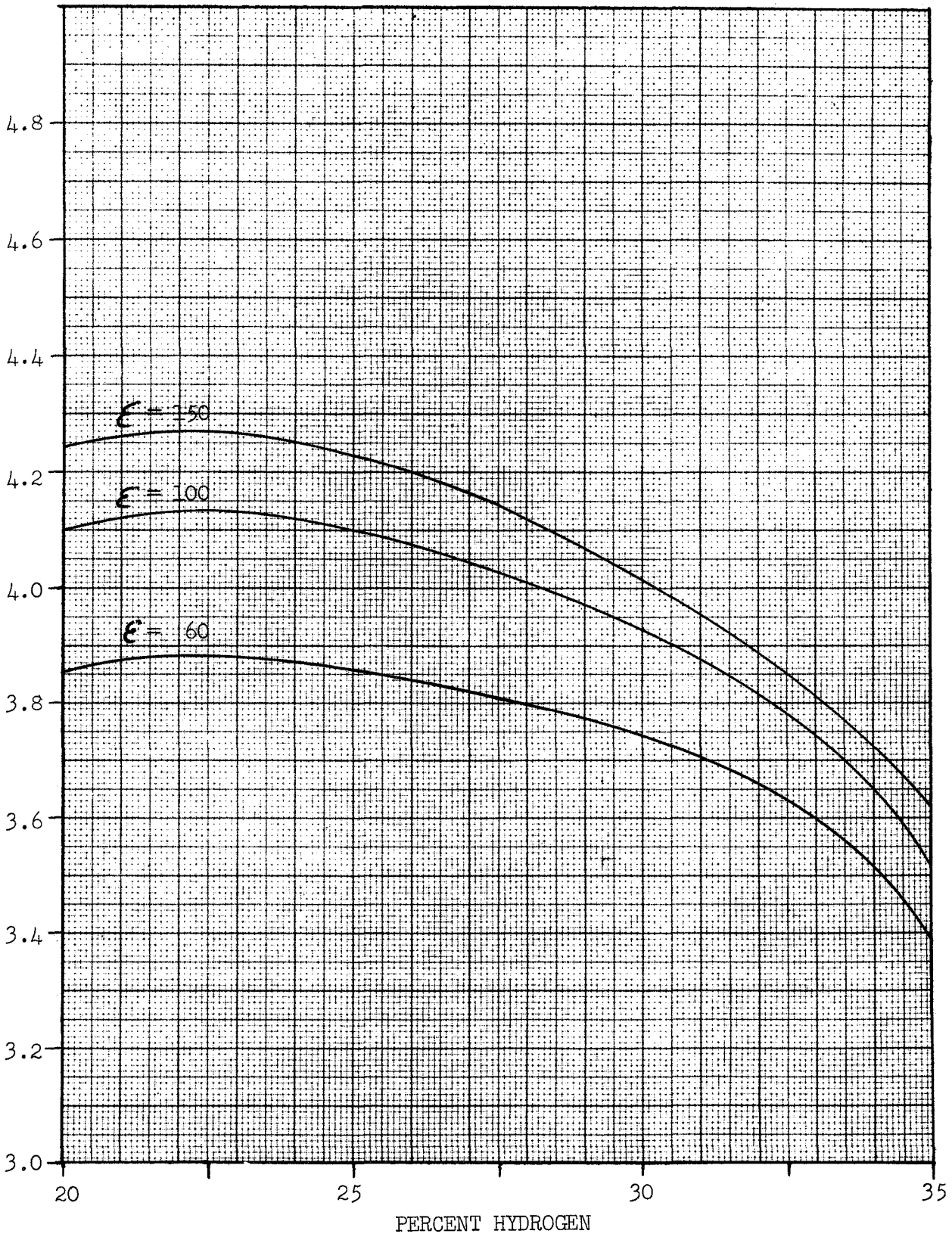

BOOSTER: ATLAS
ΔV (MISSION): 36,140 FPS
ΔV (RETRO): N/A FPS

CASE: 2C5T01
☐ H2/F2
☒ H2/F2/LI

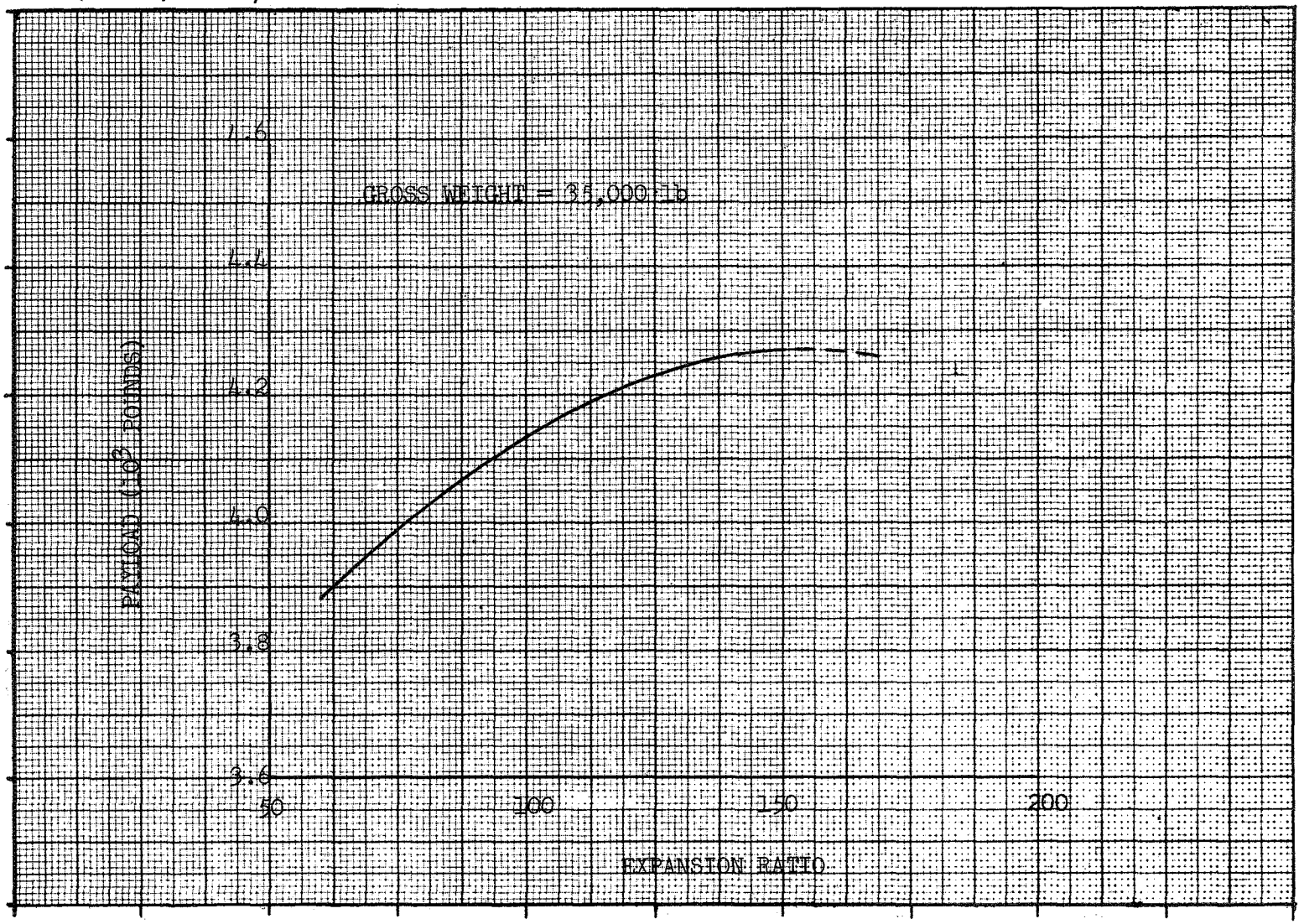

BOOSTER: ATLAS

ΔV (MISSION): 36,140 FPS

ΔV (RETRO): N/A FPS

CASE: 2C5TO1

☐ H2/F2

☒ H2/F2/LI

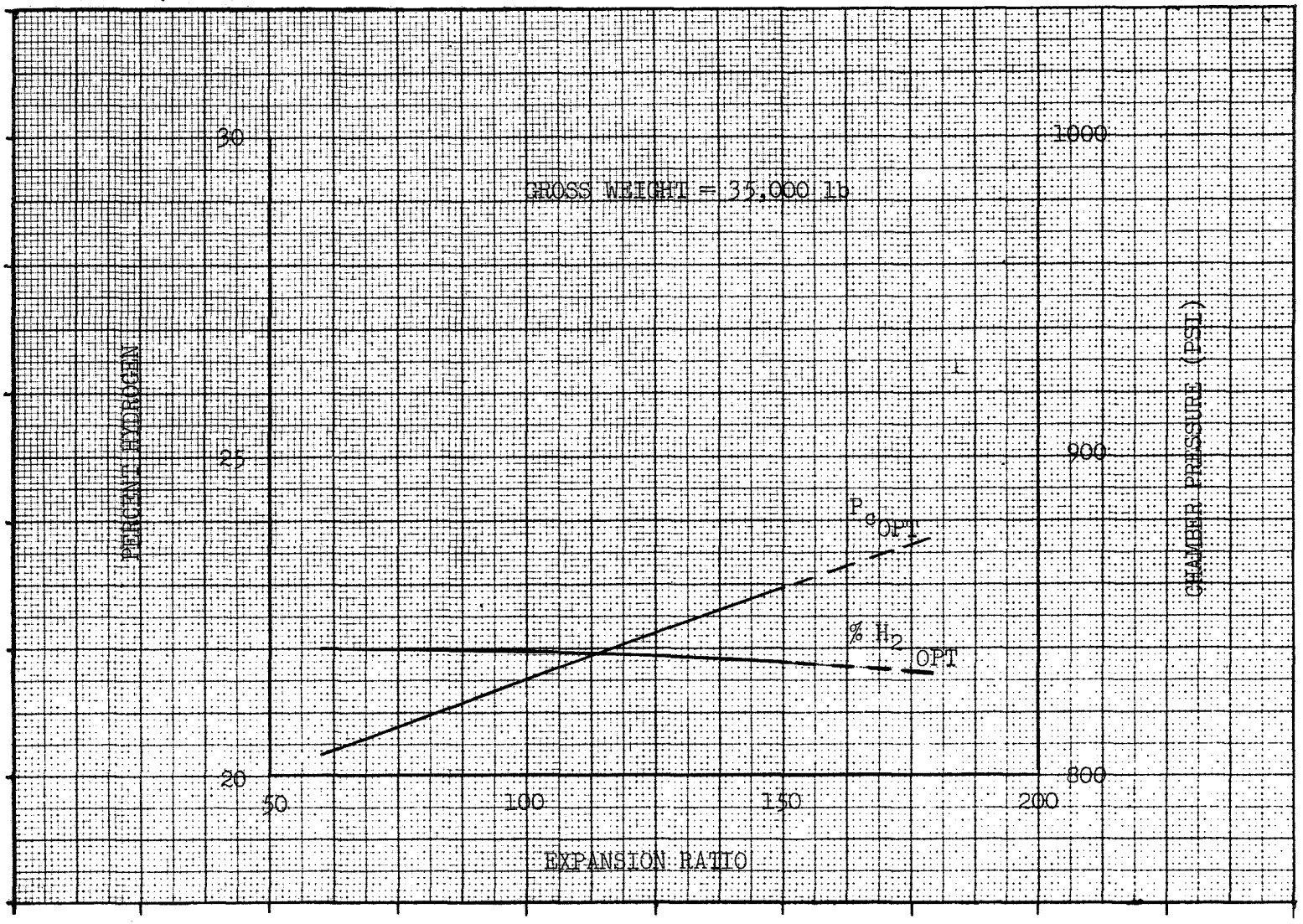

BOOSTER: ATLAS

ΔV (MISSION): 36,140 FPS

ΔV (RETRO): N/A FPS

GROSS WT: 40,000

CASE: 2C5T01

☐ H2/F2

☒ H2/F2/LI - GEL

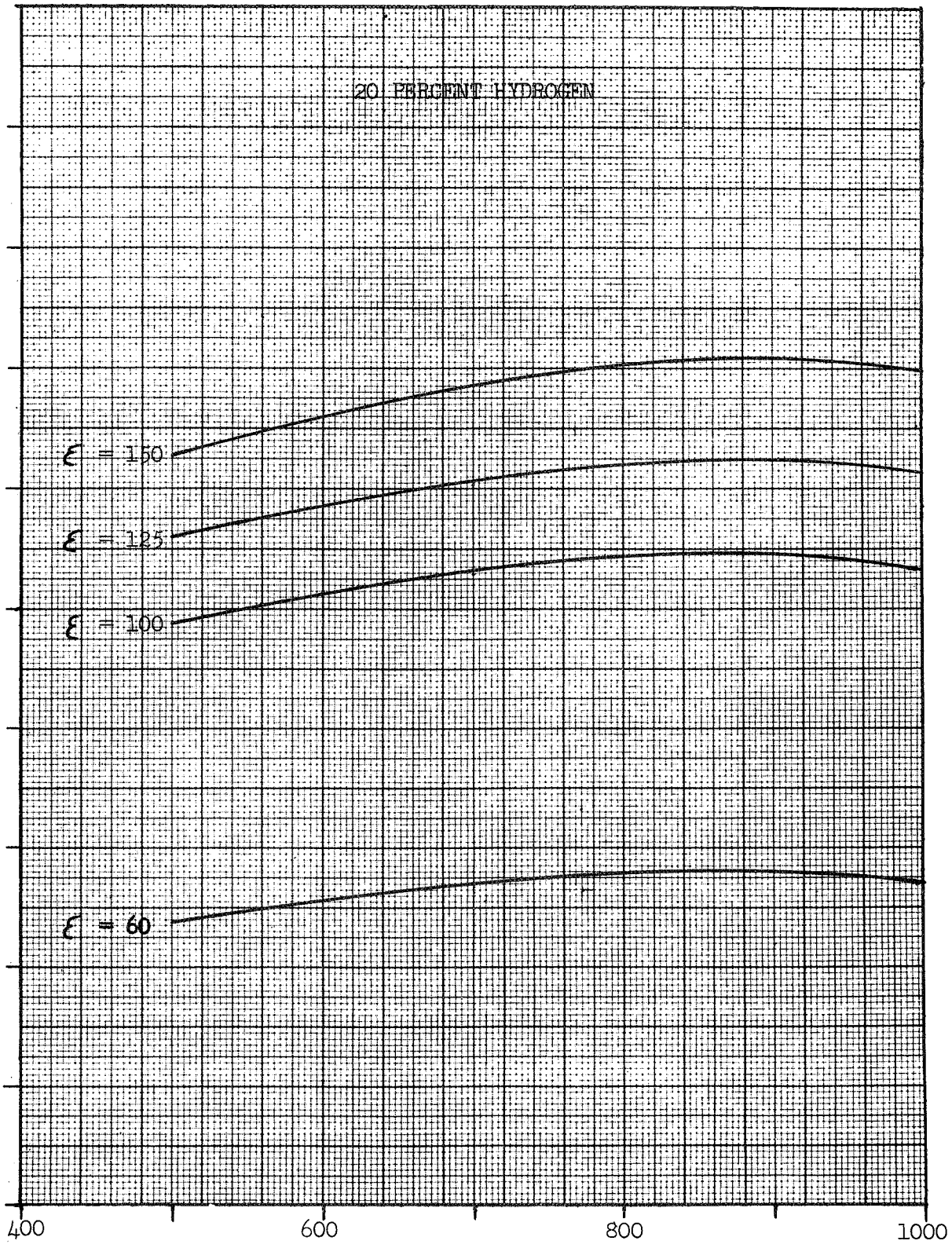

BOOSTER: ATLAS
ΔV (MISSION): 36,140 FPS
ΔV (RETRO): N/A FPS
GROSS WT: 40,000 LB

CASE: 2C5T01
☐ H2/F2
☒ H2/F2/LI - GEL

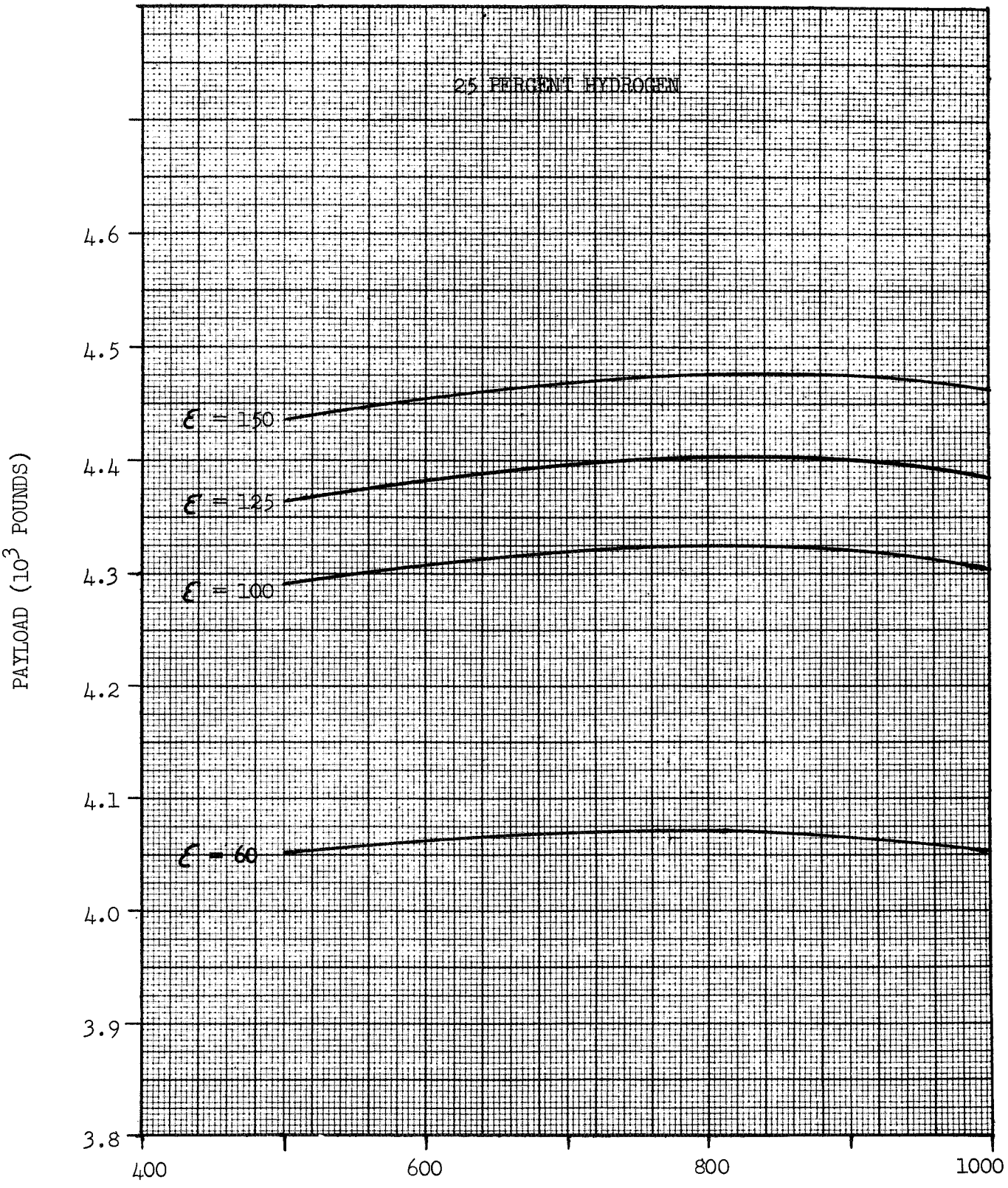

BOOSTER: ATLAS
ΔV (MISSION): 36,140 FPS
ΔV (RETRO): N/A FPS
GROSS WT: 40,000

CASE: 205T01
☐ H2/F2
☒ H2/F2/LI - GEL

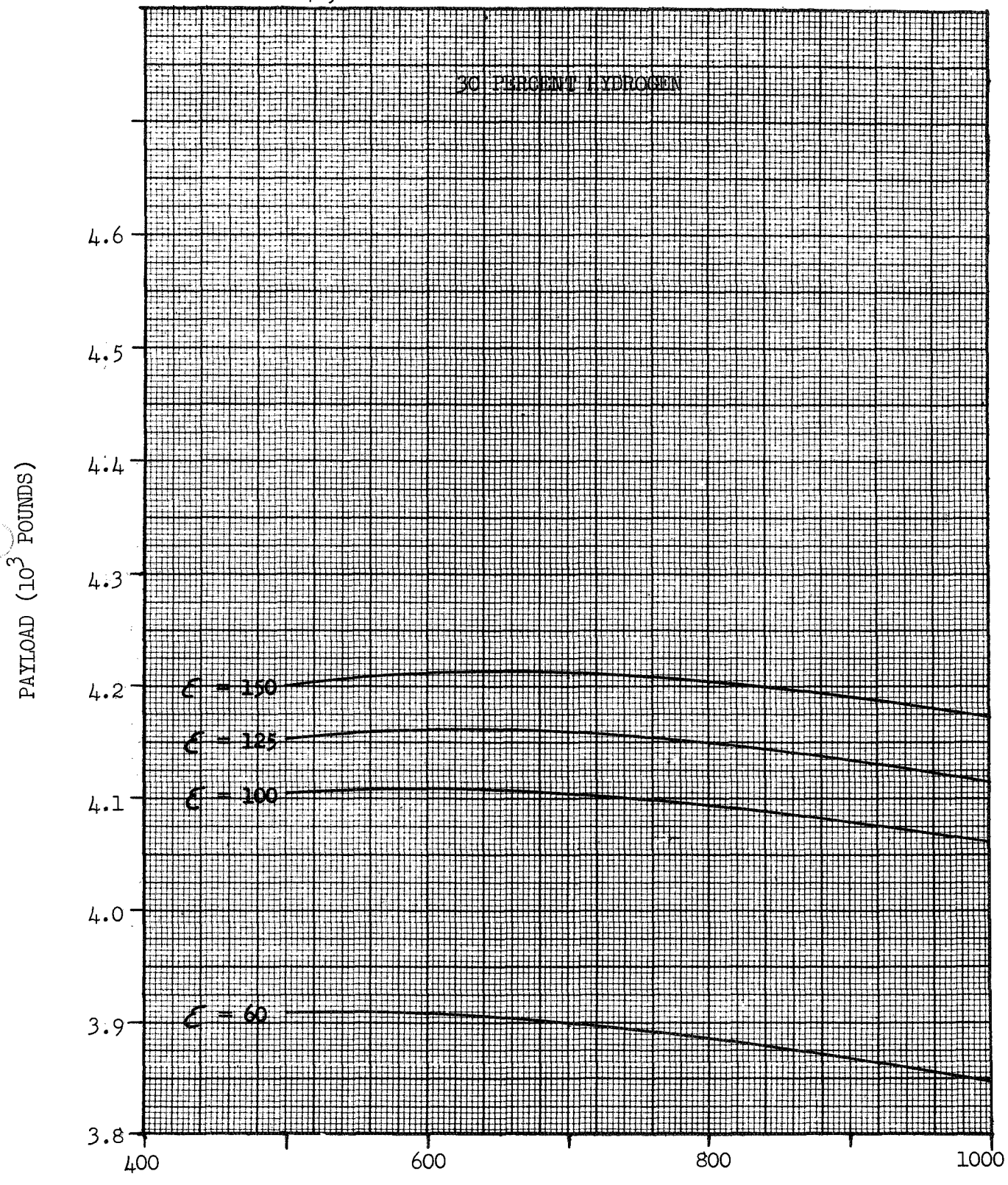

BOOSTER: ATLAS
ΔV (MISSION): 36,140 FPS
ΔV (RETRO): N/A FPS
GROSS WT: 40,000 LB

CASE: 2C5T01
☐ H2/F2
☒ H2/F2/LI - GEL

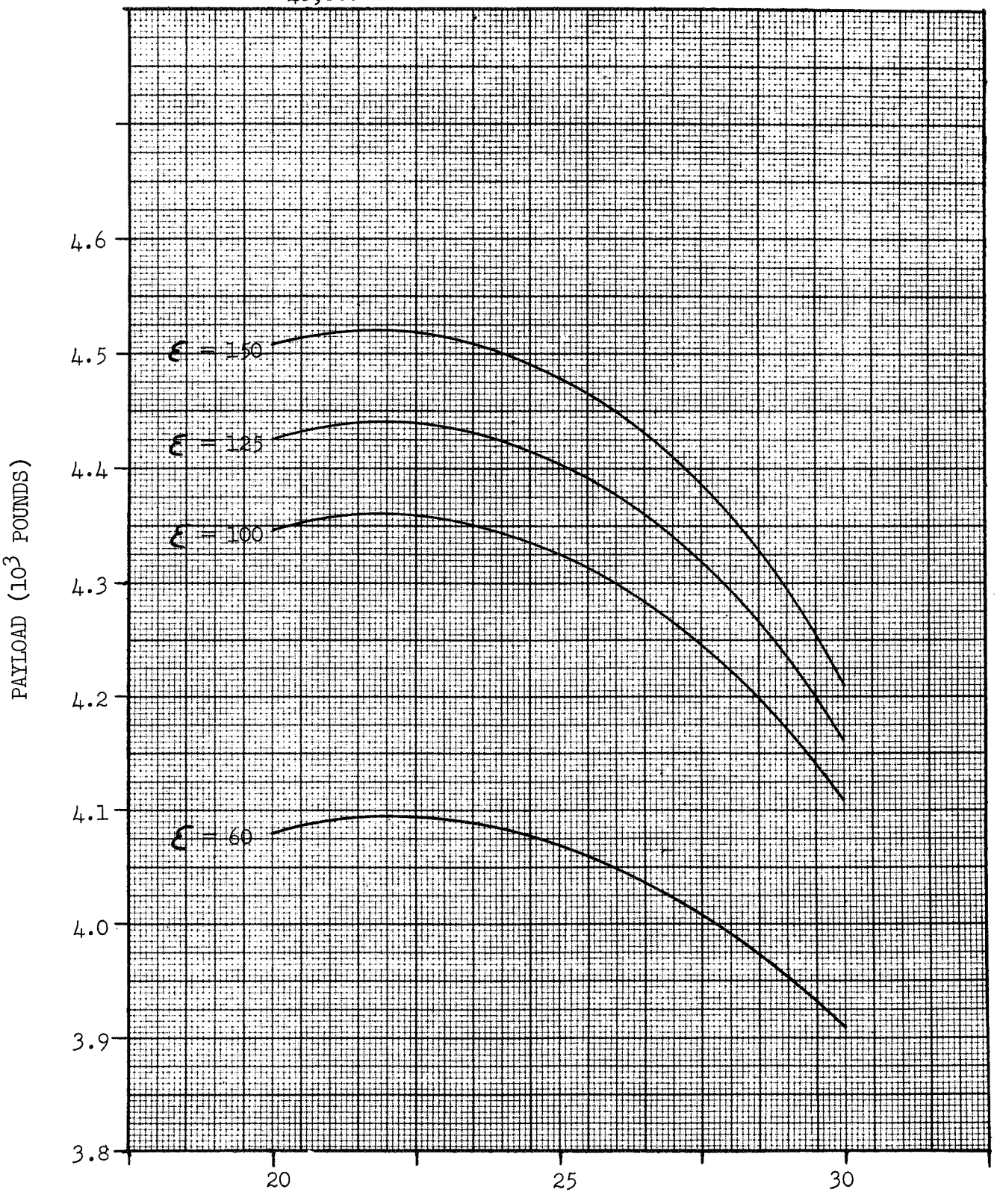

BOOSTER: ATLAS
ΔV (MISSION): 36,140 FPS
ΔV (RETRO): N/A FPS
GROSS WT: 40,000

CASE: 2C5T01
☐ H2/F2
☒ H2/F2/LI-GEL

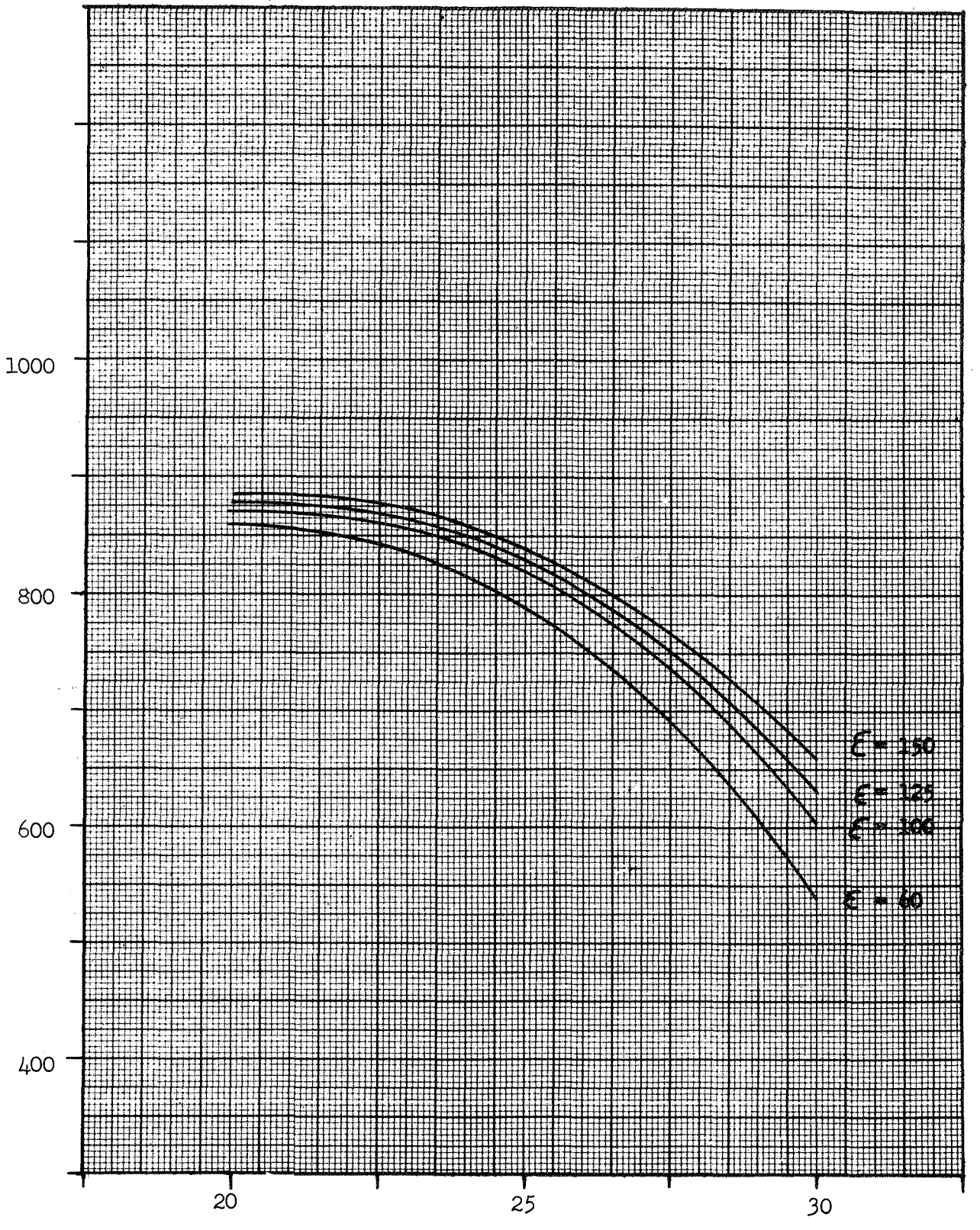

BOOSTER: ATLAS
ΔV (MISSION): 36,140 FPS
ΔV (RETRO): N/A FPS
GROSS WT: 40,000

CASE: 2C5T01
☐ H2/F2
☒ H2/F2/LI - GEL

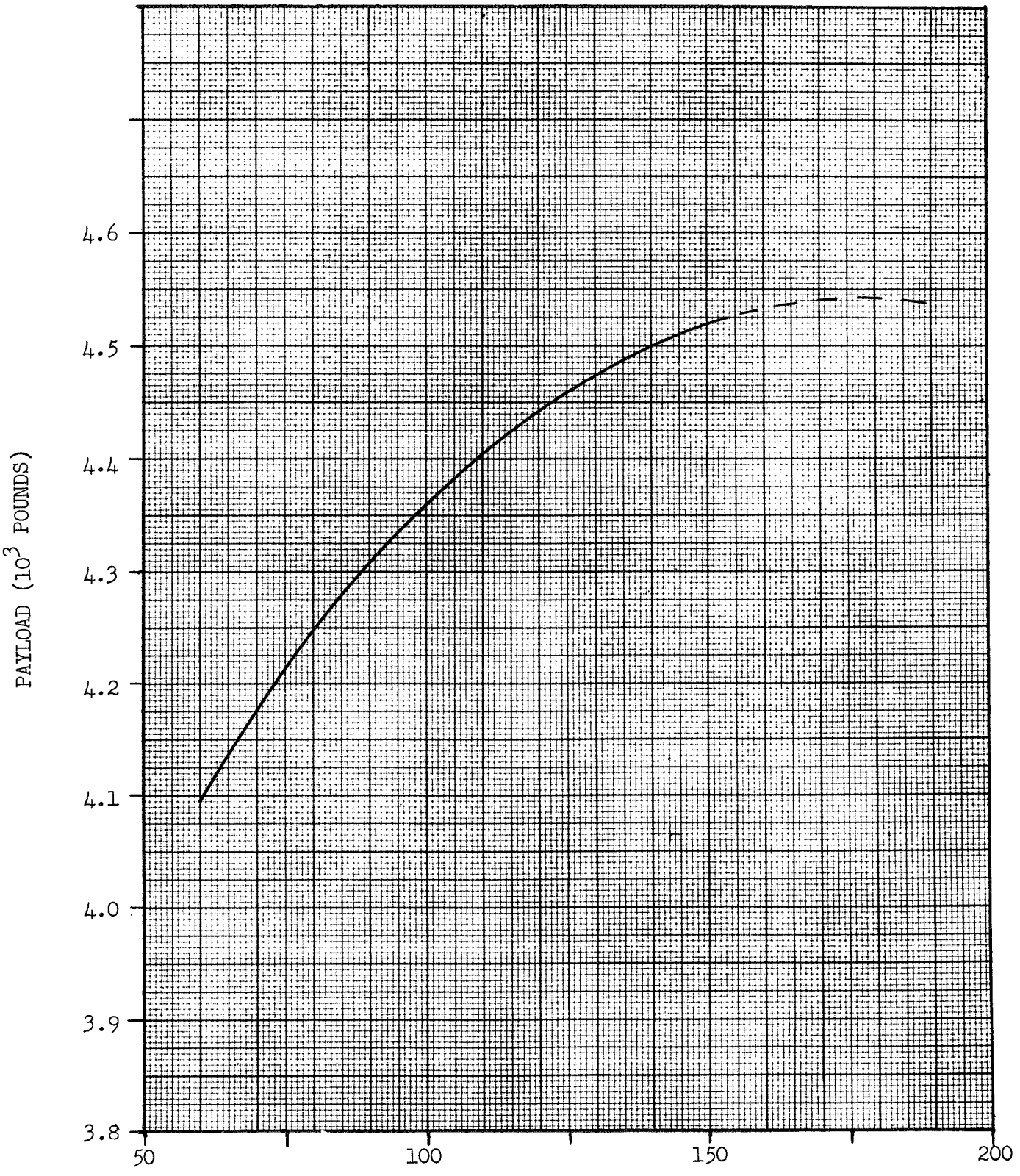

BOOSTER: ATLAS
ΔV (MISSION): 36,140 FPS
ΔV (RETRO): N/A FPS

CASE: 2C5T01
☐ H2/F2
☒ H2/F2/LI - GEL

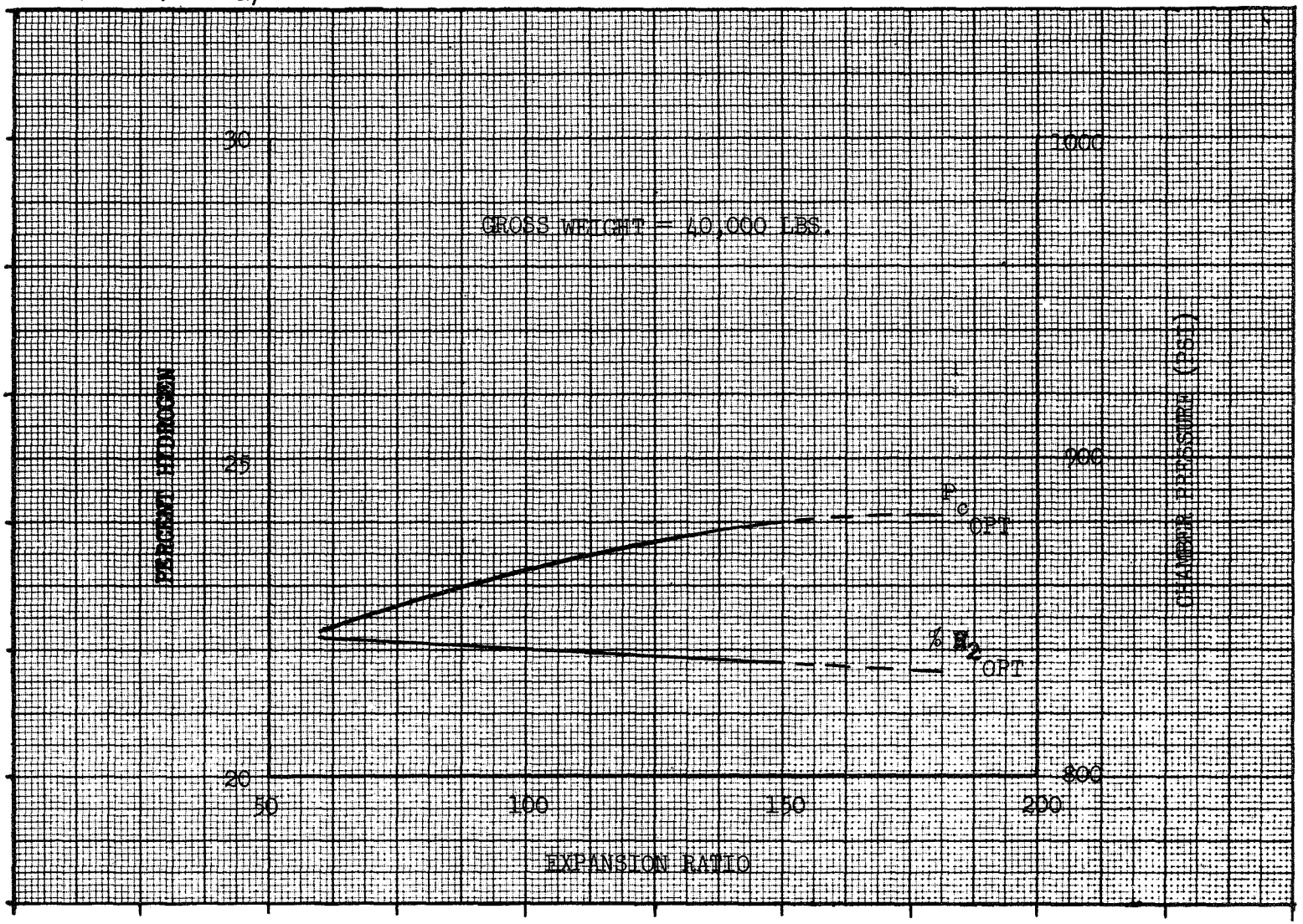

BOOSTER: ATLAS
ΔV (MISSION): 36,140 FPS
ΔV (RETRO): N/A FPS
GROSS WT: 40,000 lb

CASE: 2C5T01
☒ H2/F2
☐ H2/F2/LI

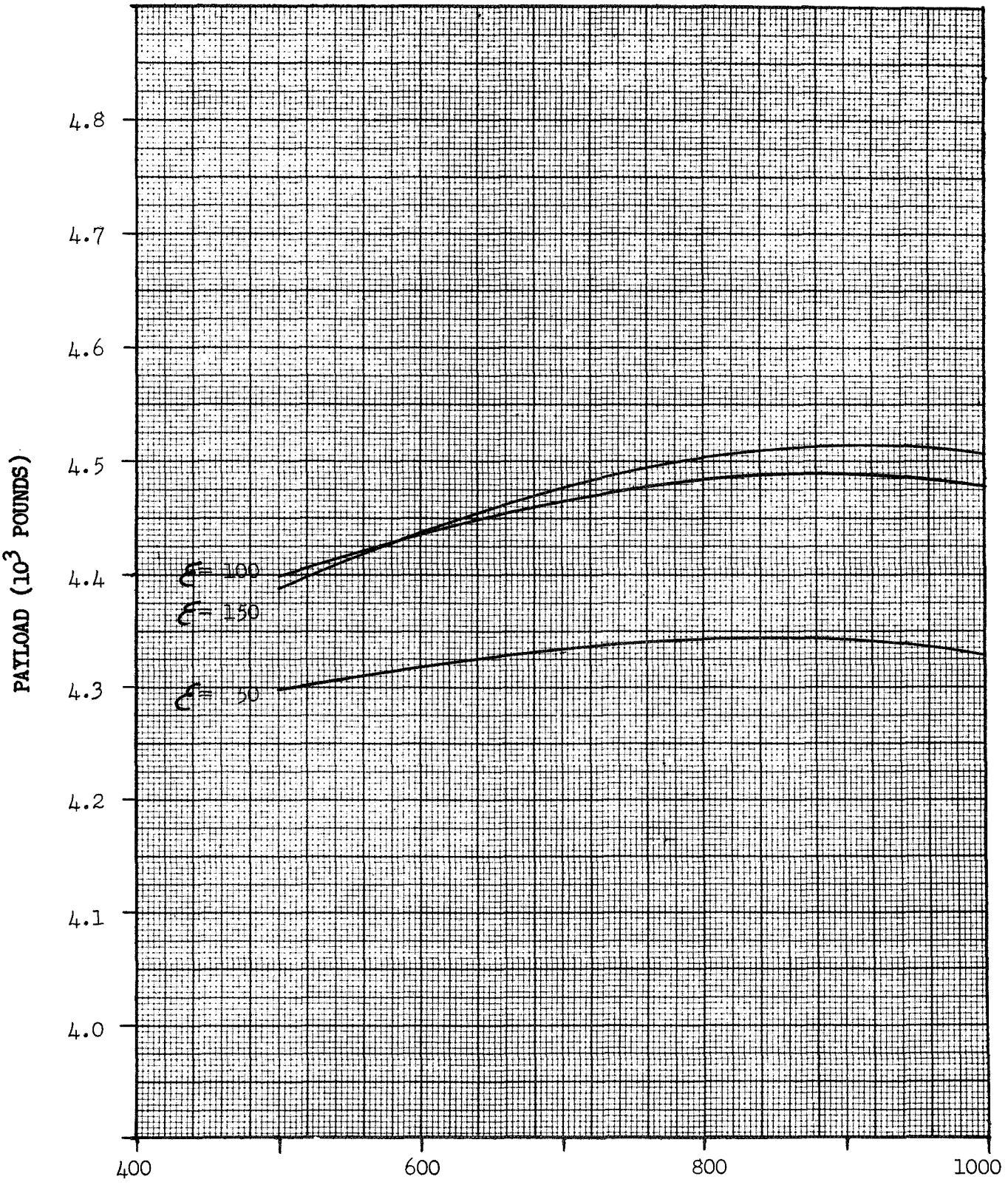

BOOSTER: ATLAS
ΔV (MISSION): 36,140 FPS
ΔV (RETRO): N/A FPS

CASE: 2C5T01
☒ H2/F2
☐ H2/F2/LI

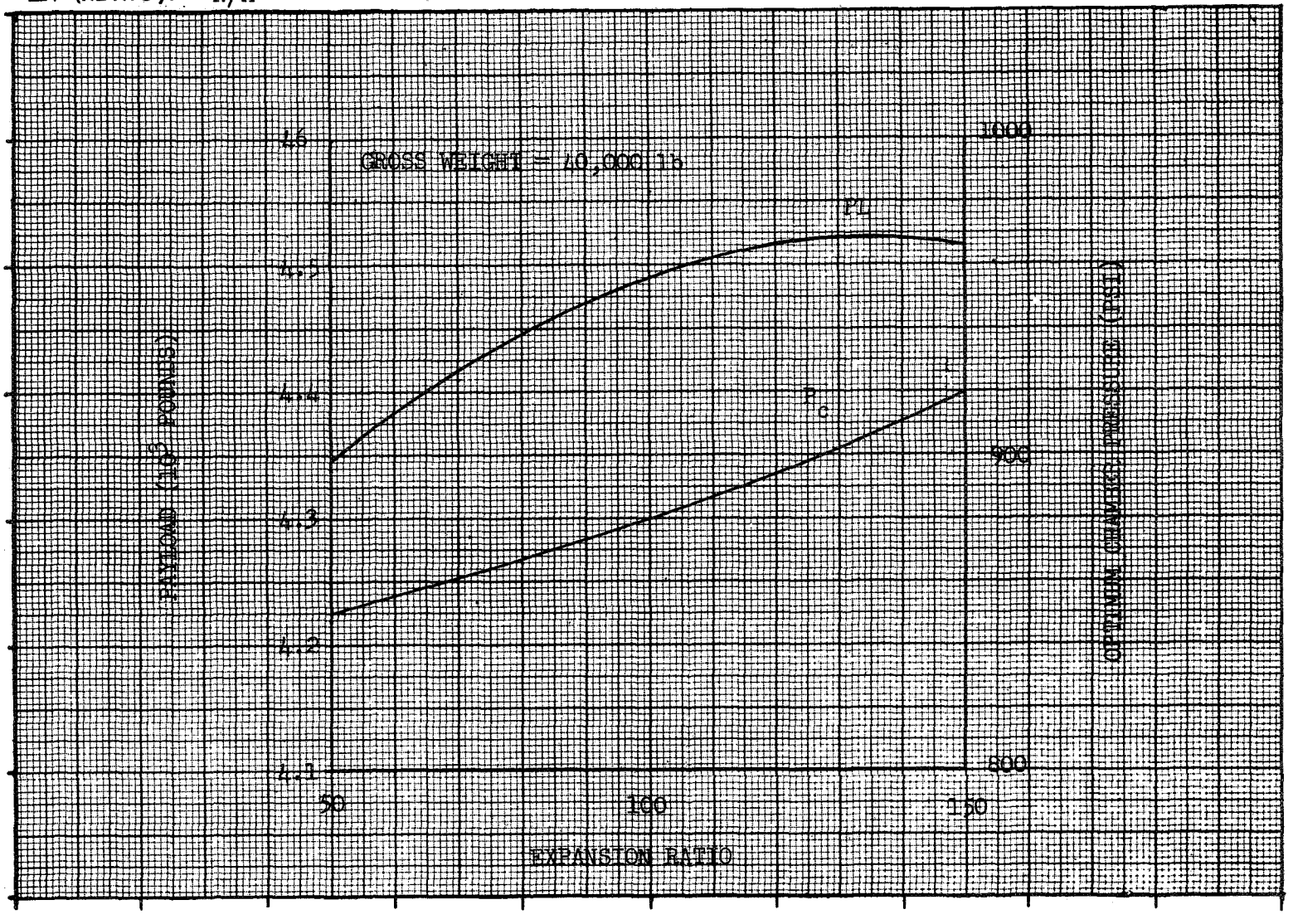

BOOSTER: ATLAS
ΔV (MISSION): 36, 140 FPS
ΔV (RETRO): N/A FPS

CASE: 2C5T01
☐ H2/F2
☐ H2/F2/LI

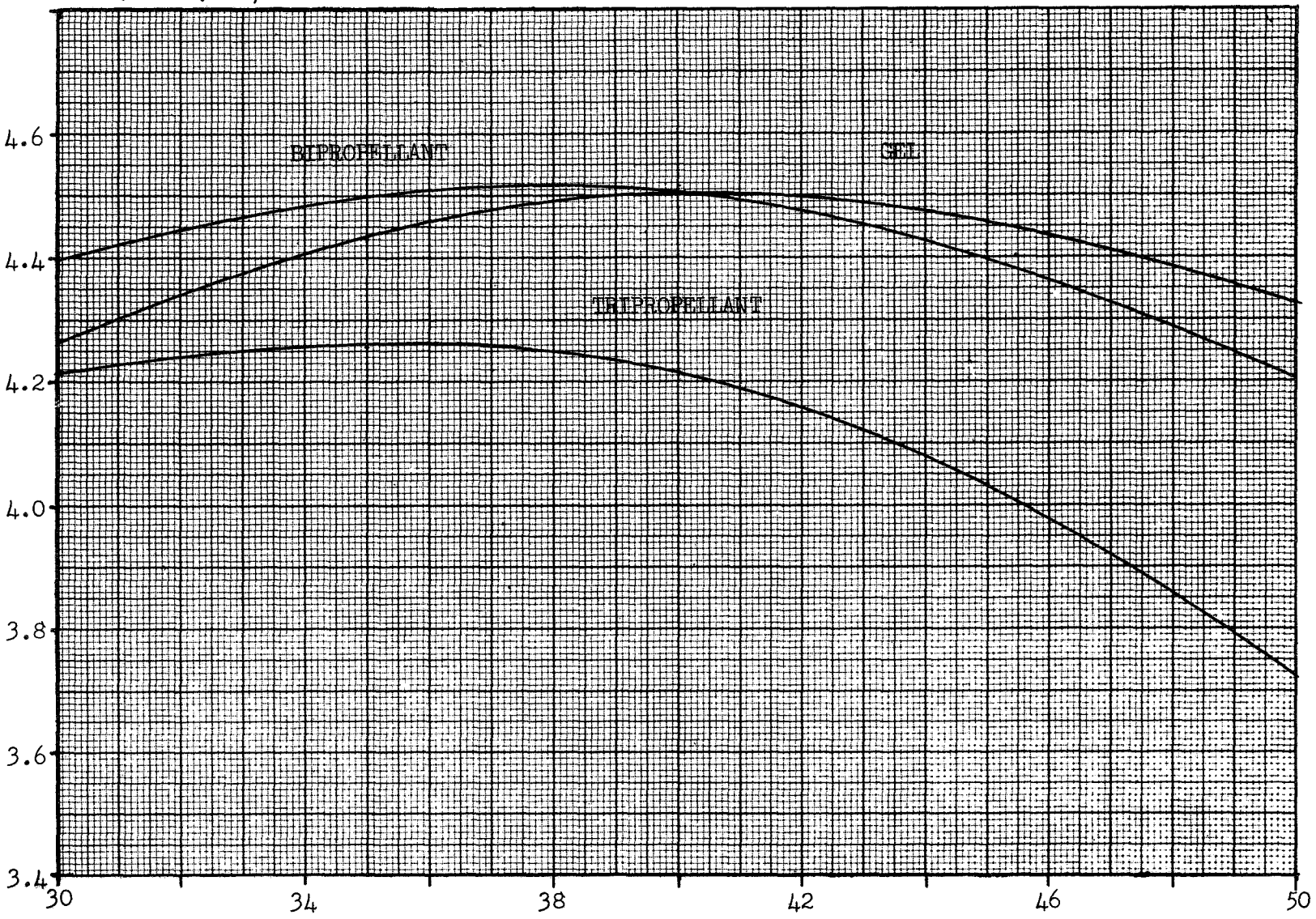

BOOSTER: Atlas/Centaur
ΔV (MISSION): 48500 FPS
ΔV (RETRO): N/A FPS
GROSS WT: 10000

CASE: 3A1T01
☐ H2/F2
☒ H2/F2/LI

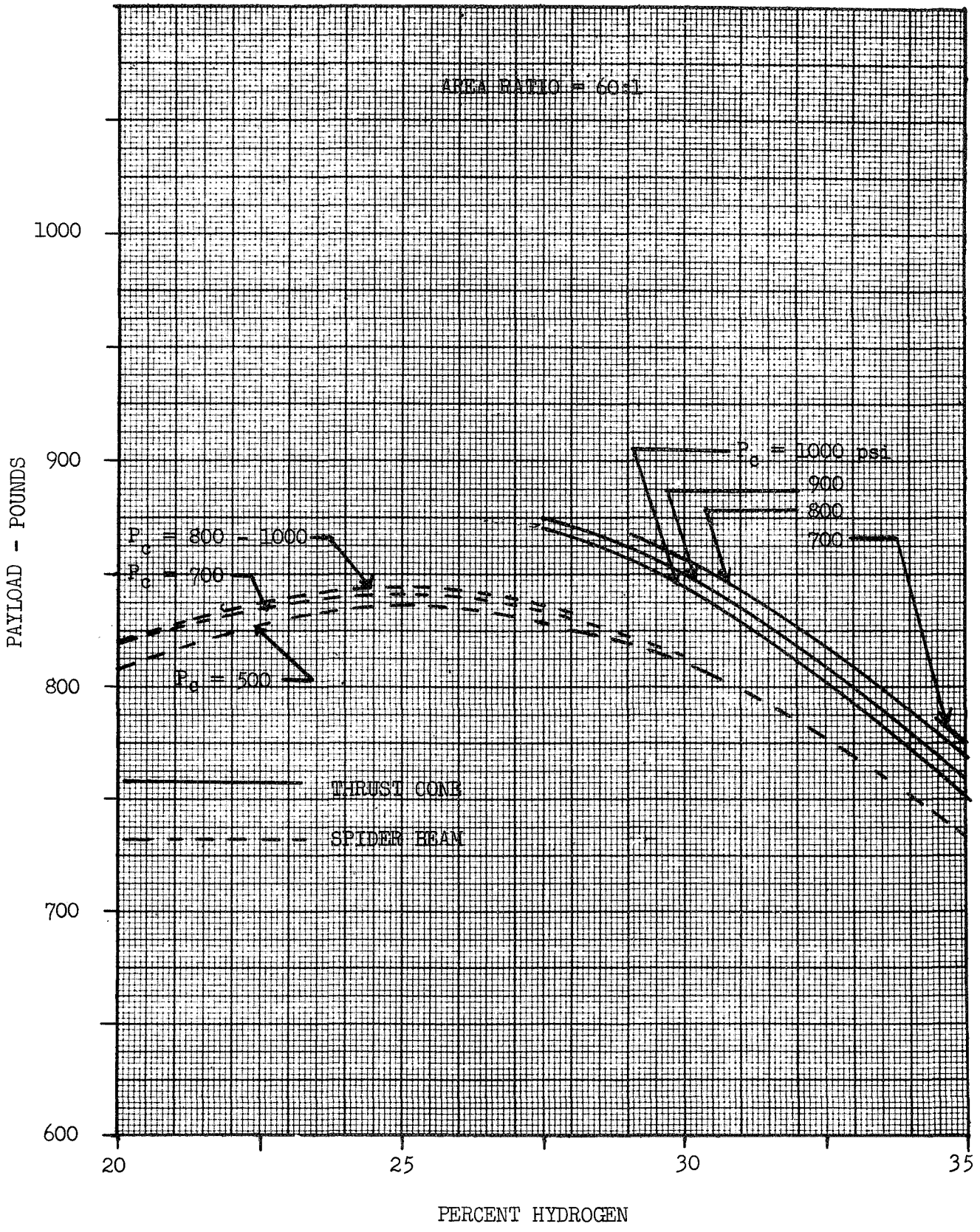

BOOSTER: Atlas/Centaur
ΔV (MISSION): 48500 FPS
ΔV (RETRO): N/A FPS
GROSS WT: 10000

CASE: 3A1T01
☐ H2/F2
☒ H2/F2/LI

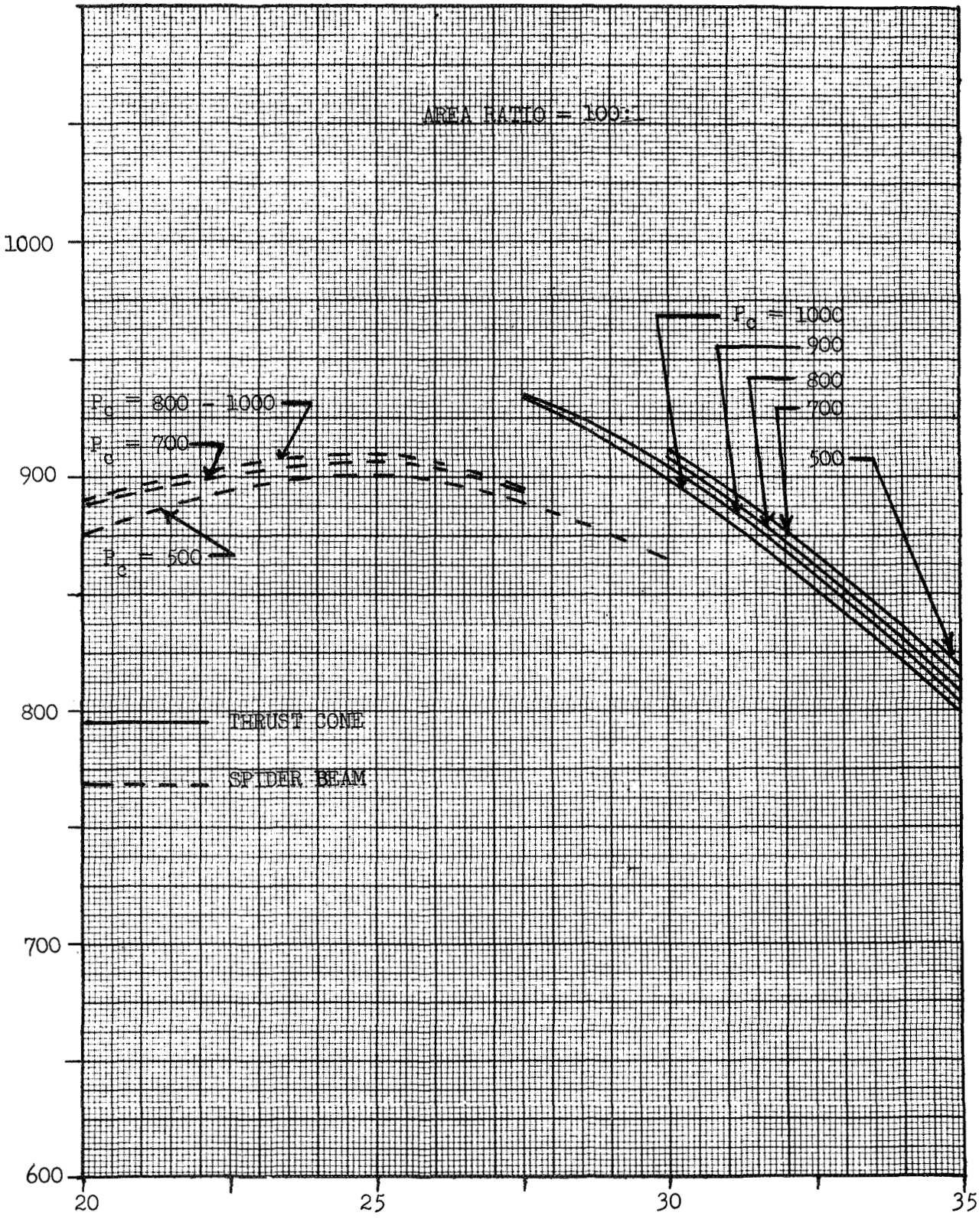

BOOSTER: Atlas/Centaur
ΔV (MISSION): 48500 FPS
ΔV (RETRO): N/A FPS
GROSS WT: 10000

CASE: 3A1T01
☐ H2/F2
☒ H2/F2/LI

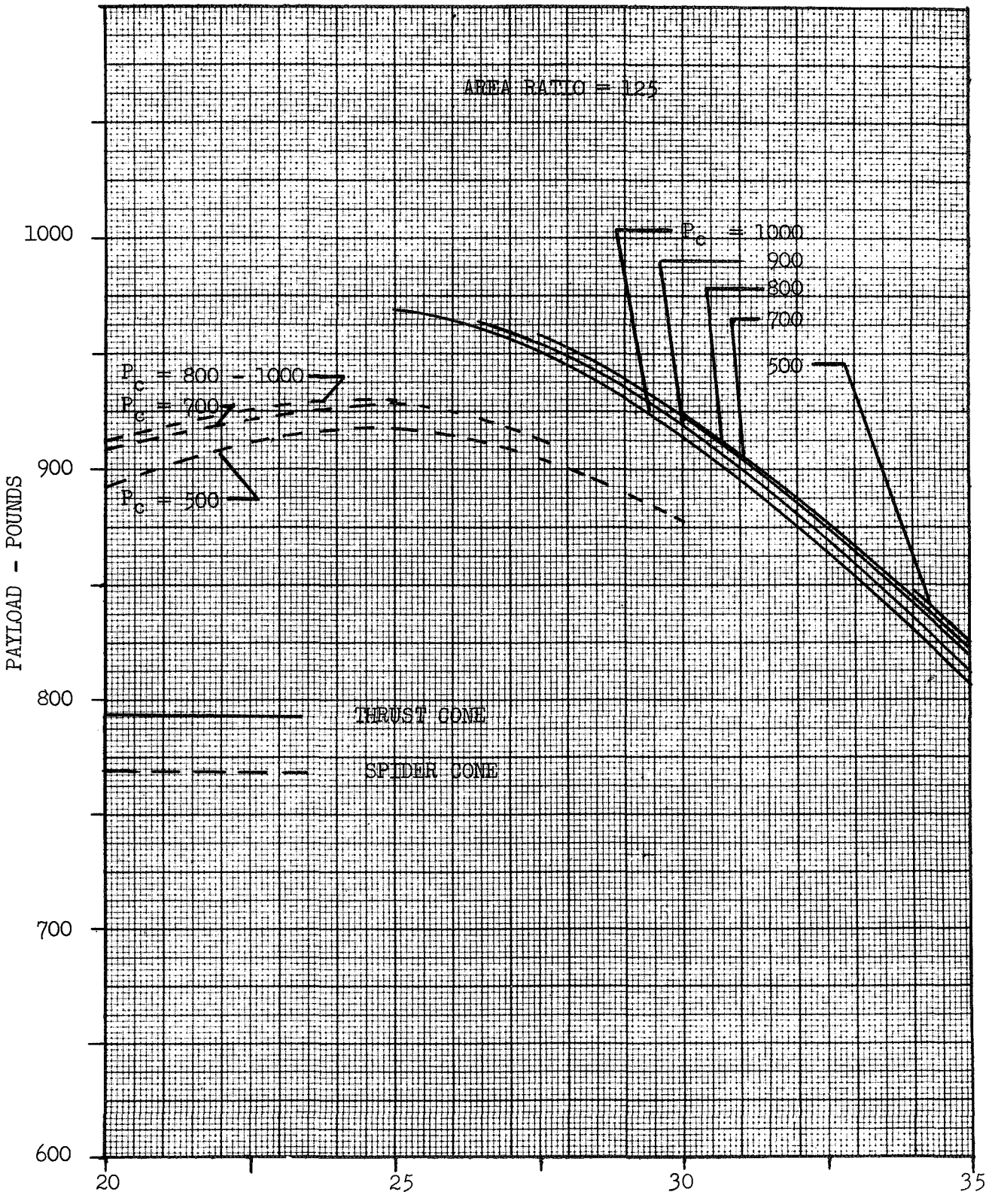

BOOSTER: Atlas/Centaur
ΔV (MISSION): 48500 FPS
ΔV (RETRO): N/A FPS
GROSS WT: 10000

CASE: 3A1T01
☐ H2/F2
☒ H2/F2/LI

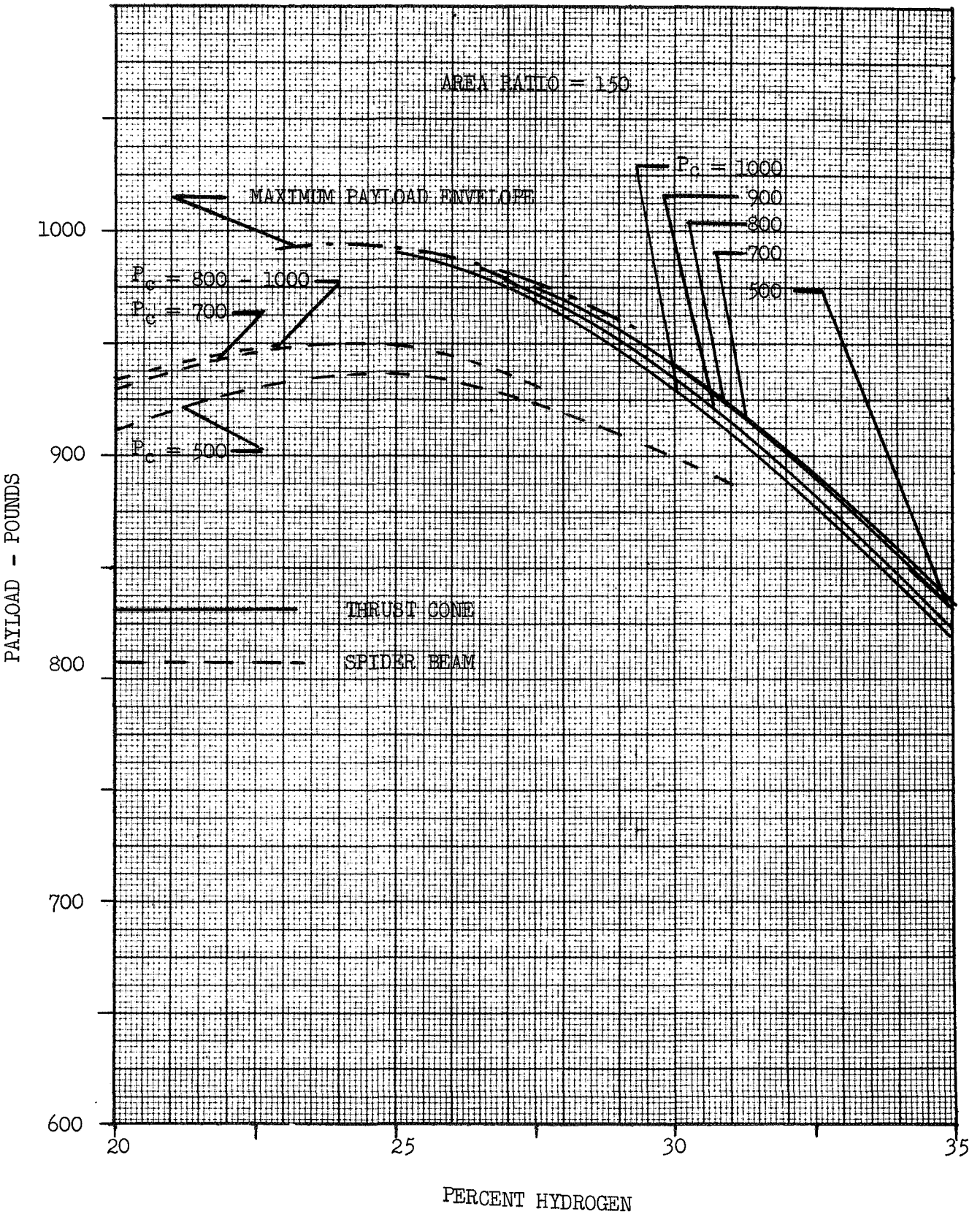

BOOSTER: ATLAS/CENTAUR
ΔV (MISSION): 48,500 FPS
ΔV (RETRO): N/A FPS
GROSS WT: 10,000

CASE: 3A1T01
☐ H2/F2
☒ H2/F2/LI

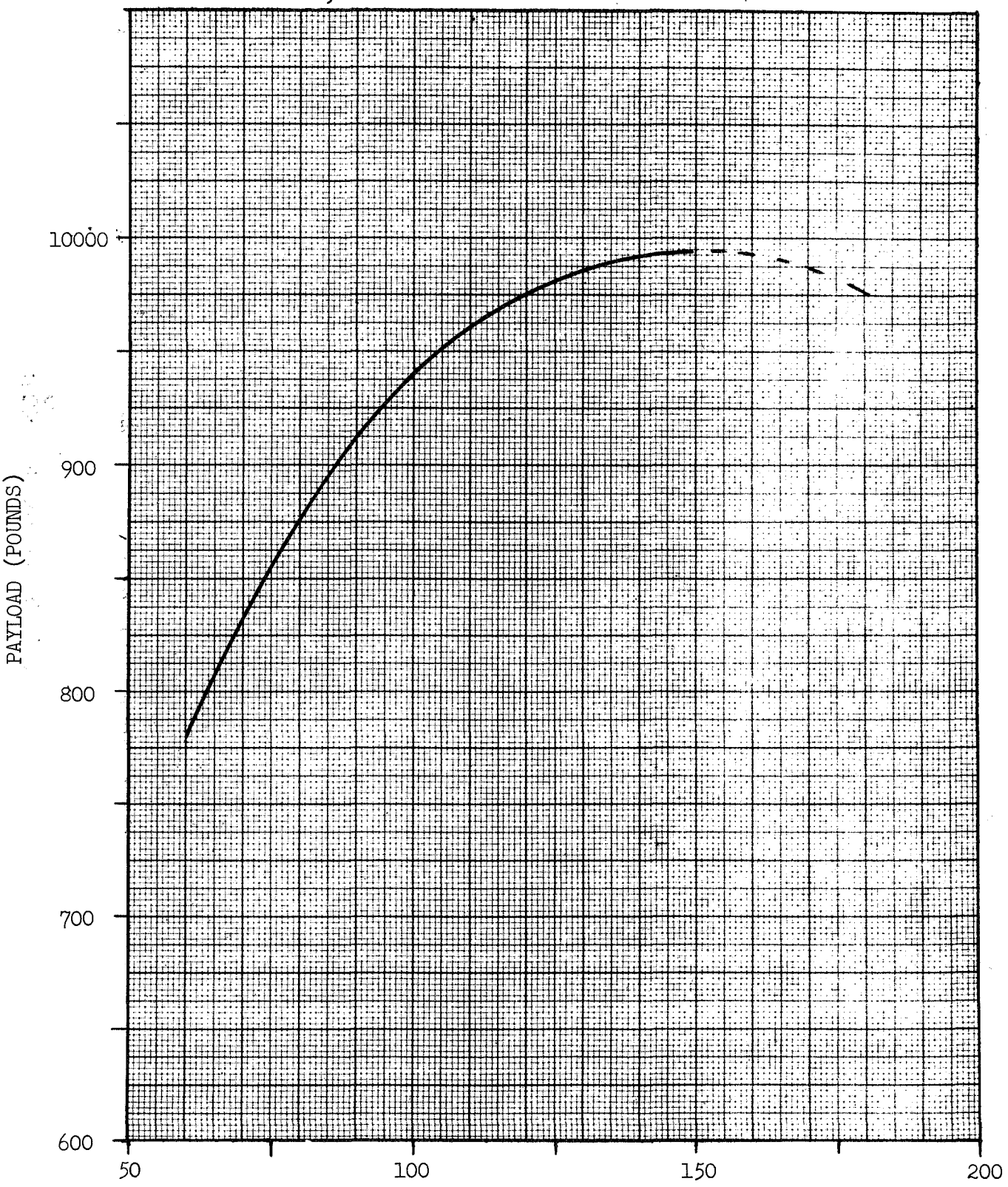

BOOSTER: Atlas/Centaur
ΔV (MISSION): 48500 FPS
ΔV (RETRO): N/A FPS

CASE: 3A1T01
☐ H2/F2
☒ H2/F2/LI

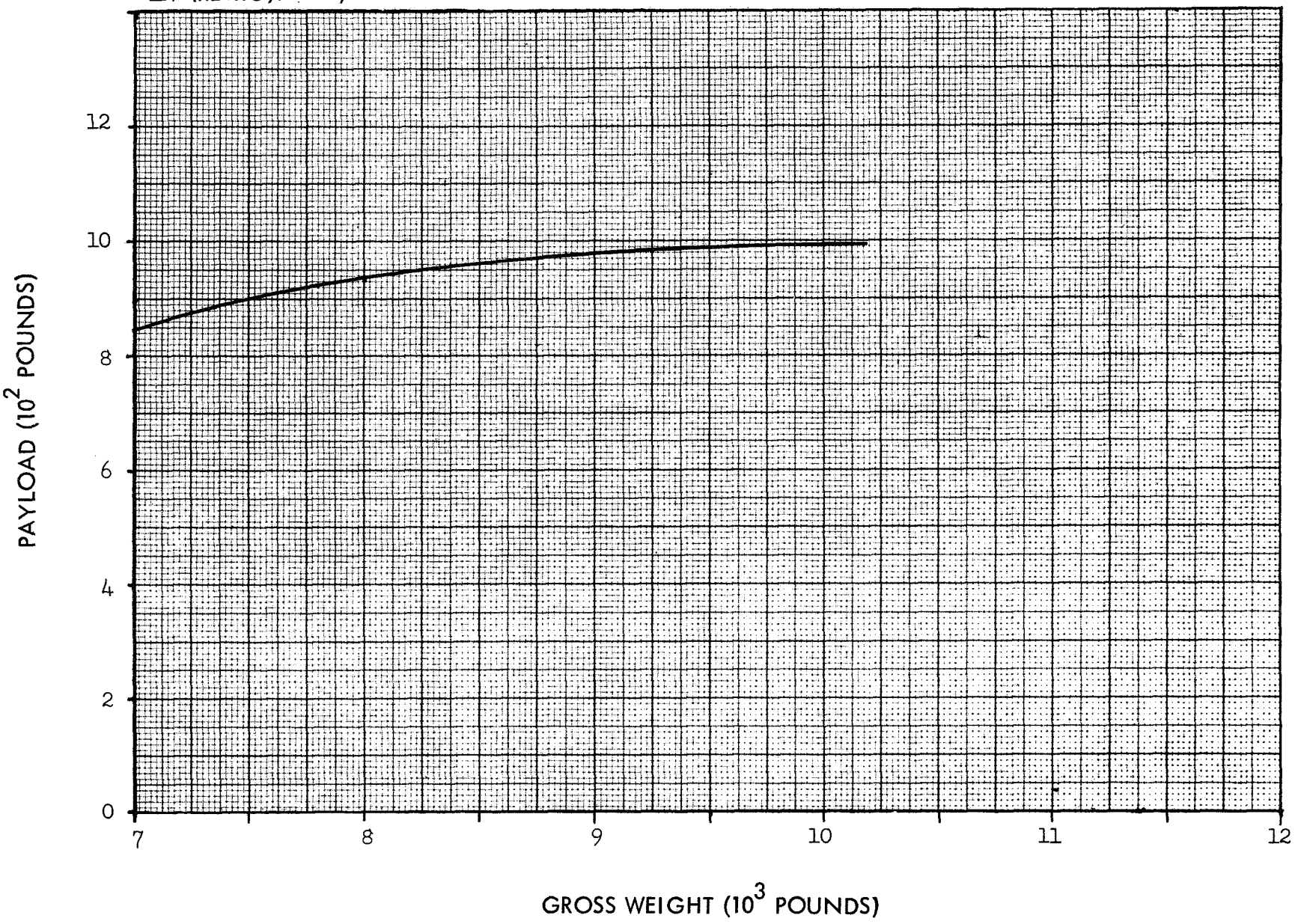

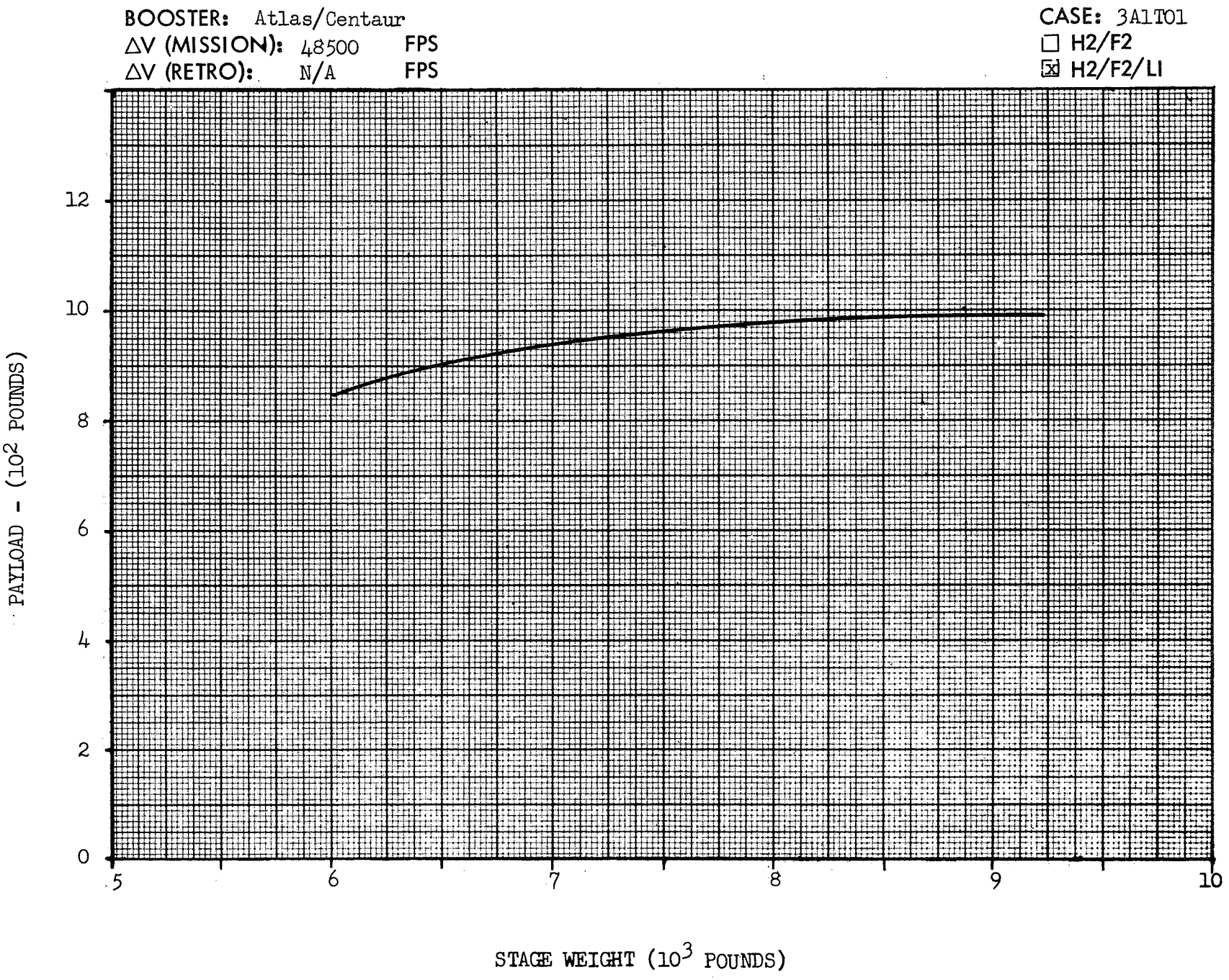
BOOSTER: Atlas/Centaur
ΔV (MISSION): 48500 FPS
ΔV (RETRO): N/A FPS
CASE: 3A1T01
☐ H2/F2
☒ H2/F2/LI
PAYLOAD - (10^2 POUNDS)
0
2
4
6
8
10
12
5
6
7
8
9
10
STAGE WEIGHT (10^3 POUNDS)

BOOSTER: Atlas/Centaur
ΔV (MISSION): 48500 FPS
ΔV (RETRO): N/A FPS

CASE: 3A1T01
☐ H2/F2
☒ H2/F2/LI

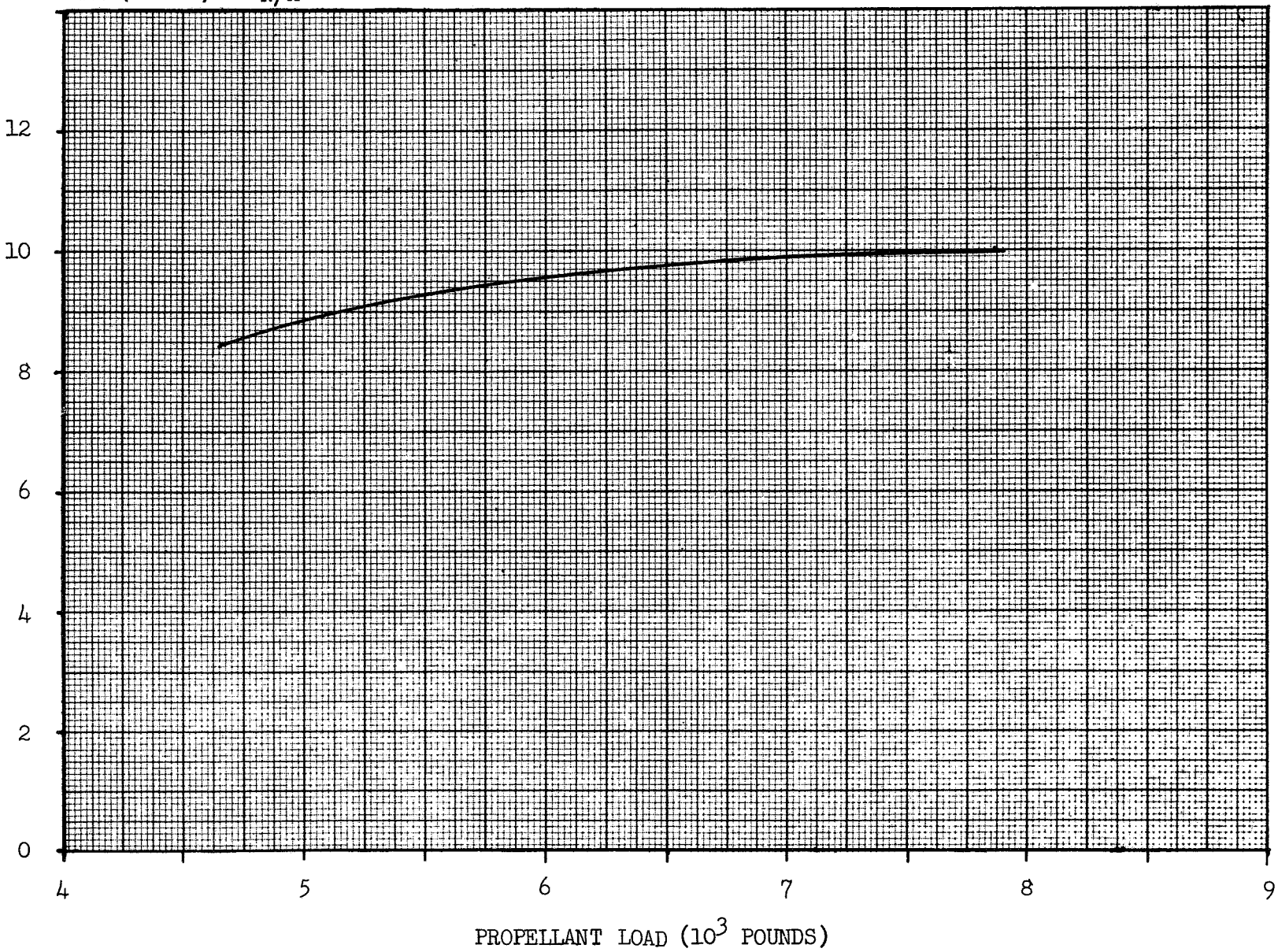

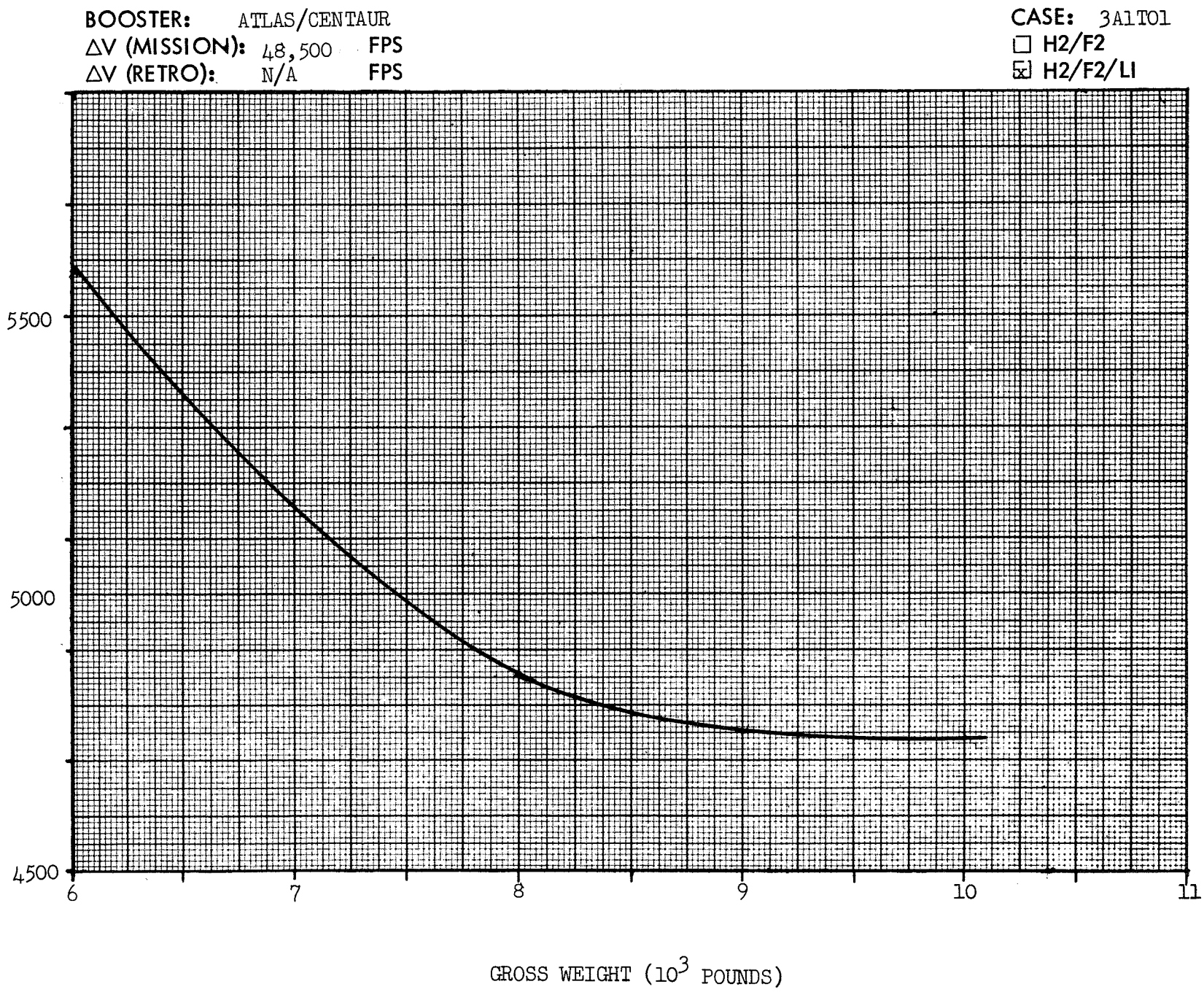
BOOSTER: ATLAS/CENTAUR
ΔV (MISSION): 48,500 FPS
ΔV (RETRO): N/A FPS
CASE: 3A1TO1
☐ H2/F2
☒ H2/F2/LI
COST EFFECTIVENESS ($/lb of Payload)
5500
5000
4500
6
7
8
9
10
11
GROSS WEIGHT (10^3 POUNDS)

BOOSTER: Atlas/Centaur
ΔV (MISSION): 36,140 FPS
ΔV (RETRO): N/A FPS

CASE: 3C1T01
☐ H2/F2
☒ H2/F2/LI

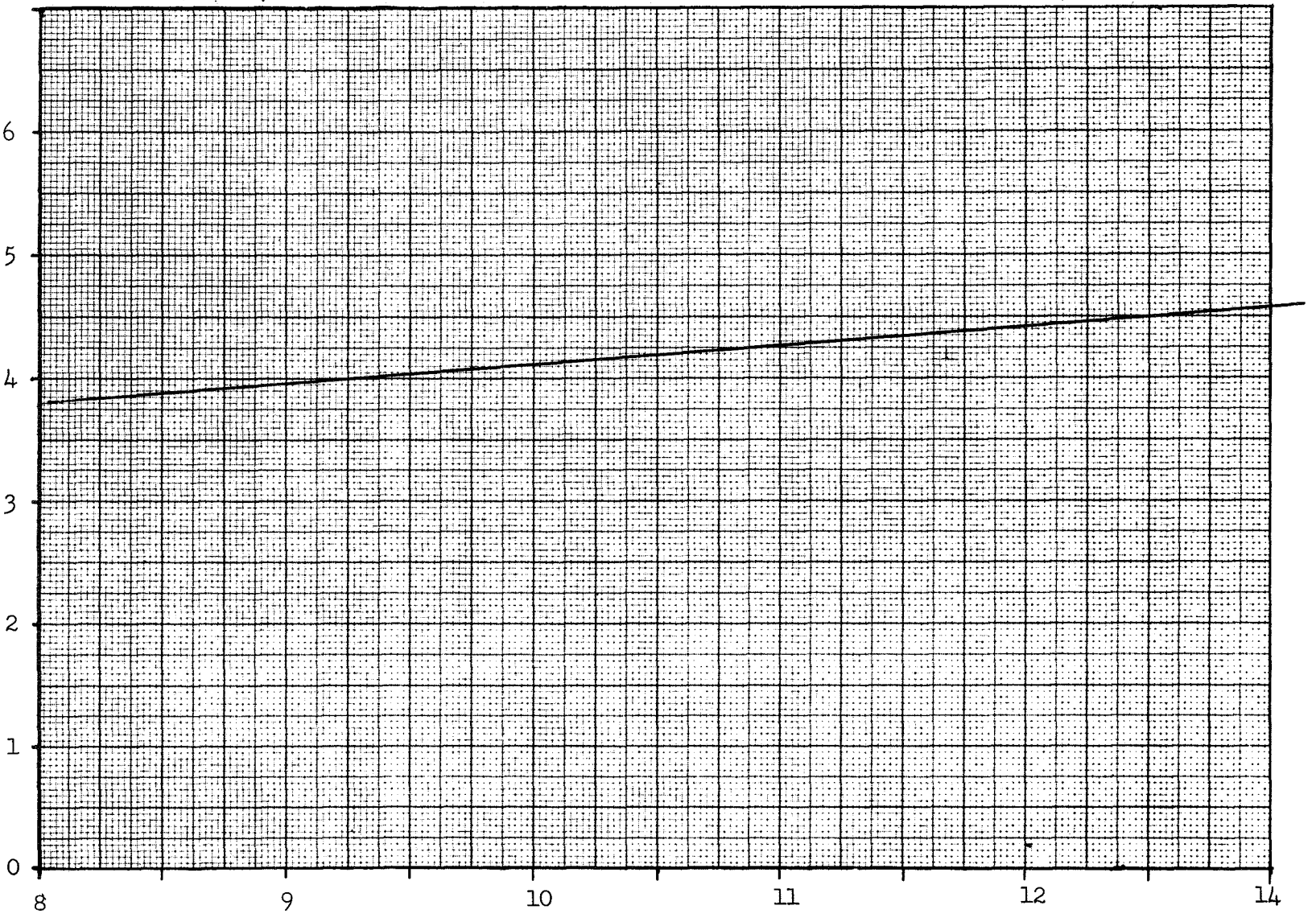

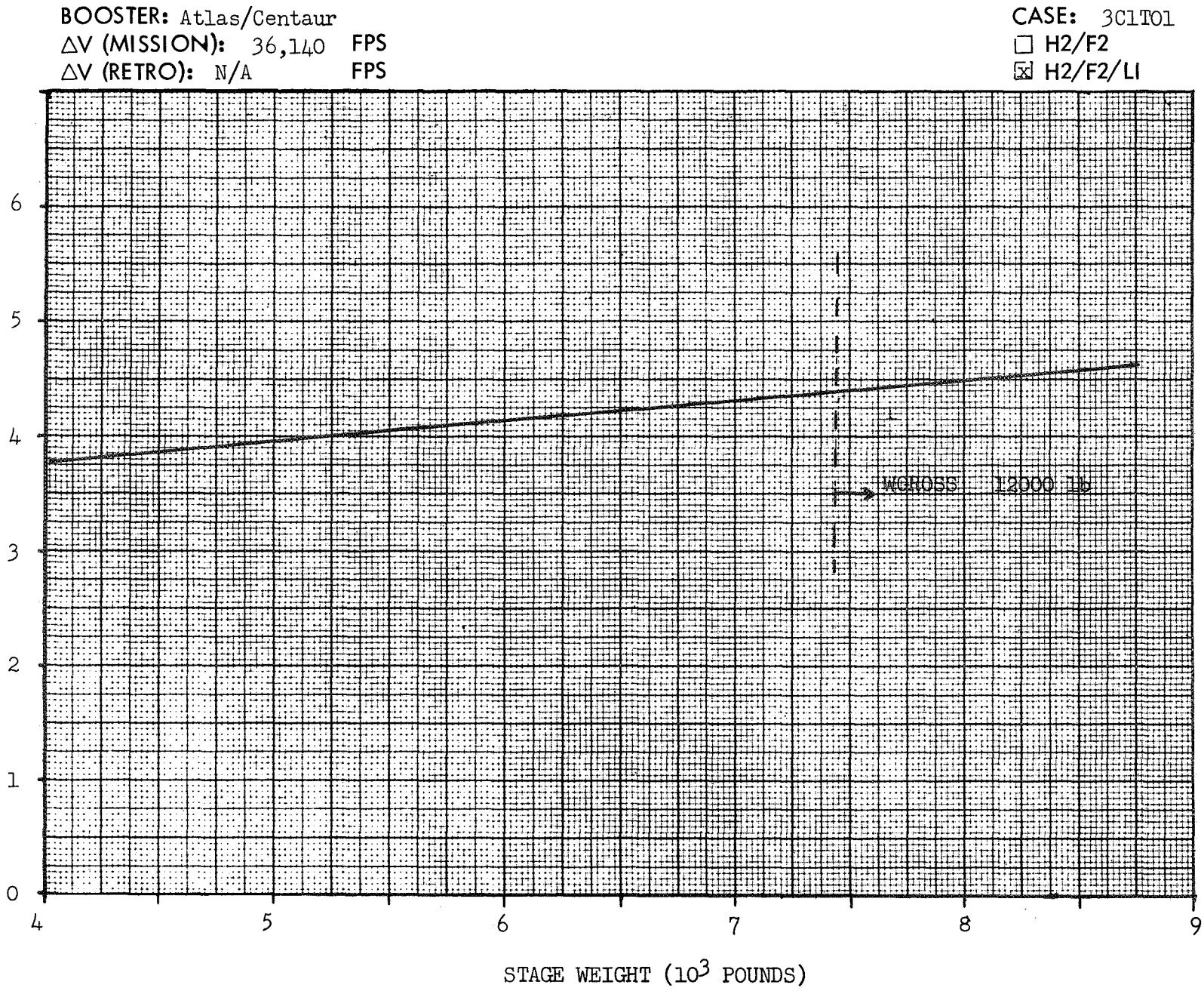
BOOSTER: Atlas/Centaur
ΔV (MISSION): 36,140 FPS
ΔV (RETRO): N/A FPS
CASE: 3C1T01
☐ H2/F2
☒ H2/F2/LI
WGROSS 12000 lb
PAYLOAD (10^2 POUNDS)
STAGE WEIGHT (10^3 POUNDS)
0
1
2
3
4
5
6
4
5
6
7
8
9

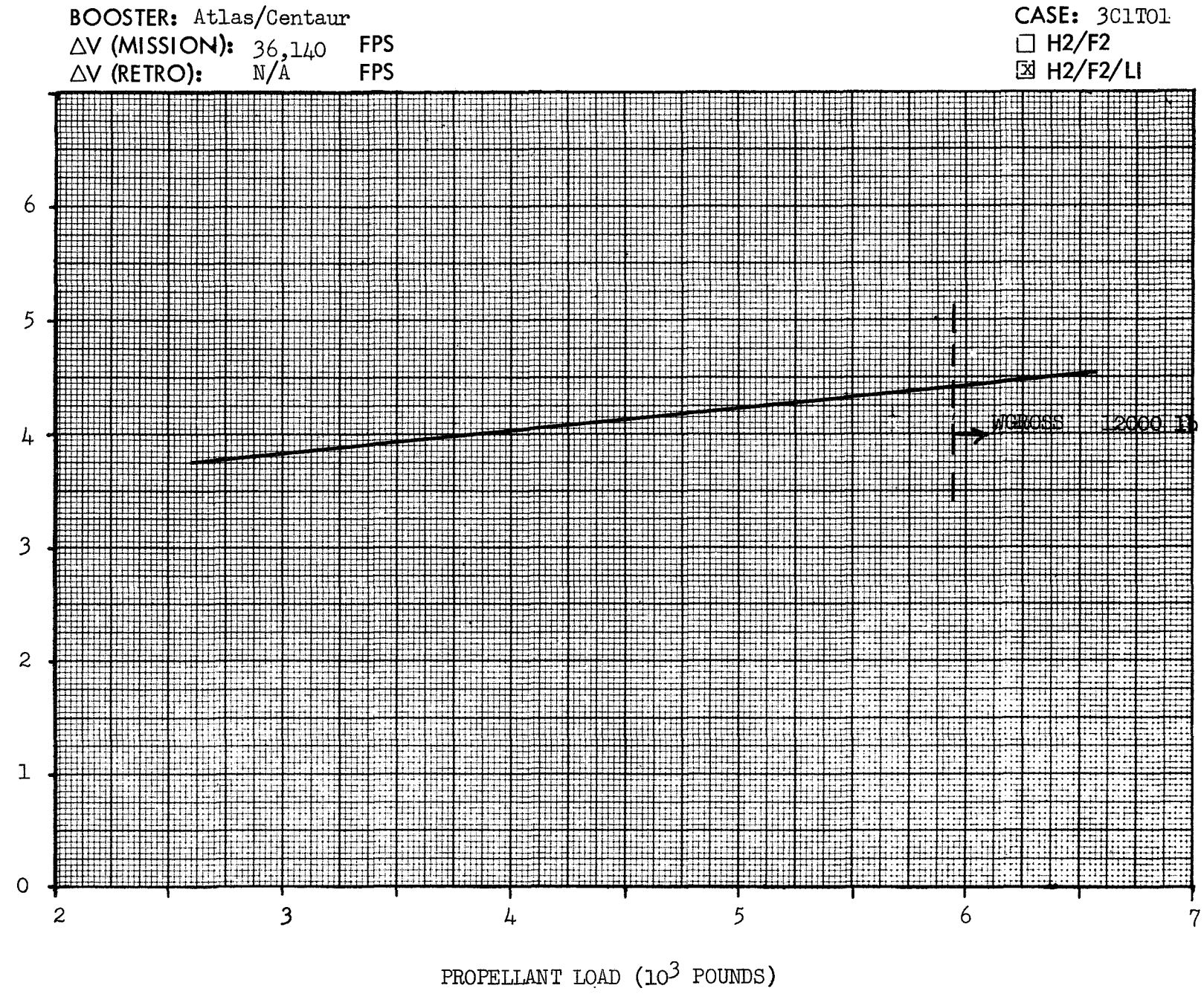
BOOSTER: Atlas/Centaur
ΔV (MISSION): 36,140 FPS
ΔV (RETRO): N/A FPS
CASE: 3C1T01
☐ H2/F2
☒ H2/F2/LI
WGROSS 12000 lb
PAYLOAD (10^2 POUNDS)
PROPELLANT LOAD (10^3 POUNDS)
0
1
2
3
4
5
6
2
3
4
5
6
7

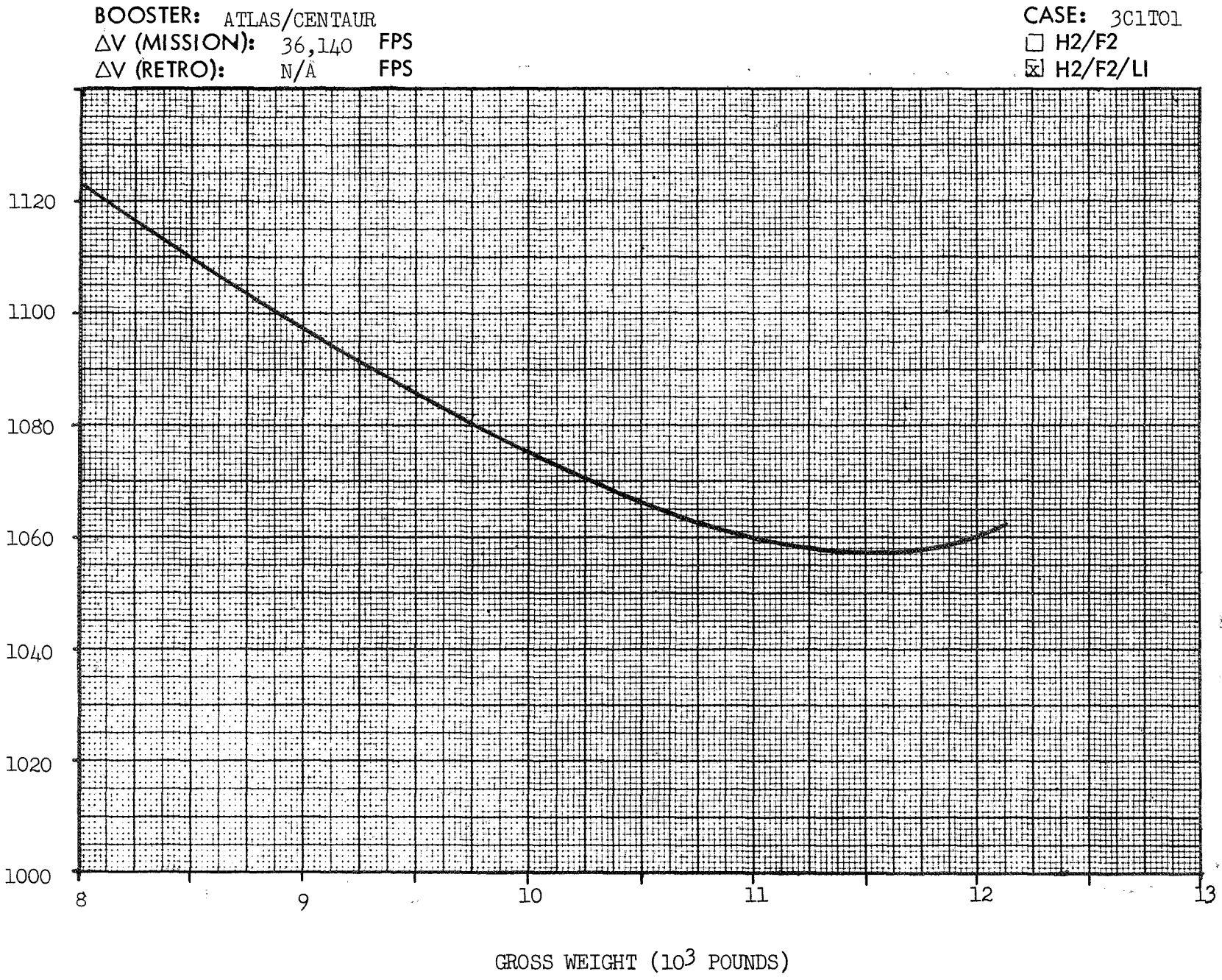
BOOSTER: ATLAS/CENTAUR
ΔV (MISSION): 36,140 FPS
ΔV (RETRO): N/A FPS
CASE: 3C1TO1
☐ H2/F2
☒ H2/F2/LI
COST EFFECTIVENESS ($/lb of Payload)
1120
1100
1080
1060
1040
1020
1000
8
9
10
11
12
13
GROSS WEIGHT (10³ POUNDS)

BOOSTER: Atlas/Centaur
ΔV (MISSION): 54500 FPS
ΔV (RETRO): N/A FPS

CASE: 3E1T01
☐ H2/F2
☒ H2/F2/LI

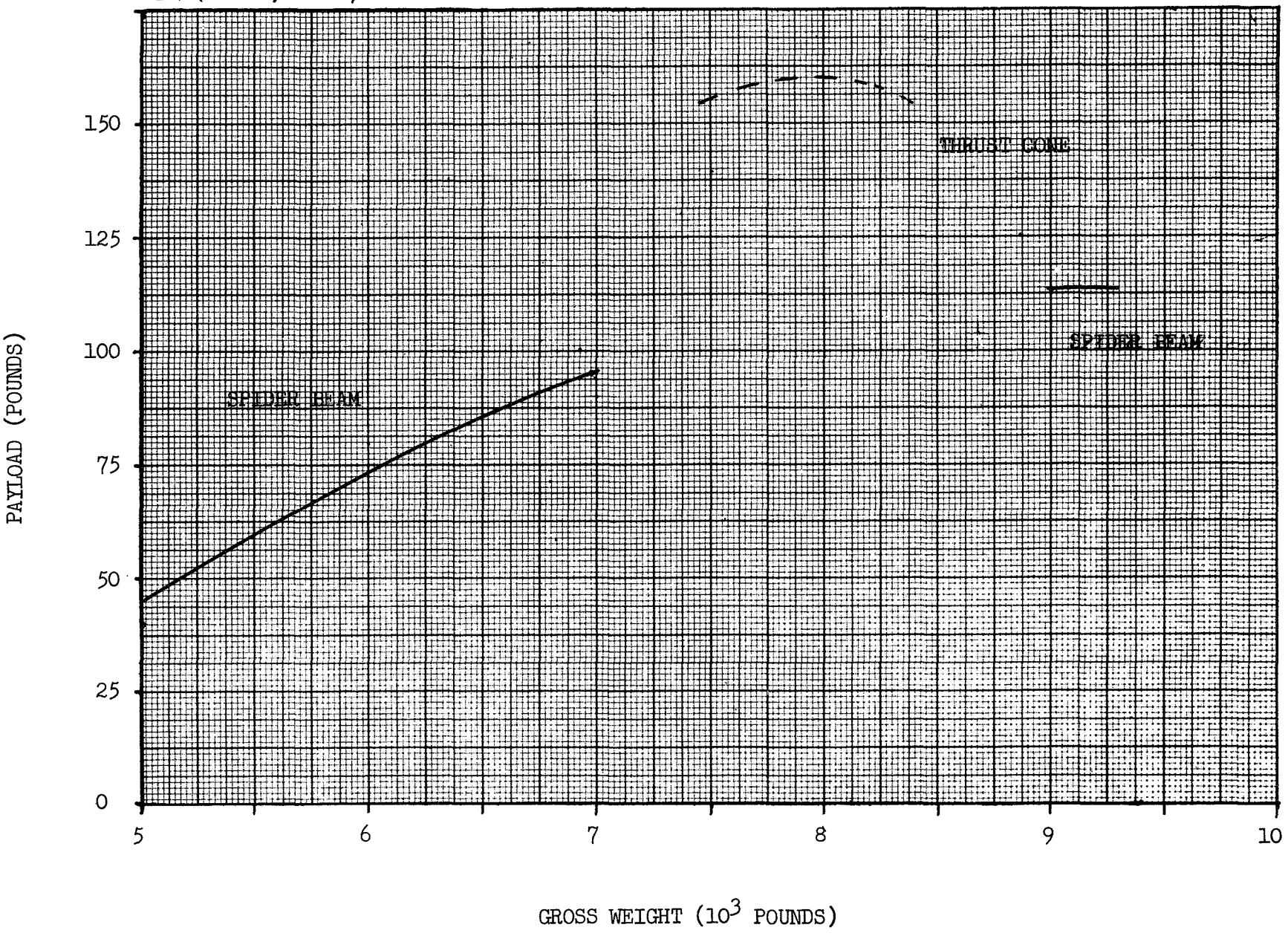

BOOSTER: Atlas/Centaur
ΔV (MISSION): 54500 FPS
ΔV (RETRO): N/A FPS

CASE: 3E1T01
☐ H2/F2
☒ H2/F2/LI

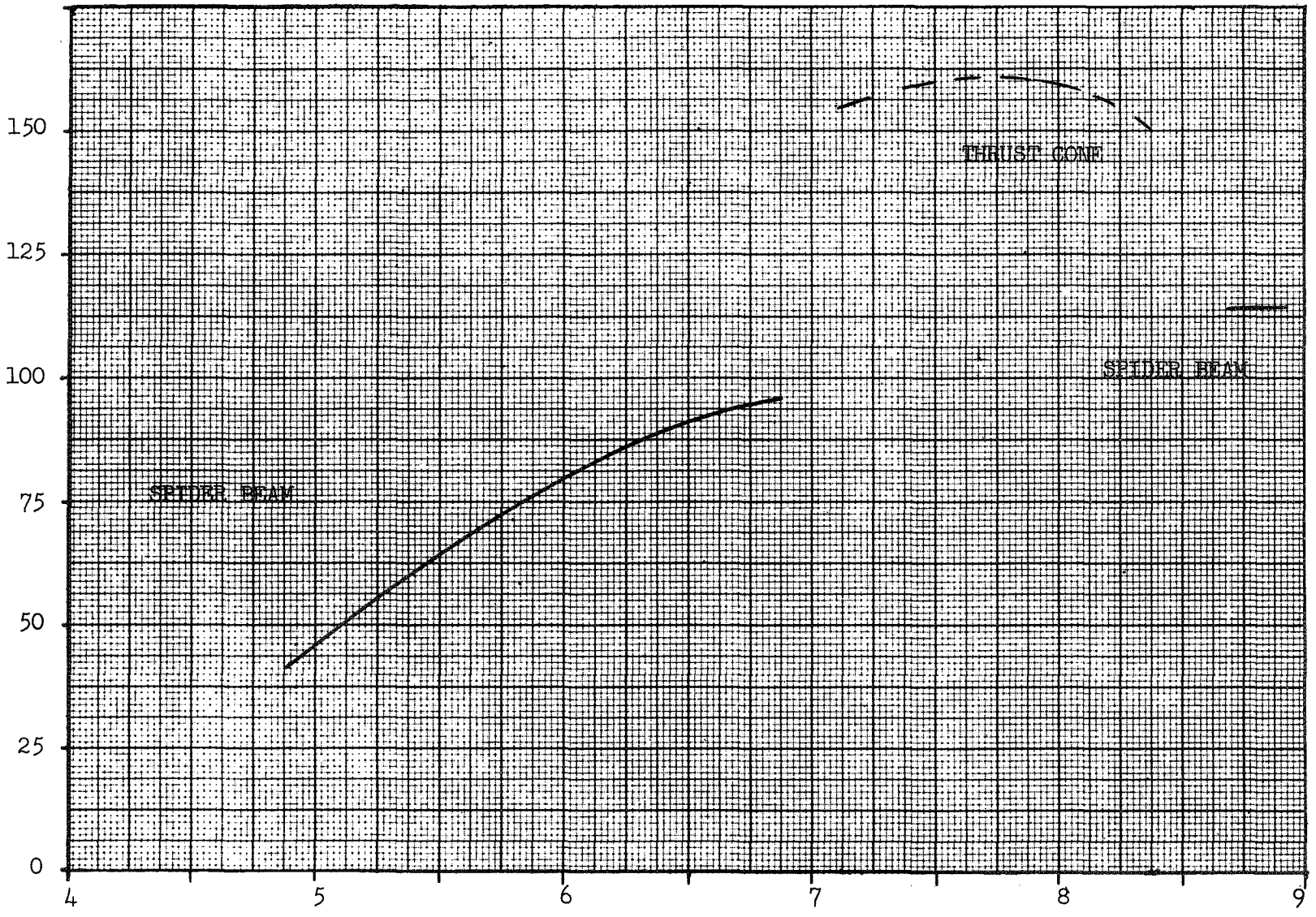

PAYLOAD (POUNDS)

STAGE WEIGHT (10^3 POUNDS)

BOOSTER: Atlas/Centaur
ΔV (MISSION): 54,500 FPS
ΔV (RETRO): N/A FPS

CASE: 3E1T01
☐ H2/F2
☒ H2/F2/LI

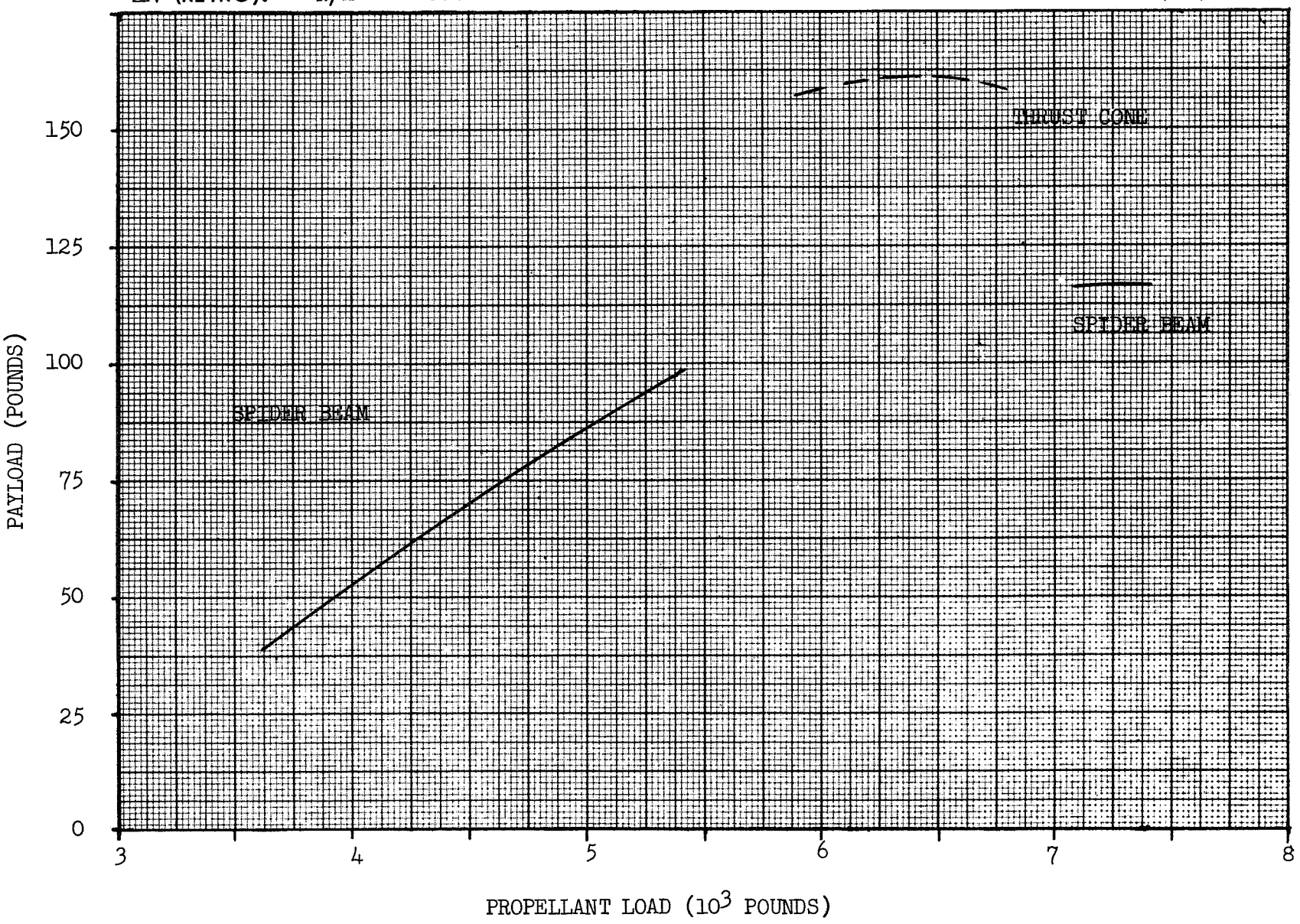

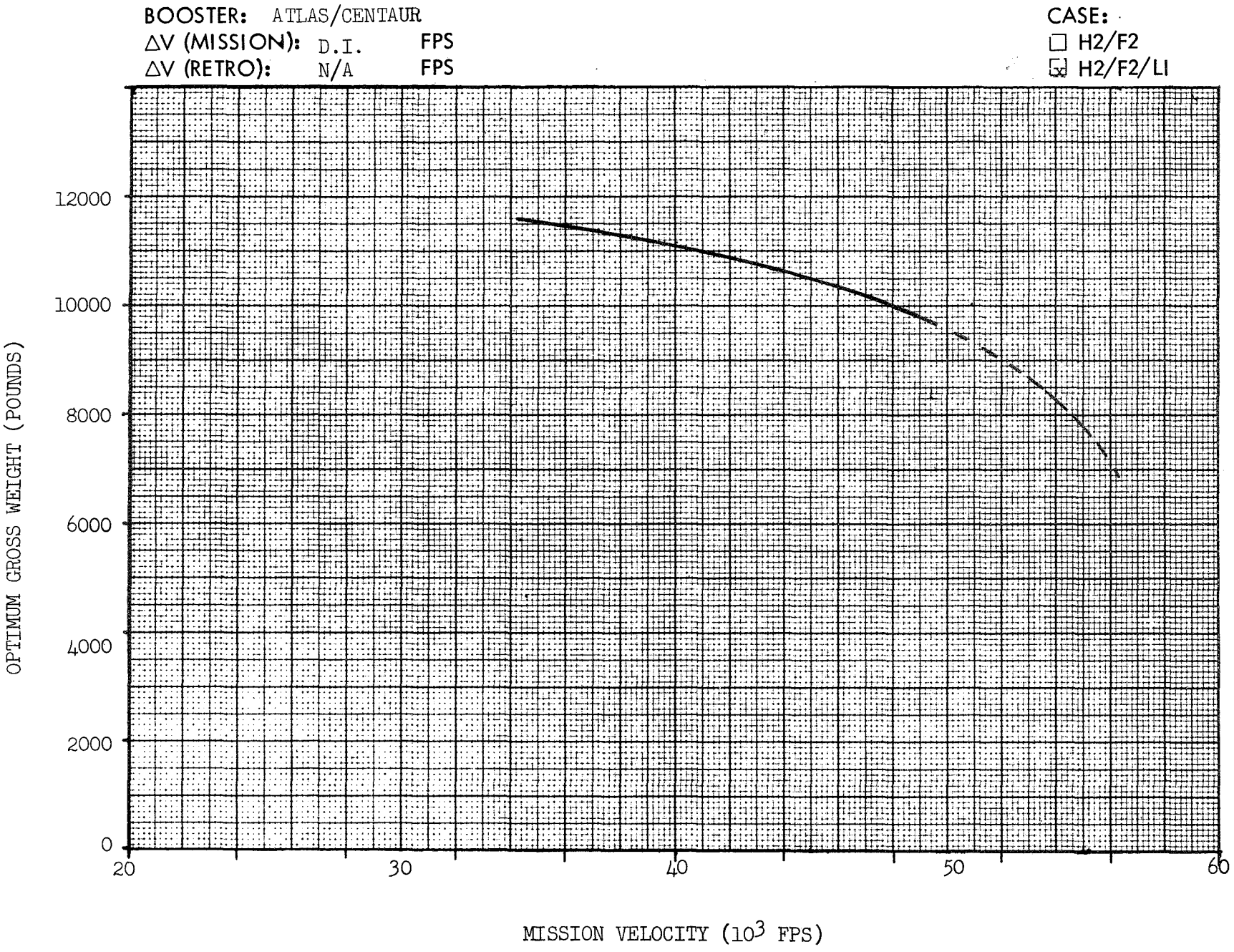
BOOSTER: ATLAS/CENTAUR
ΔV (MISSION): D.I. FPS
ΔV (RETRO): N/A FPS
CASE:
☐ H2/F2
☒ H2/F2/LI
OPTIMUM GROSS WEIGHT (POUNDS)
12000
10000
8000
6000
4000
2000
0
20
30
40
50
60
MISSION VELOCITY (10³ FPS)

BOOSTER: Atlas Centaur
ΔV (MISSION): 48,500 FPS
ΔV (RETRO): N/A FPS
GROSS WT: 10,000 LB.

CASE: 4A1T01
☐ H2/F2
☒ H2/F2/LI - GEL

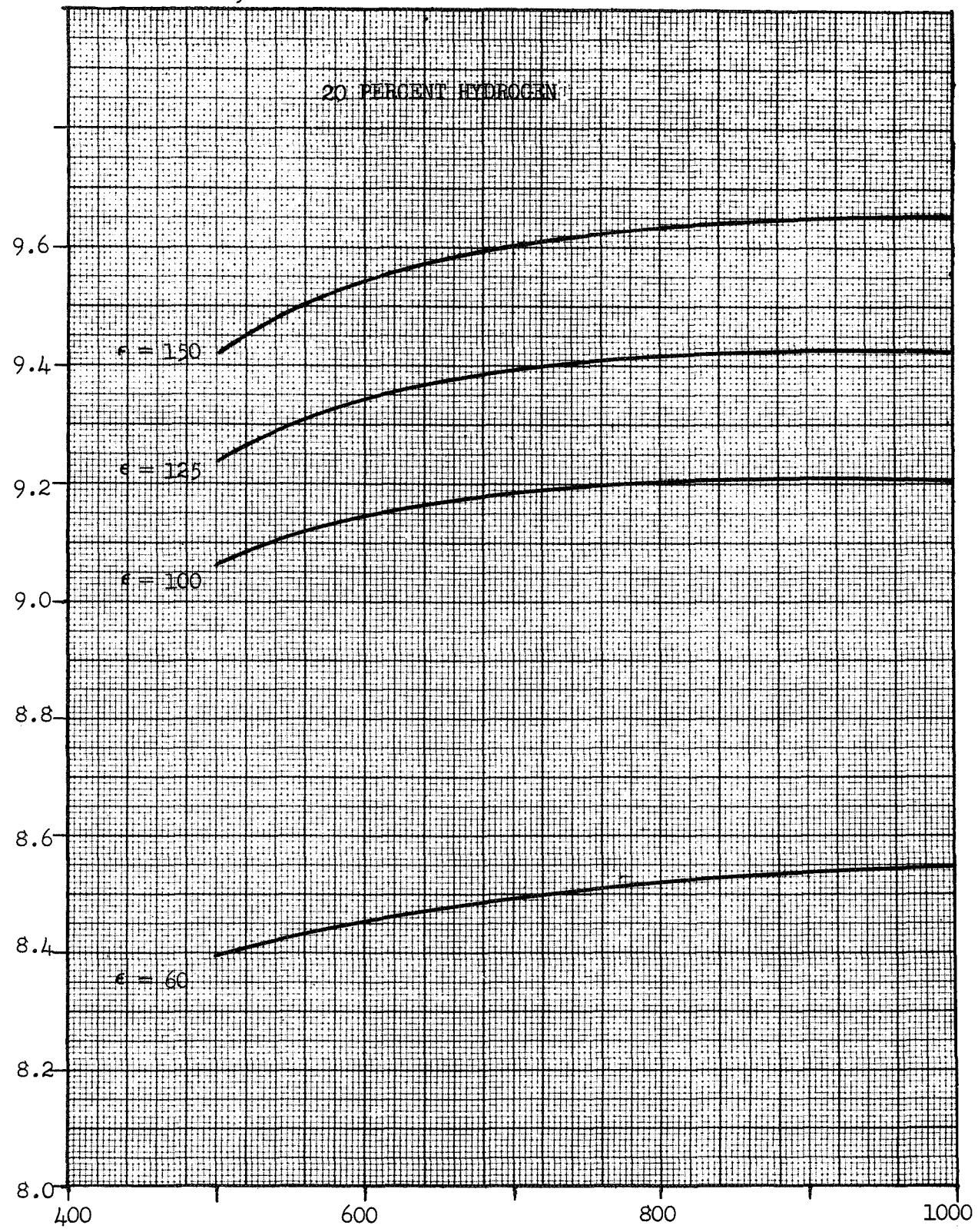

BOOSTER: Atlas Centaur
ΔV (MISSION): 48,500 FPS
ΔV (RETRO): N/A FPS
GROSS WT: 10,000 LB.

CASE: 4A1T01
☐ H2/F2
☒ H2/F2/LI - GEL

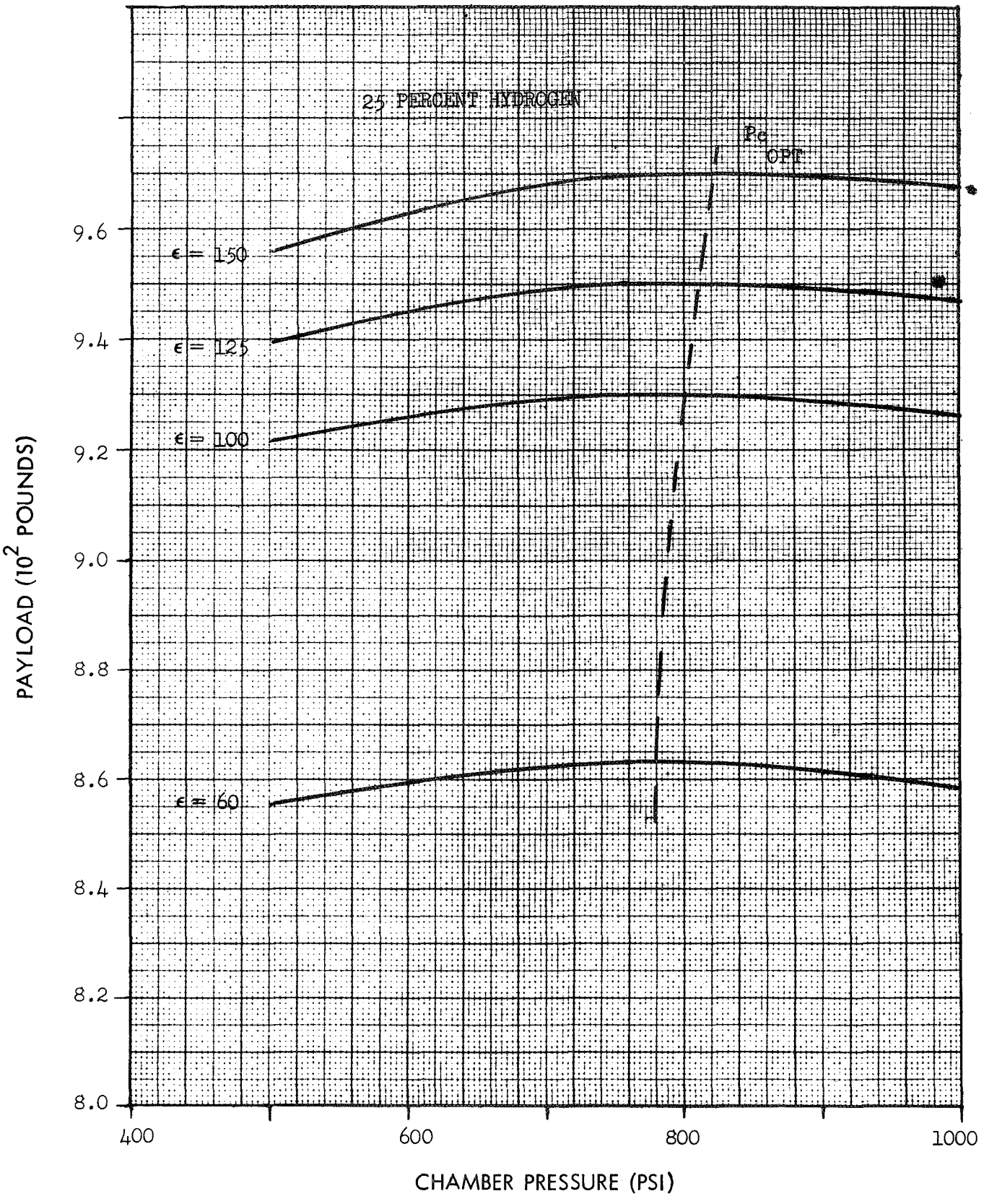

BOOSTER: Atlas Centaur
ΔV (MISSION): 48,500 FPS
ΔV (RETRO): N/A FPS
GROSS WT: 10,000 LB.

CASE: 4A1T01
☐ H2/F2
☒ H2/F2/LI - GEL

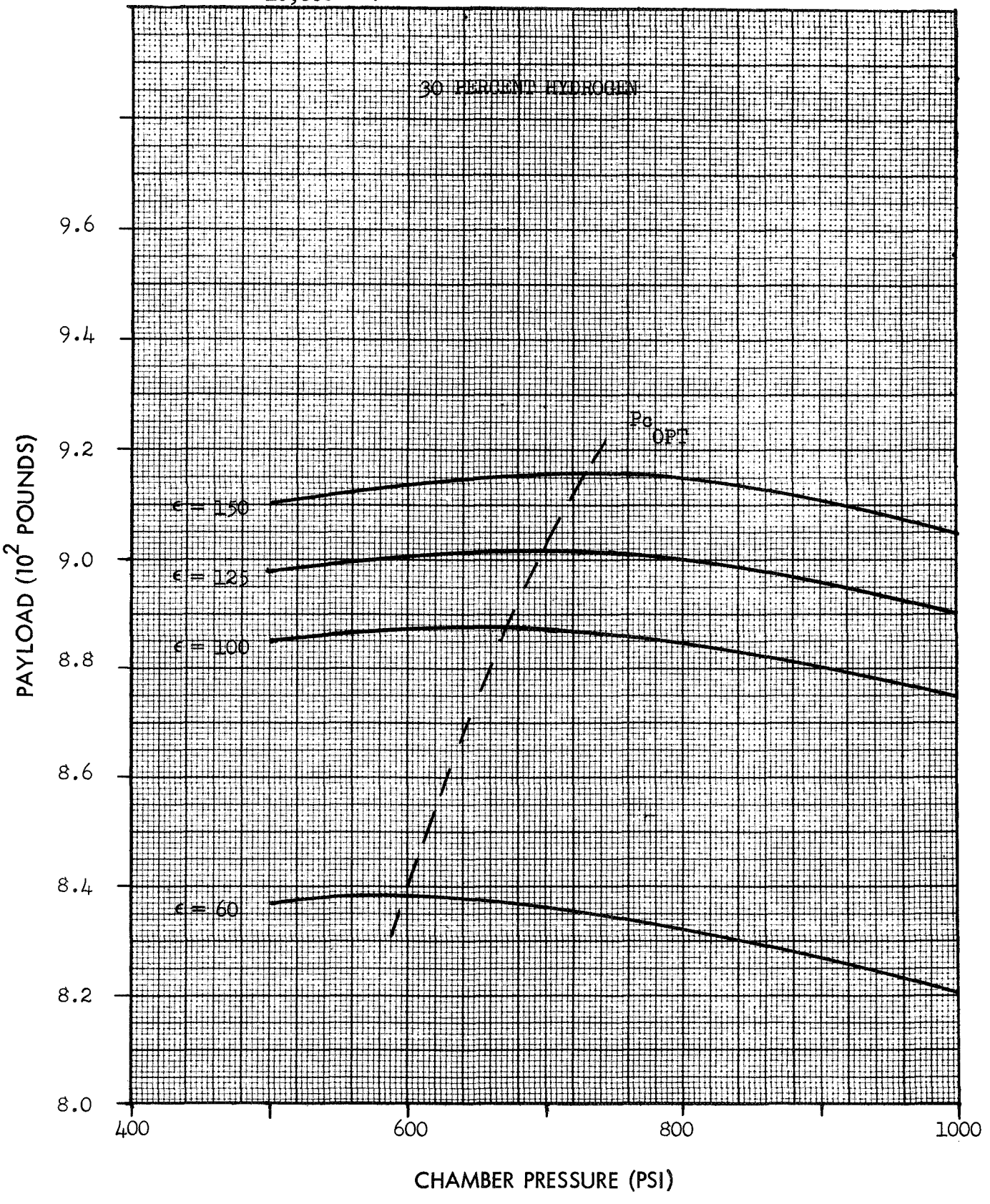

BOOSTER: Atlas Centaur
ΔV (MISSION): 36,140 FPS
ΔV (RETRO): N/A FPS

CASE: 4A1T01
☐ H2/F2
☒ H2/F2/LI - GEL

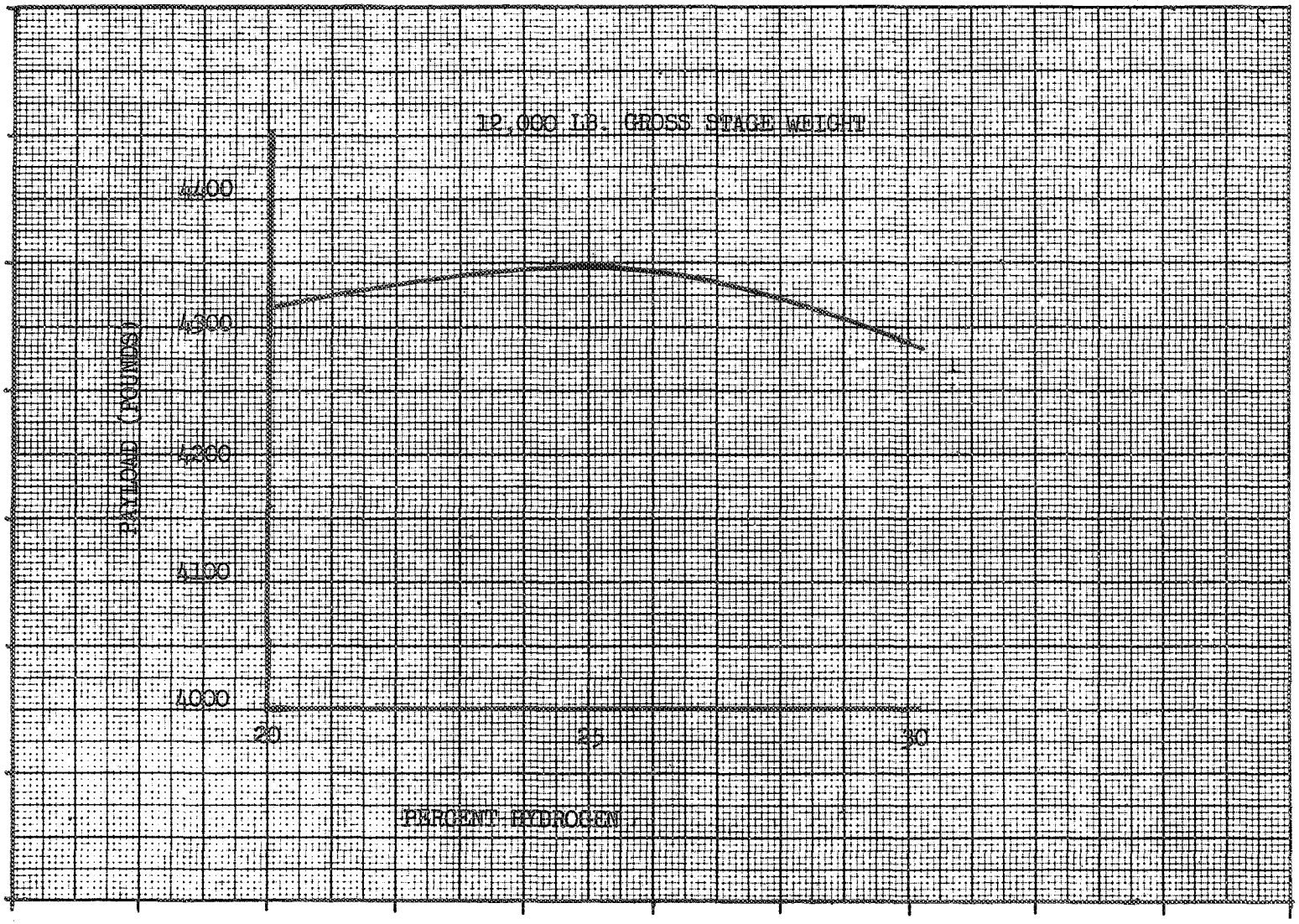

BOOSTER: ATLAS/CENTAUR
ΔV (MISSION): 48,500 FPS
ΔV (RETRO): N/A FPS
GROSS WT: 10,000

CASE: 4A1T01
☐ H2/F2
☒ H2/F2/LI-GEL

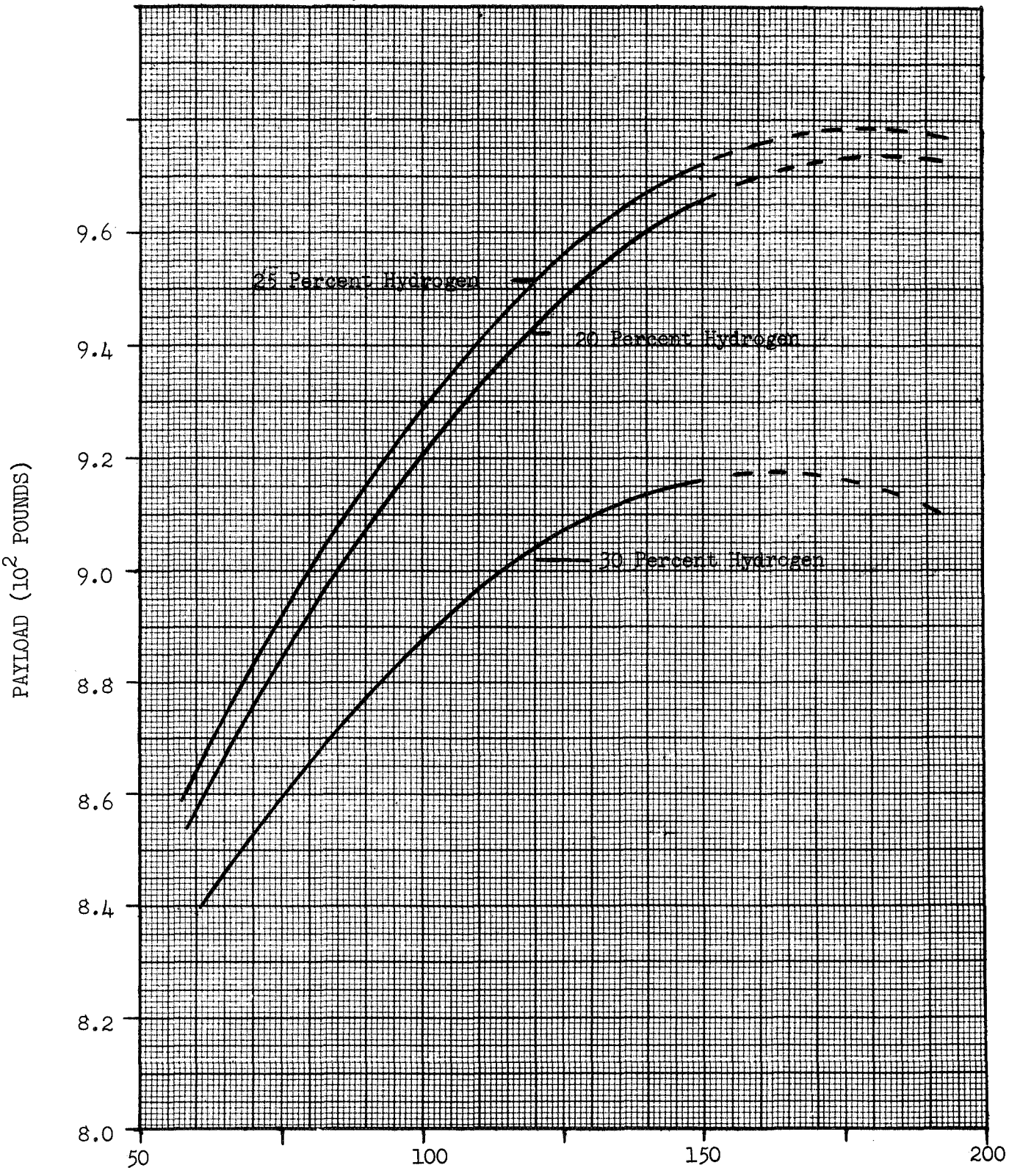

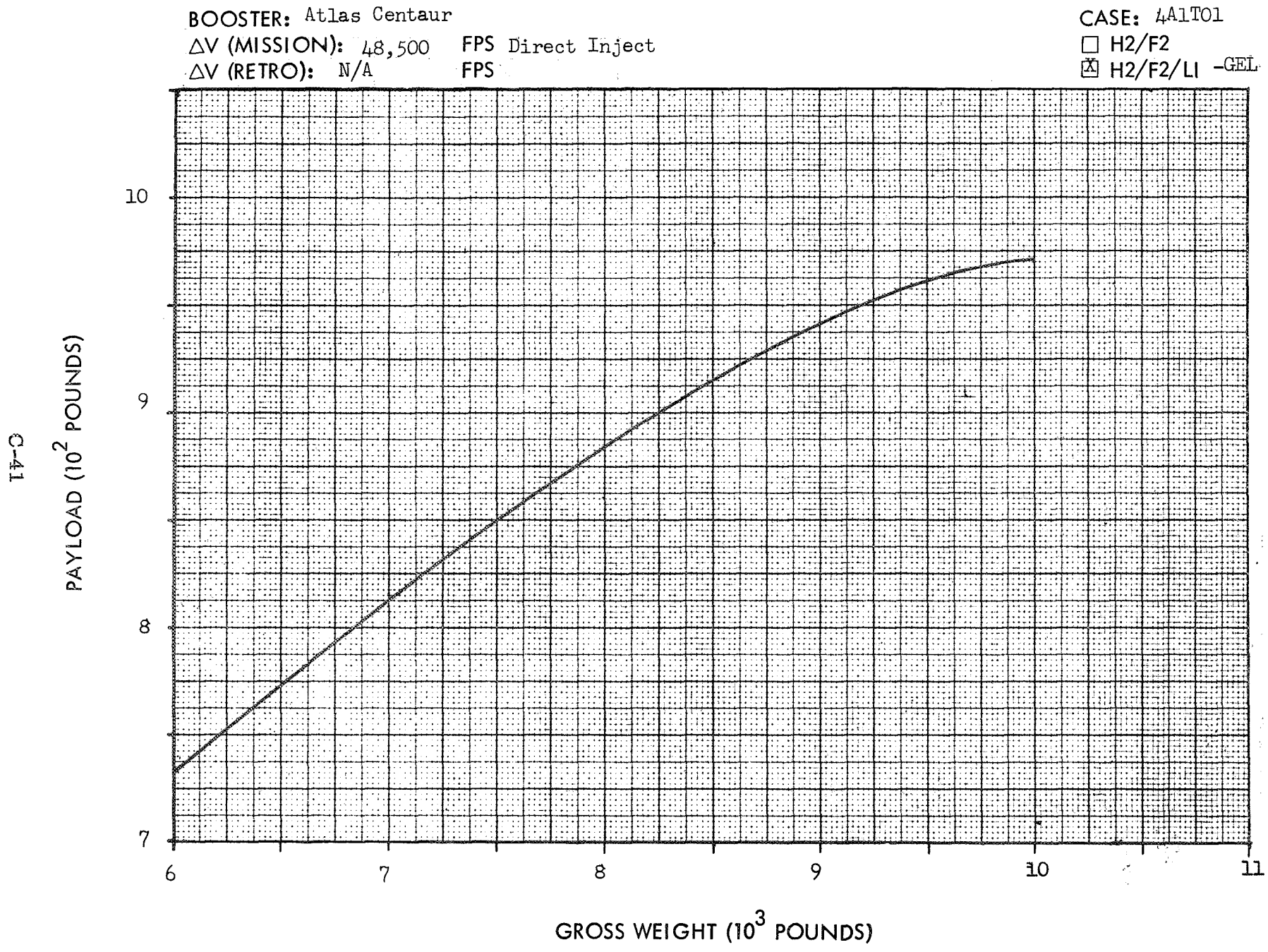
BOOSTER: Atlas Centaur
ΔV (MISSION): 48,500 FPS Direct Inject
ΔV (RETRO): N/A FPS
CASE: 4A1TO1
☐ H2/F2
☒ H2/F2/LI -GEL
PAYLOAD (10^2 POUNDS)
10
9
8
7
6
7
8
9
10
11
GROSS WEIGHT (10^3 POUNDS)

BOOSTER: Atlas Centaur
ΔV (MISSION): 48,500 FPS
ΔV (RETRO): N/A FPS

CASE: 4A1T01
☐ H2/F2
☒ H2/F2/LI – GEL

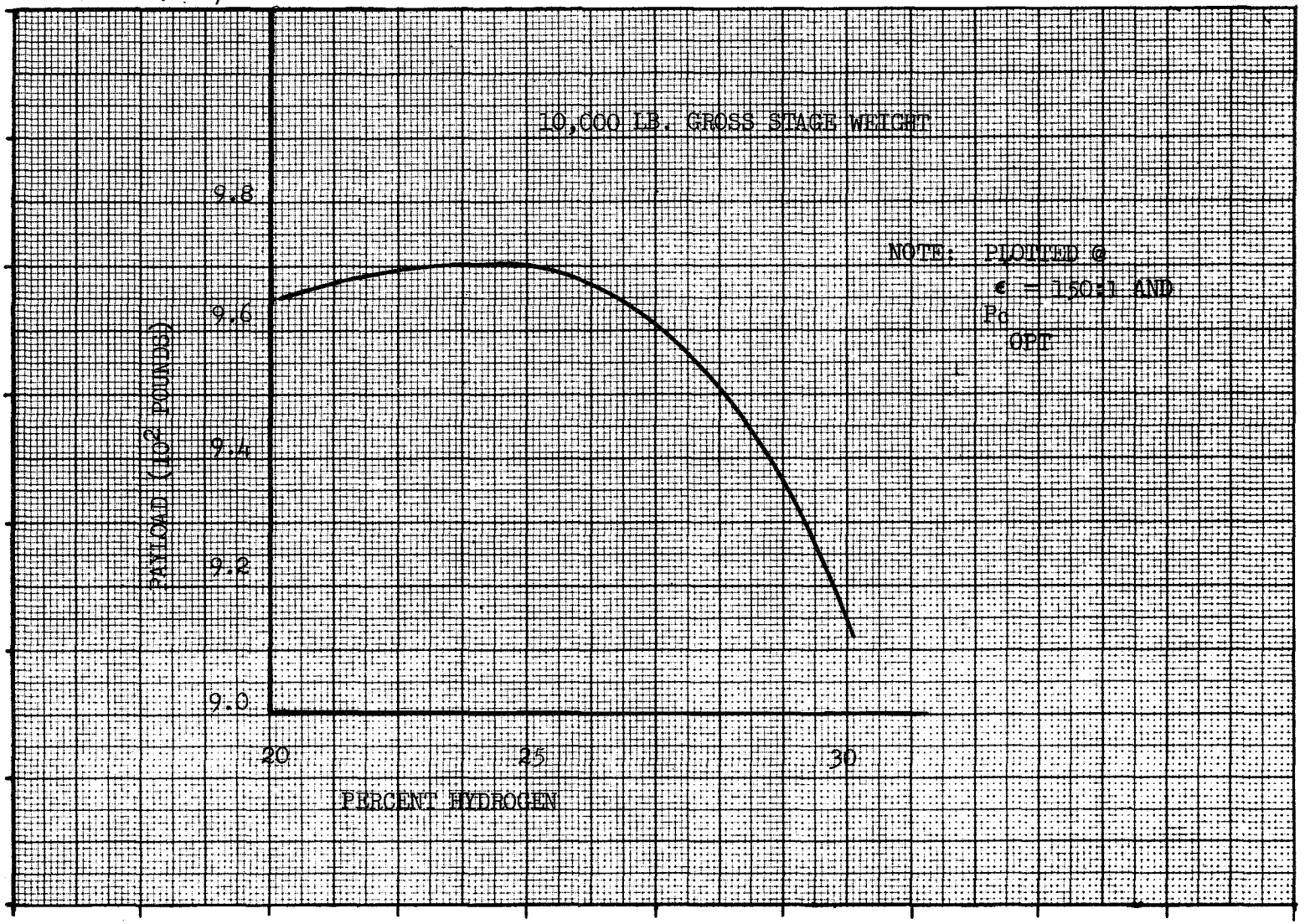

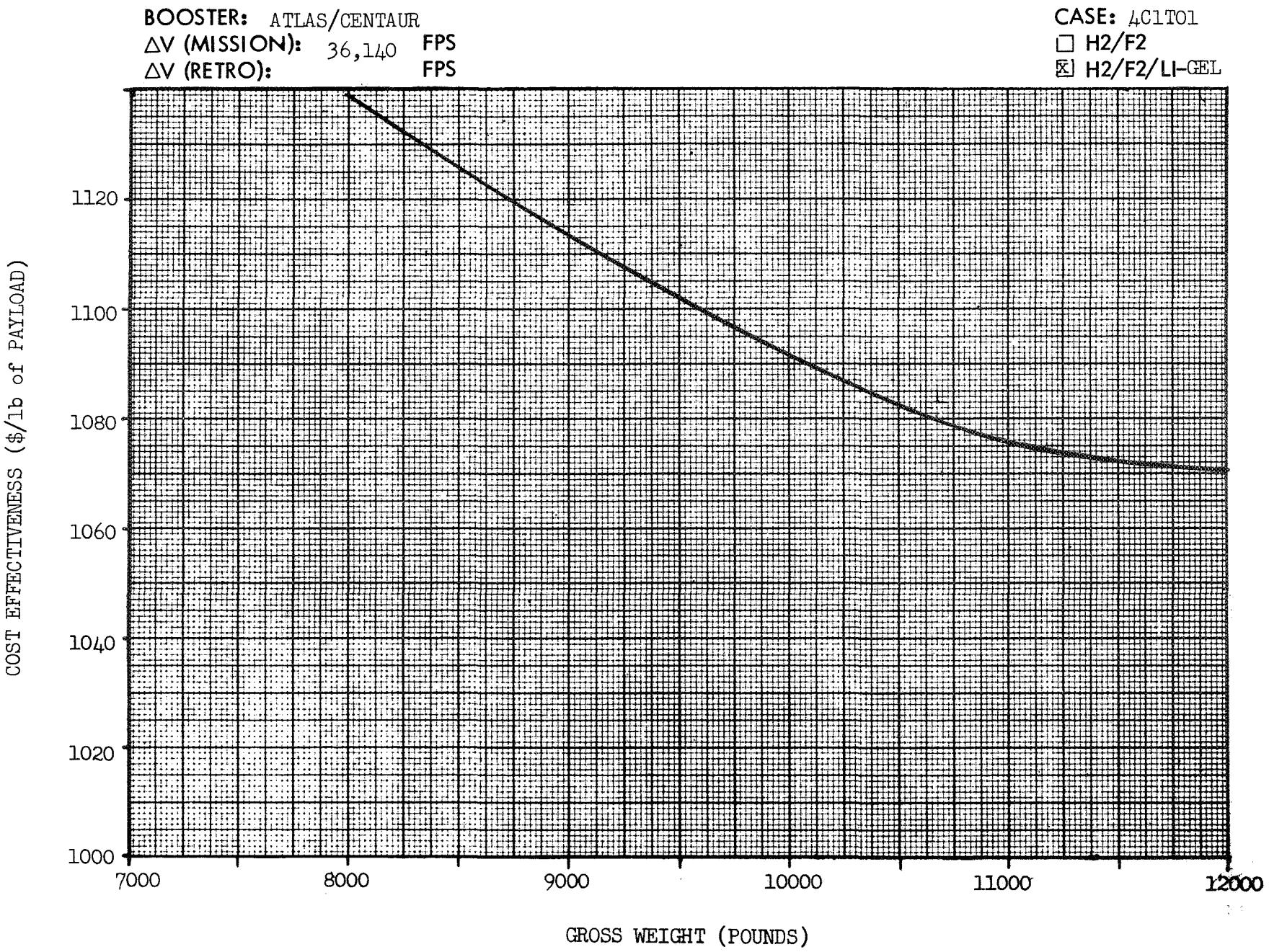
BOOSTER: ATLAS/CENTAUR
ΔV (MISSION): 36,140 FPS
ΔV (RETRO): FPS
CASE: 4C1TO1
☐ H2/F2
☒ H2/F2/LI-GEL
COST EFFECTIVENESS ($/lb of PAYLOAD)
1120
1100
1080
1060
1040
1020
1000
7000
8000
9000
10000
11000
12000
GROSS WEIGHT (POUNDS)

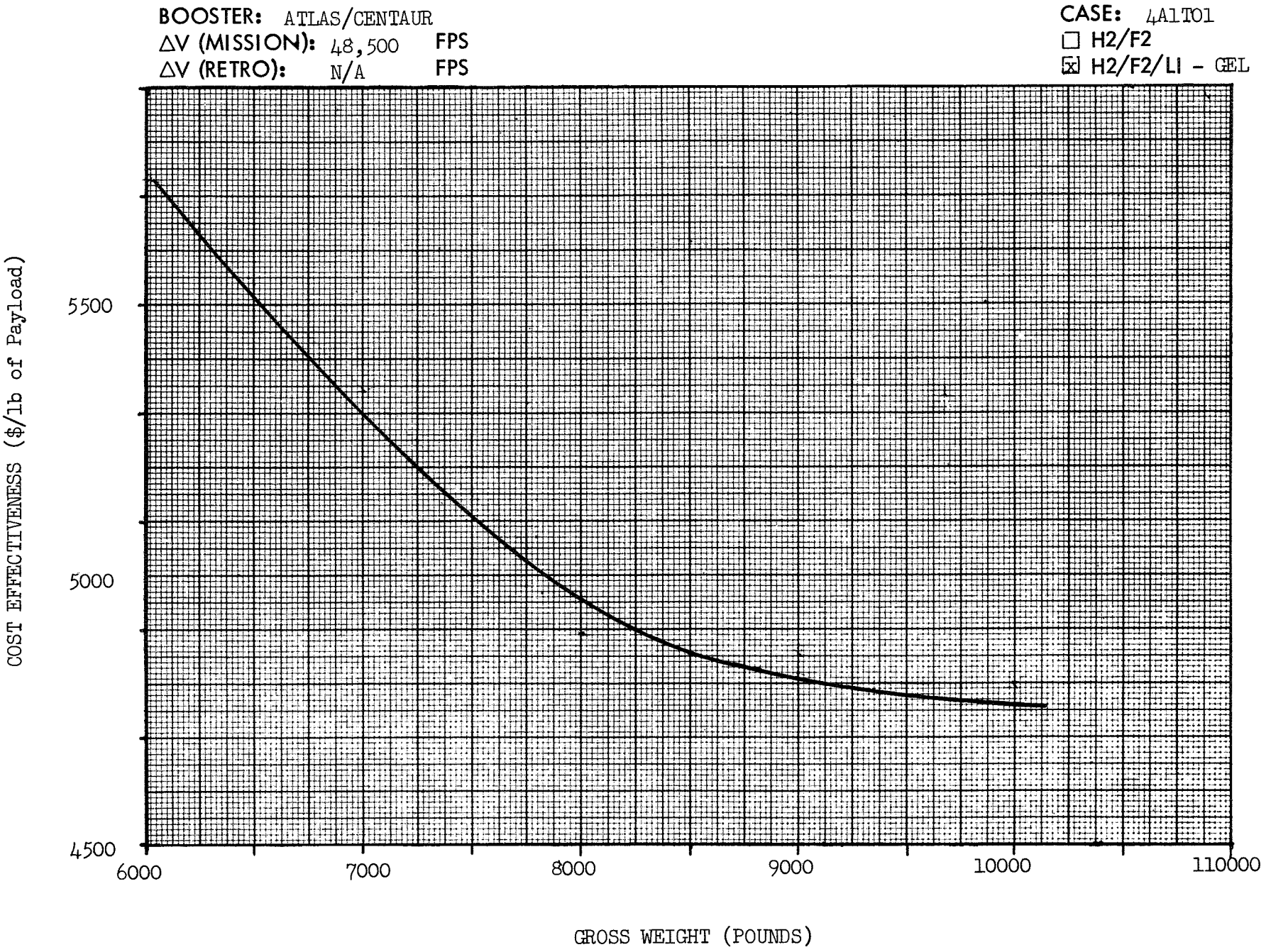
BOOSTER: ATLAS/CENTAUR
ΔV (MISSION): 48,500 FPS
ΔV (RETRO): N/A FPS
CASE: 4A1TO1
☐ H2/F2
☒ H2/F2/LI - GEL
COST EFFECTIVENESS ($/lb of Payload)
5500
5000
4500
6000
7000
8000
9000
10000
110000
GROSS WEIGHT (POUNDS)

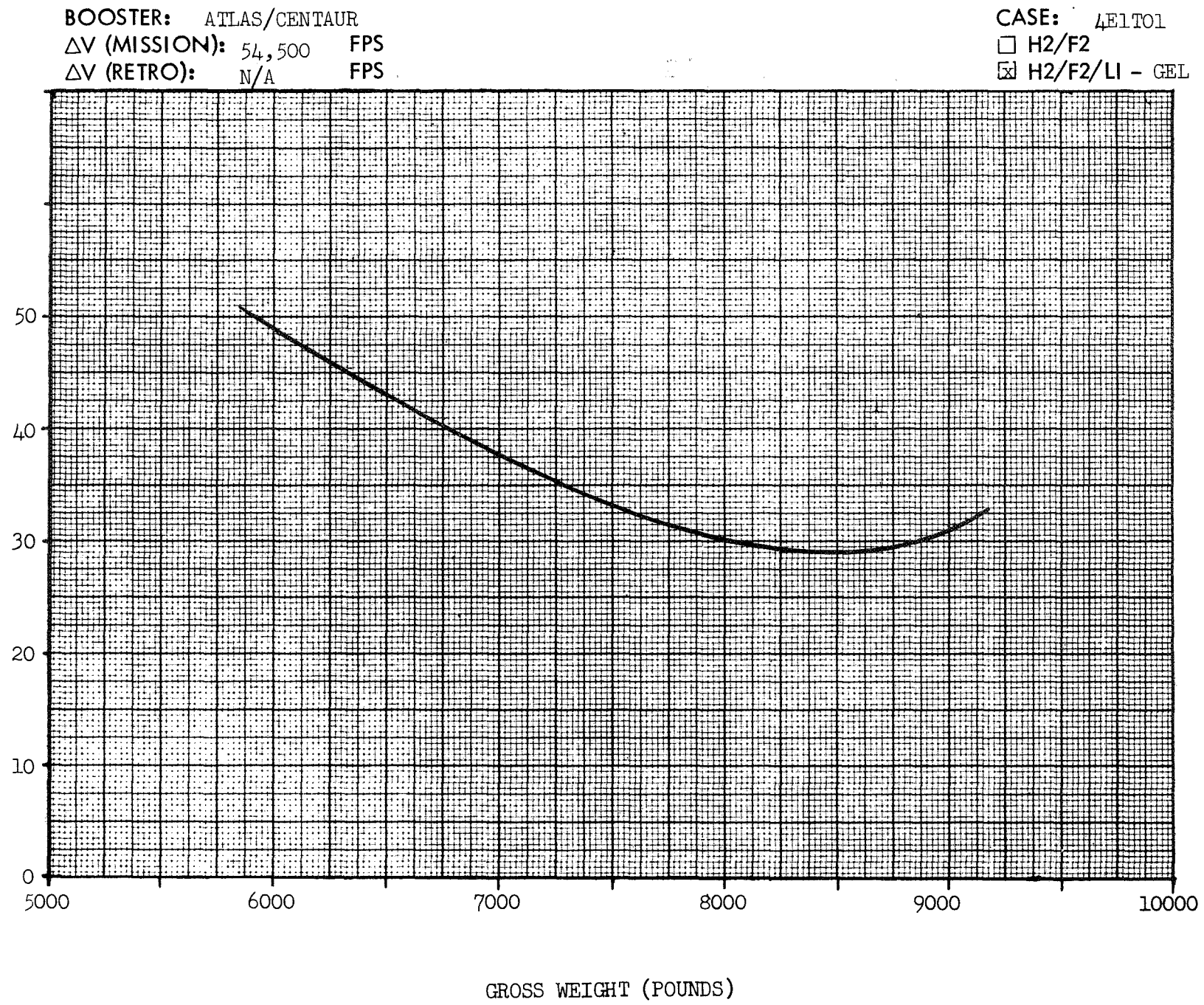
BOOSTER: ATLAS/CENTAUR
ΔV (MISSION): 54,500 FPS
ΔV (RETRO): N/A FPS
CASE: 4E1TO1
☐ H2/F2
☒ H2/F2/LI - GEL
COST EFFECTIVENESS ($/lb of Payload x 10⁻³)
0
10
20
30
40
50
5000
6000
7000
8000
9000
10000
GROSS WEIGHT (POUNDS)

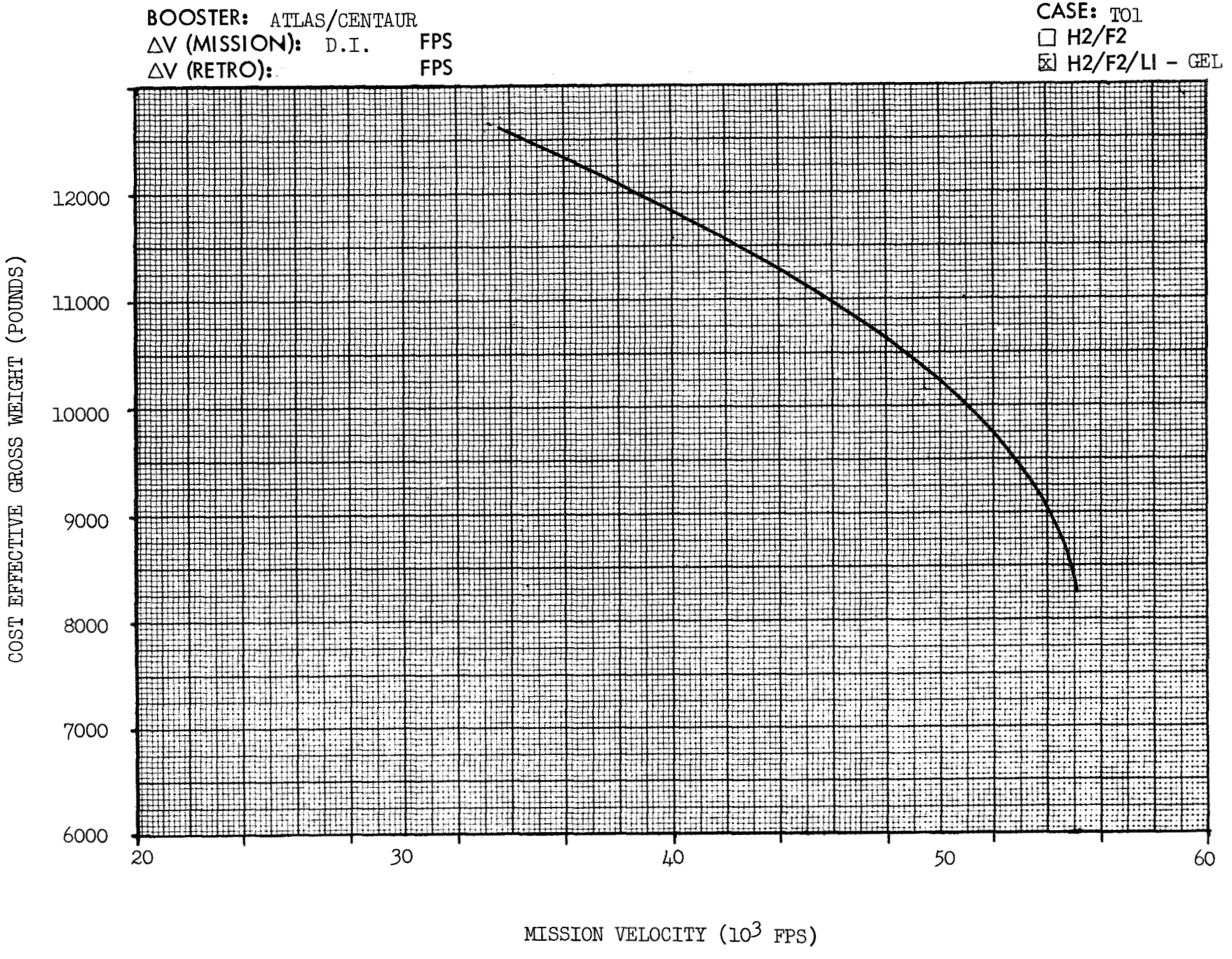
BOOSTER: ATLAS/CENTAUR
ΔV (MISSION): D.I. FPS
ΔV (RETRO): FPS
CASE: TO1
☐ H2/F2
☒ H2/F2/LI - GEL
COST EFFECTIVE GROSS WEIGHT (POUNDS)
12000
11000
10000
9000
8000
7000
6000
20
30
40
50
60
MISSION VELOCITY (10^3 FPS)

BOOSTER: ATLAS/CENTAUR
ΔV (MISSION): 36,140 FPS
ΔV (RETRO): NA FPS
GROSS WT:

CASE: 2A1TO1
☒ H2/F2
☐ H2/F2/LI

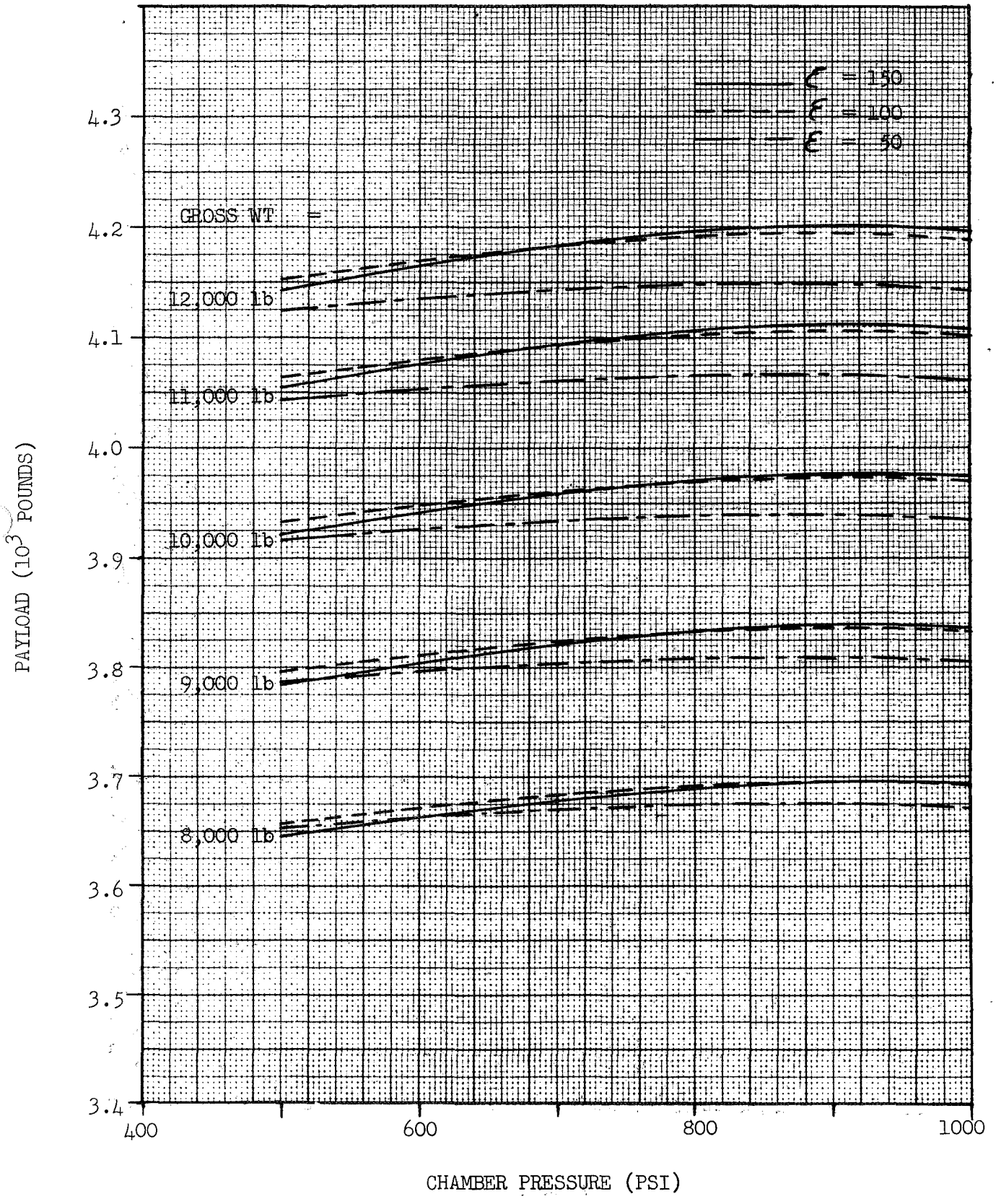

BOOSTER: ATLAS/CENTAUR
ΔV (MISSION): 36,140 FPS
ΔV (RETRO): N/A FPS
GROSS WT:

CASE: 2A1T01
☒ H2/F2
☐ H2/F2/LI

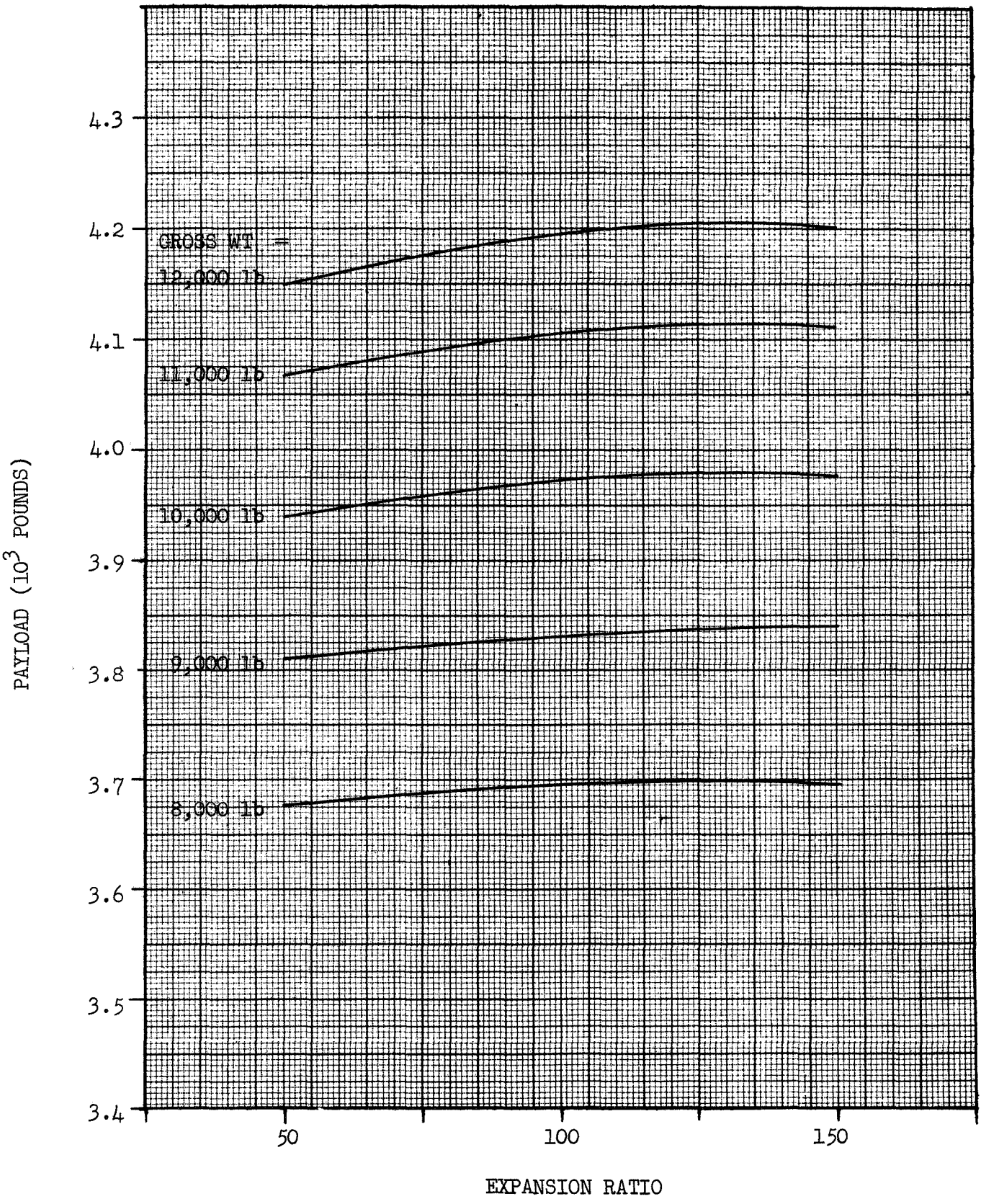

BOOSTER: ATLAS/CENTAUR
ΔV (MISSION): 36,140 FPS
ΔV (RETRO): N/A FPS

CASE: 2A1T01
☒ H2/F2
☐ H2/F2/LI

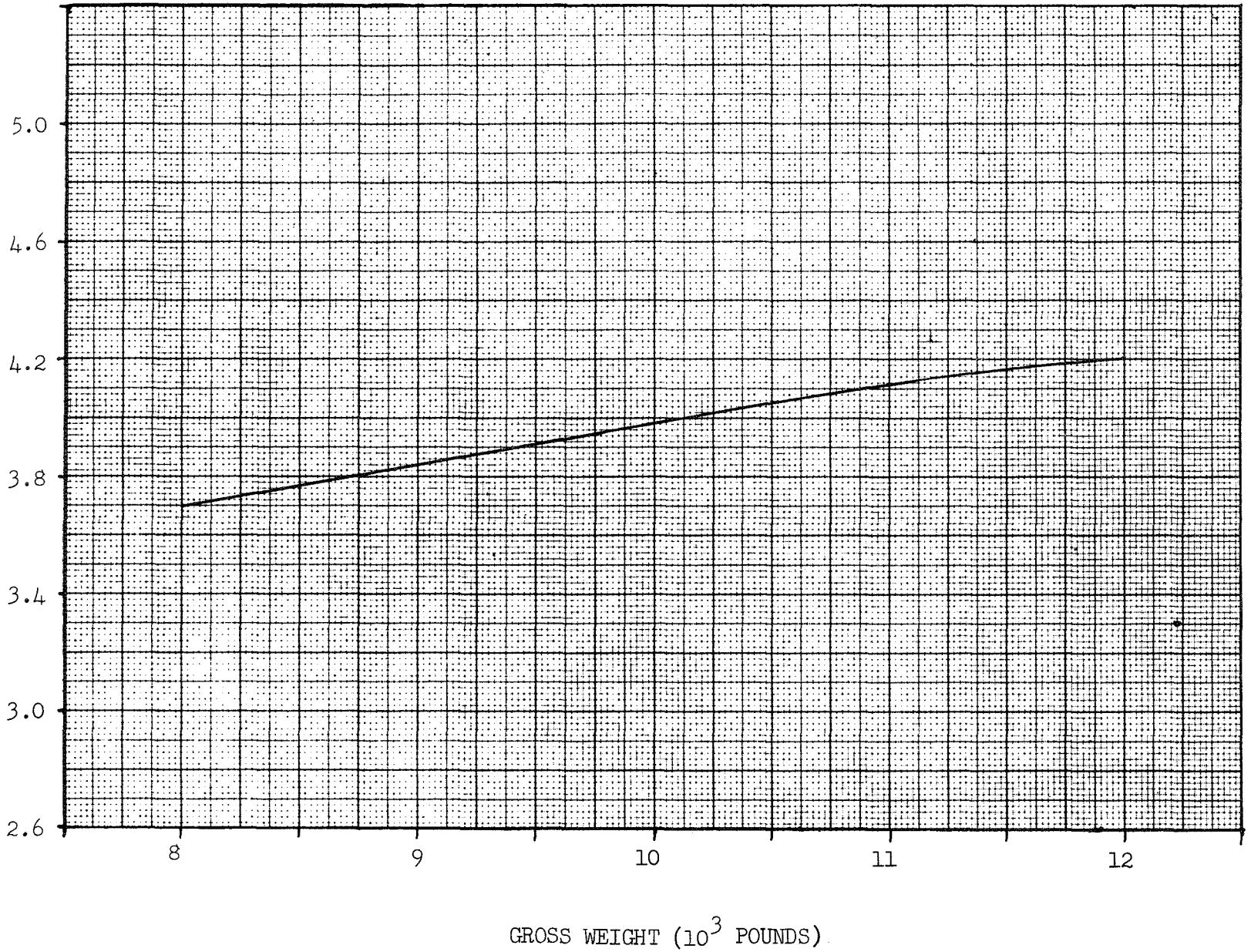

BOOSTER: ATLAS/CENTAUR
ΔV (MISSION): 36,140 FPS
ΔV (RETRO): N/A FPS

CASE: 2A1TO1
☒ H2/F2
☐ H2/F2/LI

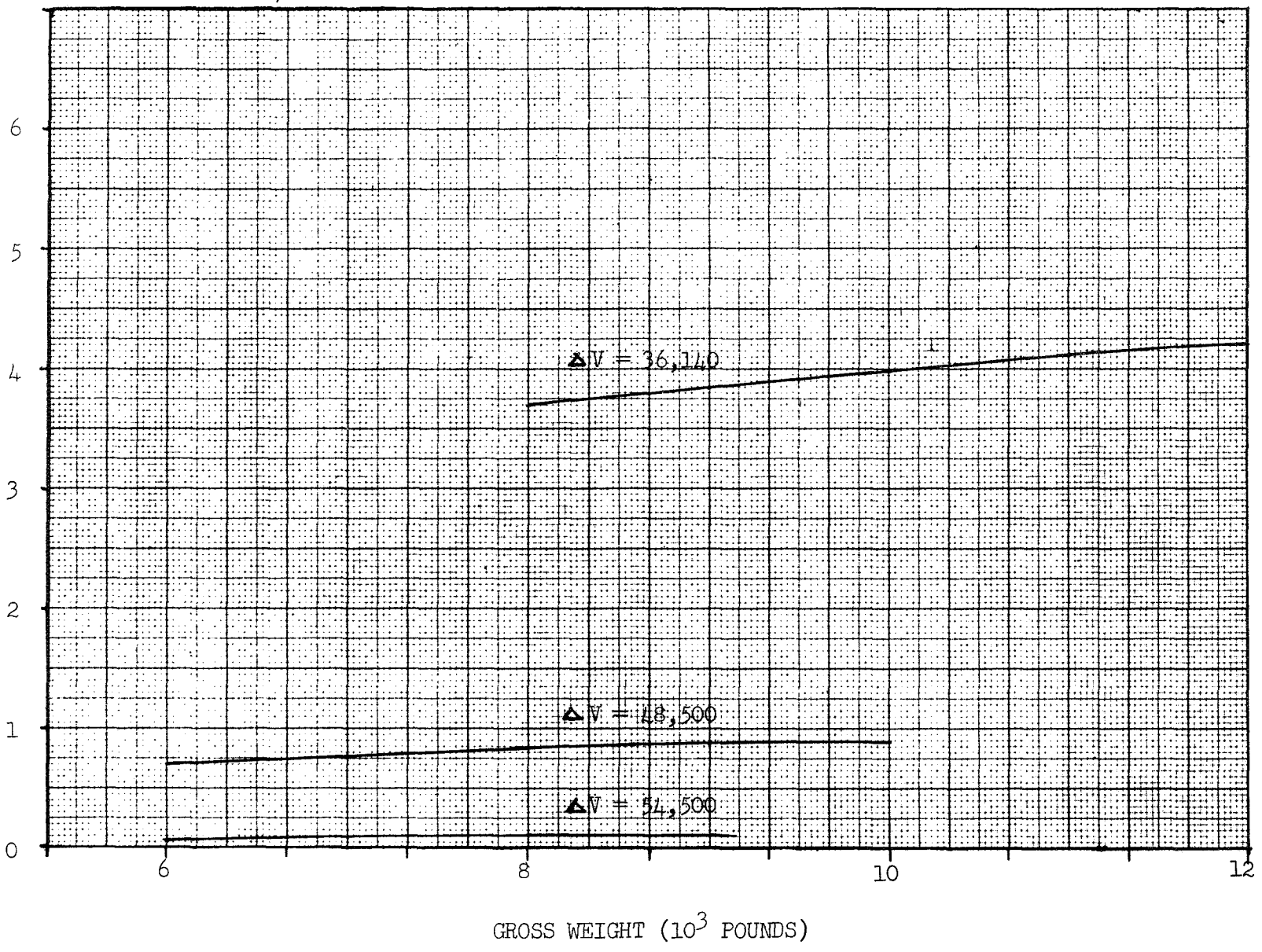

BOOSTER: ATLAS/CENTAUR
ΔV (MISSION): 36,140 FPS
ΔV (RETRO): N/A FPS

CASE: 2A1TO1
☒ H2/F2
☐ H2/F2/LI

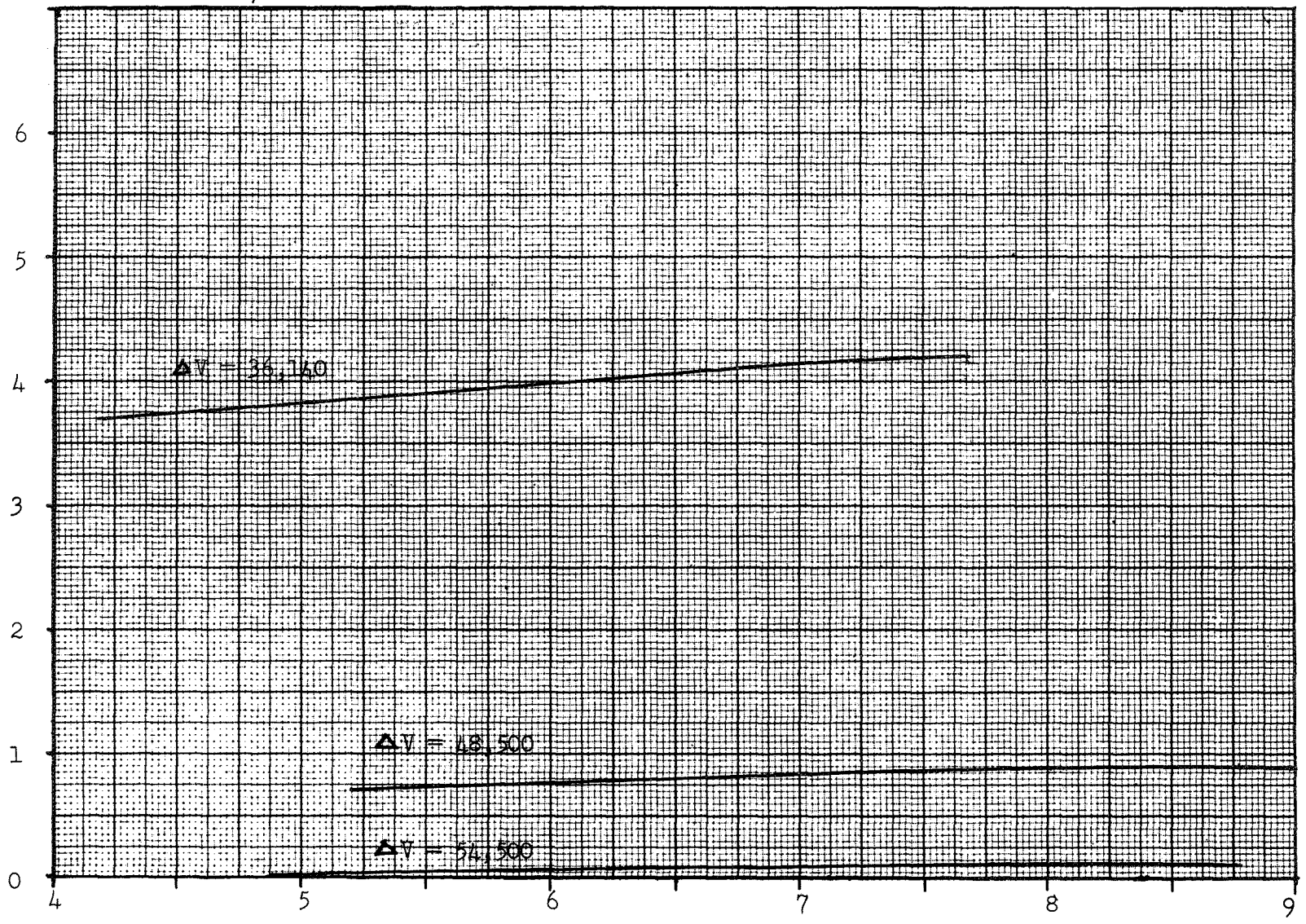

BOOSTER: ATLAS/CENTAUR
ΔV (MISSION): 36,140 FPS
ΔV (RETRO): N/A FPS

CASE: 2A1TO1
☒ H2/F2
☐ H2/F2/LI

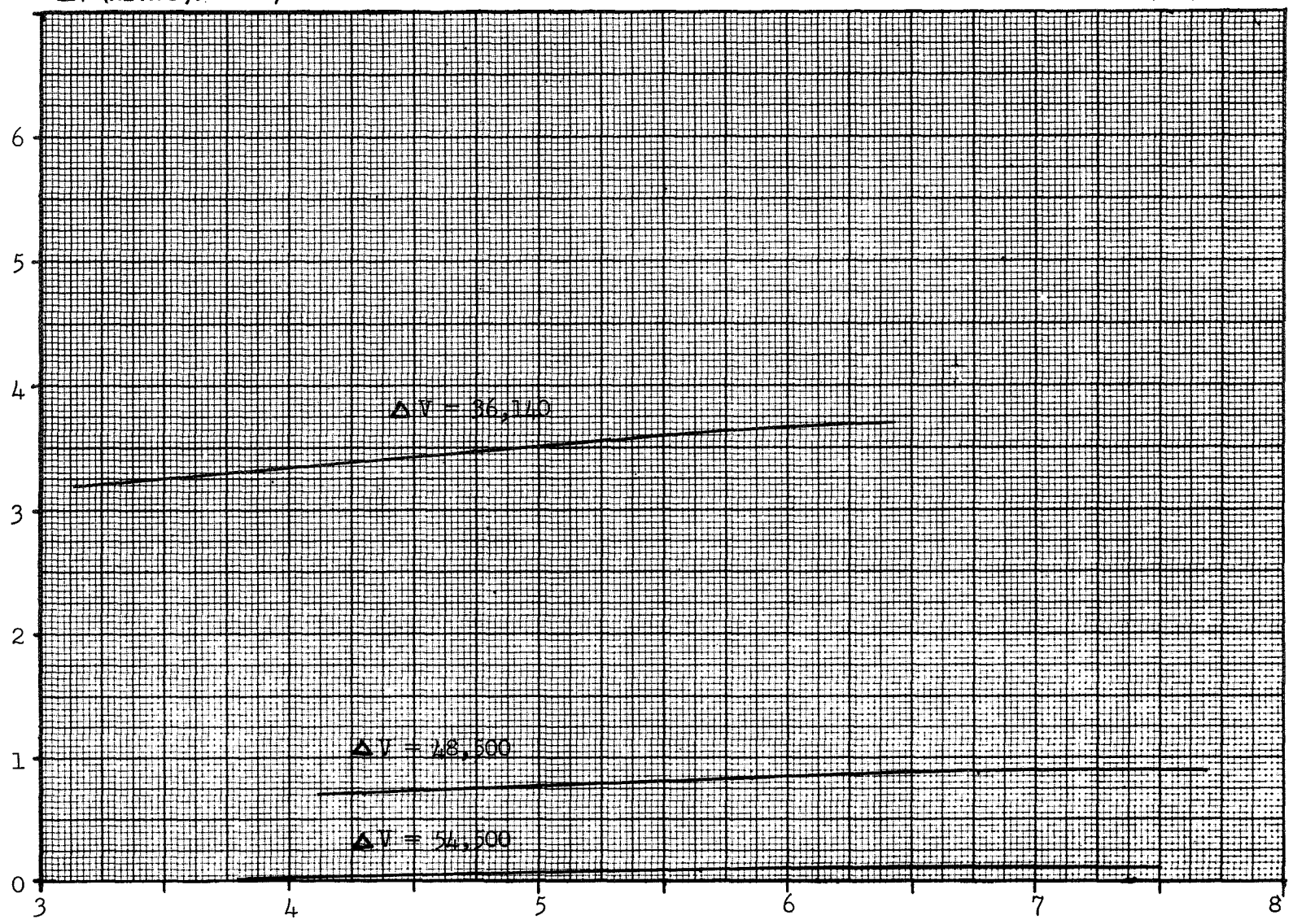

PAYLOAD (10^3 POUNDS)

PROPELLANT WEIGHT (10^3 POUNDS)

BOOSTER: T III D
ΔV (MISSION): 48,500 FPS
ΔV (RETRO): N/A FPS
GROSS WT: 20000 LB

CASE: 3A4T01
☐ H2/F2
☒ H2/F2/LI

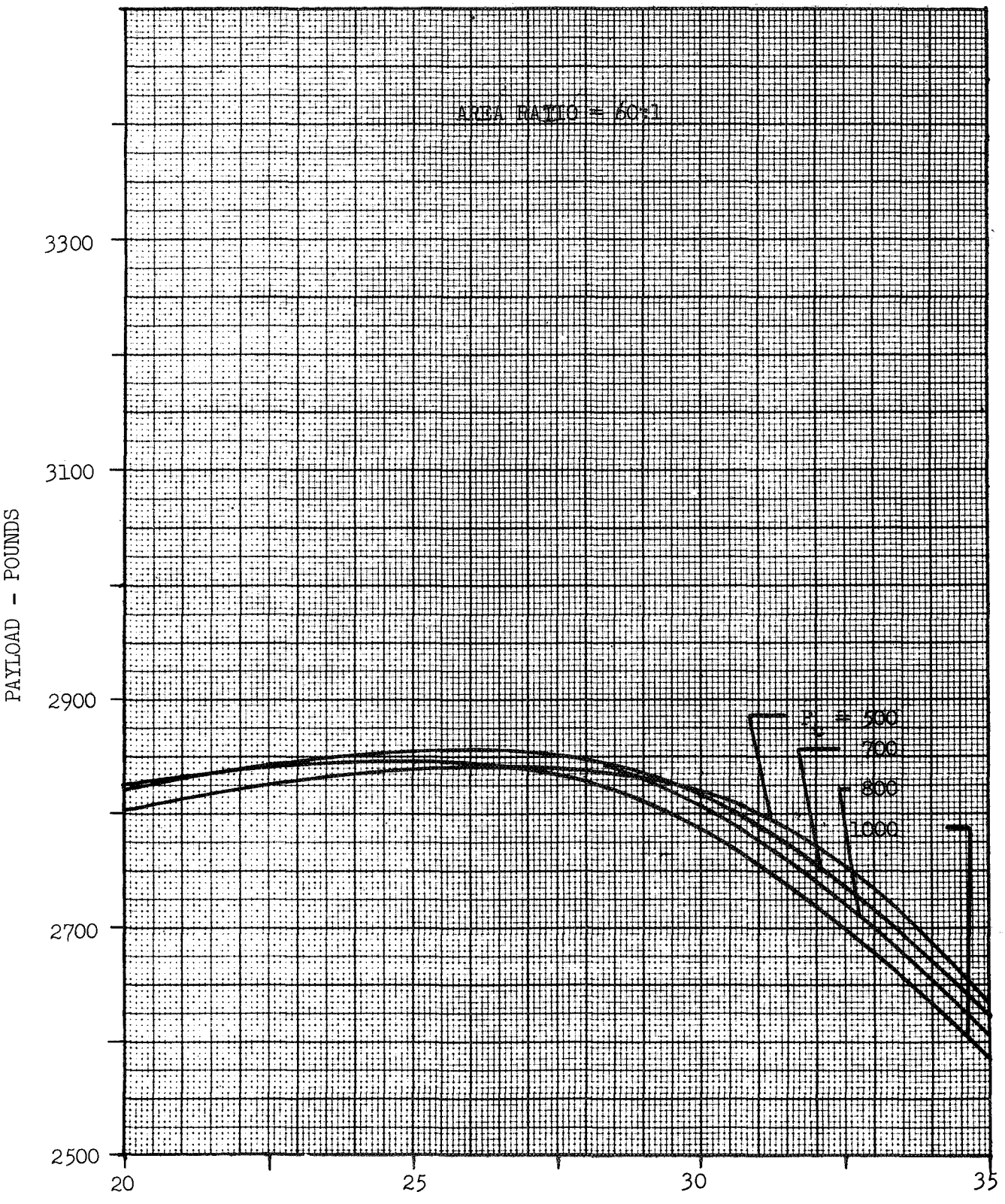

BOOSTER: T III D
ΔV (MISSION): 48,500 FPS
ΔV (RETRO): N/A FPS
GROSS WT: 20000 LB

CASE: 3A4 T01
☐ H2/F2
☒ H2/F2/LI

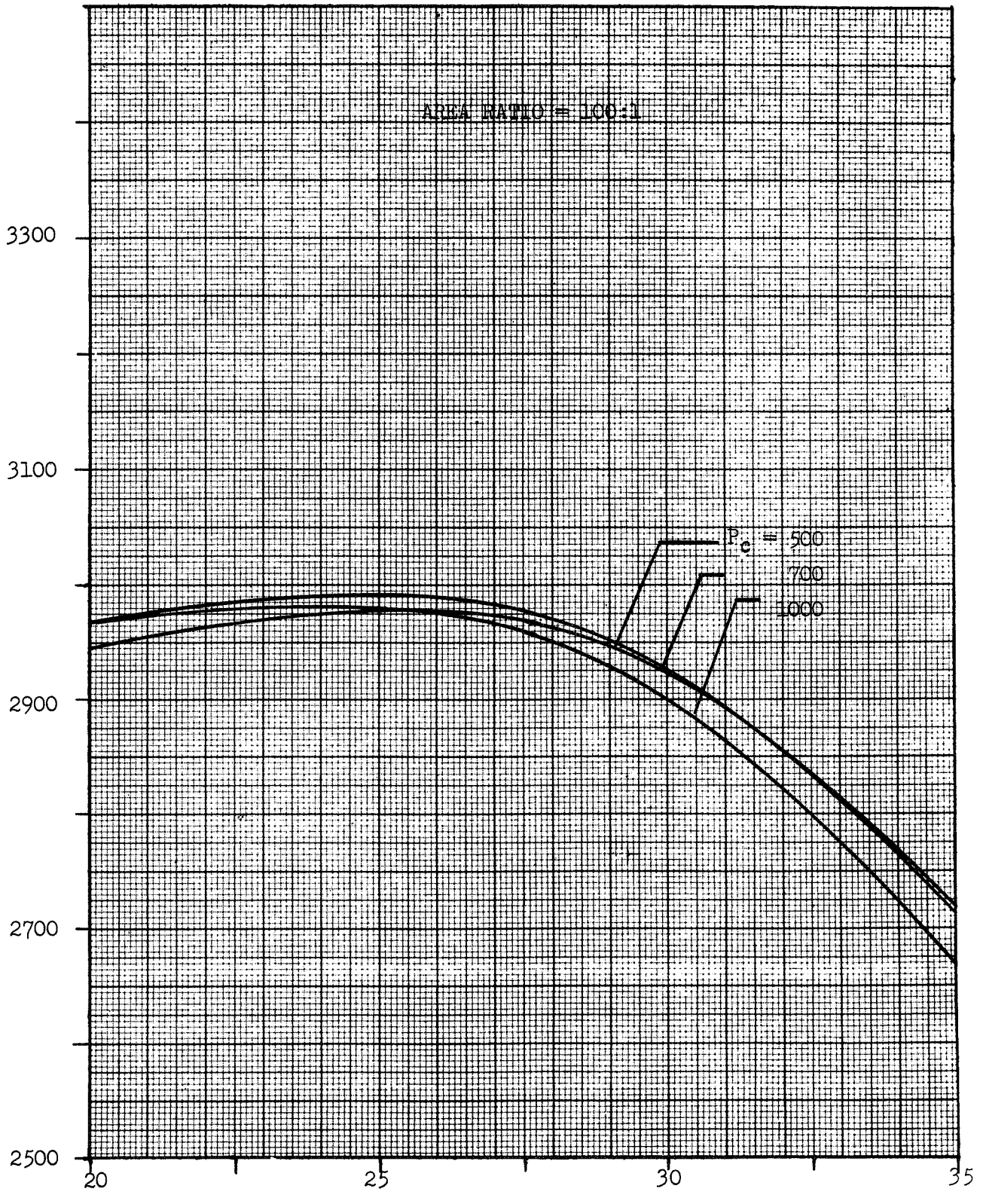

BOOSTER: T III D
ΔV (MISSION): 48,500 FPS
ΔV (RETRO): N/A FPS
GROSS WT: 20000 LB

CASE: 3A4T01
☐ H2/F2
☒ H2/F2/LI

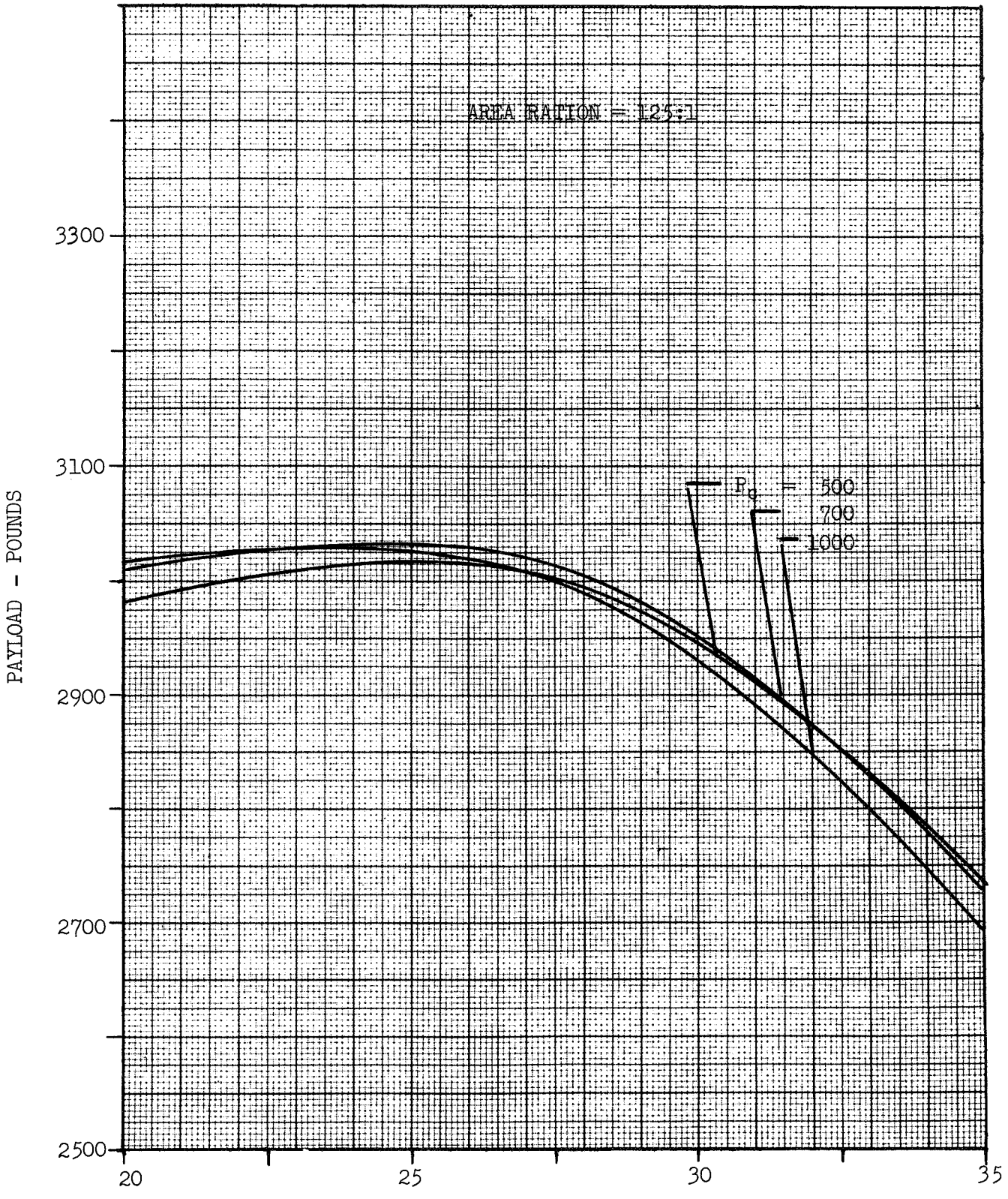

BOOSTER: T III D
ΔV (MISSION): 48,500 FPS
ΔV (RETRO): N/A FPS
GROSS WT: 20000 LB

CASE: 3A4T01
☐ H2/F2
☒ H2/F2/LI

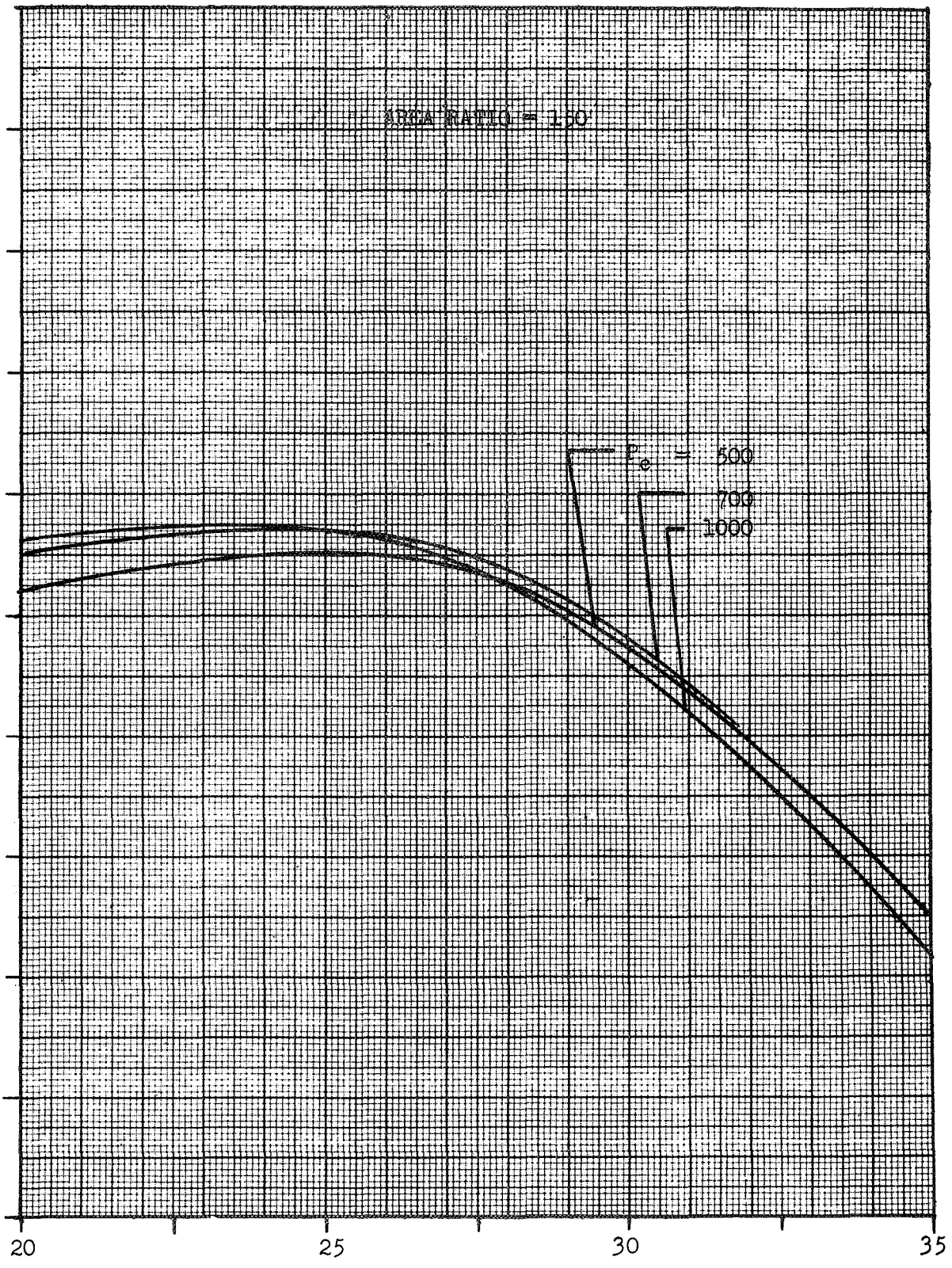

PAYLOAD - POUNDS

PERCENT HYDROGEN

BOOSTER: TITAN III D

ΔV (MISSION): 48,500 FPS

ΔV (RETRO): N/A FPS

GROSS WT: 20000

CASE: 3A4T01

☐ H2/F2

☒ H2/F2/LI

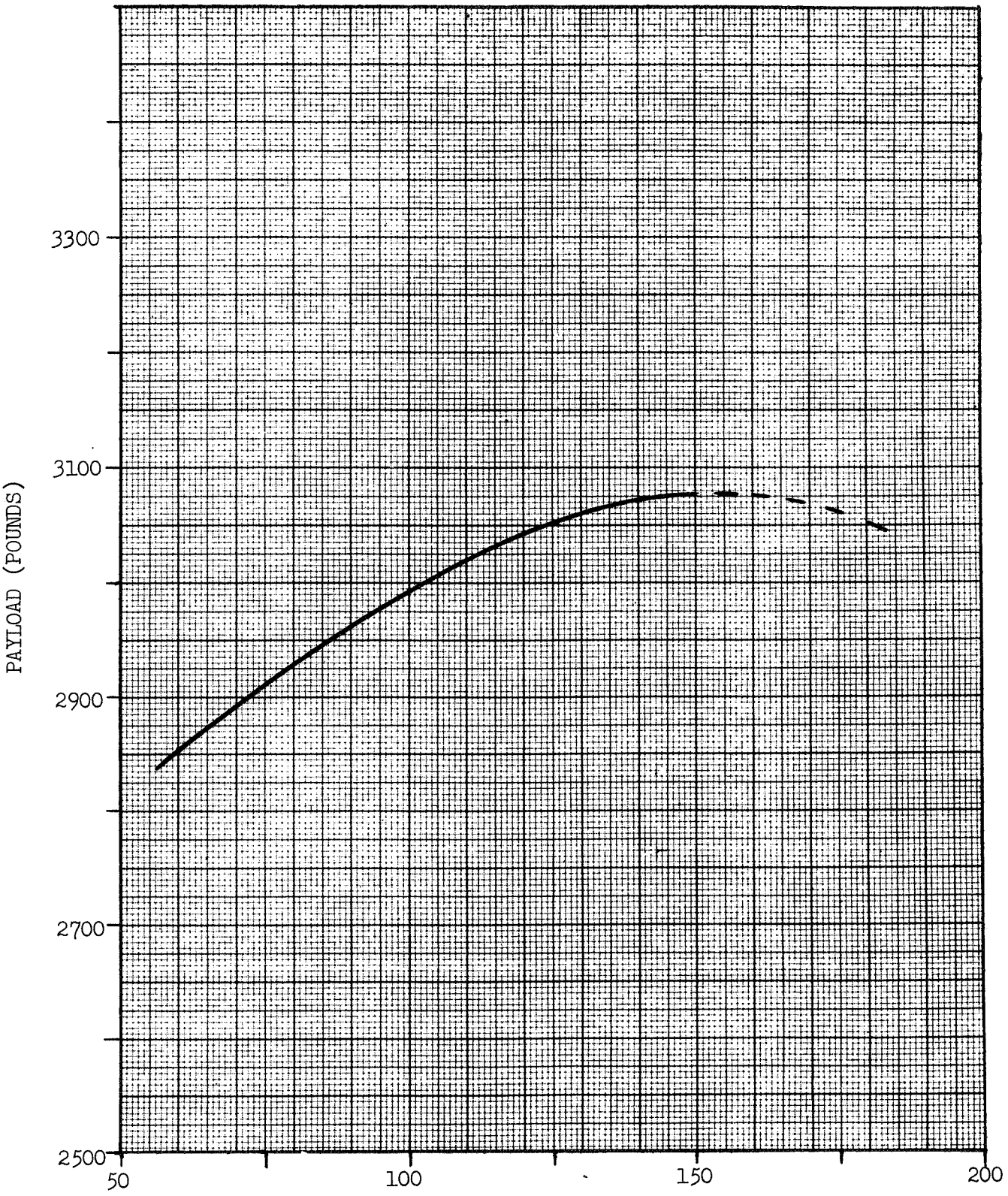

BOOSTER: T III D
ΔV (MISSION): 48,500 FPS
ΔV (RETRO): N/A FPS

CASE: 3A4T01
☐ H2/F2
☒ H2/F2/LI

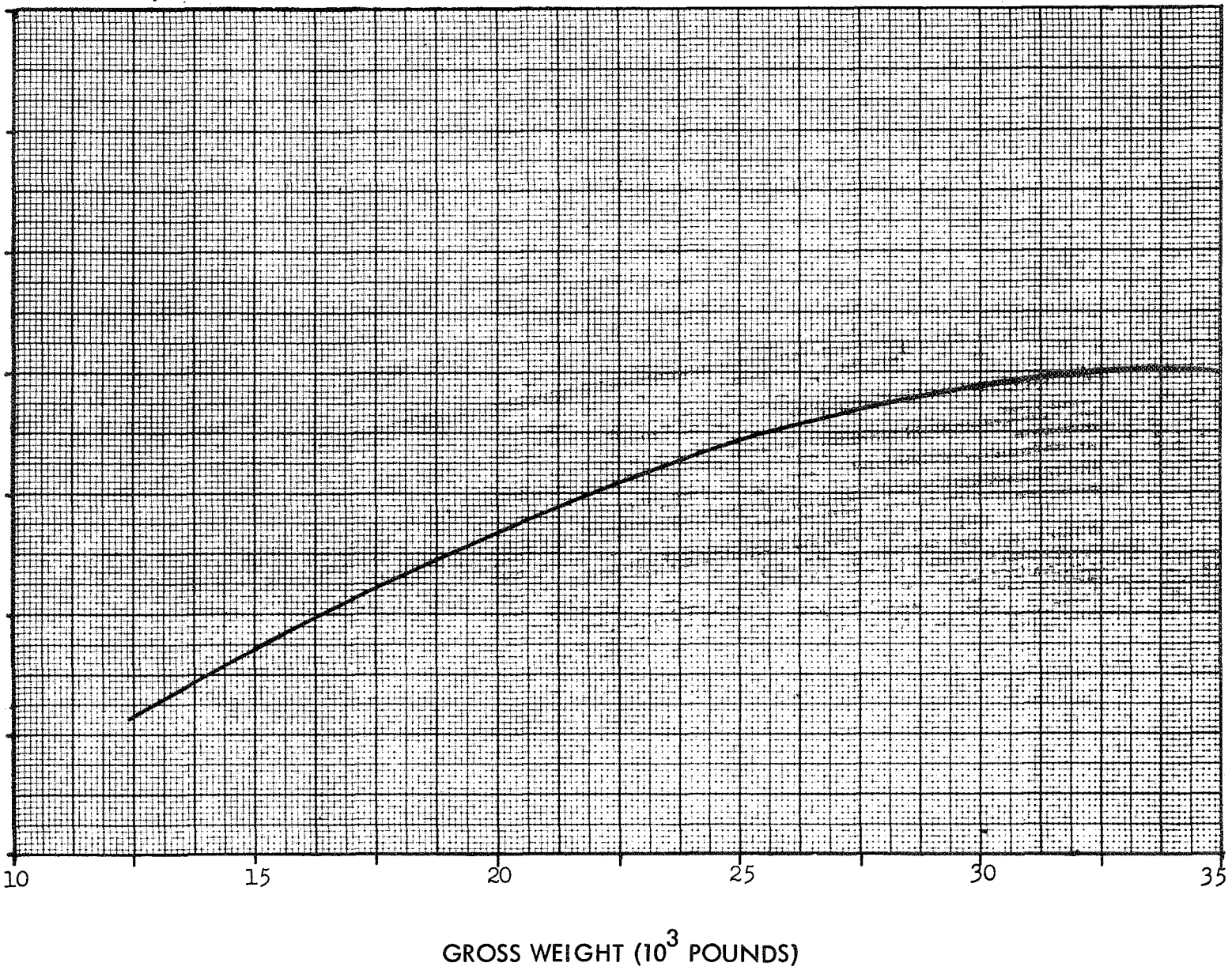

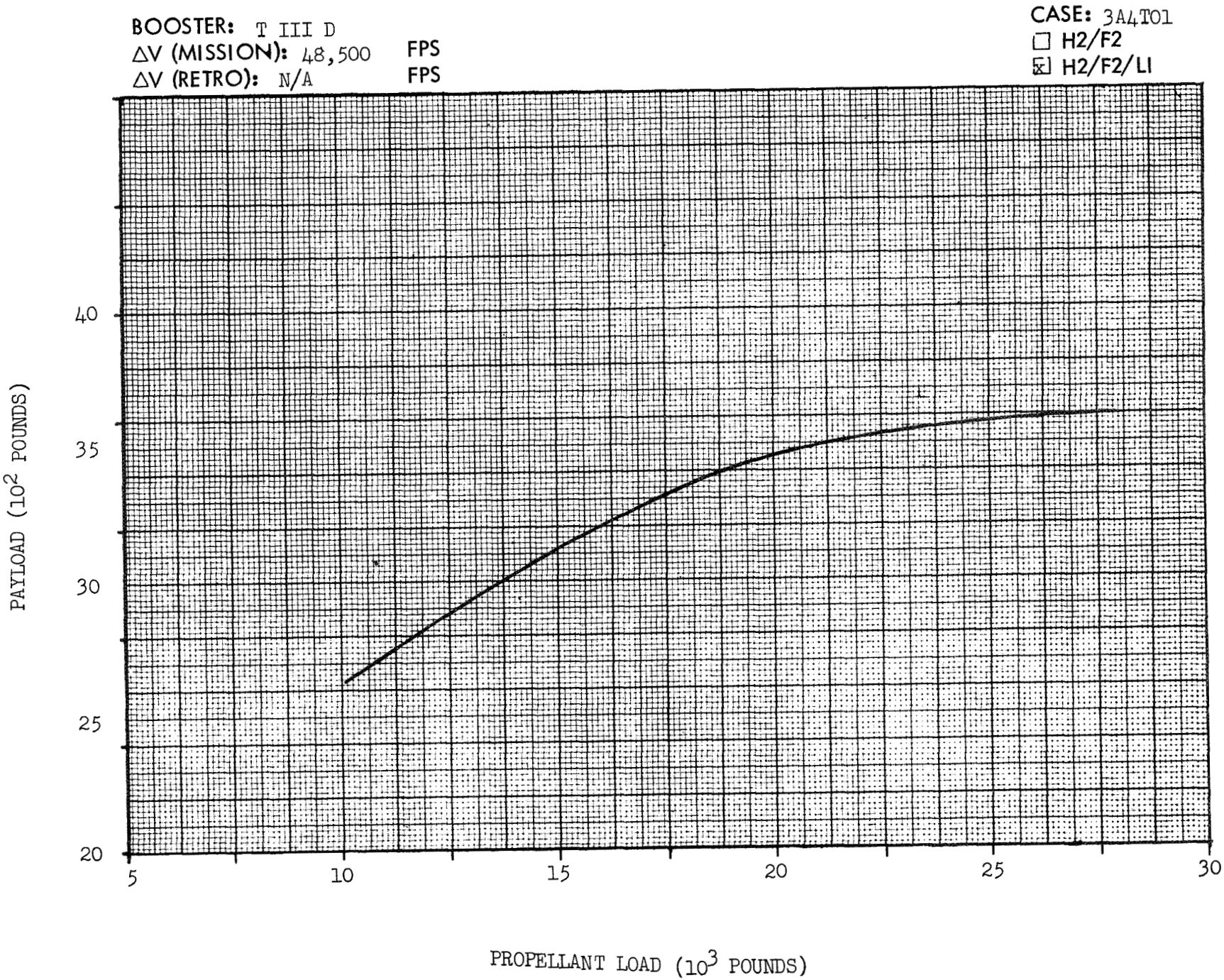
BOOSTER: T III D
ΔV (MISSION): 48,500 FPS
ΔV (RETRO): N/A FPS
CASE: 3A4T01
☐ H2/F2
☒ H2/F2/LI
PAYLOAD (10^2 POUNDS)
40
35
30
25
20
5
10
15
20
25
30
PROPELLANT LOAD (10^3 POUNDS)

BOOSTER: T III D
ΔV (MISSION): 48,500 FPS
ΔV (RETRO): N/A FPS

CASE: 3A4T01
☐ H2/F2
☒ H2/F2/LI

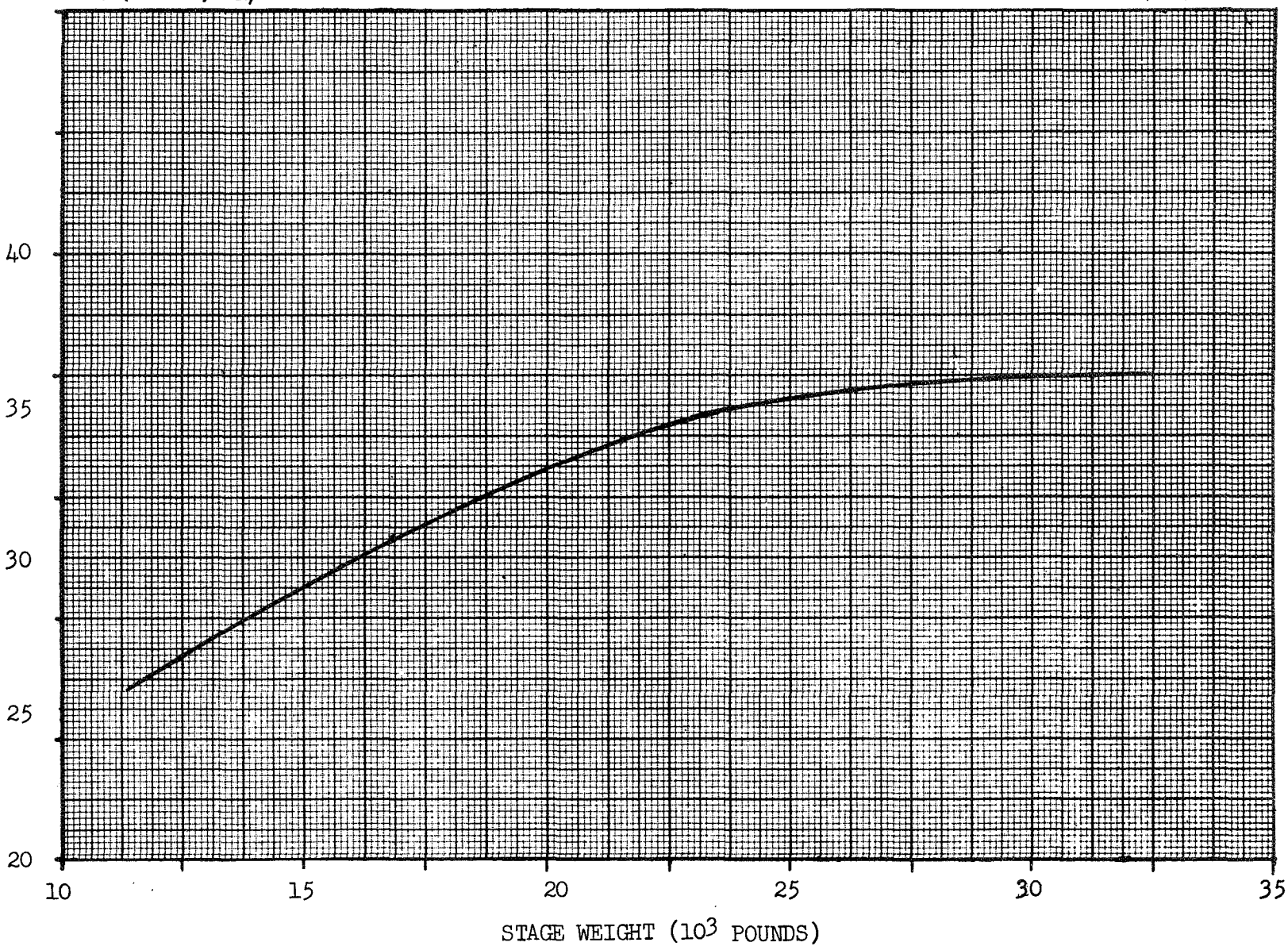

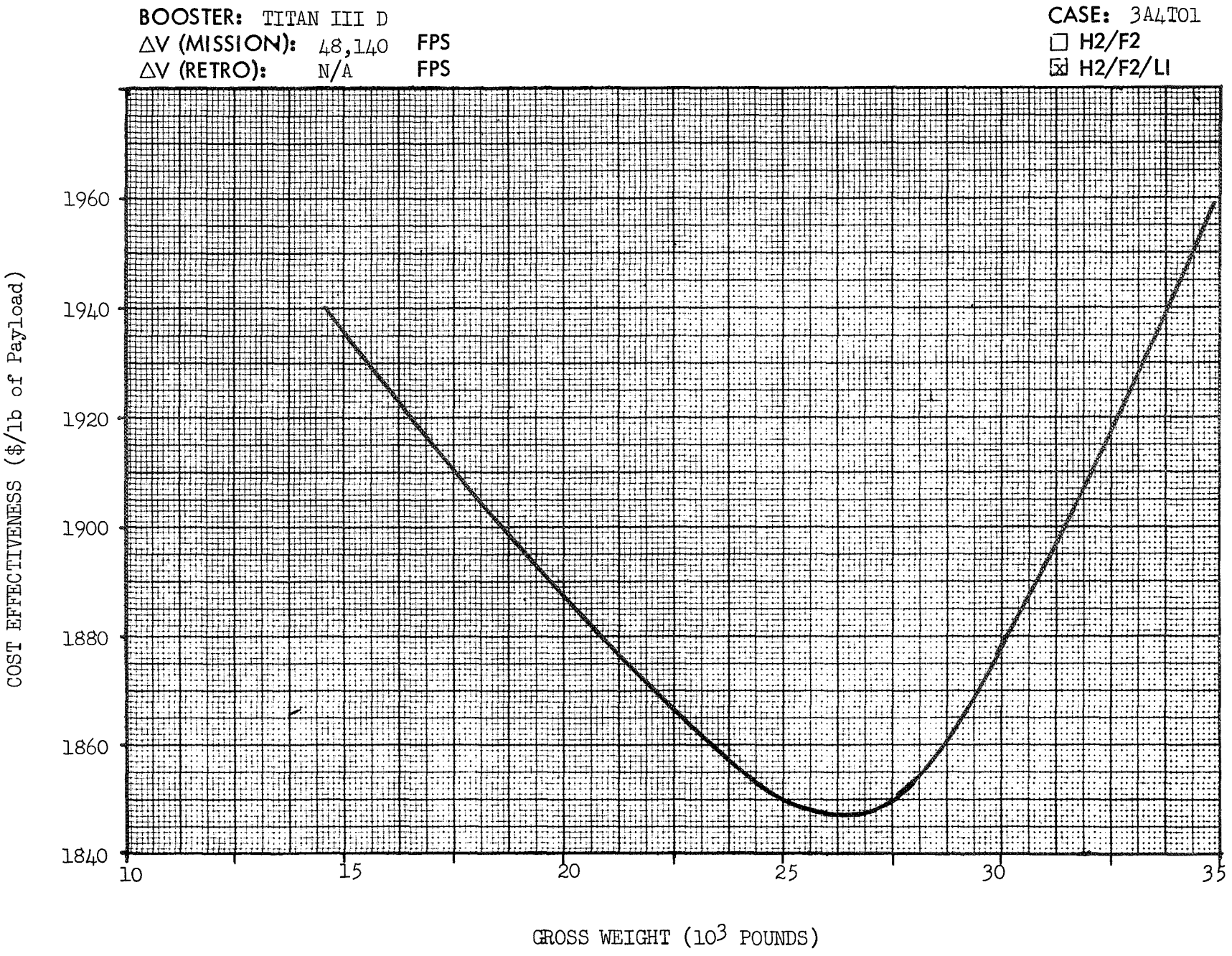
BOOSTER: TITAN III D
ΔV (MISSION): 48,140 FPS
ΔV (RETRO): N/A FPS
CASE: 3A4T01
☐ H2/F2
☒ H2/F2/LI
COST EFFECTIVENESS ($/lb of Payload)
1960
1940
1920
1900
1880
1860
1840
10
15
20
25
30
35
GROSS WEIGHT (10³ POUNDS)

BOOSTER: TITAN III D
ΔV (MISSION): 36140 FPS
ΔV (RETRO): N/A FPS

CASE: 304T01
☐ H2/F2
☒ H2/F2/LI

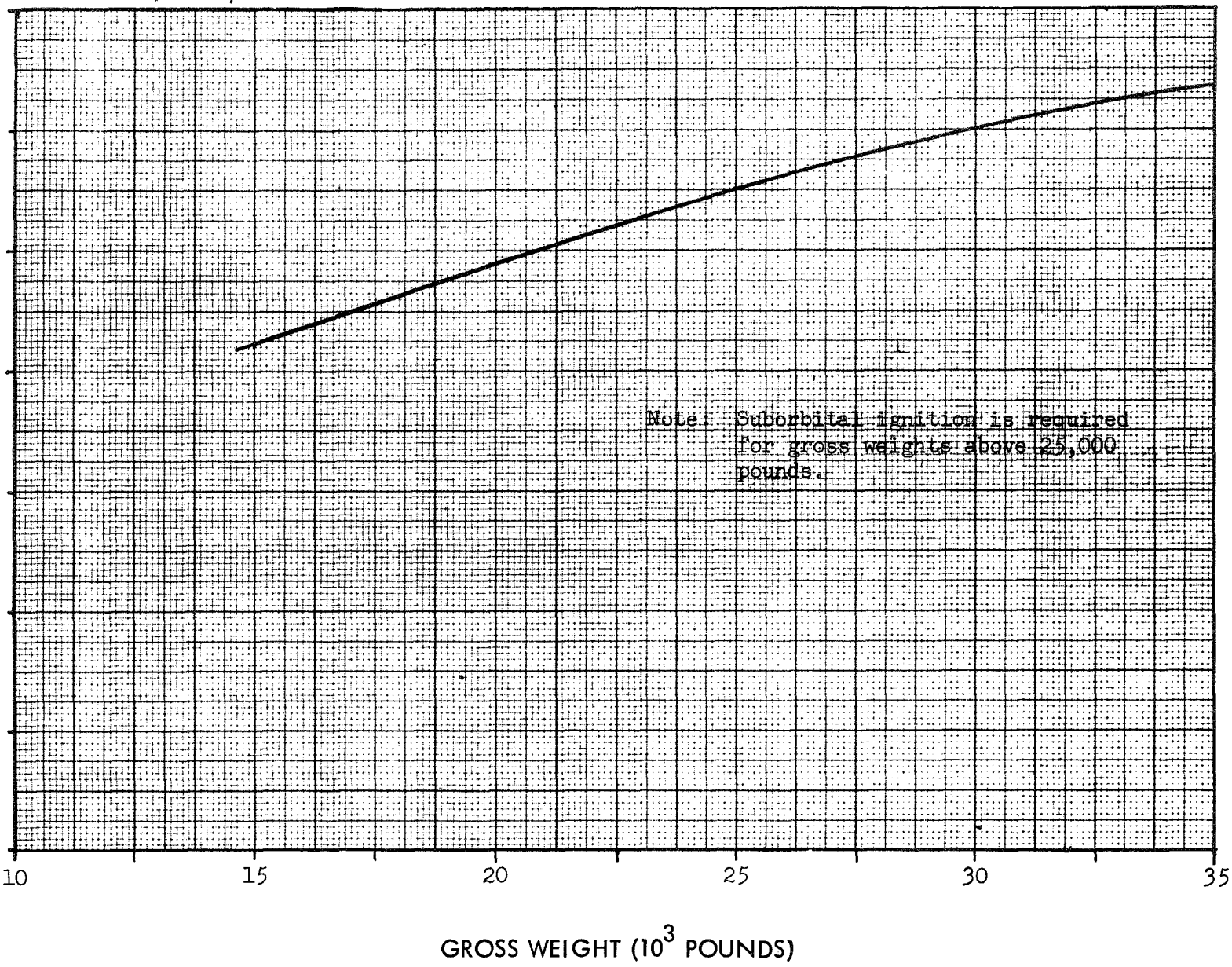

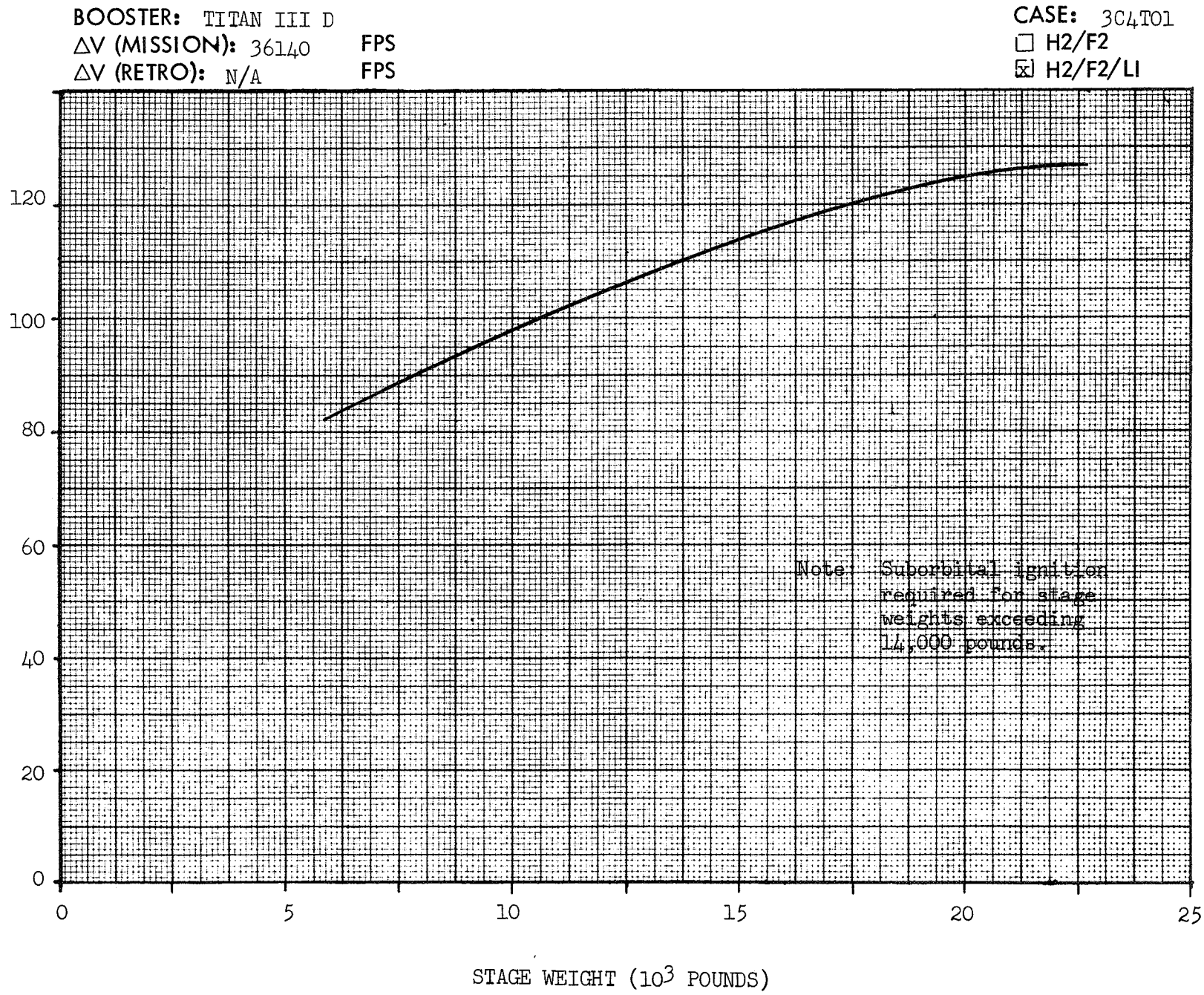
BOOSTER: TITAN III D
ΔV (MISSION): 36140 FPS
ΔV (RETRO): N/A FPS
CASE: 3C4T01
☐ H2/F2
☒ H2/F2/LI
PAYLOAD (10^2 POUNDS)
120
100
80
60
40
20
0
0
5
10
15
20
25
STAGE WEIGHT (10^3 POUNDS)
Note: Suborbital ignition required for stage weights exceeding 14,000 pounds.

BOOSTER: TITAN III D
ΔV (MISSION): 36140 FPS
ΔV (RETRO): N/A FPS

CASE: 3C4T01
☐ H2/F2
☒ H2/F2/LI

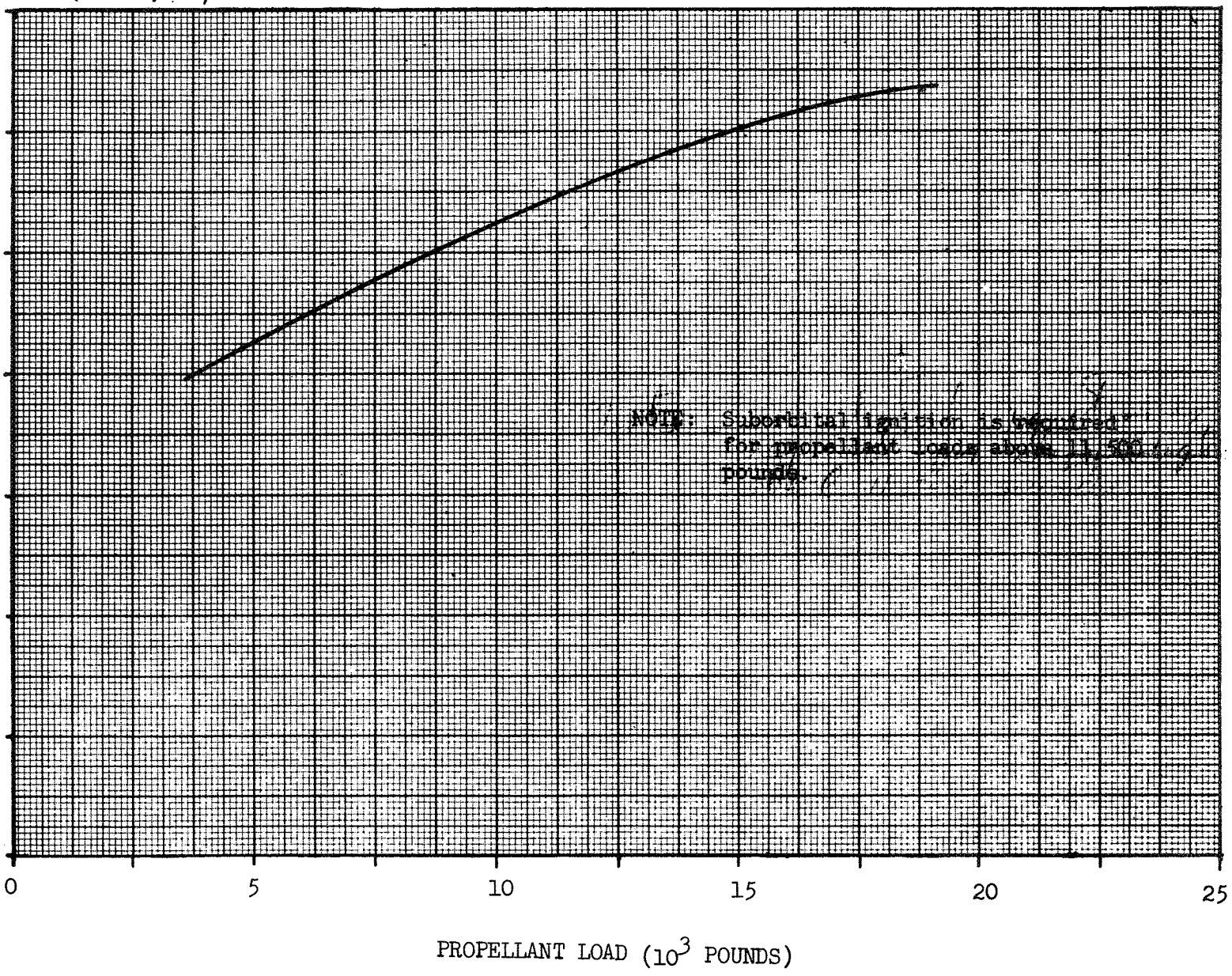

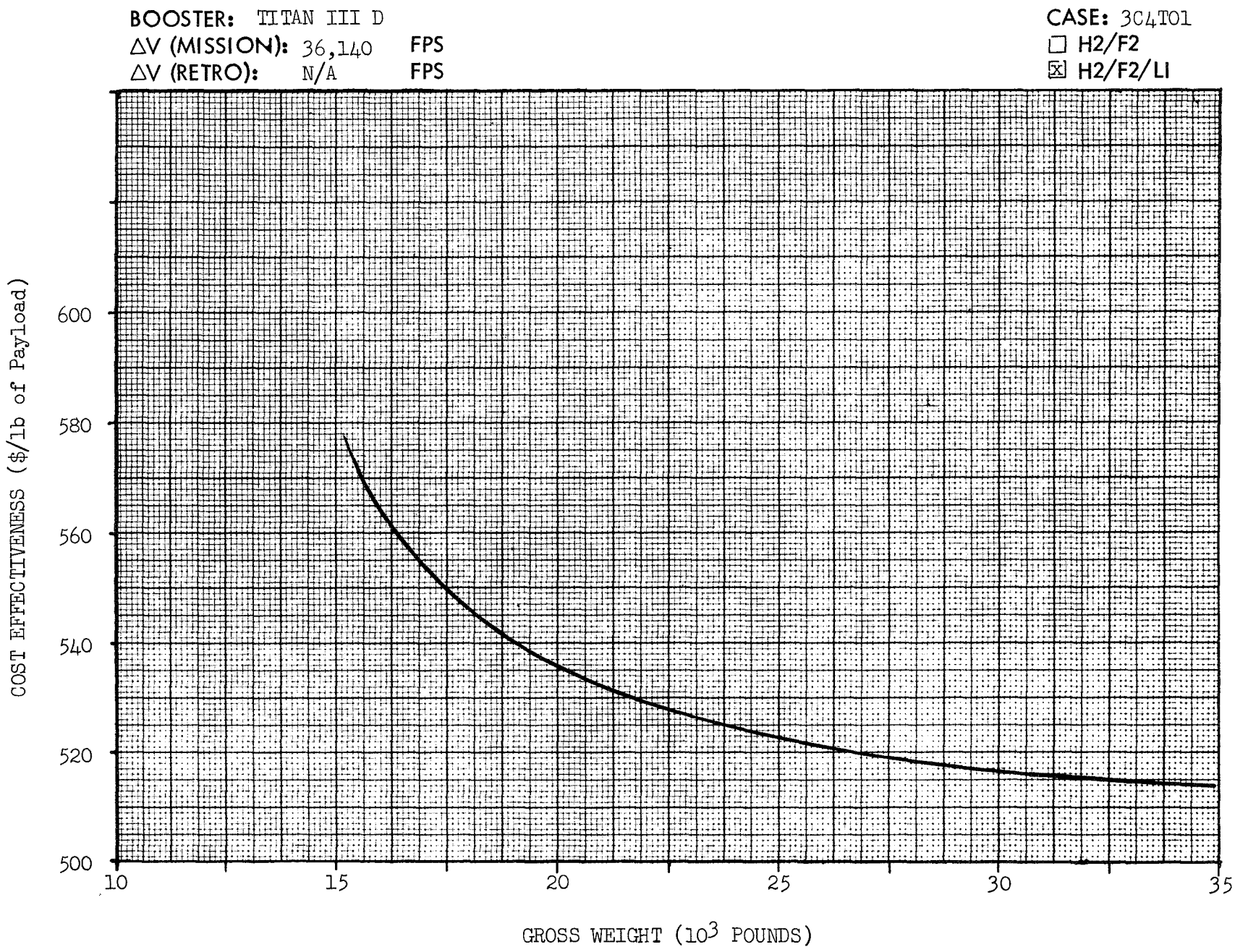
BOOSTER: TITAN III D
ΔV (MISSION): 36,140 FPS
ΔV (RETRO): N/A FPS
CASE: 3C4T01
☐ H2/F2
☒ H2/F2/LI
COST EFFECTIVENESS ($/lb of Payload)
600
580
560
540
520
500
10
15
20
25
30
35
GROSS WEIGHT (10³ POUNDS)

BOOSTER: TITAN III D
ΔV (MISSION): 54,500 FPS
ΔV (RETRO): N/A FPS

CASE: 3E4T01
☐ H2/F2
☒ H2/F2/LI

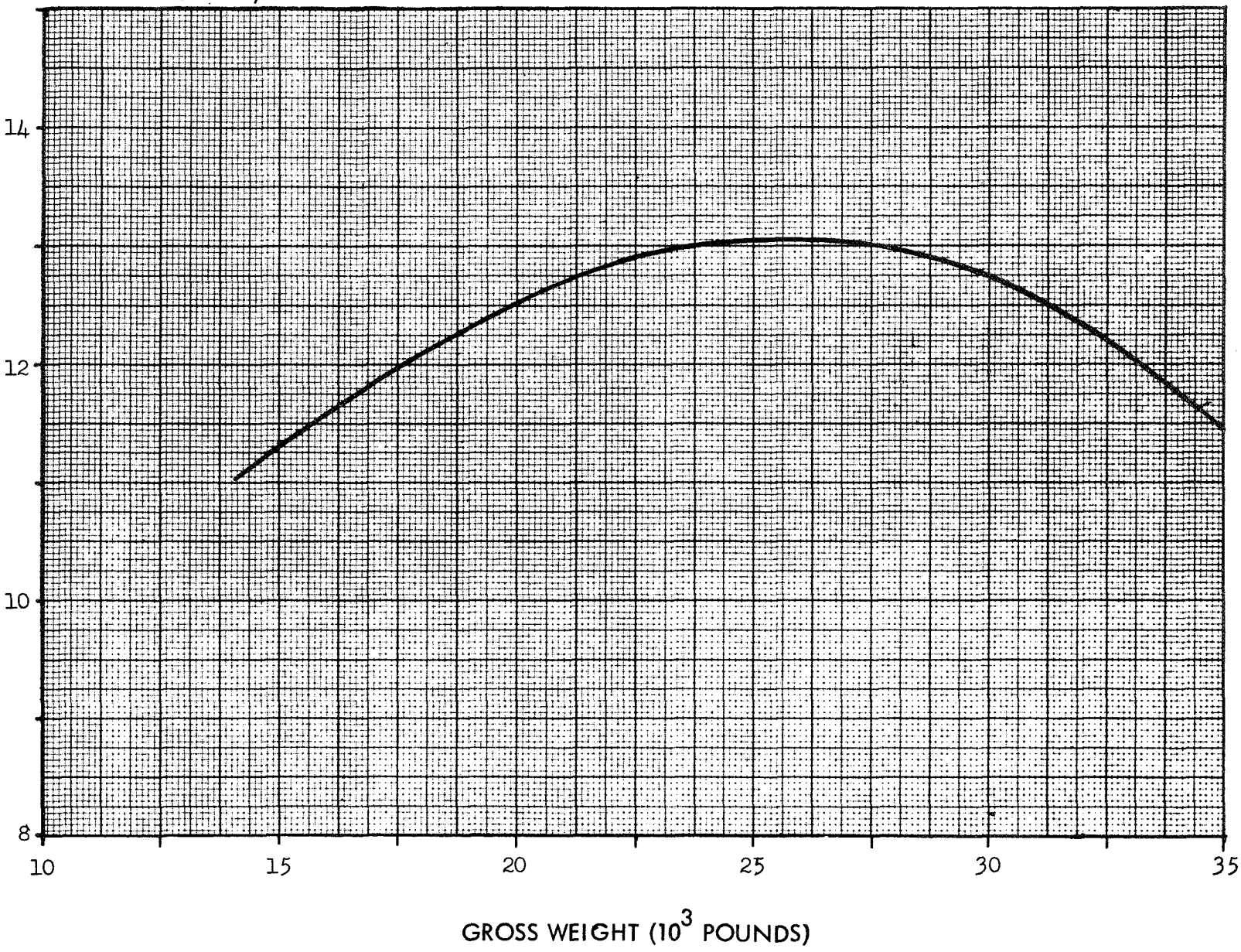

BOOSTER: TITAN III D
ΔV (MISSION): 54,500 FPS
ΔV (RETRO): N/A FPS

CASE: 3E4T01
☐ H2/F2
☒ H2/F2/LI

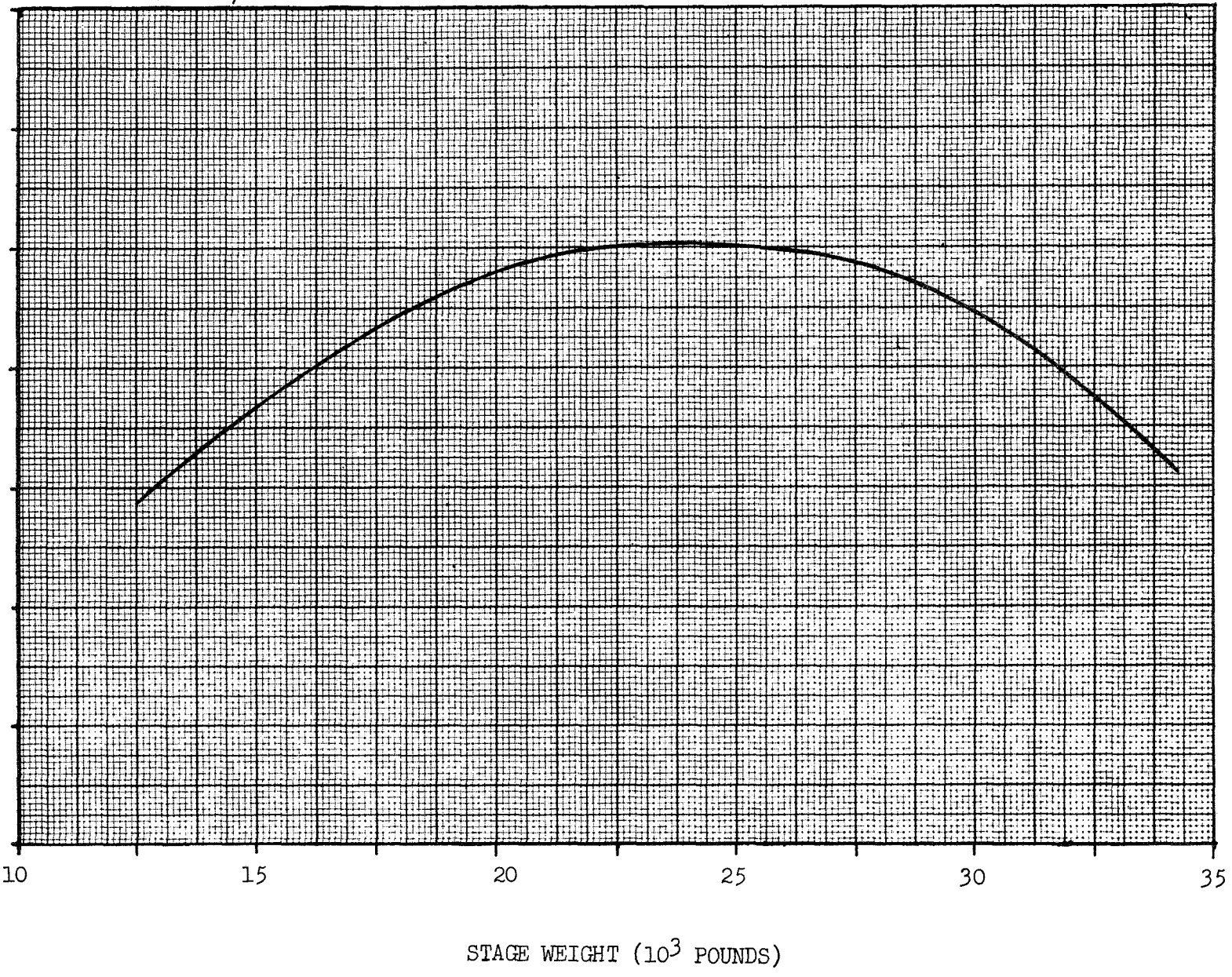

PAYLOAD (10^2 POUNDS)

STAGE WEIGHT (10^3 POUNDS)

BOOSTER: TITAN III D
ΔV (MISSION): 54,500 FPS
ΔV (RETRO): N/A FPS

CASE: 3E4T01
☐ H2/F2
☒ H2/F2/LI

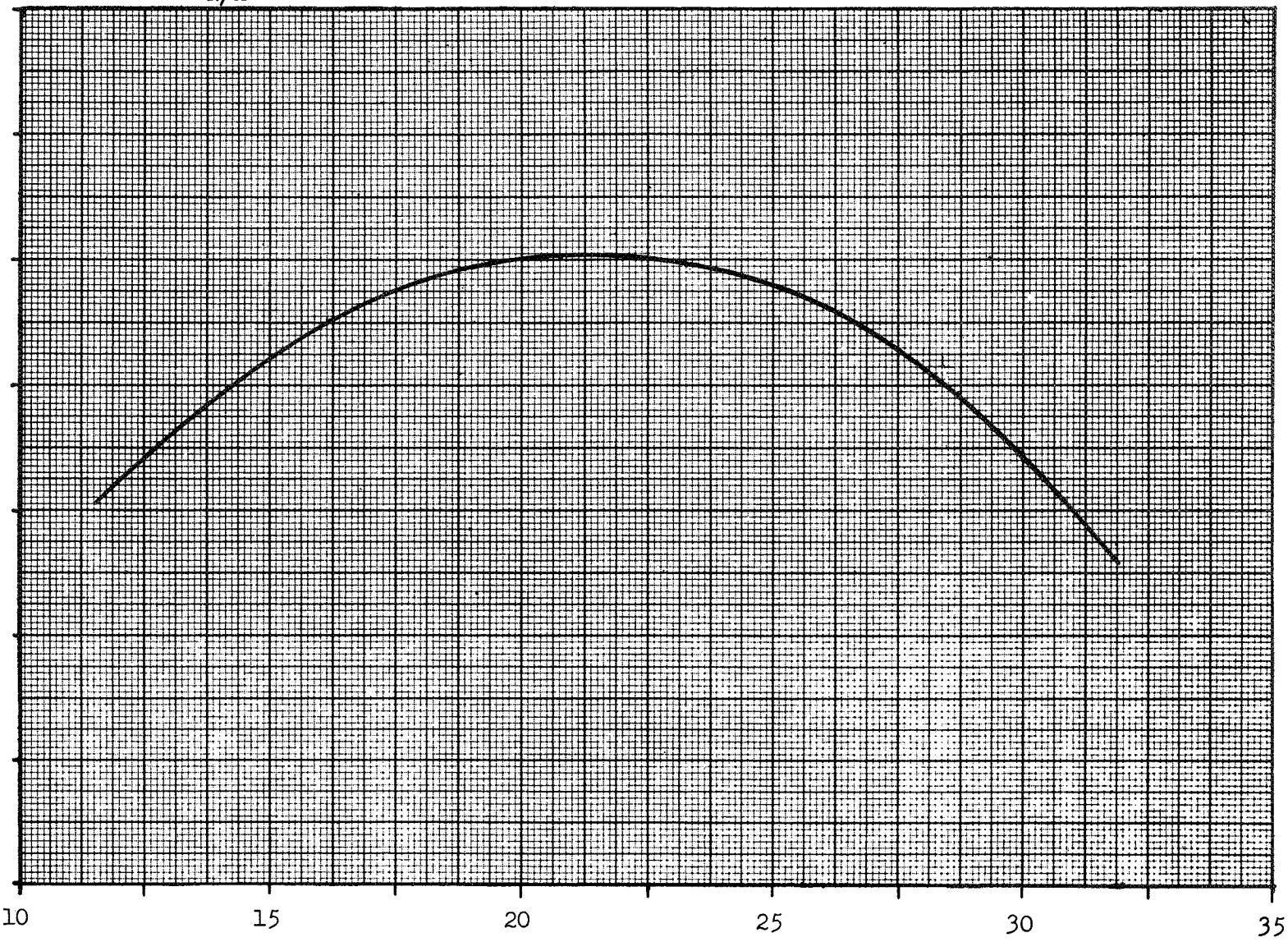

PAYLOAD (10^2 POUNDS)

PROPELLANT LOAD (10^3 POUNDS)

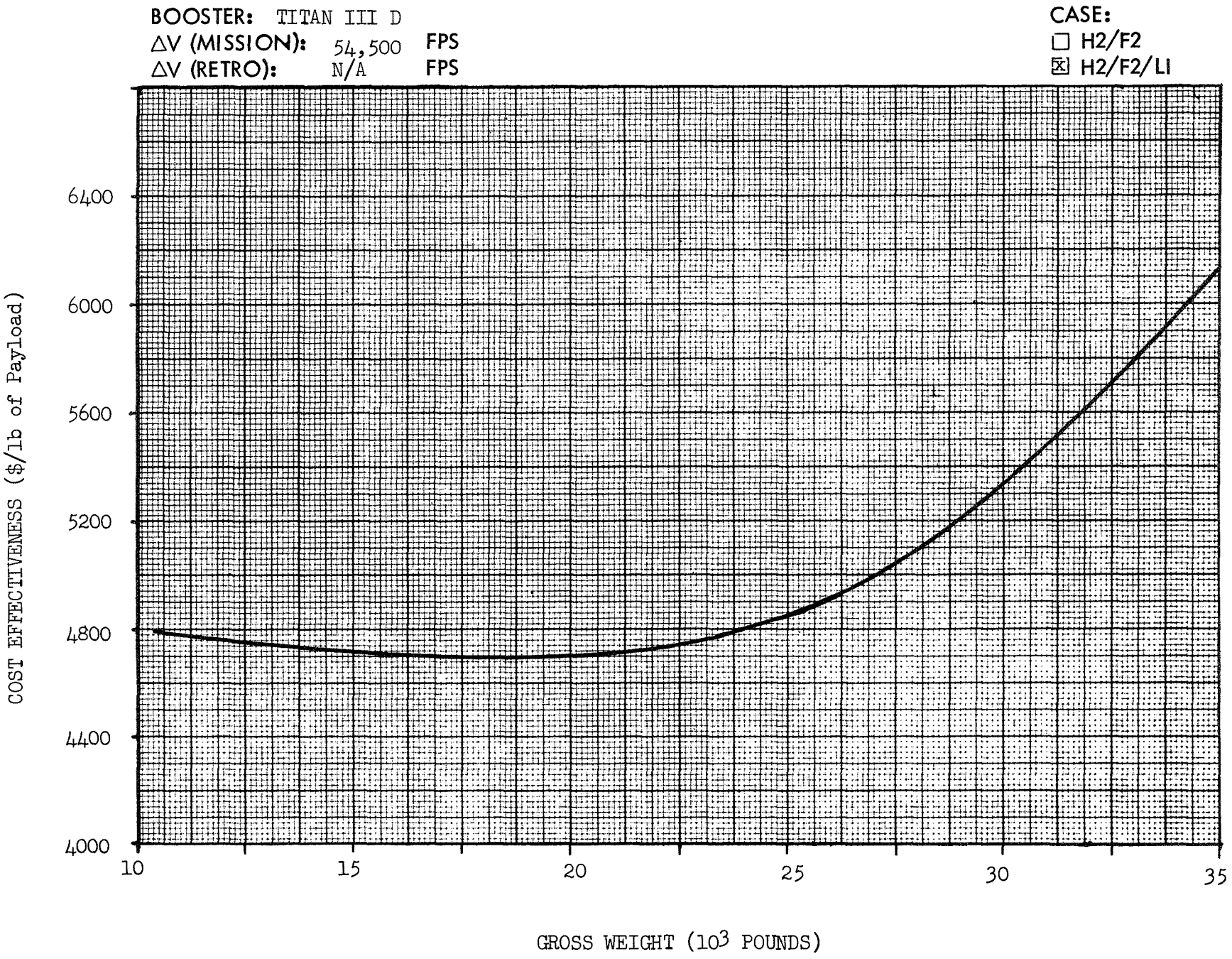
BOOSTER: TITAN III D
ΔV (MISSION): 54,500 FPS
ΔV (RETRO): N/A FPS
CASE:
☐ H2/F2
☒ H2/F2/LI
COST EFFECTIVENESS ($/lb of Payload)
6400
6000
5600
5200
4800
4400
4000
10
15
20
25
30
35
GROSS WEIGHT (10³ POUNDS)

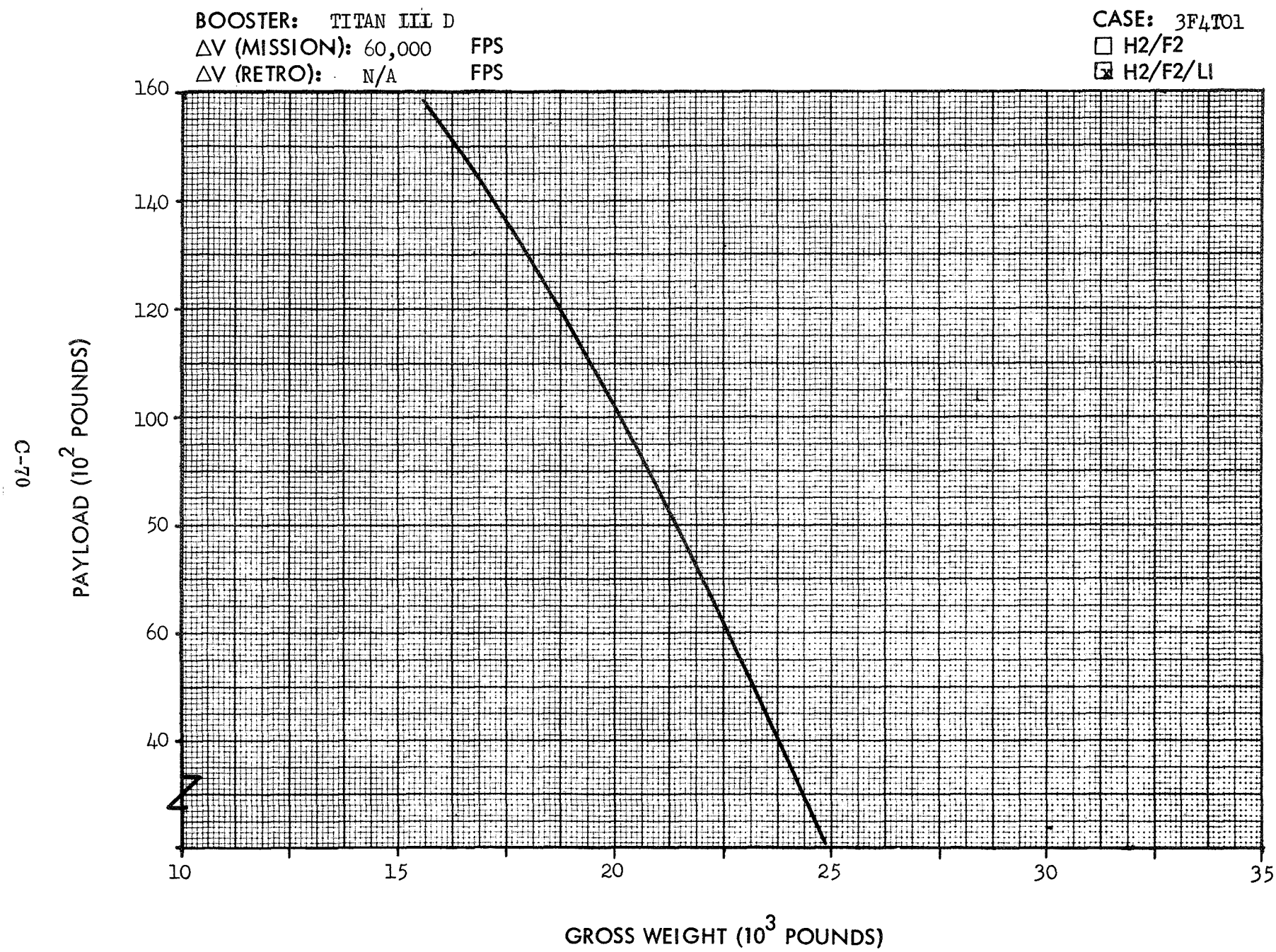
BOOSTER: TITAN IIIL D
ΔV (MISSION): 60,000 FPS
ΔV (RETRO): N/A FPS
CASE: 3F4T01
☐ H2/F2
☒ H2/F2/LI
160
140
120
100
50
60
40
10
15
20
25
30
35
PAYLOAD (10^2 POUNDS)
GROSS WEIGHT (10^3 POUNDS)

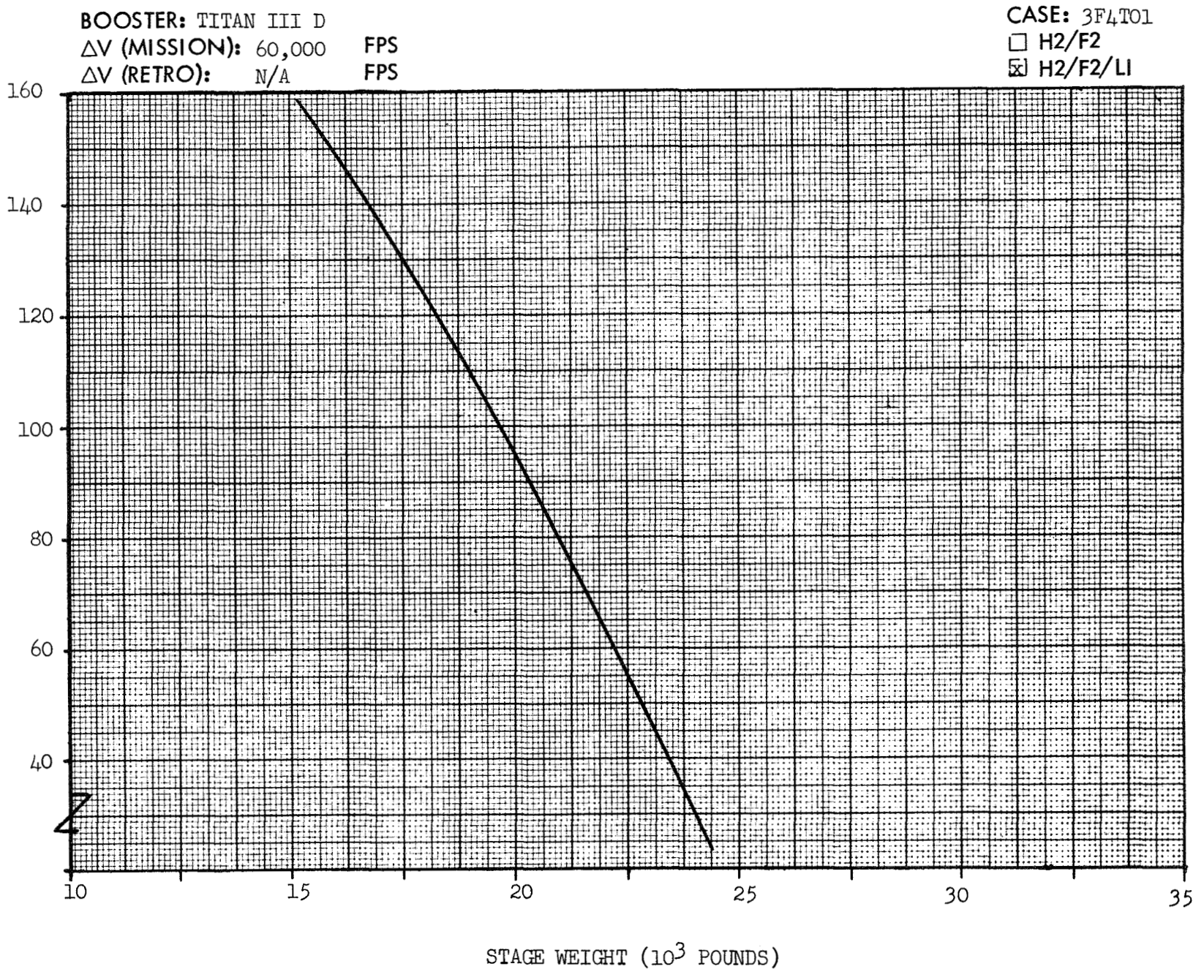
BOOSTER: TITAN III D
ΔV (MISSION): 60,000 FPS
ΔV (RETRO): N/A FPS
CASE: 3F4T01
☐ H2/F2
☒ H2/F2/LI
160
140
120
100
80
60
40
PAYLOAD (10^2 POUNDS)
10
15
20
25
30
35
STAGE WEIGHT (10^3 POUNDS)

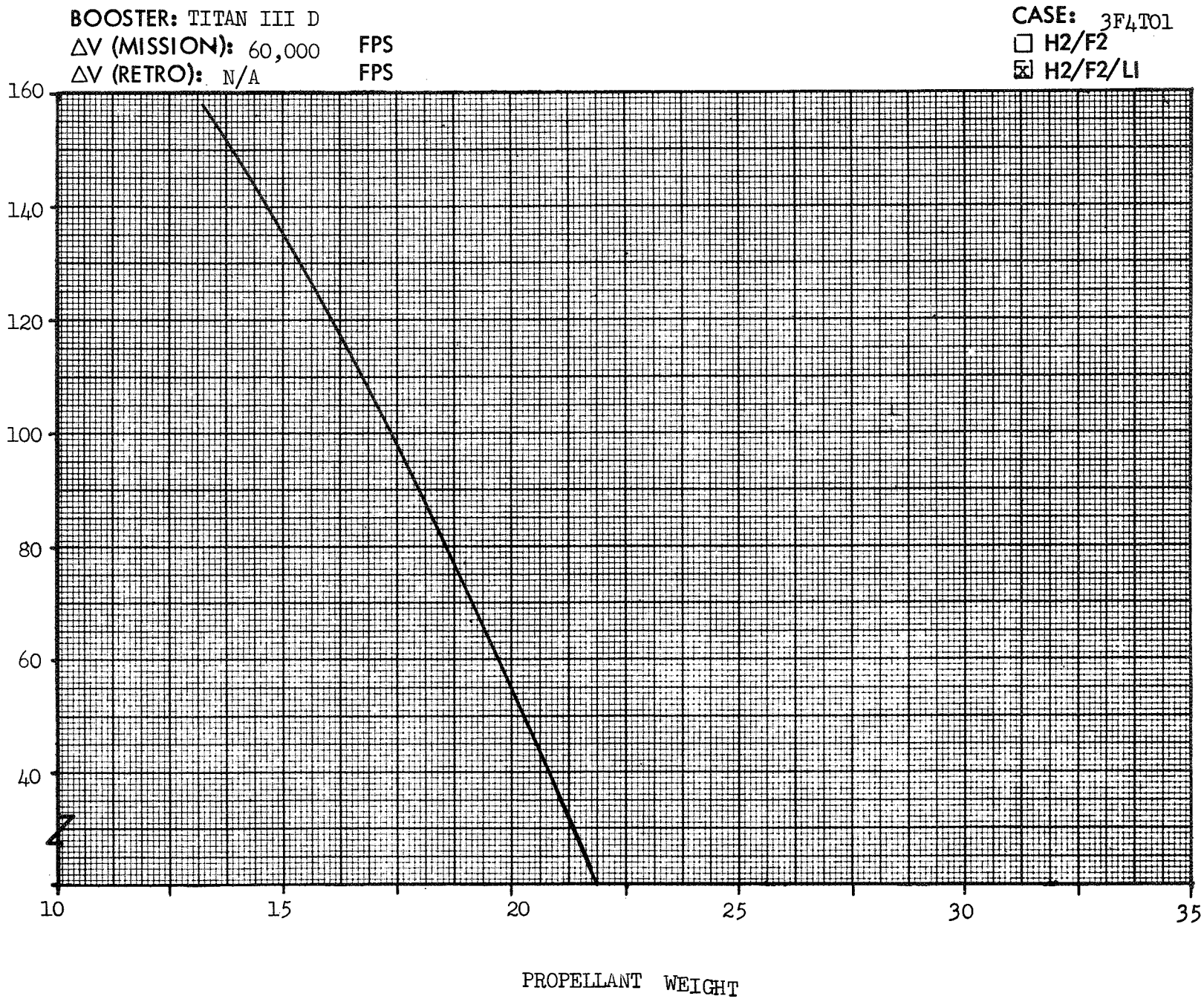
BOOSTER: TITAN III D
ΔV (MISSION): 60,000 FPS
ΔV (RETRO): N/A FPS
CASE: 3F4T01
☐ H2/F2
☒ H2/F2/LI
160
140
120
100
80
60
40
10
15
20
25
30
35
PAYLOAD (10^2 POUNDS)
PROPELLANT WEIGHT

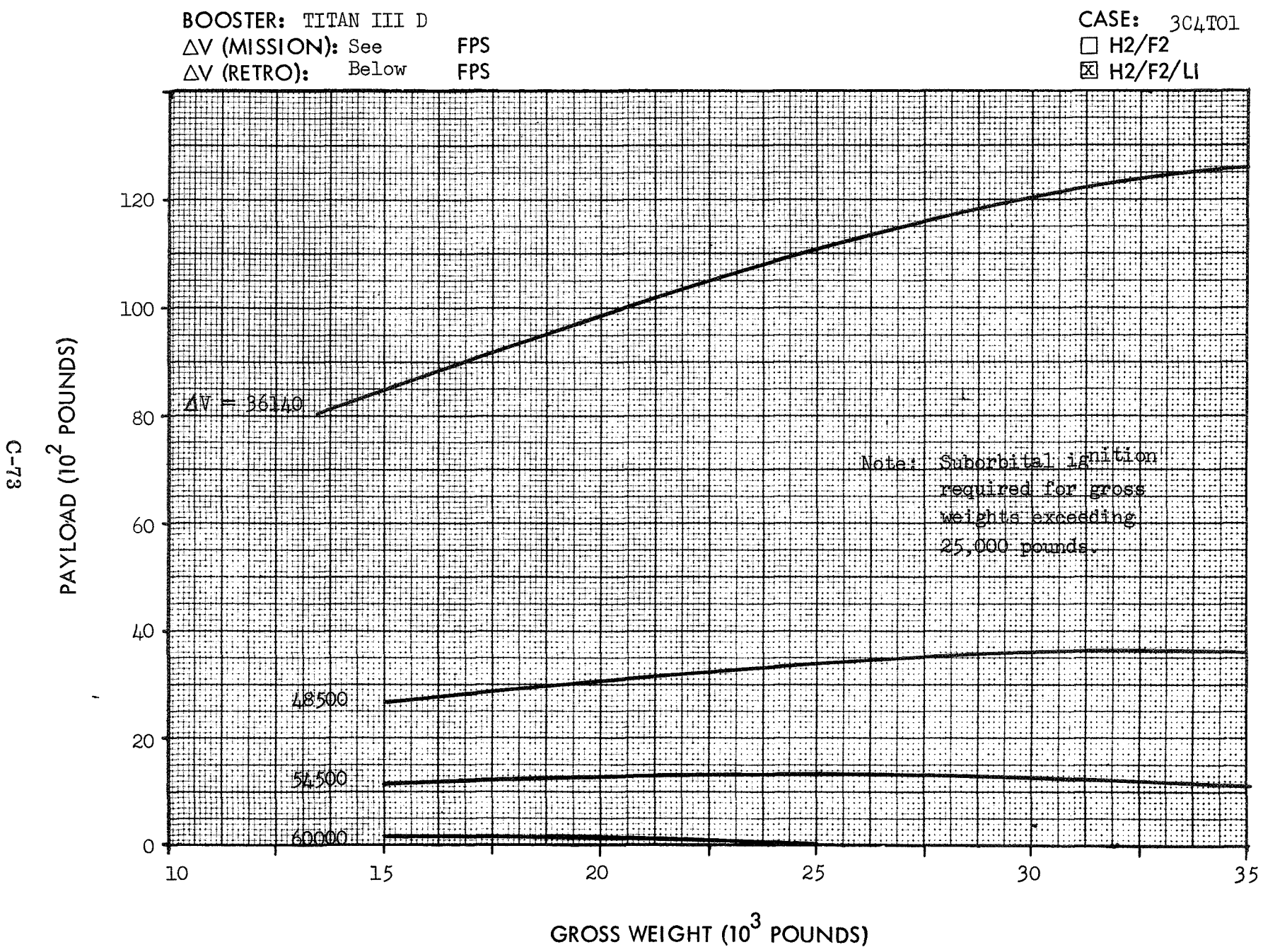
BOOSTER: TITAN III D
ΔV (MISSION): See FPS
ΔV (RETRO): Below FPS
CASE: 304T01
☐ H2/F2
☒ H2/F2/LI
PAYLOAD (10^2 POUNDS)
GROSS WEIGHT (10^3 POUNDS)
0
20
40
60
80
100
120
10
15
20
25
30
35
ΔV = 36140
48500
54500
60000
Note: Suborbital ignition required for gross weights exceeding 25,000 pounds.

BOOSTER: TITAN III D
ΔV (MISSION): D. I. FPS
ΔV (RETRO): N/A FPS

CASE:
☐ H2/F2
☒ H2/F2/LI

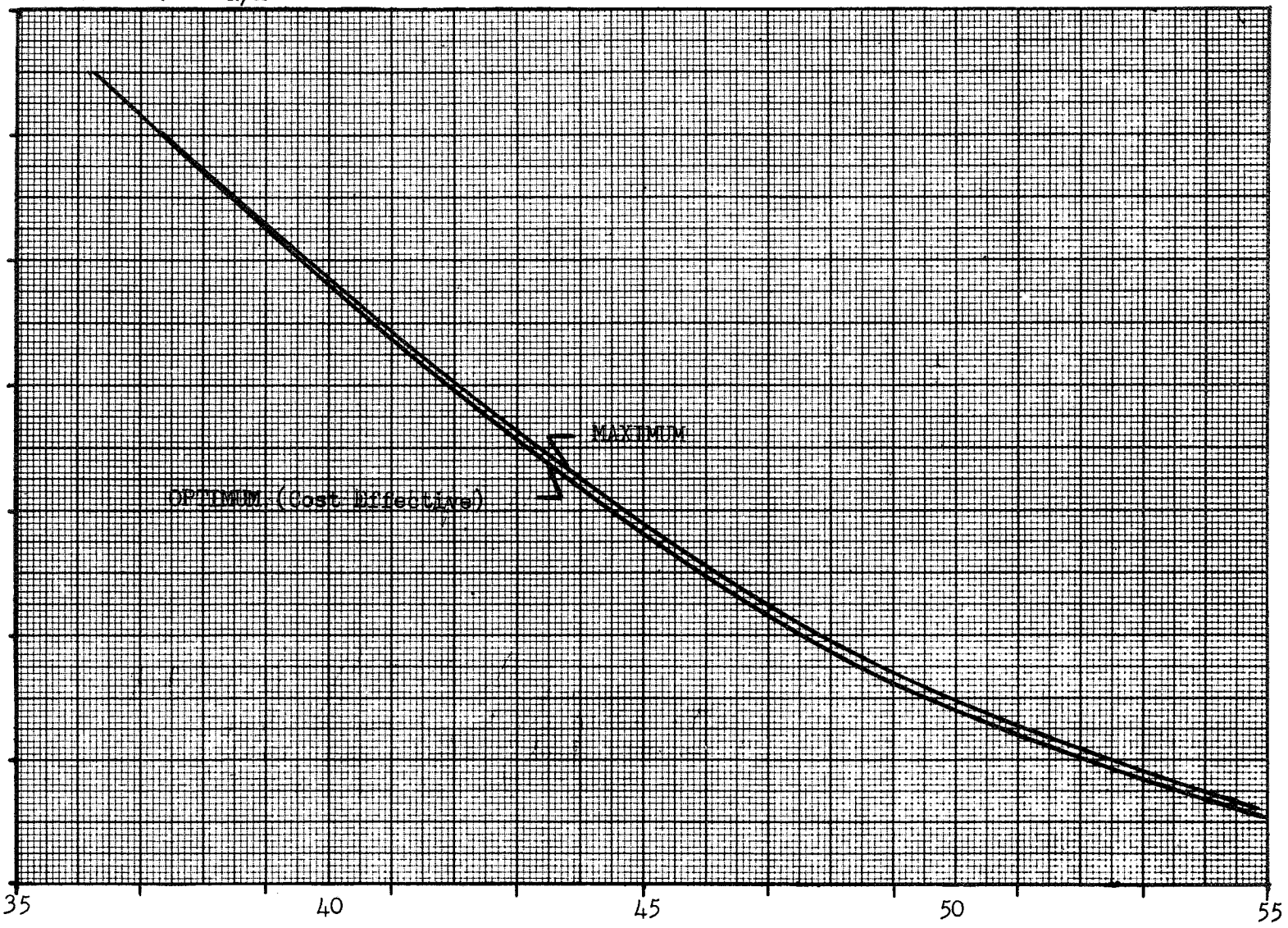

PAYLOAD (POUNDS)

MISSION VELOCITY (10^3 FPS)

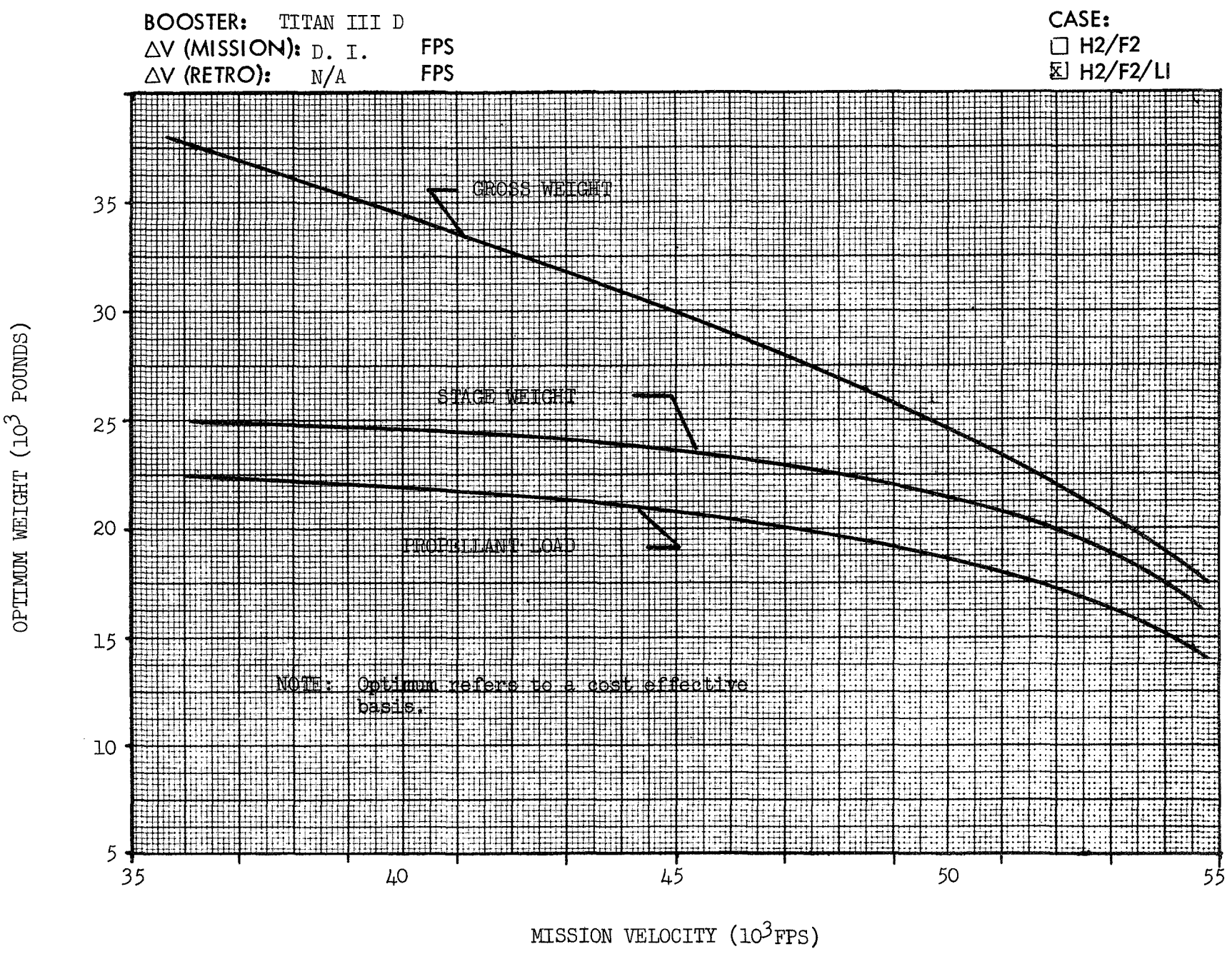
BOOSTER: TITAN III D
ΔV (MISSION): D. I. FPS
ΔV (RETRO): N/A FPS
CASE:
☐ H2/F2
☒ H2/F2/LI
GROSS WEIGHT
STAGE WEIGHT
PROPELLANT LOAD
NOTE: Optimum refers to a cost effective basis.
OPTIMUM WEIGHT (10^3 POUNDS)
MISSION VELOCITY (10^3FPS)
5
10
15
20
25
30
35
35
40
45
50
55

BOOSTER: TITAN III D
ΔV (MISSION): 48,500 FPS
ΔV (RETRO): N/A FPS
GROSS WT: 20,000

CASE: 4A4T01
☐ H2/F2
☒ H2/F2/LI-GEL

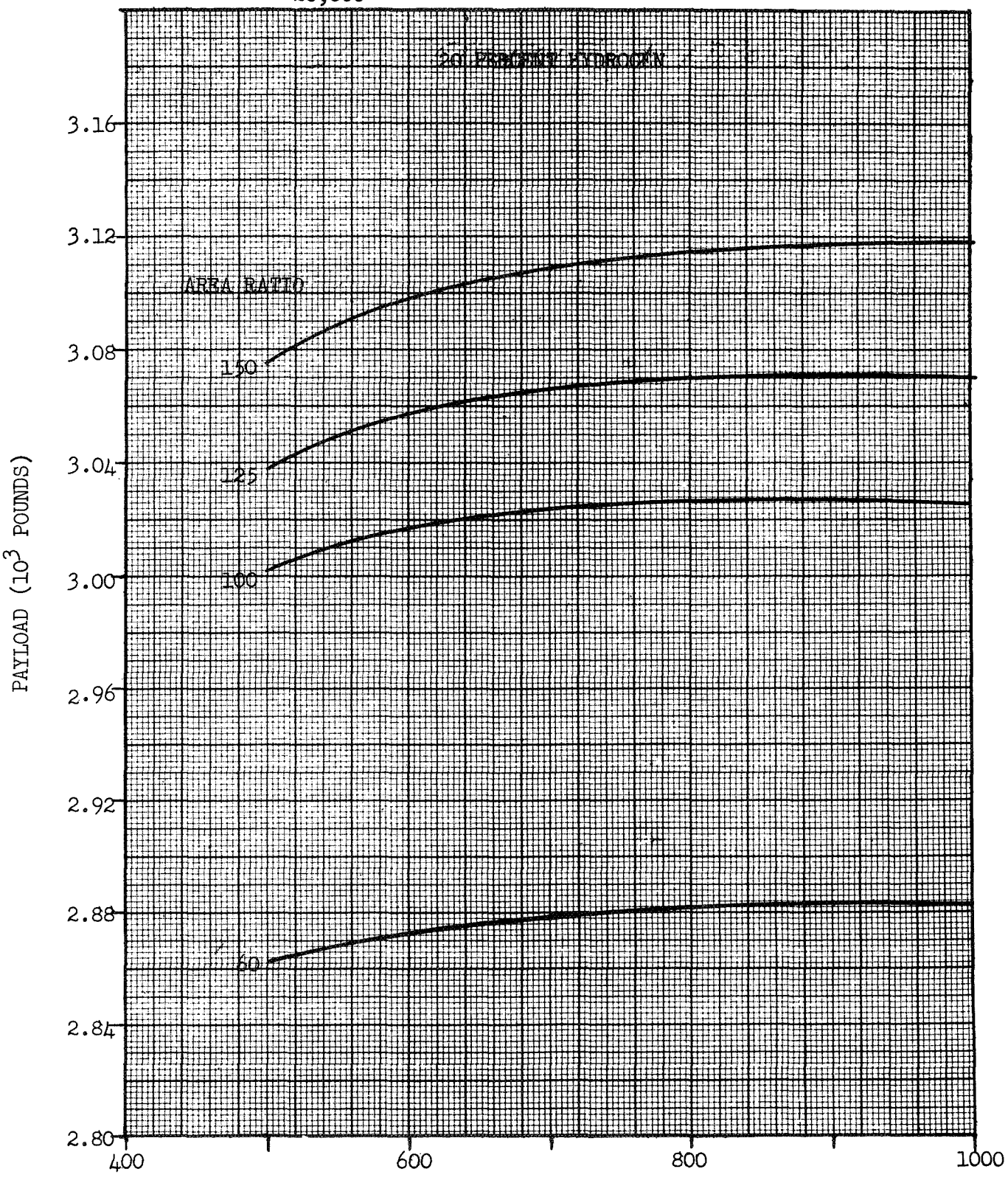

BOOSTER: TITAN III D
ΔV (MISSION): 48,500 FPS
ΔV (RETRO): N/A FPS
GROSS WT: 20,000

CASE: 4A4T01
☐ H2/F2
☒ H2/F2/LI - GEL

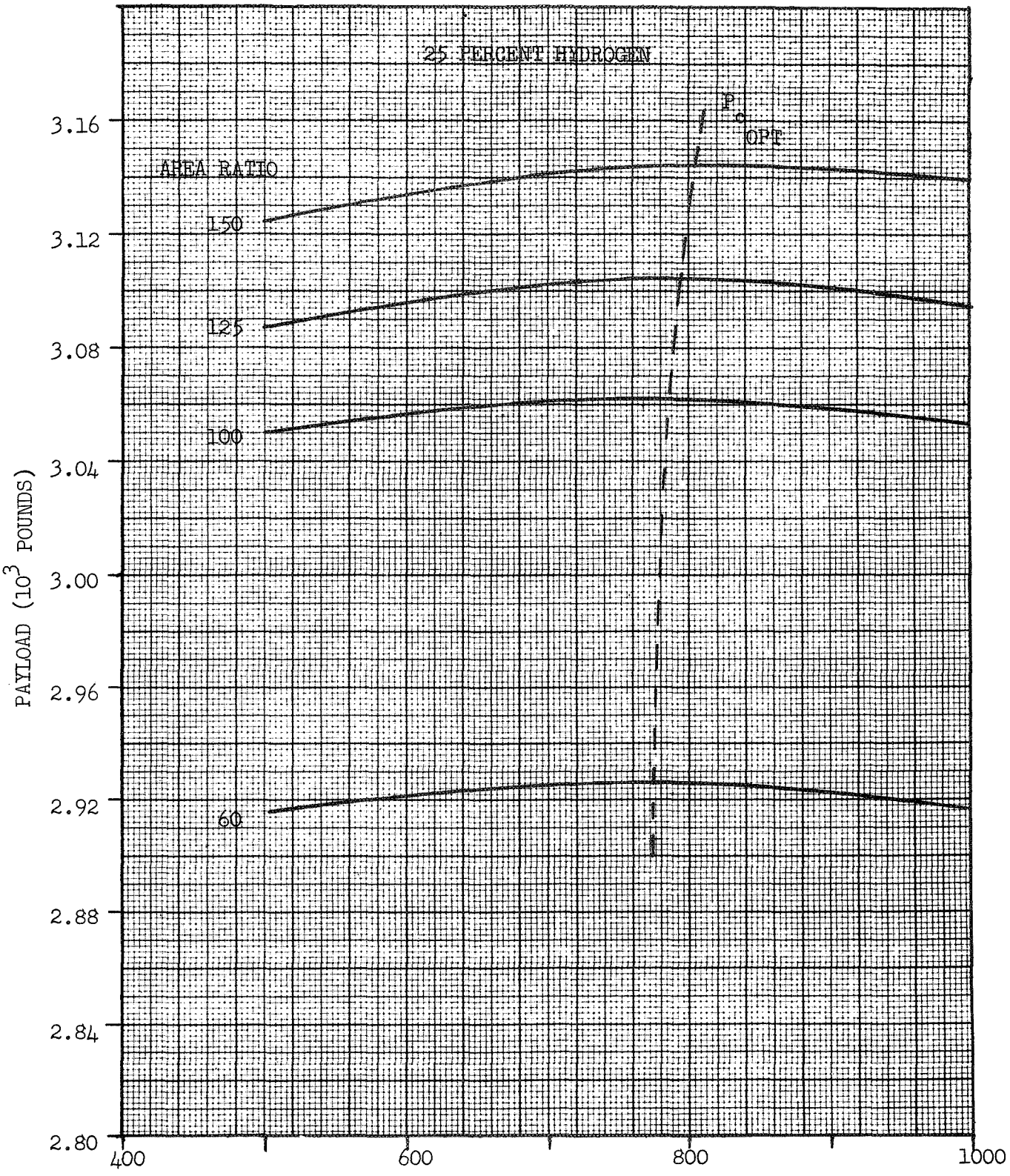

BOOSTER: TITAN III D
ΔV (MISSION): 48,500 FPS
ΔV (RETRO): N/A FPS
GROSS WT: 20,000

CASE: 4A4T01
☐ H2/F2
☒ H2/F2/LI-GEL

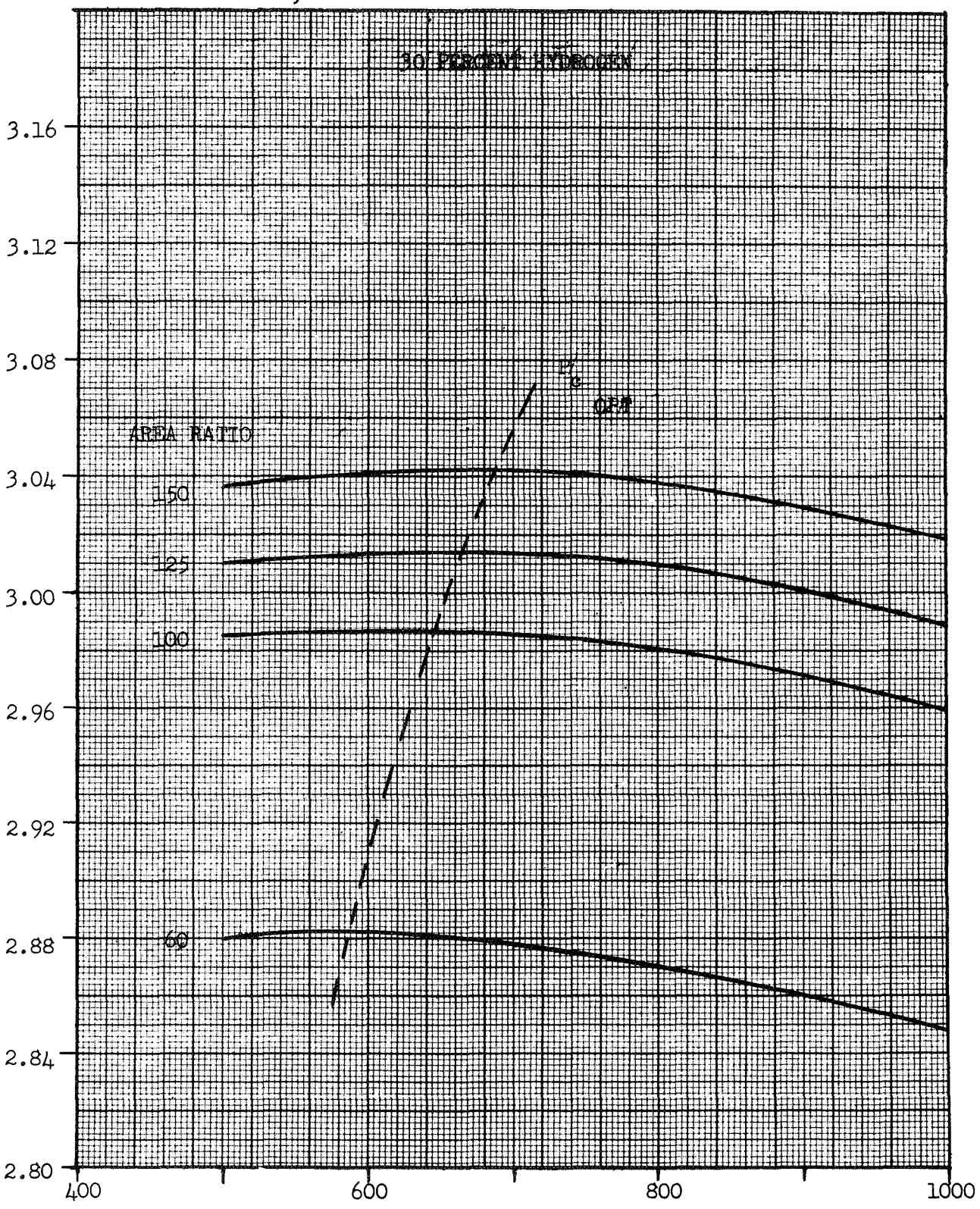

BOOSTER: TITAN III D
ΔV (MISSION): 48,500 FPS
ΔV (RETRO): N/A FPS
GROSS WT: 20,000

CASE: 4A4T01
☐ H2/F2
☒ H2/F2/LI-GEL

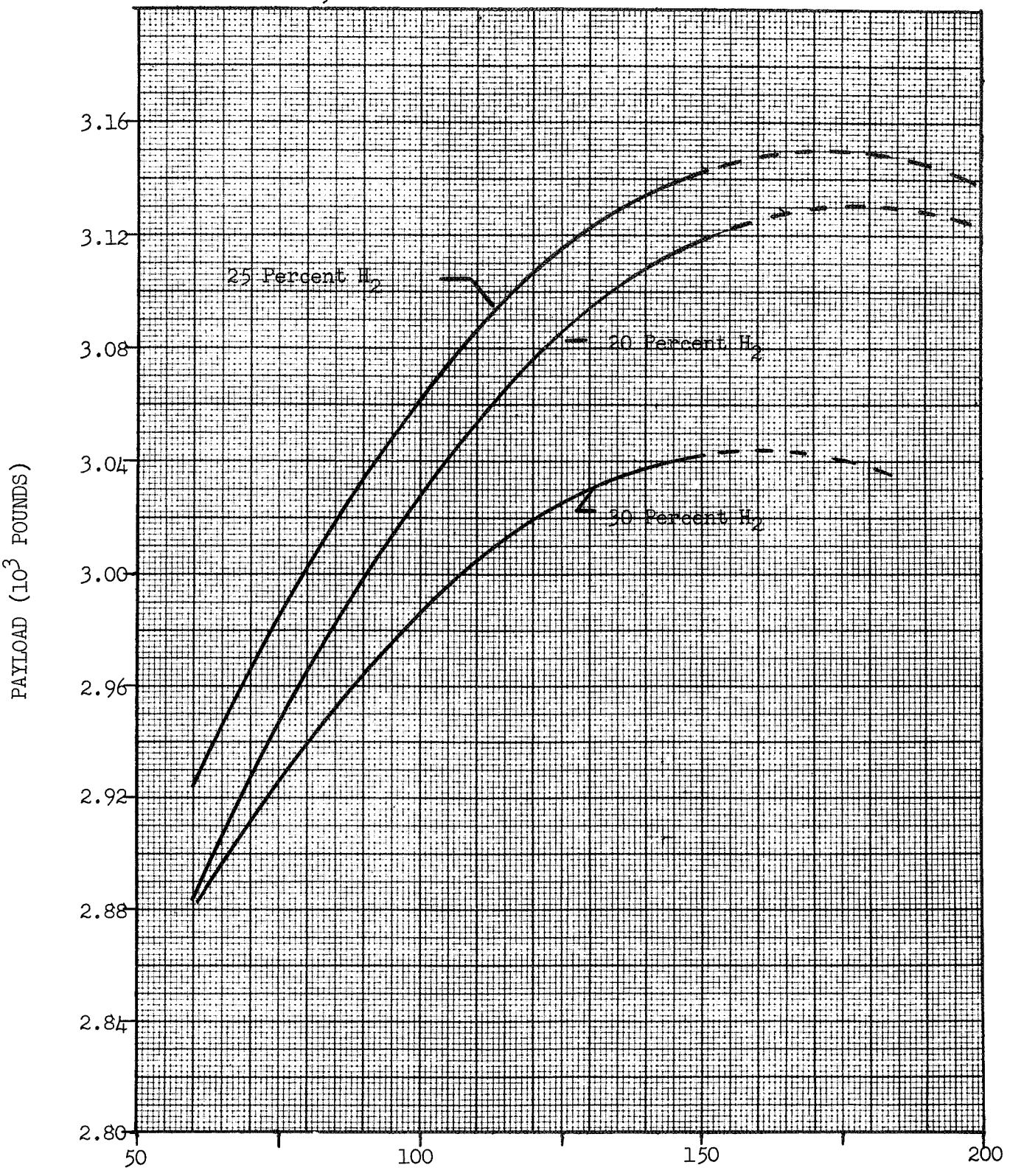

NOZZLE EXPANSION RATIO

BOOSTER: TITAN III D
ΔV (MISSION): 48,500 FPS
ΔV (RETRO): N/A FPS
GROSS WT: 20,000

CASE: 4A4T01
☐ H2/F2
☒ H2/F2/LI-GEL

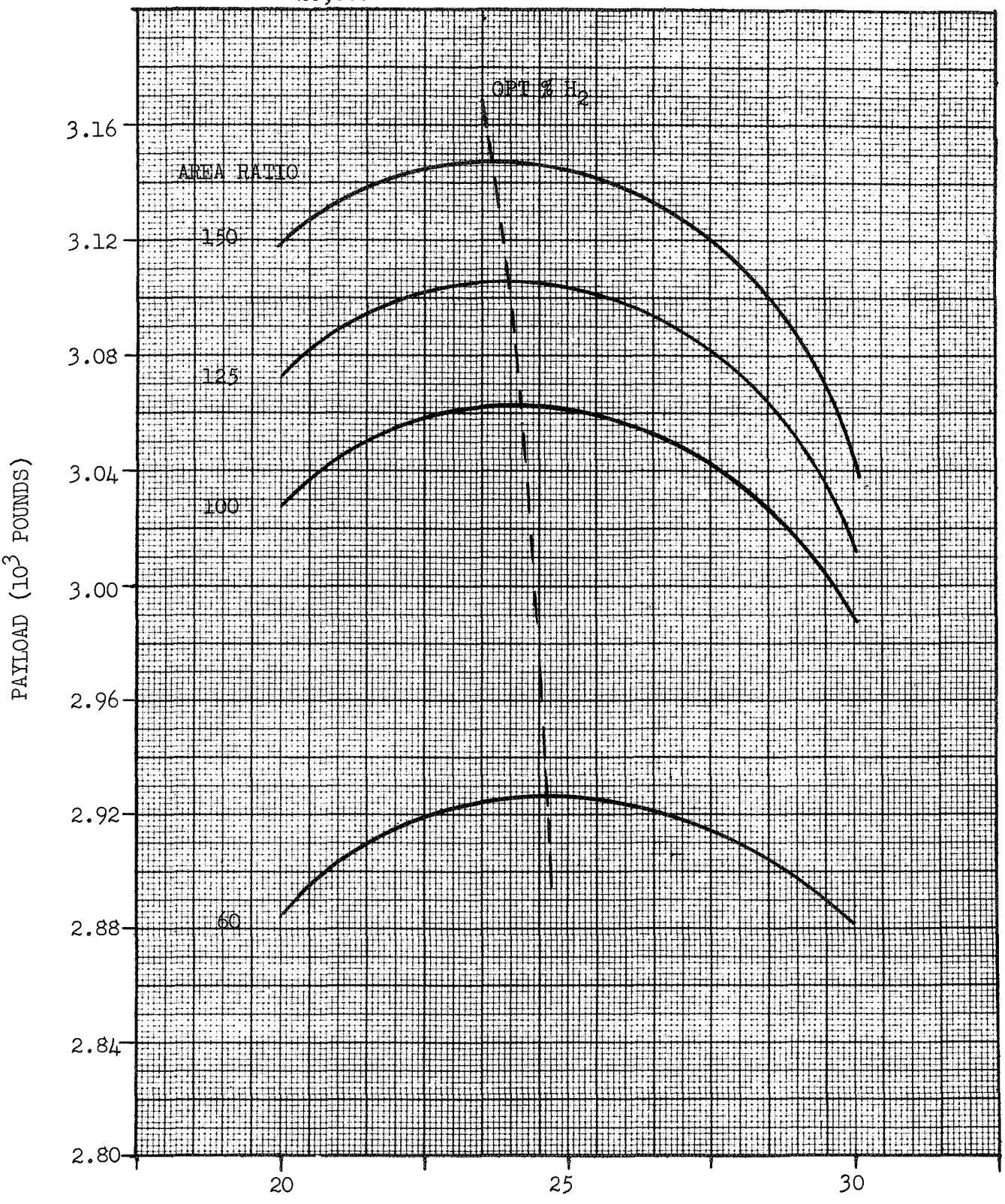

BOOSTER: TITAN III D
ΔV (MISSION): 48,500 FPS
ΔV (RETRO): N/A FPS
GROSS WT: 20,000

CASE: 4A4T01
☐ H2/F2
☒ H2/F2/LI-GEL

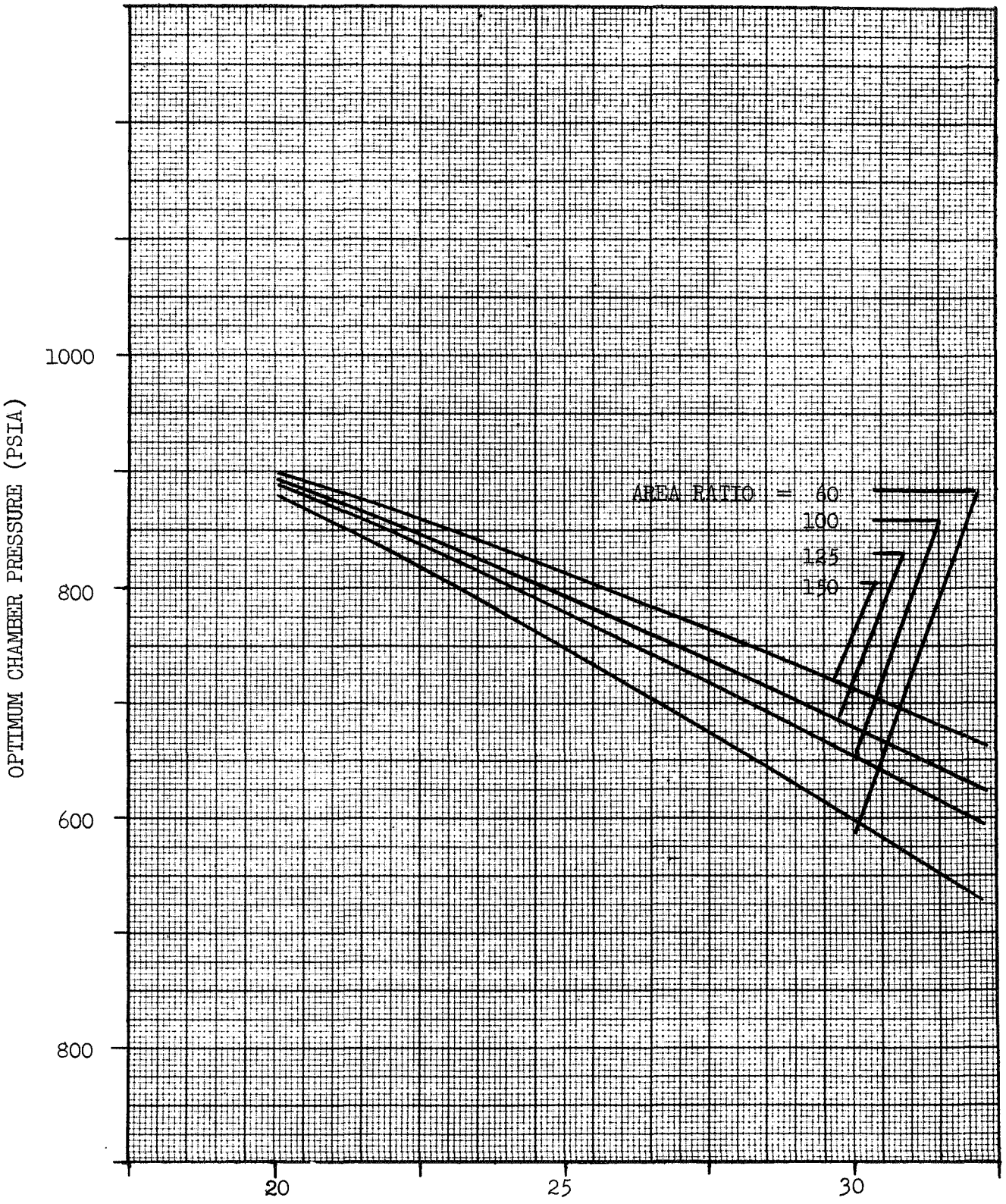

BOOSTER: TITAN III D
ΔV (MISSION): 48,500 FPS
ΔV (RETRO): N/A FPS

CASE: 4A4T01
☐ H2/F2
☒ H2/F2/LI-GEL

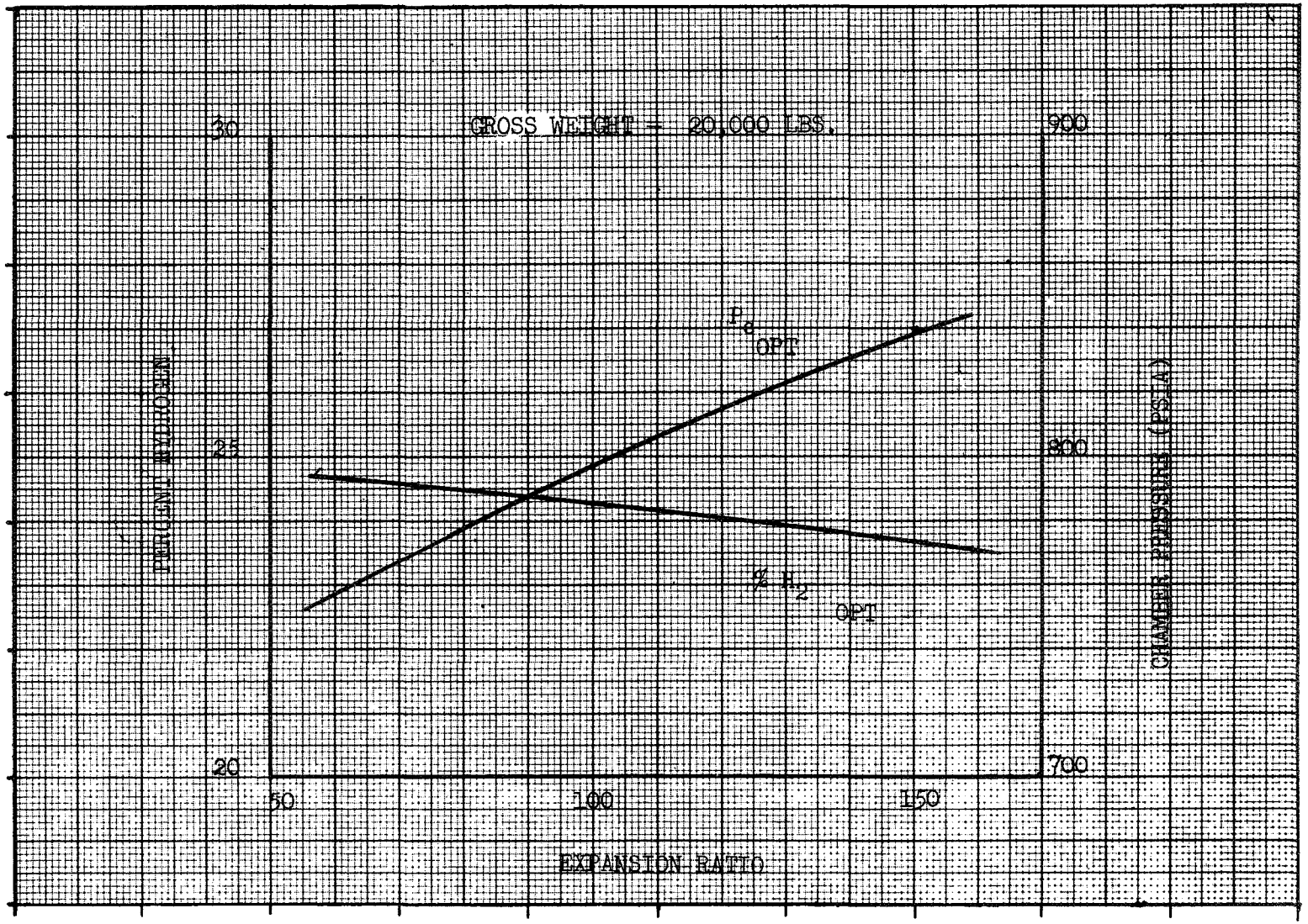

BOOSTER: TITAN III D
ΔV (MISSION): 36140 FPS
ΔV (RETRO): N/A FPS

CASE: 4C4T01
☐ H2/F2
☒ H2/F2/LI - GEL

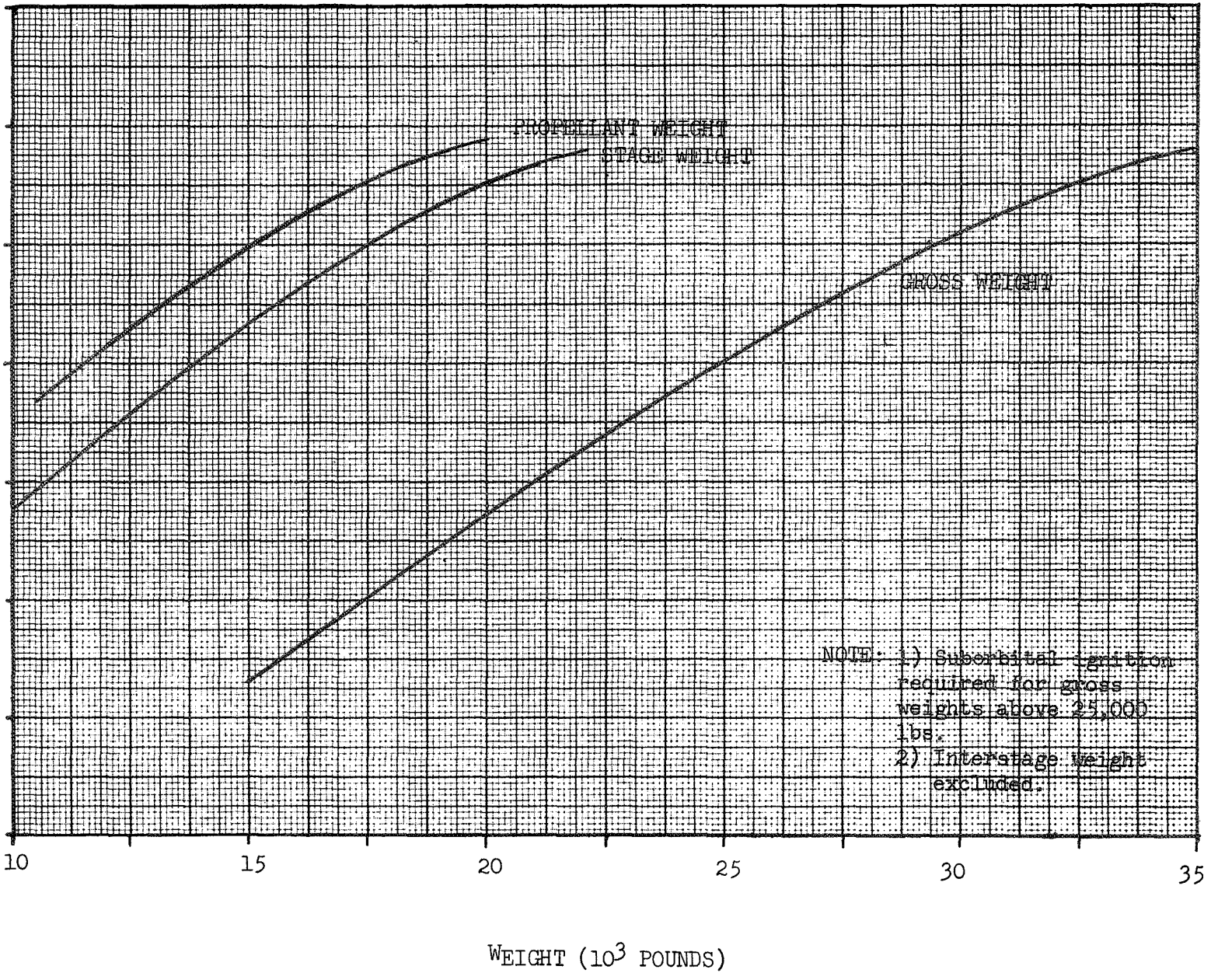

PAYLOAD (10^2 POUNDS)

WEIGHT (10^3 POUNDS)

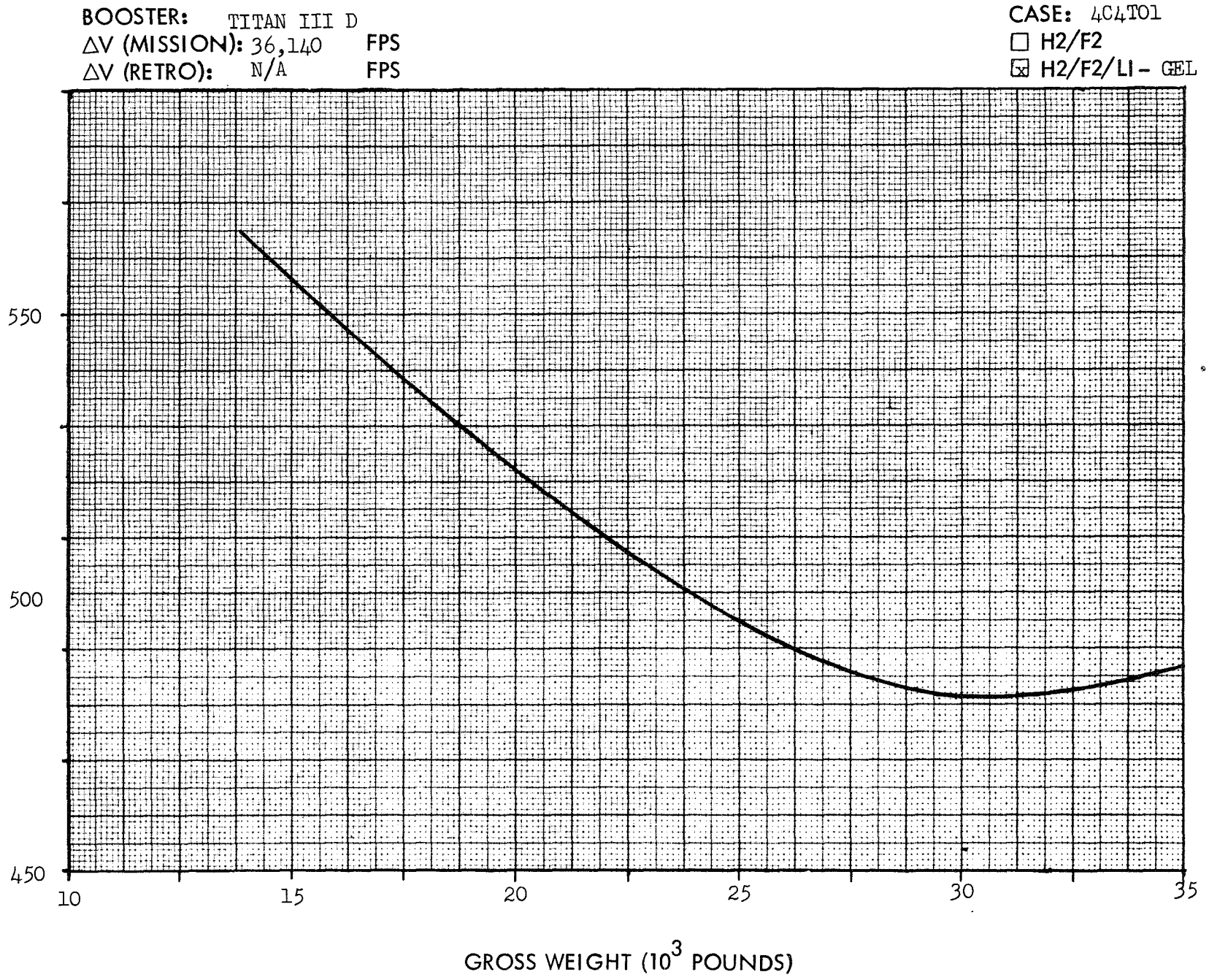
BOOSTER: TITAN III D
ΔV (MISSION): 36,140 FPS
ΔV (RETRO): N/A FPS
CASE: 4C4T01
☐ H2/F2
☒ H2/F2/LI - GEL
COST EFFECTIVENESS ($/lb of Payload)
550
500
450
10
15
20
25
30
35
GROSS WEIGHT (10^3 POUNDS)

BOOSTER: TITAN III D

ΔV (MISSION): 48,500 FPS

ΔV (RETRO): N/A FPS

CASE: 4A4T01

☐ H2/F2

☒ H2/F2/LI – GEL

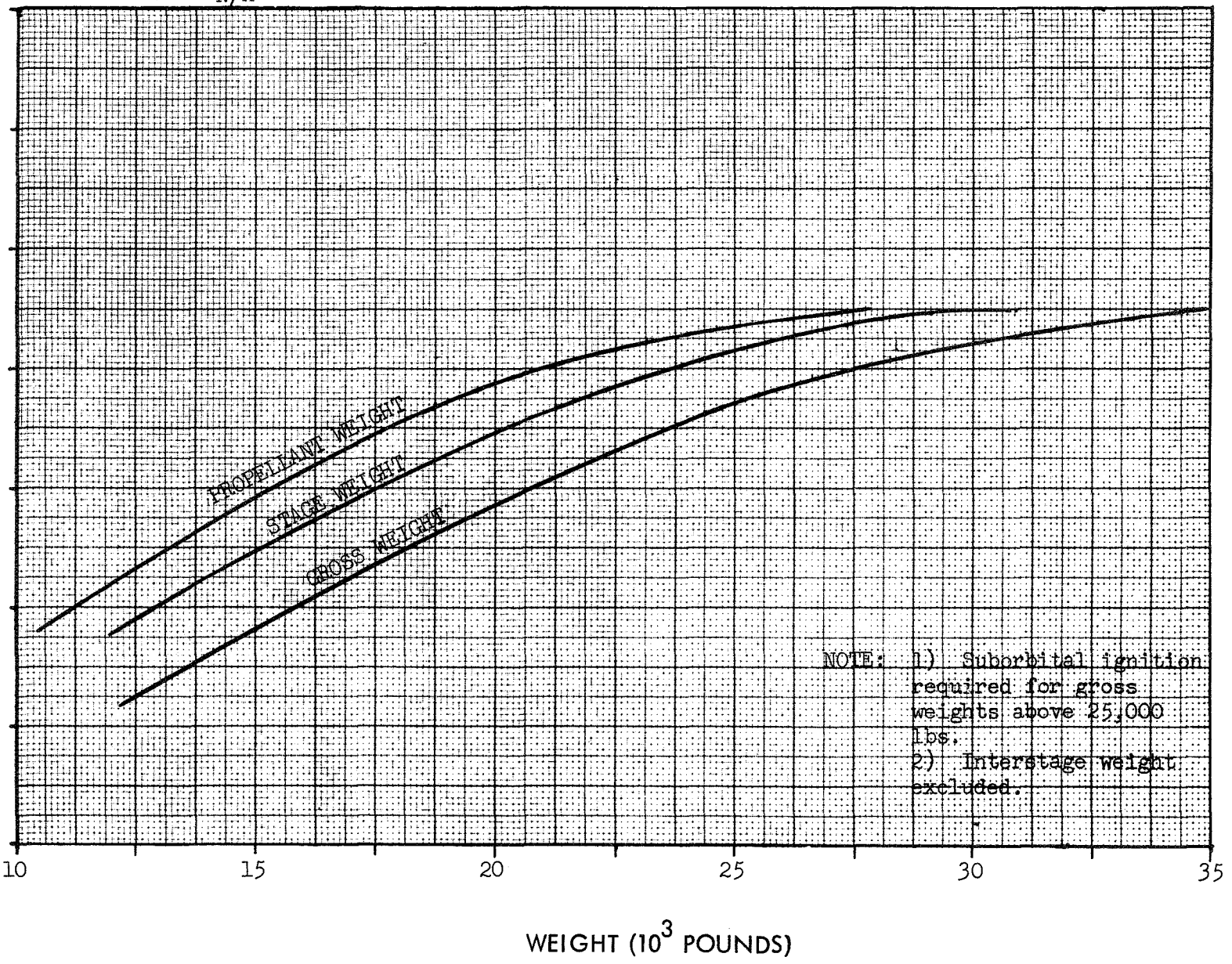

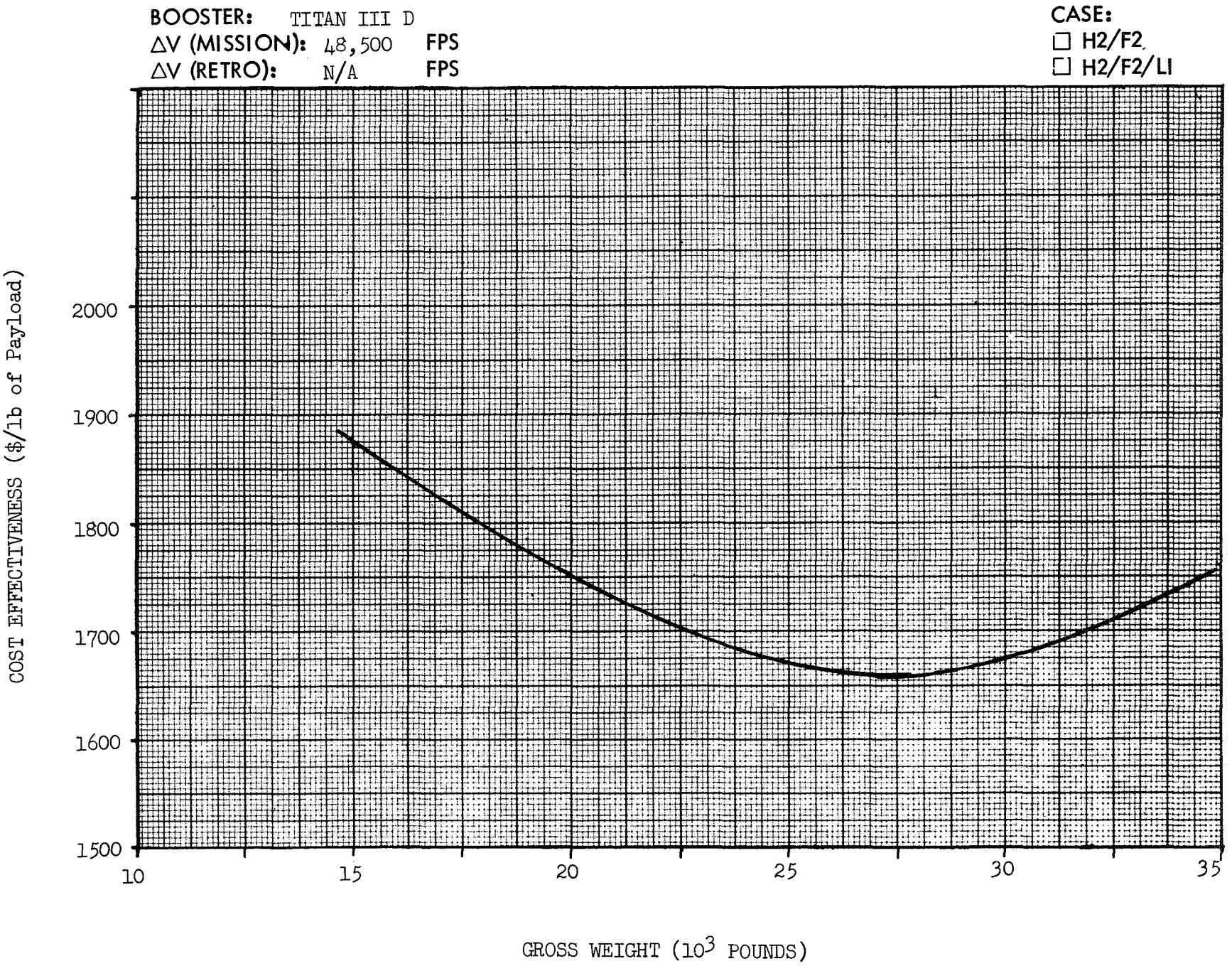
BOOSTER: TITAN III D
ΔV (MISSION): 48,500 FPS
ΔV (RETRO): N/A FPS
CASE:
☐ H2/F2
☐ H2/F2/LI
COST EFFECTIVENESS ($/lb of Payload)
2000
1900
1800
1700
1600
1500
10
15
20
25
30
35
GROSS WEIGHT (10^3 POUNDS)

BOOSTER: TITAN III D
ΔV (MISSION): 54500 FPS
ΔV (RETRO): N/A FPS

CASE: 4E4T01
☐ H2/F2
☒ H2/F2/LI - GEL

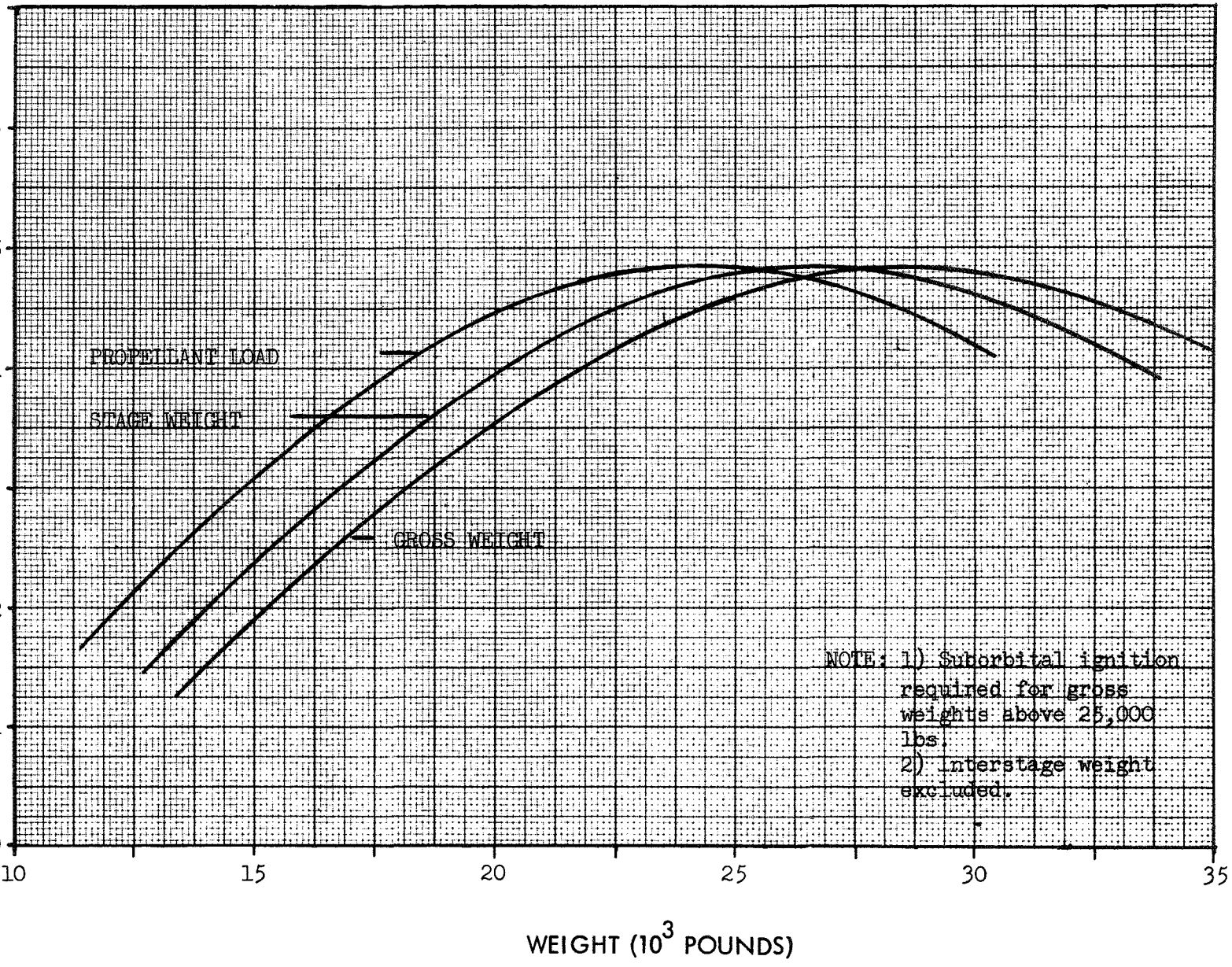

PAYLOAD (10^2 POUNDS)

WEIGHT (10^3 POUNDS)

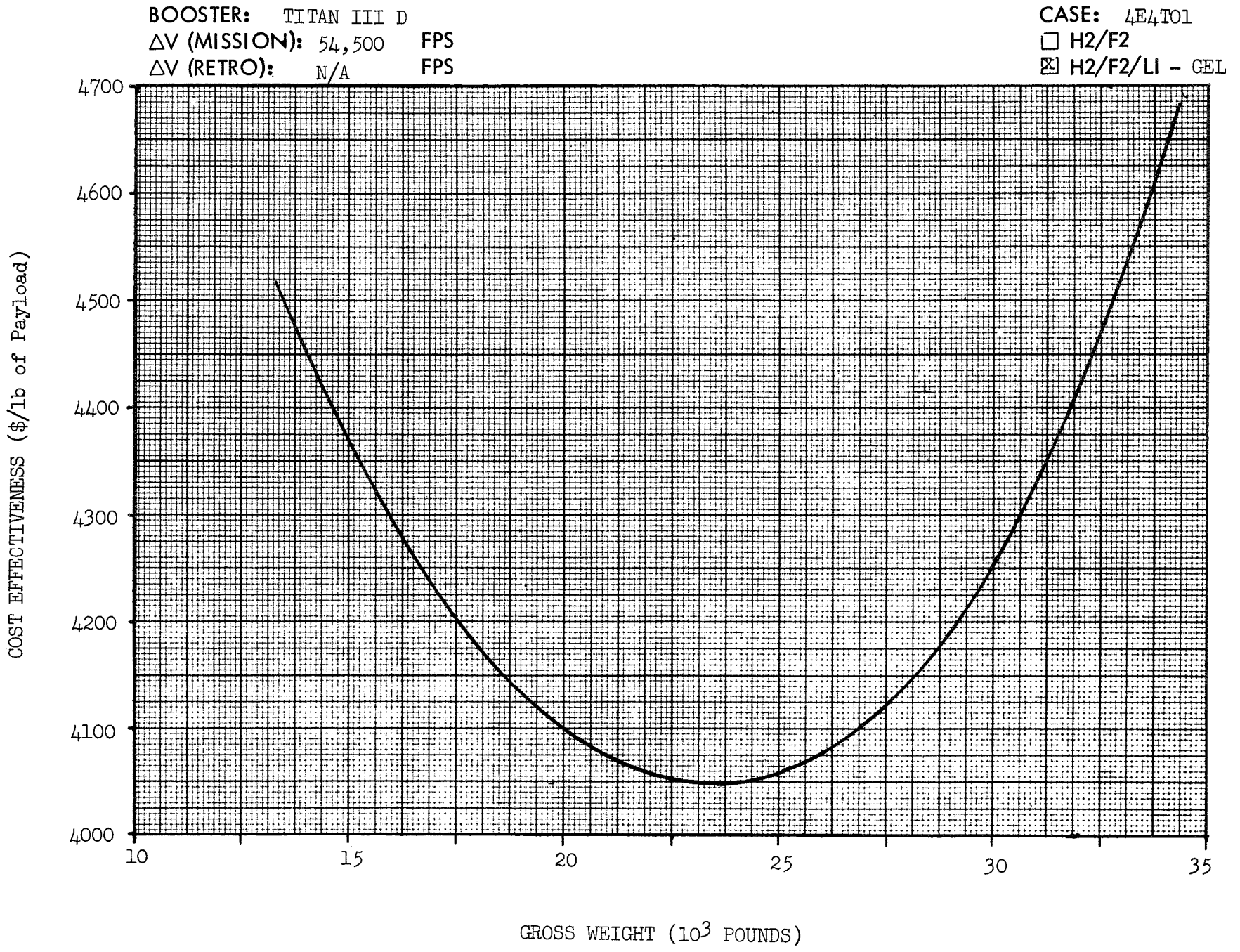
BOOSTER: TITAN III D
ΔV (MISSION): 54,500 FPS
ΔV (RETRO): N/A FPS
CASE: 4E4T01
☐ H2/F2
☒ H2/F2/LI - GEL
COST EFFECTIVENESS ($/lb of Payload)
4700
4600
4500
4400
4300
4200
4100
4000
10
15
20
25
30
35
GROSS WEIGHT (10³ POUNDS)

BOOSTER: TITAN III D
ΔV (MISSION): 60,000 FPS
ΔV (RETRO): N/A FPS

CASE: 4F4T01
☐ H2/F2
☒ H2/F2/LI - GEL

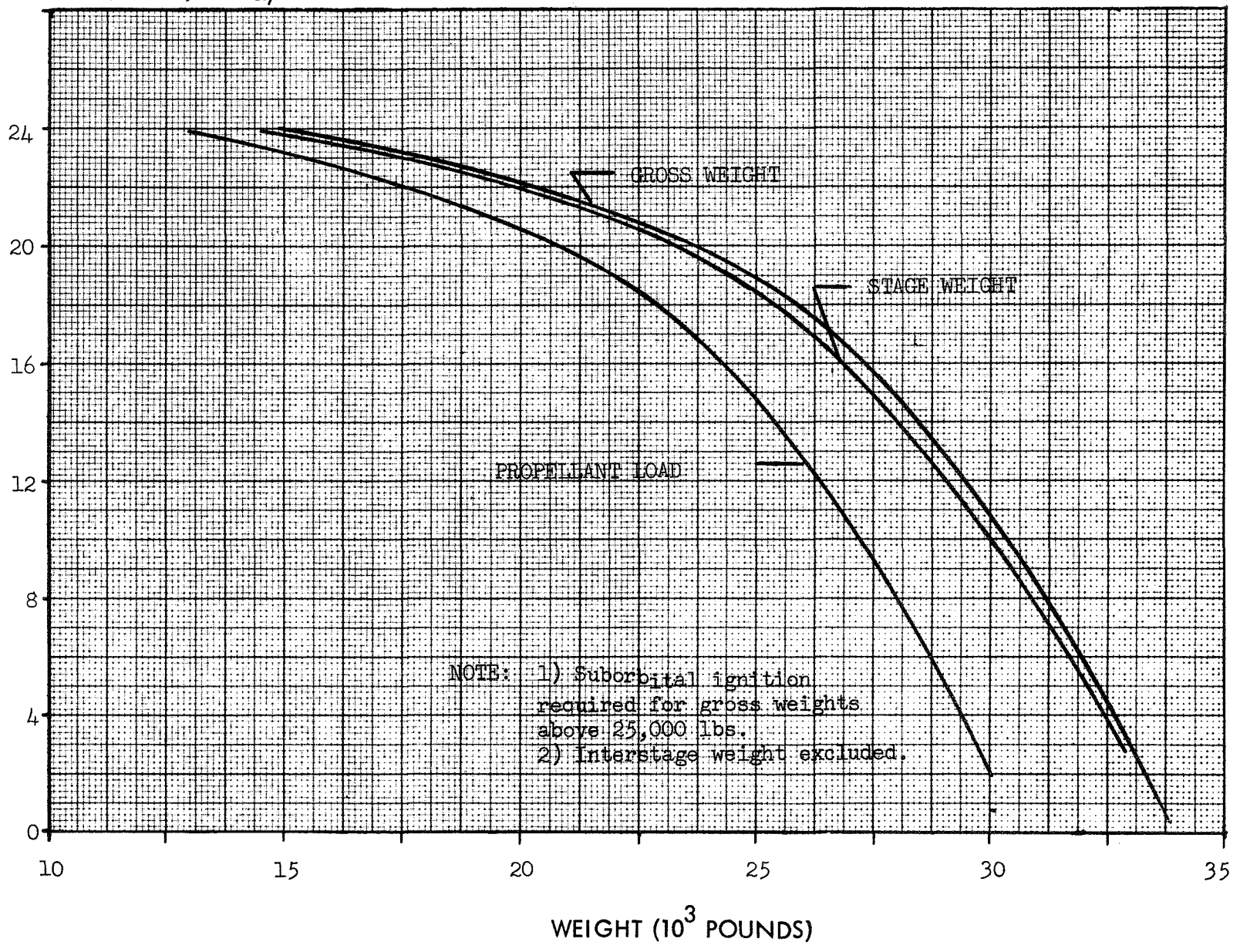

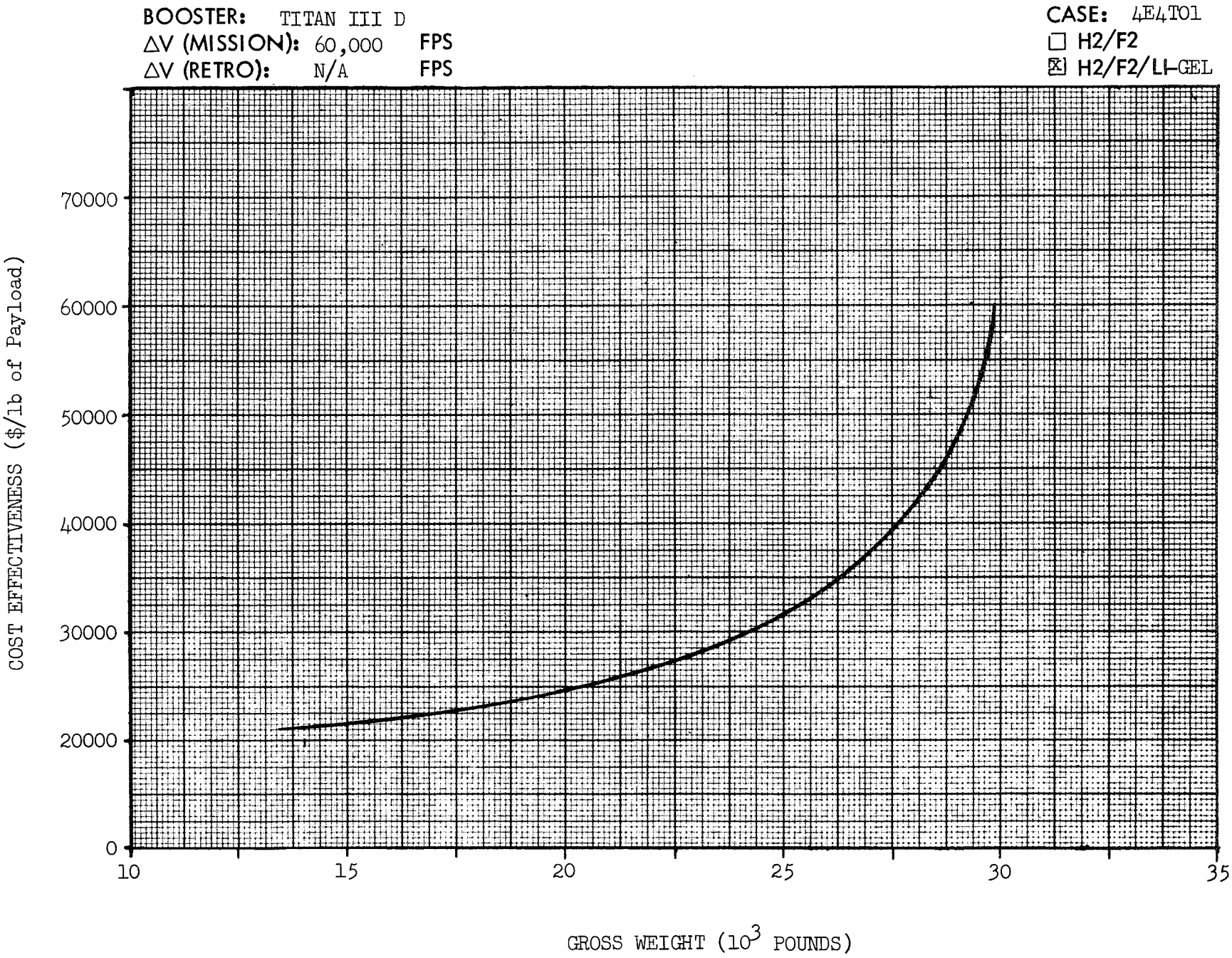
BOOSTER: TITAN III D
ΔV (MISSION): 60,000 FPS
ΔV (RETRO): N/A FPS
CASE: 4E4T01
☐ H2/F2
☒ H2/F2/LI-GEL
COST EFFECTIVENESS ($/lb of Payload)
0
20000
30000
40000
50000
60000
70000
10
15
20
25
30
35
GROSS WEIGHT (10^3 POUNDS)

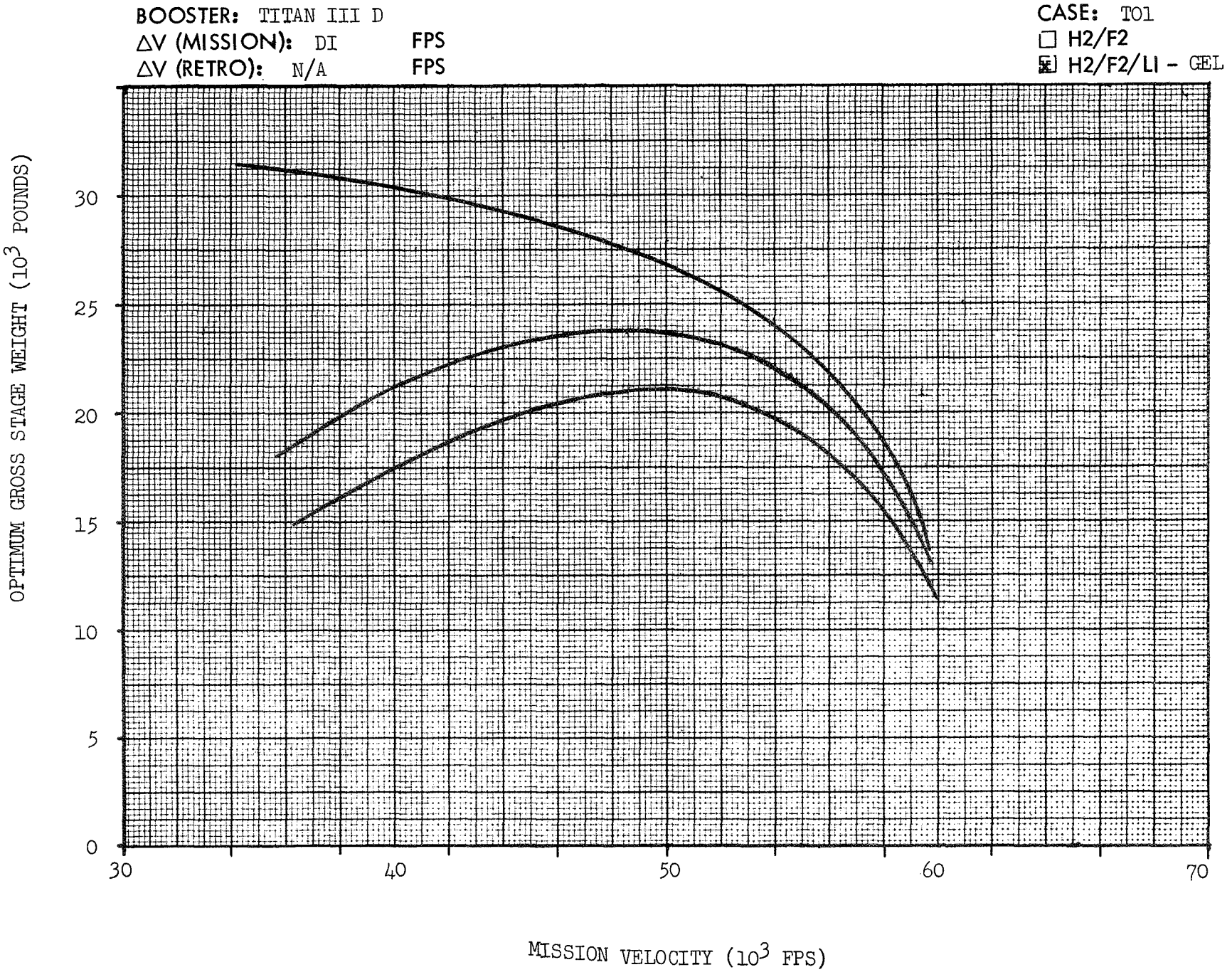
BOOSTER: TITAN III D
ΔV (MISSION): DI FPS
ΔV (RETRO): N/A FPS
CASE: T01
☐ H2/F2
☒ H2/F2/LI - GEL
OPTIMUM GROSS STAGE WEIGHT (10^3 POUNDS)
0
5
10
15
20
25
30
30
40
50
60
70
MISSION VELOCITY (10^3 FPS)

BOOSTER: TITAN III D
ΔV (MISSION): 48,500 FPS
ΔV (RETRO): N/A FPS
GROSS WT: 20000

CASE: 2C4T01
☒ H2/F2
☐ H2/F2/LI

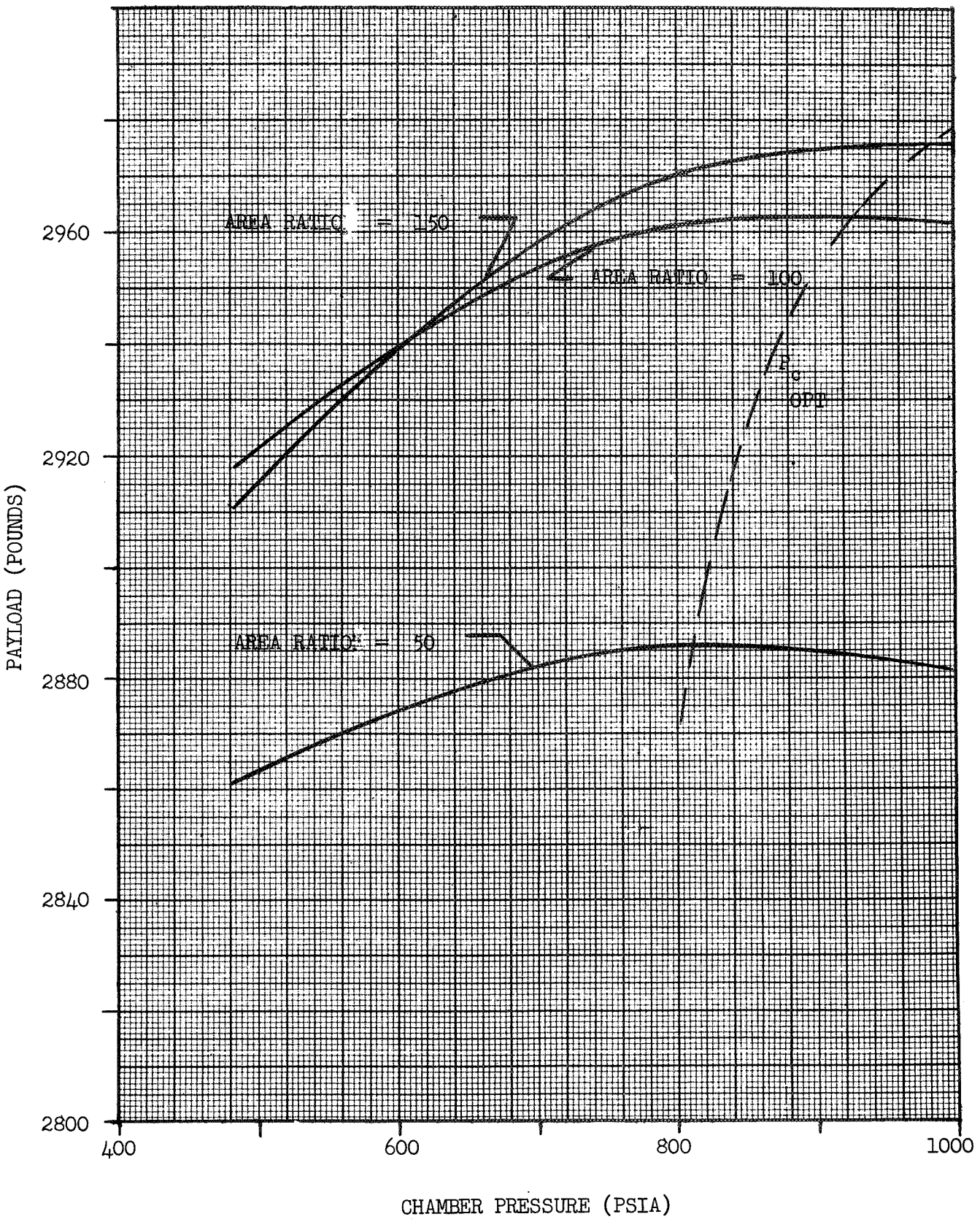

BOOSTER: TITAN III D
ΔV (MISSION): 48,500 FPS
ΔV (RETRO): N/A FPS
GROSS WT: 20000

CASE: 2C4T01
☒ H2/F2
☐ H2/F2/LI

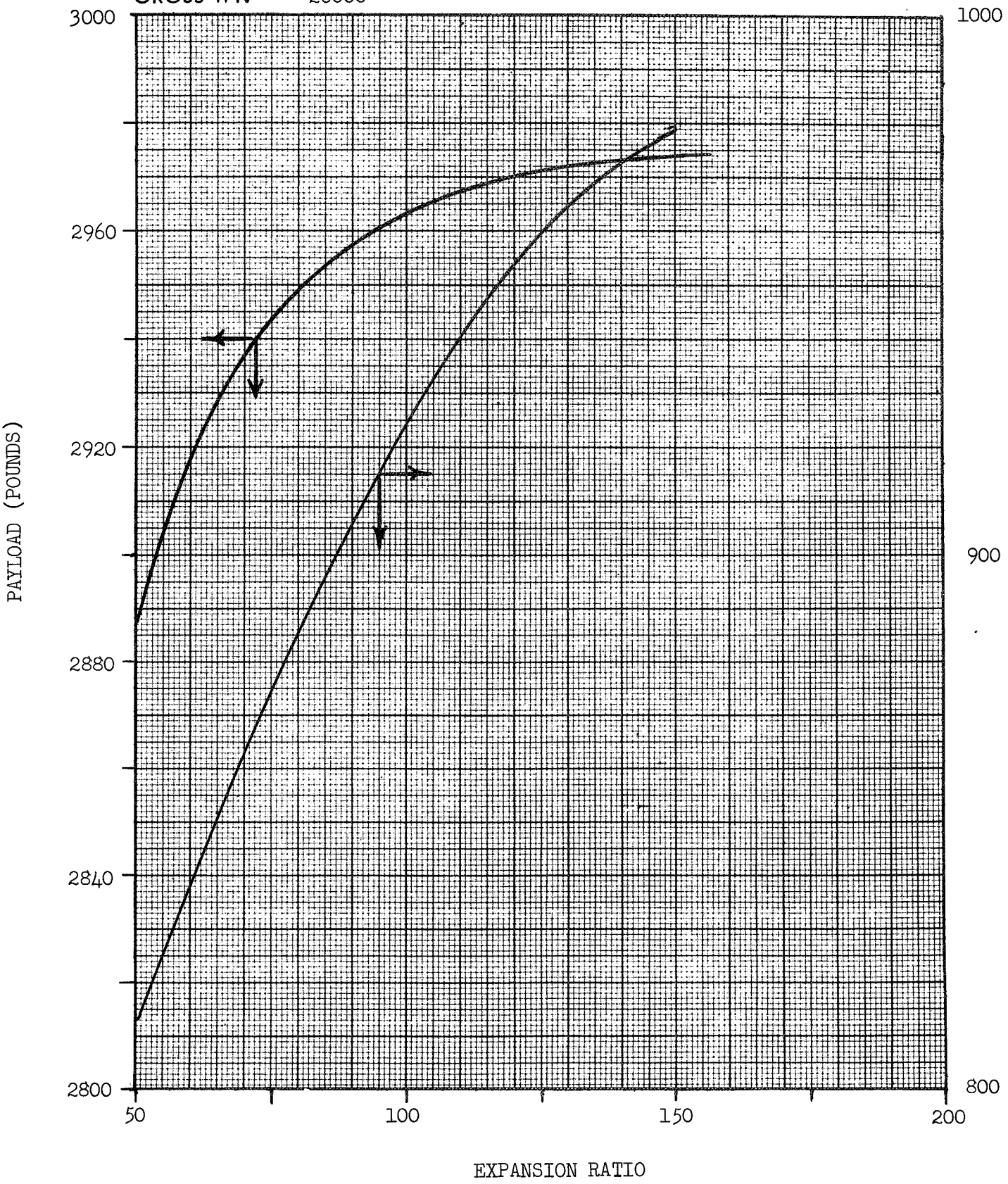

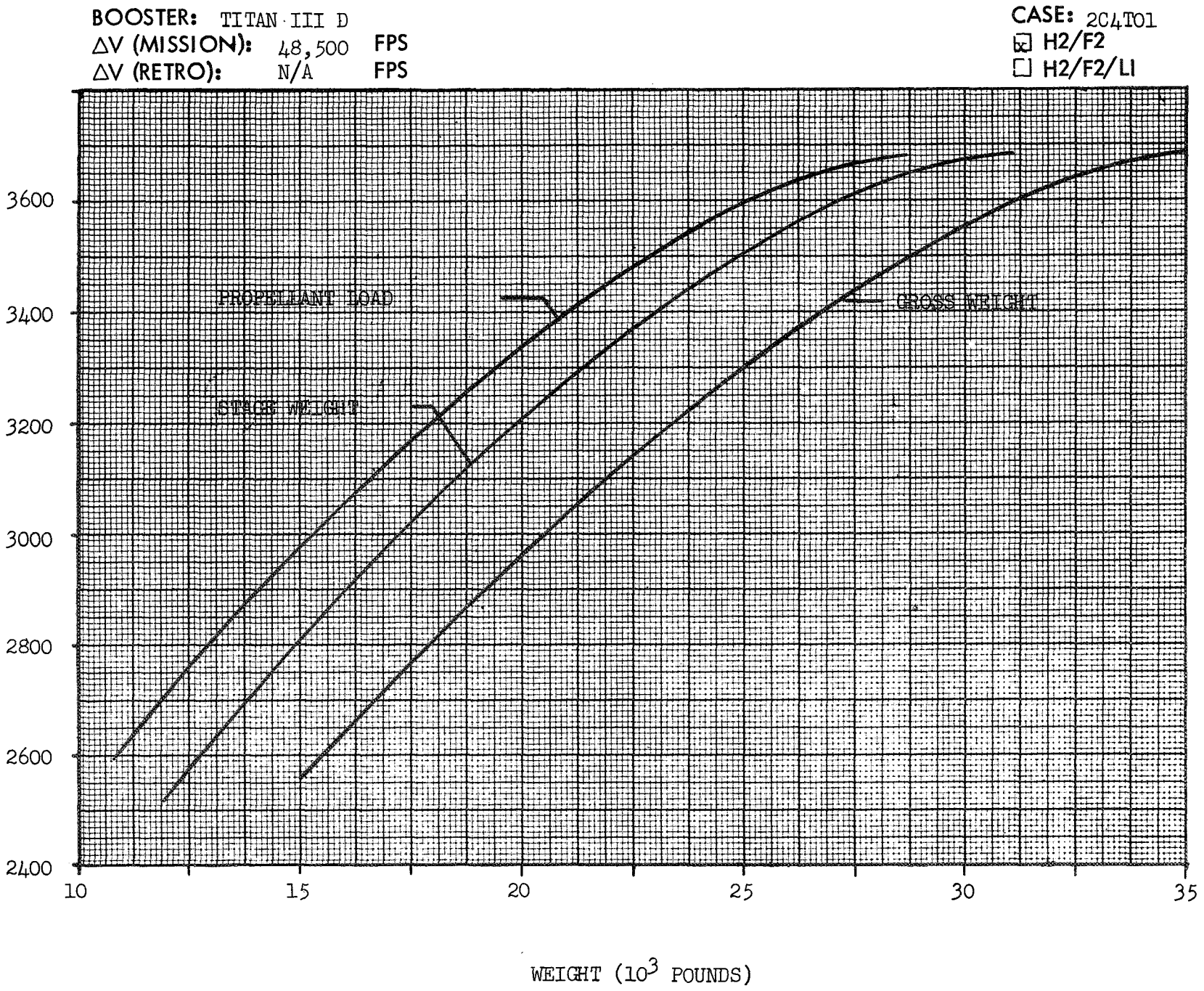
BOOSTER: TITAN III D
ΔV (MISSION): 48,500 FPS
ΔV (RETRO): N/A FPS
CASE: 2C4T01
☒ H2/F2
☐ H2/F2/LI
PROPELLANT LOAD
STAGE WEIGHT
GROSS WEIGHT
3600
3400
3200
3000
2800
2600
2400
10
15
20
25
30
35
WEIGHT (10^3 POUNDS)

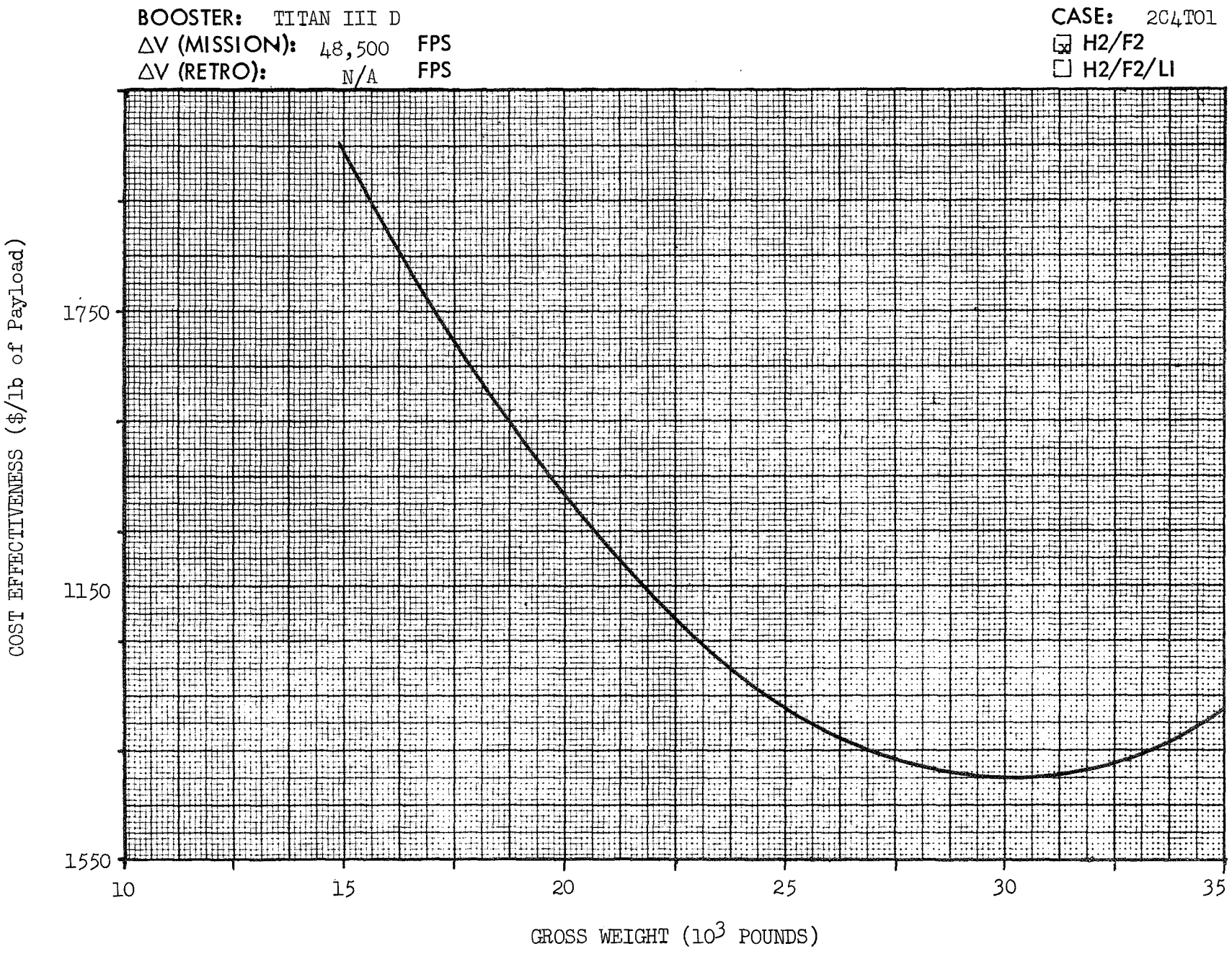
BOOSTER: TITAN III D
ΔV (MISSION): 48,500 FPS
ΔV (RETRO): N/A FPS
CASE: 2C4T01
H2/F2
H2/F2/LI
COST EFFECTIVENESS ($/lb of Payload)
1750
1150
1550
10
15
20
25
30
35
GROSS WEIGHT (10^3 POUNDS)

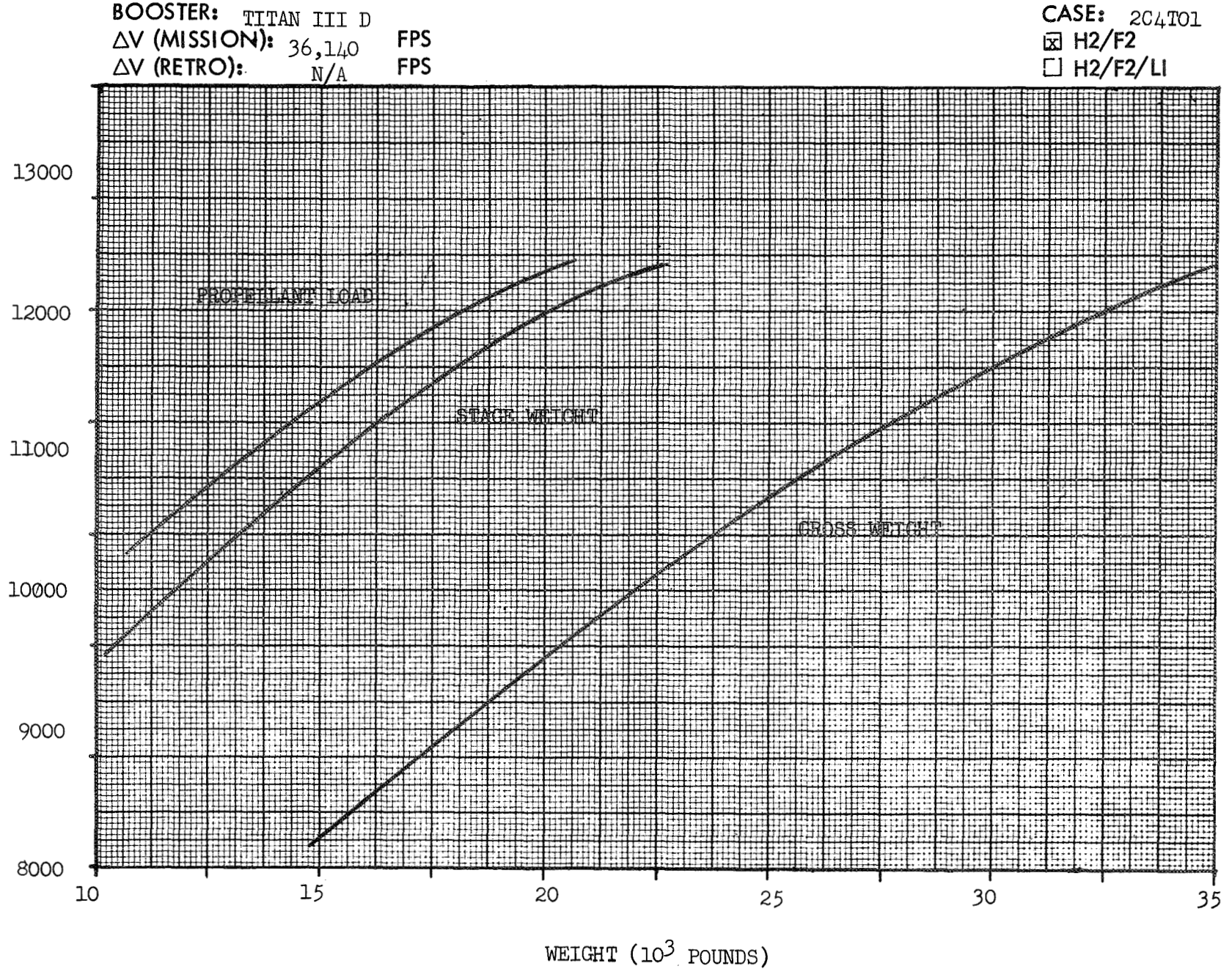
BOOSTER: TITAN III D
ΔV (MISSION): 36,140 FPS
ΔV (RETRO): N/A FPS
CASE: 2C4T01
☒ H2/F2
☐ H2/F2/LI
PROPELLANT LOAD
STAGE WEIGHT
GROSS WEIGHT
13000
12000
11000
10000
9000
8000
10
15
20
25
30
35
PAYLOAD (POUNDS)
WEIGHT (10^3 POUNDS)

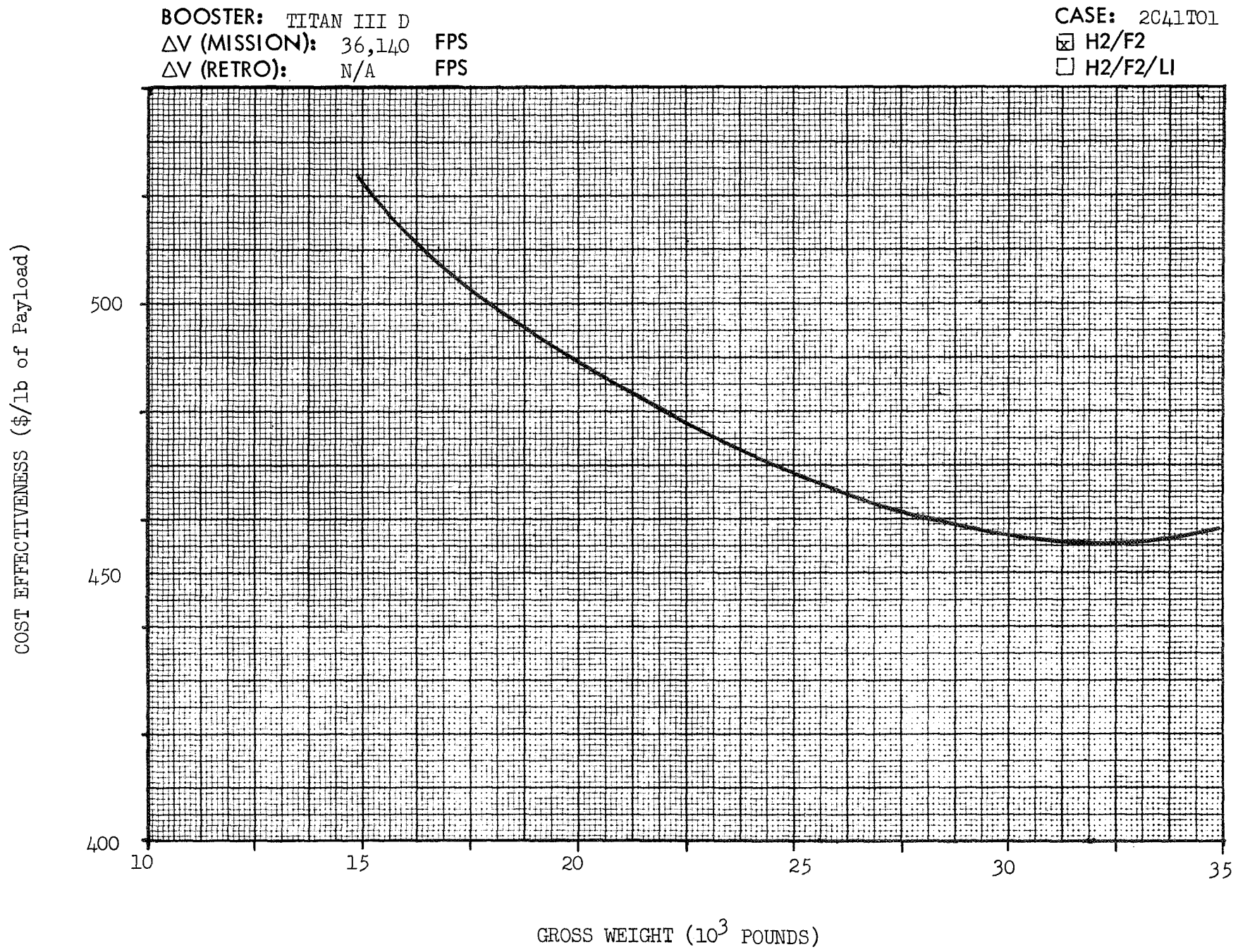
BOOSTER: TITAN III D
ΔV (MISSION): 36,140 FPS
ΔV (RETRO): N/A FPS
CASE: 2041T01
☒ H2/F2
☐ H2/F2/LI
COST EFFECTIVENESS ($/lb of Payload)
500
450
400
10
15
20
25
30
35
GROSS WEIGHT (10^3 POUNDS)

BOOSTER: TITAN III D
ΔV (MISSION): 54,500 FPS
ΔV (RETRO): N/A FPS

CASE: 2E4T01
☒ H2/F2
☐ H2/F2/LI

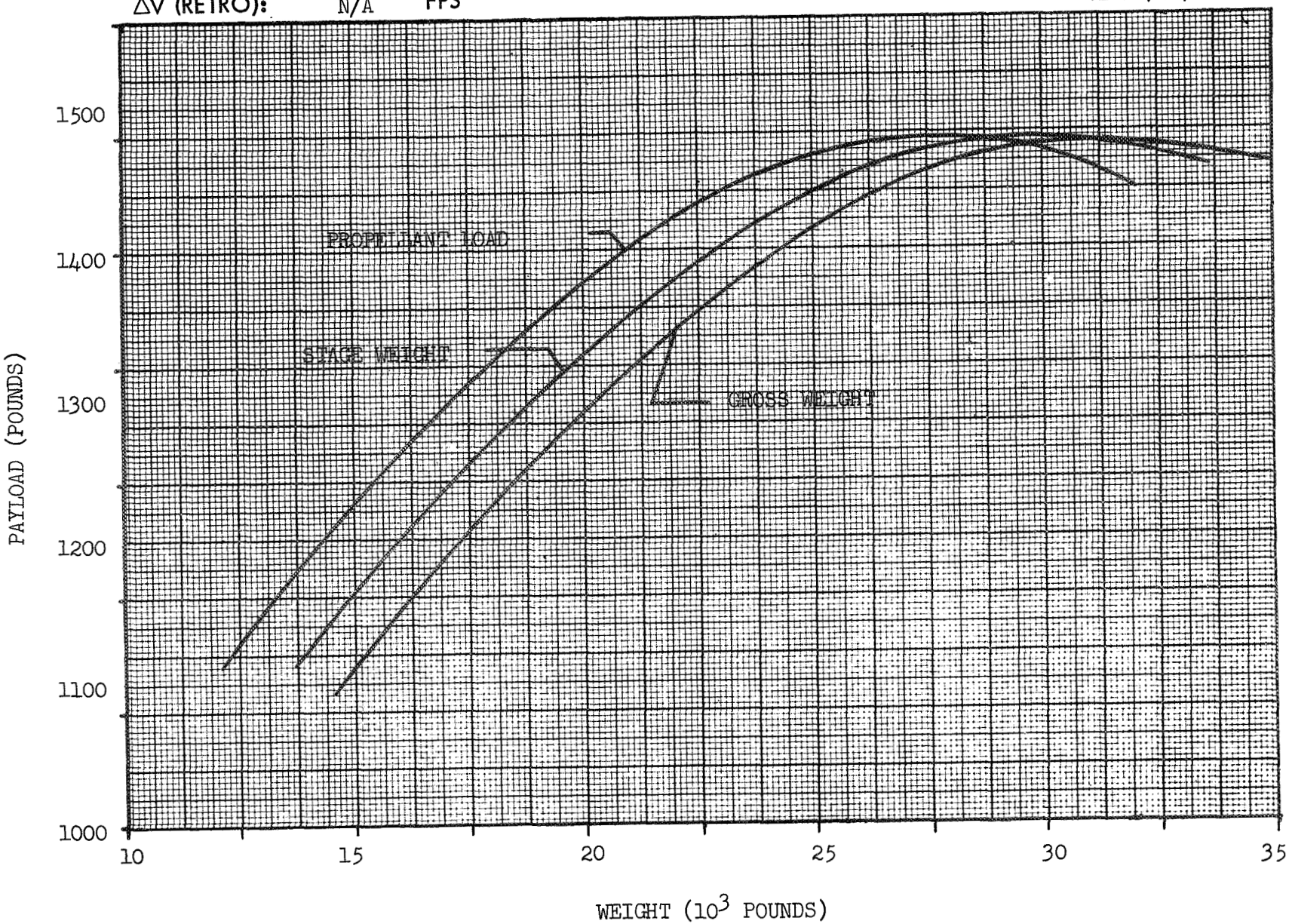

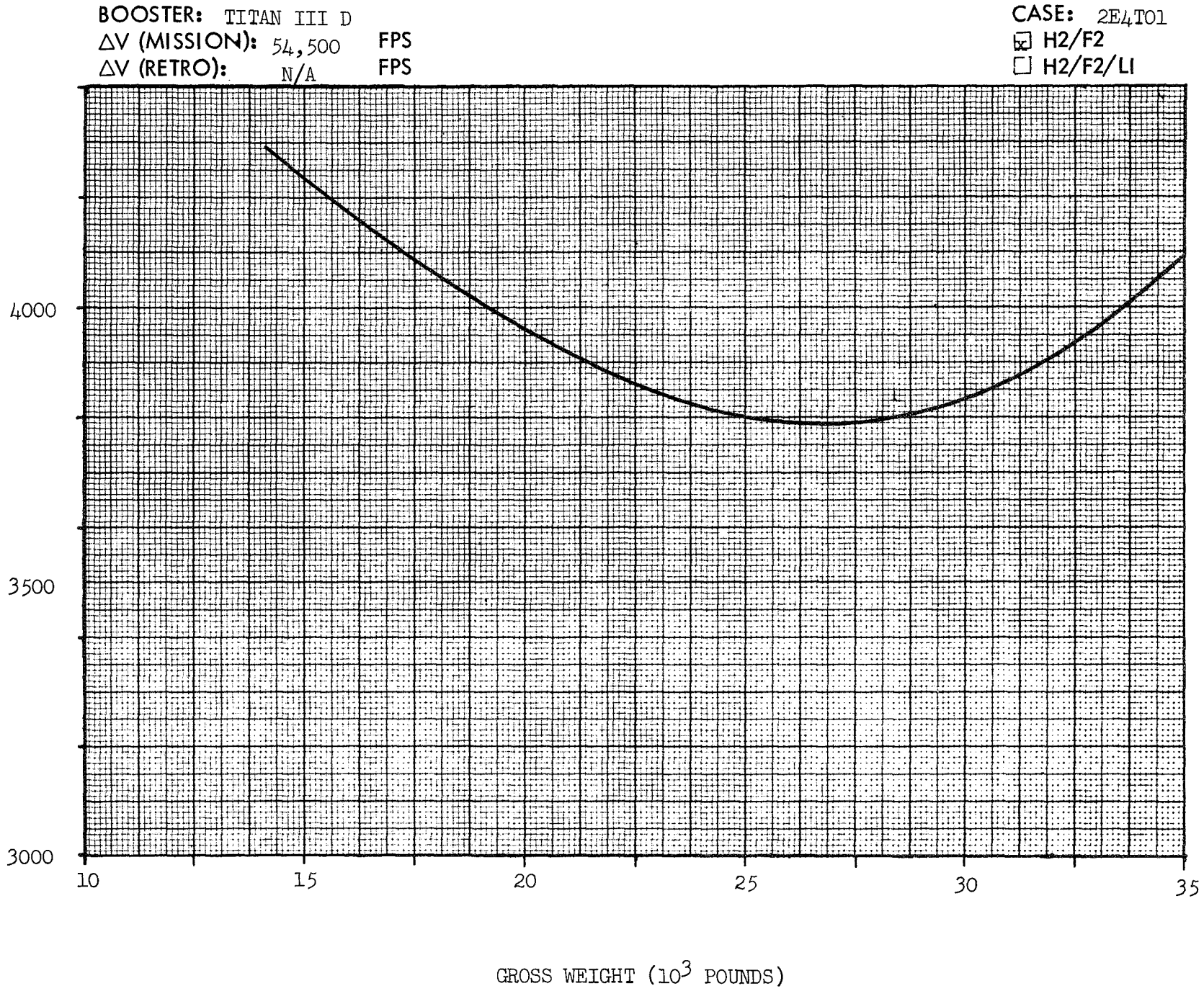
BOOSTER: TITAN III D
ΔV (MISSION): 54,500 FPS
ΔV (RETRO): N/A FPS
CASE: 2E4T01
☒ H2/F2
☐ H2/F2/LI
COST EFFECTIVENESS ($/lb of Payload)
4000
3500
3000
10
15
20
25
30
35
GROSS WEIGHT (10^3 POUNDS)

BOOSTER: TITAN III D
ΔV (MISSION): 60,000 FPS
ΔV (RETRO): N/A FPS

CASE: 4F4T01
☒ H2/F2
☐ H2/F2/LI

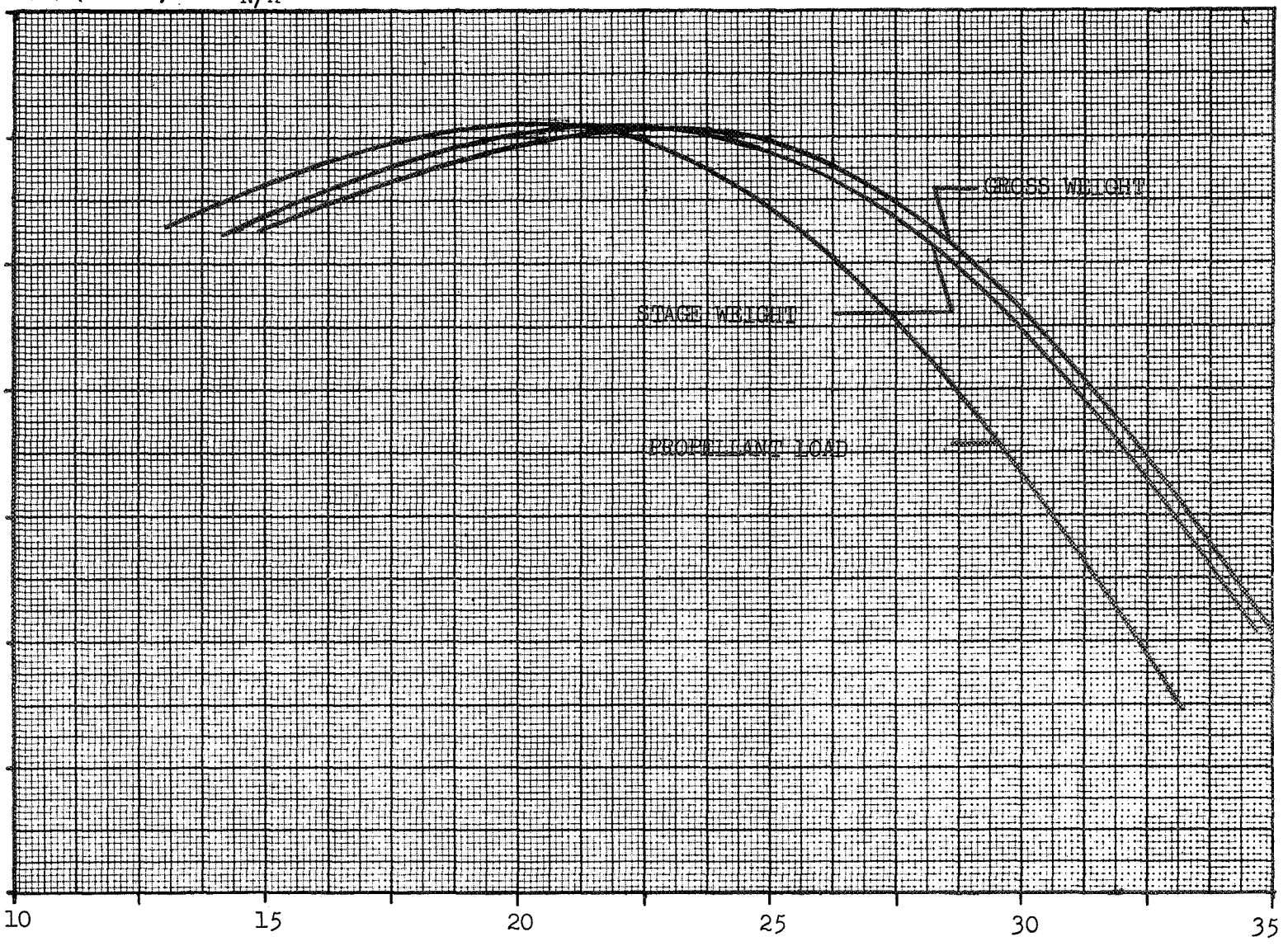

PAYLOAD (POUNDS)

GROSS WEIGHT (10^3 POUNDS)

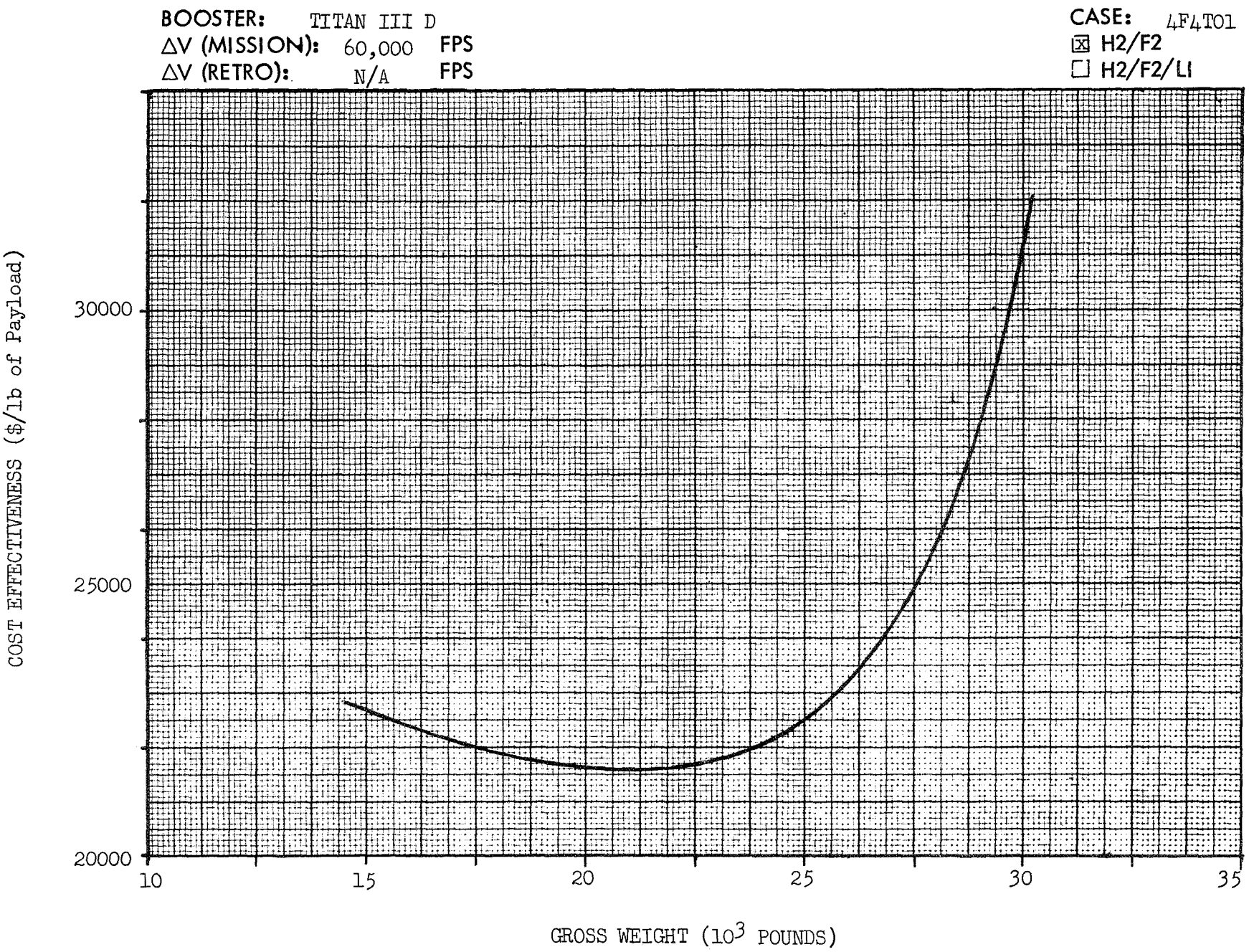
BOOSTER: TITAN III D
ΔV (MISSION): 60,000 FPS
ΔV (RETRO): N/A FPS
CASE: 4F4T01
☒ H2/F2
☐ H2/F2/LI
COST EFFECTIVENESS ($/lb of Payload)
30000
25000
20000
10
15
20
25
30
35
GROSS WEIGHT (10³ POUNDS)

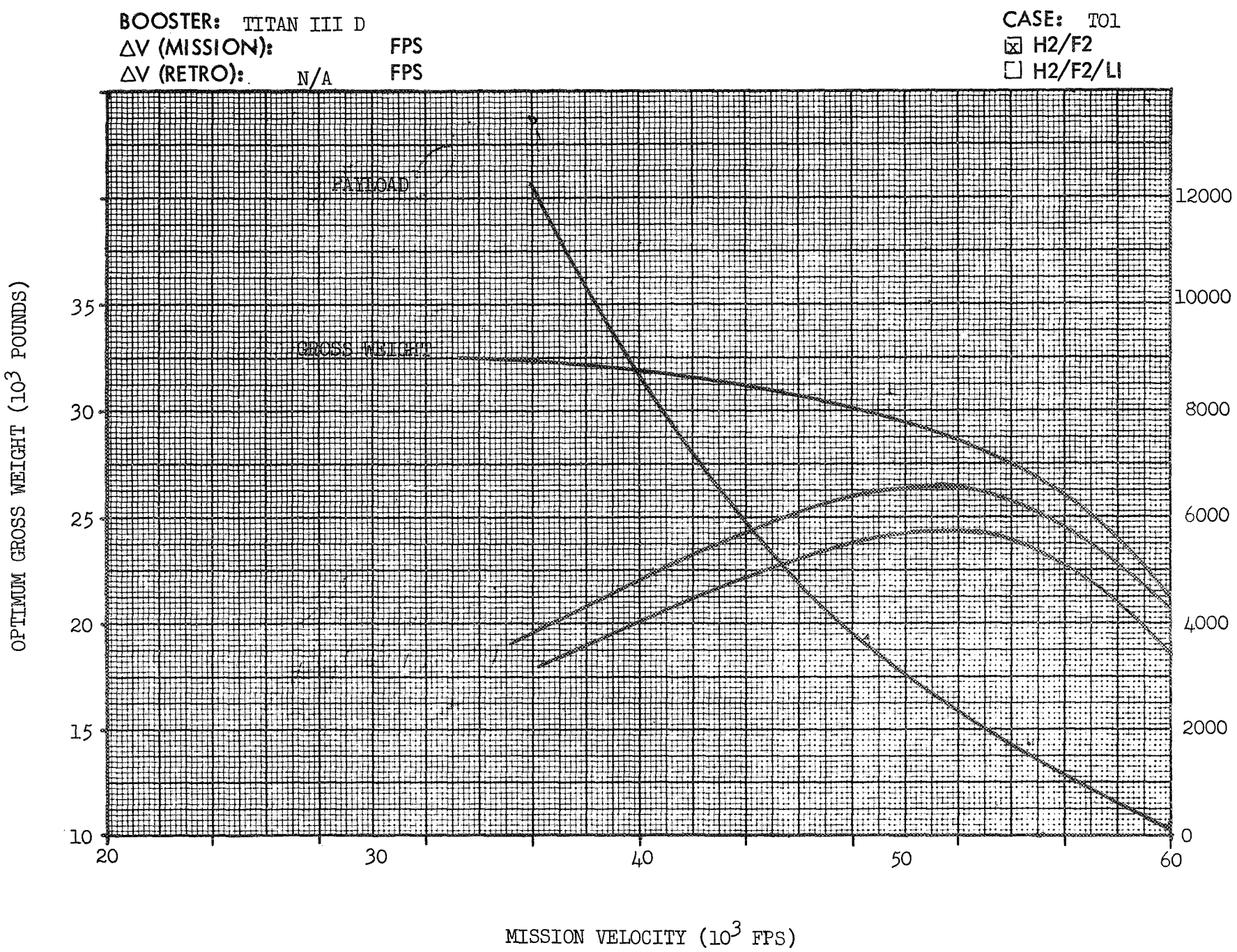
BOOSTER: TITAN III D
ΔV (MISSION): FPS
ΔV (RETRO): N/A FPS
CASE: T01
☒ H2/F2
☐ H2/F2/LI
PAYLOAD
GROSS WEIGHT
OPTIMUM GROSS WEIGHT (10^3 POUNDS)
10
15
20
25
30
35
0
2000
4000
6000
8000
10000
12000
20
30
40
50
60
MISSION VELOCITY (10^3 FPS)

BOOSTER: TITAN III D/CENTAUR
ΔV (MISSION): 48,500 FPS
ΔV (RETRO): N/A FPS
GROSS WT: 12,000 lb

CASE: 3A2T01
☐ H2/F2
☒ H2/F2/LI

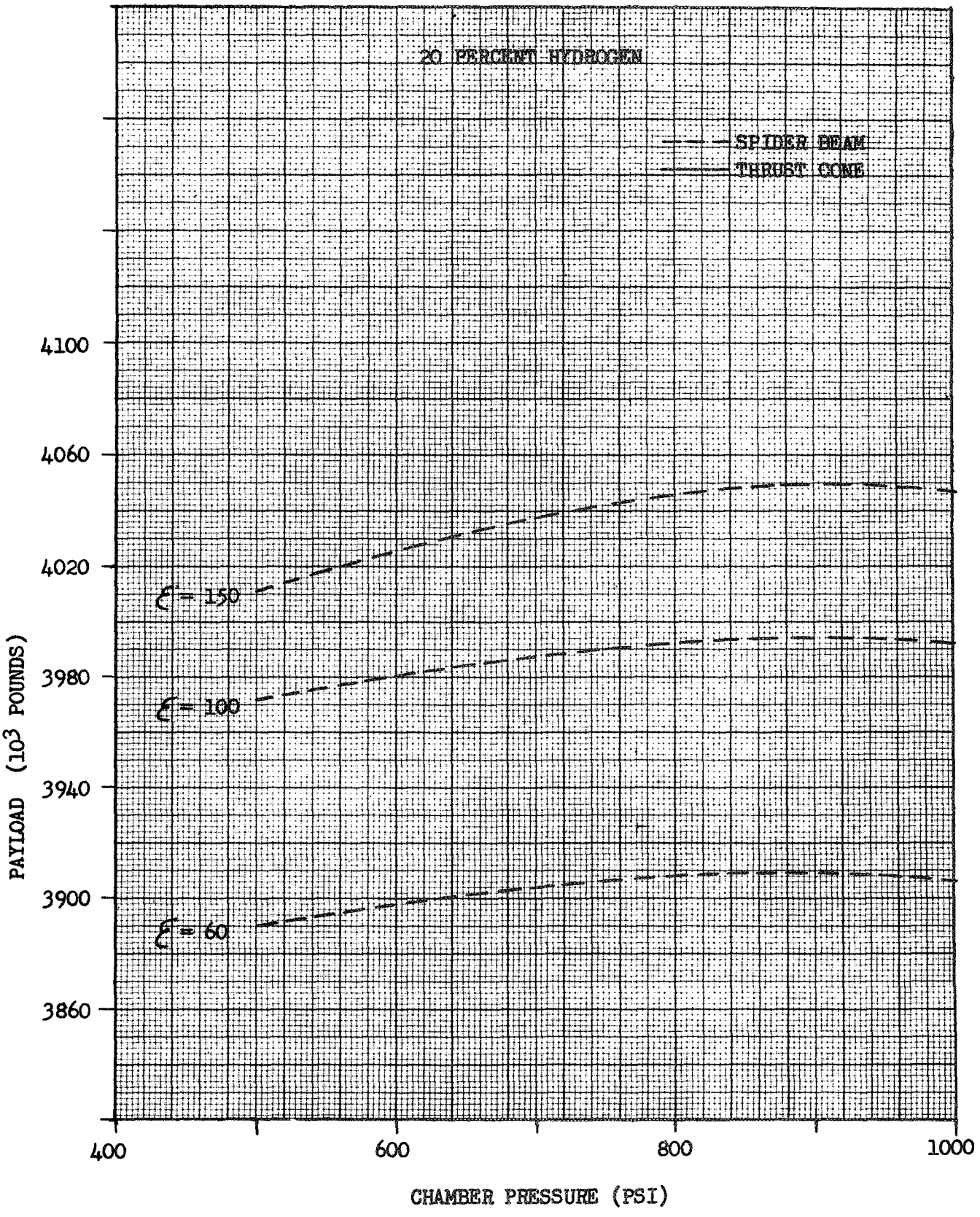

BOOSTER: TITAN III D/CENTAUR
ΔV (MISSION): 48,500 FPS
ΔV (RETRO): N/A FPS
GROSS WT: 12,000 lb

CASE: 3A2T01
☐ H2/F2
☒ H2/F2/LI

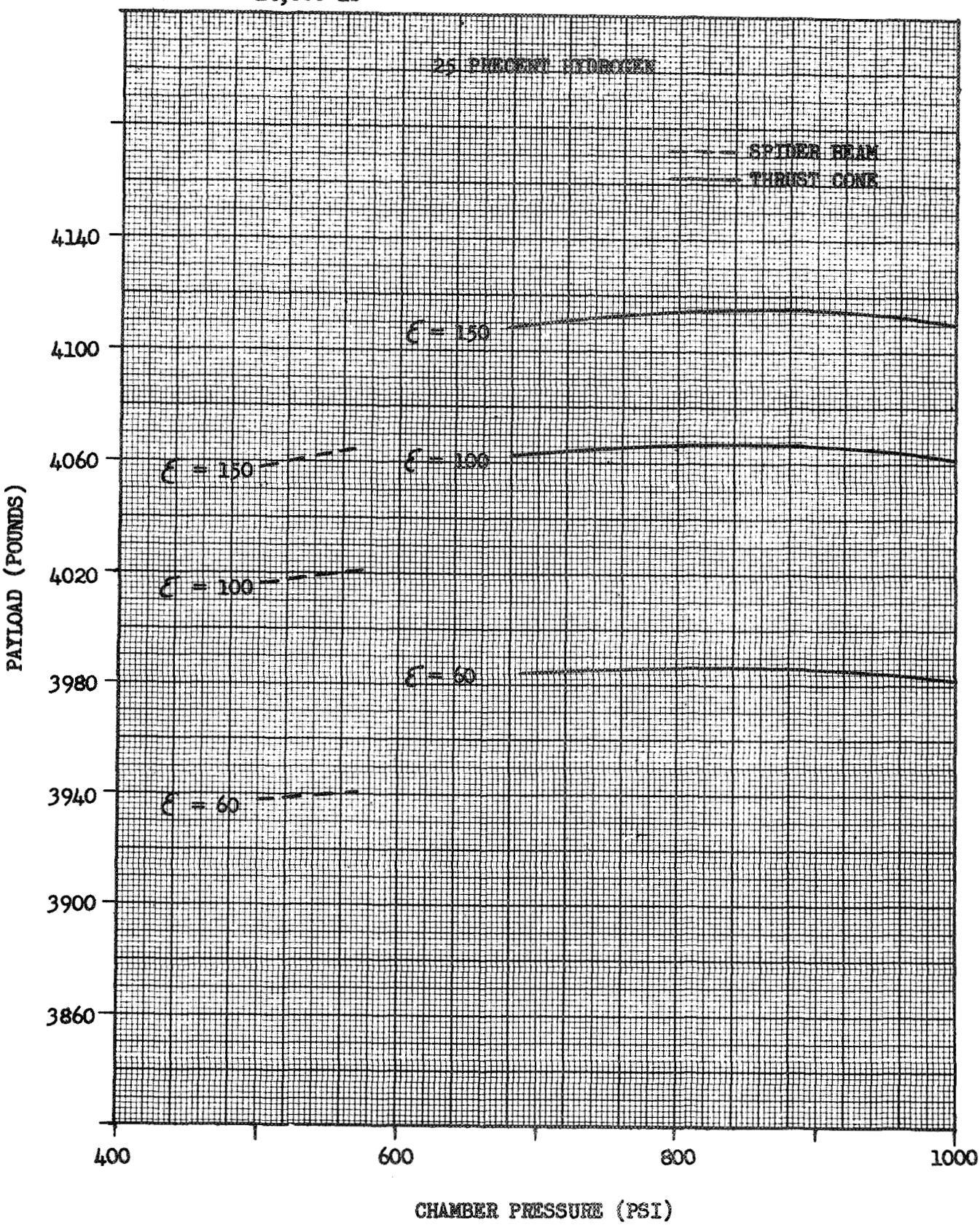

BOOSTER: TITAN III D/CENTAUR
ΔV (MISSION): 48,500 FPS
ΔV (RETRO): N/A FPS
GROSS WT: 12,000 lb

CASE: 3A2T01
☐ H2/F2
☒ H2/F2/LI

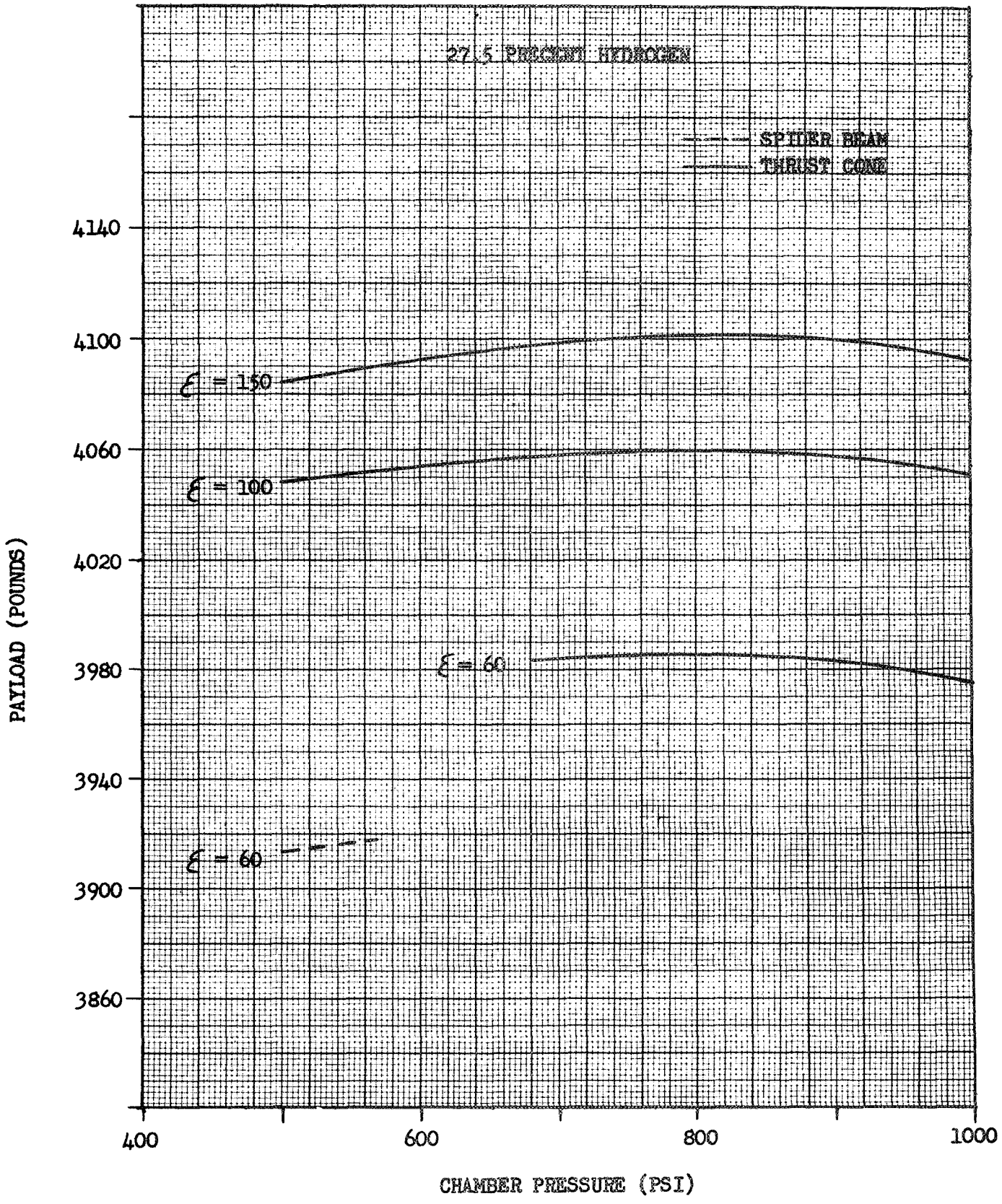

BOOSTER: TITAN III D/CENTAUR
ΔV (MISSION): 48,500 FPS
ΔV (RETRO): N/A FPS
GROSS WT: 12,000 lb

7

CASE: 3A2T01
☐ H2/F2
☒ H2/F2/LI

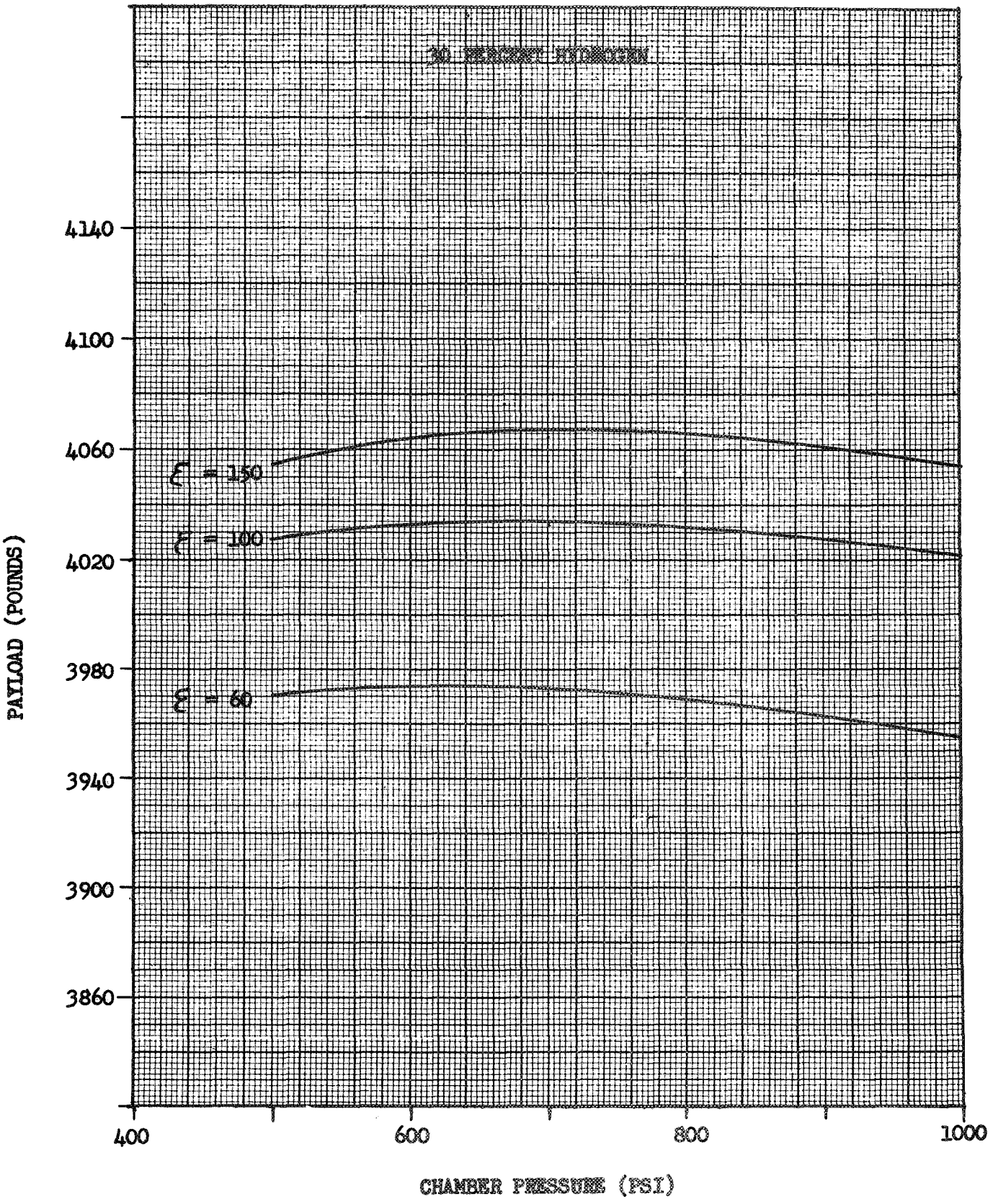

BOOSTER: TITAN III D/CENTAUR
ΔV (MISSION): 48,500 FPS
ΔV (RETRO): N/A FPS
GROSS WT: 12,000 lb

CASE: 3A2T01
☐ H2/F2
☒ H2/F2/LI

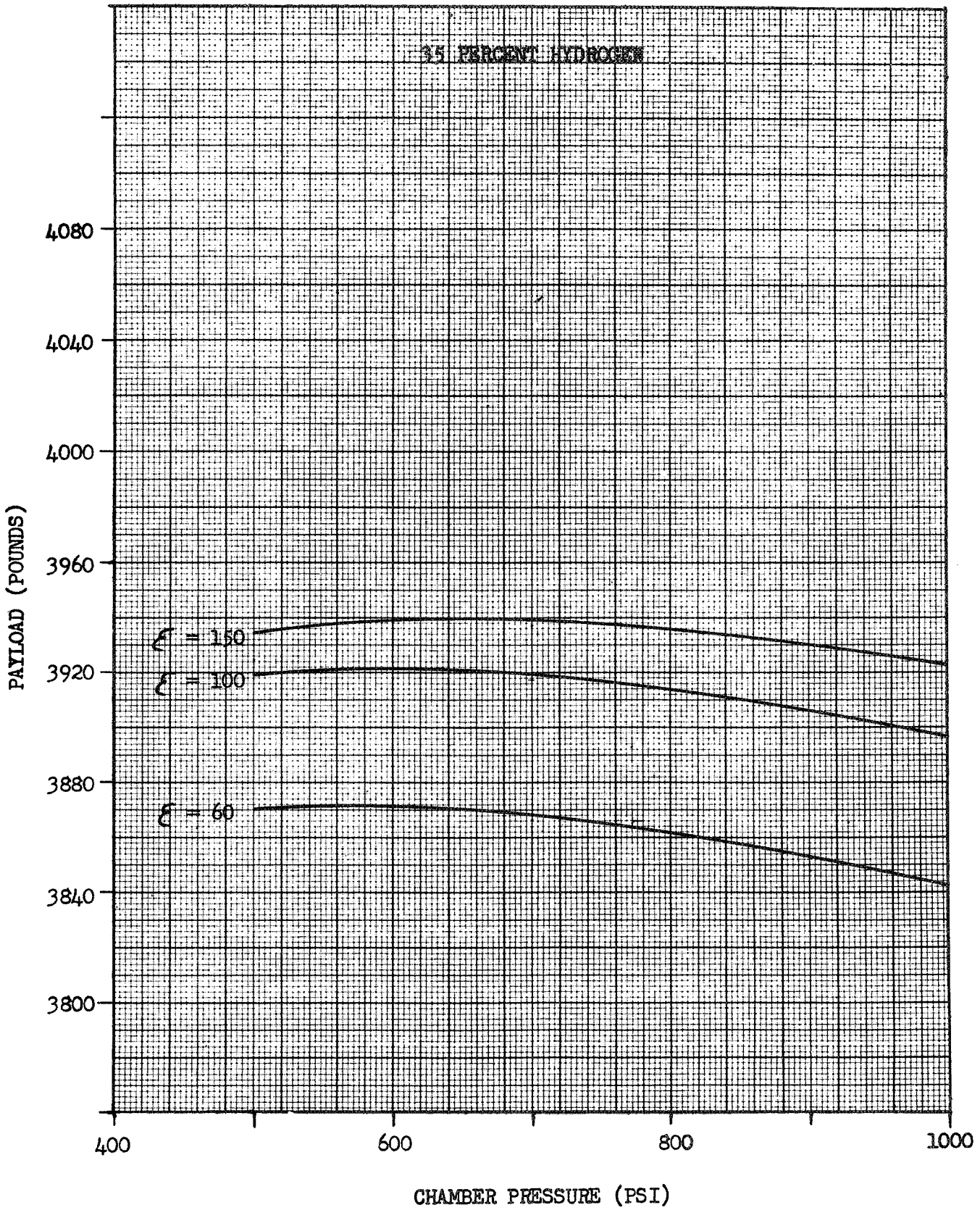

BOOSTER: TITAN III D/CENTAUR
ΔV (MISSION): 48,500 FPS
ΔV (RETRO): N/A FPS
GROSS WT: 12,000 lb

CASE: 3A2T01
☐ H2/F2
☐ H2/F2/LI

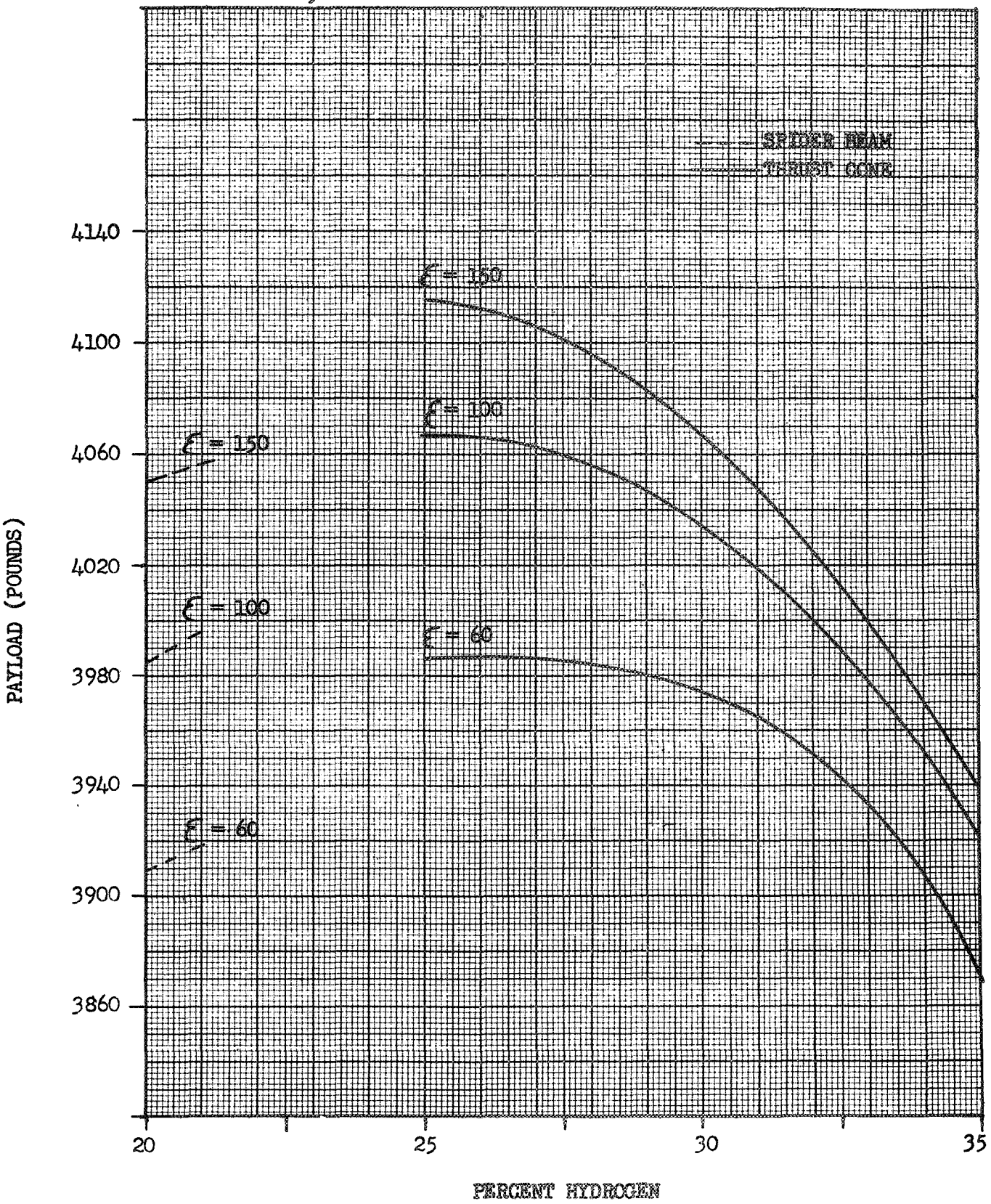

BOOSTER: TITAN III D/CENTAUR
ΔV (MISSION): 48,500 FPS
ΔV (RETRO): N/A FPS
GROSS WT: 12,000 lb

CASE: 3A2T01
☐ H2/F2
☒ H2/F2/LI

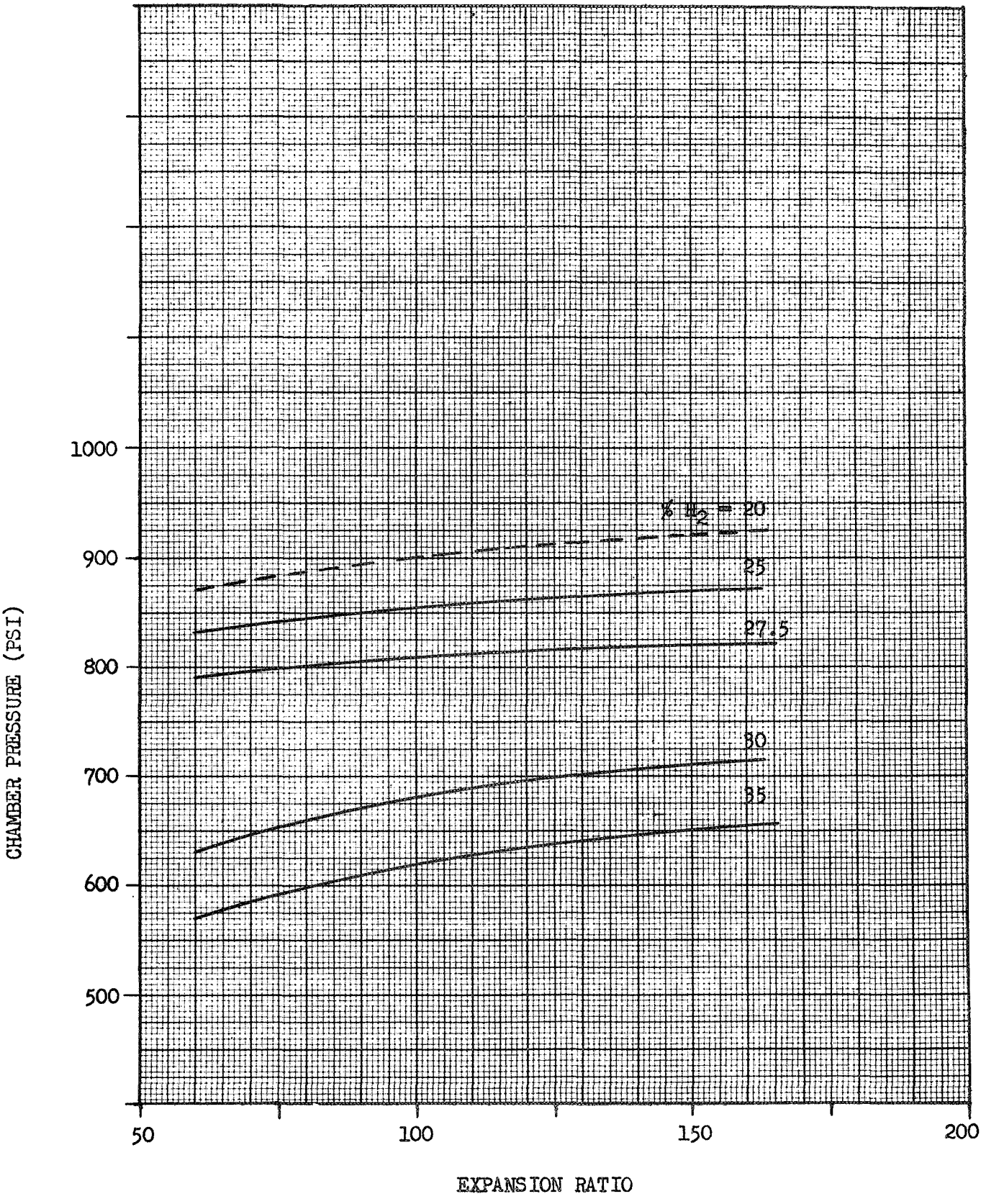

BOOSTER: TITAN III D/CENTAUR
ΔV (MISSION): 48,500 FPS
ΔV (RETRO): N/A FPS

CASE: 3A2T01
☐ H2/F2
☒ H2/F2/LI

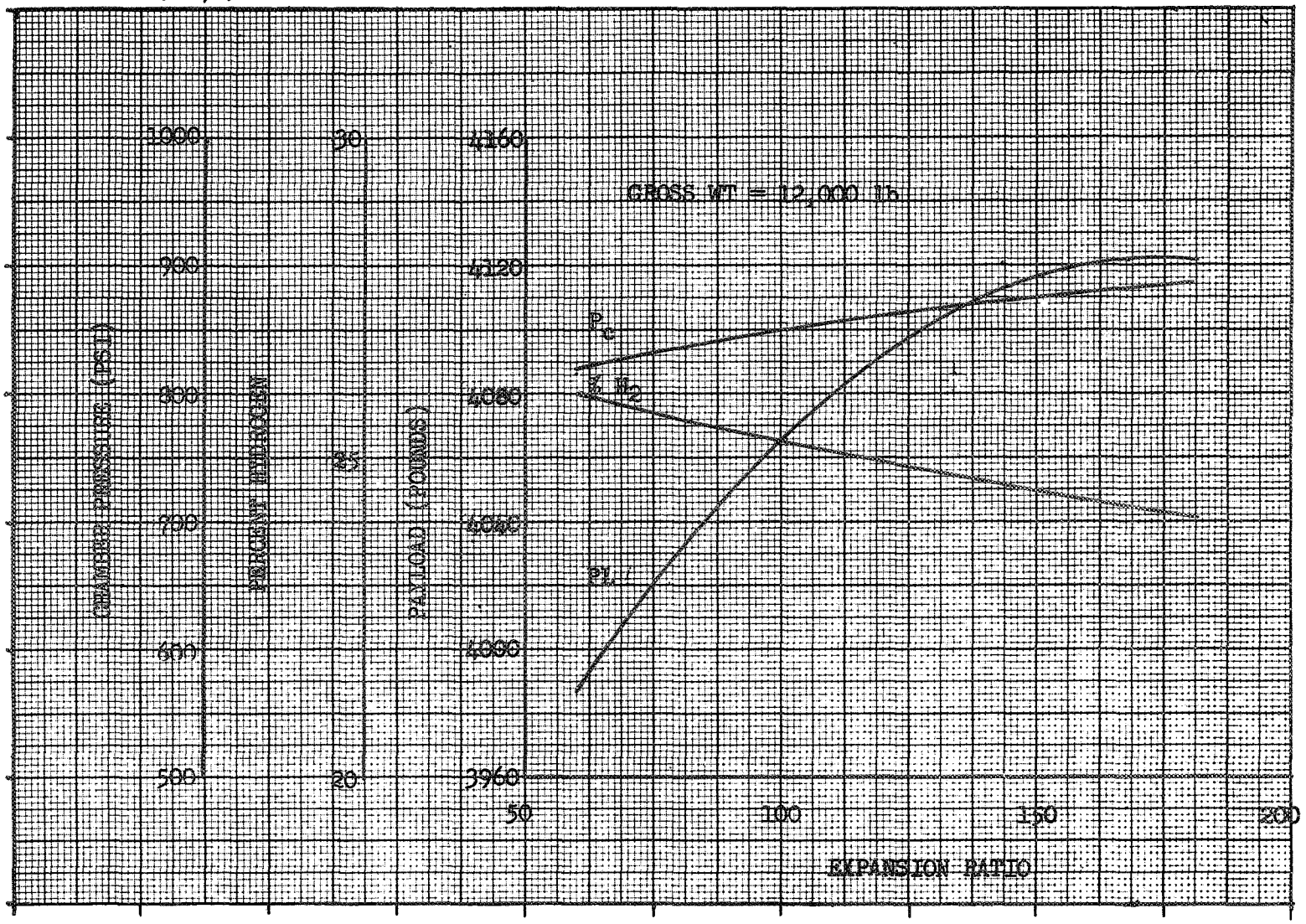

BOOSTER: TITAN III D/CENTAUR
ΔV (MISSION): 48,500 FPS
ΔV (RETRO): N/A FPS
GROSS WT: 12,000 lb

CASE: 4A2T01
☐ H2/F2
☒ H2/F2/LI-GEL

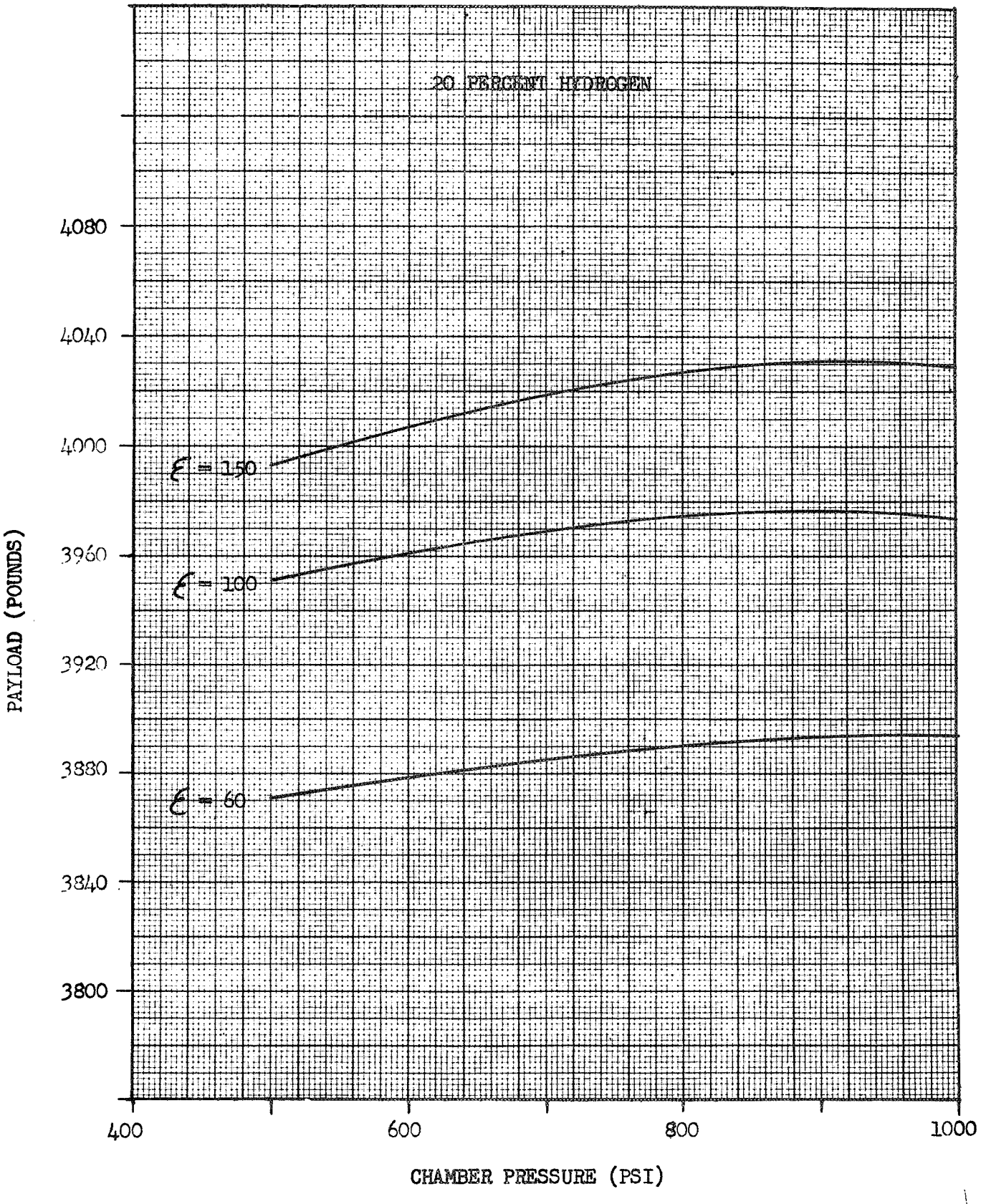

BOOSTER: TITAN III D/CENTAUR
ΔV (MISSION): 48,500 FPS
ΔV (RETRO): N/A FPS
GROSS WT: 12,000 lb

CASE: 4A2T01
☐ H2/F2
☒ H2/F2/LI - GEL

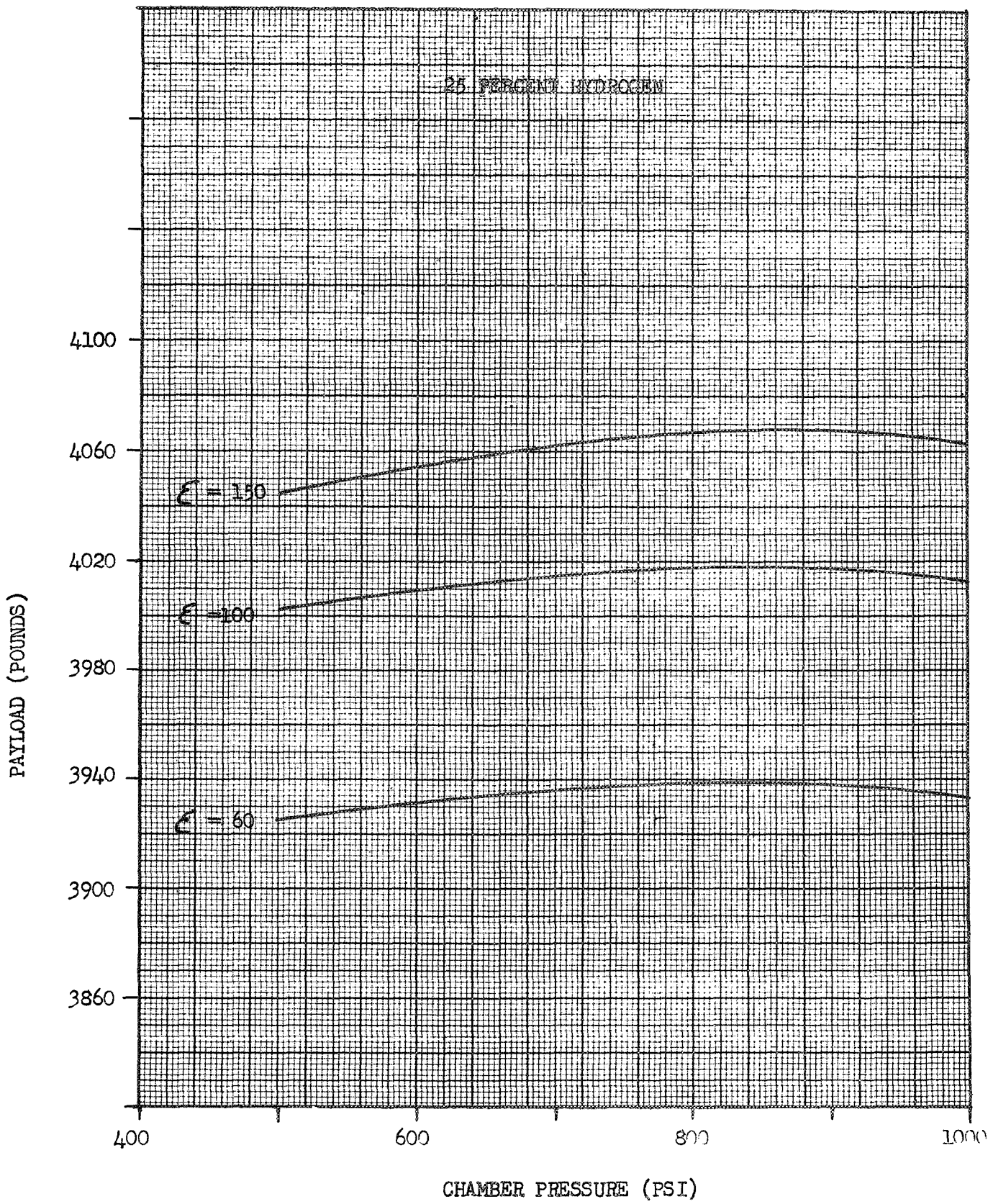

BOOSTER: TITAN III D/CENTAUR
ΔV (MISSION): 48,500 FPS
ΔV (RETRO): N/A FPS
GROSS WT: 12,000 lb

CASE: 4A2T01
☐ H2/F2
☒ H2/F2/LI - [illegible]L

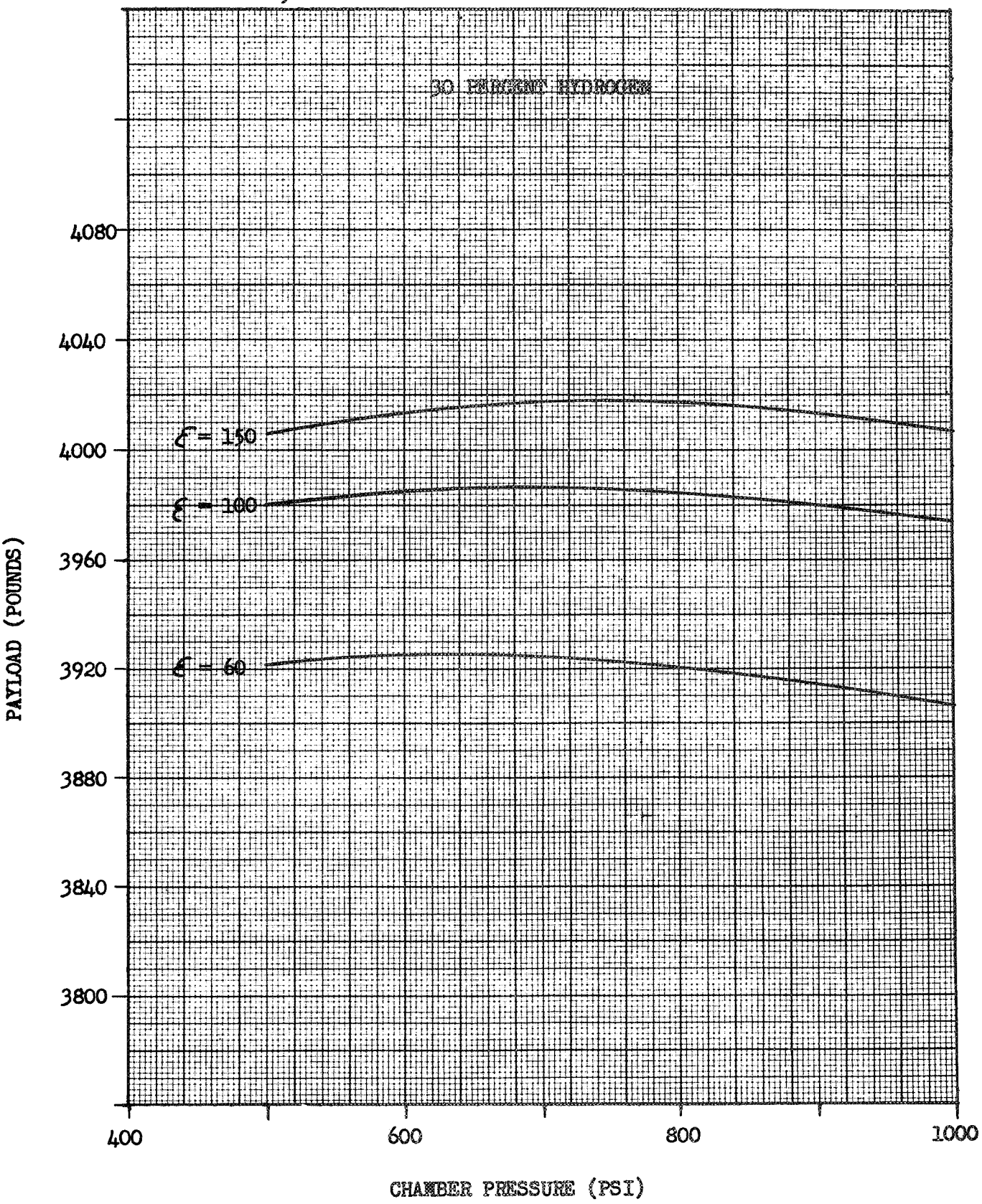

BOOSTER: TITAN III D/CENTAUR
ΔV (MISSION): 48,500 FPS
ΔV (RETRO): N/A FPS
GROSS WT: 12,000 lb

CASE: 4A2T01
☐ H2/F2
☒ H2/F2/Li - GEL

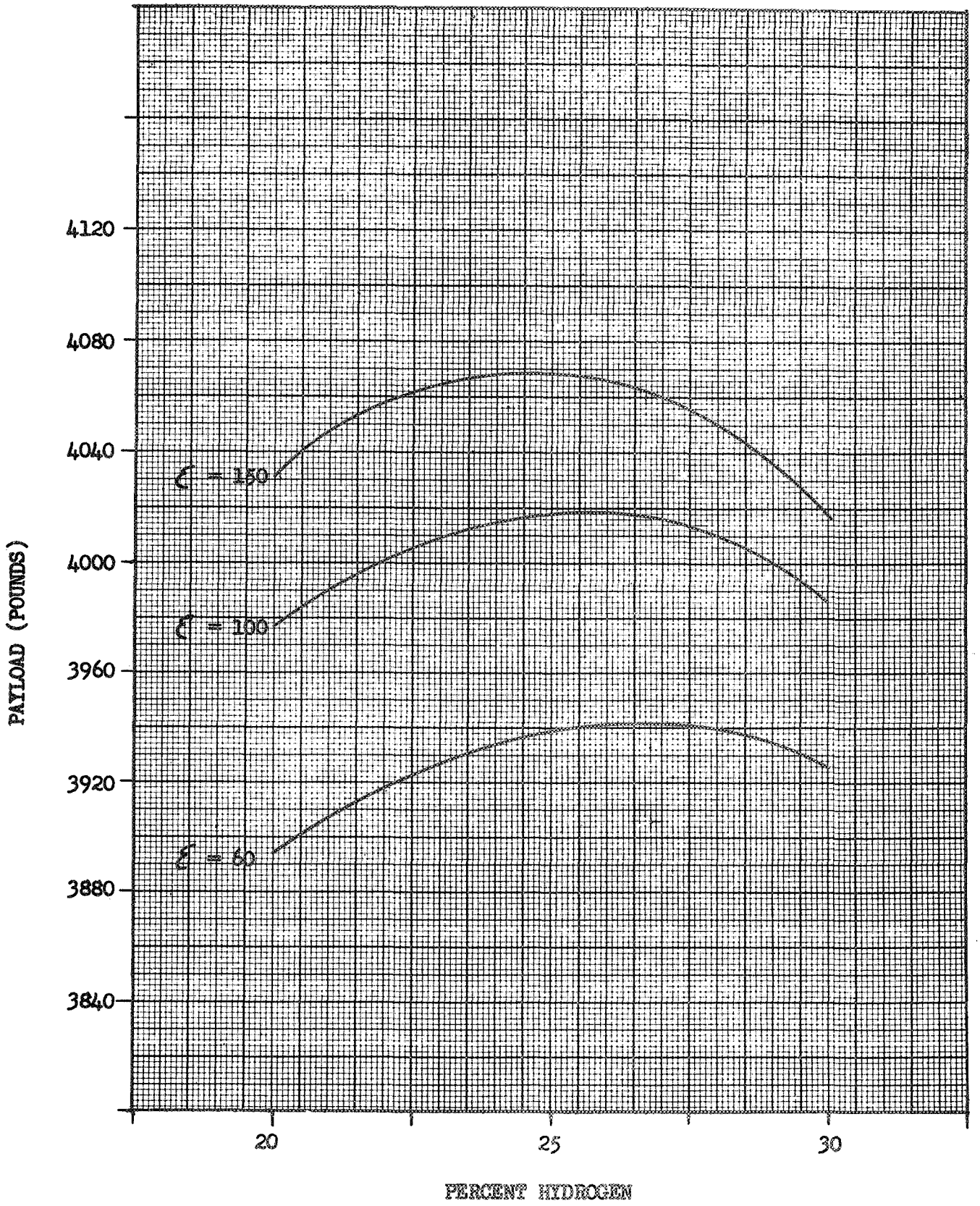

BOOSTER: TITAN III D/CENTAUR
ΔV (MISSION): 48,500 FPS
ΔV (RETRO): N/A FPS
GROSS WT: 12,000 lb

CASE: 4A2T01
☐ H2/F2
☒ H2/F2/LI - GEL

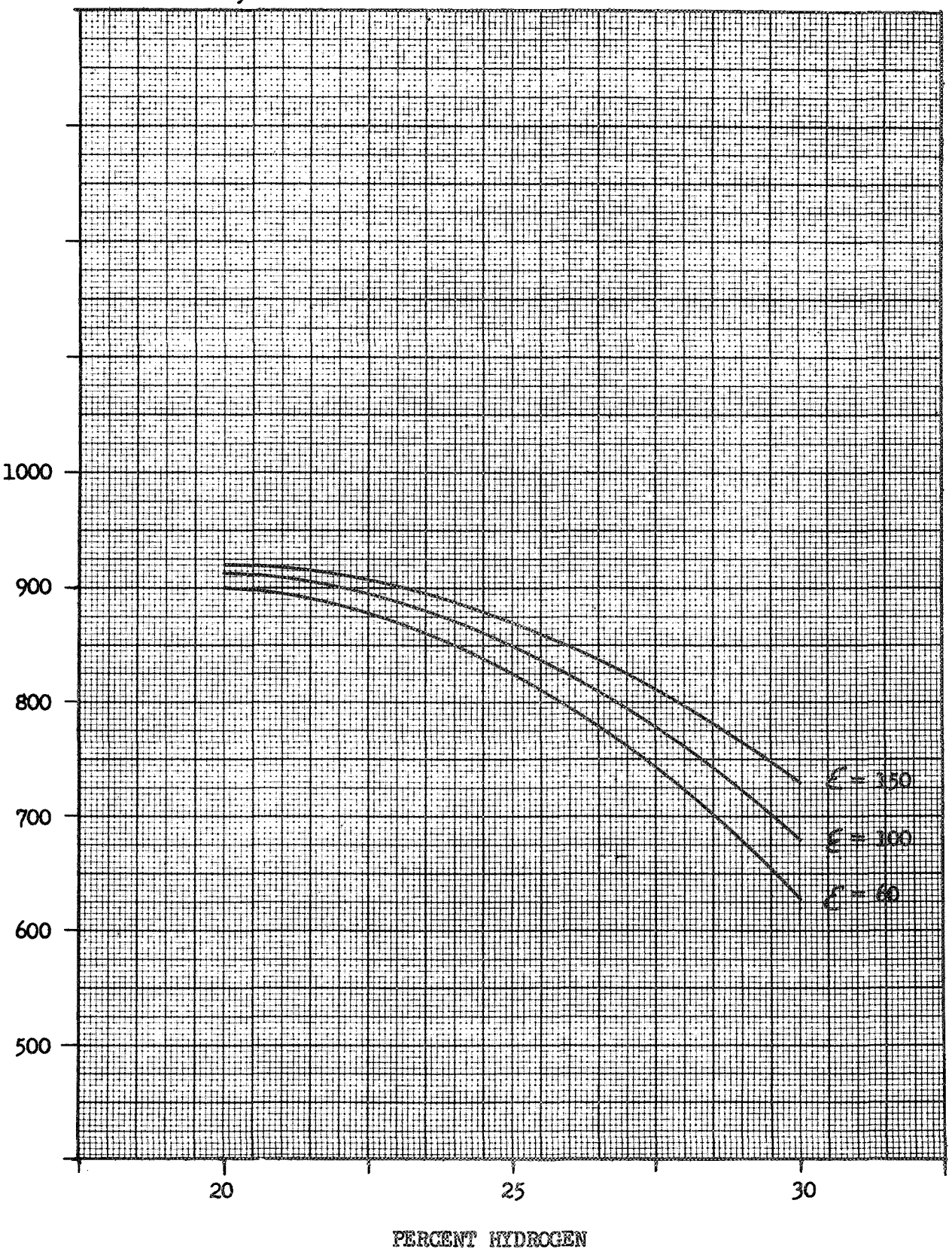

BOOSTER: TITAN III D/CENTAUR
ΔV (MISSION): 48,500 FPS
ΔV (RETRO): N/A FPS

CASE: 4A2T01
☐ H2/F2
☒ H2/F2/LI- GEL

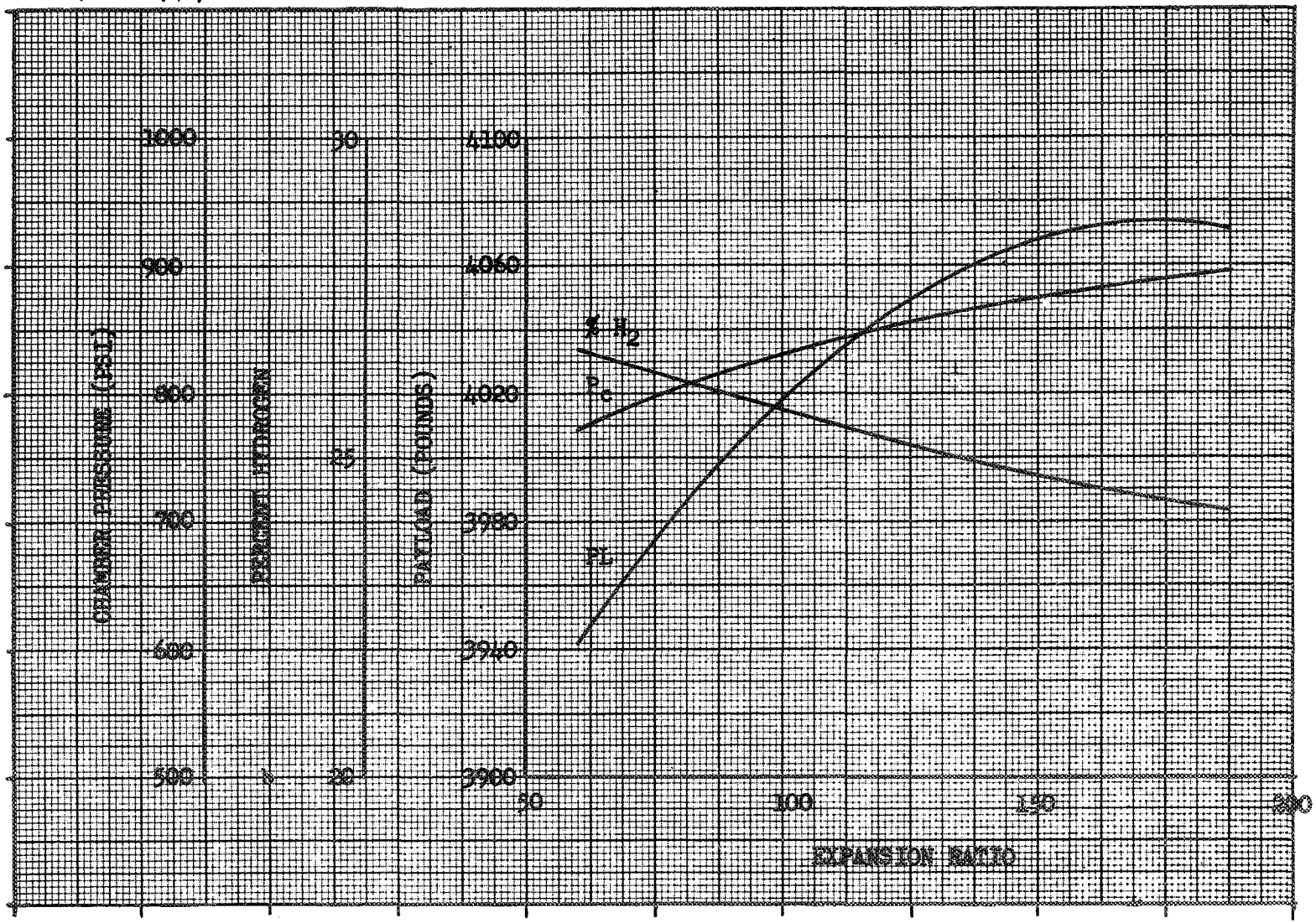

BOOSTER: TITAN III D/CENTAUR
ΔV (MISSION): 48,500 FPS
ΔV (RETRO): N/A FPS
GROSS WT: 12,000 Lb

CASE: 2A2T01
☒ H2/F2
☐ H2/F2/LI

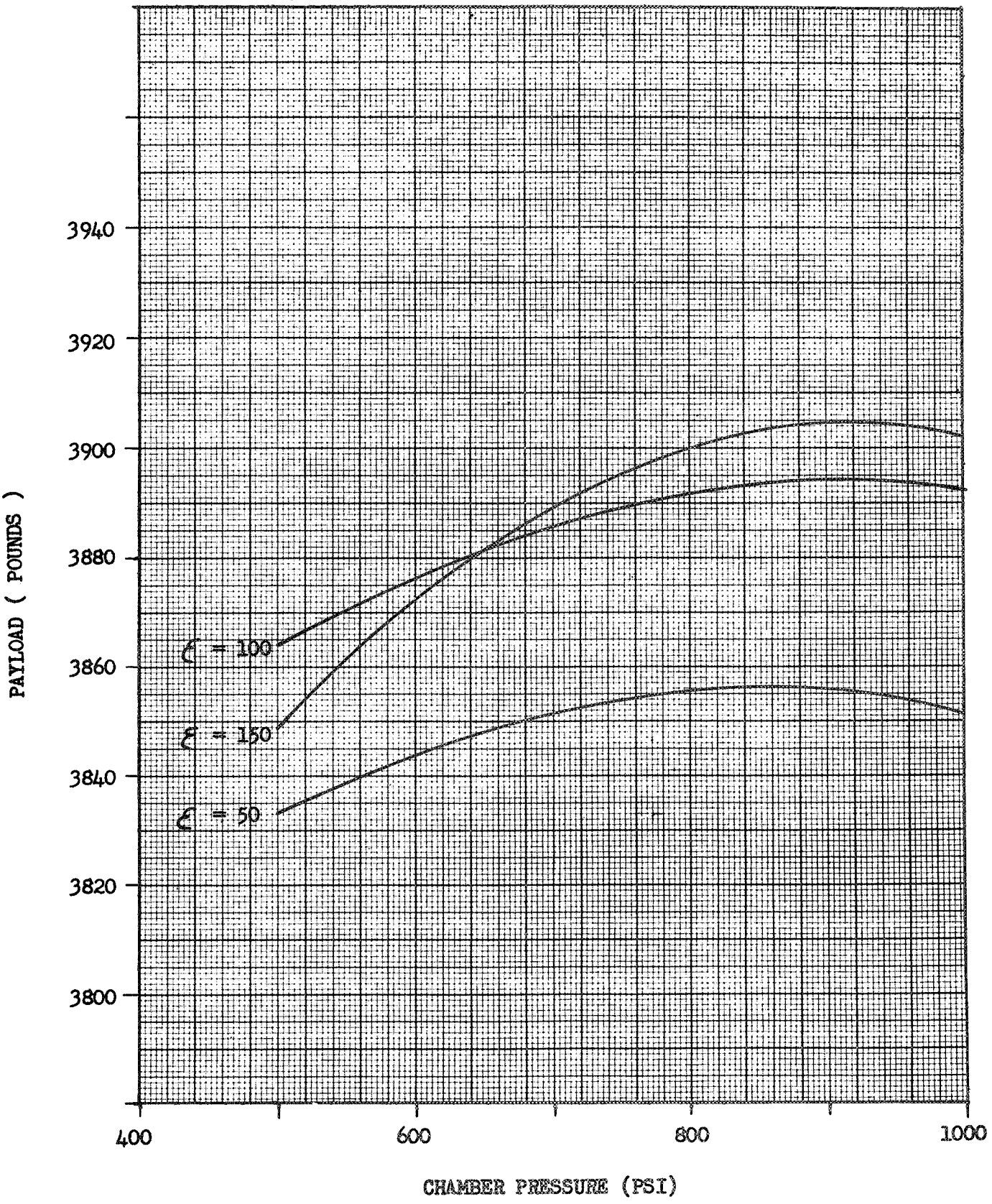

BOOSTER: TITAN III D/CENTAUR
ΔV (MISSION): 48,500 FPS
ΔV (RETRO): N/A FPS

CASE: 2A2T01
☒ H2/F2
☐ H2/F2/LI

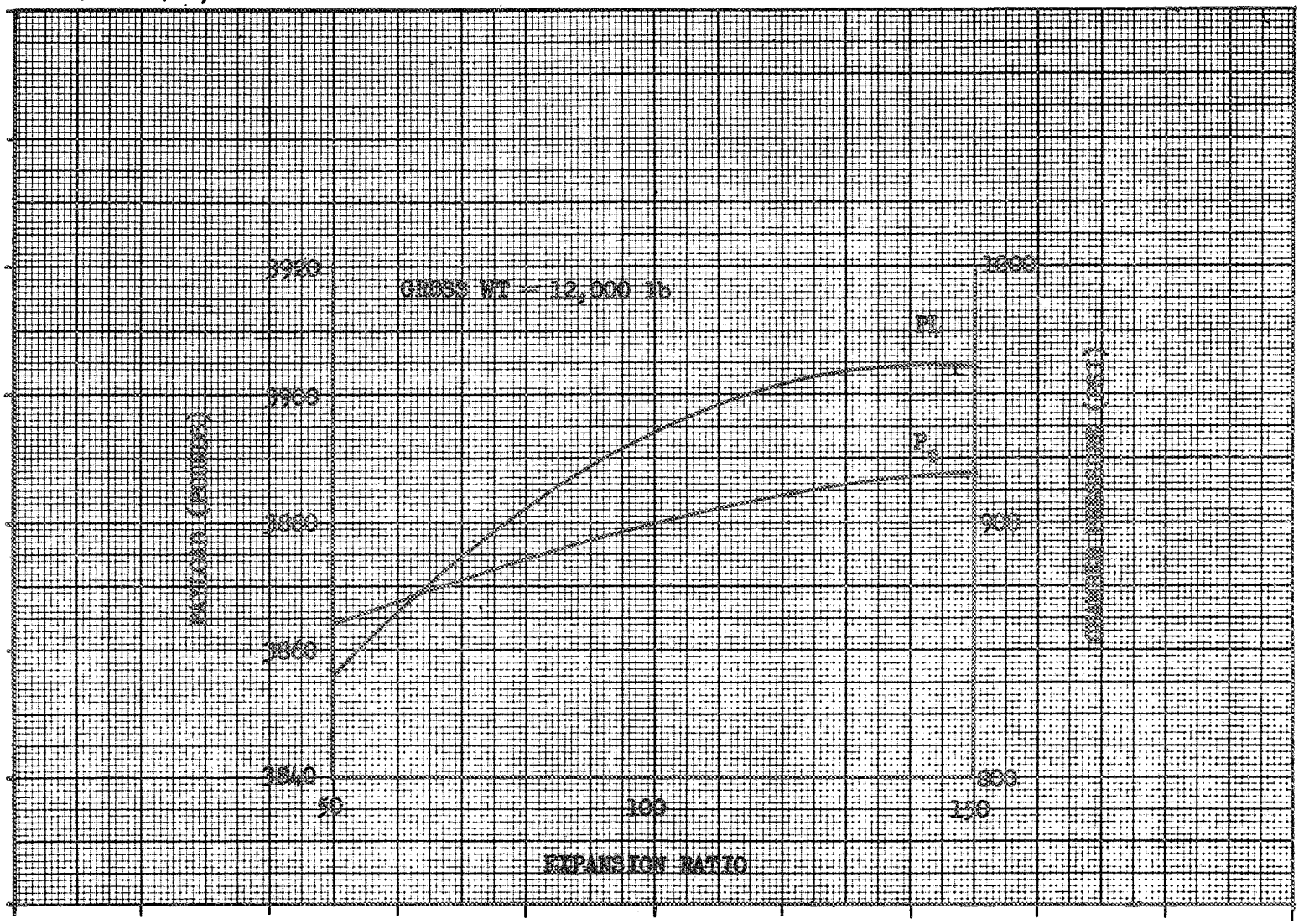

BOOSTER: 260" SRM/S-IV B
ΔV (MISSION): 48,500 FPS
ΔV (RETRO): N/A FPS
GROSS WT: 70,000 Lb

CASE: 3A3T01
☐ H2/F2
☒ H2/F2/LI

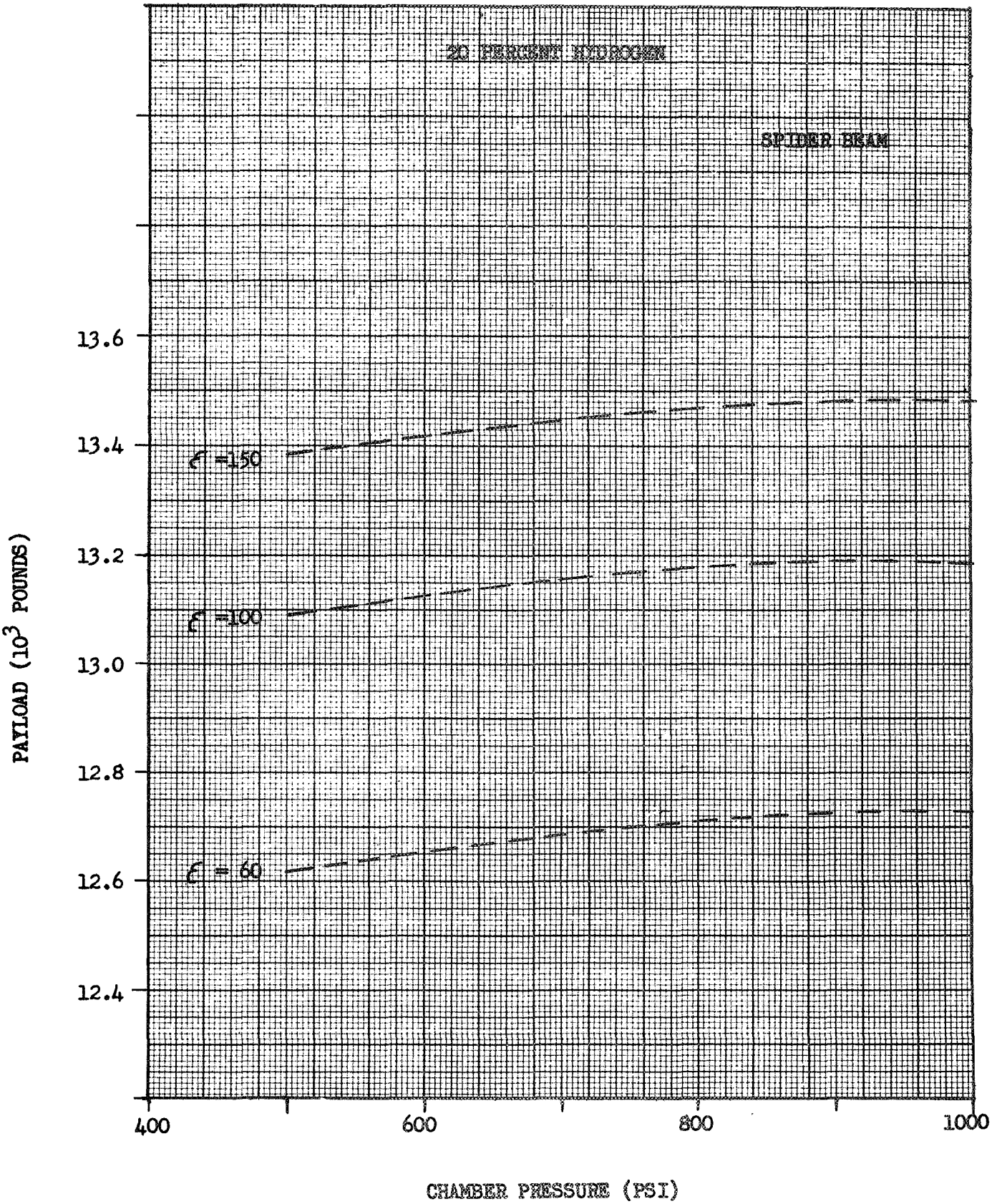

BOOSTER: 260" SRM/S-IV B
ΔV (MISSION): 48,500 FPS
ΔV (RETRO): N/A FPS
GROSS WT: 70,000 Lb

CASE: 3A3T01
☐ H2/F2
☒ H2/F2/LI

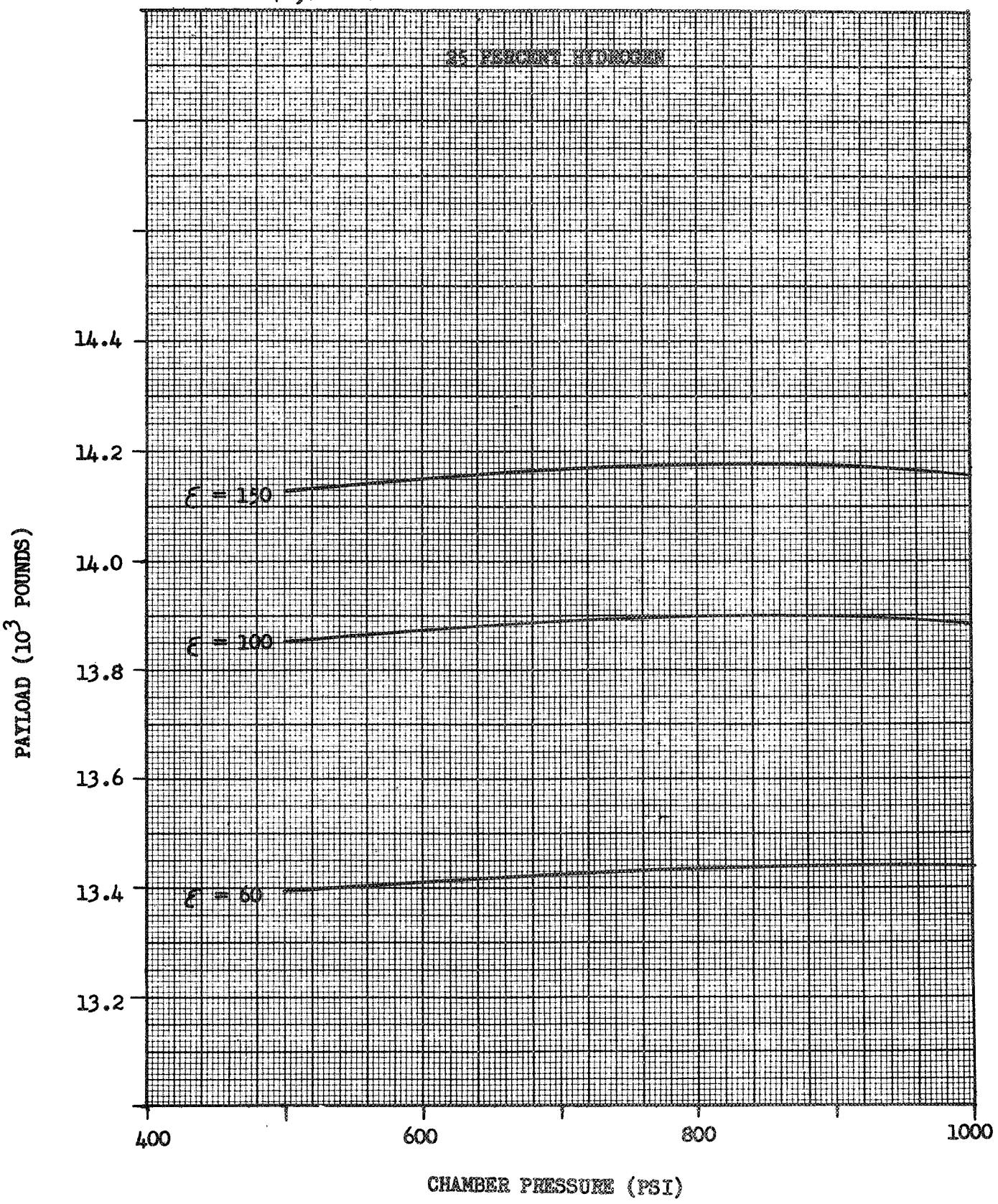

BOOSTER: 260" SRM/S-IV B
ΔV (MISSION): 48,500 FPS
ΔV (RETRO): N/A FPS
GROSS WT: 70,000Lb

CASE: 3A3T01
☐ H2/F2
☒ H2/F2/LI

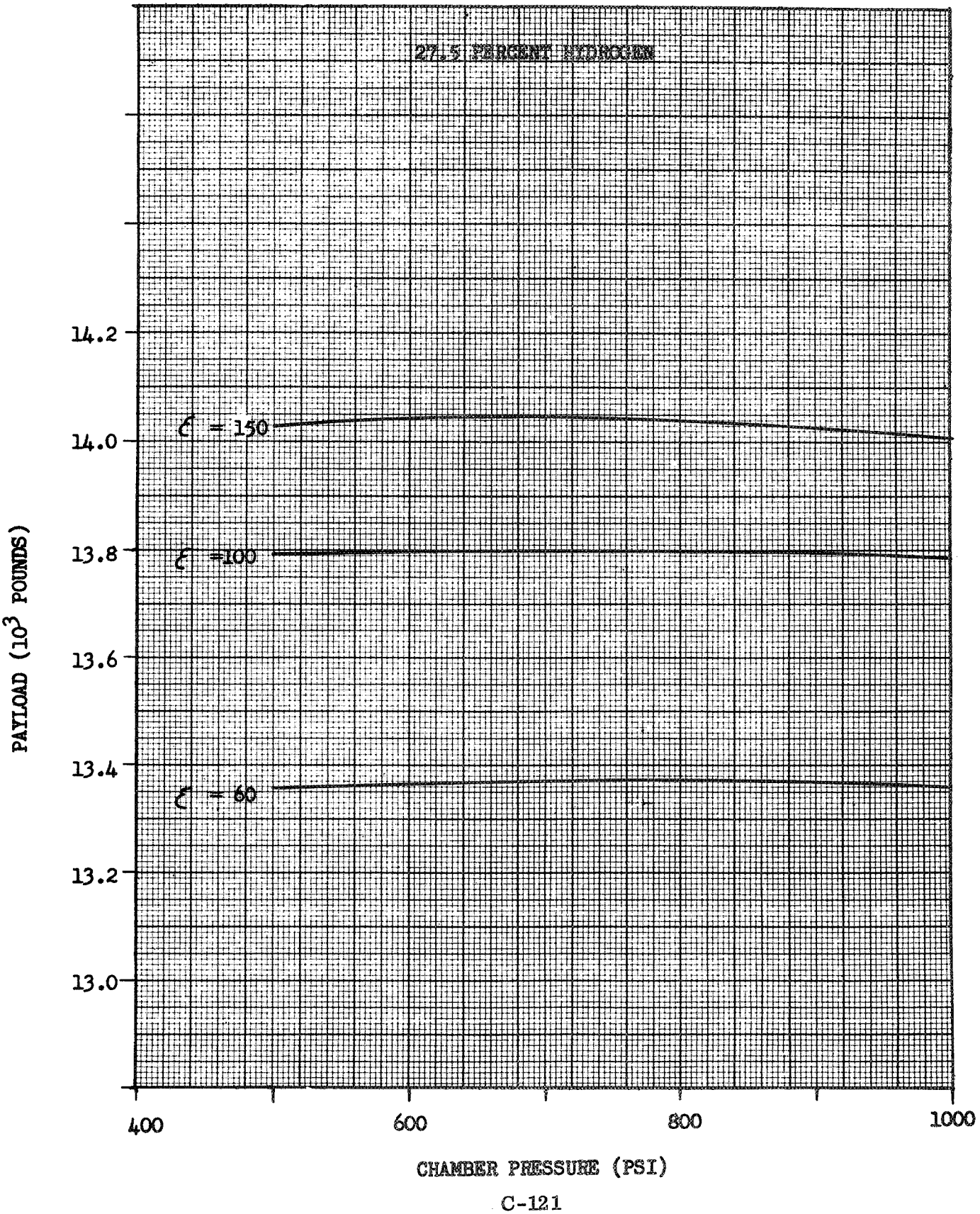

BOOSTER: 260" SRM/S-IV B
ΔV (MISSION): 48,000 FPS
ΔV (RETRO): N/A FPS
GROSS WT: 70,000 Lb

CASE: 3A3T01
☐ H2/F2
☒ H2/F2/LI

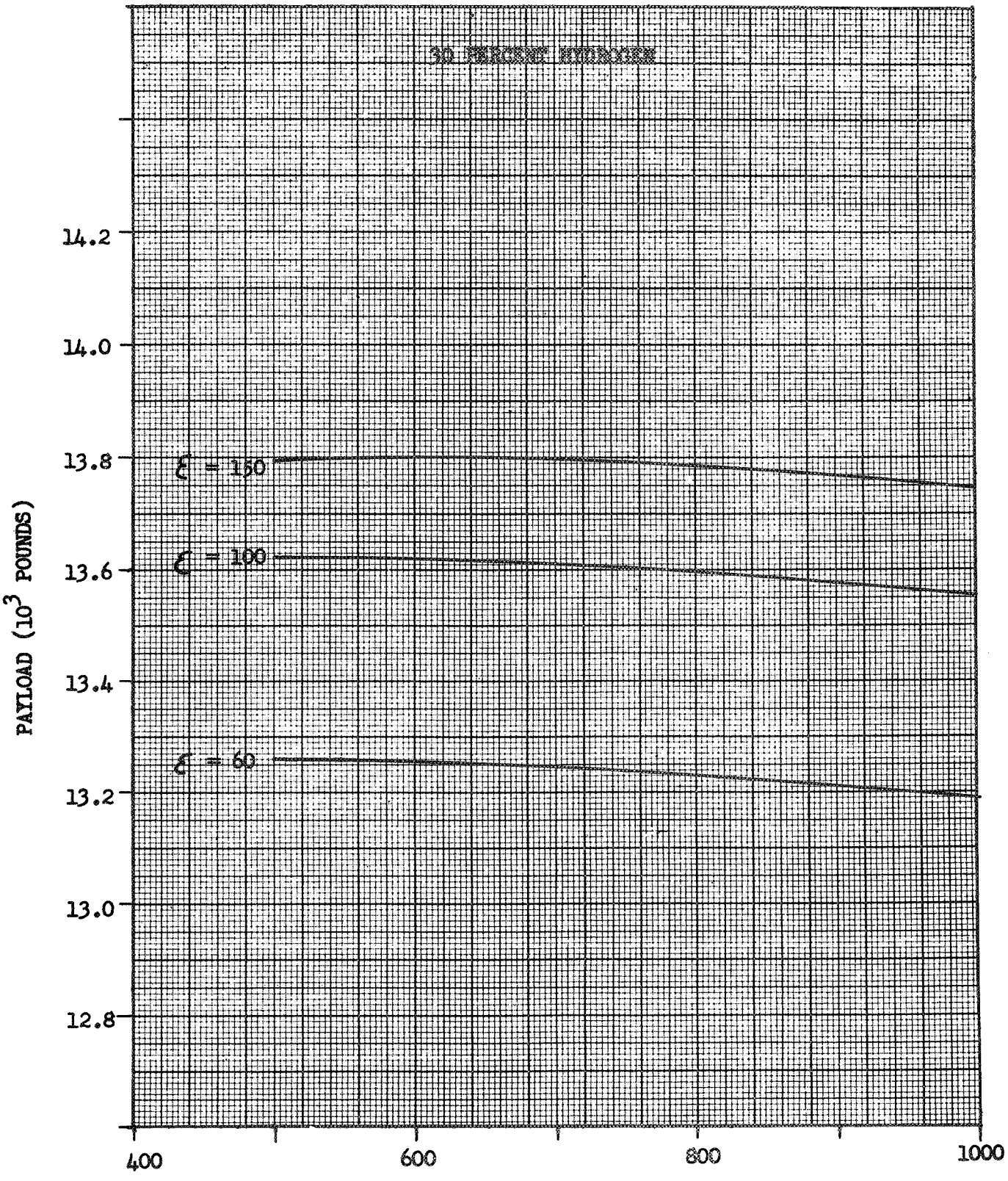

BOOSTER: 260 " SRM/S-IV B
ΔV (MISSION): 48,500 FPS
ΔV (RETRO): N/A FPS
GROSS WT: 70,000 Lb

CASE: 3A3T01
☐ H2/F2
☒ H2/F2/LI

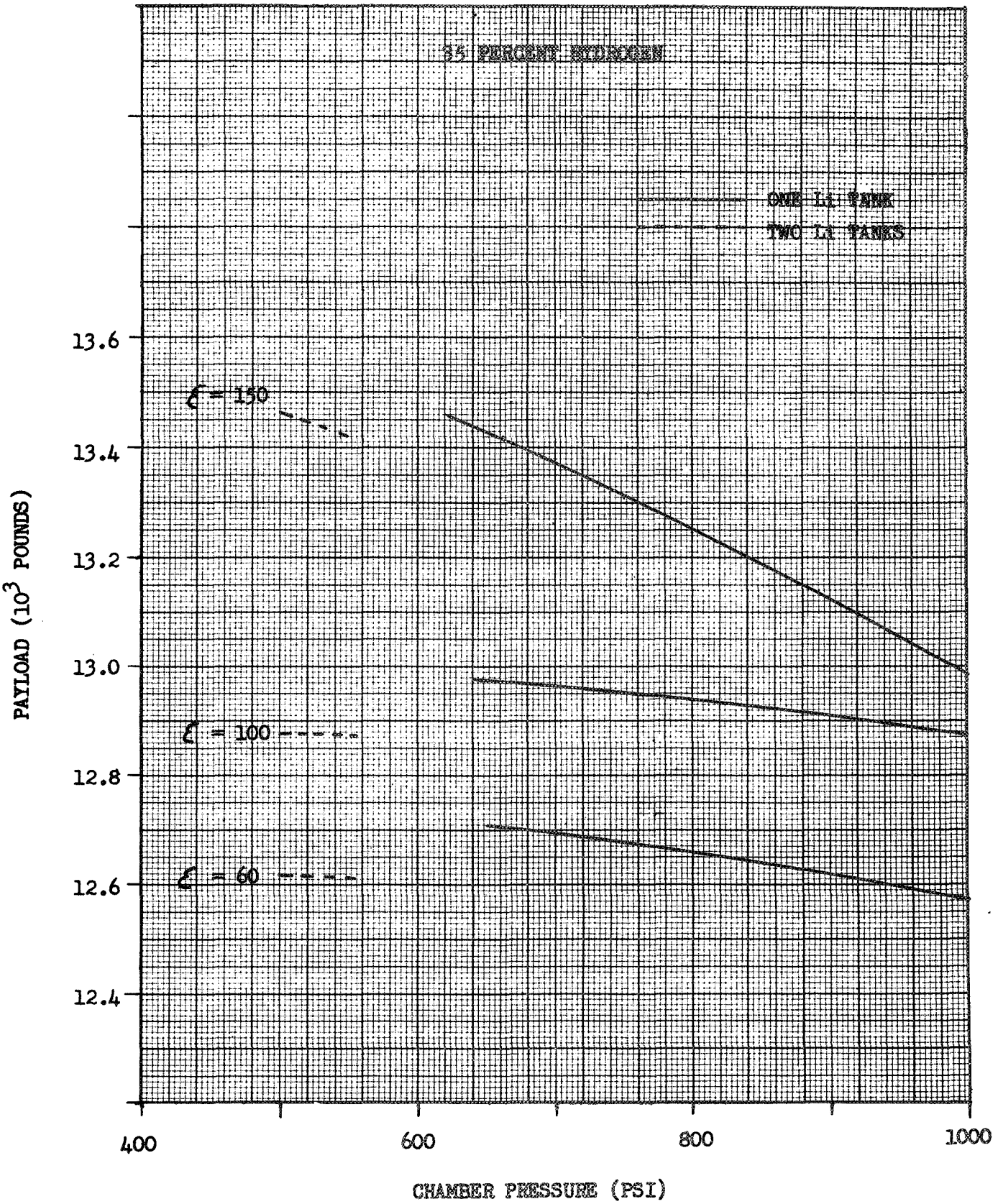

BOOSTER: 260" SRM/S-IV B
ΔV (MISSION): 48,500 FPS
ΔV (RETRO): N/A FPS
GROSS WT: 70,000 Lb

CASE:
☐ H2/F2
☒ H2/F2/LI

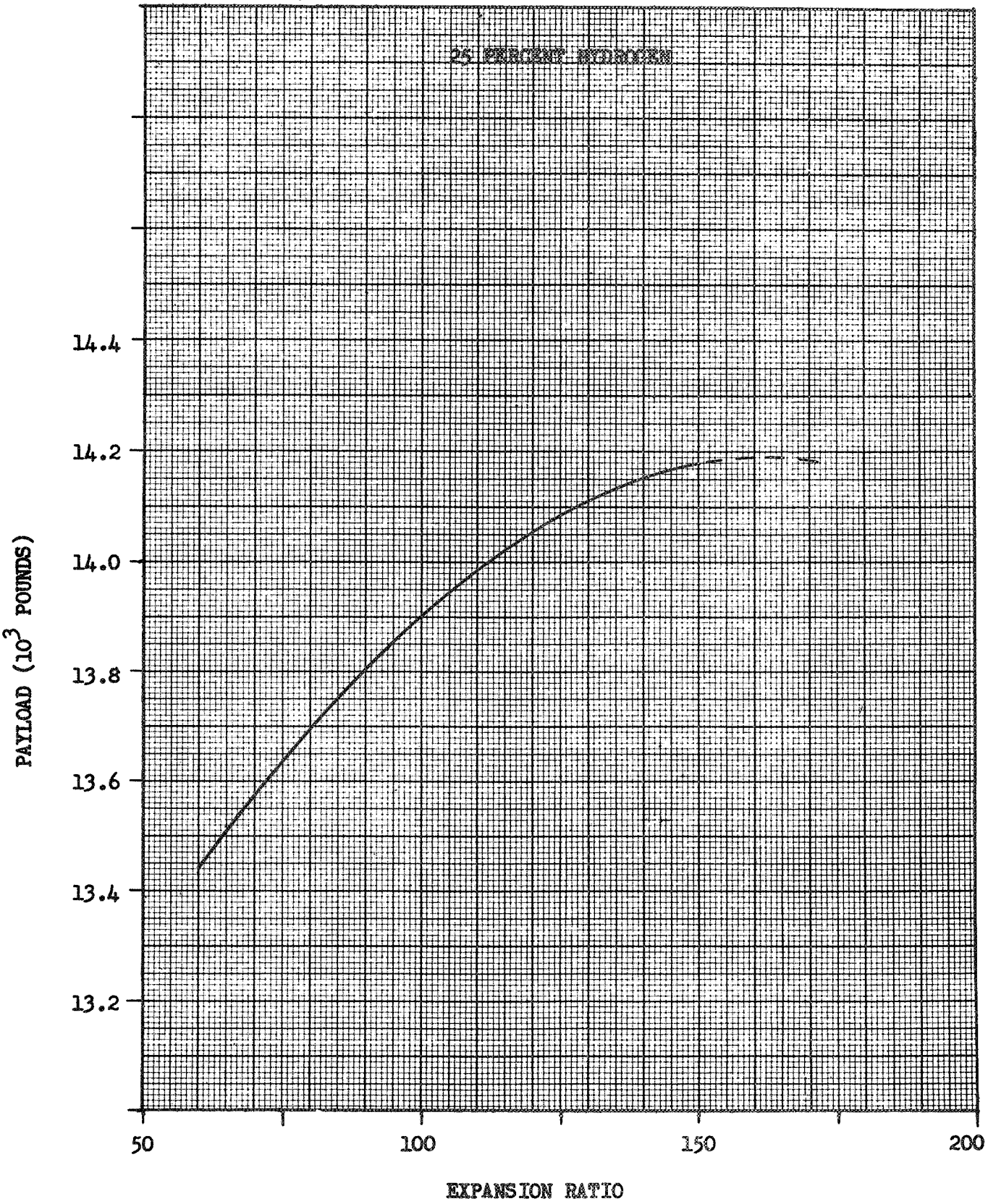

BOOSTER: 260 " SRM/S-IV B
ΔV (MISSION): 48,500 FPS
ΔV (RETRO): N/A FPS
GROSS WT: 70,000 Lb

CASE: 4A3T01
☐ H2/F2
☒ H2/F2/LI -GEL

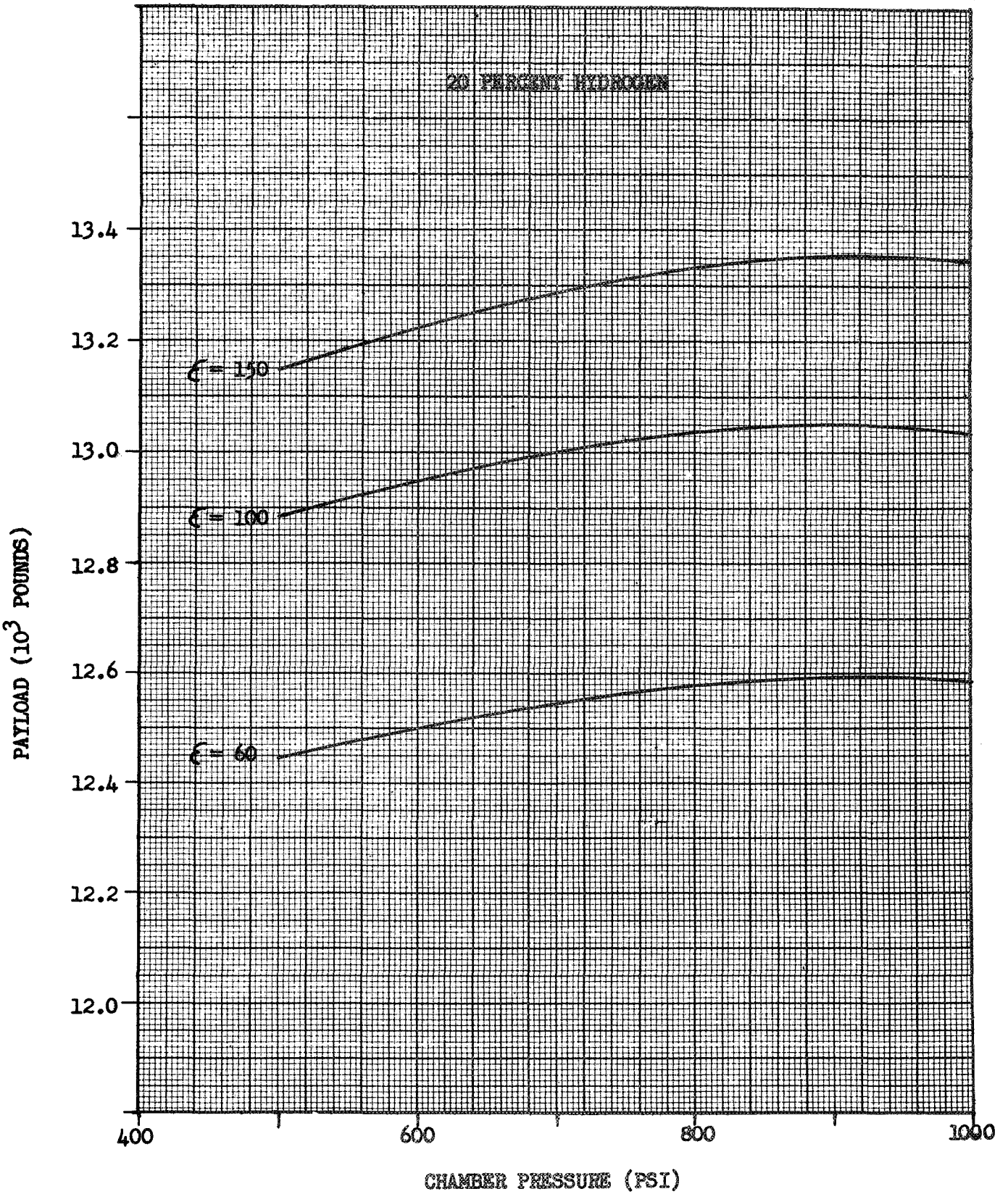

BOOSTER: 260" SRM/S-IV B
ΔV (MISSION): 48,500 FPS
ΔV (RETRO): N/A FPS
GROSS WT: 70,000 Lb

CASE: 4A3T01
☐ H2/F2
☒ H2/F2/LI -GEL

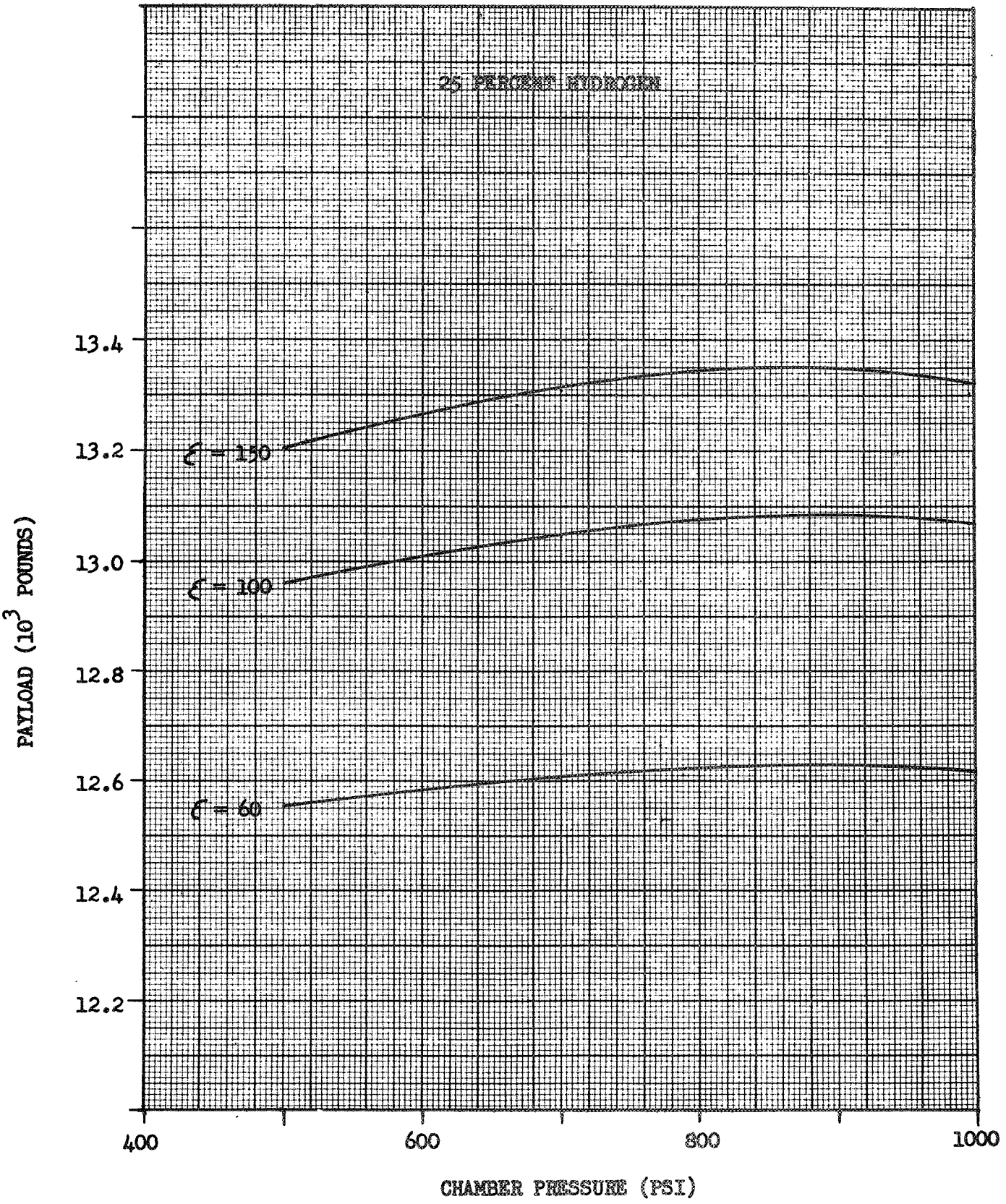

BOOSTER: 260" SRM/S-IV B
ΔV (MISSION): 48,500 FPS
ΔV (RETRO): N/A FPS
GROSS WT: 70,000 Lb

CASE: 4A3T01
☐ H2/F2
☒ H2/F2/LI -GEL

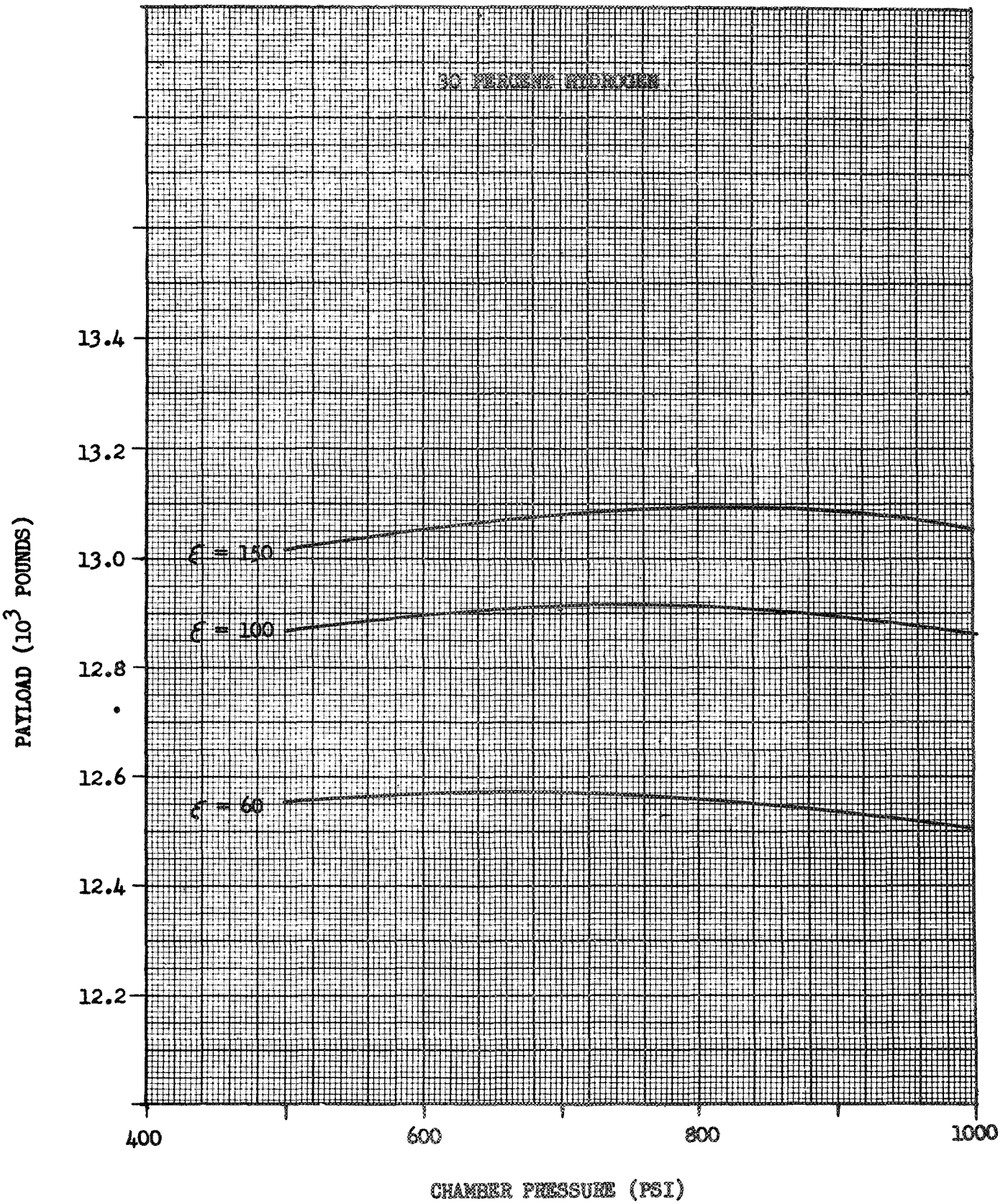

BOOSTER: 260" SRM/S-IV B
ΔV (MISSION): 48,500 FPS
ΔV (RETRO): N/A FPS
GROSS WT: 70,000 Lb

CASE: 4A3T01
☐ H2/F2
☒ H2/F2/LI - GEL

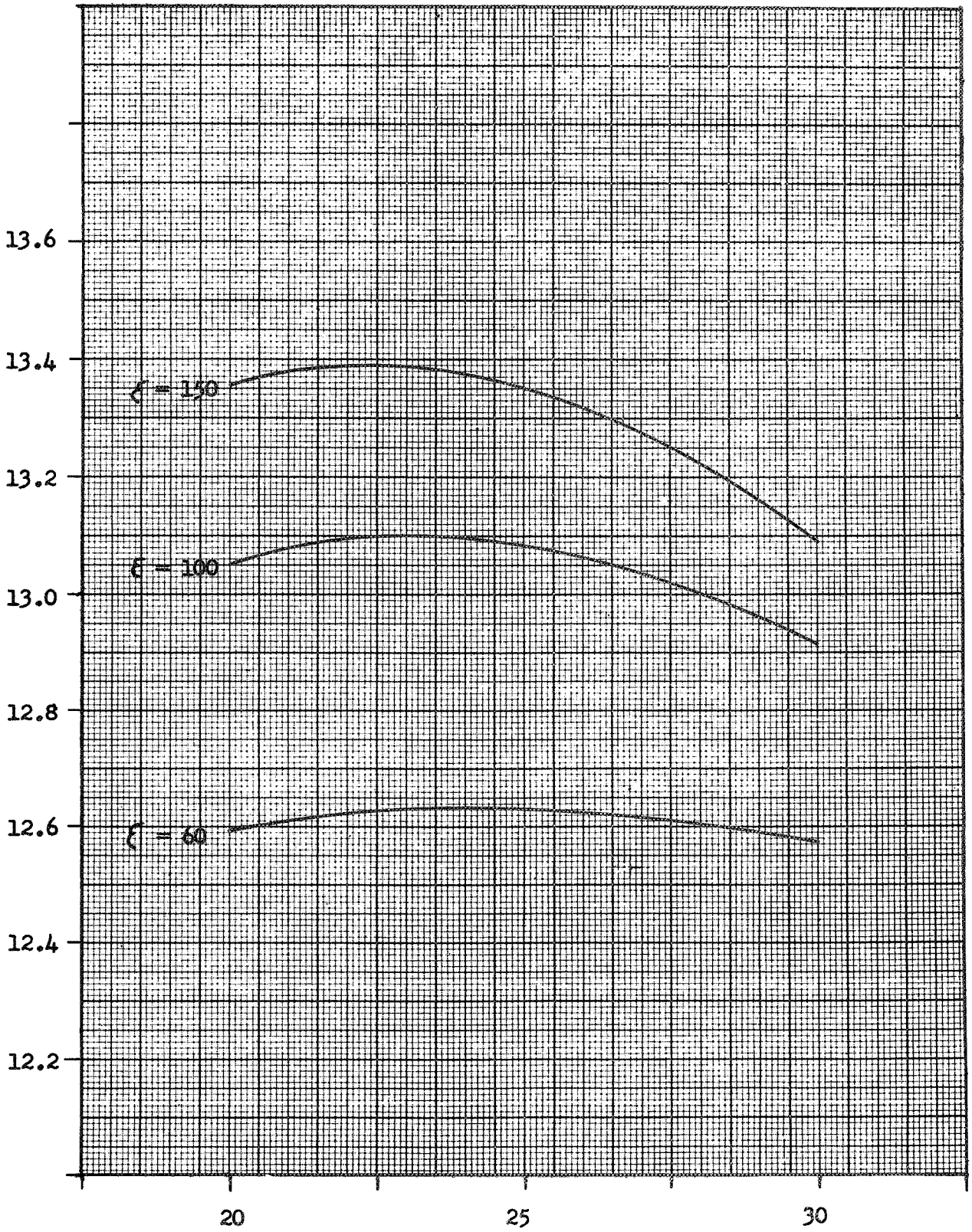

BOOSTER: 260" SRM/S-IV B
ΔV (MISSION): 48,500 FPS
ΔV (RETRO): N/A FPS

CASE: 4A3T01
☐ H2/F2
☒ H2/F2/LI - GEL

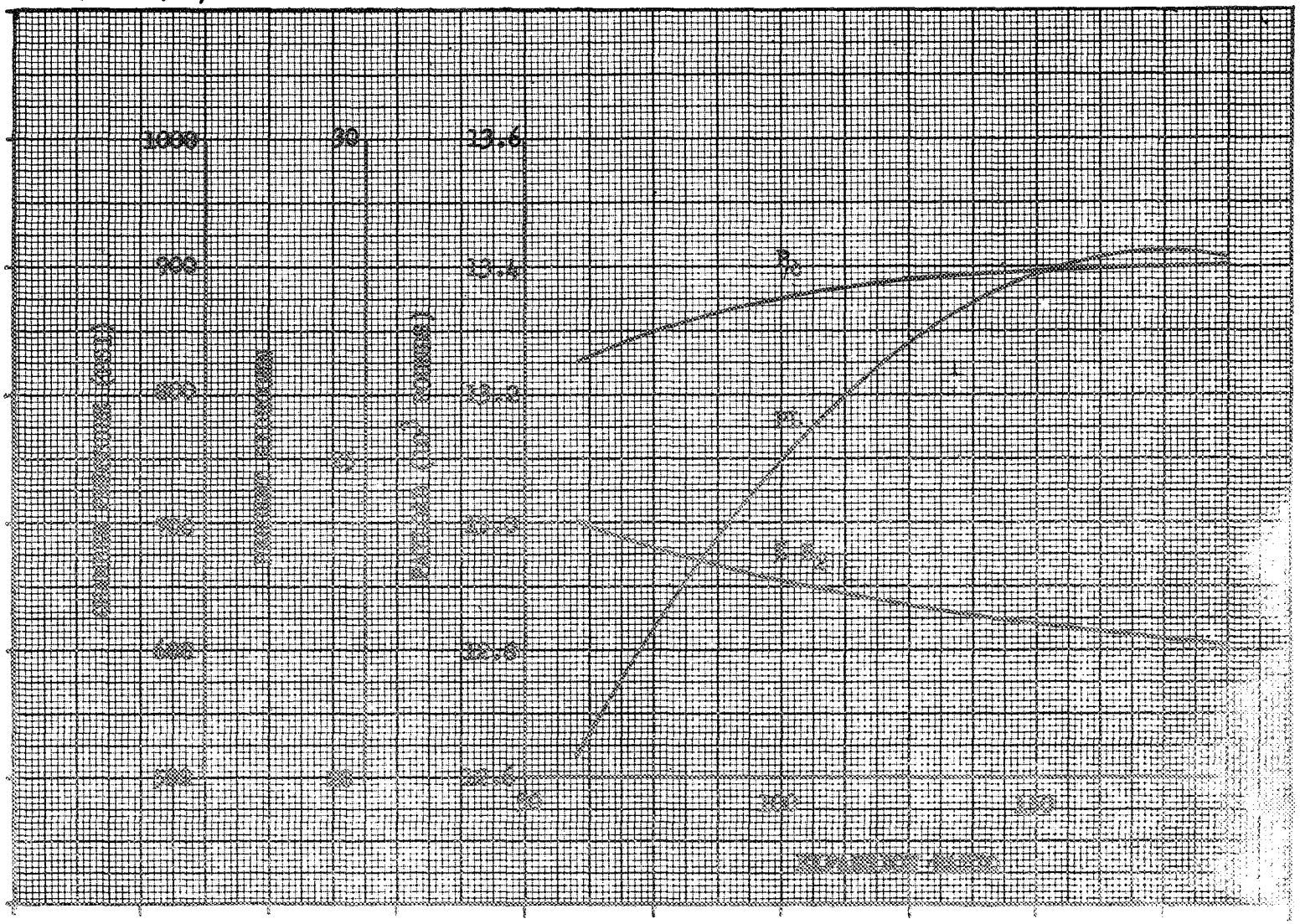

BOOSTER: 260 " SRM/S-IV B
ΔV (MISSION): 48,500 FPS
ΔV (RETRO): N/A FPS
GROSS WT: 70,000 Lb

CASE: 2A3T01
☒ H2/F2
☐ H2/F2/LI

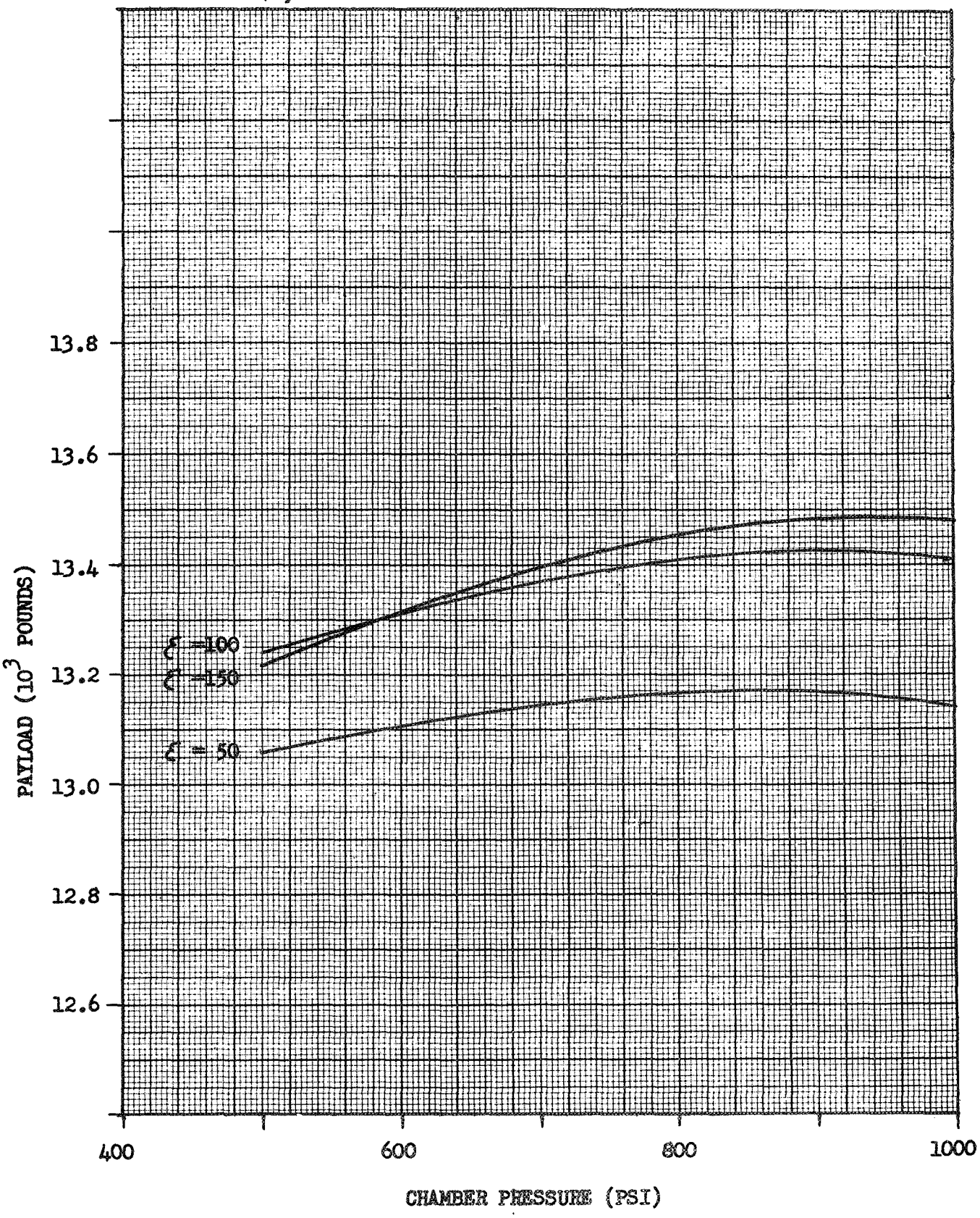

BOOSTER: 260" SRM/S-IV B
ΔV (MISSION): 48,500 FPS
ΔV (RETRO): N/A FPS

CASE: 2A3T01
☒ H2/F2
☐ H2/F2/LI

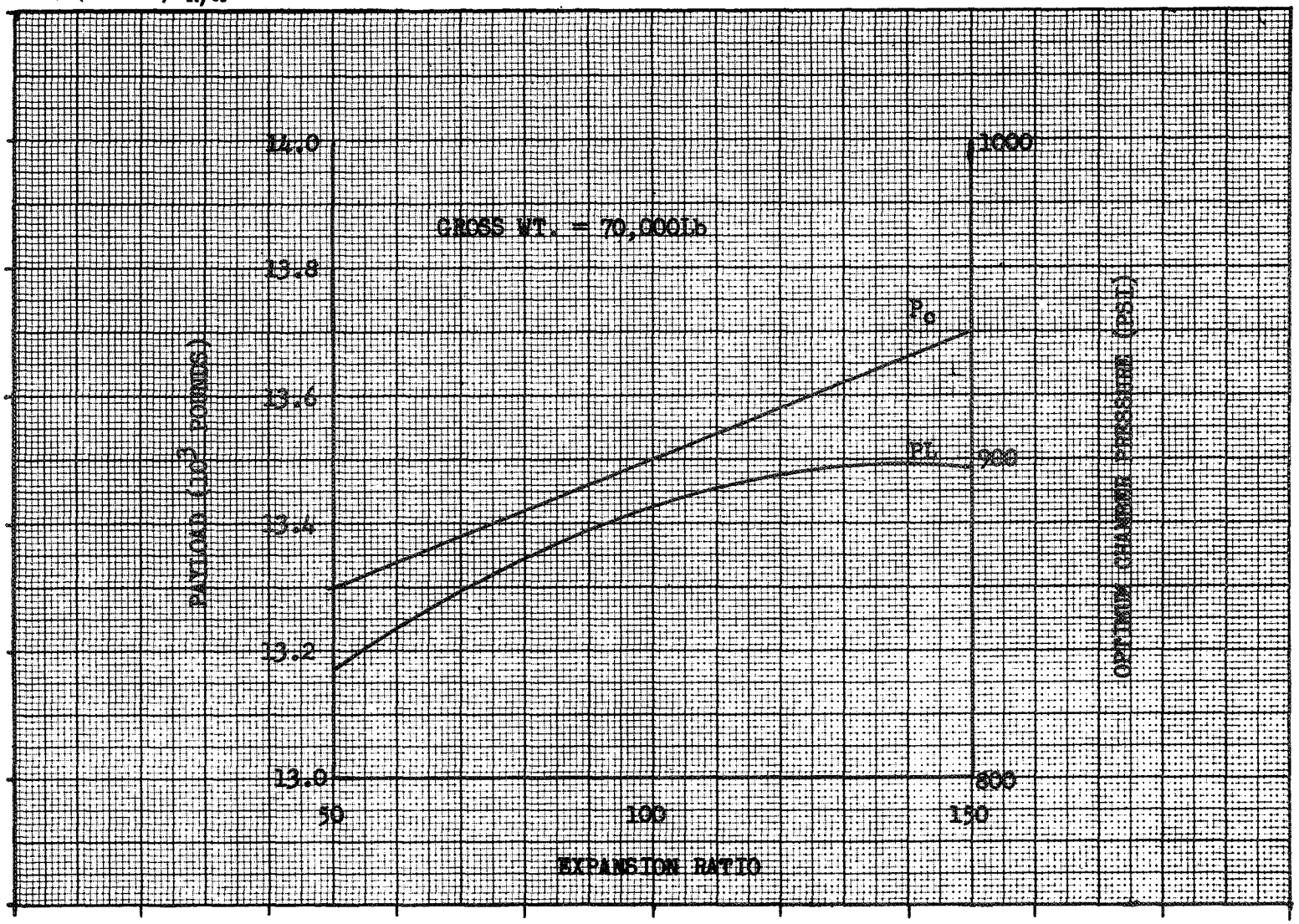

Appendix D

METEOROID SHIELD ANALYSIS

	Page
Single Burn, 205 Day Coast Mission	
Meteoroid Shield Data	D-1
Sensitivity to Meteoroid Shield Backup Sheet Selection	D-4
Sensitivity to Meteoroid Environment and Shield Design Criteria	D-5
Two Burn, 205 Day Coast Mission	
Meteoroid Shield Data	D-8
Sensitivity to Meteoroid Shield Backup Sheet Selection	D-11
Sensitivity to Meteoroid Environment and Shield Design Criteria	D-12

Table D-1. Meteoroid Shield Data

MISSION: SINGLE BURN, 205-DAY COAST

STAGE		TRIPROPELLANT		
PROPELLANT TANK		HYDROGEN	FLUORINE	LITHIUM
PROPELLANT LOAD (POUNDS)		1149	2526	922
TANK RADIUS (INCHES)		50.0	18.3	23.5
TANK CYLINDER HEIGHT (INCHES)		0.45	0	0
DOME THICKNESS (INCHES)		0.052	0.025	0.015
CYLINDER THICKNESS (INCHES)		0.103	N/A	N/A
TANK MATERIAL		Aluminum	Aluminum	Mar. Steel
MINIMUM SKIN GAUGE (INCHES)		0.025	0.025	0.015
THERMAL INSULATION THICKNESS (INCHES)		3.04	1.48	3.00
TANK SURFACE AREA (SQUARE FEET)		258.49	34.16	61.19
METEOROID DESIGN MASS (GRAMS)		3.76×10^{-3}	0.83×10^{-3}	1.28×10^{-3}
METEOROID DIAMETER (CENTIMETERS)		0.243	0.147	0.170
REQUIRED THICKNESS (INCHES)	SHIELD	0.0287	0.0174	0.0201
	BACKUP WALL	0.0391	0.0250	0.0125
DESIGN THICKNESS (INCHES)	SHIELD	0.0287	0.0250	0.0201
	BACKUP WALL (DELTA)	0.0	0.0	0.0
SPACING (INCHES)	OPTIMUM	1.742	2.719	2.107
	DESIGN	3.040	2.719	3.000
WEIGHT (POUNDS)	SHIELD	113	15	51
	BACKUP WALL (DELTA)	0	0	0
WEIGHT PER TANK (POUNDS)		113	15	51
NUMBER OF TANKS		1	2	1
TOTAL WEIGHT (POUNDS)		113	30	51
TOTAL WEIGHT FOR METEOROID PROTECTION (POUNDS)		194		

Table D-2. Meteoroid Shield Data

MISSION: SINGLE BURN, 205-DAY COAST

STAGE		GELLED H_2/Li		
PROPELLANT TANK		HYDROGEN	FLUORINE	LITHIUM
PROPELLANT LOAD (POUNDS)		1950	2762	
TANK RADIUS (INCHES)		50.0	23.7	
TANK CYLINDER HEIGHT (INCHES)		0.11	0	
DOME THICKNESS (INCHES)		0.060	0.025	
CYLINDER THICKNESS (INCHES)		0.121	N/A	
TANK MATERIAL		Aluminum	Aluminum	
MINIMUM SKIN GAUGE (INCHES)		0.025	0.025	
THERMAL INSULATION THICKNESS (INCHES)		3.12	1.25	
TANK SURFACE AREA (SQUARE FEET)		249.87	54.30	
METEOROID DESIGN MASS (GRAMS)		3.67×10^{-3}	1.17×10^{-3}	
METEOROID DIAMETER (CENTIMETERS)		0.241	0.165	
REQUIRED THICKNESS (INCHES)	SHIELD	0.0285	0.0195	
	BACKUP WALL	0.0383	0.0250	
DESIGN THICKNESS (INCHES)	SHIELD	0.0285	0.0250	
	BACKUP WALL (DELTA)	0.0	0.0	
SPACING (INCHES)	OPTIMUM	1.253	3.421	
	DESIGN	3.120	3.421	
WEIGHT (POUNDS)	SHIELD	109	24	
	BACKUP WALL (DELTA)	0	0	
WEIGHT PER TANK (POUNDS)		109	24	
NUMBER OF TANKS		1	1	
TOTAL WEIGHT (POUNDS)		109	24	
TOTAL WEIGHT FOR METEOROID PROTECTION (POUNDS)		133		

Table D-3. Meteoroid Shield Data

MISSION: SINGLE BURN, 205-DAY COAST

STAGE		BIPROPELLANT		
PROPELLANT TANK		HYDROGEN	FLUORINE	LITHIUM
PROPELLANT LOAD (POUNDS)		383	4600	
TANK RADIUS (INCHES)		36.4	28.1	
TANK CYLINDER HEIGHT (INCHES)		0	0	
DOME THICKNESS (INCHES)		0.048	0.025	
CYLINDER THICKNESS (INCHES)		N/A	N/A	
TANK MATERIAL		Aluminum	Aluminum	
MINIMUM SKIN GAUGE (INCHES)		0.025	0.025	
THERMAL INSULATION THICKNESS (INCHES)		3.68	1.04	
TANK SURFACE AREA (SQUARE FEET)		140.35	74.02	
METEOROID DESIGN MASS (GRAMS)		2.38×10^{-3}	1.48×10^{-3}	
METEOROID DIAMETER (CENTIMETERS)		0.209	0.178	
REQUIRED THICKNESS (INCHES)	SHIELD	0.0247	0.0207	
	BACKUP WALL	0.0305	0.0250	
DESIGN THICKNESS (INCHES)	SHIELD	0.0250	0.0250	
	BACKUP WALL (DELTA)	0.0	0.0	
SPACING (INCHES)	OPTIMUM	1.472	3.990	
	DESIGN	3.680	3.990	
WEIGHT (POUNDS)	SHIELD	54	34	
	BACKUP WALL (DELTA)	0	0	
WEIGHT PER TANK (POUNDS)		54	34	
NUMBER OF TANKS		1	1	
TOTAL WEIGHT (POUNDS)		54	34	
TOTAL WEIGHT FOR METEOROID PROTECTION (POUNDS)		88		

Table D-4. Sensitivity to Meteoroid Shield Backup Sheet Selection

MISSION: SINGLE BURN, 205-DAY COAST

TANKAGE		NUMBER OF TANKS	METEOROID SHIELD WEIGHT (POUNDS)		
			TYPE OF BACKUP SHEET		DELTA
			SEPARATE WALL	TANK WALL	
BIPROPELLANT	H_2 TANK	1	100	54	46
	F_2 TANK	1	59	34	25
	TOTAL	2	159	88	71
GELLED H_2/Li	H_2/Li TANK	1	207	109	98
	F_2 TANK	1	42	24	18
	TOTAL	2	249	133	116
TRIPROPELLANT	H_2 TANK	1	217	113	104
	F_2 TANK	2	50	30	20
	Li TANK	1	72	51	21
	TOTAL	4	339	194	145

Table D-5. Sensitivity to Meteoroid Environment and Shield Design Criteria

MISSION: SINGLE BURN, 205 DAY COAST
STAGE: TRIPROPELLANT

DESIGN CRITERIA		METEOROID SHIELD WEIGHT (POUNDS)		
CRITERIA	VALUE	H_2 TANK	F_2 TANK	Li TANK
PROBABILITY OF NO PUNCTURE	0.990	99	28	43
	0.995*	113	30	51
	0.999	174	40	84
RATIO OF SHIELD - BACKUP SHEET SPACING TO METEOROID DIAMETER	0.20	99	30	38
	0.30*	113	30	51
	0.40	151	30	68
METEOROID FLUX MODEL**	0.1X	99	26	38
	1X*	113	30	51
	10X	300	66	135
METEOROID VELOCITY (KM/SEC)	10	113	26	51
	20*	113	30	51
	30	117	38	58
METEOROID DENSITY (G/CC)	0.25	143	30	65
	0.50*	113	30	51
	1.00	99	30	41

* STUDY BASELINE
** INCREASE IN METEOROID MASS

Table D-6. Sensitivity to Meteoroid Environment and Shield Design Criteria

MISSION: SINGLE BURN, 205-DAY COAST
STAGE: GELLED H_2/Li

DESIGN CRITERIA		METEOROID SHIELD WEIGHT (POUNDS)		
CRITERIA	VALUE	H_2 TANK	F_2 TANK	Li TANK
PROBABILITY OF NO PUNCTURE	0.990	95	23	
	0.995*	109	24	
	0.999	162	36	
RATIO OF SHIELD - BACKUP SHEET SPACING TO METEOROID DIAMETER	0.20	95	24	
	0.30*	109	24	
	0.40	145	25	
METEOROID FLUX MODEL**	0.1X	95	21	
	1X*	109	24	
	10X	258	61	
METEOROID VELOCITY (KM/SEC)	10	109	21	
	20*	109	24	
	30	109	32	
METEOROID DENSITY (G/CC)	0.25	137	24	
	0.50*	109	24	
	1.00	95	24	

* STUDY BASELINE
** INCREASE IN METEOROID MASS

Table D-7. Sensitivity to Meteoroid Environment and Shield Design Criteria

MISSION: SINGLE BURN, 205-DAY COAST
STAGE: BIPROPELLANT

DESIGN CRITERIA		METEOROID SHIELD WEIGHT (POUNDS)		
CRITERIA	VALUE	H_2 TANK	F_2 TANK	Li TANK
PROBABILITY OF NO PUNCTURE	0.990	54	32	
	0.995*	54	34	
	0.999	79	54	
RATIO OF SHIELD - BACKUP SHEET SPACING TO METEOROID DIAMETER	0.20	54	34	
	0.30*	54	34	
	0.40	70	38	
METEOROID FLUX MODEL**	0.1X	54	28	
	1X*	54	34	
	10X	133	90	
METEOROID VELOCITY (KM/SEC)	10	54	28	
	20*	54	34	
	30	54	45	
METEOROID DENSITY (G/CC)	0.25	67	36	
	0.50*	54	34	
	1.00	54	34	

* STUDY BASELINE

** INCREASE IN METEOROID MASS

Table D-8. Meteoroid Shield Data

MISSION: TWO BURN, 205-DAY COAST

STAGE		TRIPROPELLANT		
PROPELLANT TANK		HYDROGEN	FLUORINE	LITHIUM
PROPELLANT LOAD (POUNDS)		7677	16255	5932
TANK RADIUS (INCHES)		90.8	33.4	34.6
TANK CYLINDER HEIGHT (INCHES)		0	0	0
DOME THICKNESS (INCHES)		0.060	0.025	0.015
CYLINDER THICKNESS (INCHES)		N/A	N/A	N/A
TANK MATERIAL		Aluminum	Aluminum	Mar. Steel
MINIMUM SKIN GAUGE (INCHES)		0.025	0.025	0.015
THERMAL INSULATION THICKNESS (INCHES)		3.62	1.17	3.00
TANK SURFACE AREA (SQUARE FEET)		779.89	104.44	123.67
METEOROID DESIGN MASS (GRAMS)		8.57×10^{-3}	1.91×10^{-3}	2.17×10^{-3}
METEOROID DIAMETER (CENTIMETERS)		0.319	0.194	0.202
REQUIRED THICKNESS (INCHES)	SHIELD	0.0378	0.0229	0.0239
	BACKUP WALL	0.0471	0.0250	0.0150
DESIGN THICKNESS (INCHES)	SHIELD	0.0378	0.0250	0.0239
	BACKUP WALL (DELTA)	0.0	0.0	0.0
SPACING (INCHES)	OPTIMUM	2.242	4.744	2.988
	DESIGN	3.620	4.744	3.000
WEIGHT (POUNDS)	SHIELD	450	48	123
	BACKUP WALL (DELTA)	0	0	0
WEIGHT PER TANK (POUNDS)		450	48	123
NUMBER OF TANKS		1	2	2
TOTAL WEIGHT (POUNDS)		450	96	246
TOTAL WEIGHT FOR METEOROID PROTECTION (POUNDS)		792		

Table D-9. Meteoroid Shield Data

MISSION: TWO BURN, 205-DAY COAST

STAGE		GELLED H_2/Li		
PROPELLANT TANK		HYDROGEN	FLUORINE	LITHIUM
PROPELLANT LOAD (POUNDS)		12862	17700	
TANK RADIUS (INCHES)		88.42	43.29	
TANK CYLINDER HEIGHT (INCHES)		0	0	
DOME THICKNESS (INCHES)		0.058	0.025	
CYLINDER THICKNESS (INCHES)		N/A	N/A	
TANK MATERIAL		Aluminum	Aluminum	
MINIMUM SKIN GAUGE (INCHES)		0.025	0.025	
THERMAL INSULATION THICKNESS (INCHES)		3.54	0.90	
TANK SURFACE AREA (SQUARE FEET)		738.92	170.64	
METEOROID DESIGN MASS (GRAMS)		8.23×10^{-3}	2.76×10^{-3}	
METEOROID DIAMETER (CENTIMETERS)		0.316	0.219	
REQUIRED THICKNESS (INCHES)	SHIELD	0.0373	0.0259	
	BACKUP WALL	0.0470	0.0252	
DESIGN THICKNESS (INCHES)	SHIELD	0.0373	0.0259	
	BACKUP WALL (DELTA)	0.0	0.0002	
SPACING (INCHES)	OPTIMUM	2.312	6.051	
	DESIGN	3.540	6.000	
WEIGHT (POUNDS)	SHIELD	420	83	
	BACKUP WALL (DELTA)	0	1	
WEIGHT PER TANK (POUNDS)		420	84	
NUMBER OF TANKS		1	1	
TOTAL WEIGHT (POUNDS)		420	84	
TOTAL WEIGHT FOR METEOROID PROTECTION (POUNDS)		504		

Table D-10. Meteoroid Shield Data

MISSION: TWO BURN, 205-DAY COAST

STAGE		BIPROPELLANT		
PROPELLANT TANK		HYDROGEN	FLUORINE	LITHIUM
PROPELLANT LOAD (POUNDS)		2652	29201	
TANK RADIUS (INCHES)		63.8	51.2	
TANK CYLINDER HEIGHT (INCHES)		0	0	
DOME THICKNESS (INCHES)		0.042	0.026	
CYLINDER THICKNESS (INCHES)		N/A	N/A	
TANK MATERIAL		Aluminum	Aluminum	
MINIMUM SKIN GAUGE (INCHES)		0.025	0.025	
THERMAL INSULATION THICKNESS (INCHES)		3.40	1.28	
TANK SURFACE AREA (SQUARE FEET)		393.99	240.22	
METEOROID DESIGN MASS (GRAMS)		5.15×10^{-3}	3.56×10^{-3}	
METEOROID DIAMETER (CENTIMETERS)		0.270	0.239	
REQUIRED THICKNESS (INCHES)	SHIELD	0.0319	0.0282	
	BACKUP WALL	0.0412	0.0274	
DESIGN THICKNESS (INCHES)	SHIELD	0.0319	0.0282	
	BACKUP WALL (DELTA)	0.0	0.0024	
SPACING (INCHES)	OPTIMUM	3.242	6.560	
	DESIGN	3.400	6.000	
WEIGHT (POUNDS)	SHIELD	192	123	
	BACKUP WALL (DELTA)	0	4	
WEIGHT PER TANK (POUNDS)		192	127	
NUMBER OF TANKS		1	1	
TOTAL WEIGHT (POUNDS)		192	127	
TOTAL WEIGHT FOR METEOROID PROTECTION (POUNDS)		319		

Table D-11. Sensitivity to Meteoroid Shield Backup Sheet Selection

MISSION: TWO BURN, 205-DAY COAST

TANKAGE		NUMBER OF TANKS	METEOROID SHIELD WEIGHT (POUNDS)		
			TYPE OF BACKUP SHEET		DELTA
			SEPARATE WALL	TANK WALL	
BIPROPELLANT	H_2 TANK	1	365	192	173
	F_2 TANK	1	215	127	88
	TOTAL	2	580	319	261
GELLED H_2/Li	H_2/Li TANK	1	804	420	384
	F_2 TANK	1	145	84	61
	TOTAL	2	949	504	445
TRIPROPELLANT	H_2 TANK	1	859	450	409
	F_2 TANK	2	168	96	72
	Li TANK	2	357	246	111
	TOTAL	5	1384	792	592

Table D-12. Sensitivity to Meteoroid Environment and Shield Design Criteria

MISSION: TWO BURN, 205-DAY COAST
STAGE: TRIPROPELLANT

DESIGN CRITERIA		METEOROID SHIELD WEIGHT (POUNDS)		
CRITERIA	VALUE	H_2 TANK	F_2 TANK	Li TANK
PROBABILITY OF NO PUNCTURE	0.990	378	90	207
	0.995*	450	96	246
	0.999	691	166	426
RATIO OF SHIELD - BACKUP SHEET SPACING TO METEOROID DIAMETER	0.20	300	96	164
	0.30*	450	96	246
	0.40	600	118	328
METEOROID FLUX MODEL**	0.1X	297	80	155
	1X*	450	96	246
	10X	1235	273	673
METEOROID VELOCITY (KM/SEC)	10	450	80	246
	20*	450	96	246
	30	463	128	295
METEOROID DENSITY (G/CC)	0.25	567	112	310
	0.50*	450	96	246
	1.00	357	96	196

* STUDY BASELINE
** INCREASE IN METEOROID MASS

Table D-13. Sensitivity to Meteoroid Environment and Shield Design Criteria

MISSION: TWO BURN, 205-DAY COAST
STAGE: GELLED H_2/Li

DESIGN CRITERIA		METEOROID SHIELD WEIGHT (POUNDS)		
CRITERIA	VALUE	H_2 TANK	F_2 TANK	Li TANK
PROBABILITY OF NO PUNCTURE	0.990	354	75	
	0.995*	420	84	
	0.999	650	157	
RATIO OF SHIELD - BACKUP SHEET SPACING TO METEOROID DIAMETER	0.20	282	81	
	0.30*	420	84	
	0.40	561	112	
METEOROID FLUX MODEL**	0.1X	282	66	
	1X*	420	84	
	10X	1165	254	
METEOROID VELOCITY (KM/SEC)	10	420	69	
	20*	420	84	
	30	435	116	
METEOROID DENSITY (G/CC)	0.25	334	81	
	0.50*	420	84	
	1.00	530	106	

* STUDY BASELINE
** INCREASE IN METEOROID MASS

Table D-14. Sensitivity to Meteoroid Environment and Shield Design Criteria

MISSION: TWO BURN, 205-DAY COAST
STAGE: BIPROPELLANT

DESIGN CRITERIA		METEOROID SHIELD WEIGHT (POUNDS)		
CRITERIA	VALUE	H_2 TANK	F_2 TANK	Li TANK
PROBABILITY OF NO PUNCTURE	0.990	161	102	
	0.995*	192	127	
	0.999	332	235	
RATIO OF SHIELD - BACKUP SHEET SPACING TO METEOROID DIAMETER	0.20	150	113	
	0.30*	192	127	
	0.40	256	168	
METEOROID FLUX MODEL**	0.1X	150	92	
	1X*	192	127	
	10X	581	380	
METEOROID VELOCITY (KM/SEC)	10	192	105	
	20*	192	127	
	30	231	175	
METEOROID DENSITY (G/CC)	0.25	241	159	
	0.50*	192	127	
	1.00	152	113	

* STUDY BASELINE
** INCREASE IN METEOROID MASS

Appendix E

BOOSTER VELOCITY INCREMENT VERSUS PAYLOAD

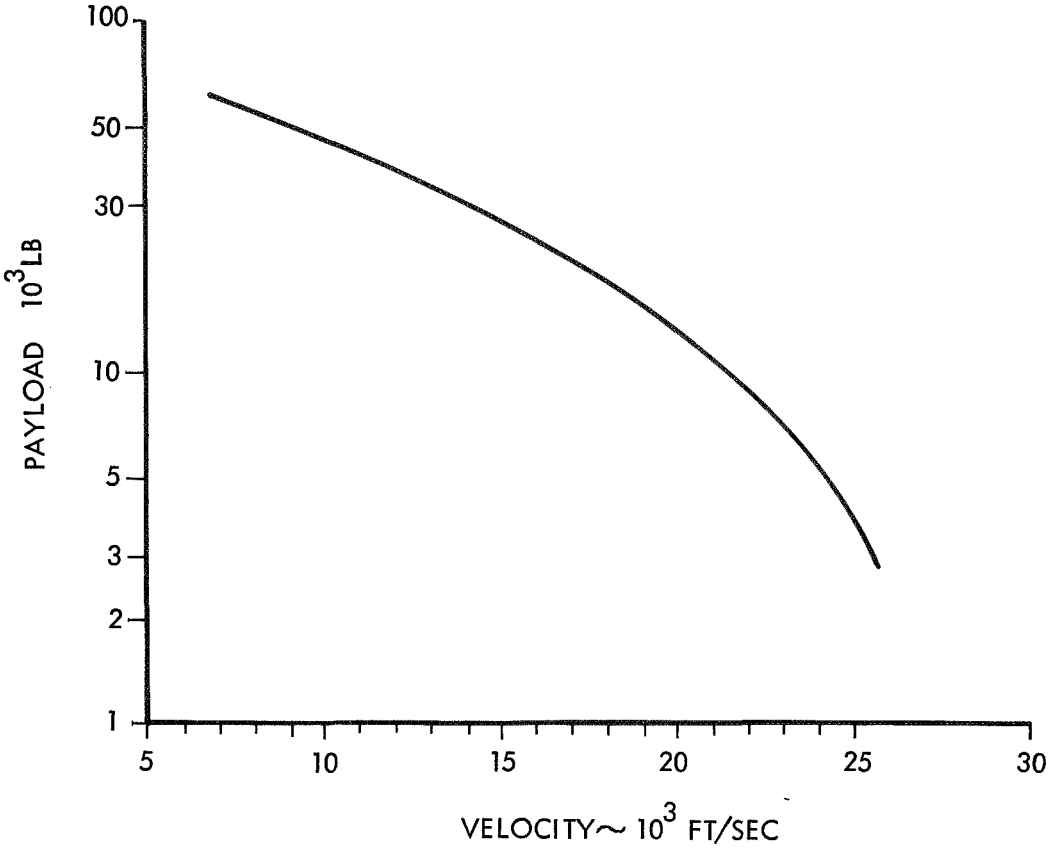

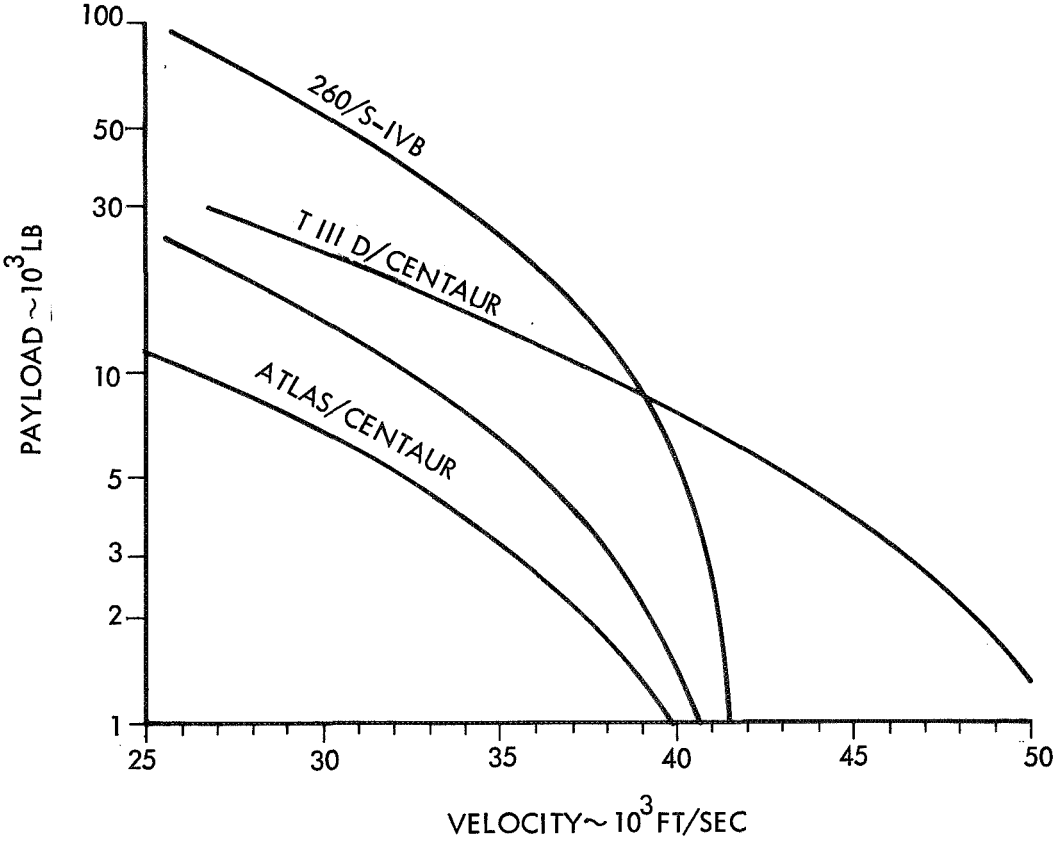

Booster Velocity vs. Payload

Appendix F

DESIGN CHARTS

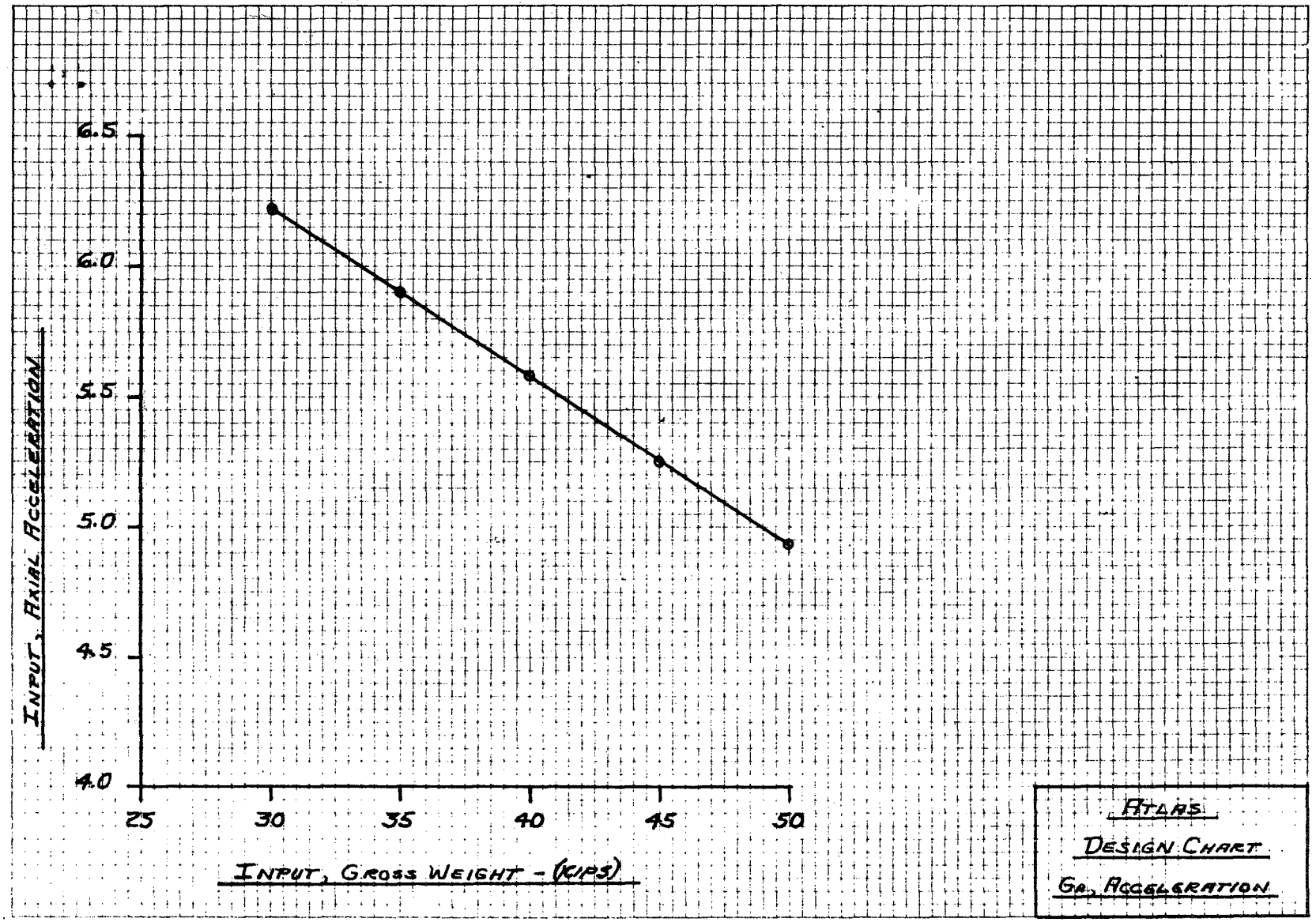
INPUT, AXIAL ACCELERATION
6.5
6.0
5.5
5.0
4.5
4.0
25
30
35
40
45
50
INPUT, GROSS WEIGHT - (KIPS)
ATLAS
DESIGN CHART
GA, ACCELERATION

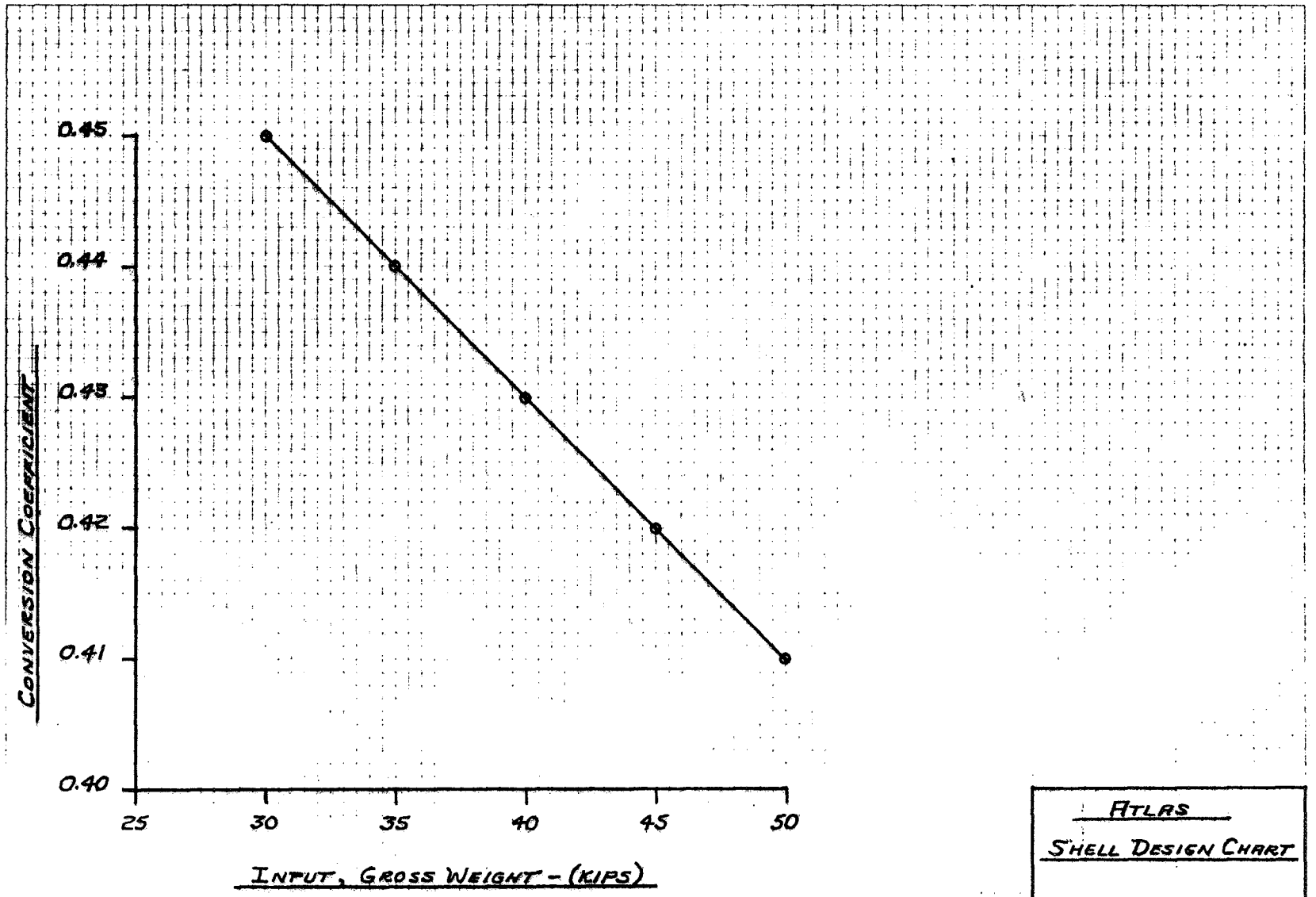

ATLAS

SHELL DESIGN CHART

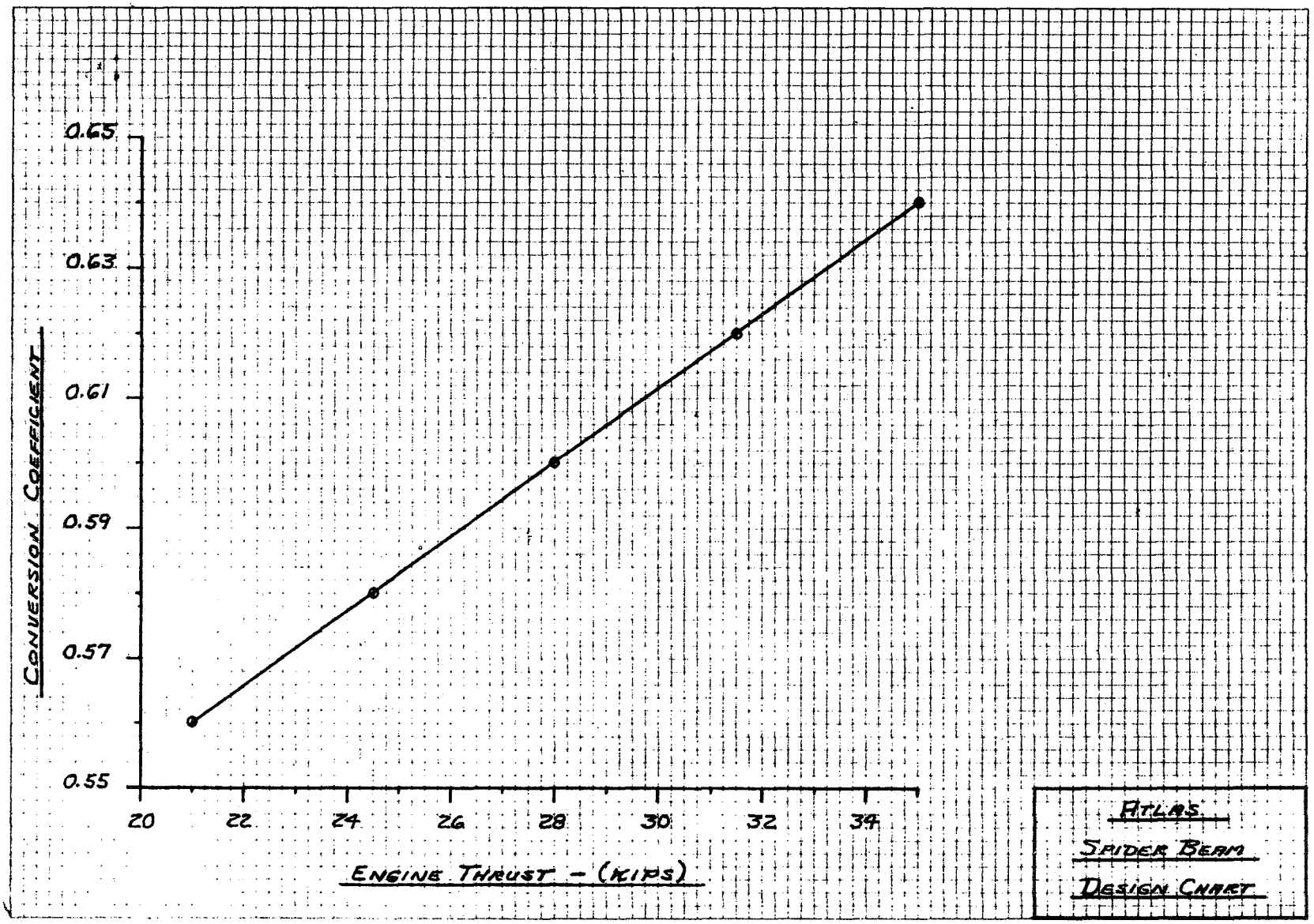
CONVERSION COEFFICIENT
0.65
0.63
0.61
0.59
0.57
0.55
20
22
24
26
28
30
32
34
ENGINE THRUST - (KIPS)
ATLAS
SPIDER BEAM
DESIGN CHART

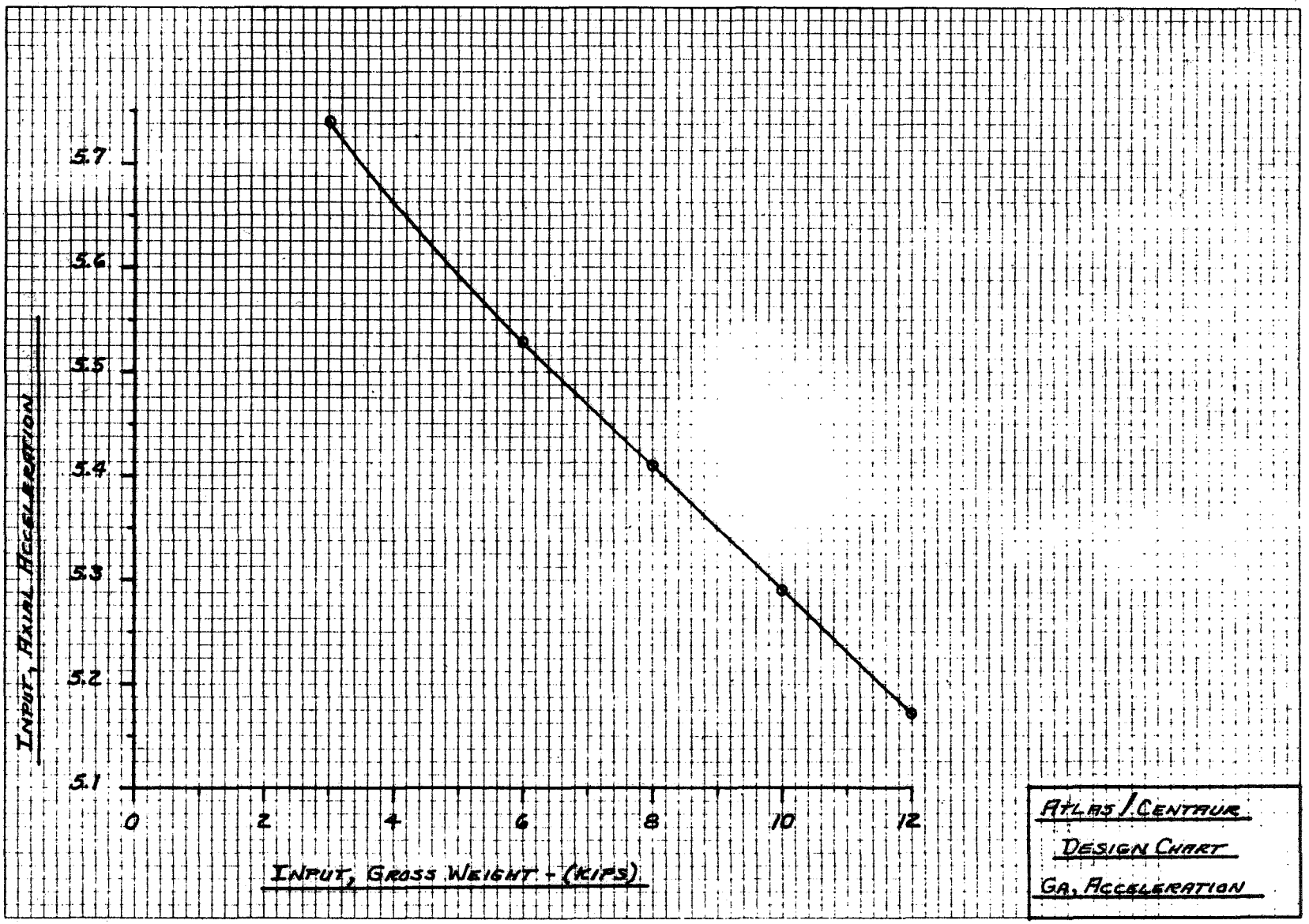
INPUT, AXIAL ACCELERATION
5.7
5.6
5.5
5.4
5.3
5.2
5.1
0
2
4
6
8
10
12
INPUT, GROSS WEIGHT ÷ (KIPS)
ATLAS / CENTAUR
DESIGN CHART
GA, ACCELERATION

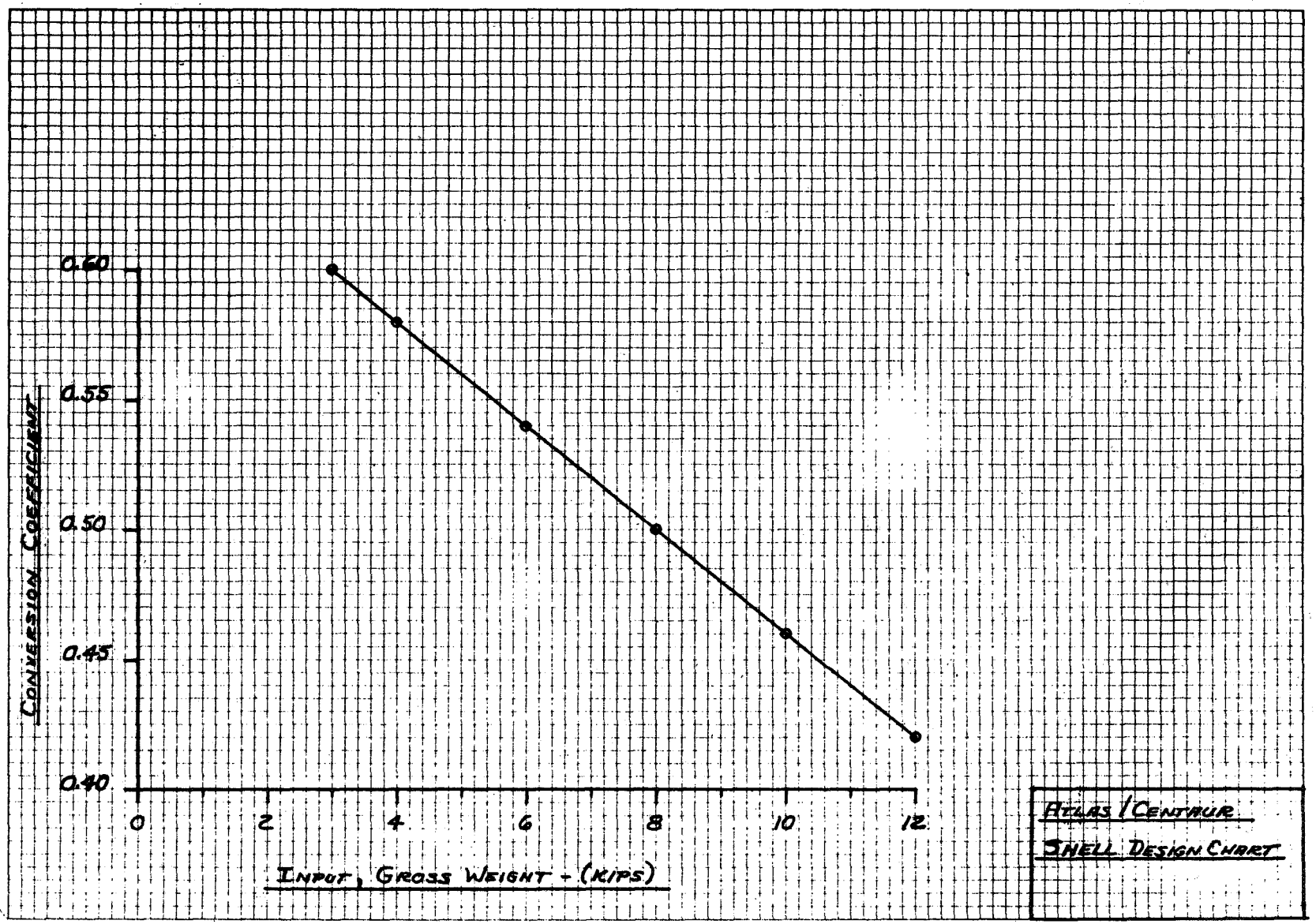
0.60
0.55
0.50
0.45
0.40
CONVERSION COEFFICIENT
0
2
4
6
8
10
12
INPUT, GROSS WEIGHT - (KIPS)
ATLAS / CENTAUR
SHELL DESIGN CHART

ATLAS/CENTAUR
SPIDER BEAM
DESIGN CHART
ENGINE THRUST - (KLBS)
CONVERSION COEFFICIENT
0.60
0.55
0.50
0.45
0.40
0
1
2
3
4
5
6
7
8
9

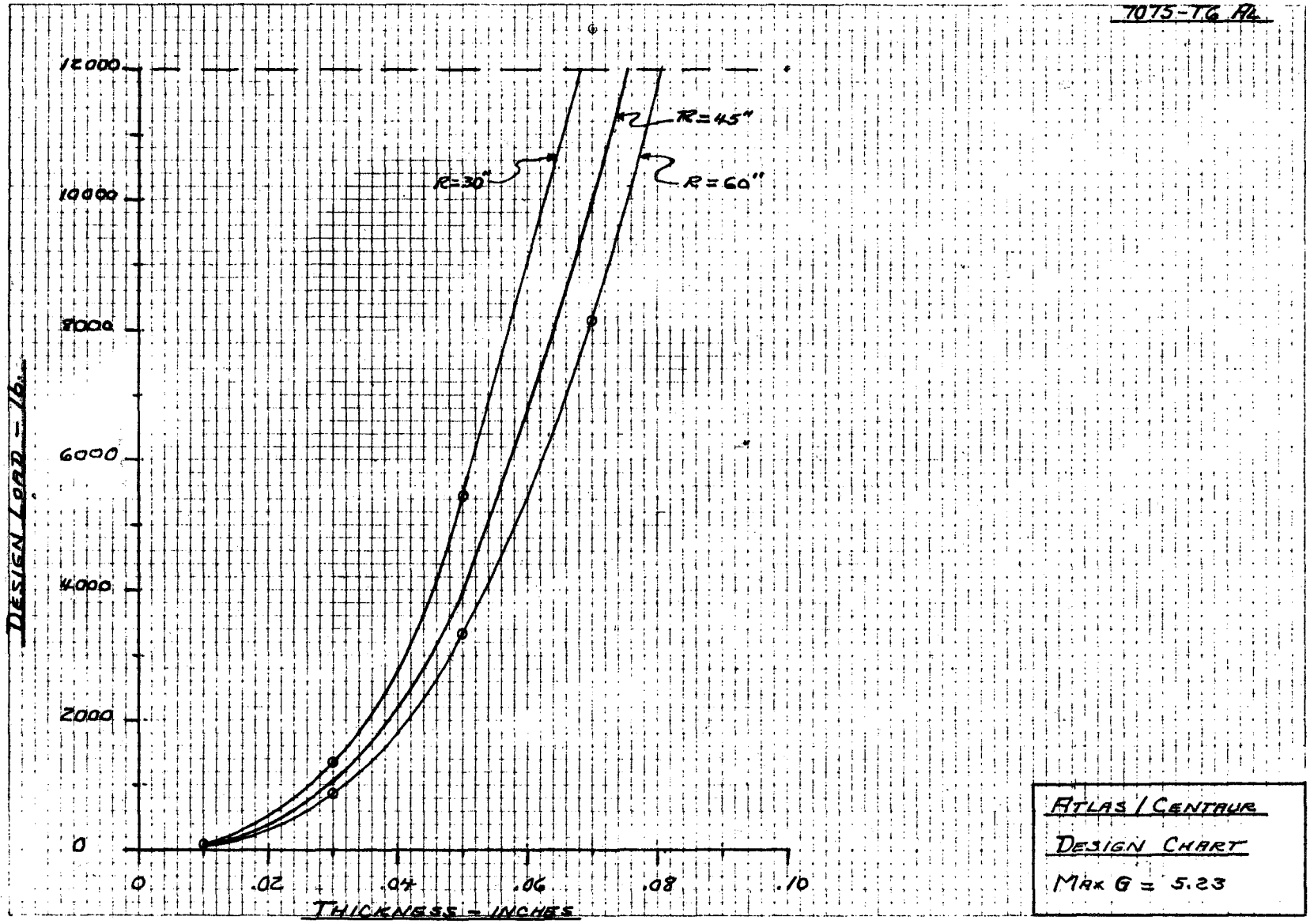
7075-T6 Al.
12000
10000
8000
6000
4000
2000
0
DESIGN LOAD = lb.
R=30"
R=45"
R=60"
0
.02
.04
.06
.08
.10
THICKNESS - INCHES
ATLAS / CENTAUR
DESIGN CHART
MAX G = 5.23

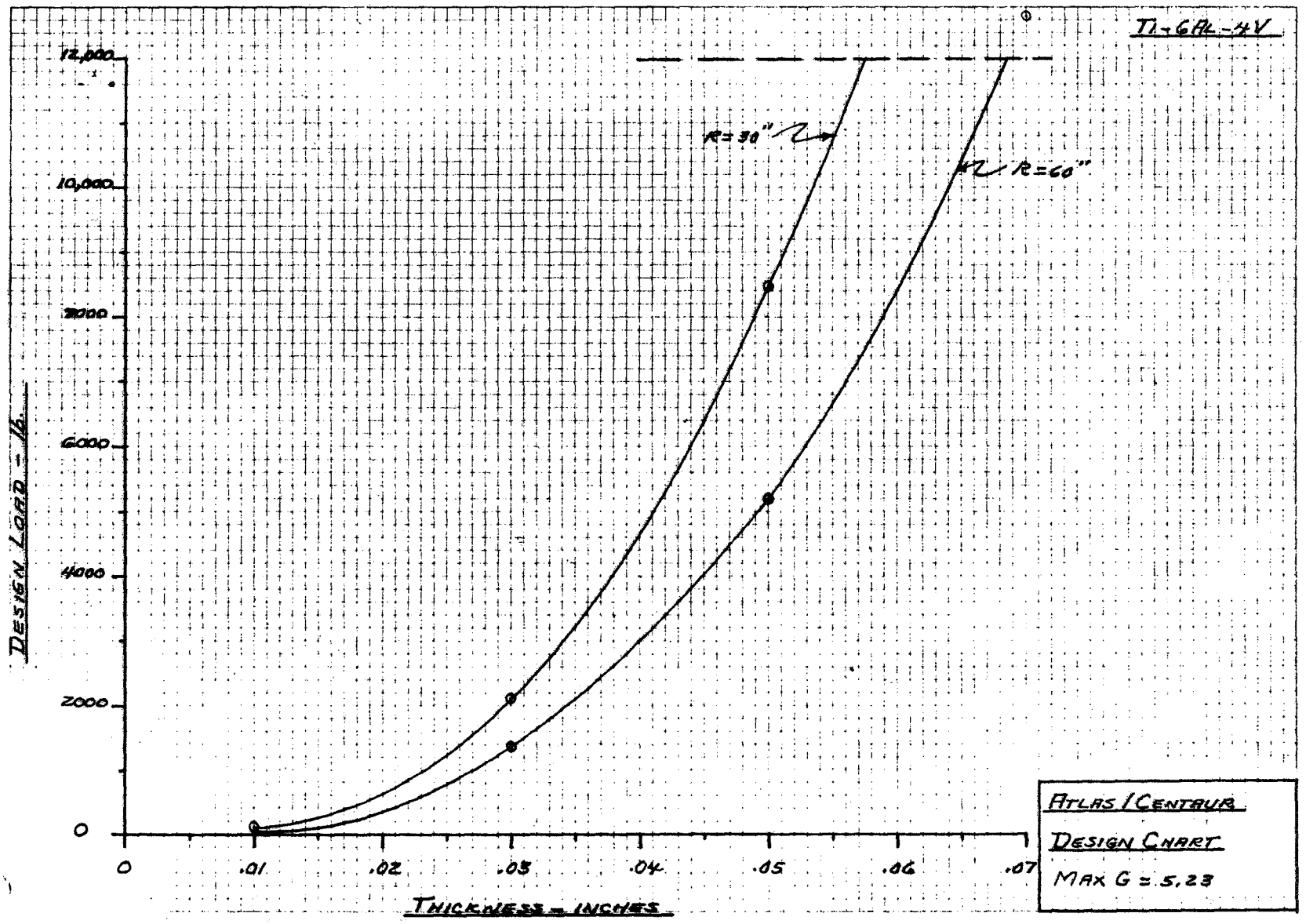
Ti-6Al-4V
R=30"
R=60"
DESIGN LOAD - lb.
12,000
10,000
8000
6000
4000
2000
0
0
.01
.02
.03
.04
.05
.06
.07
THICKNESS - INCHES
ATLAS/CENTAUR
DESIGN CHART
MAX G = 5.23

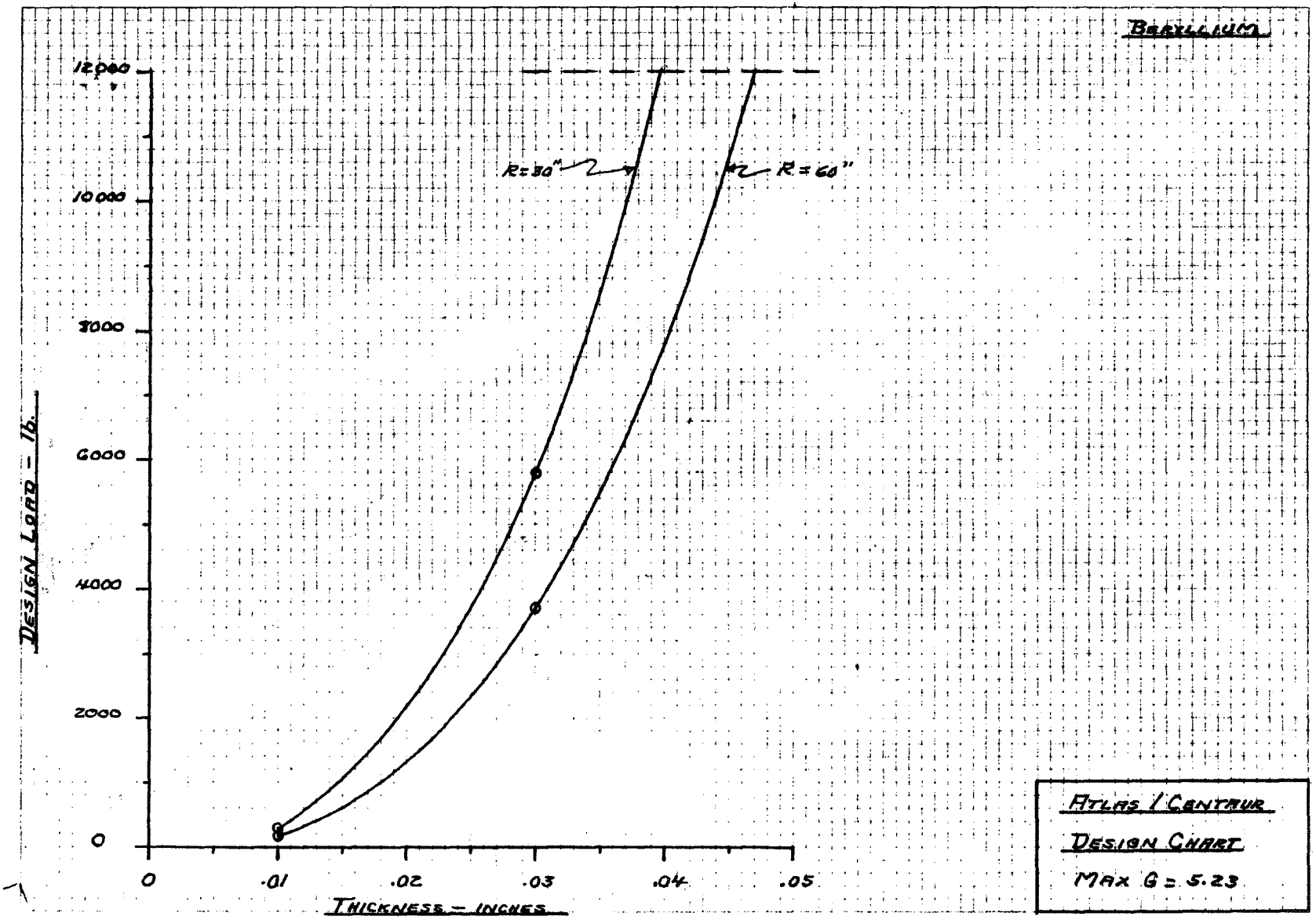
BERYLLIUM
DESIGN LOAD = lb.
12000
10000
8000
6000
4000
2000
0
R=30"
R=60"
0
.01
.02
.03
.04
.05
THICKNESS = INCHES
ATLAS / CENTAUR
DESIGN CHART
MAX G = 5.23

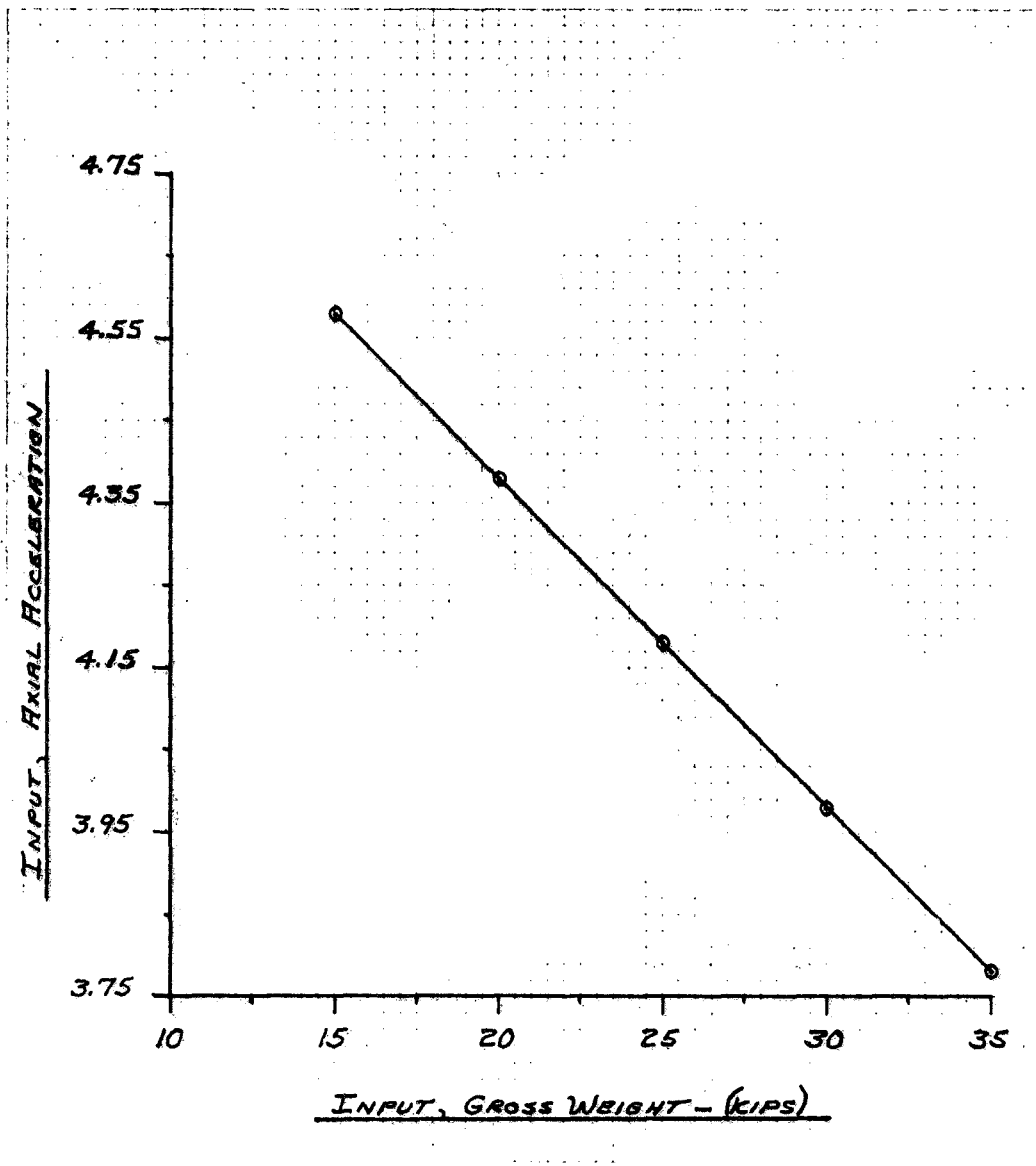

TITAN IIID
DESIGN CHART
GA, ACCELERATION

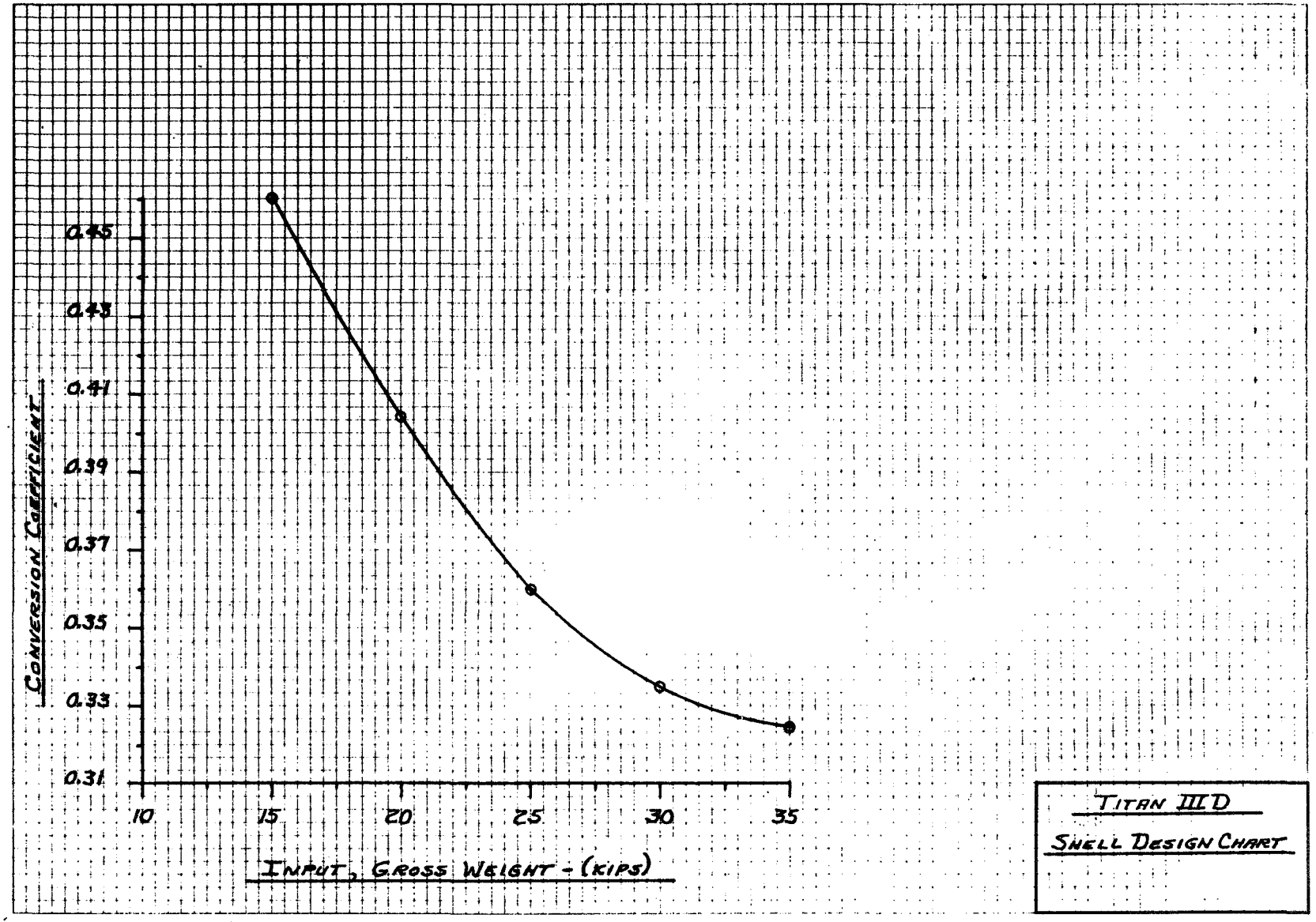
CONVERSION COEFFICIENT
0.45
0.43
0.41
0.39
0.37
0.35
0.33
0.31
10
15
20
25
30
35
INPUT, GROSS WEIGHT - (KIPS)
TITAN IIID
SHELL DESIGN CHART

TITAN IIID
SPIDER BEAM
DESIGN CHART
CONVERSION COEFFICIENT
0.63
0.61
0.59
0.57
0.55
0.53
0.51
0.49
10
15
20
25
ENGINE THRUST - (KLBS)

TIIID / CENTAUR
DESIGN CHART
GA, ACCELERATION
INPUT, GROSS WEIGHT - (KIPS)
7
8
9
10
11
12
13
14
15
INPUT, AXIAL ACCELERATION
3.40
3.45
3.50
3.55
3.60
3.65
3.70

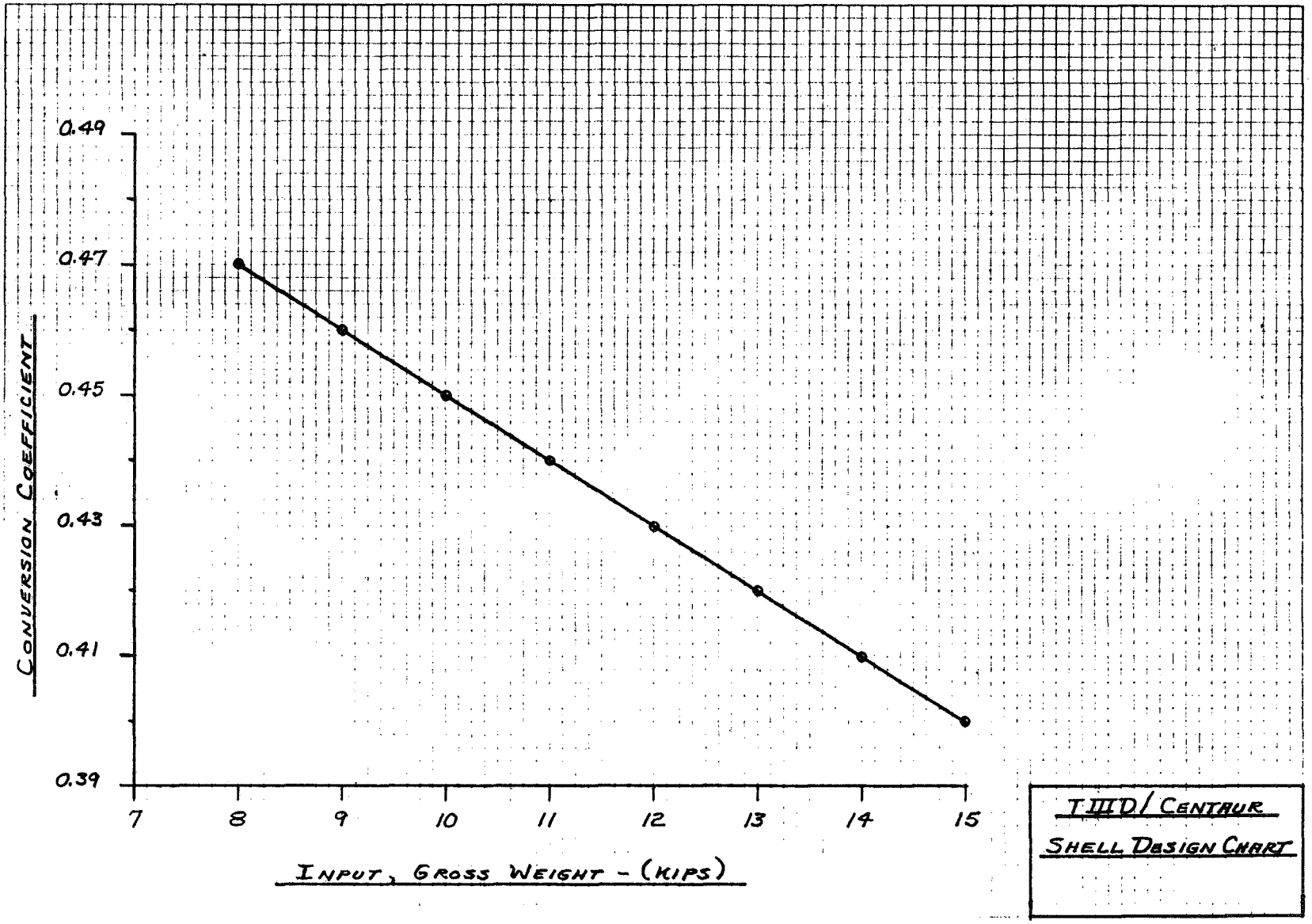
CONVERSION COEFFICIENT
0.49
0.47
0.45
0.43
0.41
0.39
7
8
9
10
11
12
13
14
15
INPUT, GROSS WEIGHT - (KIPS)
TIIID/CENTAUR
SHELL DESIGN CHART

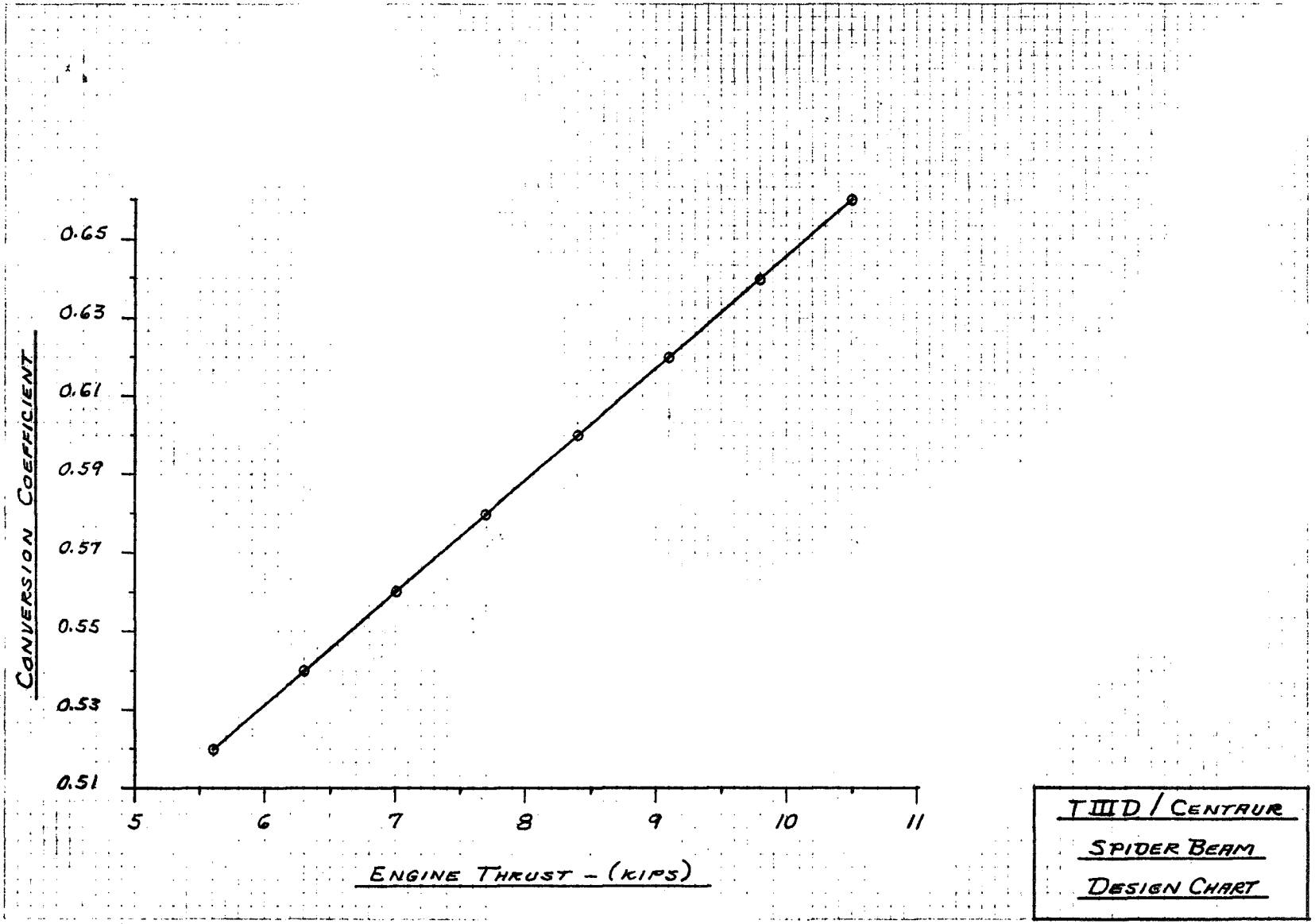
CONVERSION COEFFICIENT
0.65
0.63
0.61
0.59
0.57
0.55
0.53
0.51
5
6
7
8
9
10
11
ENGINE THRUST - (KIPS)
TIID / CENTAUR
SPIDER BEAM
DESIGN CHART

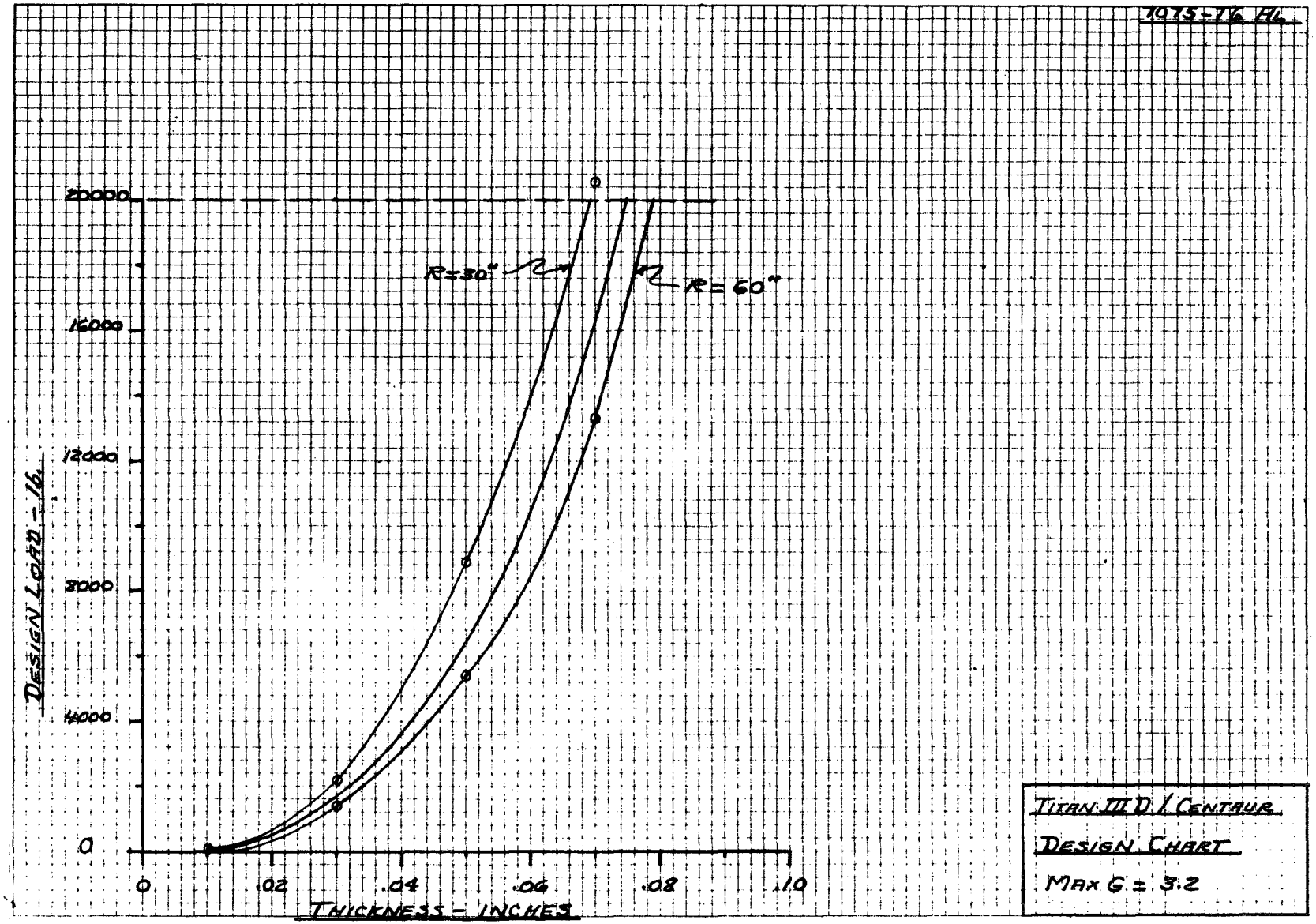
7075-T6 AL.
20000
16000
12000
8000
4000
0
DESIGN LOAD - lb.
R=30"
R=60"
0
.02
.04
.06
.08
.10
THICKNESS - INCHES
TITAN III D / CENTAUR
DESIGN CHART
MAX G = 3.2

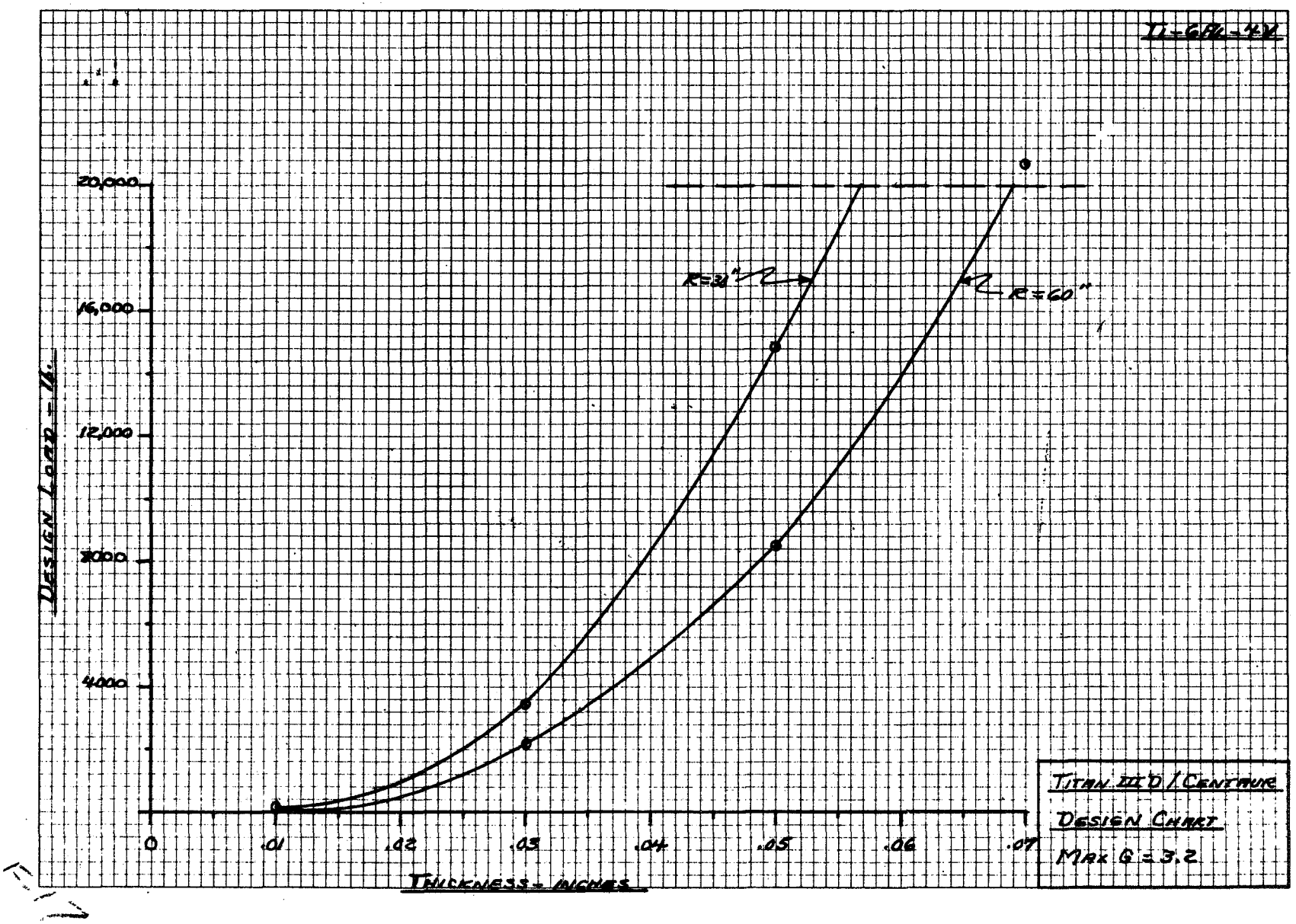
Ti-6Al-4V
20,000
16,000
12,000
8000
4000
0
.01
.02
.03
.04
.05
.06
.07
R=30"
R=60"
DESIGN LOAD - LBS.
THICKNESS - INCHES
TITAN III D / CENTAUR
DESIGN CHART
MAX G = 3.2

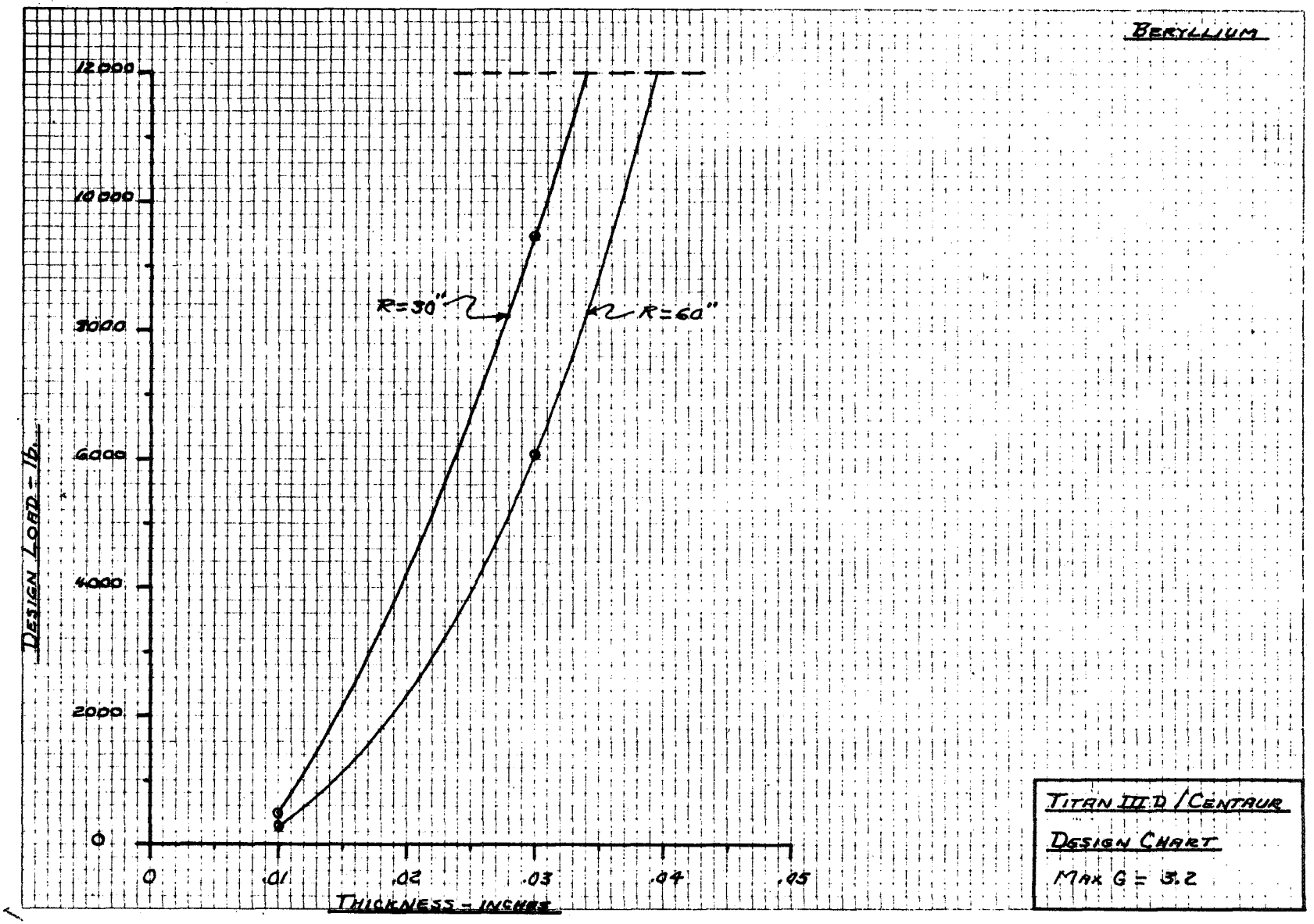
BERYLLIUM
DESIGN LOAD - lb.
12000
10000
8000
6000
4000
2000
0
R=30"
R=60"
0
.01
.02
.03
.04
.05
THICKNESS - INCHES
TITAN III D / CENTAUR
DESIGN CHART
MAX G = 3.2

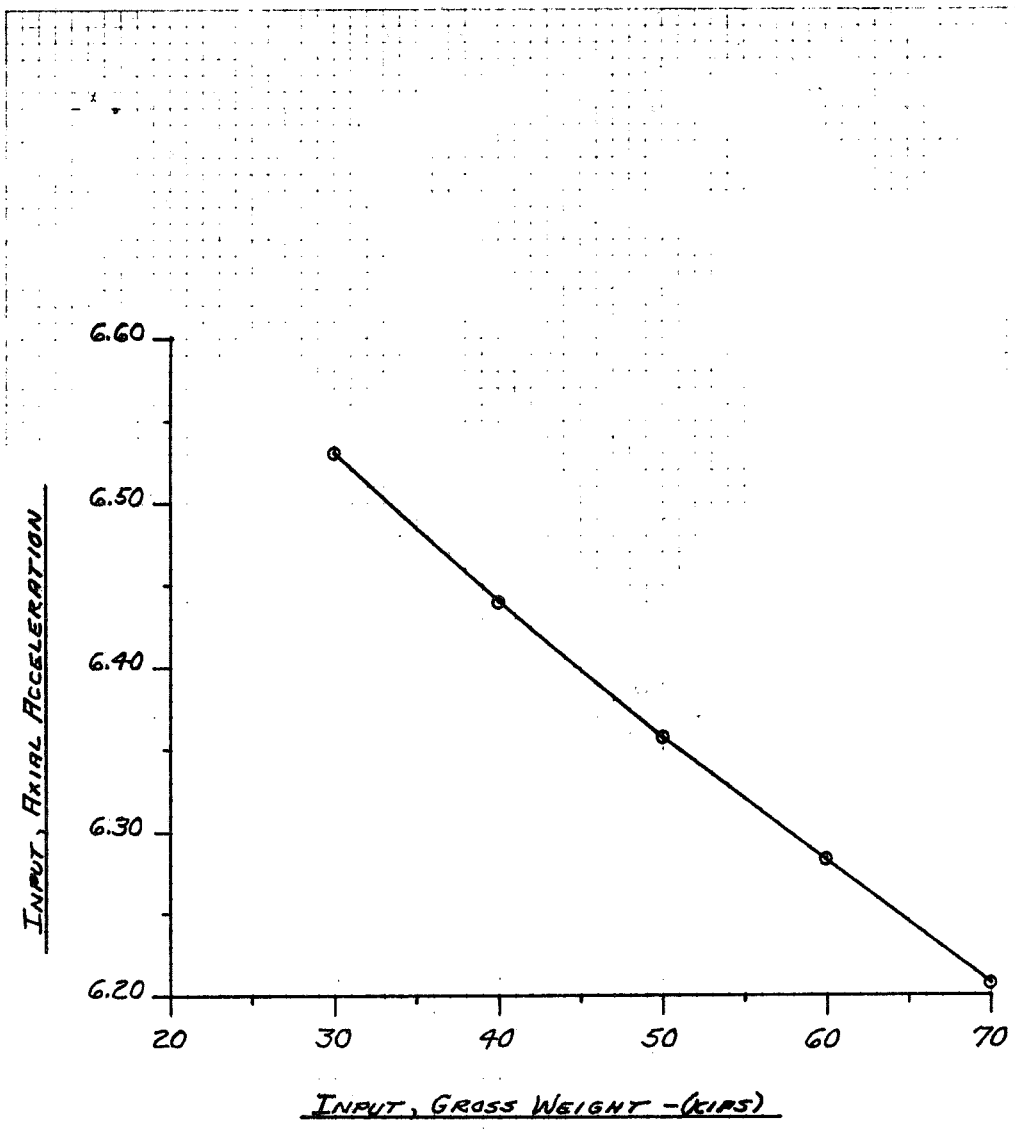

260/SIVB
DESIGN CHART
GA, ACCELERATION

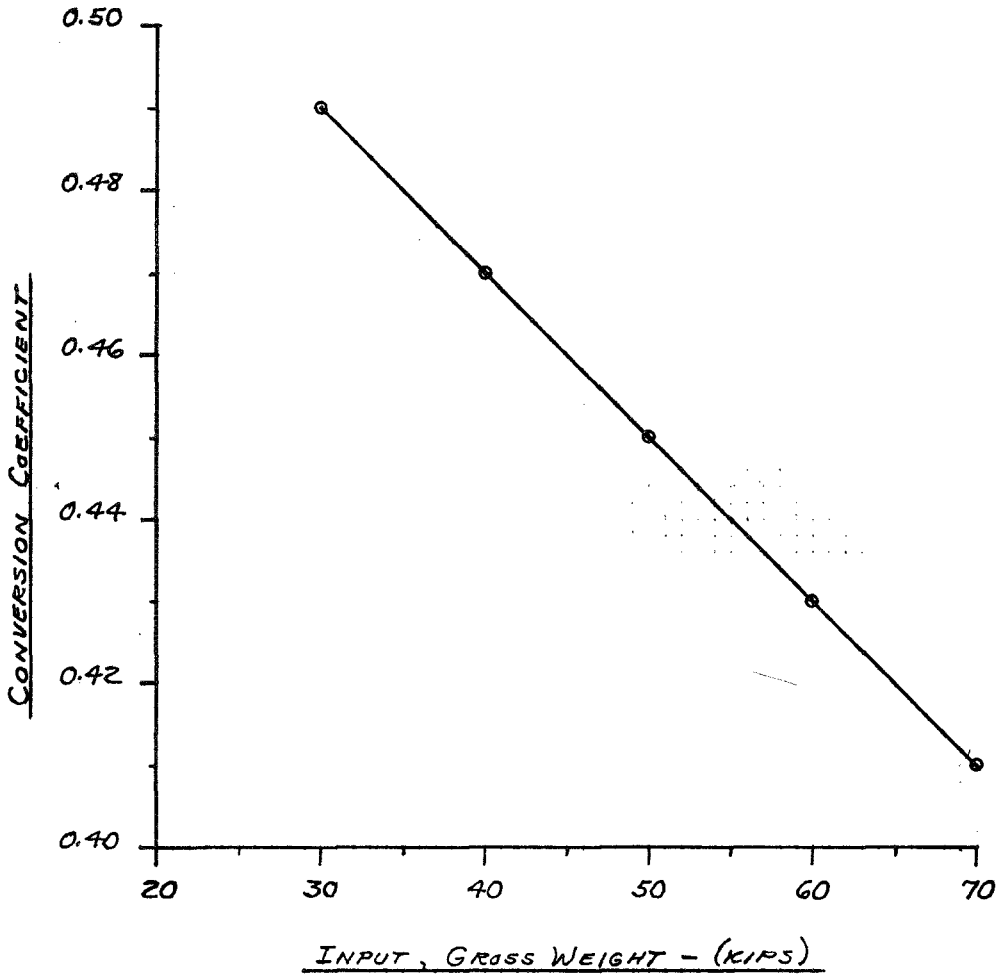

260/SIVB
SHELL DESIGN CHART

260/SIVB
SPIDER BEAM
DESIGN CHART
CONVERSION COEFFICIENT
0.56
0.54
0.52
0.50
0.48
0.46
20
25
30
35
40
45
50
ENGINE THRUST - (KIPS)

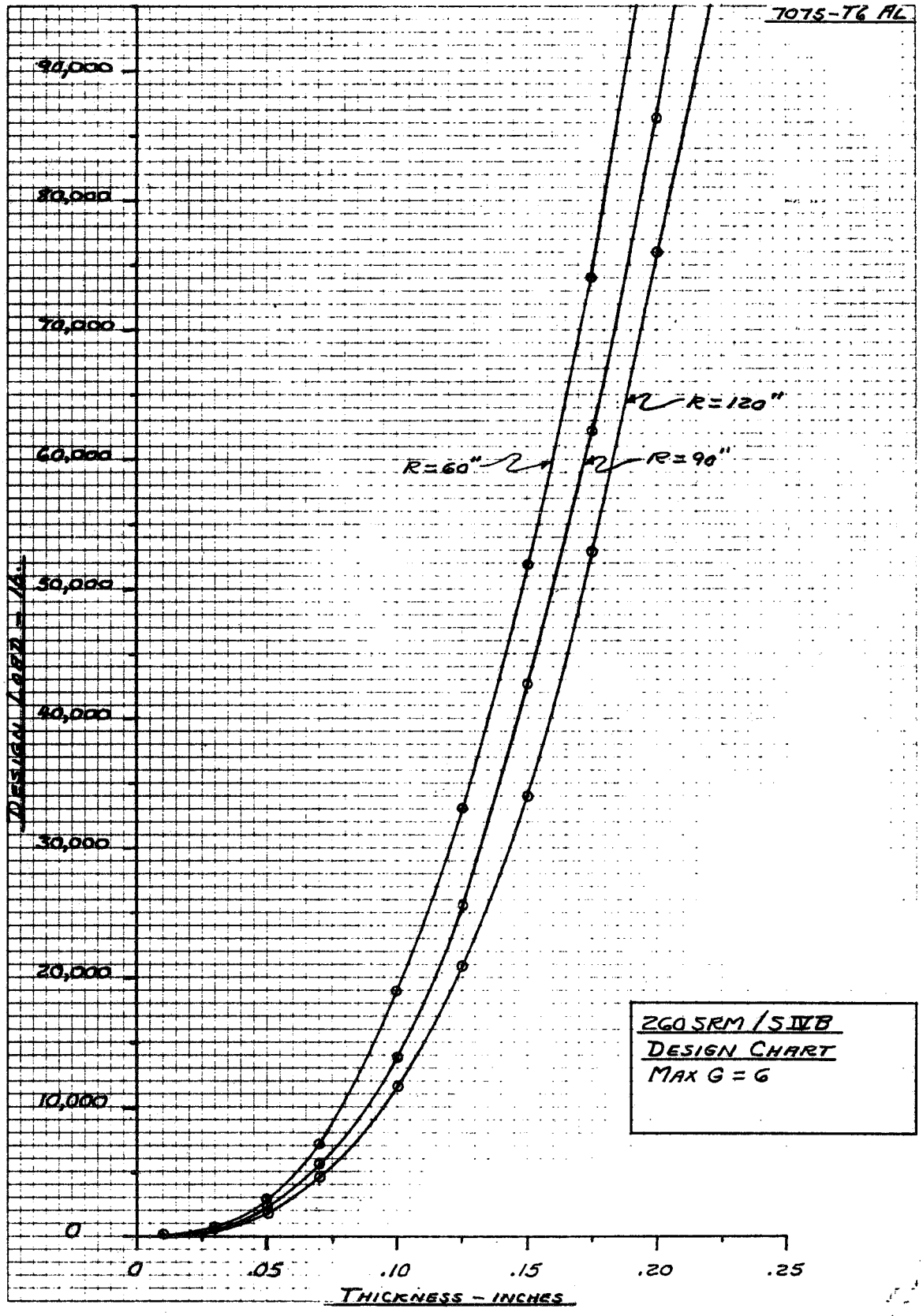
7075-T6 AL
90,000
80,000
70,000
60,000
50,000
40,000
30,000
20,000
10,000
0
DESIGN LOAD = kL
R=120"
R=90"
R=60"
0
.05
.10
.15
.20
.25
THICKNESS - INCHES
260 SRM / S IVB
DESIGN CHART
MAX G = 6

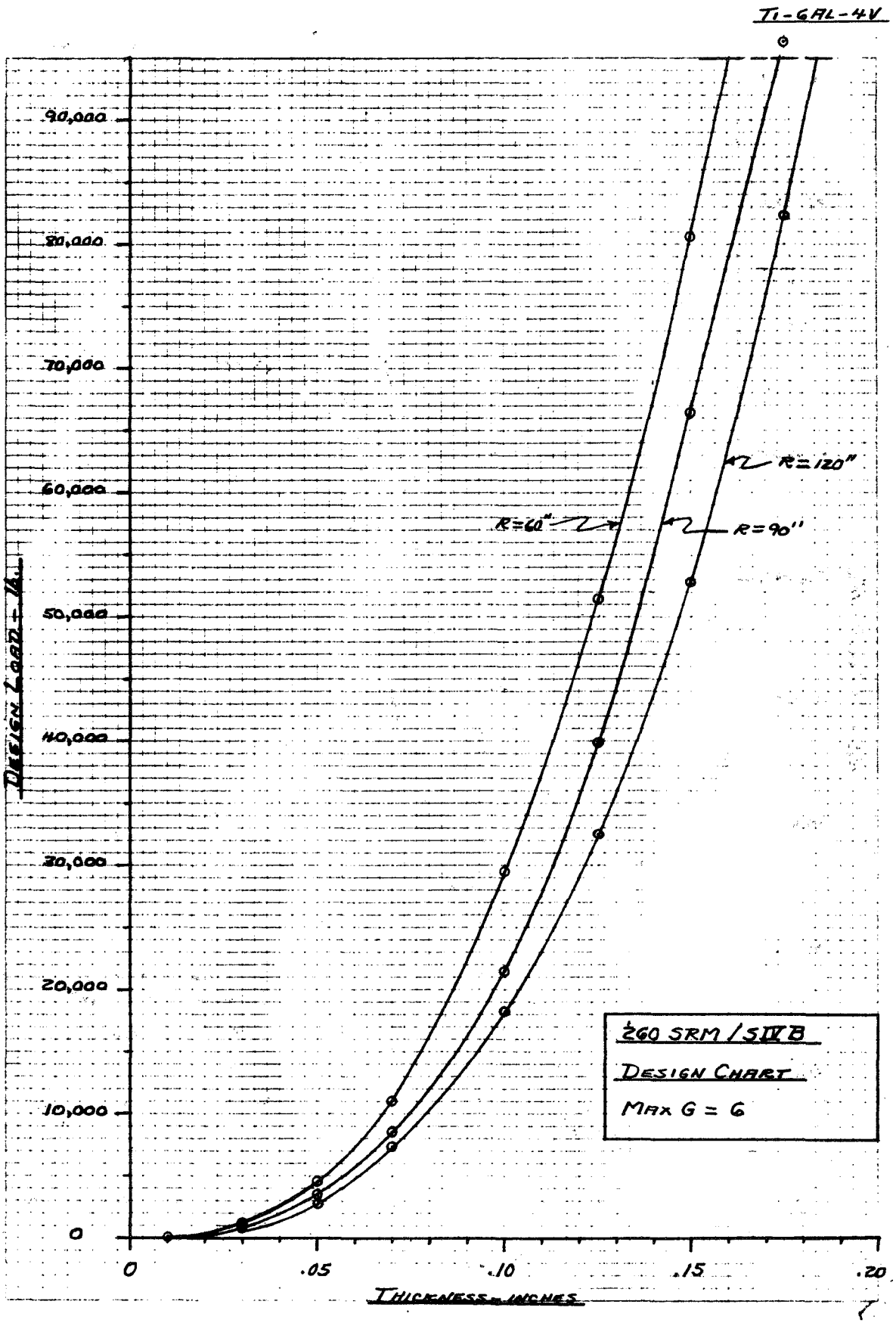
Ti-6AL-4V
90,000
80,000
70,000
60,000
50,000
40,000
30,000
20,000
10,000
0
DESIGN LOAD - LB.
R=60"
R=90"
R=120"
0
.05
.10
.15
.20
THICKNESS - INCHES
260 SRM / SIVB
DESIGN CHART
MAX G = 6

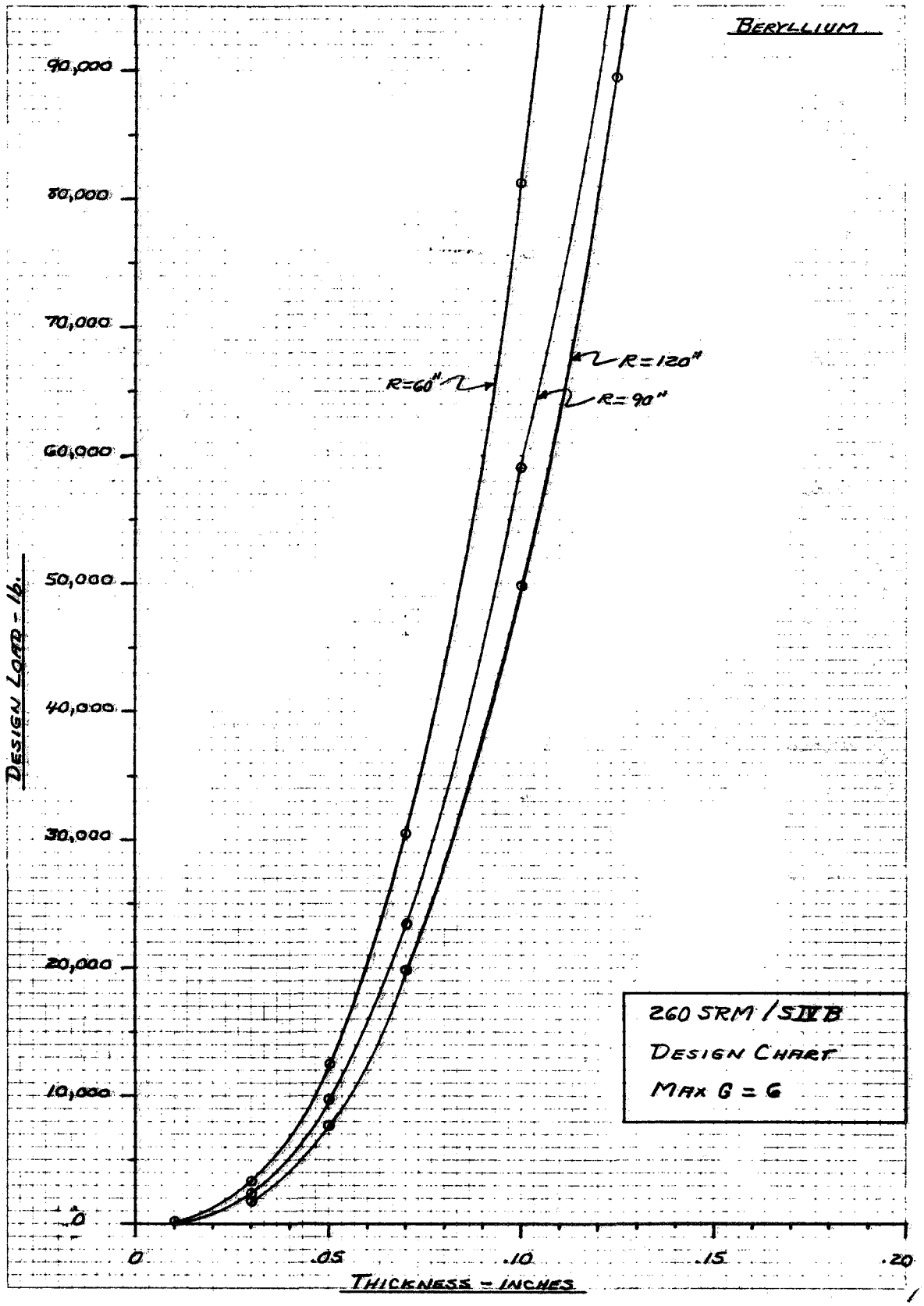
BERYLLIUM
90,000
80,000
70,000
60,000
50,000
40,000
30,000
20,000
10,000
0
DESIGN LOAD - lb.
R=60"
R=120"
R=90"
0
.05
.10
.15
.20
THICKNESS - INCHES
260 SRM / SIVB
DESIGN CHART
MAX G = 6

Stage Design Chart
Buckling Coefficients
t = 0 - .25"
R = 30 - 198"
R=30"
R=60"
R=90"
R=120"
R=150"
R=198"
C = Buckling Coefficient
Thickness - Inches
0
.05
.10
.15
.20
.25
.1
.2
.3
.4
.5

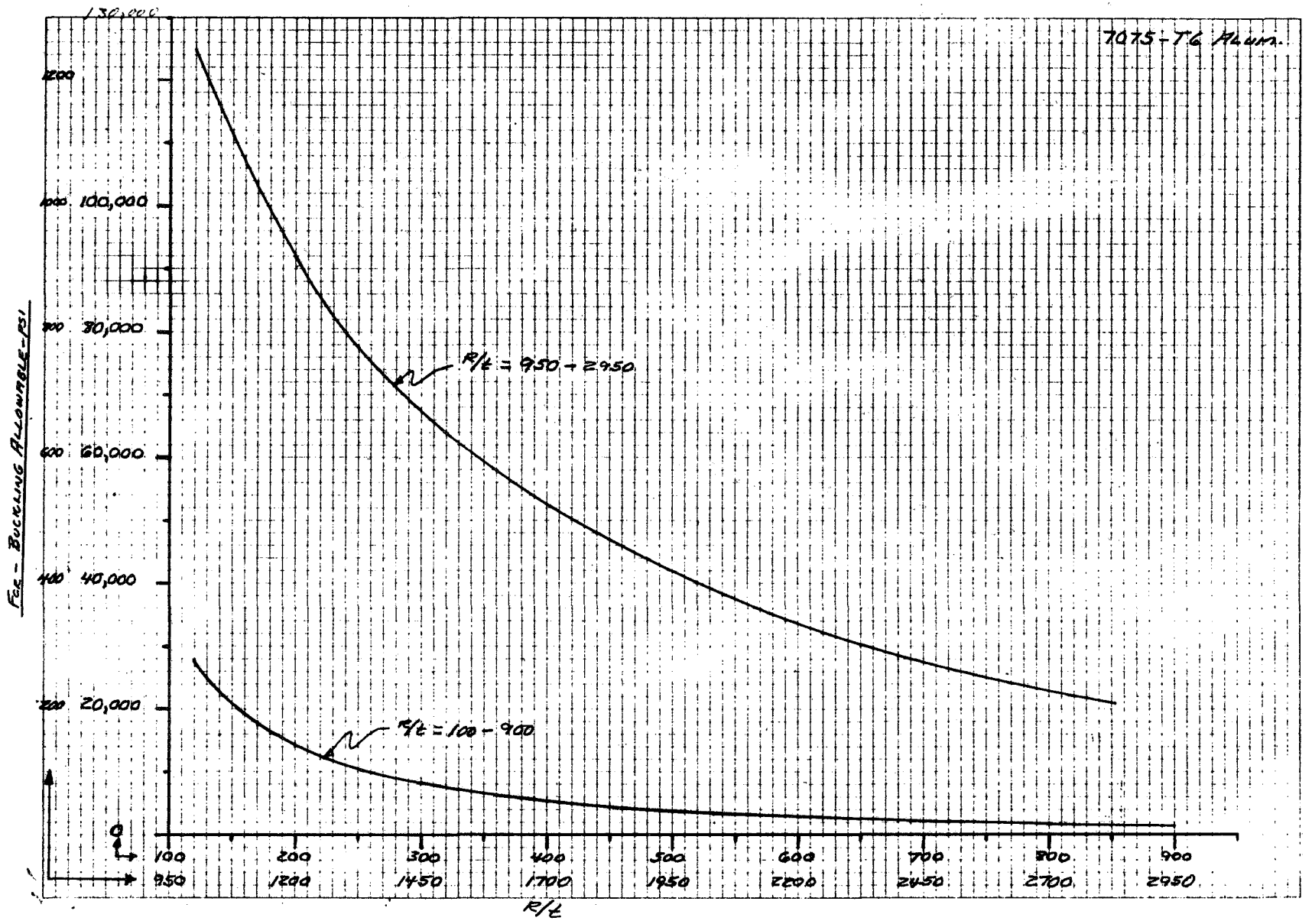
7075-T6 Aluminum
F_{cc} - Buckling Allowable - PSI
130,000
120
100 100,000
80 80,000
60 60,000
40 40,000
20 20,000
R/t = 950 - 2950
R/t = 100 - 900
Q
100 200 300 400 500 600 700 800 900
950 1200 1450 1700 1950 2200 2450 2700 2950
R/t

7075-T6 Aluminum
Semi-Monocoque Design Chart

$$F_{CR} = \frac{k_c \pi^2 E}{12(1-\mu_e^2)}\left(\frac{t}{b}\right)^2$$

$$Z = \frac{b^2}{Rt}\left(1-\mu_e^2\right)^{1/2}$$

$E = 10.4 \times 10^6$ PSI

$\mu_e = 0.33$

$R = 130''$

b = Plate Width

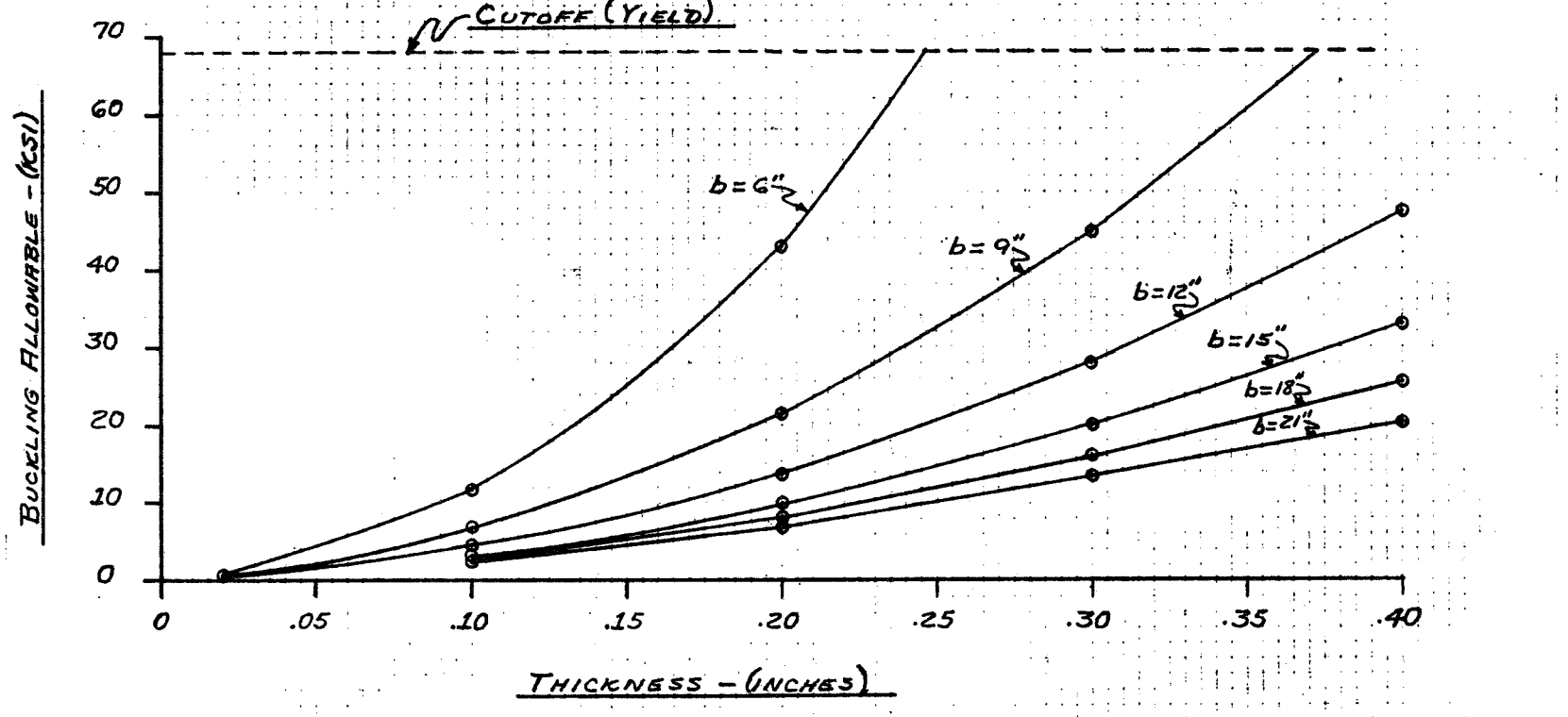

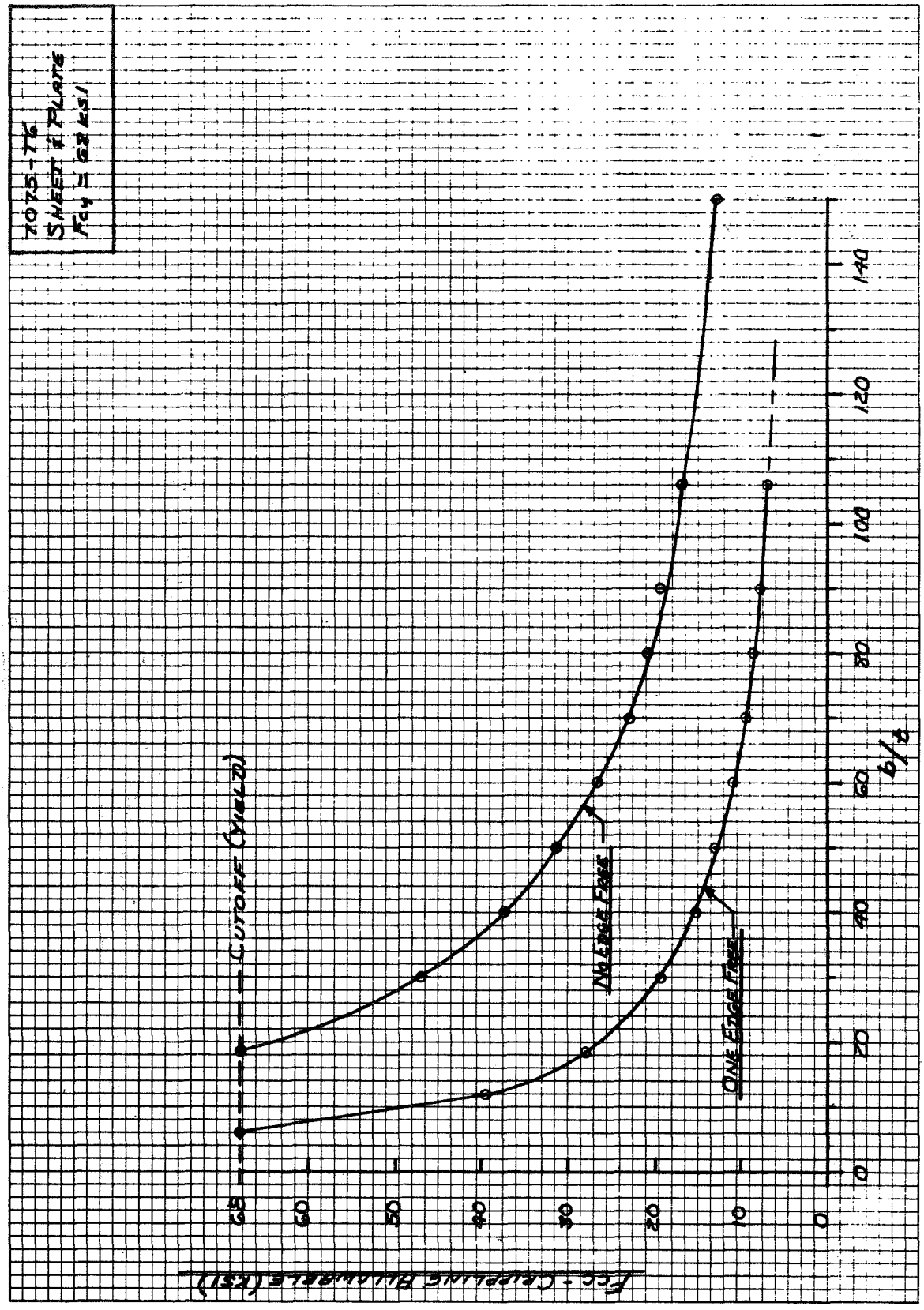
7075-T6
SHEET & PLATE
Fcy = 68 ksi
Fcc - CRIPPLING STRESS (KSI)
CUTOFF (YIELD)
NO EDGE FREE
ONE EDGE FREE
t/b
0
20
40
60
80
100
120
140
70
60
50
40
30
20
10
0

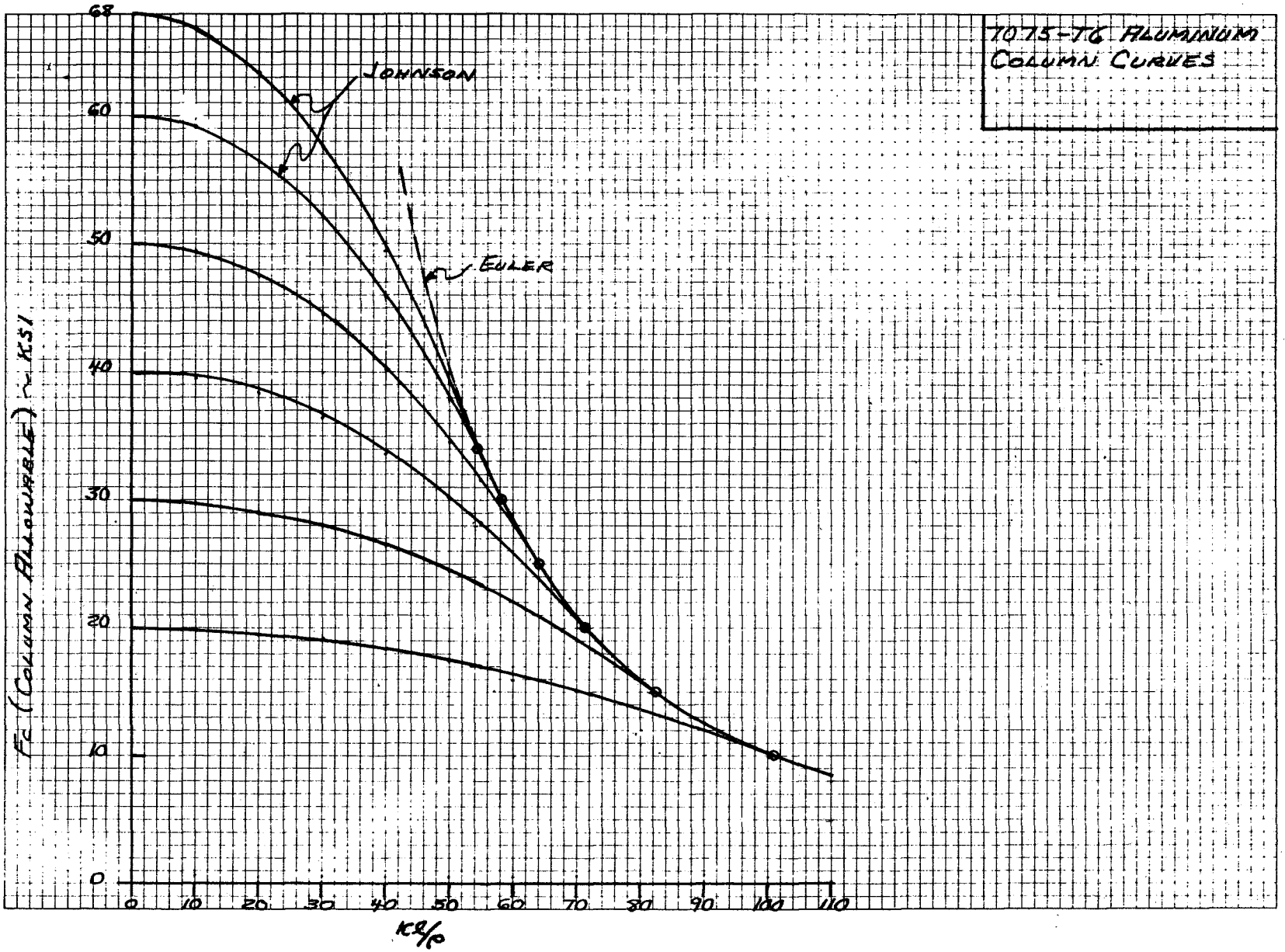
7075-T6 ALUMINUM
COLUMN CURVES
JOHNSON
EULER
F_c (COLUMN ALLOWABLE) ~ KSI
KL/ρ
0
10
20
30
40
50
60
68
70
80
90
100
110

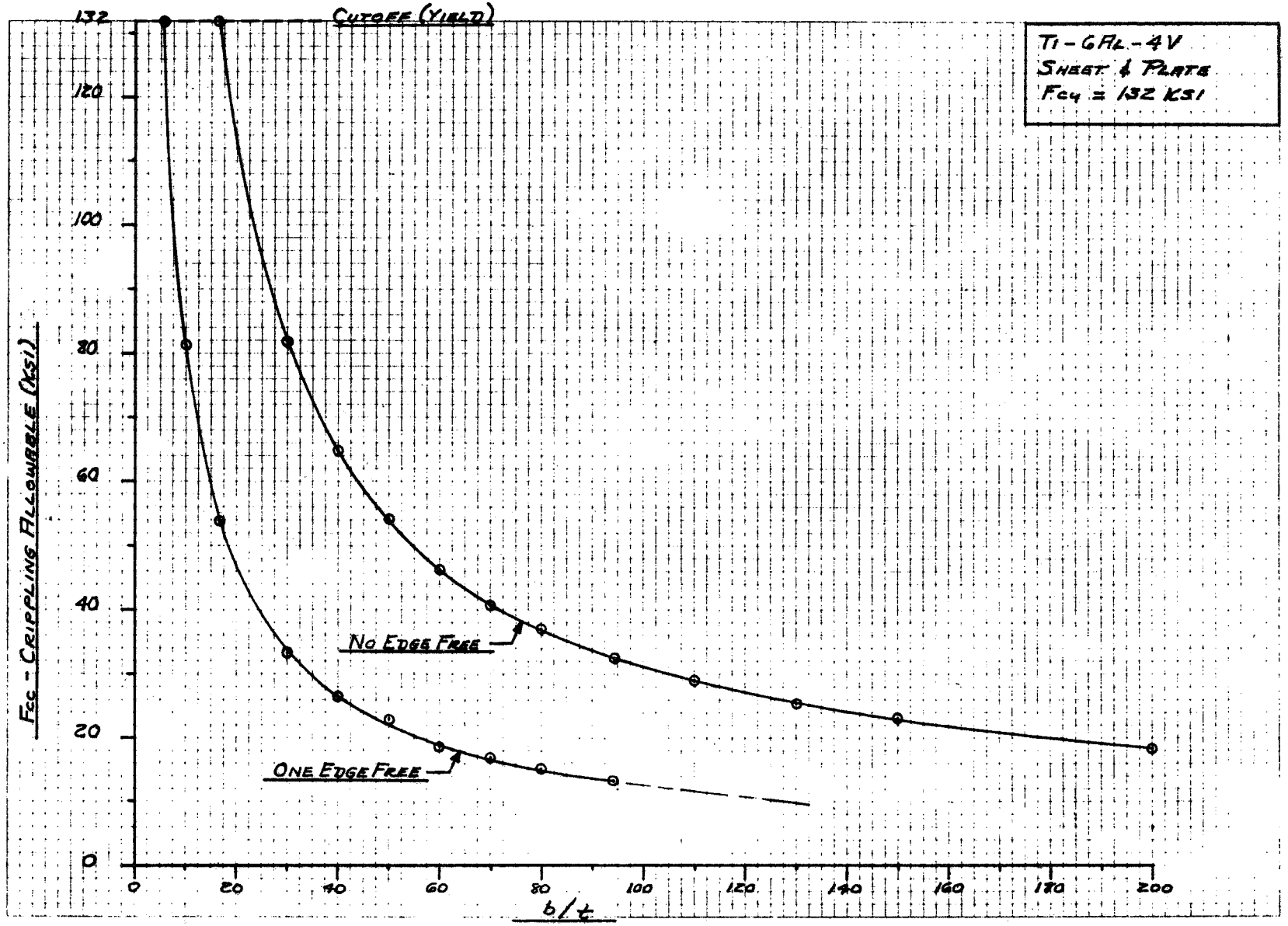
Cutoff (Yield)
Ti-6Al-4V
Sheet & Plate
Fcy = 132 KSI
Fcc - Crippling Allowable (KSI)
No Edge Free
One Edge Free
b/t
132
120
100
80
60
40
20
0
0
20
40
60
80
100
120
140
160
180
200

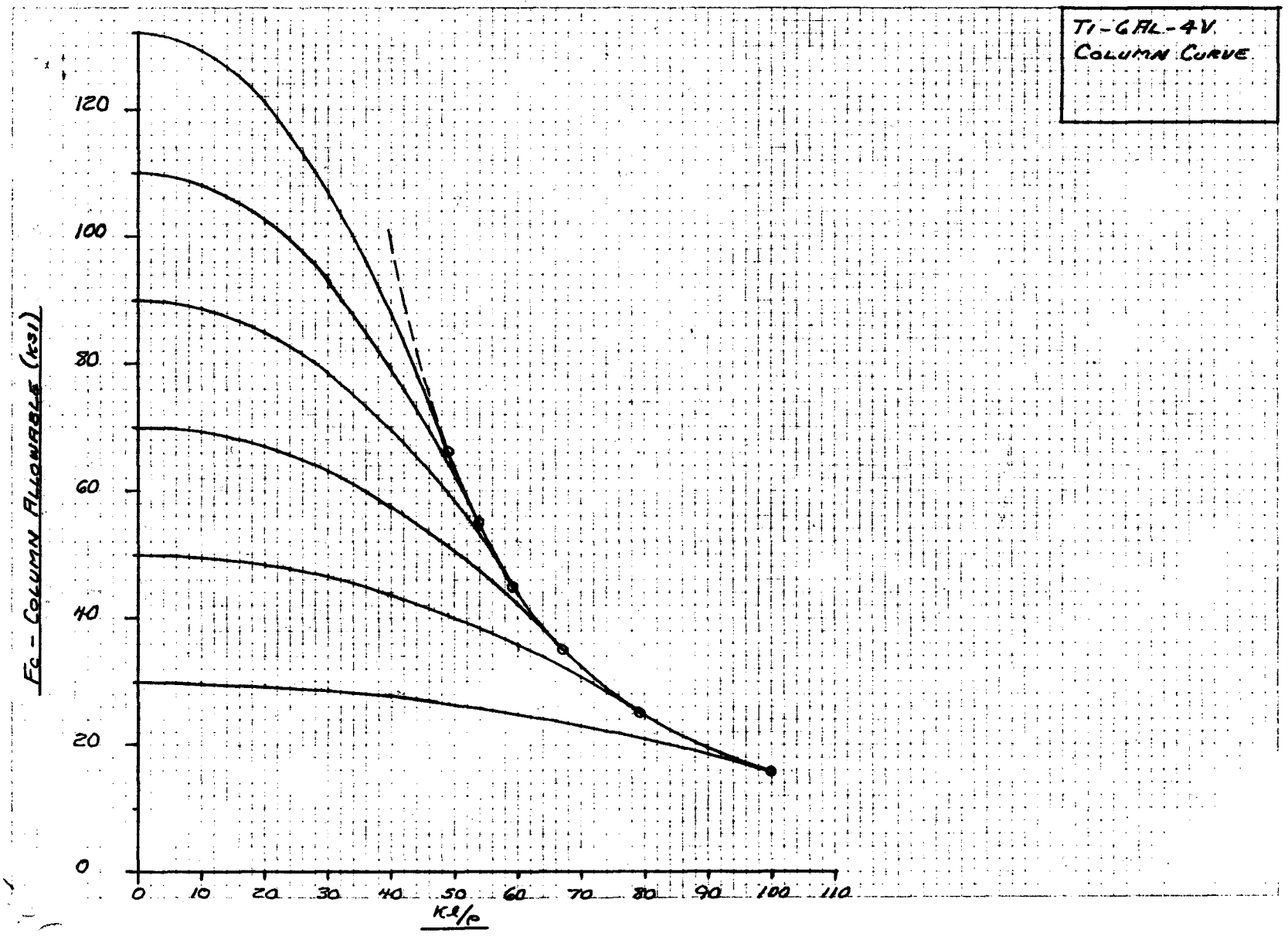
Ti-6Al-4V
Column Curve
Fc - Column Allowable (ksi)
120
100
80
60
40
20
0
0
10
20
30
40
50
60
70
80
90
100
110
Kℓ/ρ

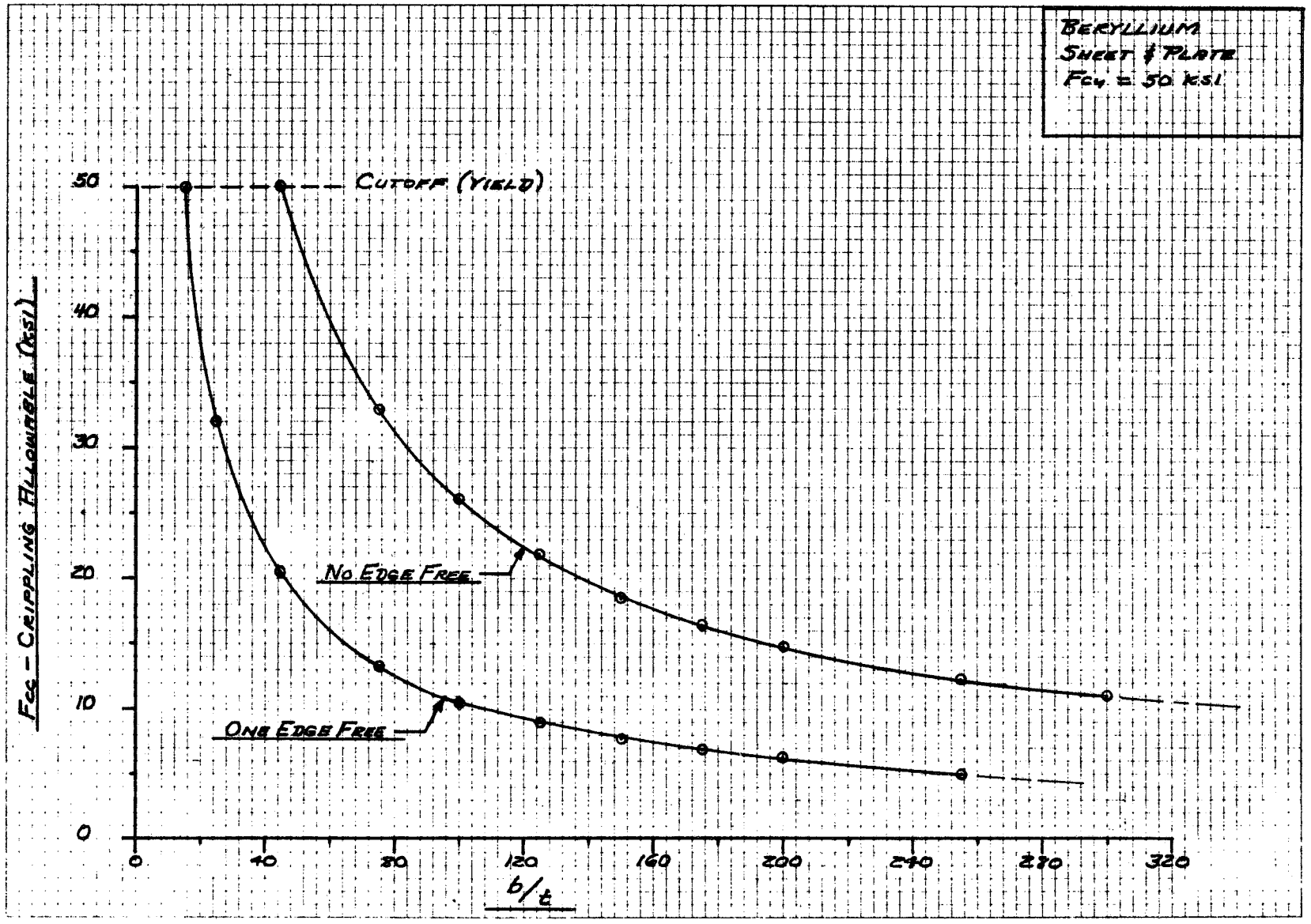
BERYLLIUM
SHEET & PLATE
F_{cy} = 50 KSI
F_{cc} - CRIPPLING ALLOWABLE (KSI)
CUTOFF (YIELD)
NO EDGE FREE
ONE EDGE FREE
50
40
30
20
10
0
0
40
80
120
160
200
240
280
320
b/t

Beryllium
Column Curve
Fc - Column Allowable (ksi)
50
40
30
20
10
0
0
25
50
75
100
125
150
175
200
225
250
kL/ρ

F-33